

EXPERT REPORT: Case No. 18 WATER 14014

for

John Winchester, High Country Hydrology

- a) Consulted for: municipal water resources planning, hydrological analyses, drought simulation, use of the 1% drought in the planning process, and technical tools and models
- b) The grounds for John Winchester's opinions are knowledge of pertinent information presented in City of Wichita's Response to Production Request of Equus Beds Groundwater Management District No.2 and City of Wichita's Responses to Intervener's Production Requests, as referenced in the summaries of the respective opinions below, and in several cases, excerpted and attached for convenience of reference.
- c) John Winchester's factual observations and opinions, as presented in the Proposal documents and summarized herein, include:
 - iii. Expert opinions based on scientific analyses:
 - 2.1 1% Drought Reconstruction - Palmer Drought Severity Index (PDSI)
 - The PDSI is utilized by the National Oceanic and Atmospheric Administration (NOAA), the United States Department of Agriculture (USDA), the United States Drought Monitor (USDM), and other agencies to classify relative drought conditions.
Proposal Attachment B - Palmer Drought Severity Index, Research Paper No. 45 is provided as Attachment A to this Report.
 - HCH found that the PDSI chronology could be used to review historic droughts of record for their intensity and duration.
Cook (1999 and 2007) constructed PDSI timeseries referenced by HCH. These reports are provided as Attachment B-1 and B-2 to this Report.
Attachment C - HCH 1% Drought Reconstruction Technical Memorandum summarizes the basis for selecting the droughts of varying duration. Attachment C of the Proposal is provided as Attachment B-3 to this Report.
 - HCH calculated that a 1% drought can be approximated by the drought of 1933 through 1940.

Layzell (2012) investigated past drought occurrences in Kansas from paleoclimate records over the last 1000 years. In terms of the long-term record of drought variability, the 1930s and 1950s droughts are not unusual. This report is provided as Attachment C-1 to this Report.

- Woodhouse & Overpeck (1998): The paleoclimatic data suggest a 1930s-magnitude Dust Bowl drought occurred once or twice a century over the past 300–400 years, and a decadal-length drought once every 500 years. This report is provided as Attachment C-2 to this Report. Table 2-2: 1% Drought Reconstruction from PDSI

- PDSI data associated with the 1930's drought demonstrate conditions similar to reconstructed 1% droughts. Table 2-2 is provided as Attachment D.

- 2.3 Integrated Water Resources Management During a 1% Drought Using MODSIM-DSS

- MODSIM-DSS is a water resources management decision support system software that can simulate networked raw water resources such as reservoirs, streams, or aquifers.

HCH was consulted to convert Burns & McDonnell's RESNET hydrologic computer simulation model to MODSIM-DSS. Discussion of the RESNET model has been presented as part of Exhibits: ASR EIS Appendices; the excerpts are presented as Attachment E-1.

Conversion and utilization of the model by HCH was done as presented in pages 1-43 of Exhibits: HCH Documents; the excerpts are presented as Attachment E-2.

The converted model was peer-reviewed by Burns and McDonnell.

Section 2.3 of the Proposal has been provided as Attachment E-3 of this Report.

- The model was updated to reflect 1% drought conditions including hydrologic components, projected future demand, and water resources assumptions.

The MODSIM-DSS model was developed to reflect observed and constructed streamflows and evaporative conditions to represent the 1930's drought.

- Figure 1 - MODSIM DSS Network GUI

- The model represents the resources as well as environmental effects.

Stream losses and gains to the adjacent aquifer are calculated from modeled conditions.

Figure 1 of the Proposal has been provided as Attachment F.

- d) John Winchester is a High Country Hydrology employee; the subdirectory Contracts provided in the City's Production of Documents discloses contractual agreements with R.W. Beck, Inc., and SAIC Energy, Environment & Infrastructure, LLC. Each company was directly engaged by the City of Wichita; these Contracts are also provided.
- e) John Winchester's qualifications are as presented in the City of Wichita's Preliminary Expert Disclosure.
- f) John Winchester's factual observations and opinions are as presented above in this Expert Report, ASR Permit Modification Proposal, cover letter, and supporting appendices.

John Winchester, High Country Hydrology

DRAFT

ATTACHMENT B
Palmer Drought Severity Index, Research Paper No. 45

U.S. DEPARTMENT OF COMMERCE

JOHN T. CONNOR, *Secretary*

WEATHER BUREAU

ROBERT M. WHITE, *Chief*

RESEARCH PAPER NO. 45

Meteorological Drought

WAYNE C. PALMER

Office of Climatology
U.S. Weather Bureau, Washington, D.C.



National Climatic Data Center
Federal Building Library
Asheville, NC 28801-2696

WASHINGTON, D.C.

FEBRUARY 1965

FOREWORD

Drought has been cited as a scourge of mankind since biblical times. It still is a major menace to world food supplies. Insect plagues, with which it ranks as a crop threat, can be fought by modern means. Drought remains an unconquered ill.

Meteorological science has not yet come to grips with drought. It has not even described the phenomenon adequately. This is certainly the first step toward understanding. And then a long road remains ahead toward prediction and, perhaps, limited control. This paper is an important step toward these goals. It presents a numerical approach to the problem and thus permits an objective evaluation of the climatological events.

Although often so classified, drought is not just an agricultural problem. It affects the city dweller, whose water may be rationed, and the industrial consumers of water as well. In fact, water is one of the most vital natural resources. Its lack, regionally or temporally, has the most profound effect on economy. In a country as large as the United States drought is likely to affect only a part of its territory at any one time. However, no section is entirely spared of droughts and occasionally substantial areas are affected. By severity and duration these events can be calamitous not only locally but for the whole economic structure. Hence knowledge of the probability of their occurrence and their course is an essential element for planning. The thorny problem of a rational land utilization is closely tied in with these considerations.

The pioneering work of the late C. W. Thornthwaite on potential evapotranspiration has underlain all modern attempts to assess the water balance. As in his work, the aim of the effort reported on in this paper remains primarily on the climatological aspects. The new method presented here is directed at a quantitative assessment of periods of prolonged meteorological anomalies. We hope it is a step forward and that it can be followed by similar analyses on a broader geographical basis.

H. E. LANDSBERG.

CONTENTS

	Page
Foreword.....	II
List of Symbols.....	V
Abstract.....	1
1. INTRODUCTION.....	1
Definitions.....	2
Points of view.....	2
Speculations concerning the definition.....	3
2. THE PROBLEM AND OBJECTIVES.....	4
3. DEVELOPMENTAL DATA USED.....	4
4. TECHNIQUES USED AND THEIR LIMITATIONS.....	6
5. PROCEDURE AND DISCUSSION.....	9
Hydrologic accounting.....	9
Potential values.....	9
Coefficient of evapotranspiration, α	11
Coefficient of recharge, β	13
Coefficient of runoff, γ	13
Coefficient of loss, δ	13
CAFEC precipitation, \hat{P}	14
Precipitation excesses and deficiencies.....	15
The climatic characteristic, K	17
The moisture anomaly index, z	18
6. THE DURATION FACTOR.....	20
The effect of time.....	20
Drought categories.....	20
The driest intervals.....	20
Determining monthly increments of drought severity.....	21
7. RE-EVALUATION OF THE WEIGHTING FACTOR.....	23
Evidence of unsatisfactory k values.....	23
A procedure for estimating mean values of K	23
K as a function of other aspects of climate.....	24
Monthly weighting factors.....	24
Final adjustment of the monthly K values.....	26
Standard deviation of d as a weighting factor.....	26
An example of the drought severity computations.....	26
8. APPLICATION OF THE DROUGHT FORMULAS TO WET PERIODS.....	28
9. END OF DROUGHT (OR WET SPELLS).....	28
Changes in the severity index.....	28
Determining the end of a drought.....	29
Determining the end of a wet spell.....	30
10. PROCEDURE FOR COMPUTING THE SEVERITY OF DROUGHT AND WET SPELLS.....	30
11. RESULTS FOR WESTERN KANSAS DROUGHTS.....	34
The drought of 1894.....	34
The drought of 1913.....	34
The drought of the 1930's.....	34
Agricultural aspects.....	34
Vegetative cover measurements.....	37
The duststorms.....	37
Disaster declaration.....	37
The 1950's drought.....	37
Drought and streamflow.....	38
Pasture feed conditions.....	39
12. DROUGHT CONDITIONS IN CENTRAL IOWA.....	40
The drought of 1934.....	40
Hydrologic data.....	40
The drought of 1936.....	41
The drought of 1947.....	42
The drought during the 1950's.....	42

	Page
13. SUMMARY OF DROUGHT PERIODS AND FREQUENCY OF DROUGHT CLASSES.....	43
Western Kansas.....	43
Central Iowa.....	44
Meaning of the drought classes.....	44
14. PROGNOSTIC VALUE OF THE INDEX.....	45
15. THE METHOD APPLIED TO NORTHWESTERN NORTH DAKOTA.....	47
Results and verification.....	47
An example of current drought analysis.....	49
16. CONCLUDING REMARKS.....	50
ACKNOWLEDGMENTS.....	50
APPENDIX A. AUXILIARY CLIMATIC INFORMATION.....	51
Geographic distribution of the climatic constants.....	51
Distribution of the moisture departures.....	51
APPENDIX B. EFFECT OF THE AVAILABLE WATER CAPACITY TERM.....	52
Purpose of the <i>AWC</i> value.....	52
Experiments at Dover, Del.....	52
Effect of unrepresentative <i>AWC</i> values.....	53
Areas with small storage capability.....	53
APPENDIX C. ANALYSIS OVER OTHER TIME OR SPACE UNITS.....	54
Weekly analyses.....	54
Results.....	54
Conclusions.....	54
Point versus area analysis.....	55
APPENDIX D. RELATIVE INSTABILITY OF THE CLIMATE OF WESTERN KANSAS SINCE THE EARLY 1930's.....	55
APPENDIX E. RECURRENCE OF SERIOUS DROUGHT IN WESTERN KANSAS.....	56
REFERENCES.....	56

LIST OF FIGURES

1. Accumulated index during the driest periods of various lengths.....	20
2. An illustration of the cumulative procedure. (A) Six relatively dry months followed by four very dry months, (B) The four very dry months by themselves.....	21
3. Mean annual weighting factor as related to average moisture demand, average moisture supply, and average absolute moisture departure.....	24
4. Mean pasture condition, western Kansas, June 1 to November 1, versus the average index, \bar{X} , for the same growing season. Data for the period 1932 to 1957.....	40
5. Mean monthly precipitation in central Iowa.....	46
6. Mean monthly precipitation in western Kansas.....	46
7. Cumulative annual number of months with $ X < 1.0$, western Kansas.....	55

LIST OF TABLES

1. Hydrologic accounting for central Iowa.....	10
2. Long-term means.....	12
3. Climatic coefficients and constants.....	12
4. Climatic analysis of moisture departures in western Kansas.....	15
5. Monthly moisture departure, <i>d</i> , western Kansas.....	16
6. Monthly moisture departure, <i>d</i> , central Iowa.....	17
7. The driest intervals.....	20
8. The amount of abnormal dryness required to maintain a given drought severity.....	22
9. Monthly weighting factor, <i>K</i> , for selected places.....	25
10. A selected 3-month dry period in 1947 in central Iowa.....	27
11. Classes for wet and dry periods.....	28
12. An example of the computational procedure for determining the beginning and ending of wet periods and dry periods and the monthly severity index of each (western Kansas data).....	31
13. Drought (and wet spell) index, <i>X</i> , western Kansas.....	35
14. Total basal cover of short grasses in an ungrazed prairie near Hays, Kansas (after Weaver and Albertson)....	37
15. Drought index values and the least amount of runoff (thousands of acre-feet) during periods of various lengths ending with the month and year shown, western Kansas.....	39
16. Drought (and wet spell) index, <i>X</i> , central Iowa.....	41
17. Drought periods, western Kansas, 1887-1962.....	43
18. Drought periods, central Iowa, 1930-1962.....	44

	Page
19. Contingency table showing May precipitation in central Iowa as a function of the index value at the end of April.....	45
20. Means, coefficients, and constants for northwestern North Dakota (1931-1960).....	47
21. Drought periods, northwestern North Dakota, 1931-1962.....	48
22. Moments of the departures, d	51

LIST OF SYMBOLS

	Page*
α coefficient of evapotranspiration.....	11
α_3 standardized third moment, a measure of skewness.....	51
β coefficient of moisture recharge.....	13
γ coefficient of runoff.....	13
δ coefficient of loss.....	13
Δ net change during a month.....	22
σ standard deviation.....	51
a a measure of kurtosis.....	51
AWC available water capacity of the soil.....	7
c a coefficient expressing the tendency to return to normal.....	22
$CAFEC$ Climatically Appropriate For Existing Conditions.....	12
d moisture departure for a particular month, $P - \hat{P}$	15
\bar{d} average monthly moisture departure.....	18
\bar{D} the mean of the absolute values of d	25
\overline{ET} computed evapotranspiration for an individual month.....	7
\overline{ET} long-term mean evapotranspiration for a calendar month.....	11
\widehat{ET} CAFEC evapotranspiration.....	14
i dummy variable denoting a particular month in a series of months.....	14
j dummy variable indicating the number of months of lag.....	29
k the first approximation of K	18
K' the second approximation of K	25
K the climatic characteristic or weighting factor.....	18
\bar{K} a mean weighting factor.....	18
L net loss of soil moisture during a month.....	7
\bar{L} long-term mean soil moisture loss for a calendar month.....	13
\hat{L} CAFEC soil moisture loss.....	14
L_s computed moisture loss from the surface layer of the soil.....	7
L_u computed moisture loss from the soil underlying the surface layer.....	7
P areal average precipitation for a particular month.....	7
\bar{P} long-term mean precipitation for a calendar month.....	11
\hat{P} CAFEC precipitation.....	14
P_e percentage probability that a weather spell has ended.....	29
\overline{PE} potential evapotranspiration for an individual month.....	7
\overline{PE} long-term mean potential evapotranspiration for a calendar month.....	11

*Page on which symbol is introduced.

	Page*	
PL	potential loss of soil moisture, $PL_s + PL_u$	10
\overline{PL}	long-term mean potential loss of soil moisture for a calendar month.....	13
PL_s	potential loss of soil moisture from the surface layer.....	10
PL_u	potential loss of soil moisture from the underlying soil.....	10
PR	potential recharge; amount of moisture required to bring the soil to field capacity....	9
\overline{PR}	long-term mean potential recharge for a calendar month.....	13
PRO	potential runoff.....	11
\overline{PRO}	long-term mean potential runoff for a calendar month.....	13
Q	Z_e plus the previously accumulated moisture anomaly: the denominator of equation (30).....	29
R	recharge; net gain in soil moisture during month.....	11
\overline{R}	long-term mean soil moisture recharge for a calendar month.....	13
\hat{R}	CAFEC soil moisture recharge.....	14
RO	computed runoff.....	9
\overline{RO}	long-term mean runoff for a calendar month.....	13
\widehat{RO}	CAFEC runoff.....	14
S	amount of available moisture in both layers of soil at the end of a month, $S_s + S_u$	9
S'	amount of available moisture in both layers of the soil at the start of a month.....	10
S_s	amount of available moisture in the surface soil layer at the end of a month.....	9
S'_s	amount of available moisture in the surface soil layer at the start of a month.....	7
S_u	amount of available moisture in the underlying soil at the end of a month.....	9
S'_u	amount of available moisture in the underlying soil at the start of a month.....	7
t	duration in months.....	21
T	areal average temperature for a particular month.....	10
U_d	the amount of dryness effective in ending a wet spell.....	30
U_w	the amount of wetness effective in ending a drought.....	29
V	accumulated values of U_d or U_w ; the numerator of equation (30).....	29
X	the index of drought (or wet spell) severity.....	21
X_1	(1) drought severity for an initial dry month.....	22
	(2) severity index for a wet spell that is becoming established. It is also the percent chance that a wet spell has begun.....	32
X_2	severity index for a drought that is becoming established. It is also the percent chance that a drought has begun.....	32
X_3	the severity index for any wet spell or any drought that has become definitely established.....	32
z	the preliminary estimate of Z	18
Z	moisture anomaly index.....	23
Z_e	the moisture anomaly required to end a "weather spell" in a single month.....	29

*Page on which symbol is introduced,

METEOROLOGICAL DROUGHT

WAYNE C. PALMER

Office of Climatology, U.S. Weather Bureau, Washington, D.C.

[Manuscript received July 23, 1962; revised June 16, 1964]

ABSTRACT

Drought can be considered as a strictly meteorological phenomenon. It can be evaluated as a meteorological anomaly characterized by a prolonged and abnormal moisture deficiency. Not only does this approach avoid many of the complicating biological factors and arbitrary definitions, it enables one to derive a climatic analysis system in which drought severity is dependent on the duration and magnitude of the abnormal moisture deficiency. Within reasonable limits, time and space comparisons of drought severity are possible. The objective of this paper is to develop a general methodology for evaluating the meteorological anomaly in terms of an index which permits time and space comparisons of drought severity.

The underlying concept of the paper is that the amount of precipitation required for the near-normal operation of the established economy of an area during some stated period is dependent on the average climate of the area and on the prevailing meteorological conditions both during and preceding the month or period in question. A method for computing this required precipitation is demonstrated. The difference between the actual precipitation and the computed precipitation represents a fairly direct measure of the departure of the moisture aspect of the weather from normal. When these departures are properly weighted, the resulting index numbers appear to be of reasonably comparable local significance both in space and time.

Successive monthly index values for past dry periods were combined by a relatively objective procedure to yield an equation for calculating drought severity in four classes—mild, moderate, severe, and extreme. The method of analysis is described and the results of applying the procedure to 76 years of western Kansas weather, 33 years of central Iowa weather, and 32 years of independent data from northwestern North Dakota are presented.

The procedure is tractable for machine data processing by weekly or monthly periods for either points or areas. When this type of climatic analysis has been carried out for a large number of contiguous areas, not only will one obtain drought severity expectancy figures but also other useful items as well. For instance, the analysis will provide wet period expectancies, maps useful in land use capability studies, and material of interest in water resources planning. In addition, some of the derived parameters will very likely prove to be useful in crop yield investigations.

1. INTRODUCTION

Drought means various things to various people, depending on their specific interest. To the farmer drought means a shortage of moisture in the root zone of his crops. To the hydrologist it suggests below average water levels in streams, lakes, reservoirs, and the like. To the economist it means a water shortage which adversely affects the established economy. Each has a concern

which depends on the *effects* of a fairly prolonged weather anomaly.

A completely adequate definition of drought is difficult to find. Not only is there disagreement as to the meaning of the word, even its spelling and pronunciation provide room for discussion. It is variously spelled as "drought" and "drouth." Recommended pronunciation for the first spelling

is "drou" (as in trout) and the second form becomes "drouth" (as in south) [3]. These interesting sidelights are indicative of the confusion that prevails.

DEFINITIONS

From previous drought studies one can assemble a number of definitions, such as:

1. A period with precipitation less than some small amount such as 0.10 in. in 48 hr. [6].

2. A period of more than some particular number of days with precipitation less than some specified small amount [16].

3. A period of strong wind, low precipitation, high temperature, and unusually low relative humidity (this has been referred to as "atmospheric drought") [7].

4. A day on which the available soil moisture was depleted to some small percentage of available capacity [68].

5. A period of time when one or all of the following conditions prevailed: (a) Pasturage becoming scarce, (b) Stock losing condition from fair order, (c) Hand feeding in vogue, (d) Agistment of stock [72].

6. Monthly or annual precipitation less than some particular percentage of normal [30].

7. A condition that may be said to prevail whenever precipitation is insufficient to meet the needs of established human activities [20].

The list could be extended, but nearly all have in common a certain arbitrariness difficult, in some cases, to defend. A surprising number ignore the protracted dry spell concept given in most dictionaries and emphasized by Linsley et al. [28], and only a few, such as the *Glossary of Meteorology* [22] and Blair [5] recognize that drought is a relative term.

It appears that the press and the general public use the term in a more consistent way than do meteorologists, climatologists, hydrologists, and the other scientists who have done work on the subject. It is worthy of note that the term does not ordinarily appear in the public press until an area has endured an unusual moisture deficiency for an extended period of time. Those journalists who use such expressions as "drought of investment capital" and "man-power drought" must assume their share of responsibility for using "drought" as a synonym for "shortage."

However, most farmers do not call a "dry spell" a drought until matters begin to become rather

serious. In spite of the differences which exist, the people in humid climates seem to mean much the same thing when they refer to drought as do the people in a semiarid region; viz, that the moisture shortage has seriously affected the *established* economy of their region. From consideration of the many facets of the problem, it is possible to formulate a generalized definition that can be used as a starting point. Drought is therefore defined here as a prolonged and abnormal moisture deficiency. This is essentially the definition given by the American Meteorological Society [22]. At the outset this definition may appear to be too generalized for any useful purpose, but examination will show that it established the guidelines necessary for further work. Foley [14] presented an excellent discussion based on a somewhat similar generalized approach.

This may be regarded as a generalized meteorological definition rather than a specific biologic or hydrologic one. In fact, many of the specialized aspects and ramifications of drought can be accommodated by the definition. This generalized definition has been chosen deliberately in order that the phenomenon may be studied in as objective a manner as possible without first having arbitrarily defined "prolonged", or "abnormal" or "moisture deficiency."

POINTS OF VIEW

Agricultural drought is probably the most important aspect of drought, but that problem is far more specialized and complicated than some investigators seem to realize. A study of agricultural drought immediately leads one into the realms of soil physics, plant physiology, and agricultural economics. Of all the available possibilities one must choose a particular one, thereby limiting the useful results to particular crops grown under specified conditions of soil and cultural practices.

Hydrologic drought, concerned as it is with reductions in stream flow and in lake and reservoir levels, depletion of soil moisture, a lowering of the ground-water table, and the consequent decrease in ground-water runoff [21], also poses specialized problems. This is far from being a purely meteorological problem. It is, in fact, more of an engineering problem which involves not only meteorology and hydrology, but geology and other geophysical sciences as well.

As a matter of fact, both agriculture and hydrology are more concerned with the effects of the moisture shortage than with the purely meteorological aspects. The onset of the effects can be immediate or delayed; likewise, recovery from a recent moisture shortage can be almost immediate or delayed, depending on the particular circumstances of the area and activity affected. For these and other reasons crop yields, pasture conditions, stream flow, lake levels, and the like are not particularly satisfactory measures of the severity of meteorological drought. Probably the severity is most closely related to some localized economic measure of the disruption of the established economy. If such a measure exists, it has not come to the author's attention. In this connection it should be mentioned that man-made drought, a demand, created by economic development, for more water than is normally available in an area, was not considered in this study. However, the procedures developed here will shed some light on the problems of such over-developed regions.

SPECULATIONS CONCERNING THE DEFINITION

During recent years the U.S. Government has recognized and provided economic aid to areas which have endured "disaster." Among the various things that can create a disaster is drought. This is not generally considered to be a moisture deficiency that causes mere inconvenience or even one that creates mild hardship, but rather a shortage of water so unusual that it creates destruction or ruin, as of life or property [31]. It is almost impossible for this degree of drought disaster to develop over a short period of time; at least two or three months of extremely unusual weather are required and ordinarily the time is much greater, say a year or more [18].

This relatively substantial fact concerning disastrous drought provides a general framework for speculation concerning the period of time involved in a definition of "prolonged"; it is apparently of the order of months. However, it

seems reasonable to postulate that a mild drought could develop in a single month.

It may at first seem that "moisture deficiency" should be easier to define than "prolonged," and in some respects it is. However, more is involved than a mere rainfall record. An area may welcome a period of dry weather if the period immediately preceding was unusually wet. The dry weather provides an opportunity for getting rid of an oversupply of water and allows the area to operate on a more normal basis—a basis which is ordinarily adjusted to the climatic averages, having been arrived at by many years of trial and error. Antecedent conditions must therefore be taken into account when evaluating the adequacy of rainfall. One indirect method for accomplishing this is through measurements or estimates of the amount of available soil moisture at the beginning of the period of little or no precipitation. Soil moisture may therefore be regarded as an *index* of antecedent weather conditions. Deficiency, of course, implies a demand which exceeds supply; however, the "abnormal" aspect must also be considered.

A thing is abnormal that deviates markedly from what has been established as some measure of the middle point between extremes. It is therefore reasonable to state that a period during which moisture need exceeds moisture supply by an *unusual* amount could be considered as a period of abnormal moisture deficiency. By this postulate of abnormality various climates can be placed on a relatively equal basis insofar as drought is concerned.

The foregoing discussion may seem to be largely a matter of semantics; however, it has served to develop a basis for a somewhat meaningful approach to the drought problem. A drought period may now be defined as an interval of time, generally of the order of months or years in duration, during which the actual moisture supply at a given place rather consistently falls short of the climatically expected or climatically appropriate moisture supply. Further, the severity of drought may be considered as being a function of both the duration and magnitude of the moisture deficiency.

2. THE PROBLEM AND OBJECTIVES

This paper does not deal with the fundamental causes of drought. Superficially one can say that drought periods are associated with periods of anomalous atmospheric circulation patterns, but the basic question concerning the physical reasons for the circulation anomalies remains. As Namias has pointed out [33] there are those who consider the circulation changes as self-evolving, while another school of thought holds that the anomalous states of the general circulation are due to extraterrestrial causes. Such controversies point out the necessity for fundamental research. Until such questions are answered and real understanding achieved, explanations of the cause of drought as well as attempts at drought prediction will be premature and inadequate.

Stated in the simplest terms the problem here is to develop a method for computing the amount of precipitation that should have occurred in a given area during a given period of time in order for the "weather" during the period to have been normal—normal in the sense that the moisture supply during the period satisfied the average or climatically expected percentage of the absolute moisture requirements during the period. In other words, the question is how much precipitation should have occurred during a given period to have kept the water resources of the area commensurate with their established use? After determining how much precipitation should have occurred, one can readily compare it with the amount that actually did occur and thereby have a measure of the departure of the moisture supply from the "normal" or climatically appropriate supply.

Unfortunately, the derivation of moisture ex-

cesses and deficiencies over a number of periods of time does not solve the problem because the duration factor must be considered and these moisture departures do not constitute a series drawn from a single statistical population [47]. Departures for a series of, say, Mays at a given place represent a different population from the September departures at the same place, and the departures for another month at a different place represent still another population. In order to develop a drought index which is relatively independent of space and time these various departures must be weighted in such a manner that they can be considered as comparable indices of moisture anomaly. The problem is to develop a weighting factor which transforms the various departures in accordance with their apparent significance in the weather and climate of the area being studied. For instance, if in central Iowa during March the actual moisture supply were one inch less than the expected moisture supply, the departure would not be of any great consequence because in their climate the spring-time precipitation generally exceeds the water requirements. On the other hand, a similar shortage in western Kansas in August or September would be very important because in this climate any abnormal moisture shortage during the summer months serves to increase the effects of the normally inadequate supply.

The final part of the problem consists of combining these derived indices of moisture anomaly into an index of abnormality for extended *periods* of drought. At the same time systematic procedures must be derived for delineating the abnormal periods.

3. DEVELOPMENTAL DATA USED

In order to develop an index which would allow space as well as time comparisons of drought statistics, two climatically dissimilar areas were chosen for initial study.

The 31 counties comprising the western one-third of Kansas were formerly grouped by the Weather Bureau into one climatological division (now subdivided into three). Therefore the temperature and precipitation data are available

[13] for the area as a unit on a monthly basis since January 1887. This region possesses a semi-arid to dry subhumid climate. The winters are rather cold and the summers rather hot with about 13 or 14 in. (70 percent) of the annual precipitation occurring during the freeze-free period of about 5½ to 6 months [58]. In addition to the availability of the data, the Kansas area was chosen because the author is well acquainted

by personal experience with the climate in that region, and it was expected, or at least hoped, that his agricultural experience in the western Great Plains [36] would enable him to make a better assessment of the implications of moisture deficiencies in that area. The western one-third of Kansas is for some purposes too large an area to be treated as a unit, but for the purposes of this developmental work that is not a particularly serious objection.

The other area studied was made up of the 12 counties of the central climatological division of Iowa. For this area as a whole the monthly temperature and precipitation data were obtained for the period January 1931 through December 1957. These data probably constitute a more homogeneous series than do the Kansas data, but the sparse data coverage in Kansas during the earlier years is not likely to bias this study to any appreciable extent. The climate of central Iowa can be classed as moist subhumid. The winters are colder than those in western Kansas and the summers are not as warm. Approximately 20 in. (65 percent) of the annual precipitation occurs during the freeze-free period of about 5½ to 6 months [57]. While both areas have a continental climate, that of central Iowa is decidedly more humid as evidenced by the following facts:

(a) Average precipitation in central Iowa exceeds that of western Kansas by about 10 in. per year.

(b) Iowa has about 40 percent more days with measurable precipitation than does the Kansas area.

(c) The relative humidity in Iowa averages 12 to 15 percent higher than it does in Kansas.

(d) Western Kansas is less cloudy than central Iowa; therefore it receives more solar radiation.

(e) Average wind speeds are somewhat greater in Kansas than in Iowa.

The point in emphasizing these differences is to show that weather which would be considered normal in western Kansas would be considered exceptionally dry were it to occur in central Iowa. Inasmuch as the economy in Iowa is not geared to such dry weather, considerable loss and hardship would result; the local people would most likely consider that they were having a disastrous drought. On the other hand, a smaller

absolute departure toward aridity would create a very serious disruption of the economy in western Kansas because an inch of rain is so much more important there than it is in Iowa. It is obvious that the effect of a moisture shortage is relative. Therefore these two areas were chosen because their climates are different and the problem is to fit both into a scheme which will produce locally meaningful measures of drought.

Some may wonder why areas have been chosen for study rather than points. Of course point data could have been used, but for developmental purposes it was easier to deal with areal averages, thereby avoiding the extreme variability of point weather. The objective here is to deal with drought, which is often prolonged and widespread, rather than with dry spells which are generally considered to be of shorter duration and more or less random in their occurrence at points. Actually, the method developed has been applied to point data (see Appendix C), but the results have more climatological meaning and may be easier to interpret if they apply to homogeneous climatological areas rather than to points.

This study is based on periods no shorter than one month. This is objectionable in that no account is taken of the distribution of precipitation within the month. Although this produces errors in the timing of computed moisture deficiencies, it is not likely seriously to bias the magnitude of the total moisture deficiency during abnormally dry periods, the item with which this study is primarily concerned. Shorter periods have been studied by machine methods and results seem to justify the preceding statement. Daily and weekly analyses are discussed in Appendix C. A very practical reason for using monthly data was that this is the form in which the data are most readily available, but more important is the fact that the use of daily or weekly data would have increased the amount of work almost to the point where this project would have become a career rather than an investigation.

The meteorological data used in this investigation were the monthly areal averages of temperature and precipitation for each individual month during the period January 1887 through December 1957 for the western one-third of Kansas and similar areal averages for central Iowa for the period January 1931 through December 1957.

4. TECHNIQUES USED AND THEIR LIMITATIONS

The water balance or hydrologic accounting approach to climatic analysis allows one to compute a reasonably realistic picture of the time distribution of moisture excesses and deficiencies. The advantages and disadvantages of various methods for computing the water balance have been too often discussed in the literature to require further detailed discussion here. Only a few general remarks seem necessary.

It is well known that evaporation is a very complicated function of the climatic elements; however, close network observational data are not available for some of the elements such as net radiation, vapor pressure deficit, and wind speeds at appropriate levels. This complication has led a number of investigators to attempt to estimate evaporation on the basis of the more numerous temperature and precipitation data. One of the foremost among these systems is that of Thornthwaite [48].

Thornthwaite's formula has been widely criticized for its empirical nature—but more widely used. It is obvious that Thornthwaite had long been aware of the physical factors involved in the evaporation and transpiration processes [49]. His empirical scheme merely provides a simple usable approximation to the climatic moisture demand. In spite of its simplicity and obvious limitations, no less an authority than Dr. H. L. Penman regards the Thornthwaite relationship as doing surprisingly well [39]. A rather complete account of the work of Thornthwaite with a long list of pertinent references has been published [50]. Although this drought study is based on this method of estimating potential evapotranspiration, there is no reason why a different method cannot be substituted as the basic working tool in a study such as this—if and when a more useful method is developed. The fact that a large number of such methods appears in the literature shows that the problem is not at all simple and that no solution so far has been found to be entirely satisfactory.

In this study potential evapotranspiration was computed from Thornthwaite's formula by means of the Palmer-Havens Diagram [37, 38] and used as a measure of the climatic demand for moisture. In order to carry out a realistic hydrologic

accounting most investigators have found it necessary to derive "actual" evapotranspiration as a function of potential evapotranspiration and the dryness of the soil. There are some difficulties involved in this question of the availability of soil moisture. An unresolved argument of considerable proportions is, and has been for many years, underway among soil physicists, plant physiologists, and others [69]. If a climatologist may be permitted an opinion in this matter, it seems that West and Perkman [71] may have pointed to the source of the disagreements in their observations concerning the extent to which the roots of plants thoroughly permeate soils under some circumstances but only partially occupy the soil under other conditions.

As there does not appear to be a universally acceptable procedure for dealing with the question of the availability of water, rules are required to convert current ignorance into working practice. An empirical procedure which Marlatt [29] tried in 1957 at this author's suggestion and found to be fairly satisfactory was adopted here. This procedure, which was also tried by Kohler [24] at about the same time or a little earlier, consists of dividing the soil into two arbitrary layers. The undefined upper layer, called surface soil and roughly equivalent to the plow layer [52], is assumed to contain 1 in. of available moisture at field capacity. This is the layer onto which the rain falls and from which evaporation takes place. Therefore, in the moisture accounting it is assumed that evapotranspiration takes place at the potential rate from this surface layer until all the available moisture in the layer has been removed. Only then can moisture be removed from the underlying layer of soil. Likewise, it is assumed that there is no recharge to the underlying portion of the root zone until the surface layer has been brought to field capacity. The available capacity of the soil in the lower layer depends on the depth of the effective root zone and on the soil characteristics in the area under study. It is further assumed that the loss from the underlying layer depends on initial moisture content as well as on the computed potential evapotranspiration (PE) and the available capacity (AWC) of the soil system. Therefore,

$$L_s = S'_s \text{ or } (PE - P), \quad (1)$$

whichever is smaller and

$$L_u = (PE - P - L_s) \frac{S'_u}{AWC}, \quad L_u \leq S'_u \quad (2)$$

where L_s = moisture loss from surface layer,
 S'_s = available moisture stored in surface layer at start of month,
 PE = potential evapotranspiration for the month,
 P = precipitation for the month,
 L_u = loss from underlying levels,
 S'_u = available moisture stored in underlying levels at start of month, and
 AWC = combined available capacity of both levels.

Further, it is assumed that no runoff occurs until both layers reach field capacity. This is, of course, not an entirely satisfactory assumption, as Kohler [24] has pointed out, and this point is further discussed below.

As previously stated, the maximum water requirements of a region are here estimated by Thornthwaite's potential evapotranspiration term. How realistic is this computed value? PE is an empirically derived quantity which, from the Seabrook data [10] and other sources [9], is estimated to be in error by as much as 100 percent or more on occasional individual days and to show an average daily absolute error of approximately 35 percent. However, as one increases the period of time considered, the average percent absolute error decreases to approximately 10 to 15 percent for periods of about 2 weeks or longer. This suggests that for the climatological analysis of monthly moisture requirements, the computed PE is not seriously in error in climates of the type being used in this investigation.

The PE concept is, by implication, applicable only during periods when vegetation is growing actively. This suggests that during the colder months PE may not be a particularly good measure of the moisture needs of an area. Considering the fact that in most temperate regions precipitation normally exceeds PE during these colder months, the question of moisture requirements becomes a problem concerning expected additions to rather than depletions of the moisture storage within a region. These additions may be viewed as additions to the soil moisture reserve or as the buildup of lake, reservoir, and ground

water storage. In these instances PE values are relatively meaningless, and one could reasonably take the view that the moisture requirement during such periods is related to some factor which we can call "potential recharge." Just as potential evapotranspiration measures the amount of moisture that could be *used* provided the supply were not limited, potential recharge would measure the amount of moisture that could be *added* provided it rained enough. The way in which this potential recharge concept has been used in this study is discussed in the following section.

By this time it is probably fairly obvious to the reader that the supply and demand concept of the economist is being used here; and, though reasoning by analogy is often misleading, this moisture problem bears certain similarities to the supply and demand problems of a manufacturing establishment. During periods of peak demand, production may be exceeded by demand and previously created inventories are relied upon to meet this demand; whether or not the demand is completely met does not, theoretically, decrease it. During periods of minimum demand, production requirements are those necessary to create suitable inventories.

In the case of the moisture problem the supply side of the picture is represented by the moisture supplied directly by precipitation during the period *plus* the amount of previously stored moisture which is withdrawn to help meet the demand of the period. Inasmuch as the lake, reservoir, and ground water withdrawal cannot be so readily estimated, the degree to which the moisture supply is augmented by previously stored moisture is herein represented by estimates of the amount of the depletion of the available soil moisture. *This procedure was used only because it is a convenient method for converting weather into specific numbers of inches of water demand and use.*

Depletions of soil moisture must be based on evapotranspiration (ET) estimates. In addition to the problems mentioned previously, estimates of ET require that one use a realistic value for the available water capacity (AWC) of the soils in the area under consideration. The AWC varies markedly from soil to soil; however, it is probably no more variable than is microclimate and for the purposes of this study of meteorological drought AWC can be taken as a value which is more or less representative of the area in general. For studies of agricultural drought specifically, AWC must be known [19], or the problem must

be solved for a wide range of capacities as was done by van Bavel and Verlinden [68]. A considerable amount of work has been done on the problem of moisture availability in soils, and a résumé of much of this work on soil water and plant growth has been published [41]. There is, however, a dearth of readily available information on even the approximate available water capacities of various soils.

The soils in question in western Kansas are predominantly of Colby series [4] and possess rather good infiltration, retention, and moisture release characteristics. An *AWC* of 6 in. was assumed for this study (1 in. in the surface layer and 5 in. in the lower layers). It is likely that 6 in. is too small a value; however, some experimenting with the use of a 4-in. *AWC* and an 8-in. *AWC* indicated that all three values would give substantially the same results in this particular study because precipitation in this area is ordinarily insufficient to provide more than 3 or 4 in. of stored moisture.

Central Iowa consists of a level to gently rolling area of dark and generally permeable soils which are quite productive. Much of the area is covered by deep soils of the Webster, Clarion, or Muscatine series. Though the Webster soils are rather poorly drained, all the soils are capable of holding fairly large amounts of available water [40]. In this study an available water capacity of 10 in. was assumed for the probable root zone in this region, with 1 in. assigned to the surface layer and 9 in. to the lower layers. Obviously, not all points in the region possess soils having an *AWC* of exactly 10 in., but this seems to be a reasonable figure to use for the area as a whole.

Another difficulty encountered in making estimates of evapotranspiration involves runoff which of course varies a great deal from place to place and depends on soil, topography, and many other factors [25]. It would be possible to incorporate

into this type of study some systematic procedure for handling runoff in a more realistic manner than has been done here. Such a complication has, in fact, been adapted for machine data processing [12]. Perhaps, in time, runoff can be computed as a function of deficiency and precipitation, somewhat along the lines suggested by Kohler and Richards [26]. However, herein it has been assumed that runoff occurred whenever precipitation fell and the full amount of available water was already stored in the soil. In the western Kansas area this procedure produced an average annual computed runoff of 0.29 in. which is about 1.5 percent of the average annual precipitation. This figure agrees rather well with the Geological Survey estimate [27]. In central Iowa, on the other hand, the computed average annual runoff was 5.58 in. which is approximately 1 in. larger than the Geological Survey estimate for this region [27]. This does not appear to be a particularly serious departure from reality, the discrepancy being only a few days of moisture supply at midsummer use rates. If this were specifically an irrigation study, an error of this size would be too large to tolerate; but for the type of climatological analysis involved here the amount of precipitation which is assigned as runoff appears to be reasonably correct. The most serious objection is that the runoff is not always allowed to occur at the proper time. These timing errors probably produce some bias in the analysis. It seems likely that in the two climates studied here the moisture situation sometimes appears slightly more favorable than it really was, particularly in summer. Remember too that this study deals with areas rather than points and inasmuch as precipitation at excessive rates seldom covers large areas [45], the climatological analysis is probably not affected as seriously as one might first suppose.

5. PROCEDURE AND DISCUSSION

In brief, the procedure, which is described in some detail in subsequent sections, consists of the following steps:

1. Carry out a hydrologic accounting by months for a long series of years.
2. Summarize the results to obtain certain constants or coefficients which are dependent on the climate of the area being analyzed.
3. Reanalyze the series using the derived coefficients to determine the amount of moisture required for "normal" weather during each month.
4. Convert the departures to indices of moisture anomaly.
5. Analyze the index series to develop:
 - a. Criteria for determining the beginning and ending of drought periods.
 - b. A formula for determining drought severity.

HYDROLOGIC ACCOUNTING

The hydrologic accounting procedure is illustrated by the central Iowa data for the years 1933-35 in table 1. The previous year, 1932, was relatively wet in central Iowa and both layers of the soil were computed to have been at field capacity at the end of December 1932. This condition persisted until April 1933 when *PE* exceeded the precipitation (*P*) by 0.47 in. Column 5 shows that this 0.47 in. was withdrawn from the surface layer (in accordance with equation (1)), thereby reducing the surface layer storage to 0.53 in. by the end of April as shown in column 7. The loss from the underlying soil was zero (col. 6) and the storage in the underlying soil remained unchanged from the previous month (col. 8). Note also that the total loss, *L*, from both soil layers is carried in column 13. There was, of course, no net recharge and no runoff so columns 11 and 15 show zero for this month. The 0.47 in., withdrawn from the surface layer at the potential rate, is added to the precipitation to give a computed evapotranspiration of 1.63 in. (col. 14). Column 9 shows that the available water in both

soil layers was reduced to 9.53 in. by the end of April.

May was rather wet and precipitation exceeded *PE* by 2.04 in. Only 0.47 in. was required to return the soil to field capacity and the remainder, 1.57 in., was assigned as runoff (col. 15). The 0.47 in. appears as a positive change in storage in the surface layer (col. 5) and since no change occurred in the underlying soils, total recharge in column 11 is also 0.47 in.

June was dry and hot and *PE* exceeded the rainfall by 5.34 in. After the inch of available moisture in the surface layer was used at the potential rate, the weather still "demanded" 4.34 in. from the soil. By equation (2) the loss from the lower portion of the soil was computed as 3.91 in. (col. 6), thereby reducing the available soil moisture to 5.09 in. (col. 9) all of which was in the lower layer (col. 8). The computed evapotranspiration (*P+L*) during June (5.94 in. in col. 14) was not far short of the *PE* for the month, but it was obtained largely at the expense of the previously stored soil moisture; column 13 shows 4.91 in. of water lost from the soil during June. The remainder of the table further illustrates this two-level moisture accounting method.

POTENTIAL VALUES

There are some items in table 1 which, although not used directly in the water balance computations, have been tabulated as part of the accounting procedure because they will be needed later. The potential recharge (*PR* col. 10) is such an item. Potential recharge can be considered as a measure somewhat similar to potential evapotranspiration, similar in that it measures some supposedly maximum condition that could exist. Just as the difference between evapotranspiration and potential evapotranspiration measures one aspect of the moisture deficiency during a period, the difference between recharge and potential recharge is related to another aspect of the moisture deficiency. Potential recharge is defined as the amount of moisture required to bring the soil to field capacity.

TABLE 1.—Hydrologic accounting for central Iowa. Available water capacity=1.00 inch in surface layer and 9.00 inches in underlying levels

1	2	3	4	5	6	7	8	9	10	11	12	13	14	15
Year	T (°F.)	P	PE	ΔS _s	ΔS _u	S _s	S _u	S	PR	R	PL	L	ET	RO
						(at end of month)								
<i>1933</i>														
January	32.3	0.90	0.01	0	0	1.00	9.00	10.00	0	0	0.01	0	0.01	0.89
February	22.6	.21	0	0	0	1.00	9.00	10.00	0	0	0	0	0	.21
March	36.3	3.22	.31	0	0	1.00	9.00	10.00	0	0	.31	0	.31	2.91
April	48.5	1.16	1.63	-.47	0	.53	9.00	9.53	0	0	1.57	.47	1.63	0
May	60.6	5.60	3.56	.47	0	1.00	9.00	10.00	.47	.47	3.26	0	3.56	1.57
June	77.8	1.03	6.37	-1.00	-3.91	0	5.09	5.09	0	0	5.83	4.91	5.94	0
July	76.3	3.57	6.22	0	-1.35	0	3.74	3.74	4.91	0	3.17	1.35	4.92	0
August	70.3	1.84	4.64	0	-1.11	0	2.63	2.63	6.26	0	1.81	1.11	2.95	0
September	69.7	3.57	4.18	0	-.16	0	2.47	2.47	7.37	0	1.10	.16	3.73	0
October	49.8	1.95	1.52	.43	0	.43	2.47	2.90	7.53	.43	.38	0	1.52	0
November	37.9	.26	.34	-.08	0	.35	2.47	2.82	7.10	0	.34	.08	.34	0
December	26.9	.89	0	.65	.24	1.00	2.71	3.71	7.18	.89	0	0	0	0
<i>1934</i>														
January	26.1	1.34	0	0	1.34	1.00	4.05	5.05	6.29	1.34	0	0	0	0
February	25.1	.59	0	0	.59	1.00	4.64	5.64	4.95	.59	0	0	0	0
March	34.4	1.01	.09	0	.92	1.00	5.56	6.56	4.36	.92	0	0	.09	0
April	50.1	.61	1.82	-1.00	-.12	0	5.44	5.44	3.44	0	1.46	1.12	1.73	0
May	70.0	.76	5.08	0	-2.33	0	3.11	3.11	4.56	0	2.76	2.33	3.09	0
June	78.4	2.10	6.53	0	-1.37	0	1.74	1.74	6.89	0	2.03	1.37	3.47	0
July	79.3	4.68	6.82	0	-.34	0	1.38	1.38	8.26	0	1.19	.36	5.04	0
August	72.9	2.83	5.25	0	-.36	0	1.04	1.04	8.62	0	.72	.34	3.17	0
September	61.1	5.59	3.02	1.00	1.67	1.00	2.61	3.61	8.96	2.57	.31	0	3.02	0
October	56.5	1.15	2.26	-1.00	-.03	0	2.58	2.58	6.39	0	1.33	1.03	2.18	0
November	41.7	5.15	.60	1.00	3.55	1.00	6.13	7.13	7.42	4.55	.15	0	.60	0
December	21.0	.34	0	0	.34	1.00	6.47	7.47	2.87	.34	0	0	0	0
<i>1935</i>														
January	20.6	1.53	0	0	1.53	1.00	8.00	9.00	2.53	1.53	0	0	0	0
February	28.5	1.44	0	0	1.00	1.00	9.00	10.00	1.00	1.00	0	0	0	.44
March	39.9	1.46	.62	0	0	1.00	9.00	10.00	0	0	.62	0	.62	.84
April	46.4	1.24	1.39	-.15	0	.85	9.00	9.85	0	0	1.35	.15	1.39	0
May	54.8	4.13	2.70	.15	0	1.00	9.00	10.00	.15	.15	2.51	0	2.70	1.28
June	65.4	8.65	4.27	0	0	1.00	9.00	10.00	0	0	3.94	0	4.27	4.38
July	78.6	4.43	6.66	-1.00	-1.11	0	7.89	7.89	0	0	6.09	2.11	6.54	0
August	72.9	1.64	5.25	0	-2.85	0	5.04	5.04	2.11	0	4.14	2.85	4.49	0
September	64.5	3.89	3.46	.43	0	.43	5.04	5.47	4.96	.43	1.74	0	3.46	0
October	50.7	3.55	1.60	.57	1.38	1.00	6.42	7.42	4.53	1.95	1.02	0	1.60	0
November	33.9	2.89	.07	0	2.58	1.00	9.00	10.00	2.58	2.58	.07	0	.07	.24
December	21.6	1.31	0	0	0	1.00	9.00	10.00	0	0	0	0	0	1.31

NOTE: Values in columns 3-15 are inches of water.

$$PR = AWC - S', \quad (3)$$

where S' is the amount of available moisture in both layers of the soil at the beginning of the month.

Potential loss (PL col. 12) expresses another measure of a maximum condition that could exist. It is defined as the amount of moisture that could be lost from the soil provided the precipitation during the period were zero. It is assumed that PE for the period and the initial soil moisture conditions were as "observed."

$$PL = PL_s + PL_u, \quad (4)$$

where $PL_s = PE$ or S'_s , whichever is smaller, and $PL_u = (PE - PL_s) S'_u / AWC$.

Potential loss allows one to evolve some measure of a condition such as existed during June 1933 in Iowa. Under the initial condition for that month (see table 1) one would expect no recharge; there-

fore the fact that none occurred is not surprising and cannot be used as a measure of the unusual dryness of the month. ET as computed was 93 percent of PE , so this small shortage does not adequately express the dry condition. The unusual thing was that nearly 50 percent of the available moisture was removed from the soil during a single month. When we compare this loss with the potential loss, it is seen that it represents about 84 percent of potential. This is an unusually large percentage, much larger than would normally be expected to occur in central Iowa in June. As will be shown later the actual loss in Iowa during June averages only 17 percent of the potential loss.

In hydrologic accounting one cannot neglect runoff because under some conditions it is the most important thing that is taking place. Having evolved measures of potential recharge and potential loss as well as potential evapotranspira-

tion, there is also a need for some measure of potential runoff, PRO .

Consider the case of April 1935 in table 1. Note that at the beginning of April the soil was at field capacity; therefore the potential recharge is zero. The month was somewhat cooler than normal and PE was only 1.39 in. Inasmuch as the 27-yr. mean April rainfall is 2.58 in., it is apparent that one could reasonably expect some runoff to have occurred during that month, even if the rainfall were a good deal below average. It turns out that $ET=PE$, $R=PR$, and the loss from the soil was only 0.15 in., 11 percent of PL ; the runoff was zero. Agriculturally speaking, there was no moisture shortage, but the fact remains that the month was a good deal drier than normal. This unusual dryness shows up in the stream-flow data. The Des Moines river, which drains the western part of the central division of Iowa, averaged 2.4 ft. below its long-term mean stage [59]. If this scheme is to measure the moisture abnormalities of the weather, it must take account of the fact that in situations such as this one the runoff was not as large as one might have expected. Having a measure of potential runoff makes it possible to handle this part of the moisture situation in a manner similar to that used for the other aspects.

Developing this turned out to be more difficult than expected. Actually, of course, the maximum runoff that could occur in a given situation (assuming $PE=0$ and following the accounting rules which are being used) would be equal to the precipitation minus the amount that could be added to the soil. It turns out that this measure cannot be used in this particular study because the approach being used requires that the actual precipitation should not be introduced at this stage of the development. After experimenting with at least a dozen measures and estimates of potential runoff, the following simple reasoning was used.

At the outset one can reasonably assume that runoff is most likely to be small when potential recharge is large and to be large when the soil is already at field capacity and recharge can, therefore, be only zero. Returning to equation (3), it is obvious that potential recharge is largest when S' is smallest and vice versa. For want of a more satisfying relationship one can assume that potential runoff is some function of the amount of soil moisture available and simply write,

$$PRO = AWC - PR = S' \quad (5)$$

This assigns "potential precipitation" as being equal to AWC . While this is not a particularly elegant way of handling this problem, it seemed to be the best that could be done at the time. It has worked out better than expected.¹

The water balance computations were carried out for 27 years of central Iowa data and for 71 years of western Kansas data. The monthly means of the various important items for both areas are shown in table 2. Note that when one processes the data in this manner, one derives a value of average soil moisture recharge as well as a value for average soil moisture loss for most months. For example, in western Kansas many Aprils show a gain in soil moisture and the 71-yr. average gain is 0.55 in. On the other hand many Aprils show a loss for the month and the 71-yr. average loss is 0.26 in. The values of potential evapotranspiration tabulated in table 2 are the averages of all the individual values. This is the reason they do not exactly correspond to the average temperature values.

COEFFICIENT OF EVAPOTRANSPIRATION, α

In humid climates,² evapotranspiration is usually nearly equal to potential evapotranspiration; but in rather dry climates the usual condition is for the evapotranspiration to fall a good deal short of the potential. This fact can be used to estimate the amount of ET that one can normally expect in any particular climate; i.e., in terms of the PE for that climate. For example, consider June in Kansas in table 2. The average PE is 5.20 in. and the average ET is 3.69 in.; therefore, the average ET is about 71 percent of average PE in western Kansas in June. This 0.71 is here called the coefficient of evapotranspiration, α

$$\alpha = \overline{ET} / \overline{PE}. \quad (6)$$

Similarly, α for June in central Iowa is about

¹ At the time of this writing so much machine work has been based on "potential precipitation" = AWC , that it would be difficult to justify a change in equation (5). However, if the job were to be done over, it now appears that the computed potential runoff would generally be closer to reality if one assigned some rather large constant value to "potential precipitation." For example, one might assume that "potential precipitation" for a month is equal to 3 times the normal precipitation for the month. If this were done, equation (5) would become $PRO = 3P - PR$.

² "Climate" as used here refers to time as well as place. Each month has a climatic average; so central Iowa has 12 climates.

TABLE 2.—Long-term means

	T (° F.)	ET	PE	R	S'	PR	RO	L	S ₁	S ₂	PL	P
Western Kansas: 1887-1957, 71 years AWC ₁ =1.00 in., AWC ₂ =5.00 in.												
January	29.8	0.04	0.05	0.34	1.33	4.67	T	0.02	0.61	0.73	0.04	0.37
February	33.3	.13	.14	.51	1.65	4.35	T	.03	.76	.89	.13	.62
March	41.6	.62	.64	.44	2.12	3.88	0.07	.21	.87	1.25	.55	.92
April	52.9	1.62	1.76	.55	2.35	3.65	.08	.26	.70	1.65	.97	1.99
May	62.3	2.90	3.38	.38	2.64	3.36	.07	.53	.59	2.05	1.46	2.83
June	72.6	3.69	5.20	.09	2.52	3.48	.06	.86	.40	2.12	1.97	2.79
July	78.4	3.61	6.37	.03	1.75	4.25	0	.85	.13	1.62	1.65	2.99
August	76.9	2.89	5.69	.02	.93	5.07	0	.44	.03	.90	.84	2.47
September	68.4	1.80	3.67	.01	.50	5.50	0	.15	.03	.47	.29	1.65
October	55.8	1.04	1.88	.25	.35	5.65	0	.04	.01	.35	.11	1.25
November	41.6	.34	.52	.35	.56	5.44	.01	.03	.13	.43	.10	.68
December	32.2	.08	.09	.46	.89	5.11	0	.02	.34	.55	.05	.52
Σ		18.76	29.39	3.43			.29	3.44				19.08
Central Iowa: 1931-57, 27 years AWC ₁ =1.00 in., AWC ₂ =9.00 in.												
January	20.5	0	0	0.58	7.49	2.51	0.58	0	0.98	6.51	0	1.16
February	24.5	.02	.02	.49	8.07	1.93	.54	0	1.00	7.07	.02	1.04
March	34.6	.26	.26	.45	8.56	1.44	1.33	0	1.00	7.56	.26	2.04
April	49.1	1.71	1.72	.28	9.01	.99	.83	.23	1.00	8.01	1.57	2.58
May	60.5	3.49	3.59	.26	9.05	.95	.90	.57	.79	8.26	3.10	4.09
June	70.4	4.89	5.19	.09	8.75	1.25	.78	.71	.65	8.10	4.24	5.06
July	75.4	5.56	6.13	0	8.13	1.87	0	2.12	.56	7.57	4.67	3.44
August	72.8	4.40	5.26	.41	6.04	3.96	.02	1.07	.05	5.99	3.13	3.75
September	64.8	3.08	3.52	.74	5.37	4.63	0	.59	.18	5.19	1.81	3.23
October	53.7	1.78	1.97	.45	5.53	4.47	.13	.27	.34	5.19	1.13	2.09
November	36.9	.30	.30	1.36	5.71	4.29	.23	.02	.44	5.27	.21	1.87
December	24.8	0	0	.73	7.04	2.96	.42	0	.84	6.20	0	1.15
Σ		25.49	27.96	5.84			5.76	5.58				31.50

0.94. These coefficients have been computed³ for each month in both regions and are shown in column 2 of table 3.⁴

These coefficients in themselves do a fairly good job of measuring the agricultural climate. For example, the fact that *ET* averages only a little over one-half of *PE* in July in western Kansas ties in with the fact that this is a very unsatisfactory region for corn production. However, in this study these coefficients are used to estimate the amount of *ET* that would be normal for a particular place after having taken account of the moisture demand (*PE*) during that month. In other words, if in western Kansas a particular June was much warmer than normal, say *PE*=6.00 in., then *ET* would have to be 0.71×6 or 4.26 in. in order that *ET* should bear its normal relation to the climatic demand for moisture. This derived evapotranspiration, 4.26 in. in this case, will be called the "CAFEC" (Climatically Appropriate For Existing Conditions) evapotranspiration. This derived evapotranspiration can

³ The coefficients were computed from long-term sums rather than from long-term means which accounts for the slight discrepancies noted when one tries to compute table 3 from table 2. The coefficients in table 3 are shown to four decimals to avoid cumulative rounding errors in subsequent calculations.

⁴ When *ET* and *PE* both equal zero, consider α=1.0; α=0 only when *ET*=0 and *PE*>0.

be compared with the *ET* as computed in the original hydrologic accounting and thereby one gains some measure of the abnormality of this particular aspect of the moisture situation. For

TABLE 3.—Climatic coefficients and constants

1	2	3	4	5	6	7
	α	β	γ	δ	k	K
WESTERN KANSAS						
January	0.9466	0.0722	0.0023	0.4694	0.99	2.58
February	.9754	.1166	.0020	.2290	1.00	2.20
March	.9679	.1136	.0317	.3730	.96	1.84
April	.9218	.1499	.0359	.2688	1.02	1.54
May	.8581	.1155	.0266	.3613	1.12	1.38
June	.7099	.0268	.0251	.4332	1.38	1.28
July	.5660	.0071	0	.5151	1.76	1.38
August	.5074	.0040	0	.5274	1.96	1.66
September	.4899	.0009	0	.5272	2.04	1.87
October	.5533	.0436	0	.3519	1.65	1.82
November	.6596	.0652	.0195	.3245	1.23	2.04
December	.9223	.0900	0	.4055	1.01	2.26
CENTRAL IOWA						
January	1.00	0.2315	0.0776	0	0.50	1.55
February	1.00	.2530	.0670	0	1.538	1.61
March	1.00	.3129	.1554	0	.48	1.41
April	.9968	.2804	.0919	0	1.495	1.14
May	.9727	.2790	.0996	0	1.835	.97
June	.9425	.0709	.0897	0	1.677	.92
July	.9081	0	0	0	1.4535	1.10
August	.8357	.1027	.0028	0	1.3418	.93
September	.8738	.1603	0	0	1.3246	1.12
October	.9035	.1012	.0244	0	1.2420	1.02
November	1.00	.0171	.0408	0	1.1150	.88
December	1.00	.2453	.0603	0	.63	1.62

example, PE in Iowa in June 1934 (see table 1) was 6.53 in. Using $\alpha=0.9425$, from table 3, the *CAFEC* evapotranspiration is 6.15 in. Note, however, that because of the initial dryness of the soil and the shortage of rainfall during June, the computed ET was only 3.47 in. The difference, 2.68 in., measures the amount by which the moisture supply failed to provide the amount of ET that, from climatic considerations, one might reasonably expect in central Iowa during such a warm June.

COEFFICIENT OF RECHARGE, β

In many places soil moisture recharge is a seasonal affair. Table 2 shows that the main recharge period in central Iowa is November through March. During this period PE is very small, and the moisture need is a need for rebuilding the moisture supply that was depleted by the weather of the past summer. Just as ET cannot exceed PE , the recharge R cannot exceed the potential recharge PR and is ordinarily a good deal less than the potential except in climates that are humid to superhumid and in areas with small water storage capability.

The ratio of the average recharge to the average potential recharge is called the coefficient of recharge, β

$$\beta = \bar{R}/\bar{PR}. \quad (7)$$

The monthly values of β are shown in table 3. They range from at or near zero during the moisture-depletion seasons of the year to as high as 32 percent during some months of the moisture-recharge season in Iowa. These coefficients, when used in conjunction with the potential recharge for a particular month, enable one to estimate the *CAFEC* recharge, i.e., the recharge that would have been climatically appropriate for the conditions of the time and place being examined. For example, PR in Iowa at the beginning of June 1934 (see table 1) was 6.89 in. The coefficient of recharge during June in Iowa is 0.0709. *CAFEC* recharge is therefore $6.89 \times 0.0709 = 0.49$ in. This is to say that the addition of 0.49 in. of moisture to the soil during June 1934 would have been climatically appropriate in view of the initial dryness of the soil. Actually, the computed recharge was zero, so the 0.49 in. represents an abnormal deficit of soil moisture recharge.

In the preceding section on the coefficient of

evapotranspiration it was shown that the expected evapotranspiration for June 1934 in central Iowa was 6.15 in. To this we can add the 0.49 in. of expected recharge and show, so far, a need for 6.64 in. of moisture. This is not a "maximum moisture need" measurement; it might better be called a "customary or established moisture use" estimate.⁵

COEFFICIENT OF RUNOFF, γ

As pointed out earlier, potential runoff is related to the initial amount of available water in the soil and for simplicity has been set equal to it as shown in equation (5). The coefficient of runoff γ can be obtained in the same manner as were previously discussed coefficients.

$$\gamma = \bar{RO}/\bar{PRO} = \bar{RO}/\bar{S}'. \quad (8)$$

The monthly values of γ for both central Iowa and western Kansas are shown in column 4 of table 3.

Returning to the trusty example of June 1934 in central Iowa, the *CAFEC* runoff can be calculated by multiplying 0.0897, the June value of γ from table 3, by 3.11, the amount of moisture in the soil at the end of May 1934 (see table 1). This gives 0.28 in. for the *CAFEC* runoff for this particular month.

Adding this to the *CAFEC* evapotranspiration and the *CAFEC* recharge for this month, we have $6.15 + 0.28 + 0.49 = 6.92$ in. This represents the amount of moisture that was needed in order to maintain the water resources of the area at a "normal" level. However, this does not represent the amount of precipitation that was "needed", because there was at the beginning of June some moisture in the soil which could be expected to supply a part of the evapotranspiration, if necessary. The computation of the "expected" loss from the soil is discussed in the following section.

COEFFICIENT OF LOSS, δ

Following the same reasoning used previously, the Coefficient of Loss δ can be determined:

$$\delta = \bar{L}/\bar{PL}. \quad (9)$$

The monthly values of δ are shown in table 3.

⁵ It is unfortunate that these rather odd expressions need be introduced, but we are not well-equipped verbally for the task of dealing with some of these concepts.

Note that during summer in Kansas the average computed moisture loss from the soil is approximately 50 percent of the average potential loss. Although the coefficients are larger in western Kansas than they are in central Iowa, the potential loss averages a good deal larger in Iowa (see table 2); therefore, the expected withdrawal of soil moisture is smaller in Kansas—as one would expect.

The example of June 1934 in Iowa can now be completed. The *CAFEC* loss from the soil = $\delta \times PL = 0.1677 \times 2.03 = 0.34$ in. This can be subtracted from the previously computed 6.92 in. of moisture needed thereby giving 6.58 in. of *CAFEC* precipitation. This is the amount of precipitation that would have maintained the water resources of the area at a level appropriate for the established economic activity of the area.

CAFEC PRECIPITATION, \hat{P}

Summarizing, we have, for any individual month the *CAFEC* quantities (denoted by a circumflex) for evapotranspiration, recharge, runoff, loss, and precipitation:

$$\hat{ET} = \alpha PE \quad (10)$$

$$\hat{R} = \beta PR \quad (11)$$

$$\hat{RO} = \gamma PRO \quad (12)$$

$$\hat{L} = \delta PL \quad (13)$$

$$\hat{P} = \hat{ET} + \hat{R} + \hat{RO} - \hat{L} \quad (14)$$

Because of the manner in which each of these components of the *CAFEC* precipitation is computed, each has a mean value equal to the mean value of its counterpart as given in table 2. This is true because,

$$\hat{ET}_i = \alpha PE_i = \frac{\sum_{i=1}^n (ET)}{\sum_{i=1}^n (PE)} PE_i,$$

and

$$\sum_{i=1}^n (\hat{ET}) = \frac{\sum_{i=1}^n (ET)}{\sum_{i=1}^n (PE)} \sum_{i=1}^n (PE).$$

Therefore

$$\sum_{i=1}^n (\hat{ET}) = \sum_{i=1}^n (ET)$$

This is to say, for example, that the 71-yr. mean value of the *CAFEC* evapotranspiration for July in western Kansas is 3.61 in., the same as the 71-yr. mean value of the evapotranspiration as determined from the original hydrologic accounting. The same reasoning holds for the other components of the *CAFEC* precipitation. (Of course, the *CAFEC* value and the "actual" value seldom agree in a particular month.)

From this it follows that the long-term mean of the *CAFEC* precipitation is equal to the long-term mean of the actual precipitation. This simply means that the average departure of the actual precipitation from the *CAFEC* precipitation is zero and no bias has been introduced. The departures in individual months therefore represent departures from the average moisture climate of the area being considered. These departures are correlated with, but are by no means identical to, the monthly departures of the precipitation from its long-term mean; in fact, on occasion the two departures may be of opposite sign. In the case of June 1934 in Iowa, the actual precipitation, 2.10 in., departed from the *CAFEC* precipitation, 6.58 in., by -4.48 in., while the departure of the actual from its long-term mean was only -2.96 in. As one would expect from considerations of the antecedent weather, and as was actually the case, the moisture situation during June 1934 in central Iowa was a good deal more serious than is represented by the -2.96 in. departure from long-term mean precipitation. As a matter of fact, the *Iowa Weekly Weather and Crop Bulletin* of July 3, 1934, carried such remarks as: ". . . more wells failing and water being bought and hauled from long distances . . .", ". . . pastures burned up . . ." and ". . . livestock fast going down in flesh . . ." [61].

It should be pointed out that on rare occasions \hat{P} turns out to be negative. This occurs only when the weather has been very wet during a season which is normally quite dry. Negative values are interpreted as indicating that the past weather has been so unusually wet that the area will remain abnormally wet for another month even though no precipitation at all occurs during the month. Although the idea of "negative pre-

precipitation" is a bit disconcerting, the few instances in which \hat{P} has been negative have produced reasonable appearing results without introducing any difficulties.

PRECIPITATION EXCESSES AND DEFICIENCIES

When the entire series of data had been reworked and the *CAFEC* precipitation had been computed for each individual month, the difference between the actual precipitation and the *CAFEC* precipitation for each month,

$$d = P - \hat{P}, \quad (15)$$

provided what appear to be meaningful measures of the departure of the moisture aspect of the weather from normal. Table 4 shows an example of the computations for a selected period from the western Kansas record. This period contains

the "infamous" year of 1934 when drought forced many of the inhabitants to leave or face starvation. This extremely long period of drought (July 1932 through October 1940) was characterized by unusually warm weather as well as exceptionally dry weather. July 1934 was the most extreme month. The *CAFEC* precipitation for this month (col. 10) was computed by equations (10) through (14) as follows:

$$\begin{aligned} \hat{P} &= (.5660 \times 7.90) + (.0071 \times 5.86) + (0 \times 0.14) \\ &\quad - (.5151 \times 0.14) = 4.44 \text{ in.} \end{aligned}$$

This unusually large value is a consequence of the extremely hot weather coupled with the initial dryness created by the hot dry weather which preceded July. Ordinarily almost 25 percent of the evapotranspiration during July comes from previously stored soil moisture, but in this case there was hardly any soil moisture; therefore,

TABLE 4.—Climatic analysis of moisture departures in western Kansas

1	2	3	4	5	6	7	8	9	10	11	12	13	14
	PE	PR	PRO	PL	$\alpha \frac{PE}{ET+}$	$\beta \frac{PR}{R+}$	$\gamma \frac{S'}{KO-}$	$\delta \frac{PL}{L=}$	\hat{P} (*)	P	d (P - \hat{P})	z (dk)	Z (dK)
<i>1932</i>													
June.....	4.80	4.67	1.33	1.06	3.41	0.12	0.03	0.46	3.10	5.56	2.46	3.39	3.15
July.....	7.04	3.91	2.09	2.09	3.98	.03	0	1.08	2.93	1.78	-1.15	-2.02	-1.59
August.....	5.97	5.66	.34	.34	3.03	.02	0	.18	2.87	1.53	-1.34	-2.63	-2.22
September.....	3.41	5.93	.07	.04	1.67	.01	0	.02	1.66	1.28	-.38	-.78	-.71
October.....	1.63	5.95	.05	.01	.90	.26	0	0	1.16	.62	-.54	-.89	-.98
November.....	.53	5.97	.03	0	.35	.39	0	0	.74	.10	-.64	-.79	-1.31
December.....	0	5.97	.03	0	0	.54	0	0	.54	.24	-.30	-.30	-.68
<i>1933</i>													
January.....	.21	5.73	.27	.21	.20	.41	0	.10	.51	.02	-.49	-.49	-1.26
February.....	0	5.92	.08	0	0	.69	0	0	.69	.18	-.51	-.51	-1.12
March.....	.94	5.74	.26	.23	.91	.65	.01	.09	1.48	.68	-.90	-.86	-1.66
April.....	1.72	5.97	.03	.01	1.58	.90	0	0	2.48	2.17	-.31	-.32	-.48
May.....	3.36	5.52	.48	.46	2.88	.64	.01	.17	3.36	3.48	.12	.13	.17
June.....	6.50	5.40	.60	.60	4.61	.14	.01	.26	4.50	.88	-3.62	-5.00	-4.63
July.....	6.91	5.99	.01	.01	3.91	.04	0	0	3.95	1.84	-2.11	-3.71	-2.91
August.....	5.41	5.99	.01	.01	2.74	.02	0	.01	2.75	4.91	2.16	4.23	3.59
September.....	4.30	5.99	.01	.01	2.11	.01	0	.01	2.11	1.33	-.78	-1.59	-1.46
October.....	2.03	5.99	.01	0	1.12	.26	0	0	1.38	.60	-.88	-1.45	-1.60
November.....	.78	5.99	.01	0	.51	.39	0	0	.90	.97	.07	.09	.14
December.....	.40	5.80	.20	.19	.37	.52	0	.08	.81	1.04	.23	.23	.52
<i>1934</i>													
January.....	.21	5.16	.84	.21	.20	.37	0	.10	.47	.11	-.36	-.36	-.93
February.....	.18	5.26	.74	.18	.18	.61	0	.04	.75	1.36	.61	.61	1.34
March.....	.82	4.08	1.92	.82	.79	.46	.06	.31	1.00	.55	-.45	-.43	-.83
April.....	2.15	4.35	1.65	.95	1.98	.65	.26	.06	2.43	.39	-2.04	-2.10	-3.14
May.....	4.60	5.23	.77	.59	3.95	.60	.02	.21	4.36	1.24	-3.12	-3.49	-4.31
June.....	6.16	5.67	.33	.33	4.37	.15	.01	.14	4.39	2.89	-2.00	-2.76	-2.56
July.....	7.90	5.86	.14	.14	4.47	.04	0	.07	4.44	.74	-3.70	-6.51	-5.11
August.....	6.54	5.99	.01	.01	3.32	.02	0	.01	3.33	1.44	-1.89	-3.70	-3.14
September.....	2.80	5.99	.01	.01	1.37	.01	0	0	1.38	1.45	.07	.14	.13
October.....	2.42	5.99	.01	0	1.34	.26	0	0	1.60	.66	-.94	-1.55	-1.71
November.....	.80	5.99	.01	0	.53	.39	0	0	.92	.66	-.26	-.32	-.53
December.....	.08	5.99	.01	0	.07	.54	0	0	.61	.15	-.46	-.46	-1.04
<i>1935</i>													
January.....	.21	5.92	.08	.07	.20	.43	0	.03	.60	.31	-.29	-.29	-.75
February.....	.32	5.82	.18	.17	.31	.68	0	.04	.95	.25	-.70	-.70	-1.54
March.....	1.26	5.89	.11	.10	1.22	.67	0	.04	1.85	.61	-1.24	-1.19	-2.28
April.....	1.57	5.99	.01	0	1.44	.90	0	0	2.34	.25	-2.09	-2.15	-3.22
May.....	2.52	5.99	.01	0	2.16	.69	0	0	2.85	4.65	1.80	2.02	2.48

* Col. 10=col. 6+col. 7+col. 8-col. 9.

TABLE 5.—Monthly moisture departures, d, western Kansas

	Jan.	Feb.	Mar.	Apr.	May	June	July	Aug.	Sept.	Oct.	Nov.	Dec.
1887	-0.21	-0.05	-1.03	1.63	-0.74	-1.24	-0.98	1.48	-0.08	-0.13	-0.29	-0.13
1888	-0.23	-0.74	.44	2.03	.87	-.57	.30	1.33	-1.13	.38	-.28	-.47
1889	.72	-.12	.38	1.35	.56	.82	.27	-.03	-1.09	1.13	-.17	-.79
1890	.10	-.26	-.96	1.57	-2.07	-2.28	-2.65	-.98	-.73	-.51	-.17	-.64
1891	.72	-.34	1.74	-.28	1.39	3.07	3.06	0	2.17	.30	-.43	.75
1892	-.04	-.64	1.33	-.64	3.52	-.22	.72	1.12	-1.12	-.57	-.37	.11
1893	-.31	-.35	-.71	-1.80	-1.74	-2.14	-.39	-.21	-.05	-.90	-.38	-.61
1894	-.22	.47	-.67	-1.33	-2.17	-1.17	-1.93	-2.08	-.05	-1.07	-.73	-.18
1895	.07	.60	-.52	-.99	-.49	1.83	3.56	-.09	-1.12	-.26	.11	-.07
1896	.45	.67	-.36	1.33	-1.32	.14	-.17	-.45	.18	.64	-.16	-.41
1897	.03	-.33	.25	2.03	-.92	-.27	.45	1.31	-.41	2.02	-.37	.03
1898	.30	-.44	-.52	-.68	-.82	1.11	.92	1.97	-.78	-.05	.02	.67
1899	0	-.08	-.02	-.93	-1.74	.28	2.72	-1.66	-.47	-.65	.92	.10
1900	-.30	.01	-.25	2.93	-.79	.52	-.12	-1.46	1.50	-.96	-.62	-.43
1901	-.18	.44	.41	1.14	-1.16	-1.91	-2.33	.22	1.25	-.41	-.75	-.22
1902	.06	-.18	-.30	-1.44	.67	.43	.24	-.02	.77	.78	-.58	0
1903	-.23	2.16	-.11	-1.03	1.98	.96	1.09	.90	-1.00	-.27	-.07	-.43
1904	-.35	-.69	-1.16	-.34	.11	1.05	.51	.41	.60	.20	-.78	.22
1905	-.37	.06	-.14	2.20	1.50	.26	2.99	-.67	.08	1.17	1.27	-.40
1906	-.06	-.31	-.69	1.20	-.80	.54	2.38	.53	1.07	1.67	.35	-.15
1907	-.05	-.39	-.92	-.05	-.91	.37	.60	.24	-.29	-.12	1.44	-.73
1908	-.33	.36	-1.03	-1.80	-1.31	1.49	.27	0	-1.06	.42	-.35	-.37
1909	-.10	-.30	.66	-1.20	-.61	2.46	.72	-1.58	.36	-.21	2.83	-.60
1910	.23	.01	-1.43	-1.31	-.28	-1.78	-.68	-.73	-.24	-.77	-.49	-.49
1911	-.40	1.30	-1.06	-1.23	-1.24	-3.61	-.21	.09	-1.15	.07	-.06	-.97
1912	-.20	1.46	1.29	-.37	-1.08	2.02	-.98	2.75	.66	-.57	-.17	-.43
1913	-.13	.31	-.47	-.35	-2.20	-.14	-2.55	-.81	1.79	-.76	.32	2.64
1914	-.23	.03	-.65	-.05	1.16	1.19	.12	2.66	-1.11	.09	-.91	-.06
1915	.10	.75	.62	1.58	3.52	2.97	4.25	4.56	1.80	.71	-.31	-.16
1916	.46	-.23	-.69	.53	-1.29	.90	-1.90	-.29	-.94	-.32	-.59	-.16
1917	-.19	-.59	-.55	-.10	-.13	-2.88	-.85	1.30	.42	-.76	-.53	-.36
1918	.05	.01	.37	.09	-.13	-2.88	-.85	1.30	.42	-.76	-.53	-.36
1919	-.18	1.18	.56	1.57	.06	.87	.94	-.77	.80	.80	-.17	2.58
1920	-.21	-.44	-.72	.49	.09	-.24	-.39	-.80	1.61	.31	.80	-.25
1921	.39	-.23	-.85	.17	-1.29	-.39	.39	.98	1.37	.06	.09	.09
1922	-.21	.01	1.02	1.52	.51	-.44	.39	-.80	.03	-1.10	-.75	.01
1923	-.52	-.58	-.41	-.25	3.85	2.57	2.08	1.37	-1.29	-1.26	.15	-.53
1924	.03	.51	2.49	-.11	-.35	-1.26	2.08	1.84	3.42	3.42	.02	.41
1925	-.25	-.45	-.88	-.89	-1.53	-2.59	-.93	1.03	.29	-.25	-.66	.72
1926	-.21	-.58	.27	-.61	-1.47	-1.56	-1.00	1.03	.99	0	.35	-.37
1927	-.26	-.02	.65	.33	-2.35	1.38	.60	-1.01	-.24	-1.28	.17	-.36
1928	-.45	.61	.39	-.53	2.46	3.88	2.87	1.55	-.25	1.67	1.12	.08
1929	.03	.21	-.41	-.27	.69	-.13	.84	-.62	1.53	1.23	1.23	-.34
1930	-.03	-.72	-.67	-.67	-.44	-.68	-.76	-.39	.01	4.32	1.20	-.12
1931	-.12	.54	1.84	.38	-.04	-.85	-1.03	-.05	-1.62	4.42	.44	-.29
1932	.69	-.32	.18	.14	-1.81	2.46	-1.15	-1.34	-.38	-.54	-.64	-.30
1933	-.49	-.51	-.90	-.31	.12	-3.62	-2.11	2.16	-.78	-.88	.07	.23
1934	-.36	.61	-.45	-2.04	-3.12	-2.00	-3.70	-1.89	-.07	-.94	-.26	-.46
1935	-.29	-.70	-1.24	-2.09	1.80	.03	-2.99	-1.69	.51	-.68	-.39	-.38
1936	-.04	-.50	-1.08	-1.63	1.25	-2.66	-3.22	-2.07	.31	-.23	-.76	-.11
1937	-.01	-.29	.01	-1.70	-2.49	-.68	-2.25	-1.94	-.69	-.14	-.57	-.25
1938	-.37	-.32	-.35	.02	1.53	-.70	-.98	-2.28	.45	-1.38	-.50	-.52
1939	-.02	.38	.60	-.94	-2.11	-1.18	-2.49	-1.64	-1.99	-1.37	-.67	-.10
1940	.23	-.19	.24	-.81	.54	-1.50	-2.33	.62	-.13	-1.19	.93	.05
1941	.68	.31	.08	1.07	1.45	3.78	3.47	1.61	1.83	1.60	-.05	.29
1942	-.02	.29	.38	3.08	-1.11	2.23	.22	.81	.31	1.58	-.35	.52
1943	-.16	-.57	-.36	-.49	-.94	-.73	-1.52	-.68	-1.13	-.63	-.60	.27
1944	1.33	.33	.95	4.91	2.44	-.38	3.56	.29	-.76	-.04	.39	.41
1945	.79	-.03	-.90	1.34	-.59	.98	.13	.09	.18	-.70	-.78	-.07
1946	-.17	-.21	.35	-2.35	.40	-1.01	-1.72	-.96	1.10	4.63	2.73	-.13
1947	.49	.23	1.01	1.01	2.49	1.56	.90	-.79	-1.49	-1.06	.47	.71
1948	.06	.80	1.56	-1.82	-.22	2.17	1.03	1.70	-.86	-.87	.88	-.20
1949	.61	.30	1.19	.23	2.50	4.32	2.65	2.66	-.14	.74	-.81	-.34
1950	-.25	-.17	-.44	-1.05	-1.00	-2.15	3.88	3.98	.12	-.46	-.52	-.55
1951	.31	.10	-.08	.05	2.78	6.15	3.34	1.90	1.79	-.05	.02	-.27
1952	-.18	-.28	.69	1.09	-.47	-3.24	-1.74	-.78	-1.34	-1.15	.20	.01
1953	-.44	-.57	-.21	-.08	-.88	-3.09	-.67	-.06	-1.54	.03	1.29	.71
1954	-.08	-.69	-.34	-1.92	.80	-2.30	-2.19	-.69	-1.40	.18	-.90	-.31
1955	.02	-.16	-.70	-.75	.57	-.17	-2.97	-1.93	.58	-1.27	-.52	-.31
1956	.13	-.21	-.80	-1.39	-2.65	-3.47	-.96	-1.61	-1.82	-.95	-.40	-.69
1957	-.18	-.68	2.13	.68	2.82	3.48	1.30	-.01	1.02	.38	.15	-.58
1958	.16	.20	2.58	.34	1.14	.72	4.44	1.76	.09	-.93	.31	-.05
1959	.36	-.08	.69	-.86	-.42	-1.58	.10	-.22	1.08	2.36	-.32	-.02
1960	1.11	1.84	.74	.03	.08	1.66	-.23	-1.12	-.01	.49	.11	.29
1961	-.36	-.51	.37	-.47	1.21	1.22	.82	1.21	-.69	-.10	1.21	.13
1962	.20	-.27	.90	-.79	-.82	3.09	2.82	.05	.71	-.57	-.15	-.22
*Σ (+)	9.50	15.35	25.07	38.09	46.63	57.66	54.08	38.81	30.38	29.97	20.40	14.41
*Σ (-)	9.21	15.16	25.04	38.12	47.57	57.65	54.04	39.61	30.38	30.00	20.37	14.25
\bar{d}	0	0	0	0	0	0	0	.01	0	0	0	0
** \bar{D}	.26	.43	.71	1.07	1.34	1.62	1.52	1.10	.86	.84	.57	.40

*Sums are for 1887-1957.

** \bar{D} is the mean of the absolute values.

additional rainfall was required if moisture use was to be "normal."

For the 35-month period beginning with July 1932 the total computed need for precipitation (col. 10) was 69.09 in. This is 14.84 in. greater than the average precipitation (54.25 in. from table 2) for such a period. Actually, the precipitation totaled only 40.66 in. (col. 11), which is 28.43 in. less than the amount that would have been climatologically appropriate for the existing conditions. The point is that although the below-average precipitation, in itself, accounts for 13.59 in. of the computed abnormal moisture deficiency, the procedure outlined here brings to light an additional abnormality of -14.84 in. which is by no means insignificant. This is the result of having taken account of temperature and the other aspects of the water balance.

THE CLIMATIC CHARACTERISTIC, K

Column 12 of table 4 shows a sample of the derived monthly moisture departures. Such values were computed for the 852 months of western Kansas data and the 324 months of central Iowa data. These values are shown in tables 5 and 6.

From practical as well as statistical considerations it is apparent that a given departure means different things at different places and at different times. We can compare a series of such departures for, say, September in western Kansas; but we cannot compare September departures with, say, February departures, or with departures computed for a different area unless we determine beforehand that the sets of data are truly comparable. This suggests that the importance or significance of each departure somehow depends on the normal moisture climate for the month and place being considered.

In order to evaluate this importance, it was assumed that the economic consequences of the driest year in central Iowa were approximately as serious for the inhabitants of central Iowa as were the consequences of the driest year in western Kansas for the inhabitants of western Kansas. It turned out that the driest period of approximately 1-yr. duration in central Iowa began with June 1933 and continued through August 1934, a period of 15 months. The computed total moisture departure for the entire 15-month period was -30.67 in. or an average of -2.045 in. per

TABLE 6.—Monthly moisture departures, *d*, central Iowa

	Jan.	Feb.	Mar.	Apr.	May	June	July	Aug.	Sept.	Oct.	Nov.	Dec.
1930.....	0.26	-0.40	-1.06	0.18	-0.22	0.09	-2.04	-2.65	-2.14	-0.20	-1.42	-1.32
1931.....	-1.44	-2.10	-1.51	-1.65	-2.26	-2.62	-.89	-1.65	2.90	.07	-1.85	2.31
1932.....	1.25	-.02	-.33	-1.07	.19	.18	-.04	3.97	-.50	.01	1.39	.76
1933.....	.11	-.46	1.36	-1.15	1.66	-4.89	-.64	-2.23	-.90	-.15	-2.42	-1.04
1934.....	-.41	-1.00	-1.32	-2.54	-5.48	-4.45	-.97	-2.20	1.61	-1.31	2.11	-.79
1935.....	.36	.59	-.71	-.87	.94	4.39	1.14	-1.57	.63	1.76	1.71	.71
1936.....	.86	.47	-.72	-.79	-1.78	-1.04	-3.97	-2.44	3.83	-.08	-.88	-.53
1937.....	1.03	.39	.14	1.28	.71	-1.05	-.95	-.23	-2.17	-.11	-1.36	-.85
1938.....	-.38	-.75	-.47	1.84	2.59	-.22	1.23	-.81	1.87	-1.48	1.11	-.03
1939.....	.02	1.42	-.39	-.67	-2.85	.76	-.50	.87	-2.41	-.70	-2.01	-1.05
1940.....	-.83	-.08	-.61	.83	-1.15	-2.37	1.60	3.65	-1.79	-.26	1.17	.56
1941.....	1.04	-.21	-.78	-1.34	-2.53	1.78	-.85	-1.36	4.35	4.03	1.05	1.70
1942.....	.29	.41	.03	-1.89	.96	1.57	2.28	1.29	1.65	-.51	.67	.69
1943.....	0	.19	.09	1.07	1.10	.84	3.00	1.95	1.09	-.03	-.27	.18
1944.....	.59	.31	.96	2.56	4.76	.80	1.81	3.21	-.07	-.95	-.33	.58
1945.....	-.23	.98	.89	2.35	3.46	-.10	-.40	-.70	1.05	-1.56	-.69	.99
1946.....	1.35	-.60	1.58	-1.90	1.02	2.57	-.24	1.99	2.03	.44	-.18	.10
1947.....	.76	-.30	-.07	3.15	1.65	7.87	-1.89	-3.39	-3.02	1.77	-.20	.49
1948.....	-1.06	1.10	1.04	-.29	-1.79	-1.92	.74	-1.47	-2.42	-.46	.56	.99
1949.....	1.68	.29	.52	-1.23	-2.41	-.50	-.99	-2.44	-.09	-.14	-2.17	.99
1950.....	-.22	.60	-1.05	.31	2.28	1.35	-.26	-.98	-1.54	-1.28	-1.74	-1.12
1951.....	-1.07	.91	2.40	3.05	.56	1.40	1.66	2.90	.42	1.54	.90	.35
1952.....	.51	-.11	2.25	-.90	.22	.36	.85	1.13	-2.07	-1.64	.64	-.01
1953.....	-.19	.77	.93	1.46	-1.16	-.12	-.16	-2.49	-2.98	-2.59	-1.77	-.94
1954.....	-1.55	-.45	-.48	.78	.99	1.66	-1.99	6.56	.49	2.56	-.84	-.05
1955.....	.03	.66	-.69	1.10	-.90	-2.59	.19	-2.57	-.55	-1.29	-2.25	-1.49
1956.....	-1.33	-1.45	-1.87	-1.41	-1.94	-3.72	-.69	-1.00	-1.73	-1.07	-1.25	-1.46
1957.....	-1.18	-1.47	-1.15	-1.06	1.10	.08	.14	-.39	-.80	.81	1.02	.07
1958.....	-.21	-.41	-1.07	-.60	-2.02	.83	6.25	-.28	1.11	-1.25	-.10	-.77
1959.....	-.33	.36	2.06	.80	2.64	-1.46	-.54	-.75	.44	.44	1.02	.42
1960.....	1.90	.43	.04	.90	2.91	-1.38	-.11	2.38	.86	.09	-1.05	-.40
1961.....	-.88	1.29	2.37	.50	-1.86	-1.36	3.38	-.33	5.24	1.40	1.64	.92
1962.....	-.49	1.12	-.02	-.33	.74	-1.93	2.63	-.47	-.76	.56	-1.53	-1.05
*Σ(+)	9.85	8.89	12.19	18.78	24.19	25.61	15.08	26.85	22.47	15.09	17.89	10.02
*Σ(-)	9.92	8.90	12.15	18.76	24.25	25.62	15.15	26.84	22.45	15.10	17.91	10.00
\bar{d}	0	0	0	0	0	0	0	0	0	0	0	0
** \bar{D}	.73	.66	.90	1.39	1.79	1.90	1.12	1.99	1.66	1.12	1.33	.74

*Sums are for 1931-1957.

** \bar{D} is the mean of the absolute values.

month. Considering the same 27 years as were considered in Iowa, the driest period of similar length in western Kansas was a 14-month period from March 1934 through April 1935. The total moisture departure for this period (see column 12, table 4) was -19.11 in. or an average of -1.365 in. per month.

On the assumption that these dry periods were of approximately equal significance locally, we can multiply each by some factor, K , and write

$$\bar{K}_{Iowa} \times \bar{d}_{Iowa} = \bar{K}_{Kan} \times \bar{d}_{Kan} \quad (16)$$

and

$$\bar{K}_{Iowa} / \bar{K}_{Kan} = \bar{d}_{Kan} / \bar{d}_{Iowa} = -1.365 / -2.045 = 0.67. \quad (17)$$

The \bar{K} 's represent averages for some, as yet, undefined characteristics of the climates of these two areas during the 14- and 15-month periods; i.e., they apply to the periods as a whole rather than to each month individually. However, for the moment they can be treated as constants to be evaluated from some measured aspects of the local climate.

From equation (17) it is apparent that \bar{K} for western Kansas must be about $1\frac{1}{2}$ times as large as \bar{K} for central Iowa. Now, the average moisture demand in the two areas is roughly the same but the average moisture supply in Iowa is roughly $1\frac{1}{2}$ times larger than in Kansas. This suggests that the values of the constants may depend on the average moisture shortage in the two places. This seems reasonable inasmuch as the less the supply, in relation to the demand, the greater the significance of a given shortage.

How can one best measure average moisture demand? In some months it can be reasonably estimated by \overline{PE} , and in some months it can be estimated by the average amount of recharge that occurs. However, in some spring and fall months \overline{PE} and \bar{R} are roughly equal and both are important. Therefore average moisture demand for any period can be estimated by $\overline{PE} + \bar{R}$.

The average moisture supply is not always dependent entirely on the precipitation. In some cases the precipitation alone does not truly represent all of the moisture supply because previously stored moisture is used also. Therefore, average moisture supply for a month or period can be measured by $\bar{P} + \bar{L}$.

The normal moisture demand for the 14-month dry period in Kansas can be found from table 2 as:

$$\sum_{n=1}^{14} \overline{PE} + \sum_{n=1}^{14} \bar{R} = 36.21 \text{ in.}$$

The normal moisture supply for the same period can also be found from table 2 as:

$$\sum_{n=1}^{14} \bar{P} + \sum_{n=1}^{14} \bar{L} = 25.90 \text{ in.}$$

If we take the ratio of demand to supply, we get $36.21/25.90 = 1.398$, which we can call \bar{K} for this 14-month period in Kansas.

Turning to the 15-month period in Iowa and following the same procedure,

$$\left(\sum_{n=1}^{15} \overline{PE} + \sum_{n=1}^{15} \bar{R} \right) / \left(\sum_{n=1}^{15} \bar{P} + \sum_{n=1}^{15} \bar{L} \right) = 50.88/53.23 = 0.956,$$

which can be considered as \bar{K} for this 15-month period in Iowa.

If this ratio of moisture demand and supply can be used as a measure of the importance of moisture departures, then according to equation (17), $\bar{K}_{Iowa} / \bar{K}_{Kan}$ should be about 0.67. It turns out that $0.956/1.398 = 0.68$, which is in surprisingly good agreement.

From the above it appears that K , the climatic characteristic, can be reasonably estimated for each of the 12 calendar months as:

$$k = (\overline{PE} + \bar{R}) / (\bar{P} + \bar{L}) \quad (18)$$

where k is a first approximation of K .

The k -values in column 6 of table 3 were computed by this equation. These numbers are intended as measures of the local significance of the moisture departures which have been derived. However, it later turned out that equation (18) did not work very well in some other climates and a different equation for K had to be derived. Since the work on the final K was dependent on this first approximation, k , the following few pages describe the development based on k and are followed by the "back tracking" which evolved the final equation for K .

THE MOISTURE ANOMALY INDEX, z

These monthly constants, the k -values, were used as weighting factors for each of the monthly moisture departures during the two dry periods

being considered. Beginning with March 1934 the departures listed in column 12 of table 4 were multiplied by the corresponding factors in column 6 of table 3 to obtain the index values shown in column 13 of table 4. When the index values, z , were algebraically added for the 14-month Kansas dry period which ended with April 1935, the sum was -25.51 . This represents an average index of -1.82 per month.

When the same procedure was followed for the 15-month dry period in Iowa, the 15-month index sum was -27.06 or -1.80 per month. This agrees very well with the average index for the driest Kansas period and suggests that the derived index values do, in fact, provide comparable measures of relative climatic abnormalities. The monthly "moisture anomaly index, z ," is therefore defined as:

$$z = dk. \quad (19)$$

What are these z values and what do they mean? They cannot be regarded as inches of departure of the moisture supply from normal as are the values in column 12 of table 4. Those departures have now been weighted and must be regarded only as index numbers. Each number expresses on a monthly basis and from a moisture standpoint the departure of the weather of the month from the average moisture climate of the month. Each has, presumably, been adjusted or weighted in such a way that the same scale—the ordinate, if you wish to think of it graphically—is applicable to all values in both areas.

Small abnormalities of moisture can occur at any time in any place. Of course, this is hardly surprising. Equally to be expected is the fact that in these climates large abnormalities very rarely occur during the cold season from November through February. The largest cold-season anomalies are positive and occur mostly in November as would be expected from the fact

that large monthly amounts of precipitation can and sometimes do occur in November. On the other hand, even a complete failure of the moisture supply during any cold month will not result in any very great departure of the moisture supply from normal because in these particular climates the cold season moisture demand or *CAFEC* precipitation is always rather small.

In Kansas and Iowa the really important negative moisture anomalies occur during the warm season. This, again, is as one would expect because the moisture requirement during summer can be rather large and, on occasion, the moisture supply can fail almost completely. Note the very large negative anomalies during July in the 1930's in western Kansas. The -6.51 in 1934 is the largest negative anomaly that has thus far been computed. This large value is a direct consequence of the extremely warm and dry weather which preceded July, coupled with the hot dry weather of July itself. The mean temperature over the area during July 1934 was an all-time record 85.6° F. and the area rainfall averaged only 0.74 in.

While central Iowa has not produced such an extremely dry single month, a number of negative anomalies of the order of -4 have occurred. Also the Iowa data show a greater tendency for long uninterrupted runs of abnormally dry months. The 15-month period which began in June 1933 and the 21-month period beginning with August 1955 were both uninterrupted by even a single wet month.

Some of the unusually wet months in both Kansas and Iowa produce some really outstanding positive anomalies. For example, it rained 12.26 in. over central Iowa in June 1947 and the anomaly index, z , was $+7.24$. Likewise, western Kansas had an index of $+8.49$ for June 1951 owing to 7.89 in. of rainfall which was 267 percent of normal and produced much flooding.

6. THE DURATION FACTOR

THE EFFECT OF TIME

As Hildreth and Thomas have pointed out [18] in most cases it is not the first year of low rainfall that is disastrous to farming and ranching, but the prolonged periods which extend for 2, 3, or 4 years in a row. The same reasoning applies if one is concerned about the hydrologic aspects of drought. A relatively short period of abnormally dry weather will lower lake and reservoir levels, but matters do not become really serious until a prolonged drought period has brought the water supply to a critically low level. Therefore, if one wishes to make a distinction between, say, mild drought and extreme or disastrous drought, the duration of the abnormally dry period must be taken into account.

DROUGHT CATEGORIES

It is reasonable, and it certainly would be convenient, to have names assigned to the various categories of drought severity just as arbitrary names and definitions have been assigned to such things as dense fog, moderate rain, and other phenomena. It appears that drought severity could be adequately expressed by four classes, mild, moderate, severe, and extreme—terms which are frequently used by the U.S. Department of Agriculture as well as by the Weather Bureau. Unfortunately, no satisfactory definitions exist for these expressions. There doesn't seem to be much hope for making even a semi-objective approach to specific definitions of "mild," "moderate," or "severe" drought; but if we assume that "extreme" drought occurred in the two areas being studied during some of the driest periods of record, we can describe extreme drought in terms of the accumulation of the monthly index values.

THE DRIEST INTERVALS

Table 7 shows some accumulated moisture anomaly index values in both central Iowa and western Kansas. These periods were selected as

TABLE 7.—The driest intervals

	From—	To—	Number of months	Σz
Kansas.....	June 1936.....	August 1936.....	3	-13.40
Do.....	May 1913.....	August 1913.....	4	-13.62
Do.....	April 1934.....	July 1934.....	4	-14.86
Do.....	May 1934.....	August 1934.....	4	-16.46
Iowa.....	April 1934.....	do.....	5	-14.14
Kansas.....	do.....	do.....	5	-18.56
Iowa.....	June 1933.....	June 1934.....	13	-23.39
Do.....	do.....	August 1934.....	15	-27.06
Kansas.....	June 1955.....	September 1956.....	16	-29.71
Do.....	do.....	October 1956.....	17	-31.28
Do.....	April 1934.....	August 1935.....	17	-31.59
Do.....	do.....	August 1936.....	29	-46.82
Do.....	do.....	September 1937.....	42	-62.55

representing the maximum rate at which the negative values of the monthly index have accumulated during various time intervals. These data are shown in figure 1. The straight solid line thereon was drawn by eye. This line itself does not show rate of accumulation of the index values; it merely indicates the approximate maximum rates which have been observed during extremely

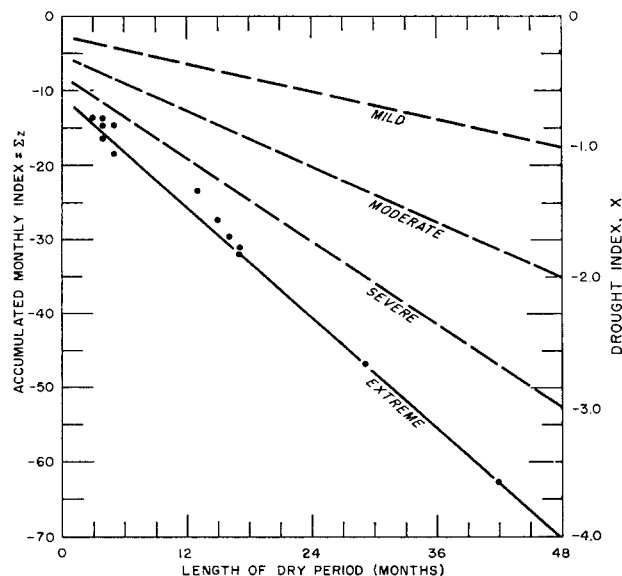


FIGURE 1.—Accumulated index during the driest periods of various lengths.

dry periods of various lengths. For instance, z -values have been known to accumulate at the rate of about -3.0 per month for 6 months, but at the average rate of only -1.5 per month over a 42-month period. Therefore, this line can represent extreme drought; i.e., an extremely dry and very unusual condition exists if $z = -12.00$ for one month as well as if $\Sigma z = -70.1$ in 4 years. This is one of a family of lines that can be drawn. Since the horizontal line at the top of this chart represents "normal," the ordinate from normal to extreme was divided into four equal lengths and the body of the graph was correspondingly divided by the dashed lines arbitrarily labeled "mild," "moderate," and "severe" drought. It is convenient to assign a numerical drought severity value of -4.0 to the line for extreme drought, -3.0 to severe drought, -2.0 to moderate drought, and -1.0 to mild drought. The solid line drawn is therefore the -4.0 line and the equation can be determined by noting that from t (duration) = 1 month and $z = -12.0$ to $t = 48$ months and $\Sigma z = -70.1$, the drought severity = -4.0 . Drought severity is therefore approximated by

$$X_i = \sum_{t=1}^i z_t / (0.309t + 2.691). \quad (20)$$

DETERMINING MONTHLY INCREMENTS OF DROUGHT SEVERITY

Equation (20) is only a first approximation to the relationship sought because it is based on algebraic sums of the index, z , over various periods of time. This is not the best way to handle the problem because this cumulative procedure causes the effect of a single month—say, a very wet month in a long series of dry months—to be directly reflected in Σz even years later. Obviously, this is unrealistic because a single wet month during a given dry summer should not, by the following summer, have any great influence on the severity of a drought which had continued during the intervening period. For instance, August 1933 was a very wet month in Kansas (see table 4) and it greatly reduced the severity of the drought that was underway. However, the drought continued and by the end of May 1934 the situation was very, very serious. But, this seriousness is not completely apparent when the z -values are accumulated and plotted on a diagram such as figure 1. In fact this procedure will create a misleading picture.

Figure 2 demonstrates how misleading the cumulative procedure can be. Figure 2A was constructed by assuming that $z = -1.0$ each

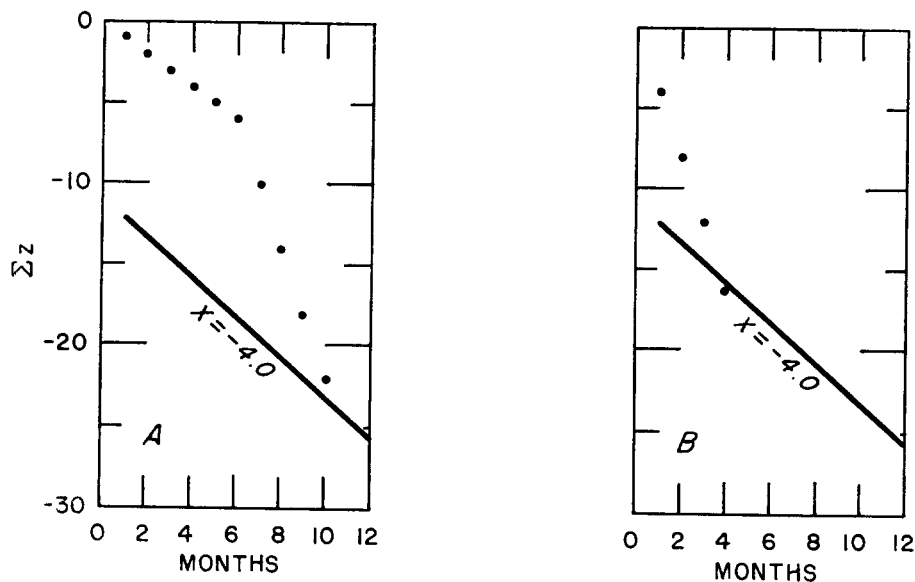


FIGURE 2.—An illustration of the cumulative procedure. (A) Six relatively dry months followed by four very dry months; (B) The four very dry months by themselves.

month for 6 months and then $z = -4.0$ during each of the following 4 months. The total accumulated value is therefore -22.0 in 10 months. Note that the 10th month does not quite reach the extreme drought line.

Now assume that the first 6 months were each very wet and that the remaining 4 months each had $z = -4.0$ as before. In this case the dry period begins with the first month in which $z = -4.0$ and these 4 dry months give the curve in figure 2B. Note that the value for the last month now falls below the extreme drought line.

We are now confronted with a result which indicates that four very dry months following six wet months produce a more serious drought than is produced by the same four very dry months following six months of relatively dry weather. Obviously, this is a fallacy. The cumulative procedure is misleading and cannot be used as a method of taking account of the duration of the dry period.

The problem must, therefore, be handled on an increment basis such that each successive month is evaluated in terms of its contribution to the severity of drought. In effect, this will eliminate direct consideration of the duration factor and bring duration in indirectly as a consequence of the accumulation of successive monthly contributions to drought severity.

In order to evaluate the contribution of each month, we can set $i=1$ and $t=1$ in equation (20) and we have,

$$X_1 = z_1/3. \quad (21)$$

Since this is an initial month,

$$X_1 - X_0 = \Delta X_1 = z_1/3. \quad (22)$$

However, this is not the whole story because in successive months a certain amount of abnormal dryness ($z < 0$) will be required merely to maintain the severity of the existing dry spell. For instance, one knows intuitively that an extreme drought will not continue in the extreme category if subsequent months are normal or only very slightly drier than normal. The question is, how much dryness is required to maintain a drought of given severity; i.e., for $\Delta X = 0$?

From equation (20) or from figure 1, it is apparent that Σz must increase as t increases in

TABLE 8.—The amount of abnormal dryness required to maintain a given drought severity

t	X_{t-1}	$\sum_{i=1}^{t-1} z_i$	ΔX_t	X_t	$\sum_{i=1}^t z_i$	z_t
2	-1.0	-3.0	0	-1.0	-3.309	-0.309
10	-1.0	-5.472	0	-1.0	-5.781	-.309
2	-3.0	-9.0	0	-3.0	-9.927	-.927
10	-3.0	-16.416	0	-3.0	-17.343	-.927

order to maintain a given value of X . The rate of increase of t is constant; i.e., t increases by 1 each month, thereby increasing the denominator by steps of 0.309. Therefore, the rate at which the index, z , must increase in order to maintain a constant value of X ($\Delta X = 0$) depends on the value of X that is to be maintained. This reasoning suggests that for all months following an initial dry month an additional term must be added to equation (22), and that the equation is of the form,

$$\Delta X_t = (z_t/3) + cX_{t-1}, \quad (23)$$

where

$$\Delta X_t = X_t - X_{t-1}.$$

The problem is to determine c . Returning to equation (20), we can compute the value of z_t which will maintain a given value of X from month to month. Table 8 shows the computed values of z in the i th month for two arbitrary values of $X_{t-1} = X_t$ and two arbitrary values of t .

If we place these values of z_t , X_{t-1} and ΔX into equation (23), we have,

$$\Delta X = 0 = (-0.309/3) - 1.0c,$$

and

$$\Delta X = 0 = (-0.927/3) - 3.0c.$$

c is therefore -0.103 and the final equation is:

$$\Delta X_t = (z_t/3) - 0.103X_{t-1}. \quad (24)$$

This equation can be used to compute the monthly contributions to drought severity. Of course, the sum of the increments gives the severity itself, i.e.,

$$X_t = X_{t-1} + \frac{z_t}{3} - 0.103X_{t-1}. \quad (25)$$

7. RE-EVALUATION OF THE WEIGHTING FACTOR

EVIDENCE OF UNSATISFACTORY K VALUES

Originally, this study was carried through to completion on the basis of the equations shown above. Results for western Kansas and central Iowa appeared reasonable and realistic. However, when the entire method was subsequently applied to other areas with rather different types of climate, some of the results were definitely peculiar and unrealistic. For example, in Kansas and Iowa the most extreme drought periods produced maximum drought index values around -5.0 to -6.0 . These seemed reasonable inasmuch as the system is designed to indicate extreme drought whenever the index exceeds -4.0 . However, an analysis for the southern climatological division of Texas produced index values ranging as large as -10.23 . Such values were obviously rather far from the expected maximum around -6.0 . On inspection it was found that some of the monthly weighting factors were inflating the departures, the d values, in an unrealistic fashion.

The other analysis that showed peculiar results was done for western Tennessee by Mr. M. H. Bailey, then State Climatologist for Tennessee. The worst flood in the history of the area (January 1937) produced an index, X , only slightly larger than zero. Again, the k values were at fault. They were so small that even huge moisture departures were rendered quite insignificant when multiplied by the weighting factor, k . In this particular January in western Tennessee, rainfall averaged 19.35 in. over the area and $P - \hat{P}$ was a huge $+12.26$ in. As will be shown later on, this system should measure unusually wet periods as well as unusually dry periods. Obviously, the index, X , should receive a large positive increment during this extremely wet month. From equation (22)⁶ one can see that this will occur only if K for January (see eq. (19)) is of the order of 0.5 to 0.7, say, 0.6. Actually, k had been computed (by eq. (18)) as 0.051 for January.

⁶ From here on z becomes Z and k becomes K in equations 19 through 25, as these are the final estimates of these indices.

PROCEDURE FOR ESTIMATING MEAN VALUES OF K

It seemed the simplest procedure for re-evaluating the weighting factor was to use equation (20) to determine what ΣZ should be for extreme drought over a 12-month period. It turned out that for $X = -4.0$ and $t = 12$ months, the sum of the weighted departures should be -25.60 . If we again assume that the driest 12-month period represents extreme drought in any area, we can obtain a new 12-month mean weighting factor, \bar{K} , by dividing -25.60 by the 12-month sum of d for the driest periods of record.

Referring to table 5, it will be noted that the driest 12-month period in western Kansas began with May 1934 and continued through April 1935. The sum of the d values for this period is -16.62 . A period almost as dry began with March 1956 and extended through February 1957. This 12-month sum of d was -15.60 . Averaging these two, to eliminate a little of the sampling variability, gives a mean 12-month sum of d of -16.11 . Dividing -25.60 (12-month ΣZ for extreme drought) by -16.11 gives 1.59. This is \bar{K} for western Kansas. It is a mean weighting factor—the mean of the 12 monthly weighting factors.

In central Iowa the driest 12-month periods were June 1933 through May 1934 and August 1955 through July 1956 (see table 6) when the 12-month sums of d were -23.02 and -20.56 . The mean is -21.79 . When we divide -25.60 by -21.79 we get 1.17 for \bar{K} is central Iowa.

By this time analyses and a monthly table of d values were available for nine different areas, viz, the climatological divisions of northwestern North Dakota, western Kansas, central Iowa, Texas High Plains, Edwards Plateau of Texas, southern Texas, western Tennessee, west central Ohio, and a point analysis for Scranton, Pa. The values computed for \bar{K} ranged from 1.06 in western Tennessee to 1.73 in northwestern North Dakota. In addition, there is the previously mentioned estimate that K for January in western Tennessee should be around 0.6 if the 1937 case is to look at all reasonable.

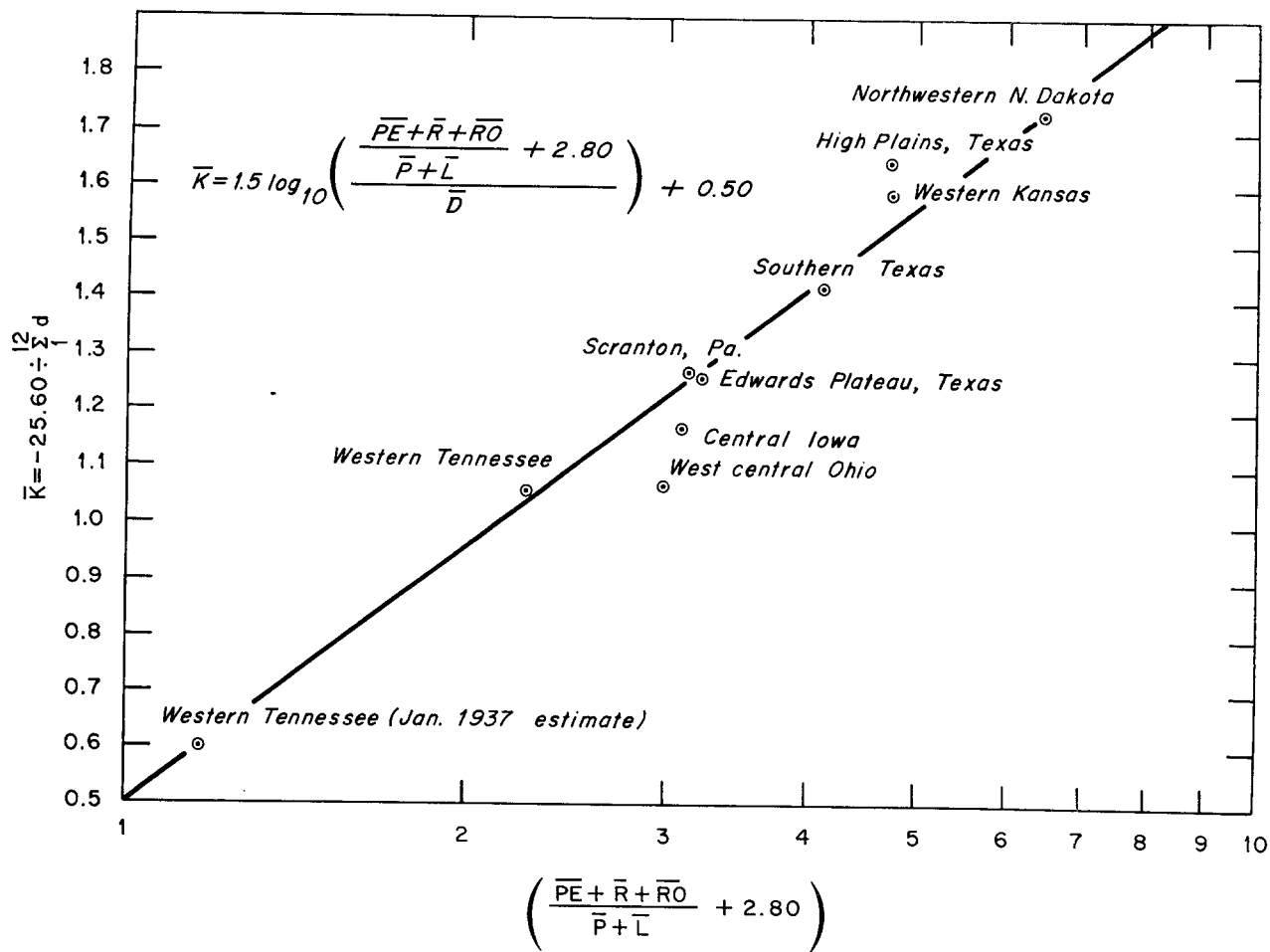


FIGURE 3.—Mean annual weighting factor as related to average moisture demand, average moisture supply, and average absolute moisture departure.

K AS A FUNCTION OF OTHER ASPECTS OF CLIMATE

From an inspection of the failures of the original k values it was apparent that K should depend on average water supply, $\bar{P} + \bar{L}$, as originally used. It was also apparent that the average runoff, $\bar{R}\bar{O}$, should be considered as a part of the moisture "demand" in addition to the average potential evapotranspiration, $\bar{P}\bar{E}$, and the average recharge, \bar{R} . Also, it was apparent that K varies inversely with \bar{D} , the mean of the absolute values of d .

After some experimenting with various empirical relationships, the semi-logarithmic plot shown in figure 3 was evolved. No doubt, greater scatter would result if more stations or areas were

added. This relationship may be fortuitous, but it seems reasonable. The problem is also complicated by sampling variability.

The K values in figure 3 were based on the driest 12-month periods in these various places and the abscissa is made up of mean values for the entire period of record analyzed, the 30 years 1931-1960 in most cases. For example, $\bar{P}\bar{E}$ is average annual PE divided by 12, and the other mean values were computed in the same fashion.

MONTHLY WEIGHTING FACTORS

The next step was to apply this empirical relationship to each of the 12 calendar months in each of the various places and thereby derive the 12 K values for each place. These results are

shown in table 9. In this table D is the monthly mean of the absolute values of d , and K' is the weighting factor computed for each month by the equation developed from figure 3; viz,

$$K' = 1.5 \log_{10} \left[\left(\frac{\overline{PE} + R + \overline{RO}}{\overline{P} + \overline{L}} + 2.80 \right) / \overline{D} \right] + 0.50. \quad (26)$$

TABLE 9.—Monthly weighting factor, K , for selected places

	Jan.	Feb.	Mar.	Apr.	May	June	July	Aug.	Sept.	Oct.	Nov.	Dec.	Sum
WESTERN TENNESSEE													
\overline{D}	3.24	1.89	1.45	1.40	1.50	1.70	1.60	1.25	1.68	1.31	1.92	1.88	-----
K'	.60	.95	1.13	1.15	1.11	1.05	1.12	1.34	1.10	1.21	.95	.96	-----
$\overline{DK'}$	1.94	1.80	1.64	1.61	1.67	1.78	1.79	1.68	1.85	1.59	1.82	1.80	20.97
K	.51	.80	.95	.97	.94	.86	.94	1.13	.93	1.02	.80	.81	-----
WEST CENTRAL OHIO													
\overline{D}	1.93	1.00	1.04	1.20	1.40	1.74	1.36	1.18	1.31	1.11	1.16	1.09	-----
K'	.94	1.37	1.34	1.25	1.15	1.01	1.19	1.29	1.22	1.31	1.27	1.31	-----
$\overline{DK'}$	1.81	1.37	1.39	1.50	1.61	1.76	1.62	1.52	1.60	1.45	1.47	1.43	18.53
K	.90	1.31	1.28	1.19	1.10	.96	1.14	1.23	1.16	1.25	1.21	1.25	-----
CENTRAL IOWA													
\overline{D}	0.73	0.66	0.90	1.39	1.79	1.90	1.12	1.99	1.66	1.12	1.33	0.74	-----
K'	1.58	1.64	1.44	1.16	.99	.96	1.31	.95	1.06	1.31	1.18	1.55	-----
$\overline{DK'}$	1.15	1.08	1.30	1.61	1.77	1.82	1.47	1.89	1.76	1.47	1.57	1.15	18.04
K	1.55	1.61	1.41	1.14	.97	.94	1.28	.93	1.04	1.28	1.16	1.52	-----
SCRANTON, PA.													
\overline{D}	0.86	0.70	0.81	0.96	1.30	1.35	2.27	1.60	1.43	1.29	1.27	0.95	-----
K'	1.47	1.60	1.51	1.40	1.20	1.19	.86	1.09	1.18	1.21	1.21	1.40	-----
$\overline{DK'}$	1.26	1.12	1.22	1.34	1.56	1.61	1.95	1.74	1.69	1.56	1.54	1.33	17.92
K	1.45	1.58	1.49	1.38	1.18	1.17	.85	1.07	1.16	1.19	1.19	1.38	-----
EDWARDS PLATEAU, TEXAS													
\overline{D}	1.16	0.85	0.95	1.40	1.61	1.90	1.59	1.14	2.08	1.61	0.77	1.10	-----
K'	1.28	1.48	1.42	1.18	1.09	1.06	1.27	1.58	1.01	1.13	1.56	1.32	-----
$\overline{DK'}$	1.48	1.26	1.35	1.65	1.75	2.01	2.02	1.80	2.10	1.82	1.20	1.45	19.89
K	1.14	1.31	1.26	1.05	.96	.94	1.13	1.40	.90	1.00	1.39	1.17	-----
SOUTHERN TEXAS													
\overline{D}	0.97	0.80	0.63	1.39	1.33	1.55	1.23	1.49	1.73	1.36	0.66	0.90	-----
K'	1.41	1.53	1.76	1.29	1.29	1.29	1.57	1.41	1.15	1.30	1.73	1.47	-----
$\overline{DK'}$	1.37	1.22	1.11	1.79	1.72	2.00	1.93	2.10	1.99	1.77	1.14	1.32	19.46
K	1.28	1.39	1.60	1.17	1.17	1.17	1.43	1.28	1.04	1.18	1.57	1.33	-----
WESTERN KANSAS													
\overline{D}	0.26	0.43	0.71	1.07	1.34	1.62	1.56	1.10	0.86	0.84	0.57	0.40	-----
K'	2.25	1.92	1.60	1.34	1.20	1.12	1.20	1.45	1.63	1.59	1.78	1.97	-----
$\overline{DK'}$.58	.58	1.14	1.43	1.61	1.81	1.87	1.60	1.40	1.34	1.01	.79	15.41
K	2.58	2.20	1.84	1.38	1.54	1.28	1.38	1.66	1.87	1.82	2.04	2.26	-----
TEXAS HIGH PLAINS													
\overline{D}	0.51	0.42	0.63	0.86	1.50	1.48	1.40	0.89	1.28	1.22	0.52	0.65	-----
K'	1.81	1.94	1.70	1.54	1.15	1.23	1.33	1.66	1.37	1.32	1.85	1.66	-----
$\overline{DK'}$.92	.81	1.07	1.32	1.72	1.82	1.86	1.48	1.75	1.61	.96	1.08	16.40
K	1.95	2.09	1.83	1.66	1.24	1.32	1.43	1.79	1.48	1.42	1.99	1.79	-----
NORTHWESTERN NORTH DAKOTA													
\overline{D}	0.20	0.23	0.33	0.67	1.04	1.48	0.98	0.81	0.91	0.59	0.38	0.19	-----
K'	2.42	2.33	2.08	1.64	1.37	1.14	1.48	1.66	1.59	1.81	2.00	2.45	-----
$\overline{DK'}$.48	.54	.69	1.10	1.42	1.69	1.45	1.34	1.45	1.07	.76	.47	12.46
K	3.43	3.30	2.95	2.33	1.94	1.62	2.10	2.35	2.25	2.57	2.84	3.47	-----

Mean=17.67

As mentioned previously, the mean values used in the development of this equation were average annual values divided by 12. In applying equation (26) to compute monthly weighting factors the mean values used are means for one of the 12 calendar months.

FINAL ADJUSTMENT OF THE MONTHLY K VALUES

If equation (26) is producing reasonably "correct" values for use in equation (19), then the average annual sum of the weighted average departures should be about the same for all places analyzed. Table 9 shows these weighted average departures, \overline{DK} for each month and their sum for the 12 months. These sums agree fairly well, but not well enough. The disagreement indicates that the departures are being given more weight in some places than in others. For example, the Tennessee weighting factors must be too large while the North Dakota weighting factors must be too small. This discrepancy was demonstrated by using the K' values to compute drought severity (using equation (19) and (25)) for some of the driest periods of record in each of these places. As an example, drought index values computed on the basis of K' indicated that drought in western Tennessee becomes more extreme than does drought in northwestern North Dakota or western Kansas. This did not seem reasonable and suggested that the weighting factors needed further adjustment.

The annual sums of \overline{DK} in table 9 range from 12.46 to 20.97. The mean sum for the nine areas is 17.67. If all weighting factors are adjusted so that all the annual sums of $\overline{DK}=17.67$, drought analysis results should be more comparable. The K values shown in table 9 were computed on this basis. For example, for January in west Tennessee, $0.51=(17.67/20.97)0.60$. This can be expressed as,

$$K = \frac{17.67}{\sum_1^{12} \overline{DK}} K' \quad (27)$$

This completes the derivation of the weighting factors. They apparently establish reasonable comparability between areas, but there seems no way of assuring that they establish more than fair to good comparability between months. No doubt it would have been better to base the con-

stant, 17.67, on analyses from many more places, but quite a range of climates is represented by these nine areas and the value 17.67 seems to work fairly well.

STANDARD DEVIATION OF d AS A WEIGHTING FACTOR

Some surely wonder why the standard deviation of d was not used as a weighting factor, thereby permitting one to deal with a standardized variable. This, of course, was tried, but results were definitely unrealistic partly because some of the distributions of d are rather skewed. Another likely factor is that the local significance of a given moisture departure is not solely dependent on its place in the distribution of departures. For example, the standard deviation of d is 1.64 in. in October in western Tennessee and it is also 1.64 in. in July in southern Texas. In the Tennessee case average moisture demand, $\overline{PE} + \overline{R} + \overline{RO}$, is 3.27 in. and average moisture supply, $\overline{P} + \overline{L}$, is 2.99 in. On the other hand, southern Texas has an average July moisture demand of 7.57 in., but an average moisture supply of only 2.13 in. Here demand is about $3\frac{1}{2}$ times supply, while in Tennessee they are roughly equal. It seems obvious that a given moisture shortage would not be equally significant in both places. We would be assuming equality if we used the standard deviation as a weighting factor.

AN EXAMPLE OF THE DROUGHT SEVERITY COMPUTATIONS

At this point it is probably time to stop and take stock of the relationships which have been developed. It seems likely that a short example will best illustrate some of the more important steps. The year 1947 was a rather unusual one for central Iowa. April, May, and June were very wet and July, August, and September were very dry. The data for the 3 dry months are shown in table 10.

Inasmuch as June had been very wet, the *CAFEC* precipitation computed by equation (14) was only 2.81 in. for July. However, the actual precipitation was so small that the departure (by equation (15)) was -1.89 in. The final climatic characteristic, K , for July in central Iowa is (table 3) 1.28, therefore, the July anomaly was (by equation (19)) -2.42 . The next three columns in table 10 show the parts of equation (24). Since this was the first dry month, the drought

TABLE 10.—A selected 3-month dry period in 1947 in central Iowa

Month	Actual precip. P	Comp. precip. \hat{P}	Clim. char. K	Moisture anomaly Z	Severity for month $Z/3$	Index to maintain severity $-.103X_{t-1}$	Change in severity ΔX	Drought index X
July.....	0.92	2.81	1.28	-2.42	-0.81	0.0	-0.81	-0.81
August.....	1.36	4.75	.93	-3.15	-1.05	.08	-.97	-1.78
September.....	1.28	4.30	1.04	-3.14	-1.05	.18	-.87	-2.65

index for the previous month was, of course, zero. The change in drought severity due to the dryness in July was therefore -0.81 . We have previously defined mild drought as beginning when the severity index reaches -1.0 ; therefore the index value of -0.81 indicates that the drought was still not serious at the end of July. For convenience we can call this "incipient" drought, a condition which we will now arbitrarily define by a severity index value between -0.50 and -1.0 . Inasmuch as the drought index is only 81 percent as large as is required to establish mild drought, we can state that there is an 81 percent probability that this July marks the beginning of a drought period. Not until the severity index reaches -1.0 can we say with certainty that (by definition) a drought began in July. This provides a very convenient method for methodically determining the beginning of drought periods. In addition, it provides a basis for preparing statements expressing the probability that a drought *has* begun. The tendency for persistence during drought makes such probability statements worthwhile from a practical standpoint.

Table 10 shows that the dry August intensified the drought (equation (25)) and matters were beginning to get a little serious by the end of the month. The drought reached a severity of -1.78 , which is classed as mild, but it was approaching moderate severity. By the end of September a moderate drought existed. The comments published in the *Iowa Weekly Weather and Crop Bulletins* [62] agree reasonably well with this analysis. Early in August there seems to have been a good deal of concern about the fact that the area was rapidly running out of moisture and that crop damage might become serious unless rains came in the next week or 10 days. By the

end of August it was apparent that the dry weather had produced serious damage to some crops and that pastures were no longer supplying adequate forage for livestock. By the end of September there were general complaints of dry soil, delayed seeding, and poor pastures, but the growing season had essentially ended and the agricultural remarks cease to be particularly useful in estimating drought severity. However, as far as one can tell, moderate drought appears to be a reasonable classification for the September weather. It is difficult to estimate the severity of meteorological drought from remarks concerning agricultural conditions because fortuitous rains sometimes produce very satisfactory yields of some crops during seasons which were, as a whole, much drier than normal. Also there seems to be a tendency for exaggeration in crop condition reports. A week of hot, dry weather seems to foster reports that the crops are practically ruined, while rain of less than 1 in. the following week may lead to forecasts of a bumper crop. This is one of the reasons it was necessary to start this drought analysis development with selected cases in which it was so dry that there could be no disagreement as to the fact that the drought was very serious from all standpoints—agricultural as well as hydrologic.

By way of comparison it is interesting to see what happens to the examples of figure 2 when one analyzes these data by equation (25). At the end of the sixth month in figure 2A the drought severity is -1.54 ; at the end of the 10th month it is -5.55 . The four very dry months increase the severity by 4.01 and produce an extreme drought condition. On the other hand, the four very dry months in figure 2B give a drought severity of -4.53 at the end of the fourth month.

8. APPLICATION OF THE DROUGHT FORMULAS TO WET PERIODS

It seems reasonable to assume that the abnormal moisture deficiencies which could create, say, a moderate drought would have created a moderately wet period had they been positive rather than negative moisture departures. In other words, could not the drought equations be applied to wet periods merely by changing the signs where necessary? For example, equation (15) yields positive departures as well as negative. Also by equation (19) the monthly moisture anomaly Z , may be positive as well as negative. Likewise, equation (25) will give positive values when the monthly index is positive. Inasmuch as the equations will provide a measure of wetness the following categories were more or less arbitrarily set up, and are given in table 11.

Originally the objective of this study was to deal only with abnormally dry periods, but this proved to be not entirely feasible. It is difficult to determine the beginnings and endings of dry

TABLE 11.—Classes for wet and dry periods

X	Class
≥ 4.00	Extremely wet.
3.00 to 3.99	Very wet.
2.00 to 2.99	Moderately wet.
1.00 to 1.99	Slightly wet.
.50 to .99	Incipient wet spell.
.49 to -.49	Near normal.
-.50 to -.99	Incipient drought.
-1.00 to -1.99	Mild drought.
-2.00 to -2.99	Moderate drought.
-3.00 to -3.99	Severe drought.
≤ -4.00	Extreme drought.

periods unless one also recognizes and takes account of the wet periods. For example, a relatively dry month such as August 1935 in central Iowa (see table 6) will appear as a separate drought period unless one recognizes that this month constituted only a slight and probably beneficial interruption in a fairly long period of unusually wet weather.

9. END OF DROUGHT (OR WET SPELL)

Generally speaking, the beginning of drought closely follows the onset of an extended period of unusually dry weather. It follows, therefore, that the end of meteorological drought should coincide with the time when some rather major and fairly abrupt readjustment in the large-scale circulation pattern begins to produce weather which is normal or wetter and continues so for a significant length of time. This return to normal weather terminates the meteorological drought, but it does not ordinarily end the effects of the drought. The effects may linger for weeks or months or even years depending on which effects are considered [70]. These persistent effects constitute a separate problem which is outside the scope of this study.

CHANGES IN THE SEVERITY INDEX

If a drought has been going on and the weather turns consistently normal or wetter, the severity index will, by equation (25) eventually reach zero. However, it does not seem reasonable to require that the index drop all the way to zero before concluding that a drought has definitely ended. From examination of a number of cases this seems to be too stringent a requirement. For example, a drought that was just barely established, say

$X = -1.10$, would, by equation (25), require $Z = +2.97$ in order to reduce the index to zero in a single month. This seems like an excessive requirement, but it is plainly so if one computes the number of months of exactly normal weather ($Z=0$) required to bring X to zero. This can also be done from equation (25). We find that X reduces from -1.10 to -0.99 in 1 month, to -0.52 in 7 months, and approaches zero in about 3 years. Obviously, one would consider the drought over long before the end of 1 year of normal weather, let alone 3 years. On the other hand, if one ends drought as soon as the index is numerically less than -1.0 , normal weather would end the -1.10 drought in a single month. This is a little extreme in the other direction, because it would certainly not be a definite fact that a drought had ended merely because one month had been normal.

From the speculations above it would appear reasonable to assume that drought ends when the severity index reaches some value between 0 and -1.0 . In order to have some consistency and at the same time not risk breaking long drought periods into a number of short but barely separate drought periods, the lower limit of incipient drought, -0.50 , was chosen as the value of X

which will be considered to definitely end a drought. In other words, as soon as the severity index reaches the "near normal" category, which lies between -0.50 and $+0.50$, no drought exists.

DETERMINING THE END OF A DROUGHT

In the previous section it was assumed that drought can be considered as definitely terminated as soon as the drought index reaches the "near-normal" category. The question, then, is, how much moisture would be required to reduce the severity of a given drought to -0.50 ? This can be solved by substituting the appropriate values into equation (25). Let $X_i = -0.50$, then

$$-0.50 = X_{i-1} + Z/3 - 0.103X_{i-1}$$

and

$$Z = -2.691X_{i-1} - 1.50.$$

Therefore, the Z -value that will end a drought in a single month is:

$$Z_e = -2.691X_{i-1} - 1.50. \quad (28)$$

By saying that drought has definitely ended when $X = -0.50$, we are also saying that there is some algebraically smallest value of Z which could occur month after month and eventually produce $X = -0.50$ for month after month. When this occurs $\Delta X = 0$ and $X_{i-1} = -0.50$, so by equation (24) one finds that $Z = -0.15$. This indicates, and quite reasonably so, that a drought period can end even though the weather is consistently just slightly drier than normal. Therefore, any value of $Z \geq -0.15$ will tend to end a drought, and the "effective wetness" is:

$$U_w = Z + 0.15 \quad (29)$$

(After a drought has definitely begun ($X \leq -1.00$), equation (29) applies to the first "wet" month; i.e., the first month having $Z \geq -0.15$. U_w should then be computed for each successive month until the computations show either a 0 percent or a 100 percent likelihood that the drought has ended.)

If the amount of wetness required to end a drought in the first wet month (Z_e from equation (28)) is greater than the effective wetness (U_w from equation (29)) for that month, the drought severity will decrease, but the drought has not definitely ended. However, since the drought severity will have been diminished by the first wet month, it will not require as much wetness to end it the second month; i.e., Z_e will be smaller

the next month and the total amount of wetness required to end the drought will be the new Z_e computed for the i th month plus the previously accumulated wetness, viz,

$$Z_e + \sum_{j=0}^{j=j^*} U_{i-j} - U_i$$

where

$U = U_w$, i refers to the i th month; i.e., the month being considered, j indicates the number of months of lag; e.g., U_{i-j} at $j=1$ refers to the value of U_w in the preceding month, and $j=j^*$, the upper limit of the summation, indicates that U_w is to be summed back in time to and including the value at the j^* month, where the j^* month is the first month of the current wet spell. If $\sum U_w < 0$, $\sum U = 0$. Otherwise, one comes out with negative probabilities. (See table 12, column 5.)

The percentage probability ⁷ that a drought has ended is therefore:

$$P_e = \frac{\sum_{j=0}^{j=j^*} U_{i-j}}{Z_e + \sum_{j=0}^{j=j^*} U_{i-j} - U_i} \times 100 = \frac{100V}{Q}. \quad (30)$$

Now it frequently happens that a drought period is temporarily interrupted by a month or so of abnormally wet weather. Such occurrences nearly always give rise to speculations that the drought has ended. From the strictly soil moisture standpoint of agricultural drought, the drought has ended, at least temporarily; but from the meteorological standpoint or even from an economic standpoint the short wet spell may turn out to be of little consequence. The wet August of 1933 in western Kansas is a good example of a temporary interruption of a serious drought. The drought had begun in July 1932 and by the end of July 1933 the drought index stood at -4.07 , which is extreme drought for the area as a whole. August 1933 was cool and wet over the area. The average precipitation was 4.91 in. and the index for the month was $Z = +3.59$. This was, however, far from enough moisture really to end the drought. From equation (28) one can compute that Z_e , the amount needed to end the drought in August, was $+9.45$. From equation (29), the effective wetness, $U_w = +3.74$, and from

⁷ P_e actually expresses moisture received as a percentage of the amount of moisture required definitely to terminate a drought. Of course, the probability that a particular drought has ended is either zero or 1.0, but it is convenient to think of P_e as the probability that a drought has ended.

equation (30) the probability that the drought had ended turns out to be 40 percent. The drought index stood at -2.45 at the end of August. However, the dry weather was resumed in September and October (see table 5), and the probability that the drought had ended had dropped to 12 percent by the end of October. Subsequent dry weather reduced the probability to zero in the spring of 1934. If, however, the wet August had been followed by continued wet weather, the probability that the drought had ended would have reached 100 percent and *the last month of drought would have been the last month in which the probability was not greater than zero*; i.e., July 1933.

DETERMINING THE END OF A WET SPELL

In order to treat wet periods methodically in the same fashion as dry periods, some sign changes are required in the equations for computing the probability that a dry spell has ended. To determine the index, Z_e , which will end a wet spell in a single month, an equation similar to equation (28) must be developed. In this case one can substitute $X = +0.50$ in equation (25) and get:

$$Z = -2.691X_{i-1} + 1.50. \quad (31)$$

This gives a measure of the amount of abnormal dryness ($-Z$) required to reduce the severity of a wet spell to $+0.50$ in a single month.

Just as a drought period can end even though the weather is consistently just slightly drier than normal, a wet period can also end with the weather continuing very slightly wetter than normal. By substituting $\Delta X = 0$ and $X_{i-1} = +0.50$ in equation (24) one gets the value of Z which will tend to end a wet spell. The "effective dryness" becomes:

$$U_d = Z - 0.15. \quad (32)$$

Equation (30) for determining the probability that a drought has ended can be used to compute the probability that a wet spell has ended.⁸

The following section describes the procedure for using these equations to make a complete climatological analysis of the moisture aspects of the weather. The term, severity, which is ordinarily applied to drought rather than to wet periods, is here applied to both. This may not be a very accurate use of the term, but it is convenient, and there does not seem to be a satisfactory word to use in place of it.

⁸ In equation (30), $U = U_d$ for the case in which the termination of a wet spell is being considered.

10. PROCEDURE FOR COMPUTING SEVERITY OF DROUGHT AND WET SPELLS

In order to carry out the computations for determining monthly drought severity, X , from a long series of monthly values of the index, Z , one must keep track of the wet spells as well as the dry spells. Therefore, a number of things must be computed for each month. For example, when there is no drought or wet spell going on, one must each month compute the "probability" that a wet spell or a dry spell has begun. After this probability has reached 100 percent and a drought or a wet spell is actually underway, one must examine each month in turn to determine the probability that the spell has ended and at the same time determine the probability that a spell of the opposite sign has begun.

The computations are really quite simple. Were they being made by hand, simultaneous computations of various items would not be

necessary because one could easily go back and pick up anything that later turned out to be important, but for machine data processing the simultaneous computations save time in the long run. The computational routine will be explained by describing an example.

Table 12 shows a 40-month period from the western Kansas record. It was necessary to turn so far back into history for the example, because it was difficult to locate a short period that would illustrate most of the points that can come up.

There are four sub-routines illustrated. Columns 3 to 8 show the routine for computing the probability that a drought or a wet spell has ended. Columns 10 to 12 show the routine for computing the probability that a wet spell has begun. Columns 13 to 15 show the routine for computing the probability that a drought has

TABLE 12.—An example of the computational procedure for determining the beginning and ending of wet periods and dry periods and the monthly severity index of each (western Kansas data)

1	2	3	4	5	6	7	8	9	10	11	12	13	14	15	16	17	18	19
Month	Z	$\frac{U_n}{Z_{+15}}$	$\frac{U_d}{Z_{-15}}$	V*	Z _e	Q**	P _e	Z _e 3.0	$\frac{-103}{X_{i,i-1}}$	ΔX_i	X _i	$\frac{-103}{X_{2,i-1}}$	ΔX_i	X _i	$\frac{-103}{X_{3,i-1}}$	ΔX_i	X _i	X
1888																		
April	3.13			0			0	1.04	-0.03	1.01	1.28			0	-0.13	0.27	1.28	1.28
May	1.20			0	-2.67	-2.67	0	0.40			0			0			1.55	1.55
June	-0.73		-0.88	0	-1.59	-2.47	33	-0.24			0			0			1.15	1.15
July	2.41		0.25	0	-1.59	-2.47	26	0.14			0	0.02	0.16	0			1.17	1.17
August	2.21		2.05	0	-3.32	-3.32	68	0.74			0	0.01	0.75	0			1.79	1.79
September	-2.11		-2.26	0	-3.32	-3.32	54	0.23			0	0.07	0.30	0			1.91	1.91
October	0.69		-0.54	0	-1.72	-3.21	80	0.19			0	0.04	0.40	0			1.05	1.05
November	-0.57		-0.72	0	-1.33	-3.05	100	0.35			0	0.06	0.15	0			0.75	0.75
December	-1.06		-1.21	0	-0.52	-2.96	0	0.12			0	0.06	0.29	0			0	0
1889																		
January	1.86			0			0	0.62			0.62			0			0	0
February	-0.28			0	-0.09	-0.09	0	0.23			0.47			0			0	0
March	0.70			0	-0.18	-0.18	0	0.19			0.65			0			0	0
April	0.88			0	-0.77	-0.77	0	0.77			0.77			0			0	0
May	1.77			0	-0.26	-0.26	0	0.26			0.95			0			0	0
June	1.05			0	-0.35	-0.35	0	0.35			1.10			0			1.10	1.10
July	0.37			0	-1.49	-1.49	13	0.12			0			0			1.11	1.11
August	-0.05		-0.20	0	-1.49	-1.49	100	0.02			0			0			0.98	0.98
September	2.04		-2.19	0	-1.14	-1.34	0	0.68			0.69			0			0	0
October	0.06			0	-2.39	-2.39	0	0.12			0.74			0			0	0
November	0.35			0	-0.74	-0.74	0	0.60			0.06			0			0	0
December	-1.79			0	-0.68	-0.68	0	0.12			0.06			0			0	0
1890																		
January	2.6			0			0	0.09			0.14			0			0	0
February	-0.57			0	-1.19	-1.19	0	0.19			0.05			0			0	0
March	1.77			0	-0.59	-0.59	0	0.59			0.06			0			0	0
April	2.42			2.57	1.51	1.51	100	0.81			0.81			0			0	0
May	2.86			2.57	1.51	1.51	0	0.95			0			0			0	0
June	-2.92			0	-0.94	-0.94	0	0.04			0			0			0	0
July	2.86			0	-1.22	-1.22	0	0.22			0			0			0	0
August	-3.06			0	-0.54	-0.54	0	0.54			0			0			0	0
September	1.63			0	-0.46	-0.46	0	0.46			0			0			0	0
October	-1.37			0	-0.31	-0.31	0	0.31			0			0			0	0
November	0.93			0	-0.12	-0.12	0	0.12			0			0			0	0
December	-0.35			0	-0.48	-0.48	0	0.48			0			0			0	0
1891																		
January	1.86			2.01	7.00	7.00	29	0.62			0.62			0			0	0
February	-0.75			1.41	4.45	6.46	22	0.25			0.31			0			0	0
March	3.20			4.76	4.50	5.91	81	1.07			1.35			0			0	0
April	-0.43			4.48	1.00	5.76	78	0.14			1.07			0			0	0
May	1.92			6.55	1.11	5.59	100	0.64			1.60			0			0	0
June	3.93			0	1.00	5.59	0	1.31			0			0			0	0
July	4.22			0	1.00	5.59	0	1.74			0			0			0	0

*V = numerator of eq. (30) = $\sum U_n$ or $\sum U_d$.
 **Q = denominator of eq. (30) = $\sum Z_n + \sum V_{i-1}$.

begun. Columns 16 to 18 show the computations for determining the severity of any wet spell or any drought that *has been established*.

Prior to the period shown in table 12, the weather had been slightly dry and "near normal." The index value, Z , for March 1888 was $+0.81$ and had produced a severity index value of $+0.27$. This value of X_1 (which would have appeared in col. 12) indicated a 27 percent chance that a wet spell had begun with March. April was rather wet with $Z=3.13$ (see col. 2 of table 12) so no "probability of end" computations are necessary. April was the second wet month in this spell and the next step is to determine the probability that a wet spell has begun. This is done by equation (25) and turns out to be 1.28 as shown in column 12. Without, at this point, going into the details, column 15 shows that there is a 0 percent probability that a drought has begun. However, a wet spell has been definitely established; therefore $X_3=X_1$, and subsequent computations for this spell are transferred to columns 16-18. (Remember that X_3 is reserved for indicating the severity of any wet spell or any drought which has become definitely established; i.e., $X_1 \geq 1.00$ or $X_2 \leq -1.00$). Column 19 will be discussed later. So, at the end of April we have a wet spell underway.

By the end of May the wet spell has continued and intensified as shown by the fact that $X_3=1.55$.

June was drier than normal; $Z=-0.73$. The first operation is to determine the probability that this dry month has ended the wet spell. From equation (31) $Z_e=-2.67$. By equation (32) one finds that $U_a=-0.88$, as shown in column 4. This is the first dry month, so $V=U_a$, and by equation (30) we get a 33 percent chance that the wet spell has ended. The computations for this particular wet spell have been shifted from column 12 to column 18, so $X_1=0$. Inasmuch as this was a dry month, it may turn out to be the beginning of a drought period, provided that this wet spell ends. The drought severity index, X_2 in column 15, turns out to be -0.24 (from equation (25)). This shows a 24 percent chance that a drought has begun. We must continue to compute X_3 until this particular wet spell ends. Column 18 shows that the dry month has reduced the wet spell index to 1.15.

July, being a little wetter than normal, reduces the probability that the wet spell has ended to 26 percent. It also reduces the probability that

a drought has begun to 8 percent (col. 15). Even though there is only a 26 percent chance that this wet spell has ended, we must compute the probability that July marks the beginning of another wet spell, because under certain rare circumstances a value of X_1 for this month will be needed later on. For example, this or any wet spell will have ended if the weather is near normal month after month. When this happens, it turns out that the best measure of the weather (X in col. 19) must be obtained from the computed values of X_1 and X_2 . Therefore, both must be computed at every opportunity.

August ends all questions about a drought beginning or a near-normal period being underway, because it was so wet that P_e dropped to 0 percent. Since the probability of ending dropped to zero, we must wait for a subsequent dry period to end the existing wet spell. Note also that when $P_e=0$, X_1 and X_2 also equal zero.

We do not have to wait long for another dry period. September 1888 was rather dry and starts a new "ending period." Looking ahead we note that by the end of December P_e has reached 100 percent. Actually $P_e > 100$ percent, so it is entered as 100. Therefore a wet spell has been delineated as beginning with March and extending through August 1888. April, May, June, July, and August qualify as "slightly wet" (refer to table 11). Having defined the beginning and ending of the wet spell, we can now determine the proper values for X (col. 19). During the early portion of the wet spell, before X_1 reached 1.00 (not shown), $X=X_1$; thereafter $X=X_3$ until August, the last wet month.

Inasmuch as the period September through December 1888 was essentially dry and finally produced $P_e=100$ percent, the X_3 values entered for September, October, and November are of interest only in that they enable one to compute the values in column 6. By December there is no more interest in X_3 ($P_e=100$ percent) for this past wet spell; so $X_3=0$.

September began a 9-month period in which neither a drought nor a wet spell became established. X_1 and X_2 were computed at every opportunity, of course, and during most months we have two severity index values, one indicating slightly wetter than normal, the other indicating slightly drier than normal. Which one best represents the weather for each month?

If one accumulates the Z values from September

1888 through June 1889 and prepares a time graph of the accumulated sum at the end of each month, the following points will be readily apparent. Note in column 2 that the period September through December 1888 was predominantly dry and that the wetness index, X_1 in column 12, became zero during December. During December and on back through this predominantly dry period assign $X=X_2$.

Following the slightly dry period was a period which was, in general, a bit wet. This wet period began in January 1889 and continued through July 1889. During this period the drought index, X_2 , was gradually approaching zero and finally reached zero in March of 1889. During March and on back through this predominantly wet period assign $X=X_1$.

The next month, April, was wetter than normal, so X_2 is again zero and $X=X_1$. For the same reason $X=X_1$ in May. June produces an X_1 value >1.00 , so $X_3=X_1$ and $X=X_3$. July was wet also, and X_1 is set to zero, $X_2=0$, and $X=X_3$. August was slightly drier than normal and produces a small chance (13 percent) that the wet spell has ended. X_1 remains zero, but X_2 is -0.02 . Uncertainty exists as to whether the wet spell has ended or not. There is no way of knowing (at the end of August) whether X should equal 0.98 or -0.02 . The assignment of the X value for August must await further developments.

September was rather dry; P_e reaches 100 and answers the question left over from August. The wet spell ended; therefore, $X=-0.02$ in August and -0.70 in September.

October was wet. This again reduces X_2 to zero, so $X=X_1$. November was also slightly wet and again $X=X_1$.

December was dry and began what later turned out to be a brief mild drought. However, during December and on through January 1890, the computations give values for both X_1 and X_2 . (X_3 has remained at zero because no drought or wet spell has become established during this period.) Again there is a period of uncertainty as to whether X should equal X_1 or X_2 . By the end of February X_1 dropped to zero, so we assign $X=X_2$ in February and also for the preceding January and December.

This systematic procedure of assigning the value of X in accordance with the times when X_1 and X_2 equal zero enables one to obtain an index value for each month when no drought or wet spell is

underway. This somewhat arbitrary rule almost always assigns what appear to be reasonable values for the final index, X . Once in a while one can argue that the wrong value has been assigned, but in such cases X_1 and X_2 are both so small that there isn't really much room for argument either way.

March 1890 established mild drought and $X_3=X_2$ and $X=X_3$. April put an abrupt end to the drought as shown by $P_e=100$ percent. For April X_3 again becomes zero and $X=X_1$.

May 1890 marks the beginning of another drought period of 8 months duration. This drought reached its greatest severity, -3.22 , by the end of September. The next 3 months were drier than normal, but not sufficiently dry to maintain the severity that was reached in September, and the severity generally decreased until the abnormally wet weather beginning with January 1891 brought an end to this drought period. By May it was definitely established (col. 8) that the drought had ended and that another wet spell had begun.

If the above discussion seems confusing at first, please recall that table 12 covers a period which was selected to illustrate all aspects of the many problems that can arise. During many rather long periods of the record, such as that shown in table 4, the only computations consistently required are those for X_3 because a serious drought is underway and only occasionally does one encounter a month that is sufficiently wet to require computation of the probability that the drought has ended. The slightly wet May 1933 in Kansas produced a 6 percent probability that the drought had ended, but this dropped to zero the following month. The wet August 1933 produced a 40 percent probability that the drought had ended, but the probability never got above 47 percent (in February 1934) and by the following spring it again became zero, thereby bringing an end to the computations of P_e , X_1 , and X_2 .

August 1933 in Kansas raised one problem that is not included in the example in table 12. This month produced a 40 percent probability that the drought had ended, and it also produced an X value of 1.20 which indicates that a wet spell has begun. However, in this case—and a very few others like it—the drought did not end, and we cannot use this as the beginning of a wet spell unless the drought ends. In such instances X_3

does not equal X_1 and the X_1 computations must be continued in column 12 until P_e reaches zero or 100 percent or until X_1 returns to zero.

It might be well to point out that tables 1, 4, and 12 make up the work sheet that one uses to make these computations.

II. RESULTS FOR WESTERN KANSAS DROUGHTS

The monthly index computations were carried out for western Kansas for the 71-yr. base period, 1887-1957, and later for the years 1958-1962. The values of X are listed in table 13. Let us examine the index values for some of the individual months to see what one might conclude as to their reasonableness or representativeness.

As has been pointed out previously, there is hardly any satisfactory means for checking the validity of index values which indicate "mild" or "moderate" drought. However, "extreme" drought produces conditions which can be recognized and more or less agreed upon.

THE DROUGHT OF 1894

It is difficult to locate any very concrete information concerning the drought of 1894 in western Kansas, but the following statements are indicative of the situation. Tannehill [43] wrote, ". . . the great drought of 1894 brought complete crop failure and disaster [to the Great Plains]. As many as 90 percent of the settlers abandoned their farms in some areas." In the Department of Agriculture *Yearbook* for 1894 [11] we find, "During the prevalence of this hot period [in late July 1894] the prospects for crops [over portions of Kansas and Nebraska], already unfavorable on account of prolonged drought, were greatly reduced. Much corn was completely dried up and cut for fodder."

From other sources [13] it is apparent that western Kansas was included in these rather general statements. At any rate 1894 has gone down in history as a year of disastrous drought and it seems reasonable to assume that the drought was "extreme" during at least the latter part of the summer. In table 13 the index indicates extreme drought (> -4.00) from July through December 1894.

THE DROUGHT OF 1913

The next serious dry period in western Kansas reached its peak of severity in August 1913.

Fortunately, the drought months during 1913 did not follow directly on the heels of the very dry period of 1910 and 1911; the intervening year of 1912 was abnormally wet. Even so, 1913 produced some memorable comments in the *Monthly Weather Review* of August 1913 [17]. For example, "The month [of August] will long be remembered as one of the most disastrous from an agricultural standpoint ever experienced." Also, "The drought of the summer of 1913 was one of the most damaging droughts that Kansas has experienced since authentic weather records were begun in the State." And, ". . . with the possible exception of the summer of 1874, the summer of 1913 stands alone as the driest the State [as a whole] has experienced since the early fifties. . . ." The index shows moderate drought in July and extreme drought in August.

THE DROUGHT OF THE 1930's

Agricultural Aspects.—The drought during the 1930's was the longest and most serious of record in western Kansas. Between August 1932 and October 1940 the index indicates 38 months of extreme drought. There is a great deal of information about this drought period and its effects. Many books and innumerable articles have been written. One useful source of information of an agricultural nature is the *Weekly Weather and Crop Bulletin* [65]. From the Kansas reports representative remarks pertinent to the western third of the State are listed below.

- July 25, 1933----- Corn needing rain badly and some greatly damaged.
- Aug. 1, 1933----- Pastures poor or dried up, cattle being shipped out in some localities. Stock water scarce in many places.
- June 26, 1934----- Needing rain badly in all parts.
- July 3, 1934----- Hot and dry. All crops need rain badly. Corn condition critical, crop badly stunted. Pastures insufficient to support livestock in much of west.
- July 17, 1934----- Corn stunted and burned until

TABLE 13.—Drought (and wet spell) index, X, western Kansas

	Jan.	Feb.	Mar.	Apr.	May	June	July	Aug.	Sept.	Oct.	Nov.	Dec.
1887	-0.18	-0.20	-0.81	-0.84	-0.34	-0.83	-1.19	0.82	-0.05	-0.12	-0.31	-0.38
1888	-0.54	-1.02	.27	1.28	1.55	1.15	1.17	1.79	-.70	-.40	-.55	-.84
1889	.62	.47	.65	.77	.95	1.10	1.11	-.02	-.70	-.69	-.74	-.60
1890	-.45	-.59	-1.12	.81	-.95	-1.79	-2.83	-3.08	-3.22	-3.20	-2.90	-3.16
1891	.62	.31	1.35	1.07	1.60	2.75	4.21	3.78	4.74	4.43	3.68	3.87
1892	3.44	3.56	4.01	3.27	4.55	3.99	3.91	4.13	-.70	-.98	-1.13	-.93
1893	-1.10	-1.25	-1.56	-2.32	-2.88	-3.49	-3.31	-3.09	-2.80	-3.06	-2.96	-3.12
1894	-2.99	-2.34	-2.51	-2.93	-3.63	-3.76	-4.26	-4.97	-4.49	-4.68	-4.70	-4.08
1895	-3.60	-2.71	-2.75	-2.98	-2.90	.78	2.34	2.15	-.70	-.79	-.64	-.62
1896	-.17	-.64	-.79	-.03	-.64	-.51	-.54	-.73	-.54	-.09	-.19	-.48
1897	.03	.27	.39	1.39	.83	.62	.77	1.41	1.00	2.13	-.25	.02
1898	.28	-.32	-.61	-.91	1.32	1.65	1.90	1.27	2.37	2.10	1.89	2.20
1899	0	-.06	-.06	-.53	-1.28	.12	1.32	-.92	-1.12	-1.39	.63	-.65
1900	.32	.59	.38	1.84	-.36	-.10	-.15	-.94	.93	-.58	-.94	-1.16
1901	-1.19	.03	.28	.84	-.53	-1.29	-2.23	-1.88	-.91	-1.07	-1.47	-1.49
1902	-1.29	-1.29	-.98	-1.62	.31	.46	.52	.46	.89	1.27	-.39	-.35
1903	-.51	1.58	1.74	2.43	2.43	2.58	2.81	3.02	-.62	-.72	-.70	-.95
1904	-1.17	-1.56	-2.11	-2.06	.05	.49	.67	.83	1.11	1.12	-.53	-.17
1905	.47	.46	.32	1.42	1.96	1.87	3.06	2.37	2.18	1.86	2.52	1.96
1906	1.71	1.30	1.59	2.05	1.47	1.55	2.48	2.51	2.92	3.63	3.50	-.11
1907	-.07	-.35	-.87	-1.27	-1.56	.16	.42	.51	-.18	-.23	-.51	-.55
1908	.21	.45	-.63	-1.49	-1.94	.64	.69	.62	-.66	.25	1.14	-.28
1909	-.34	-.52	-.07	-.68	-.89	1.05	1.27	-.87	-.22	.33	1.98	2.23
1910	2.20	1.98	-.88	-1.46	-1.44	-2.05	-2.58	-1.93	-2.19	-2.71	-2.95	-3.02
1911	-3.05	-1.79	-2.26	-2.46	-2.78	-4.03	-3.71	-3.28	-3.66	-3.24	-2.95	-.73
1912	.45	1.47	2.11	2.08	1.37	2.09	2.32	3.60	3.64	-.35	-.43	-.71
1913	-.75	-.44	-.68	-.79	-1.72	-1.90	-2.87	-4.12	1.12	-.54	.70	2.62
1914	-.20	-.16	-.54	-.51	.53	.56	.66	.81	-.69	-.57	-1.13	-1.06
1915	.09	.63	.95	1.66	3.11	4.06	5.69	7.53	7.87	7.49	6.51	5.86
1916	5.66	-.17	-.57	-.24	-.81	-.35	-1.18	-1.22	-1.68	-1.70	-1.92	-1.84
1917	-1.81	-2.05	-2.18	-2.01	-1.87	-2.58	-3.16	-2.66	-2.13	-2.37	-2.49	-2.50
1918	-2.20	-1.96	-1.53	-1.32	-1.24	-2.34	-2.17	-2.58	.48	.92	.71	2.58
1919	2.16	2.81	2.86	3.38	3.06	3.11	3.22	2.17	2.95	2.84	3.09	2.58
1920	2.13	1.59	.99	1.14	1.06	.85	.58	.95	1.46	2.14	1.96	1.83
1921	1.98	-.17	-.67	-.51	-1.05	.17	.33	-.44	-.37	-1.00	-1.41	-1.25
1922	-1.30	.01	.64	1.35	1.44	-.19	-.06	-.50	-1.25	-1.88	-1.59	-1.83
1923	-2.09	-2.30	-2.31	-2.20	1.77	2.69	3.37	3.78	4.54	6.14	5.52	5.26
1924	4.75	4.63	5.68	-.06	-.21	-.73	-.70	-.72	-.47	-.57	-.96	-.32
1925	-.50	-.78	-1.24	-1.57	-2.11	-3.00	-3.12	-2.23	-1.38	-1.24	-.87	-1.06
1926	-1.13	-1.44	-1.12	-1.31	-1.86	-2.34	-2.56	-2.86	-2.72	-3.22	-2.77	-2.43
1927	-2.40	-2.16	-1.54	-1.21	-2.17	.59	.81	1.64	.01	-.67	-1.08	-1.24
1928	-1.50	.45	.64	.30	1.40	2.92	3.94	4.39	3.78	4.40	4.71	4.25
1929	3.84	3.59	2.97	2.52	2.58	2.25	2.18	1.62	2.05	2.16	2.78	-.26
1930	-.26	-.76	-1.09	-1.32	-.98	-1.24	-1.46	-1.53	.01	2.63	3.18	2.94
1931	2.54	2.68	3.53	3.37	-.02	-.38	-.81	-.70	-1.64	-1.80	.30	-.05
1932	.63	.34	.41	.44	-.85	1.05	-.53	-1.22	-1.33	-1.52	-1.80	-1.84
1933	-2.07	-2.23	-2.55	-2.45	-2.14	-3.46	-4.07	-2.45	-2.69	-2.94	-2.59	-2.15
1934	-2.24	-1.56	-1.68	-2.56	-3.74	-4.20	-5.47	-5.96	-5.31	-5.33	-4.96	-4.80
1935	4.56	4.60	4.89	5.46	4.07	3.64	4.65	5.11	4.26	4.23	3.52	3.45
1936	-3.12	-3.17	-3.50	-3.98	-2.99	-3.81	-4.90	-5.55	-4.79	-4.44	-4.50	-4.12
1937	-3.71	-3.54	-3.17	-3.71	-4.48	-4.31	-4.90	-5.47	-5.34	-4.87	-4.76	-4.46
1938	4.92	4.11	3.90	3.49	-2.43	-2.48	-2.67	-3.65	-2.99	-3.52	-3.50	-3.53
1939	-3.19	-2.58	-1.94	-2.22	-2.96	-3.16	-3.98	-4.48	-5.26	-5.55	-5.44	-4.80
1940	-4.11	-3.83	-3.29	-3.37	-2.77	-3.12	-3.87	-3.13	-2.89	-3.31	.63	.61
1941	1.13	1.24	1.16	1.59	2.10	3.49	4.73	5.13	5.74	6.12	5.46	5.10
1942	4.55	4.29	4.08	5.24	4.19	4.71	4.32	4.33	4.07	4.61	3.90	3.89
1943	-.14	-.55	-.71	-.89	-1.23	-1.41	-1.96	-2.14	-2.62	-2.73	-2.86	-.20
1944	1.32	1.42	1.85	4.18	4.87	4.21	5.42	5.02	4.03	3.59	3.49	3.44
1945	3.77	3.36	2.46	2.90	2.33	2.51	2.31	2.12	2.01	-.42	-.91	-.87
1946	-.93	-.98	-.67	-1.81	-1.44	-1.72	-2.33	-2.62	.69	3.43	4.94	4.33
1947	4.30	4.03	4.23	4.31	5.02	5.17	5.05	4.09	2.74	1.82	1.95	2.28
1948	2.10	2.47	3.18	1.92	1.62	2.38	2.60	3.27	2.39	1.61	1.18	.91
1949	1.34	1.42	2.00	1.91	2.86	4.40	5.17	6.11	5.39	5.28	-.55	-.75
1950	-.88	-.91	-1.09	-1.52	-1.82	-2.55	1.78	3.80	3.48	2.84	2.20	1.56
1951	1.67	1.57	1.36	1.25	2.40	4.77	5.82	6.27	6.74	6.02	5.41	4.65
1952	4.02	3.40	3.47	3.67	-.22	-1.58	-2.22	-2.02	-2.65	-3.08	-2.62	-2.34
1953	-2.48	-2.64	-2.50	-2.28	-2.45	-3.52	-3.47	-3.14	-3.78	-3.37	-2.14	-1.39
1954	-1.32	-1.69	-1.73	-2.54	-1.91	-2.69	-3.42	-3.45	-3.96	-3.44	-3.70	-3.55
1955	-3.16	-2.95	-3.08	-3.15	-2.57	-2.38	-3.50	-4.21	-3.42	-3.84	-3.79	-3.63
1956	-3.15	-2.98	-3.16	-3.55	-4.40	-5.43	-5.31	-5.65	-6.20	-6.14	-5.78	-5.70
1957	-5.26	-5.22	1.31	1.53	2.67	3.87	4.07	3.64	3.91	3.74	3.45	2.65
1958	2.52	2.41	3.74	3.52	3.68	3.61	5.28	5.71	5.18	4.09	3.88	3.44
1959	3.40	2.99	3.10	2.34	1.91	1.04	.98	.76	1.35	2.64	2.15	1.91
1960	2.66	3.74	3.80	3.43	3.12	3.51	3.04	2.11	1.88	1.99	1.86	1.89
1961	1.39	.88	1.02	.67	1.16	1.56	1.78	2.27	1.61	1.38	2.06	1.95
1962	1.92	1.52	1.91	1.30	.79	2.03	3.12	2.83	2.98	-.35	-.41	-.54

- almost ruined. Pastures too poor to support livestock.
- Aug. 7, 1934..... Conditions worst ever known in many places. Corn not sufficient growth even for fodder in many western counties.
- Aug. 14, 1934..... Pastures generally bare. Distressed animals being shipped out in increasing numbers.
- Sept. 4, 1934..... Russian thistles being put up as fodder.
- Oct. 9, 1934..... Winter wheat sowing delayed by dryness and crop making little growth.
- Nov. 27, 1934..... Wheat fields bare in nearly all of western third.
- Feb. 27, 1935..... Severe duststorms.
- Apr. 16, 1935..... Severe duststorms; practically no pastures in western half.

- May 7, 1935----- Duststorms [continue] frequent in western half; wheat crop very poor to poor in western half and deteriorating.
- May 28, 1935----- Rain. Pastures greening.
- July 2, 1935----- Moderate rains in northwest, southwestern counties are needing moisture.
- July 30, 1935----- Dry. Much [of corn crop] damaged beyond recovery. Pastures deteriorating rapidly in west.
- Aug. 27, 1935----- Corn in southwest counties not worth cutting. Grain sorghums badly stunted. Pastures deteriorating.
- Oct. 29, 1935----- Wheat very poor to poor in extreme west.
- Nov. 19, 1935----- Forage scarce in most of western half where wheat pastures poor.
- Mar. 17, 1936----- Duststorms again reported.
- Apr. 21, 1936----- Many [wheat] fields bare.
- May 26, 1936----- Pastures much improved.
- June 23, 1936----- Wheat badly damaged.
- July 28, 1936----- Little [corn] in the western half will be fit for forage.
- Sept. 1, 1936----- Pastures brown and scanty.
- Nov. 24, 1936----- Wheat needs moisture rather badly; some soil blowing. Pastures scanty.
- Dec. 1, 1936----- Wheat deteriorating. Moderate duststorms.
- Mar. 2, 1937----- Considerable damage from previous duststorms. Substantial moisture badly needed.
- Apr. 27, 1937----- Duststorms frequent.
- May 25, 1937----- Wheat deteriorated in most of west and greatly damaged in southwest.
- June 22, 1937----- Pastures weedy in west [from previous rains].
- July 20, 1937----- Corn stunted and not tasseling.
- Aug. 31, 1937----- Soil moisture very deficient. Pastures dried badly.
- Sept. 28, 1937----- Duststorms in southwest.
- Nov. 16, 1937----- Duststorms. Wheat deteriorating.
- Dec. 7, 1937----- Wheat deteriorating in southwest.
- Apr. 26, 1938----- Duststorms.
- June 28, 1938----- Corn making satisfactory growth. Pastures improving.
- Aug. 30, 1938----- Soil very dry; corn badly burned.
- Sept. 20, 1938----- Soil moisture sufficient for early growth [of wheat].
- Nov. 15, 1938----- Many wheat fields bare, some showing drill rows and, in favored localities, covers ground; root system there poor.
- Dec. 6, 1938----- Wheat deteriorated.
- Jan. 10, 1939----- Heavy duststorms.
- Feb. 21, 1939----- [More] duststorms.
- Mar. 14, 1939----- Sufficient topsoil moisture for present needs and outlook is improved.
- Apr. 11, 1939----- Soil moisture now ample except in some western counties. Winter wheat improved; rank growth in southwest.
- May 2, 1939----- Winter wheat deteriorated.
- May 23, 1939----- Lack of rain being felt in west, especially in southwest where condition serious. Wheat deteriorated.
- Aug. 1, 1939----- Corn deteriorated; bulk in west damaged beyond recovery.
- Sept. 5, 1939----- Record-breaking heat, soil moisture badly depleted. Condition of all crops declined. Wheat seeding halted account dry soil.
- Oct. 17, 1939----- Severe duststorms. Pastures very poor.
- Oct. 31, 1939----- [Still] waiting for rain [before seeding winter wheat]. Sowing so far has been done in dust.
- Nov. 28, 1939----- Much [wheat] not germinated, seeding still underway.
- Dec. 19, 1939----- Winter wheat condition generally lowest on record. Duststorms.
- Mar. 5, 1940----- Moisture ample for current needs.
- Apr. 30, 1940----- Moisture deficient in western third, especially in southwest where duststorms [occurred]. Wheat fair in west.
- May 28, 1940----- Wheat crop poor and weedy. Pastures growing well.
- July 2, 1940----- Hot winds shriveled [wheat].
- July 30, 1940----- Severe damage to corn; half to three-fourths tassels burned white. Grain sorghums deteriorating. Pastures not sufficient to support livestock.
- Aug. 13, 1940----- Rain adequate for current needs. More than half of corn [Statewide] past help. Pastures poor, but will revive.
- Aug. 27, 1940----- Soil mostly too dry [for wheat seeding]. Pastures poor.
- Oct. 1, 1940----- Topsoil moisture sufficient to abundant. Bulk of wheat up to excellent stands.
- Oct. 29, 1940----- Moisture badly needed. Wheat growth slowed. Pastures dry.
- Dec. 3, 1940----- Soil moisture penetrated to 1 to 2 feet or more. Wheat good to excellent condition with sufficient moisture to carry it through the winter.
- Dec. 24, 1940----- [Wheat] prospects better than for a considerable number of years.

When one compares these remarks with the index values for the corresponding months in table 13, it becomes apparent that the index numbers are fairly representative of the severity of the agricultural drought. Consider, for instance, the fall of 1939. Many accounts of this great drought of the 1930's fail to point out that this was the worst fall season that occurred. The index indicates extreme drought, and the published remarks during October, November, and December substantiate it: pastures were very

poor; it was too dry to plant wheat; and dust storms raged nearly every week.

Vegetative Cover Measurements.—Weaver and Albertson [70] have presented so many observations and interesting details of the effects of drought on the plant communities of the Great Plains that it is difficult to select an illustrative example. However, the basal cover measurements which they made annually (apparently in the fall) for over two decades in an ungrazed area near Hays, Kans. are indicative of the seriousness of the drought that prevailed in the 1930's and again in the 1950's. (Hays lies just to the east of the western Kansas area studied here.)

The most interesting feature of the figures in table 14 is the fact that they show that the drought in the 1930's was essentially continuous until revival of the vegetation began in 1941. The data (not shown) from the moderately grazed and overgrazed plots at Hays show a much more rapid deterioration of basal cover during the initial drought years. The overgrazed plot was reduced from 80 percent cover in 1932 to 30 percent cover in 1934. The minimum of 3 percent was reached in 1936. Some slight increase in cover took place in 1937, 1938, and 1939, but by 1940 the cover was only 14 percent. Incidentally, recovery in 1941 was slightly more rapid than on the ungrazed area.

The Duststorms.—Other aspects of the drought picture in western Kansas during the early 1930's have been pieced together by Johnson [23]. He paints a fairly vivid picture of the trials and tribulations of those people who were struggling to eke out a living from the land during those dry years. From Johnson as well as from the numerous publications of Albertson and co-workers at Kansas State College, Fort Hays, it is very clear that much of the notoriety associated with the years of 1934-1936 is a direct result of

the unusually strong winds which created the terrible duststorms during those years. The wind combined with the drought to produce the disastrous conditions *and* the publicity. Other years have been about as dry and nearly as warm, but they lacked the strong winds, and the droughts were therefore less spectacular as well as less damaging.

Disaster Declaration.—On June 19, 1934 Congress passed an emergency appropriation bill providing funds for the purchase of drought-stricken livestock. This program got underway at approximately the same time that the index indicates the existence of an extreme drought condition. Apparently at that time there was recognition that an extreme and disastrous condition had developed. On this basis one could postulate that extreme drought may well have coincided with the conditions which led to an official designation of "drought disaster area."

THE 1950's DROUGHT

The drought which began in Kansas in 1952 was a very serious matter by the summer of 1953. At the end of June the drought index indicates a severe drought. On the last day of June the Disaster Designation Committee of the U.S. Department of Agriculture, on the basis of first-hand reports from the drought area, declared all 31 counties of western Kansas a disaster area. Although the index does not show extreme drought it is interesting to note that the index value is very close to the value it had when drought disaster was recognized in 1934.

By the end of September 1953 the drought situation was even more critical. The index is -3.78 and the agricultural reports [66] indicate a serious shortage of feed with farmers faced with the choice of selling part of their breeding herds or buying high-priced feed. Table 14 shows the astonishing decrease in measured basal cover that had occurred during 1953. Also the streamflow records (table 15) indicate that only 1956 and 1939 produced less runoff during September than did 1953.

In September of 1954 the moisture shortage was apparently more pronounced; but, the published Crop Bulletins for that period are unfortunately rather vague. The comments are so general that it is difficult to tell very much about the specific situation in the western part of

TABLE 14.—Total basal cover of short grasses in an ungrazed prairie near Hays, Kansas (after Weaver and Albertson [70])

Year	Percent cover						
1932.....	89	1938.....	30	1944.....	95	1950.....	91
1933.....	86	1939.....	22	1945.....	93	1951.....	90
1934.....	85	1940.....	20	1946.....	89	1952.....	93
1935.....	65	1941.....	56	1947.....	88	1953.....	38
1936.....	58	1942.....	94	1948.....	93	1954.....	20
1937.....	26	1943.....	90	1949.....	92		

Kansas. From reading all the reports one is aware that the area was very dry with delayed wheat seeding, feed shortages, and poor prospects in general.

The streamflow data for September 1954 show very slightly more runoff than during September 1953, but apparently this was the result of fairly heavy rains between the eastern border of the area and the gaging station at Beloit. The basal cover data in table 14 give a specific bit of information which reinforces the idea that very serious drought conditions existed in September 1954.

In 1955 the spring rains again produced some temporary alleviation of the drought, but during July the situation became critical and the *Kansas Weekly Weather and Crop Reports* [63] of August 2 indicate that the crop, pasture, and hay prospects were fading rapidly, with supplemental livestock feeding on the increase. By the end of August (report of Aug. 30) it was apparent that many grain sorghum fields would not head, corn would not produce grain, and the pastures were supplying practically no feed at all. Further evidence of the extreme drought during August is the fact that the runoff for the month established a record low for August (see table 15).

The moisture situation was dismal all during 1956. The spring was dry and the summer and fall were drier. The total runoff for the year, computed by the method described in the next section, was the lowest of record. The following remarks [67] illustrate the extreme seriousness of the drought in western Kansas.

- May 28, 1956..... Pastures furnishing little or no grazing.
- July 2, 1956..... Dry soil delayed planting [of grain sorghums] and stands poor. Rain urgently needed. Supplemental feeding of livestock still necessary. Drought intensified.
- July 30, 1956..... Grain sorghums at a standstill; plants firing. Corn tassels turned white and stalks firing.
- Aug. 27, 1956..... Droughty conditions steadily increasing. Crops continue to deteriorate. Many sorghum fields beyond help. No available soil moisture to 4 ft. at Garden City.
- Sept. 10, 1956..... Supplemental feeding general and liquidation of herds increasing.
- Sept. 17, 1956..... Drought situation aggravated by 100° weather. A few plantings [of wheat] emerged to uneven

stands, but plants beginning to die. Herds being liquidated.

- Sept. 24, 1956..... Seeding being delayed. Much damage to seedbeds [by severe dust-storms]. Wheat plants dying. Kansas River last three days lowest stage of record.
- Oct. 8, 1956..... All major streams at near-record low flows.
- Oct. 22, 1956..... Fields [for wheat] powder dry and seeding awaiting rains.
- Oct. 29, 1956..... Strong winds and dust severely damaged newly emerged [wheat] seedlings. Winter roughage supplies critically low.
- Nov. 12, 1956..... [Wheat] seeding continues in southwest and west central where soil powder dry.

When one compares the above remarks with the appropriate index values in table 13, it becomes apparent that the index values are relatively representative of the general agricultural situation. An index value of -4.00 seems to correspond reasonably well with "extreme" drought.

DROUGHT AND STREAMFLOW

Records of rates of streamflow can also be examined to determine whether or not such data show a useful relationship to drought severity. However, the available data pertinent to the western third of Kansas are far from satisfactory inasmuch as the stream-gaging stations are so located that the measured flow is not by any means dependent on only this area.

Four drainage basins are represented in the western third of Kansas [42]. An area in the northwestern corner, the equivalent of four or five counties, lies in the Upper Republican River basin and the drainage is toward the northeast. There are no long-record gaging stations which could be used to represent the runoff from this relatively small area. A similar situation exists in the southwestern part of the State where the Cimarron River carries the runoff from seven or eight counties. Here too no records are available for the period of concern in this study.

At Garden City, Kans., there is a long record of runoff on the Arkansas River [54]. This record is not particularly well suited for the purposes of this study because it represents too large an area, but it appears to be about the only one that can be used for this portion of the State.

With the exception of the previously mentioned counties in the northwest, the northern half of the western third of Kansas is drained by the Smoky Hill, the Saline, and the Solomon Rivers. Good runoff records exist for all three rivers [55]. The long-record stations are all a little too far east of our area, but the data may be at least partially indicative of the runoff from the area of concern.

The stations used were at Ellsworth, on the Smoky Hill River, Tescott on the Saline River, and Beloit on the Solomon River. The records of monthly runoff in thousands of acre feet were tabulated for these three stations and for Garden City for the period May 1929–August 1950 and the period October 1952–September 1957. No effort was expended in weighting or adjusting these records because even at best one could hardly expect to get more than a rough indication of the runoff from the study area. Therefore the runoff from the four stations was merely added to obtain a single value for each month. From these records table 15 was prepared. The three lowest index values for each month from table 13 have also been entered on table 15 for convenience.

From this table a number of things are apparent. First, the record low runoff for the 1–5-month period ending with April occurred in 1935. One can see also that the most serious April drought, as indicated by the index, also occurred in 1935.

The lowest 1-month and 2-month runoff values for the other months appear to coincide reasonably well with the lowest index values. For instance,

the least April and May runoff (11,600 acre feet) occurred in 1937. The index, -4.48 , also indicates the most serious May drought occurred that same year. Also, the least May and June runoff occurred in 1933 with 1956 not far behind (see footnote, table 15). The driest June according to the index was 1956 which was also the year with the least 3-month total runoff.

The remaining months in the table show much the same sort of thing. Considering the crude method of handling the only partially representative runoff information, the correspondence between years of very low index numbers and years of very small runoff is rather encouraging, but not unexpected. Both are a consequence of about the same climatic elements.

The reader will no doubt have noticed that the largest negative index value occurred in 1956 rather than in 1934 or 1936 as might have been expected. The runoff data for the periods ending with September seem to confirm that this dryness in 1956 was at least as extreme as that during the drought in 1934. As previously mentioned, some effects were worse in 1934 than in 1956 because of the wind and dust in 1934.

PASTURE FEED CONDITIONS

At the beginning of each month during the period April 1 to November 1 the United States Department of Agriculture receives numerous reports on pasture feed conditions in each State.

TABLE 15.—Drought index values and the least amount of runoff (thousands of acre-feet) during periods of various lengths ending with the month and year shown, western Kansas

	Length of period (months)										Year and amount of the 3 lowest index values for the month		
	1		2		3		4		5				
	Yr.	Amt.	Yr.	Amt.	Yr.	Amt.	Yr.	Amt.	Yr.	Amt.			
April.....	1935	2.9	1935	5.2	1935	8.0	1935	10.2	1935	12.5	-5.46	-3.98	-3.71
May.....	1937	6.9	1937	11.6	1937	22.8	1934	38.9	1956	45.8	-4.48	-4.40	-4.07
June.....	1933	5.3	1933	43.1	1956	56.4	1940	65.3	1940	68.2	-5.43	-4.31	-4.20
July.....	1934	9.8	1933	25.6	1933	63.4	1933	88.4	1933	95.6	-5.47	-5.31	-4.90
August.....	1955	5.0	1934	15.5	1940	88.9	1956	122.6	1956	128.7	-5.96	-5.65	-5.55
September.....	1956	1.0	1956	18.4	1934	45.3	1956	110.5	1956	123.6	-6.20	-5.34	-5.31
October.....	1939	1.5	1956	2.7	1956	20.1	1934	47.9	1956	112.2	-6.14	-5.55	-5.33
November.....	1939	2.1	1939	3.6	1956	5.9	1956	23.3	1934	50.4	-5.78	-5.44	-5.96
											1956	1939	1934

^a 39.1 in 1956.
^b 50.3 in 1956.
^c also 1937.

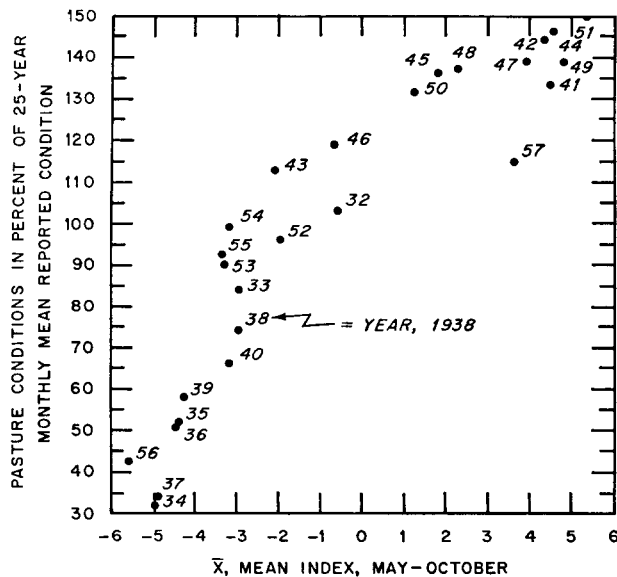


FIGURE 4.—Mean pasture condition, western Kansas June 1 to November 1, versus the average index \bar{X} for the same growing season. (Data for period 1932–57.)

These subjective reports are expressed in terms of percent of normal condition, where “normal” indicates not the average but the expected condition under very favorable weather.

These monthly data for the western third of Kansas for 1932 through 1957 were obtained from the United States Department of Agriculture Crop Reporting Board by personal communication. Each monthly value represents approximately 200 individual reports. These data apparently contain some month-to-month and season-to-season fluctuations and trends which are in part dependent on the outlook and state of mind of the observers. It is suspected that

the reports tend to show an exaggerated response to month-to-month weather changes. For example, from other accounts, such as table 14, there is evidence that pastures became gradually poorer and poorer during the drought in the 1930's. However, these condition reports show a very abrupt drop to a minimum of 11 percent of normal during 1934 followed by an improvement to 30 to 50 percent of normal during 1939.

In addition there are month-to-month trends in the data which indicate that a given percentage does not mean the same thing from month to month. For example, the average reported conditions for 25 years were as follows:

	Percent		Percent
Apr. 1.....	64	Aug. 1.....	62
May 1.....	64	Sept. 1.....	60
June 1.....	68	Oct. 1.....	59
July 1.....	69	Nov. 1.....	62

In order to remove this variability all the monthly values were recomputed in terms of mean reported condition. For example, a report of 34 percent of normal on June 1 becomes 50 percent of mean reported condition.

From these monthly values of mean reported condition it was possible to obtain a mean value for the period June 1 to November 1 for each year. Figure 4 shows the relation between this measure of pasture condition and the average April to October index (from table 13). The poorer condition in the 1930's as compared to the 1950's may be related to the amount of wind. The relatively poor condition in 1957 is the result of the poor condition (55 percent) that existed in the spring of this wet year. All in all, the index appears to be relatively representative of pasture conditions in western Kansas. No effort was made to investigate similar relationships in other areas.

12. DROUGHT CONDITIONS IN CENTRAL IOWA

The monthly index values for central Iowa for the period 1930–1962⁹ are shown in table 16. Only in 1931, 1934, 1936, 1956, and early 1957 does the index indicate really serious drought. Crops were rather poor in 1931, especially in the northern part of the area and average corn yield for the entire area was only 38.9 bushels per acre.

⁹ 1930 and the years since 1957 were analyzed using the coefficients from the base period, 1931–57.

THE DROUGHT OF 1934

The severity of the drought in 1934 is evidenced by the following remarks [61] concerning the agricultural situation in central Iowa.

May 15, 1934..... Intense duststorms; meadows poor; hay and oats practically ruined; farm crop outlook poorest in memory; water scarce on great many farms.

TABLE 16.—Drought (and wet spell) index, X, central Iowa

	Jan.	Feb.	Mar.	Apr.	May	June	July	Aug.	Sept.	Oct.	Nov.	Dec.
1930	0.13	-0.21	-0.69	-0.55	-0.56	-0.47	-1.29	-1.98	-2.48	-2.31	-2.62	-3.02
1931	-3.26	-3.81	-3.94	-3.97	-4.12	-4.45	-4.14	-4.09	1.13	1.14	2.99	3.85
1932	4.10	3.67	3.13	2.40	2.21	2.04	1.85	2.89	-2.76	2.48	2.76	2.87
1933	2.63	2.11	2.53	-4.4	.54	-1.53	-1.64	-2.16	-2.25	-2.08	-2.81	-3.05
1934	-2.95	-3.19	-3.48	-4.09	-5.11	-5.98	-5.77	-5.86	.56	-.56	2.82	3.34
1935	.49	.76	.35	-.63	.30	1.65	1.97	1.28	1.37	1.98	2.44	2.55
1936	2.73	2.71	-.34	-.60	-1.12	-1.33	-2.88	-3.34	1.33	1.16	.70	.90
1937	1.34	1.41	1.33	1.68	1.74	-.33	-.71	-.71	-1.39	-1.30	-1.70	-1.95
1938	-1.95	-2.15	-2.15	.70	1.47	1.25	1.64	1.21	1.74	.93	1.26	1.11
1939	1.01	1.67	-.18	-.41	-1.29	-.92	-1.04	-.60	-1.43	-1.58	-2.20	-2.52
1940	-2.69	-2.45	-2.49	-1.91	-2.09	-2.61	-.68	1.74	.94	.73	1.10	1.27
1941	1.68	-.11	-.47	-.93	-1.65	-.92	-1.19	-1.49	1.51	3.07	3.16	3.69
1942	3.43	3.31	2.98	1.95	2.06	2.24	2.98	3.07	3.32	3.20	3.13	3.16
1943	2.83	2.64	2.41	2.57	2.67	2.65	3.56	3.77	3.76	3.36	3.11	2.88
1944	2.88	2.75	2.92	3.59	4.76	4.52	4.82	5.32	4.75	3.85	3.32	3.27
1945	2.81	3.05	3.15	3.72	4.46	3.97	3.39	3.26	3.28	2.27	1.76	2.07
1946	2.58	2.04	2.57	1.55	1.72	2.35	2.28	1.98	2.49	3.10	2.95	2.56
1947	2.69	2.25	1.99	2.99	3.21	5.35	-.81	-1.78	-2.65	.76	-.08	-.02
1948	-.57	.59	1.02	-.11	-.68	-1.21	-.77	-1.15	-1.87	-1.88	.22	.45
1949	1.27	1.30	1.41	-.47	-1.20	-1.24	-1.53	-2.13	-1.88	-1.75	-2.41	-2.66
1950	-2.50	-1.97	-2.26	.12	.85	1.18	-.11	-.40	-.89	-1.35	-1.88	-2.26
1951	-2.58	.49	1.57	2.57	2.49	2.67	3.10	3.68	3.45	3.75	3.71	3.51
1952	3.41	3.00	3.75	3.02	2.78	2.60	2.69	2.76	-.72	-1.35	.25	.21
1953	.09	.49	.88	1.34	-.88	-.38	-.41	-1.14	-2.05	-2.95	-3.33	-3.47
1954	-3.91	-3.75	-3.59	.30	.59	1.05	.09	2.12	2.07	2.95	-.32	-.32
1955	-.31	.30	-.32	-.26	-.52	-1.28	-1.07	-1.76	-1.77	-2.14	-2.79	-3.25
1956	-3.61	-4.02	-4.49	-4.57	-4.73	-5.41	-5.14	-4.92	-5.01	-4.95	-4.92	-5.15
1957	-5.23	-5.48	-5.46	-5.30	-4.39	-3.91	-3.45	-2.97	-2.94	-2.28	-1.66	-1.45
1958	-1.41	-1.48	-1.83	-1.87	-2.33	.26	2.90	2.51	2.63	1.83	1.60	1.05
1959	.77	.88	1.76	1.88	2.54	1.82	1.40	1.03	1.07	1.15	1.42	1.48
1960	2.31	2.30	2.08	2.21	2.92	2.19	1.91	2.45	2.50	2.28	1.64	1.17
1961	.60	1.23	2.21	2.17	1.35	.78	2.14	1.82	3.45	3.69	3.94	4.00
1962	3.34	3.60	3.22	2.76	2.72	1.84	2.77	-.15	-.39	-.11	-.69	-1.15

- June 5, 1934..... Pastures parched to tinder, feed situation acute; some corn dying; livestock being sold for lack of pasture; one-half or more of the farmers [in Polk Co.] having to haul water.
- June 19, 1934..... Pastures brown; corn fair; oats short and light.
- July 3, 1934..... Corn rolled; small grain withered; more wells failing [in Hamilton Co.] and water being bought and hauled from long distances; pastures burned up; barley hardly tall enough to cut and very thin; wheat yield 5 to 20 bushels.
- July 17, 1934..... Rain; pastures greening; corn now growing; oats and barley very poor.
- July 31, 1934..... Oats yield 3 to 15 bushels per acre with quality very poor to fair; corn suffering; hauling water still in vogue [in Hamilton Co.]; cattle picking up since pastures improved; water situation [in Polk Co.] becoming more critical every day.
- Aug. 14, 1934..... Corn badly hurt, some being cut for fodder; tomatoes and cucumbers not setting; potatoes not doing anything; forage not growing well; pastures very short and furnish practically no feed; practically every farmer [in Polk Co.] hauling water.
- Aug. 28, 1934..... Corn will yield 10 to 40 bushels, only fair quality; ground too hard and dry for fall plowing; much of the corn crop going into silage or fodder.

When one compares the remarks above with those which applied to western Kansas, it may appear that 1934 did not produce extreme drought in central Iowa. However, the weather was *extreme for Iowa*; at no other period during the years studied was the moisture shortage in that area so disastrous. The drought index seems to be measuring this drought situation rather accurately.

Hydrologic Data.—It was not possible to locate any stream-gaging station or combination of stations that would reasonably represent the runoff from this relatively small area. The Des Moines River and the Iowa River both pass through the area but the gaging-station records probably reflect conditions outside the area at least as much as inside it. The Skunk River originates in and drains the central portion of the area, but the only long-record station is at Augusta about 75 or 80 miles to the southeast of the area of concern.

THE DROUGHT OF 1936

Fortunately, only July and August were extremely hot and dry, but they produced a very serious agricultural situation. By the third week in July there were reports [65] of moderate drought damage to corn. By late July it was estimated that the corn crop had been reduced by one-fourth and there were no good pastures. Rains in early September came too late for much of the corn, but produced a good supply of fodder and helped

pastures. Corn yields turned out to be better than expected. The index reached its largest value, -3.34, in August.

THE DROUGHT OF 1947

In September of 1947 there were complaints [62] of pastures dry and short, corn and soybean crops being injured by drought, and soil too dry for fall plowing and seeding. But the situation did not approach the seriousness of the extreme drought of 1934. The index, -2.65, at the close of September also indicates a much less serious drought than in 1934.

THE DROUGHT DURING THE 1950's

During most of the first half of the summer of 1953 growing conditions were ideal [62]. (Note that the index indicates this as a period of mostly near-normal weather.) The moisture shortage began to develop about the middle of the growing season, and ". . . by the end of the season it was quite dry over the entire State, with some areas in critical condition." In October "Reports of dry wells are common over the State." "The fire hazard has increased, . . . communities have banned all outdoor fires."

The really serious dryness occurred so late in the year that the agricultural reports are very meager, but from the quoted reports above one can estimate that the drought was quite serious. Apparently it lasted all winter because the first *Iowa Weekly Weather and Crop Bulletin* of the spring of 1954 (April 5) reported, "water is still being hauled for livestock."

Noteworthy dryness returned in late 1955, and 1956 brought the most serious drought since the 1930's. The following selected excerpts from the Crop Bulletins [67] are more or less indicative of the agricultural situation in central Iowa during the 1956 growing season. Most of the reports were worded in such general terms that one cannot tell what area of the State they apply to; only a few contain remarks specifically pertinent to the problem being considered here.

- May 28, 1956----- Some late corn and soybeans not germinating because of a lack of moisture. Pastures and meadows need rain.
- June 4, 1956----- Poor yields on first cutting of alfalfa; oats heading only 6 to 8 in. tall. Only 1.4 in. of available moisture in 5-ft. root zone of alta fescue at Ames.

- June 11, 1956----- Corn and soybeans look good; pastures very dry and furnishing little forage.
- June 18, 1956----- Oat crop light; pastures very dry; yields of first cutting of alfalfa generally poor; some stands of red clover did not survive the dry fall and winter; corn generally not showing drought damage yet.
- June 25, 1956----- Oats being harvested as hay or pasture.
- July 16, 1956----- Corn in excellent condition; second cutting of alfalfa short with poor yields.
- July 23, 1956----- Corn and soybeans developing unevenly; excellent prospects where rains received, but prospects declining in drier spots.
- July 30, 1956----- Hay fields damaged by lack of moisture, some too far gone to recover if rains came now. Soybeans hurting for rain. Many meadows too dry to furnish forage. Rains badly needed in most of State.
- Aug. 6, 1956----- Corn prospects deteriorated in drier spots. Many clover seedlings destroyed by drought. Only 0.9 in. of available soil moisture in top 5 ft. at Ames.
- Aug. 20, 1956----- Corn crop uneven with best prospect in years in some areas, while other areas need rain to avoid further deterioration. Fall plowing retarded by dry soil.
- Aug. 27, 1956----- Crop prospects very uneven; some areas damaged beyond help by drought. Only 1.5 in. of available soil moisture (to 5 ft.) at Ames on August 31.
- Sept. 24, 1956----- Fall plowing and wheat seeding at a standstill because of dry soil.
- Oct. 8, 1956----- No available moisture to 5 ft. under alta fescue at Ames. Wheat only 50 percent planted, latest in 10 yr.

As they stand these remarks are not very informative; however, 1956 produced the least rainfall recorded for central Iowa during any year from 1930-60. It therefore seems likely that such remarks as "in the drier areas" included central Iowa. Insofar as the soil moisture measurements at Ames are representative, they certainly indicate an unusually dry condition at every sampling date.

As further evidence of the drought in central Iowa all rivers draining the area reached or almost reached record low stages during the latter half of 1956 [60]. As measured at Augusta the Skunk River equaled its 41-yr. record low in October, November, and December. The Iowa River at

Wapello was near its 42-yr. record low stage in both October and November. At Des Moines the Des Moines River equaled its 60-yr. record low in October and very nearly equaled it in July, September, and November.

The combined evidence indicates very unusual dryness in central Iowa during 1956. The index values show extreme drought from February 1956 through May 1957. This classification seems reasonable.

13. SUMMARY OF DROUGHT PERIODS AND FREQUENCY OF DROUGHT CLASSES

Tables 17 and 18 were prepared from tables 13 and 16. These tables show the month in which each of the various drought periods became established in western Kansas and central Iowa and the last dry month in each drought period. Also, the maximum value of the drought index has been tabulated for each period, as well as the number of months of mild, moderate, severe, and extreme drought as defined in table 11. The total duration of each drought period does not in every instance agree with the sum of the number of months in each class because on occasion a month or so in the incipient class occurred in the middle

of a long drought period. July 1948 in central Iowa (see table 16) is an example of this.

WESTERN KANSAS

In western Kansas the median duration of drought is about 4 months, but the distribution is very skewed and the mean is about 12 months. A total of 339 months of drought occurred in the 76 years. This is 37 percent of the time. From table 13 one can also determine that a wet spell was underway in 37 percent of the months and that near-normal conditions existed in 12 percent of the months. It may at first seem unrealistic to have

TABLE 17.—Drought periods, western Kansas, 1887-1962

Start		End		Maximum severity	Number of months				
Year	Month	Year	Month		Mild	Moderate	Severe	Extreme	Total
1887	July	1887	July	-1.19	1				1
1888	February	1888	February	-1.02	1				1
1890	March	1890	March	-1.12	1				1
1890	June	1890	December	-3.22		2	3		6
1892	November	1895	May	-4.97	4	12	8	6	31
1899	May	1899	May	-1.28	1				1
1899	September	1899	October	-1.39	2				2
1900	December	1901	January	-1.19	2				2
1901	June	1902	April	-2.23	8	1			11
1904	January	1904	April	-2.11	2	2			4
1907	April	1907	May	-1.56	2				2
1908	April	1908	May	-1.94	2				2
1910	April	1911	November	-4.03	4	9	6	1	20
1913	May	1913	August	-4.12	2	1		1	4
1914	November	1914	December	-1.13	2				2
1916	July	1918	August	-3.16	12	13	1		26
1921	May	1921	May	-1.05	1				1
1921	October	1922	January	-1.41	4				4
1922	September	1923	April	-2.31	4	4			8
1925	March	1927	May	-3.22	12	11	3		27
1927	November	1928	January	-1.50	3				3
1930	March	1930	August	-1.53	5				6
1931	September	1931	October	-1.80	2				2
1932	August	1940	October	-5.96	8	22	30	39	99
1943	May	1943	November	-2.86	3	4			7
1946	April	1946	August	-2.62	3	2			5
1950	March	1950	June	-2.55	3	1			4
1952	June	1957	February	-6.20	6	17	23	11	57
Number of months					101	101	74	58	339
Percent of 912 months					11	11	8	6	37

Months of Beginning and Ending of Drought

	Jan.	Feb.	Mar.	Apr.	May	June	July	Aug.	Sept.	Oct.	Nov.	Dec.
First month	1		4	4	4	3	2	1	3	1	3	1
Last month	3	2	1	3	6	1	1	4	0	3	2	2

TABLE 18.—Drought periods, central Iowa, 1930-1962

Start		End		Maximum severity	Number of months				
Year	Month	Year	Month		Mild	Moderate	Severe	Extreme	Total
1930	July	1931	August	-4.45	2	3	5	4	14
1933	June	1934	August	-5.98	2	5	3	5	15
1936	May	1936	August	-3.34	2	1	1		4
1937	September	1938	March	-2.15	5	2			7
1939	May	1940	June	-2.69	5	7			14
1941	May	1941	August	-1.65	3				4
1947	August	1947	September	-2.65	1	1			2
1948	June	1948	October	-1.88	4				5
1949	May	1950	March	-2.66	6	5			11
1950	October	1951	January	-2.58	2	2			4
1952	October	1952	October	-1.35	1				1
1953	August	1954	March	-3.91	1	2	5		8
1955	June	1958	May	-5.48	10	6	4	16	36
1962	December				1				1
Number of months					45	34	18	25	126
Percent of 396 months					11	9	5	6	32

Months of Beginning and Ending of Drought

	Jan.	Feb.	Mar.	Apr.	May	June	July	Aug.	Sept.	Oct.	Nov.	Dec.
First month	0	0	0	0	4	3	1	2	1	2	0	1
Last month	1	0	3	0	1	1	0	4	1	2	0	0

three-fourths of the time devoted to either a drought or abnormally wet weather; but it is a well-known fact that normal or average weather does not occur very frequently, even on a monthly basis. This, coupled with the tendency for persistence, helps to explain the high percentage of abnormal conditions.

Table 17 also shows that western Kansas has mild drought during 11 percent of the months, moderate drought in 11 percent, severe drought in 8 percent, and extreme drought in 6 percent of the months.

At the bottom of table 17 is an auxiliary tabulation showing the number of times (out of the 28 drought periods) that each of the calendar months established a drought period. Spring and early summer account for about half of the drought beginnings, but apparently there is no really preferred time of beginning, so the information is neither startling nor particularly useful.

On the other hand it was a little surprising to find that almost one-third of the drought periods ended with April or May. This may be useful information in that it suggests that if a drought continues through May there is a good chance that June and July will also be drought months. There seems to be a slight tendency for the change to normal or wetter weather to occur during September, but the evidence is rather meager.

CENTRAL IOWA

The shorter record from central Iowa produced only the 14 drought periods shown in table 18. From this table and table 16 the following facts are evident.

Mild drought occurred 11 percent of the time, moderate drought 9 percent, severe drought 5 percent, and extreme drought 6 percent of the time. Drought was underway in 32 percent of the months, and a wet spell was underway in 50 percent of the months. In 11 percent of the months the weather was near-normal. (The remainder were "incipient.")

The average duration of drought was about 9.6 months, but the median was about 7 months. Half the droughts became established in May or June and all but three started between May and September. With the possible exceptions of March and August no month seems to have been a particularly preferred final drought month.

From these facts it is apparent that drought is almost as frequent in central Iowa as in western Kansas, but it is a little dangerous to make comparisons between the two areas because the analyses cover unequal periods of record.

MEANING OF THE DROUGHT CLASSES

On the basis of available evidence it appears

that the drought index values are reasonably comparable in their local significance both in space and time. It seems reasonable to postulate that a drought index of -4.0 spells economic disaster in any region in which the established economy is significantly dependent on the vagaries of weather for its moisture supply.

As a point of departure the following descriptions of the consequence of each of the four classes of drought are proposed. These descriptions are more or less ecological and are probably not as close to being universally applicable as is the drought index itself. However, they may be useful for certain purposes.

14. PROGNOSTIC VALUE OF THE INDEX

This index apparently measures something that might be of value in forecasting. Inasmuch as it provides a single number which is a function of many aspects of the current and recent weather, it seems likely that the index could, under certain circumstances, be useful in predicting the precipitation for the following month.

Figure 5 shows that not only does precipitation average much less during drought periods than during wet periods, but also that the two regimes show some remarkable departures from the average precipitation climate of central Iowa. For example, the fact that February produces near normal precipitation, on the average, during wet periods warrants some investigation. Can one use the previous index value as an indicator that February precipitation is not likely to exceed the normal by any substantial amount?

Monthly precipitation forecasts are ordinarily issued in terms of "light," "near-normal" or "heavy." These classes are defined in such a way that each contains 1/3 of the total number of occurrences. For central Iowa the February limit for "light" for this 33-yr. period is about 0.58 in. and "heavy" includes all amounts in excess of about 1.25 in.

There were 13 years during this period when the index was $>+1.50$ at the end of January. These 13 cases were followed by 5 Februaries which had "light" precipitation, 6 with "near-normal" precipitation, and 2 with "heavy" precipitation. This suggests only a 15 percent probability of heavy February precipitation when the index is greater than $+1.50$ at the end of January.

Mild drought: Some of the native vegetation almost ceases to grow.

Moderate drought: The least drought-resistant members of the native plant community begin to die and the more xerophytic varieties start to take their place.

Severe drought: Only the most xerophytic varieties of native vegetation continue to grow. And vegetal cover decreases.

Extreme drought: Drought-resistant varieties gradually give way to open cover. More and more bare soil is exposed.

Table 19 shows the relationship between May precipitation and the index value at the end of April. The class limits for May are shown in the table. Of particular interest is the fact that the index at the end of April was positive in 16 of the 33 years, and in only 2 of those 16 years did "light" precipitation occur during the following May. Even more surprising is the fact that in 13 of the 16 cases (81 percent) the May precipitation was greater than the long-term mean with 8 of the 16 falling into the "heavy" category. Equally surprising is the fact that in 12 of the 17 Mays which followed Aprils having a negative index value the precipitation was less than the long-term mean. "Light" precipitation was observed in about half of these cases and only 3 years produced "heavy."

This relationship seems too good to be true and very likely it is to some extent fortuitous, but the chance of its breaking down completely on subsequent data seems a bit remote.

This relationship suggests a number of things.

TABLE 19.—Contingency table showing May precipitation in central Iowa as a function of the index value at the end of April, 1930-62

Index value at end of April	May precipitation				Total
	Light <3.00 in.	Near normal <Mean >Mean		Heavy >4.80 in.	
X > 0.....	2	1	5	8	16
X < 0.....	9	3	2	3	17
Total.....	11	11		11	33

As far as drought is concerned there does not appear to be much chance of April being the last of a drought period. As a matter of fact one can determine from table 16 that 12 of the 15 Aprils having a negative index were followed by Mays which added to the droughtiness.

Of course, the factor that is being reflected in these relationship is persistence. It may be that this index is a more useful parameter for studying certain types of persistence relationships than is precipitation by itself.

Another subject for speculation arises here. Perhaps the persistence in the moisture aspect of this continental climate is related to the sources of the precipitation. It may well be that a good deal of the precipitation in continental climates represents moisture re-evaporated from land areas. This portion may be more substantial than some authorities have surmised. If it is, it would afford a partial explanation of the persistence of wet and dry periods. Begemann and Libby [2], from studies of the tritium content of rainfall, estimated that about one-third of the rain in the upper Mississippi Valley is ocean water and about two-thirds represents re-evaporated surface water.

As can be seen from figure 5, the July precipitation during drought periods in central Iowa does not average as much as it does during wet periods. Also, the difference between June and July is much less during drought periods than in the mean or during wet periods. This is an interesting difference which bears looking into.

The most striking thing that one finds on examination of the data is that there were 7 years when the *June* precipitation was less than the *July* normal with a drought underway at the end of June; and in all of these cases the July precipitation exceeded the June precipitation with the average difference being 1.98 in. Further, the July rainfall was normal or above in all but one of these 7 years.

Figure 5 also shows a large percentage difference in November precipitation between wet periods and drought periods. Apparently drought is rather persistent during the fall months because there were 12 years when drought was underway at the end of October and 9 of these were followed by Novembers in which the precipitation was below normal, the average departure being about 1 in.

Figure 6 shows a decrease in the average rainfall

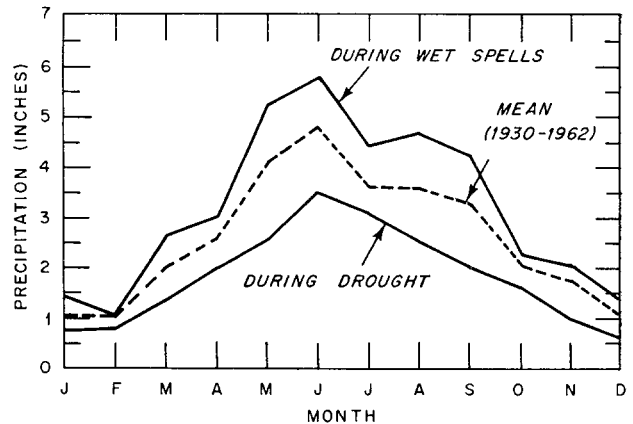


FIGURE 5.—Mean monthly precipitation in central Iowa.

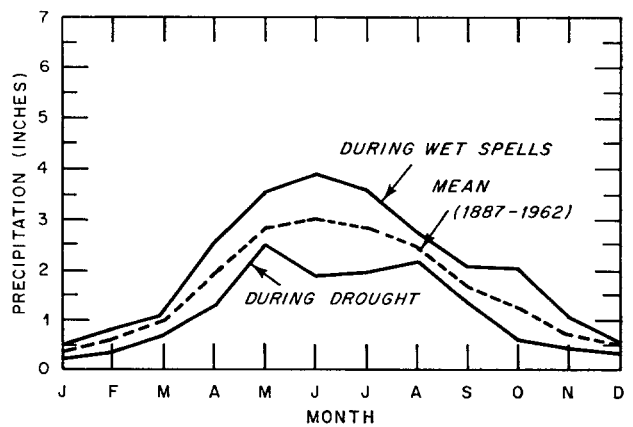


FIGURE 6.—Mean monthly precipitation in western Kansas.

from May to June in western Kansas during drought. This is in contrast to both the average change and the change during wet periods. On examination of the data it turns out that the drought index at the end of May was negative in 42 of the 76 years. In 30 of the 42 years the subsequent rainfall during June was less than the 76-yr. mean. There were 30 years when the May index was < -1.00 and 77 percent were followed by drier than average Junes.

The unusual dryness of October during drought periods in Kansas led to further examination of those years. There were 28 years when drought was underway at the end of September and 26 (93 percent) were followed by below average rainfall during October. In 24 of the years the Octo-

ber rainfall totaled less than 1 in. over the area. So, in Kansas too, we find some evidence that the index may be useful in forecasting.

These few examples demonstrate the need for further study of these and similar aspects of the usefulness of the index values.

15. THE METHOD APPLIED TO NORTHWESTERN NORTH DAKOTA

RESULTS AND VERIFICATION

In order to determine whether or not this method of analysis would provide reasonable final results in an area other than those on which it was primarily based, the data from the northwestern climatic division (six counties) of North Dakota were analyzed for the 30 years beginning with 1931. The derived means, coefficients, and constants are shown in table 20.

This Dakota area was chosen for analysis in 1961 because a drought was underway at the time, and it seemed timely to study an area in which drought was a problem of current concern. As it turned out this was not a particularly satisfactory region for a test because of the difficulty of locating auxiliary information for judging the reasonableness of the final index values.

Streamflow in this region (the Souris River) is almost completely regulated by controlled lakes and reservoirs. In addition, a number of new dams were built during the 1930's and there seems reason to believe that some of the low flows recorded at that time were a consequence of the flow being impounded behind newly constructed dams upstream.

The agricultural reports are at times a little misleading because the crops are so dependent on June precipitation. Ordinarily, almost one-fourth

of the annual precipitation comes in June, and a hot dry June has a tremendous effect. As long as crops are deteriorating day by day, the agricultural reports stress the urgent need for moisture; but after the crops are harvested or dried up, published complaints of a moisture shortage diminish unless the shortage is so severe that even drinking water must be hauled in.

Table 21 summarizes the drought periods in northwestern North Dakota. The index reached its maximum negative value, -6.66 , in August 1934 during the 20-month drought which began in August 1933. Note that this drought was in the extreme class 60 percent of the time. This drought was mostly in the mild class until April 1934 when the index, -2.41 , showed it as moderate. By the end of the very dry May (rainfall 0.76 in.) the drought was in the extreme class with an index of -4.11 . The next 11 months (except one) were all abnormally dry and the drought severity increased. The following index values were computed: June, -4.76 ; July, -6.24 ; August, -6.66 ; September, -6.04 ; October, -6.26 ; November, -6.13 ; December, -5.69 . Drought severity continued to decrease in the following months, but moisture remained abnormally short until May 1935 when the drought ended. There is evidence that the drought in 1934 definitely reached an extreme severity.

TABLE 20.—Means, coefficients and constants for northwestern North Dakota, 1931-1960

$AWC_c=1.00$ in., $AWC_u=5.00$ in.

	Jan.	Feb.	Mar.	Apr.	May	June	July	Aug.	Sept.	Oct.	Nov.	Dec.
<i>T</i>	6.3	10.5	21.4	40.5	53.2	61.3	69.2	66.9	56.1	44.4	26.0	13.6
<i>ET</i>	0	0	T	.86	2.40	3.52	3.46	2.32	1.25	.64	.02	0
<i>PE</i>	0	0	T	.91	2.95	4.26	5.52	4.69	2.68	1.13	.02	0
<i>R</i>41	.39	.59	.40	.13	.32	0	0	.21	.21	.54	.37
<i>S</i>	1.76	2.16	2.56	3.15	3.30	2.69	2.44	1.11	.64	.67	.81	1.35
<i>PR</i>	4.24	3.84	3.44	2.85	2.70	3.31	3.56	4.89	5.36	5.33	5.19	4.65
<i>RO</i>01	T	.01	.02	0	.15	0	0	0	0	0	0
<i>L</i>	0	0	0	.25	.91	.57	1.33	.48	.17	.07	T	0
<i>PL</i>	0	0	T	.80	1.64	1.83	2.08	.86	.28	.17	.01	0
<i>P</i>42	.40	.61	1.02	1.80	3.43	2.13	1.85	1.26	.77	.55	.37
<i>α</i>	1.00	1.00	1.00	.9410	.8142	.8272	.6272	.4953	.4647	.5672	.9492	1.00
<i>β</i>0970	.1029	.1727	.1400	.0467	.0976	0	0	.0392	.0385	.1040	.0800
<i>γ</i>0042	.0017	.0050	.0064	0	.0565	0	0	0	0	0	0
<i>δ</i>	0	0	0	.3180	.4450	.3141	.6396	.5546	.5967	.4368	.5172	0
<i>K</i>	3.43	3.30	2.95	2.33	1.94	1.62	2.10	2.35	2.25	2.57	2.84	3.47

TABLE 21.—Drought periods, northwestern North Dakota, 1931–1962

Start		End		Maximum severity	Number of months				
Year	Month	Year	Month		Mild	Moderate	Severe	Extreme	Total
1931	March	1932	September	-5.05	2	6	4	7	19
1933	August	1935	April	-6.66	6	2		12	21
1935	September	1935	October	-1.45	2				2
1936	June	1937	August	-4.14	1	1	12	1	15
1938	September	1938	September	-1.01	1				1
1939	September	1941	March	-2.18	13	2			19
1946	April	1946	September	-2.40	2	4			6
1949	April	1949	September	-2.00	4	1			6
1952	April	1953	February	-3.44	1	5	5		11
1955	October	1959	August	-5.30	17	5	8	4	47
1960	September	1962	April	-5.67	7	1	4	3	16
Number of months					56	27	33	27	163
Percent of 368 months					15	7	9	7	42

Months of Beginning and Ending of Drought

	Jan.	Feb.	Mar.	Apr.	May	June	July	Aug.	Sept.	Oct.	Nov.	Dec.
First month	0	0	1	3	0	1	0	1	4	1	0	0
Last month	0	1	1	2	0	0	0	2	4	1	0	0

Bavendick [1] leaves no doubt of this. He wrote:

It was not until June [1934] that any semblance of normal precipitation occurred and even that month showed a deficiency [59 percent of 30-yr. mean]. To further aggravate the situation, duststorms of unprecedented severity occurred during April and May. Much of the livestock was shipped out of the State due to lack of feed. Drought was so severe that plans for the evacuation of farmers from western North Dakota were seriously discussed. . . . Many cattle died from lack of feed and water and from dust which accumulated in their lungs and stomach. Some persons died from "dust pneumonia" caused by an accumulation of dust in their lungs.

As was the case in Kansas the effects of the abnormal moisture deficiency were greatly increased by the windstorms and dust, but the driest spring and summer on record certainly seems a likely candidate for the classification of extreme drought.

Turning to the drought in 1961, we find serious complaints of drought as the hottest and driest June on record reduced the wheat crop to about one-fourth of average. There were a few local showers in July and those areas enjoyed some temporary relief, but this was followed by the driest and hottest August on record. The following selected comments from the *North Dakota Weekly Weather and Crop Report* of August 29, 1961 [64] illustrate the seriousness of the drought at this time.

"Stock water situation is serious with many hauling water to livestock [in Burke Co.]. [The same was true in Mountrail Co.] Wheat yields averaged 4 to 7 bushels with a variation of 1.5 to

17 bushels. [Much of this was summer-fallowed wheat.] Very little barley and oats was harvested. Wells and dugouts are being constructed. Majority of [Renville] County remains extremely dry. Fall tillage delayed because of dry weather. Everything is at a standstill."

By way of comparison, the computed drought index values during 1961 were as follows: May, -1.16; June, -3.11; July, -4.14; August, -5.67. The peak severity during this drought was the -5.67 at the end of August. Severity decreased during subsequent months until the drought ended with April 1962.

This drought does not appear to have been as devastating as the drought of 1934, and from a crop yield standpoint the drought of 1936 ($X = -3.28$ at the end of July) was apparently more serious [1] than this one in 1961. There are many reasons why the effects were not as serious in 1961. In the first place there is a good deal more know-how these days for coping with the problems of dryland agriculture. There is evidence here that the Great Plains Conservation Program [53] has already met with some success in its objective—"to assist farmers and ranchers to develop for themselves a land use program which will help them avert many of the hazards that come with the recurring droughts common to the region." In addition, the availability of livestock feed on soil-bank acreages greatly alleviated the stockmen's problems in 1961. This feed was made available for haying and grazing by an official

U.S. Department of Agriculture action in late June declaring this a drought disaster area.

This action—possibly necessitated by the wording of the soil-bank law—led to much confusion concerning the seriousness of the drought during June and July. Some noted this disaster designation and visualized conditions similar to those in the dustbowl days of the 1930's in the southern Plains.

Conditions in July 1961 were by no means as serious as those which prevailed at the peak of the droughts in the southern Plains in the 1930's and in the 1950's. Descriptions such as [56] bear this out. The index also reflects this fact. At the end of July 1961 the index showed -4.14 in northwestern North Dakota. This value compares with the western Kansas values of -5.96 in August 1934 and -6.20 in September 1956.

It is also interesting to note that in the Kansas cases the index was around -3.5 to -4.0 when disaster was declared, but in the case of northwestern North Dakota the index was only about -3.00 . There seems to be some evidence that the index provides a better estimate of the severity of this drought than does the disaster declaration. However, one must always bear in mind that this index is a function of the anomalous weather rather than of the *effects* of the weather. Agriculturally, one might be justified in considering the June weather as a calamity, but from a meteorological standpoint the drought at the end of June could not reasonably be placed in the same category with the drought of 1934.

AN EXAMPLE OF CURRENT DROUGHT ANALYSIS

During the summer of 1961 there was a considerable amount of public interest in the drought in the northern Great Plains and the Prairie Provinces of Canada. A period of showery weather began early in July and immediately there were reports that the drought had ended. On the basis of this analysis an article was prepared [35] pointing out that the weather of June had already used nearly all the antecedent moisture so that above normal July rainfall was required if the evapotranspiration was to be normal. It was further demonstrated that July had increased rather than ended the water shortage in this area. Early in August another article was released [34] pointing out the strong climatological likelihood for the drought gradually

becoming worse during August. This article was based, in large part, on equation (14) which estimates the amount of precipitation needed for "normal" weather. It turned out that August had provided this much rain only eight times during the last 30 years, with most of the eight occurring during years in which most months were wetter than normal. From this it was concluded that the drought was more likely to become worse than to end during August. Actually, this turned out to be the driest and hottest August in 30 years and the drought became more extreme by September 1.

During September it rained 2.79 in. over the area. This was, by equations (29) and (30), far from being enough moisture definitely to establish an end to the long period of drought, but it did produce a 27 percent probability that the drought had ended. At that time there was no way of being certain that September was not just an interruption in the long drought. In fact, October and November were among the driest of record and both reduced the probability that the drought had ended. By the first of December the probability had been reduced to 9 percent with no prospect of its reaching 100 percent before the following spring. The unhappy truth is that under the existing circumstances there was no way of making a reasonable estimate as to whether this very serious drought period had ended or if the area was destined to suffer through another hot dry summer. This is in marked contrast to the situation in July and early August when there existed relatively high probabilities that the drought would get worse before it got better.

Actually, the change from prevailing dry weather to unusually wet weather did not take place until May of 1962. It turned out, therefore, that the wet weather of September 1961 was only a brief interruption in the dry weather. That this would be the case was suspected in early winter, but there was no certainty until the following spring. This demonstrates that the need for reliable seasonal weather forecasts remains. However, under certain circumstances this method does provide a useful substitute.

In general this method of analysis seems to have provided fairly good results in North Dakota. There seems no way of measuring exactly how well the index is describing the moisture variable. The best one can say is that the results seem reasonable both in time and in comparison with the results obtained in Kansas and Iowa.

16. CONCLUDING REMARKS

To a large extent this drought analysis method requires strict adherence to the procedures which have been described. Any radical departure from these procedures will produce values of Z which are incompatible with the equations for determining drought severity. However, there is no reason why one could not use a different method for computing potential evapotranspiration. Any method of monthly hydrologic accounting which is more refined and realistic than the method used here would likely produce as good or better results, but a cruder method might introduce bias or inconsistencies.

The method was specifically designed to treat

the drought problem in semiarid and dry sub-humid regions. Extrapolation beyond the circumstances for which it was designed may lead to unrealistic results. Some regions are so near to being a desert that there is really little point in attempting drought analysis. At the other extreme are the very humid regions where, again, "abnormal dryness" has very little meaning.

In conclusion, this method of climatic analysis must be regarded as only a step in measuring and describing meteorological drought. Real understanding can only follow measurement and description. Prediction and control await understanding.

ACKNOWLEDGMENTS

The author is pleased to thank Dr. H. Landsberg, Director of Climatology, for providing time and facilities for carrying out this work. In addition, his unfailing words of encouragement are greatly appreciated. Mr. Milton L. Blanc proved to be a most patient listener who could always be counted on for helpful suggestions,

pertinent questions, and stimulating discussion. Without his interest and advice this work might never have been completed. To these two men the writer is particularly grateful, though it is not to be implied that they are in any way responsible for whatever errors, fallacies, and similar detractions may still exist.

APPENDIX A.—AUXILIARY CLIMATIC INFORMATION

GEOGRAPHICAL DISTRIBUTION OF THE CLIMATIC CONSTANTS

The analytical technique described in this paper is rather long and tedious. The large amount of work required stems largely from the necessity for carrying out the hydrologic accounting for a long series of years in order to compute the five constants that are required for each calendar month. However, once the constants have been determined, a current drought analysis can be carried out without reference to a long historical record. If present plans can be carried out, the historical record will be analyzed for a network covering the United States. From these machine analyses 60 maps will be prepared showing each of the five constants for each calendar month.

Maps of α , the coefficient of evapotranspiration, should provide a reasonably good delineation of the agricultural capabilities of various "systems," where a system represents a particular combination of precipitation, temperature, and soil.

Likewise, from a study of maps of δ , the coefficient of soil moisture loss, one could, with some additional work, mathematically demonstrate the advantages of cultural practices which increase the available water capacity of some soils.

DISTRIBUTION OF THE MOISTURE DEPARTURES

Table 22 shows the moments of the distributions of the moisture departures for each calendar month for the three areas studied. As one would expect, the standard deviation, σ , shows that the greatest dispersion occurs during the summer months. Note the secondary minimum during July in central Iowa.

In order to test the distributions for normality, two statistics, α_3 and a , which are measures of skewness and flatness have been computed. α_3 is the standardized third moment and $a = \Sigma|d|/n\sigma$ is a measure which is highly correlated with the fourth moment [46]. On comparison of these values with Geary and Pearson's table [15] it is seen that the number of a values which fall outside the 5 percent limit is approximately the same as the number which would be expected by chance or if there were no departure from normality.

However, these distributions show a rather large amount of skewness. This is indicated by the disproportionately large number of α_3 values which exceed the 5 percent limit. This skewness is partly a result of the fact that the moisture

TABLE 22.—Moments of the departures, d

	Jan.	Feb.	Mar.	Apr.	May	June	July	Aug.	Sept.	Oct.	Nov.	Dec.	May to Aug.
WESTERN KANSAS													
n	71	71	71	71	71	71	71	71	71	71	71	71	71
\bar{d}	0	0	0	0	0	0	0	0	0	0	0	0	0
$\sigma(d)$35	.56	.87	1.38	1.65	2.06	1.93	1.44	1.21	1.20	.77	.60	5.54
$\alpha_3(d)$	1.321	1.234	.721	.788	.447	.435	.320	.643	.203	1.814	1.526	2.353	.624
$a(d)$753	.767	.821	.778	.813	.802	.789	.767	.815	.704	.746	.672	.784
NORTHWESTERN NORTH DAKOTA													
n	30	30	30	30	30	30	30	30	30	30	30	30	30
\bar{d}	0	0	0	0	0	0	0	0	0	0	0	0	0
$\sigma(d)$25	.30	.42	.87	1.34	2.05	1.21	1.04	1.30	.72	.47	.25	4.57
$\alpha_3(d)$173	.822	.640	-.436	-.115	1.172	.176	.259	1.673	.689	.822	.992	.204
$a(d)$801	.759	.796	.773	.779	.720	.779	.782	.701	.813	.809	.747	.758
CENTRAL IOWA													
n	27	27	27	27	27	27	27	27	27	27	27	27	27
\bar{d}	0	0	0	0	0	0	0	0	0	0	0	0	0
$\sigma(d)$91	.84	1.11	1.63	2.22	2.67	1.47	2.46	2.03	1.50	1.65	.94	5.99
$\alpha_3(d)$	-.049	-.617	.496	.473	-.194	.571	-.282	.807	.318	.746	.636	.302	.325
$a(d)$805	.784	.812	.853	.808	.711	.762	.808	.820	.745	.804	.789	.860

departure distribution has the precipitation distribution as a component. Precipitation is rather skewed because it has a lower bound of zero. The skewness in the moisture departures results in a few occurrences of large departures, especially large positive departures.

Since the addition of non-normal distributions produces a distribution which approaches normality, the "summer months," May through August, have been combined to produce a single climatological series for each of the three areas. The moments for these three distributions of total moisture departure for the 4-month period are shown in the last column of table 22. On referring to Geary and Pearson's table one finds the values of both α and α_3 are reasonably close to their expected value in a normal distribution. From these tests it was concluded that the normal distribution could be used to represent the 4-month moisture departures.

The mean and the standard deviation contain all the information needed to estimate the normal distribution in the population from a normal sample. In the samples with which we are dealing here the mean is zero. This is very convenient inasmuch as one must determine only the standard

deviation in order to estimate the probability that any particular moisture departure will be exceeded during this 4-month period. It therefore seems likely that a map of the standard deviation could be prepared as soon as a sufficient number of areas have been analyzed and that the map would be all that is required in order to prepare probability statements concerning the "summer" moisture departures. Such information might be very useful for the planning of hydrologic structures.

It may well be that for crop yield investigations the moisture departure, d ,—for the appropriate phenological periods—is the most useful variable in this study. For instance, the moisture departure in June 1961 in northwestern North Dakota was -3.69 in. This very abnormal moisture deficiency during a critical month was the most important variable responsible for the much below normal wheat yields in that area. Of course the moisture variable is only one of the factors affecting crop yields, but in the drier regions it is one of the most significant. In the wetter areas, such as central Iowa, yield reductions may often be related to the positive moisture departures at planting and harvesting times.

APPENDIX B.—EFFECT OF THE AVAILABLE WATER CAPACITY TERM

PURPOSE OF THE *AWC* VALUE

As mentioned earlier in this paper, the computed soil moisture is used primarily as a device for taking account of antecedent weather. It allows one to derive a number which is regarded as an index of the amount of previously stored water available for future use. If the assigned available water capacity is too small, we tend to underestimate the amount of water in storage. On the other hand, too large an available capacity will, in humid climates where runoff is large, lead to an overestimation of the supply of water available. That is, the computations will show water in storage for some time after the actual supply has diminished to the point where the local economy is beginning to suffer. In semiarid regions the *AWC* value is not so critical, and little difficulty is introduced by assuming too large a value for *AWC* in such areas of little runoff.

EXPERIMENTS AT DOVER, DELAWARE

While it has been known all along that reasonable final results required the use of a fairly realistic value for *AWC*, it was not entirely clear as to the effect on the drought index of using an unrealistic *AWC* value. Therefore, we analyzed a 44-yr. period of Dover data, with assumed values of *AWC* of 2.0 in., 4.0 in., and 8.0 in. That is, the complete analysis from water balance book-keeping through the final drought index values was carried out three times, the only difference being the assigned value of *AWC*. Apparently, somewhere around 4.0 to 6.0 in., could be considered as realistic for that area.

Results were somewhat unexpected. The analysis using $AWC = 2.0$ in. produced a maximum drought severity index of -3.45 , thereby indicating that extreme drought never occurred during this 44-yr. period. The analysis using $AWC = 4.0$

in. gave a maximum drought severity index of -4.51 , and $AWC = 8.0$ in. gave a maximum index of -6.17 . When one recalls that the driest year in 30 years was to be used to define extreme drought, it is apparent that either this 44-yr. period was a very biased sample or the assigned AWC value of 2.0 in. was somehow limiting the method.

EFFECT OF UNREPRESENTATIVE AWC VALUES

Why should an AWC value that is too small tend to limit the method's capability for showing large departures from normal? If, for the moment, we assume a ridiculously small value for AWC , say 0.10 in., it is apparent that the main effect is a loss of the capability for taking account of antecedent weather. One dry day or one completely dry year will produce the same result, viz, no water in storage. Likewise, a wet day or a wet year will produce full storage. In either instance the system is no longer capable of taking adequate account of past weather. As the assigned storage becomes smaller and smaller, we begin to lose a part of the basis for estimating the amount of rain needed. Finally, all estimates will tend to lie very close to the normal precipitation itself, irrespective of the dryness or wetness of the past. Large values of the moisture departure (the d values) are therefore ruled out, which also rules out large drought index values.

If, in humid climates, the assigned storage capability is too large, rather than too small, it will allow insufficient runoff during wet periods, introduce fictitious water supplies and over-optimistic expectations during dry periods, and thereby tend to make the area appear more humid than it actually is. As a consequence, drought severity will tend to be somewhat inflated. It does not appear, now, that the consequences from the use of too large a storage capacity are as misleading as those stemming from the use of too small a storage capacity. Actually, the system is not as sensitive to this factor as this dissertation might suggest. In general, the Dover results for $AWC = 4.0$ in. and $AWC = 8.0$ in. were very similar. It was only the results from using $AWC = 2.0$ in. that seemed to be markedly different.

AREAS WITH SMALL STORAGE CAPABILITY

What sort of results can we expect in an area—particularly a humid area—which actually has a rather small capability for storing water? In the first place, the analysis indicates that, as far as water is concerned, cumulative weather has little significance. This lack of an adequate moisture carryover capability makes it impossible to fully utilize the humid climate. Such an area has a water use expectation characteristic of a more arid climate which does have an adequate capability for the carryover of water. During periods of high moisture demand the small amount in storage is soon exhausted, and, even though the area is very dry, there is no expectation that a large moisture recharge will take place—in spite of the fact that the humid climate is capable of producing such a recharge. The outcome is that the full extent of the abnormal wetness or dryness of the climate cannot be completely utilized or taken into account; therefore, there is no opportunity for cumulative weather to build up to a point where the index indicates either extreme wetness or extreme drought.

In view of the "droughty soil" concept, this is a rather surprising development. However, if one recognizes that expectations are actually diminished by the lack of an adequate water storage facility, the reasonableness of the result is quite apparent. On a relative basis, an area which lacks an adequate capability for storing water is not as affected by prolonged dry weather as is an adjoining area which has this capability. This, too, may at first seem illogical; however, on a relative basis, it is true because the favored area is accustomed to and expects an adequate supply of water at all times. If the supply cannot meet the demand, a serious disruption of the economy takes place. On the other hand, the less-favored area is accustomed to frequent water shortages; the demands and operations are geared to the fact that water shortages are to be expected. Therefore, while drought may become apparent sooner in the area of little moisture carryover capability, it will never reach the peak severity that will, in time, occur in the more favored area. This interpretation seems to conform to reality, and this is the sort of result the drought index will show.

APPENDIX C.—ANALYSIS OVER OTHER TIME OR SPACE UNITS

WEEKLY ANALYSES

The foregoing discussion applies entirely to the use of monthly temperature and precipitation data as input. Inasmuch as monthly hydrologic accounting is a rather crude way of estimating the water balance [51] some experiments were conducted using weekly, and even daily, data as input.

It turned out that the daily accounting followed by weekly summarization and weekly drought severity computations introduced some difficulties, much unnecessary detail, and considerable expense without producing results which were appreciably different from those obtained from the use of weekly input data. This "daily-weekly" approach was soon abandoned.

As far as procedure is concerned, the weekly analysis was carried out by the same steps that were used in the monthly analysis. The main difference was that the long-term means of P , PE , etc. were computed for each of the 52 standard climatological weeks, whereas the monthly program requires such means only for the 12 months.

Originally, it had been estimated that the weekly constants and weekly equations could be derived from the monthly constants and equations. However, the problem is not that simple and the weekly work required the repetition of all the steps used to develop the monthly equations and constants.

Results.—Weekly analyses were compared with monthly analyses at two stations, Gothenburg, Nebr. and Ames, Iowa. The weekly system gave more detail; it came closer to pinpointing the time when events such as the beginning of a drought happen; and it allows one to keep up with a currently developing situation. But, overall results were, from a climatological standpoint, very similar to those obtained from monthly data with only a fraction of the work and expense.

Briefly, the weekly results and the monthly results were in agreement over 90 percent of the time; i.e., when one system indicated drought underway, the other system generally agreed. Also, the systems seldom disagreed by as much as 2 percent as to the percentage of time each

class of drought (mild, moderate, etc.) existed. The two indications of maximum drought severity (62 cases) never differed by more than 0.7 of a drought class and the mean absolute difference was about 0.2 of a drought class. The average difference between the two indications of the time of occurrence of the most severe point in each of the 62 drought periods was about 11 days. In general, when the two sets of drought index values were plotted against time, the agreement looked very good, both at Ames and at Gothenburg.

Conclusions.—On the basis of the records analyzed from both weekly and monthly input data, it appears that results are not very much different. The weekly data provide more detail and apparently get just a little closer to a realistic measure, but for climatological purposes the differences are slight. The monthly analysis can be done manually without spending too much time. On the other hand, weekly analysis requires much more than four times as much work. Either could be done by machine, but of course it costs more to do the job by weeks. Also, weekly data are not readily available either in published form or on punch cards. One main advantage of weekly analysis is that it enables one to keep up with a current drought.

However, it has been found possible to accomplish much the same "weekly" result by using the monthly system in such a way that the middle of the monthly interval successively moves ahead by about one-fourth of a month. That is, drop the first 8 days of the month, add the first 8 days of the next month and compute on the basis of the new "month", etc. The coefficients for the mid-points of these new "months" can be graphically determined from a plot of the previously computed monthly coefficients. This procedure requires that one carry on 3 *independent* sets of "monthly" analyses in addition to the regular monthly analysis. This scheme is not as difficult as it seems and it does enable one to keep up with a currently developing drought situation and to capture some of the detail that is lost in a regular monthly analysis.

POINT VERSUS AREA ANALYSIS

Although this method of drought analysis is based on areal data, it is of interest to determine its applicability to single station data within the area. Studies have been made for a few points, but at this writing there is only one area-single point comparison which is available.

Since only one case (in Iowa) has been analyzed, it must be realized that the results are tentative.

APPENDIX D.—RELATIVE INSTABILITY OF THE CLIMATE OF WESTERN KANSAS SINCE THE EARLY 1930'S

If one accumulates the monthly values of d or Z for western Kansas and plots them against time, the curve shows rather a large amplitude since the early 1930's as compared to the preponderance of relatively small oscillations in the previous years. Of course, the index values in table 13 show the same sort of thing. Prior to 1932 a fairly sizable number of months show an index value indicating near normal or only an incipient wet or dry condition. However, since 1932 small index values are rather rare.

This can be demonstrated in a crude fashion by counting the number of months with $|X| < 1.0$ each year and plotting the cumulative total against time. Such a plot appears in figure 7.

This figure shows that the period 1887 through 1932 was *not* marked by numerous large anomalies. At the end of this 46-yr. period, 223 months, about 5 per year, had had small index values. In other words the weather was definitely abnormal only 60 percent of the time.

However, since 1932 the climate has been noteworthy for the absence of near-normal weather. In fact, more than 11 months per year have produced either drought or unusually wet conditions. It is easy to see how the area gained its "feast or famine" reputation in recent years.

Unfortunately, there is no handy explanation for this apparent shift in the frequency of abnormal weather. It may continue and it may not. The warming trend in mean annual temperatures

The conclusions are that the analysis at a point tells one a good deal about the weather and climate of a sizable surrounding area. This is, of course, not so true in more rugged terrain. Likewise, areal analysis gives a fairly good picture of the dry and wet periods at points within the area. For climatological purposes areal analyses are probably adequate, and it is likely that future work will be concentrated on areal analyses.

in the latitude zone 40° to 70° N. seems to have come to an end at about this time [32]. Also, an apparent increase in the frequency of tropical storms in the north Atlantic began in the early 1930's [8]. Are these various events coincidental? Probably not, but we simply do not yet know enough about the fundamentals of atmospheric actions and interactions really to explain what, if anything, has taken place. Only when such things can be adequately explained will there be hope for prediction on a time scale measured in years or decades.

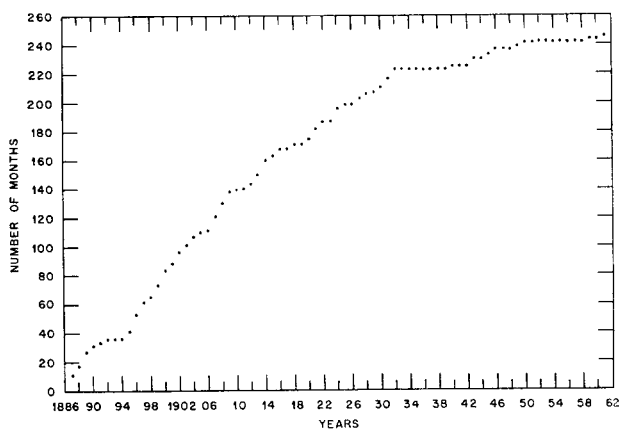


FIGURE 7.—Cumulative annual number of months with $|X| < 1.0$, western Kansas.

APPENDIX E.—RECURRENCE OF SERIOUS DROUGHT IN WESTERN KANSAS

Although no effort was made to discover "cycles of drought," the relative regularity of the occurrence of severe and extreme drought in western Kansas is rather striking. From table 13 one can see that the index indicated extreme drought in 1894, 1913, 1934 (and following years), and in 1954 (and following years). These four fairly regularly spaced occurrences of extreme drought may be accidental. However, when one recalls that the discussion of the drought of 1913 [17] mentioned damaging drought in 1874 and in the early 1850's, there appears to be sufficient evidence to lead one to speculate concerning the possibility that an extreme drought will again occur in western Kansas sometime between 1972 and 1975. We have no basis or method for estimating the probability of such an occurrence, but

one could reasonably think it may be greater than the 6 percent probability of extreme drought shown in table 17.

It is interesting to note that Tannehill reached a similar conclusion in 1954 [44]. In a study of the long-range prospects for rainfall in the United States he concluded that ". . . another dry cycle in this country should begin near the middle of the 1970's, probably in 1975." Tannehill, too, was concerned with the occurrence of widespread, disastrous drought, the sort of thing that produces dustbowls and dry reservoirs.

The only thing that seems to be certain is that future years will sooner or later bring a recurrence of extreme drought in the area. The question is, when? On the basis of past history the early 1970's may be years one might well anticipate.

REFERENCES

1. F. J. Bavendick, *Climate and Weather in North Dakota*, Water Conservation Commission, Bismarck, N. Dak., 1952, pp. 14-15.
2. F. Begemann and W. F. Libby, "Continental Water Balance, Ground Water Inventory and Storage Times, Surface Ocean Mixing Rates and World-Wide Water Circulation Patterns from Cosmic Ray and Bomb Tritium," *Geochimica et Cosmochimica Acta*, vol. 12, 1957, pp. 277-96.
3. J. F. Bender, compiler, *NBC Handbook of Pronunciation*, Thomas Y. Crowell Co., New York, 1943, 289 pp.
4. O. W. Bidwell, "Major Soils of Kansas," *Circular 336*, Kansas Agricultural Experiment Station, Manhattan, Kans., July 1956, 13 pp.
5. T. A. Blair, *Climatology*, Prentice-Hall, New York, 1942, p. 37.
6. G. Blumenstock, Jr., "Drought in the United States Analyzed by Means of the Theory of Probability," *Technical Bulletin No. 819*, U.S. Department of Agriculture, April 1942, p. 5.
7. G. E. Condra, "Drought, Its Effects and Measures of Control in Nebraska," *Nebraska Conservation Bulletin No. 25*, University of Nebraska, Conservation and Survey Div., April 1944, p. 1.
8. G. W. Cry, W. H. Haggard and H. S. White, "North Atlantic Tropical Cyclones," *Technical Paper No. 36*, U.S. Weather Bureau, 1959, 214 pp. (see p. 6).
9. W. L. Decker and J. F. Gerber, "Comparison of Estimated Values of Evapotranspiration," *Final Report on Contract CWB-8807*, University of Missouri, Columbia, Mo., 1957, 51 pp.
10. Drexel Institute of Technology, "Summary of Climatic Observations, 1956," *Publications in Climatology*, vol. X, No. 2, Laboratory of Climatology, Centerton, N.J., 1957. Also vol. V, No. 7; vol. VI, No. 6; vol. VIII, No. 2; and vol. IX, No. 4.
11. H. H. C. Dunwoody, "Weather Conditions of the Crop of 1894," *Yearbook of the U.S. Department of Agriculture, 1894*, U.S. Department of Agriculture, Washington, D.C., 1895, p. 532.
12. D. J. Fieldhouse and H. H. Englebrecht, "Calculating the Need for Irrigation in Delaware," paper presented at Second National Conference on Agricultural Meteorology, New Haven, Conn., Oct. 1958.
13. S. D. Flora, *The Climate of Kansas*, *Report of the Kansas State Board of Agriculture*, vol. LXVII, No. 285, June 1948, pp. 29 and 183.
14. J. C. Foley, "Droughts in Australia," Commonwealth of Australia, Bureau of Meteorology, *Bulletin No. 43*, Sept. 1957, 281 pp.
15. R. C. Geary and E. S. Pearson, *Tests of Normality*, Biometrika Office, London, 1958, p. 8, tables 3 and 4.
16. Great Britain Meteorological Office, *The Meteorological Glossary*, Published by the authority of the

- Meteorological Committee, Chemical Publishing Co., New York, 1951, 253 pp.
17. M. W. Hayes, "Climatological Data for August 1913, District No. 6, Missouri Valley," *Monthly Weather Review*, vol. 41, No. 8, Aug. 1913, pp. 1192-1193.
 18. R. J. Hildreth and G. W. Thomas, "Farming and Ranching Risk as Influenced by Rainfall. 1. High and Rolling Plains," MP-154, Texas Agricultural Experiment Station, College Station, Tex., Jan. 1956, p. 4.
 19. J. L. Holcombe and F. H. Wiegmann, "Drought Intensity and Irrigation Needs for Cotton in the St. Joseph Area," *D.A.E. Circular* No. 185, Louisiana State University and A. and M. College, Department of Agricultural Economics, Dec. 1955, 47 pp.
 20. J. C. Hoyt, "Drought of 1936, with Discussion of the Significance of Drought in Relation to Climate," U.S. Geological Survey, *Water Supply Paper* No. 820, 1938, p. 1.
 21. W. G. Hoyt, "Droughts," Chapt. 12 in "Hydrology," vol. IX in *Physics of the Earth*, National Research Council, McGraw-Hill Book Co., New York, 1942, pp. 579-591.
 22. R. E. Huschke, editor, *Glossary of Meteorology*, American Meteorological Society, Boston, Mass., 1959, 638 pp.
 23. V. Johnson, *Heaven's Tableland, The Dustbowl Story*, Farrar, Straus and Co., New York, 1947, 288 pp.
 24. M. A. Kohler, "Meteorological Aspects of Evaporation Phenomena," International Union of Geodesy and Geophysics, Association of Scientific Hydrology, *Publication* No. 45, General Assembly of Toronto, 1957, vol. 3, pp. 421-436.
 25. M. A. Kohler and R. K. Linsley, "Predicting the Runoff from Storm Rainfall," *Research Paper* No. 34, U.S. Weather Bureau, Sept. 1951, 10 pp.
 26. M. A. Kohler and M. M. Richards, "Multi-Capacity Basin Accounting for Predicting Runoff from Storm Precipitation," *Journal of Geophysical Research*, vol. 67, No. 13, Dec. 1962, pp. 5187-5197.
 27. W. B. Langbein and others, "Annual Runoff in the United States," U.S. Geological Survey, *Circular* 52, June 1949, 14 pp.
 28. R. K. Linsley, Jr., M. A. Kohler, and J. L. H. Paulhus, *Applied Hydrology*, McGraw-Hill Book Co., Inc., New York, 1959, 689 pp. (see p. 581).
 29. W. E. Marlatt, A. V. Havens, N. A. Willets, and G. D. Brill, "A Comparison of Computed and Measured Soil Moisture under Snap Beans," *Journal of Geophysical Research*, vol. 66, No. 2, Feb. 1961, pp. 535-541.
 30. J. K. McGuire and W. C. Palmer, "The 1957 Drought in the Eastern United States," *Monthly Weather Review*, vol. 85, No. 9, Sept. 1957, pp. 305-314.
 31. G. and C. Merriam Co., *Webster's Dictionary of Synonyms*, Springfield, Mass., 1942.
 32. J. M. Mitchell, Jr., "Recent Secular Changes of Global Temperature," *Annals of the New York Academy of Sciences*, vol. 95, Art. 1, New York, Oct. 5, 1961, p. 240.
 33. J. Namias, "Some Meteorological Aspects of Drought," *Monthly Weather Review*, vol. 83, No. 9, Sept. 1955, pp. 199-205.
 34. W. C. Palmer, "Drought and Climatology," *Weekly Weather and Crop Bulletin, National Summary*, vol. XLVIII, No. 32, Aug. 7, 1961.
 35. W. C. Palmer, "End of Drought?," *Weekly Weather and Crop Bulletin, National Summary*, vol. XLVIII, No. 30, July 24, 1961.
 36. W. C. Palmer, "Weather Service to Agriculture in the Western Great Plains," *Bulletin of the American Meteorological Society*, vol. 37, No. 9, Nov. 1956, pp. 458-461.
 37. W. C. Palmer and A. V. Havens, "A Graphical Technique for Determining Evapotranspiration by the Thornthwaite Method," *Monthly Weather Review*, vol. 86, No. 4, Apr. 1958, pp. 123-128.
 38. W. C. Palmer and A. V. Havens, "Palmer-Havens Diagram for Computing Potential Evapotranspiration by the Thornthwaite Method," U.S. Department of Agriculture, Soil Conservation Service, Portland, Oreg., 1960.
 39. H. L. Penman, "Evaporation: An Introductory Survey," *Netherlands Journal of Agricultural Science*, vol. 4, 1956, pp. 9-29.
 40. W. H. Pierre and F. F. Riecken, "The Midland Feed Region," *Yearbook of Agriculture, 1957, Soil*, U.S. Department of Agriculture, Washington, D.C., 1958, pp. 535-546.
 41. L. A. Richards and C. H. Wadleigh, "Soil Water and Plant Growth," Chapt. 3 in *Soil Physical Conditions and Plant Growth*, B. T. Shaw, editor, American Society of Agronomy, Monograph II, Academic Press, New York, 1952, pp. 73-251.
 42. Subcommittee on Hydrology of the Inter-Agency Committee on Water Resources, "River Basin Maps Showing Hydrologic Stations," *Hydrologic Activities Bulletin* No. 11, Washington, D.C., April 1961, 79 pp.
 43. I. R. Tannehill, *Drought: Its Cause and Effects*, Princeton University Press, Princeton, N.J., 1946, p. 46.
 44. I. R. Tannehill, "More Dry Years Ahead," *Country Gentleman*, Curtis Publishing Co., Philadelphia, Pa., vol. 124, No. 9, Sept. 1954.
 45. H. C. S. Thom, "The Analytical Foundations of Climatology," U.S. Weather Bureau manuscript, Jan. 1954, pp. 24-25.
 46. H. C. S. Thom, "Seasonal Degree-Day Statistics for the United States," *Monthly Weather Review*, vol. 80, No. 9, Sept. 1952, pp. 143-147 (see p. 144).
 47. H. C. S. Thom, with the assistance of the Working Group on Statistical Requirements and Methods in Climatology, WMO-CCL, "Three Chapters on Climatological Analysis," U.S. Weather Bureau manuscript, Aug. 1960, 62 pp.
 48. C. W. Thornthwaite, "An Approach toward a Rational Classification of Climate," *Geographical Review*, vol. 38, 1948, p. 55-94.
 49. C. W. Thornthwaite and B. Holzman, "Measurement of Evaporation from Land and Water Surfaces," *Technical Bulletin* No. 817, U.S. Department of

- Agriculture, Soil Conservation Service, May 1942, 143 pp.
50. C. W. Thornthwaite and J. R. Mather, "The Water Balance," *Publications in Climatology*, vol. 8, No. 1, Drexel Institute of Technology, Laboratory of Climatology, Centerton, N.J., 1955, 104 pp.
 51. C. W. Thornthwaite, J. R. Mather, and D. B. Carter, *Three Water Balance Maps of Eastern North America*, Resources for the Future, Washington, D.C., Nov. 1958, 47 pp. + 3 maps.
 52. U.S. Agricultural Research Administration, "Soil Survey Manual," U.S. Department of Agriculture *Handbook* No. 18, Aug. 1951, p. 185.
 53. U.S. Department of Agriculture, "Program for the Great Plains," developed by the U.S. Department of Agriculture with the cooperation of the Great Plains Agricultural Council, U.S. Department of Agriculture, *Miscellaneous Publication* No. 709, Jan. 1956, P. IV.
 54. U.S. Geological Survey, "Compilation of Records of Surface Waters of the United States through September 1950," *Geological Survey Water-Supply Paper* 1311, 1955, Also Papers 1280, 1340, 1391, 1441 and 1511.
 55. U.S. Geological Survey, "Compilation of Records of Surface Waters of the United States through September 1950," *Geological Survey Water-Supply Paper* 1310, 1958. Also *Water-Supply Papers* 1280, 1340, 1390, 1440 and 1510.
 56. *U.S. News and World Report*, "Parched Plains: First Hand Report," United States News Publishing Corp., Washington, D.C., vol. LI, No. 6, Aug. 7, 1961, pp. 71-73.
 57. U.S. Weather Bureau, "Climates of the States, Iowa," *Climatology of the United States*, No. 60-13, May 1959.
 58. U.S. Weather Bureau, "Climates of the States, Kansas," *Climatology of the United States*, No. 60-14, Nov. 1959.
 59. U.S. Weather Bureau, *Climatological Data, Iowa Section*, U.S. Department of Agriculture-U.S. Weather Bureau, Des Moines, Iowa, April 1935.
 60. U.S. Weather Bureau, *Daily River Stages*, vol. 52, 1956, Washington, D.C.
 61. U.S. Weather Bureau, *Iowa Weather and Crop Bulletin*, published weekly in cooperation with Iowa Department of Agriculture, Des Moines, Iowa, 1934.
 62. U.S. Weather Bureau, *Iowa Weekly Weather and Crop Bulletin*, published weekly in cooperation with U.S. Department of Agriculture, Bureau of Agricultural Economics, and Iowa Department of Agriculture, Des Moines, Iowa. Issues: Aug. 1947, Sept. 1947, Sept. 1948, Aug. 1949, Sept. 1949, Oct. 1953, Nov. 1953.
 63. U.S. Weather Bureau, *Kansas Weekly Weather and Crop Reports*, published weekly in cooperation with U.S. Department of Agriculture, Marketing Service; Kansas State Board of Agriculture, and Agriculture Extension Service of Kansas State College, Topeka, Kans., Aug. 1955.
 64. U.S. Weather Bureau, *North Dakota Weekly Weather and Crop Report*, published weekly in cooperation with U.S. Department of Agriculture, Statistical Reporting Service and North Dakota State University Extension Service, Fargo, N. Dak., Aug. 29, 1961.
 65. U.S. Weather Bureau, *Weekly Weather and Crop Bulletin*, No. 30, 1933 through No. 52, 1940, Washington, D.C.
 66. U.S. Weather Bureau, *Weekly Weather and Crop Bulletin National Summary*, vol. XL, No. 41, Oct. 12, 1953.
 67. U.S. Weather Bureau, *Weekly Weather and Crop Bulletin, National Summary*, vol. XLIII, Nos. 22-46, May 28-Nov. 12, 1956.
 68. C. H. M. van Bavel and F. J. Verlinden, "Agricultural Drought in North Carolina," North Carolina Agricultural Experiment Station, *Technical Bulletin* No. 122, 1956, 60 pp.
 69. F. J. Veihmeyer and A. H. Hendrickson, "Does Transpiration Decrease as Soil Moisture Decreases?" *Transactions of the American Geophysical Union*, vol. 36, June 1955, pp. 425-448.
 70. J. E. Weaver and F. W. Albertson, *Grasslands of the Great Plains*, Johnsen Publishing Co., Lincoln, Nebr., 1957, pp. 139 and 153.
 71. E. S. West and O. Perkman, "Effects of Soil Moisture on Transpiration," *Australian Journal of Agricultural Research*, vol. 4, No. 3, 1953, pp. 326-332.
 72. R. C. L. White, "Drought and Effective Rainfall Frequency in Pastoral New South Wales, West of the Wheat Belt," *Meteorological Study* No. 5, Bureau of Meteorology, Melbourne, Australia, 1955, p. 2.

U.S. DEPARTMENT OF COMMERCE
WEATHER BUREAU
WASHINGTON, D.C. 20235

POSTAGE AND FEES PAID

Drought Reconstructions for the Continental United States*

EDWARD R. COOK

Tree-Ring Laboratory, Lamont-Doherty Earth Observatory, Columbia University, Palisades, New York

DAVID M. MEKO

Laboratory of Tree-Ring Research, The University of Arizona, Tucson, Arizona

DAVID W. STAHL AND MALCOLM K. CLEAVELAND

Tree-Ring Laboratory, Department of Geography, University of Arkansas, Fayetteville, Arkansas

(Manuscript received 8 December 1997, in final form 25 June 1998)

ABSTRACT

The development of a 2° lat \times 3° long grid of summer drought reconstructions for the continental United States estimated from a dense network of annual tree-ring chronologies is described. The drought metric used is the Palmer Drought Severity Index (PDSI). The number of grid points is 154 and the reconstructions cover the common period 1700–1978. In producing this grid, an automated gridpoint regression method called “point-by-point regression” was developed and tested. In so doing, a near-optimal global solution was found for its implementation. The reconstructions have been thoroughly tested for validity using PDSI data not used in regression modeling. In general, most of the gridpoint estimates of drought pass the verification tests used. In addition, the spatial features of drought in the United States have been faithfully recorded in the reconstructions even though the method of reconstruction is not explicitly spatial in its design.

The drought reconstructions show that the 1930s “Dust Bowl” drought was the most severe such event to strike the United States since 1700. Other more local droughts are also revealed in the regional patterns of drought obtained by rotated principal component analysis. These reconstructions are located on a NOAA Web site at the World Data Center-A in Boulder, Colorado, and can be freely downloaded from there.

1. Introduction

Drought occurrence remains a serious concern in the United States (U.S.). In 1996, the most severe drought of the past 20 years struck the Southwest. Such events place huge demands on rural and urban water resources and quality, and place huge burdens on agricultural and energy production. The 1996 drought was preceded by a severe drought in the late 1980s in California (Roos 1994; Haston and Michaelsen 1997), in 1986 in the Southeast (Bergman et al. 1986; Cook et al. 1988), in 1976–77 in the West (Namias 1978; Matthai 1979), in the 1960s in the Northeast (Namias 1966; Cook and Jacoby 1977), in the 1950s in Texas (Namias 1955; Stahl and Cleaveland 1988), and in the 1930s in the

northern Great Plains (Warrick 1980; Stockton and Meko 1983). Clearly, drought is a common occurrence in the U.S. and can occur anywhere. Understanding the causes of drought, especially the severe multiyear events, is necessary if reliable methods of forecasting are to be developed. A major difficulty in using the available meteorological records to model drought in the U.S. is the limited time span covered by such records. There are often too few realizations of proposed forcing mechanisms of drought in the short instrumental records to test any of them in a statistically rigorous way. We hope to alleviate this problem through the use of centuries-long, annual tree-ring chronologies.

In this paper we describe the development of a gridded network of drought reconstructions covering the continental U.S. that is derived from a large collection of climatically sensitive tree-ring chronologies. The reconstructions cover the period 1700–1978 and are based on the Palmer Drought Severity Index (PDSI; Palmer 1965), a well-known and widely used measure of drought and wetness. Previous efforts in reconstructing drought from tree rings in the U.S. have been highly successful (e.g., Blasing and Duvick 1984; Cook and

* Lamont-Doherty Earth Observatory Contribution Number 5896.

Corresponding author address: Dr. Edward R. Cook, Lamont-Doherty Earth Observatory, Palisades, NY 10964.
E-mail: drdendro@ldeo.columbia.edu

Jacoby 1977; Cook et al. 1988; Cook et al. 1992; Graumlich 1993; Haston and Michaelsen 1994, 1997; Meko 1992; Mitchell et al. 1979; Stahle and Cleaveland 1988; Stahle et al. 1985, 1988; Stockton and Meko 1975, 1983; Woodhouse and Meko 1997). However, most of these efforts have only involved reconstructing local or regional drought histories. Earlier efforts by Fritts (1976, 1991) to reconstruct seasonal temperature and precipitation across the U.S. met with limited success because the tree-ring data used were restricted to western North America. Since that pioneering work, the coverage of tree-ring chronologies across the U.S. has increased enormously. Consequently, an effort to expand these drought reconstructions in a homogeneous way to the entire continental U.S. was initiated by Meko et al. (1993) and developed further by Cook et al. (1996).

We will describe in considerable detail the method used to develop the continent-wide grid of drought reconstructions and provide a number of results that document the generally high fidelity of the tree-ring estimates. This has been done in an effort to make the reconstructions as useful as possible to climatologists and modelers who might want to use these data for studying past temporal and spatial patterns of drought and their association with hypothesized forcing functions. To this end, the drought reconstructions have already been used with considerable success to reevaluate the putative connection between a bidecadal drought area rhythm in the western U.S. and solar/lunar tidal forcing (Mitchell et al. 1979; Cook et al. 1997). In addition, they are presently being used to study and better understand the teleconnection between drought/wetness and the El Niño–Southern Oscillation in the U.S. (Ropelewski and Halpert 1986; Cook et al. 1999; Cole and Cook 1998).

Much of what we have produced is, in a sense, an extension of the work done by Karl and Koscielny (1982; referred to hereafter as KK) in their study of drought in the U.S. The research of KK was based on a 60-point grid of instrumental PDSI data covering the period 1895–1981. In so doing, they described some important temporal and spatial features of drought in the U.S. As will be shown, our tree-ring reconstructions faithfully capture most of the properties of drought described by KK. In the process, the drought database for the U.S. has been extended back in time by a factor of 3 on a much denser 154-point grid, which allows for more detailed temporal and spatial analyses.

2. The PDSI grid

The PDSI grid used in this study is 2° lat \times 3° long and is patterned after a study of runoff and drought across the United States by Langbein and Slack (1982). This grid is shown in Fig. 1. It is based on 1036 single-station monthly PDSI records estimated from the Historical Climatology Network (Karl et al. 1990) and modified according to Guttman (1991). However, the Death

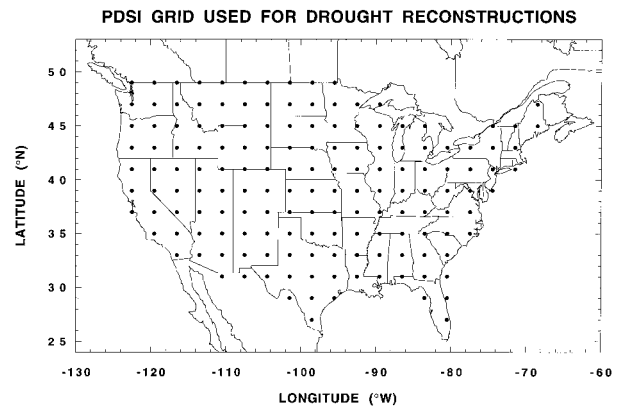


FIG. 1. Map of the continental U.S. showing the locations of the PDSI grid points used in this study. The grid spacing is 2° lat. \times 3° long, and totals 155 points.

Valley, California, record was deleted prior to gridding because of anomalously high (e.g., >20) monthly PDSI values in 1958. All stations used begin no later than 1925 and end no earlier than 1989.

The choice of the gridding dimension was a trade-off between spatial resolution and the desire to reduce the size of the PDSI network. A $2^\circ \times 3^\circ$ grid reduces the PDSI network to about 15% of its original size. Yet, the spatial definition of the grid should still be high enough to capture mesoscale patterns of wetness and dryness and to resolve regional drought patterns found by KK using a coarser 60-point PDSI grid.

Following Meko et al. (1993) and Cook et al. (1996), the single-station records were interpolated to the 155 grid points using inverse-distance weighting of the form

$$\text{PDSI}_k = \left(\sum_{j=1}^m \frac{\text{PDSI}_j}{d_j} \right) / \left(\sum_{j=1}^m \frac{1}{d_j} \right), \quad (1)$$

where m is the number of stations within a given search radius of grid point k , PDSI_j is the j th PDSI station record, and d_j is the distance of station j from grid point k . The first 3 yr of data were deleted from each station record to eliminate starting-value transience in computing the monthly PDSIs (N. Guttman 1994, personal communication). Then, a 150-km search radius was used to locate stations local to each grid point. All stations found within that radius were used. If at least five stations were not found within 150 km, then the five closest stations were used. A minimum distance of 30 km was used in $1/d$ to avoid excessively weighting stations very close to the grid points. As stations dropped out prior to 1928, the weights of the remaining series were renormalized for interpolation to gridpoint k . This enabled the preservation of pre-1928 PDSI data for regression model validation.

Because the individual stations used in the grid have varying starting years, the first year of data available at each grid point varies over space. All of the grid points have data back to 1913. Prior to 1913, the number of

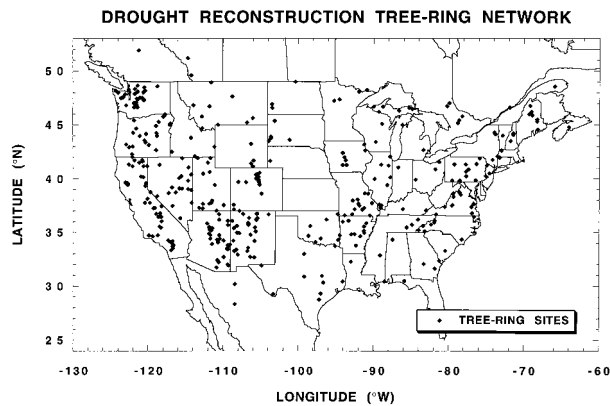


FIG. 2. Map of locations of the 425 annual tree-ring chronologies used in this study. Some of the locations represent more than one chronology. All of the series cover the common time period 1700–1979.

grid points with data declines to 143 by 1903, 97 by 1895, 38 by 1890, and 10 by 1874 due to the changing beginning years of the instrumental PDSI data over the grid. The quality of the grid also varies over space, with the weakest areas located in the northern Great Basin and Rocky Mountains regions (Cook et al. 1996).

The PDSI data were gridded on a monthly basis. Yet, past experience indicates that summer (i.e., June–August) PDSI relates better to tree rings on average than to any single month when comparisons are made over large geographic areas. Cook et al. (1992) found that the peak correlation between PDSIs and tree rings shifted from June for chronologies south of Virginia, to July in the Virginia–New York region, and even to August for some chronologies in northern New England and Canada. This shift was attributed to regional differences in phenology (i.e., the timing of tree growth) associated with the northward march of the growing season in spring and to the time required for evapotranspiration demand to significantly draw down the soil moisture supply. Consequently, we also used summer PDSI here as the best drought index to reconstruct across the United States.

3. The tree-ring network

The tree-ring chronologies used here to reconstruct past drought across the continental U.S. number 425 now, an increase of 177 over those used by Meko et al. (1993) in their examinations of spatial patterns of tree growth. Many of the new chronologies were developed after the start of that study. Others were not included for a variety of reasons. We have chosen to include virtually all available chronologies that begin no later than 1700 and end no earlier than 1979, a criterion previously established by Meko et al. (1993). Figure 2 shows the distribution of sites across the United States. The distribution is highly patchy due, in part, to the uneven distribution of forested land. In addition, the

distribution of tree species in the network is highly regional due to the natural distribution of forest communities and species range limits in the U.S. See Cook et al. (1996) for more details. Not all of these chronologies will be useful predictors of drought. However, the screening process described and tested below for retaining candidate tree-ring predictors of PDSI will guard against including those chronologies not statistically related to drought.

Prior to regression analysis, the tree-ring chronologies were put through a process of variance stabilization described in Meko et al. (1993). Variance stabilization was done to reduce the effects of changing sample size on the variance of the tree-ring chronology, especially in the early portions of chronologies below, say, six individual measurement series. This removed a potential artifact from the data that is unlikely to be related to changing climatic variability.

4. Calibration/verification results

The method used to reconstruct the PDSI grid from tree rings is point-by-point regression (PPR). As implemented here, PPR is simply the sequential, automated fitting of single-point principal components regression models of tree rings to a grid of climate variables. The sequential nature of PPR differentiates it from joint space–time methods used to simultaneously relate two fields of variables, such as canonical regression (Glahn 1968; Fritts et al. 1971), orthogonal spatial regression (Briffa et al. 1986; Cook et al. 1994), and singular value decomposition (Bretherton et al. 1992). Mathematical details of the PPR method and tests of its implementation are described in the appendixes at the end of the paper.

The PPR method is based on the premise that only those tree-ring chronologies proximal to a given PDSI grid point are likely to be true predictors of drought at that location, where “true” implies a causal relationship between tree rings and drought that is stable through time. The rationale behind this premise is our understanding of drought in the U.S. as a regional- or mesoscale phenomenon (see KK for mapped regions). Consequently, synoptic-scale teleconnections between tree rings and drought, while statistically significant during any given calibration period, may not be stable through time. This “local control” over the reconstruction of each gridpoint PDSI is not possible with the joint space–time reconstruction methods mentioned above.

In the PPR method, a fixed search radius around each grid point defines the zone of local control exercised by the method in selecting candidate tree-ring predictors of PDSI. A second level of control is also applied in the form of a screening probability, which eliminates tree-ring chronologies from the candidate pool that are poorly correlated with drought. Here we examine the statistical fidelity of the PDSI reconstructions based a 450-km search radius and a screening probability $\alpha =$

0.10, selected after the extensive testing described in appendix B. The statistics used for this purpose are the same as those described for those tests: the explained variance (R_c^2) over the 1928–78 calibration period, the squared Pearson correlation (R_v^2) over the pre-1928 verification period, the reduction of error (RE) in the verification period, and the coefficient of efficiency (CE) over the verification period. See appendix B for the mathematical definitions of these statistics. All four tests are measures of fractional variance in common between actual and reconstructed PDSI. In this sense, they are comparable. However, they differ markedly in their relative performances. As will be seen, the calibration period R_c^2 always overestimates the true fidelity of the tree-ring estimates of drought, while in the verification period, R_v^2 usually indicates better fidelity in the estimates than RE and CE. Among the verification statistics used here, the CE is the most rigorous (Cook et al. 1994).

A PDSI grid point passed the R_c^2 test if it was successfully calibrated by tree rings following the procedures outlined in appendix A; it passed the R_v^2 test if the Pearson correlation between actual and estimated PDSI in the verification period was significant at the 95% one-tailed confidence level; and it passed the RE or CE if either was >0 . See appendixes A and B for details. For the R_c^2 test, 154 of 155 grid points were successfully calibrated. The only grid point not calibrated was the one in southern, subtropical Florida, where there are no tree-ring chronologies. For the R_v^2 test, 147 grid points of the remaining 154 were successfully verified. In contrast, the number of RE and CE tests that passed dropped from 147 to 133 and 124 grid points, respectively. So, the verification test results indicate that the tree-ring reconstructions of drought are significantly related to actual PDSI over most of the grid. The median R_c^2 , R_v^2 , RE, and CE fractional variances are 0.55, 0.36, 0.31, and 0.22, respectively. The decreasing trend in these test statistics follows exactly the expected level of rigor of the regression model calibration and validation tests.

As good as these verification results are, they are probably understating the true skill of the tree-ring reconstructions at some grid points. The instrumental PDSI data in the verification period are not likely to be as homogeneous as those in the calibration period due to widely variable station record lengths and fewer station observations per year. In addition, some of the single station records used in the grid may be inhomogeneous. Consider, for example, two stations used in the PDSI grid in Nevada: Battle Mountain Airport (40°37'N, 116°52'W, elevation 1381 m) and Elko Federal Aviation Administration (FAA) Airport (40°50'N, 115°47'W, elevation 1548 m). These stations are only 53 and 63 km from the grid point in north-central Nevada (see Fig. 1) and are weighted most heavily in this five-station gridpoint average. Over the 1928–78 calibration period, the summer average PDSIs of these nearby stations have a correlation of 0.67. However, in the

1894–1927 precalibration period common to both stations, their correlation drops catastrophically to 0.05. Most of the loss of fidelity is in the pre-1910 data. If the comparison is made over the 1910–27 period only, the correlation improves somewhat to 0.27, but in either case the correlations are not statistically significant ($p < 0.05$). With regard to the tree-ring estimates of PDSI, the calibration R_c^2 is 0.69, while the verification period RE and CE are -0.67 and -0.95 , respectively. In this case, there is little doubt that the poor quality of the pre-1928 instrumental PDSI data is contributing strongly to the negative tree-ring verification. Given the extremely high quality and drought sensitivity of the tree-ring chronologies in the Great Basin, it is almost certain that the trees are doing a better job at estimating regional drought and wetness than are the meteorological stations in northern Nevada prior to 1928. It is likely that similar instrumental data problems exist elsewhere in the grid, but we have not yet quantified the impact of this source of error on the verification statistics.

5. Spatial patterns of calibration and verification

The calibration/verification results provided above were summaries for the entire drought grid. We now take a detailed look at the spatial patterns of the fractional variance statistics to see how homogeneous the results are across space.

Figure 3 shows the contoured maps of these statistics. The R_c^2 map indicates that the regression models for large areas of the U.S. explain 50%–70% of the grid-point PDSI variance. The weakest calibration areas are in the upper Midwest and in northern New England. The R_v^2 map indicates that the drought estimates over virtually all of the United States covary significantly with the actual PDSI data in the verification period. That is, any R_v^2 value in excess of 0.10 (i.e., a simple $r > 0.32$) is statistically significant using a one-tailed test and $\alpha = 0.05$. The RE and CE maps reveal more clearly some weak areas in the reconstruction grid. Specifically, there are some regions (e.g., the Great Basin, the upper Midwest, and the central Great Plains) with RE and CE both <0 . Since these regions verified reasonably well in the R_v^2 map, the loss of fidelity is probably due mainly to differences in mean level between the actual and estimated PDSIs over the verification period. This suspicion was largely verified by a series of equality-of-means tests of the verification data. Figure 4 shows maps of the mean differences between the actual and estimated PDSIs (upper map) and the corresponding t -test probabilities for those differences (lower map). Most of the differences fall in the range of ± 0.50 PDSI units, which are rarely significant even for $\alpha = 0.20$. The largest region of significant differences ($p < 0.10$) is located in the Great Basin and Wyoming–Montana areas where the RE and CE statistics are conspicuously negative.

Similar verification problems in the RE and CE maps

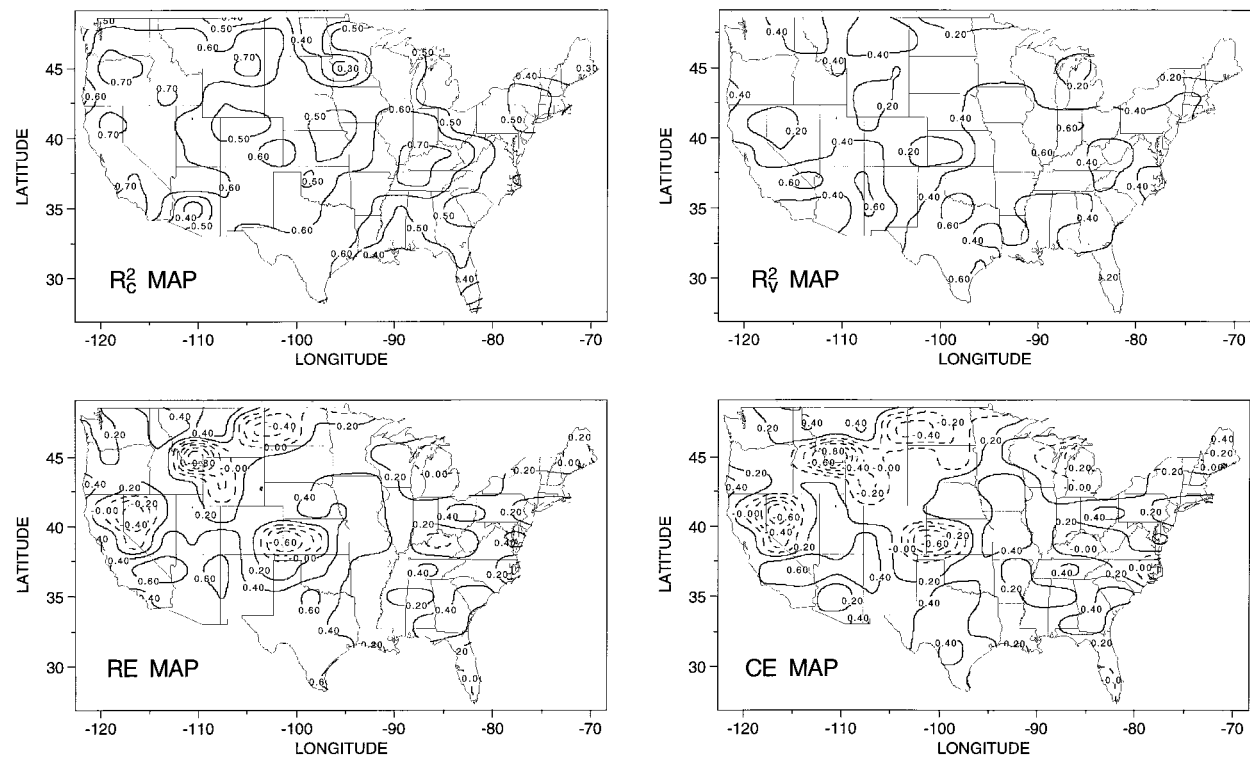


FIG. 3. Contour maps of the R_c^2 , R_v^2 , RE, and CE gridpoint fractional variance statistics. The calibration map shows that 50%–70% of the PDSI variance was calibrated by tree rings over most of the U.S. The R_c^2 , RE, and CE maps indicate, as expected, that there has been some loss of fidelity in the verification period. However, PDSI estimates over most of the U.S. is also verify significantly. The areas of negative RE and CE are mostly in areas where the mean levels of the actual and estimated PDSIs differ significantly ($p < 0.10$; see Fig. 4).

around the Great Basin were also found by Cook et al. (1996) in their earlier tests of the PPR method. Their analyses of the gridded instrumental PDSI data indicated that the regions of weak verification in Fig. 3 could be due in part to decreasing quality of the instrumental data, the Great Basin being the most likely case in point (Cook et al. 1996). However, it is also true that the quality and coverage of tree-ring data is somewhat poor in the other areas that do not verify well. Therefore, the gridpoint reconstructions in these regions should be used with more caution than those where the verification tests are all significant. The quality of these reconstructions should improve if new tree-ring chronologies can be developed in areas of poor coverage.

Finally, we examined the degree to which the reconstructions preserved the pattern of PDSI variability across the U.S. For example, it is known that drought variability is generally greater in the western half of the U.S. However, there is no guarantee that the reconstructions have preserved the spatial pattern of drought variability because of variance lost by regression. Yet, such information is important to retain if one is to make meaningful comparisons of drought variability over different time periods in the reconstructions. Figure 5 shows the contoured maps of gridpoint standard deviations for the actual and estimated PDSIs over the calibration period. There appears to be a high degree of

similarity between the two maps, even down to the local level of detail. Indeed, the maps have a correlation of 0.91. The preservation of the standard deviation pattern is due to the reasonably homogeneous pattern of calibrated variance shown in the R_c^2 map. Thus, the reconstructions ought to be quite useful for studying changing patterns of drought variability across the U.S. over the past three centuries.

6. Additional spatial comparisons

The calibration/verification results for the PPR method indicate that the PDSI reconstructions are generally valid expressions of drought over the United States. However, the PPR method does not contain any explicit spatial component other than that related to the search radius. The spatial relationships of drought in the United States (*sensu* KK) extend over regions that are generally larger than the 450-km search radius used here. Thus, while the individual gridpoint reconstructions are reasonably accurate in a temporal sense, they are not necessarily guaranteed to be valid in a spatial sense beyond the scale of the search radius used here. For this reason, we will describe here a number of analyses that collectively indicate that the spatial patterns of drought have also been well reconstructed by the PPR method.

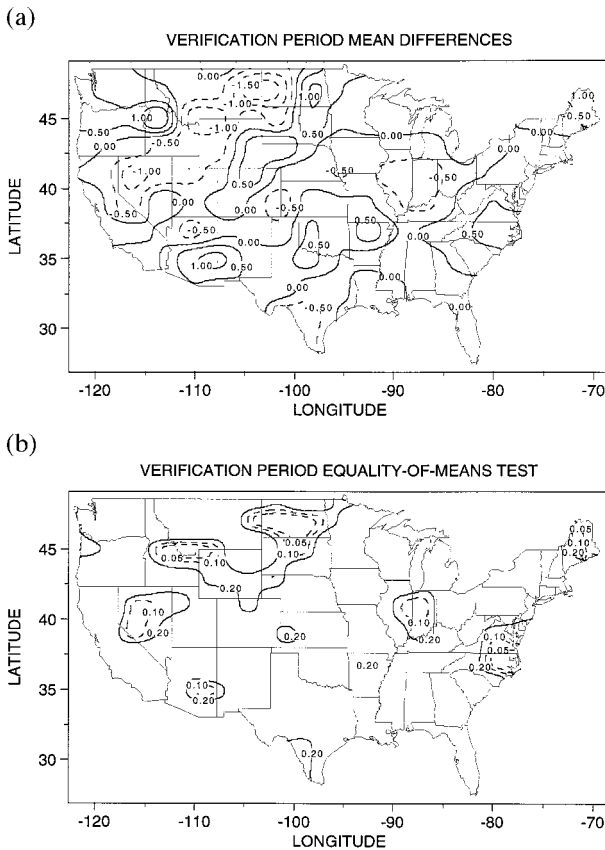


FIG. 4. Equality-of-means tests in the verification period. The contoured mean differences in PDSI units are shown in the upper map. The contoured *t*-test probabilities of those mean differences are shown in the lower map for regions where $p < 0.20$, $p < 0.10$, and $p < 0.05$. Most of the regions that have significantly different ($p < 0.10$) means also have negative REs and CEs (see Fig. 3).

a. Mean field, correlation, and congruence analyses of yearly PDSI maps

First, we will describe the degree to which the yearly maps (or spatial patterns) of reconstructed PDSI agree with those based on the gridded instrumental data. For this purpose, we will compare (a) the mean PDSI fields over time, (b) the relative spatial patterns using the Pearson correlation coefficient, and (c) the absolute spatial patterns using the congruence coefficient. The reconstructed patterns will be compared to two gridded instrumental PDSI datasets: the original one used for calibration purposes and a new one based on climate division PDSI data not directly used for calibration purposes. Comparisons using the former will be made over the 1874–1981 time period for which there are at least 10 grid points of actual and reconstructed PDSI data, while the latter has data for all grid points back to 1895 only. The rationale for using the gridded climate division data for additional tests is discussed next.

As described earlier, the single-station instrumental PDSI records used in the grid vary in length over space.

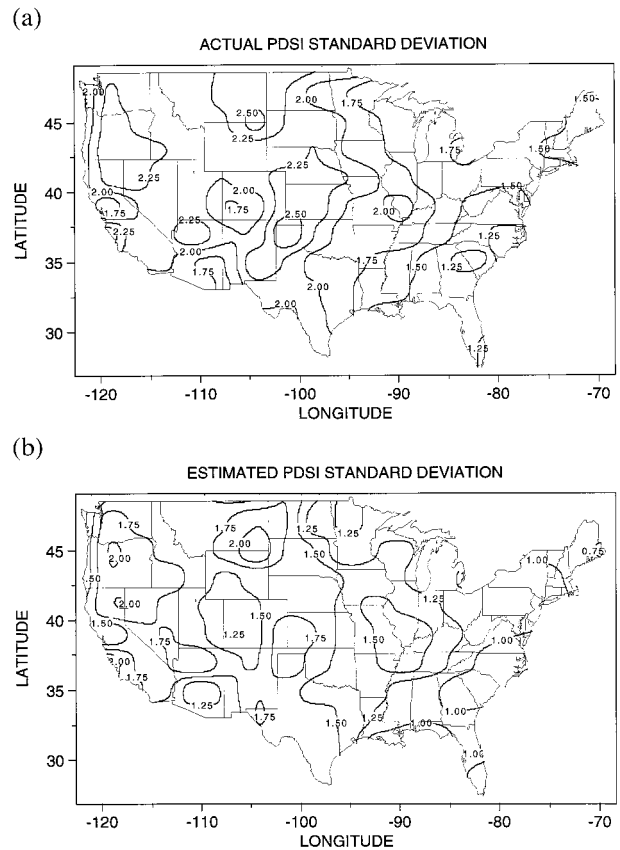


FIG. 5. Contour maps of the standard deviations of the actual and estimated PDSIs. These maps show the excellent degree to which the tree-ring estimates have preserved the spatial patterns of drought variability over the U.S.

Thus, some grid points have much longer records than others. The ending years of the tree-ring chronologies also constrain the end year of analysis. This is revealed in Fig. 6a, which shows the number of grid points with actual and reconstructed PDSI data as a function of time. The maximum number (154) covers the period 1913–78. After 1978, the number of reconstructed grid points declines precipitously to 10 by 1981 due to the ending years of the tree-ring chronologies used. Prior to 1913, the number of grid points declines to 143 by 1903, 97 by 1895, 38 by 1890, and 10 by 1874, all due to the changing beginning years of the instrumental PDSI data over the grid. The quality of the instrumental PDSI grid declines back in time as well because the number of single-station records used to estimate the gridpoint values for each year decreases as shorter records drop out of the gridding process. For these reasons, some degradation in the map comparisons ought to be expected, which is unrelated to the true fidelity of the tree-ring estimates.

In contrast, the gridded climate division data are available for all 154 grid points back to 1895 (Fig. 7a), and the number of single-station records represented in the climatic division summaries is generally greater than

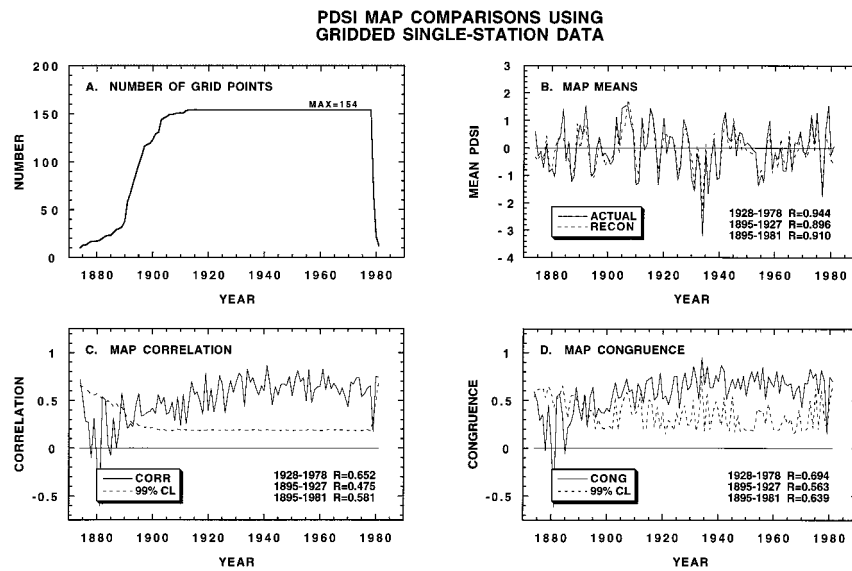


FIG. 6. Annual map comparisons of the actual and estimated PDSIs. The actual PDSI data are from the single-station grid used for calibration and verification. The number of grid points available for comparison each year is shown in (a). Note the steep drop-off in the number of available grid points prior to 1903. The grand mean PDSI averaged over all available grid points for each year is shown in (b). Note the very high correlations between the actual and estimated grand means in both the calibration and precalibration periods. The series of annual map correlations and congruences are shown in (c) and (d), respectively. The 99% confidence limits for each were determined by randomization tests. Most of the annual map comparisons exceed the 99% confidence level by wide margins.

that available from the Historical Climate Network alone. Consequently, the map comparisons (especially before 1928) ought to be more robust using the gridded climatic division data. Finally, the relationships between the actual and reconstructed data over the 1928–78 cal-

ibration period have been optimized in a least squares sense only for the single-station grid. The gridded climate division data, while highly related to the single-station grid, do not suffer from this constraint. Therefore, these additional spatial comparisons should pro-

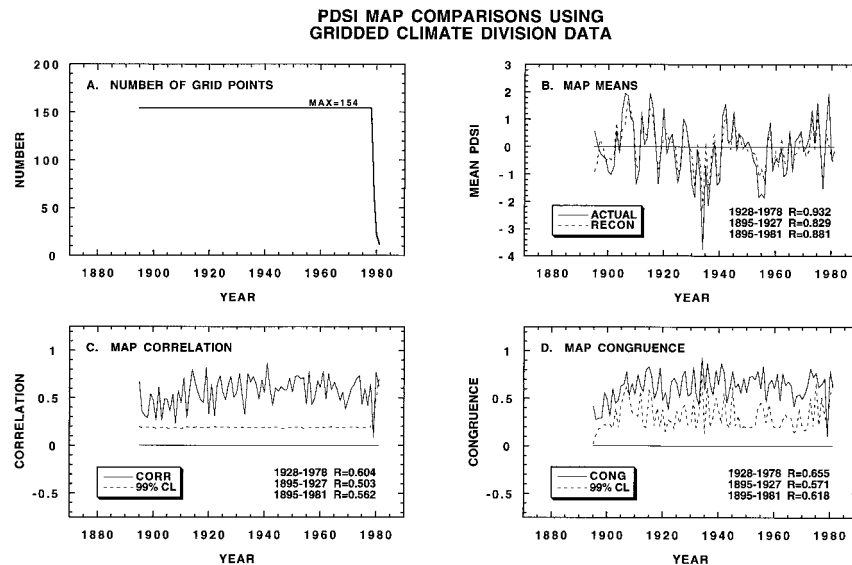


FIG. 7. Annual map comparisons of the actual and estimated PDSIs. This time the actual data are gridded climate division PDSI data, which all begin in 1895. These data avoid the steep pre-1903 loss of grid points in the single-station grid (Fig. 6a). See the Fig. 6 caption for more details.

vide a less biased evaluation of the true fidelity of the reconstructed PDSI maps.

1) MEAN FIELD COMPARISONS

A simple first-order comparison of the actual and reconstructed PDSI maps can be made by simply comparing the mean fields over time. That is, for each year all of the available gridpoint values are averaged together, separately for the actual and reconstructed data. The resulting grand mean time series are shown in Figs. 6b and 7b for the single-station and climate division grids, respectively. Although the single-station data go back to 1874, correlations between the mean actual and reconstructed series have only been calculated back to 1895 for comparison with the climatic division grid results.

There is a high degree of similarity between the mean series in each case. First, for the single-station grid, the correlation between actual and reconstructed PDSI is 0.944 over the 1928–78 calibration period. The correlation then drops to 0.896 in the 1895–1927 precalibration (i.e., verification) period, but is still highly significant. And over the entire 1895–1981 period, the correlation is 0.889. For the climate division grid, the correlations are comparable: 0.932 for the 1928–78 calibration period, 0.829 for the 1895–1927 precalibration period, and 0.881 overall. Clearly, the mean PDSI fields are well estimated by tree rings back to 1895 at least and even where the number of grid points drops to 10 in the 1874–94 period (see Fig. 6b). The similarity of the calibration period correlations based on the different grids indicates that, at this spatial scale of comparison, there is no significant least squares fitting bias in the reconstructions. These results are highly encouraging. However, this analysis does not reveal how well the spatial patterns that make up the mean fields have been replicated each year by the tree rings. To determine this, we will use map correlation and congruence analyses.

2) MAP CORRELATION

To test the relative agreement between actual and reconstructed PDSI maps, we used the Pearson product-moment correlation coefficient. First, we normalized each gridpoint reconstruction using its calibration period mean and standard deviation. This was done to avoid any regional bias in the map correlations due to spatial variations in the PDSI standard deviation (see Fig. 5). Then, for each year i of the n -yr overlap period between actual and reconstructed PDSI, we calculated

$$r_{pq} = \frac{\sum (p_k - \bar{p})(q_k - \bar{q})}{\left[\sum (p_k - \bar{p})^2 \sum (q_k - \bar{q})^2 \right]^{1/2}}, \quad (2)$$

where the summation extends over the $k = 154$ PDSI

grid points, p_k and q_k are the actual and reconstructed PDSI values at grid point k , respectively, and \bar{p} and \bar{q} are the mean fields for each year i , for example, those shown in Fig. 6b. Because the mean fields are subtracted from the gridpoint values, the information contained in them, which is a real component of drought over the coterminous United States, does not contribute to the estimate of r_{pq} .

Figure 6c shows the time series of map correlations (solid line) for the single-station grid. Also included is the one-tailed 99% confidence level (dashed line) estimated by randomizing the reconstructed PDSIs and calculating the correlation of this randomized field with the actual data. This was done 5000 times for each year. The resulting significance levels are very close to that which would have been obtained by the standard t test of the correlation coefficient. Note that back to 1889, where the number of grid points exceeds 30, the map correlations all exceed the 99% level. On average, the highest correlations occur during the 1928–78 calibration period ($\bar{r} = 0.652$), a result that is probably related to the least squares optimization. Prior to 1928, the correlations decline systematically (e.g., $\bar{r} = 0.475$ over the 1895–1927 precalibration period), a result that is consistent with the difference in the pointwise calibration/verification statistics reported earlier. Prior to 1889, the map correlations are mostly nonsignificant, in some cases catastrophically so. This result is probably a combination of a number of things that are at least partly unrelated to the overall quality of the PDSI reconstructions. Some of the longest (i.e., pre-1889) instrumental PDSI records come from the eastern U.S., where the calibration/verification statistics are relatively weak. So, a decline in spatial correlation is not too surprising when that restricted area contributes the most to the correlation analyses. And it is also likely that the quality of the actual gridded data declines back in time as the number of individual station records used in the grid declines.

The map correlations based on the climate division grid are shown in Fig. 7c. Except for 1979, when the number of grid points is small, all correlations exceed the 99% significance level. The average map correlation over the 1928–78 calibration period ($\bar{r} = 0.604$) is somewhat weaker than that based on the single-station grid ($\bar{r} = 0.652$), a result that is probably related to the lack of prior least squares fitting bias here. However, there is less evidence of the systematic decay in the map correlations prior to 1928 in this case, and the average correlation over the 1895–1927 period ($\bar{r} = 0.503$) actually exceeds that based on the single-station grid ($\bar{r} = 0.475$).

3) MAP CONGRUENCE

The map correlations are very useful for describing how well the spatial patterns of drought covary in a relative sense. However, because the mean fields are a

true component of drought variability over time (see Figs. 6b and 7b), it is desirable to include this information in the spatial analyses as well. To do this, we have used the congruence coefficient, which was originally developed as a measure of the similarity between two factor patterns in multivariate research (Richman 1986; Broadbrooks and Elmore 1987). The congruence coefficient is computed for each year of the overlap period as

$$c_{pq} = \frac{\sum p_k q_k}{\left[\sum p_k^2 \sum q_k^2 \right]^{1/2}}, \quad (3)$$

where p_k and q_k are the actual and reconstructed PDSI values at grid point k . Note that the only difference between c_{pq} and r_{pq} is the lack of \bar{p} and \bar{q} here. Thus, the means are not removed in computing c_{pq} , leading some earlier studies to describe the congruence coefficient as an unadjusted correlation coefficient (Broadbrooks and Elmore 1987). The theoretical range that c_{pq} may take is the same as r_{pq} . However, the presence of \bar{p} and \bar{q} in the calculation of congruence means that c_{pq} tends to be biased toward 1.0 relative to r_{pq} (Richman 1986). There is no theoretical sampling distribution for testing the significance of c_{pq} because of its partial dependence on \bar{p} and \bar{q} , which are random variables in their own right. Several studies have used Monte Carlo methods to generate empirical limits for c_{pq} (e.g., Broadbrooks and Elmore 1987). Here, we have generated our own significance levels using the randomization procedure described for the correlation coefficient.

Figure 6d shows the map congruence coefficients over time for the single-station grid, along with the empirical 99% confidence levels. The results are qualitatively similar to that found by correlation alone. The highest average congruence occurs in the 1928–78 calibration period ($\bar{c} = 0.694$), followed by declining but still significant congruence from 1895 to 1927 ($\bar{c} = 0.563$). Prior to 1895, congruence remains significant back to 1889 and then becomes very poor. A close comparison of the correlation and congruence plots reveals that, as expected, there is a small positive bias in the estimates of the latter (e.g., $\bar{r} = 0.581$ and $\bar{c} = 0.639$, respectively, over the 1895–1981 period). Perhaps the greatest difference in the two analyses is in the estimates of the confidence levels. The dependence of c_{pq} on \bar{p} and \bar{q} has resulted in a highly variable and erratic series of confidence levels that are clearly related to the variability between the mean fields shown in Fig. 6b.

The map congruences based on the climate division grid are shown in Fig. 7d. These results are again qualitatively similar to the correlation results. As before, there is greater long-term stability in map congruence using this grid for comparison with the reconstructed maps, and, except for 1979, all congruences exceed the 99% confidence level. All other details concerning the

map correlations above are similar here; for example, the average map congruence for the 1928–78 calibration period ($\bar{c} = 0.655$) is weaker than that based on the single-station grid ($\bar{c} = 0.694$), but the average congruence over the 1895–1927 period ($\bar{c} = 0.571$) actually exceeds that based on the single-station grid ($\bar{c} = 0.563$). None of these results indicate any serious deficiency in the annual PDSI maps produced by the tree-ring estimates.

4) DISCUSSION

The analyses shown in Figs. 6 and 7 indicate that the spatial patterns of PDSI in the reconstructions have captured those in the actual data with high ($p < 0.01$) statistical fidelity. Prior to 1895 some of the differences between the actual and reconstructed PDSI clearly arise from the deterioration of the instrumental PDSI coverage in time and space. The mean fields of the reconstructions have been estimated extremely well back as far as it is possible to test them, while the more detailed reconstructed annual maps are significantly related to the actual PDSI fields back to 1895 at least. The correlations between the actual and reconstructed mean fields are higher than the mean calibration and verification results of the individual grid points using PPR. This result indicates that the gridpoint reconstructions contain more “local noise” than do larger-scale averages of PDSI, with the mean fields studied here being the limiting case of averaging over all grid points (i.e., a continental-scale average). Averaging gridded climate reconstructions spatially to improve the signal-to-noise ratio has been used with considerable success (e.g., Fritts 1991; Mann et al. 1998) and is clearly justified if the main interest is in climate variability at spatial scales larger than that initially reconstructed. However, how one averages the reconstructions spatially to preserve insights into the physical climate system needs to be carefully considered. One approach to this problem is to use rotated principal component analysis (Richman 1986) to objectively define the natural regional drought climatologies in the United States (*sensu* KK). In the next section, we will use rotated principal component analysis to demonstrate that the regional drought patterns found by KK in their instrumental data can be reproduced well in most cases by our PDSI reconstructions.

b. Rotated principal component analysis

Rotated principal component analysis (RPCA) is a powerful tool for objectively decomposing spatial arrays of climate data into natural regional clusters or patterns (e.g., Barnston and Livezey 1987). Richman (1986) reviewed this topic in detail and performed a number of Monte Carlo experiments to test the performance of a number of rotation methods. We have used two of the recommended rotation methods here: orthogonal vari-

Reconstructed PDSI Varimax Factors (1700-1978)

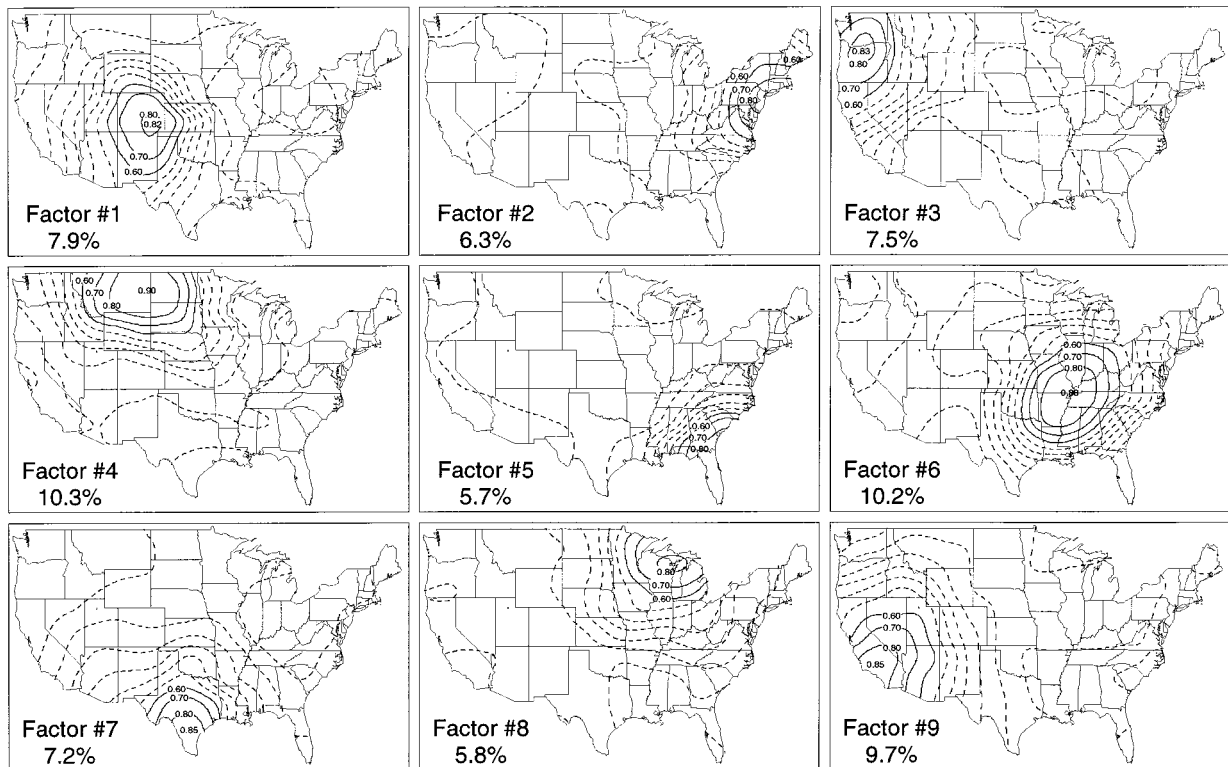


FIG. 8. Reconstructed summer drought varimax factors for the U.S. (1700–1978). The percent variance accounted for by each is indicated in each map. Most of these factors agree well with those of KK based on monthly instrumental PDSIs. The largest discrepancy is with our factor 1, located mainly over Colorado, which has replaced the “southwest” factor of KK, located mainly over Arizona. This discrepancy is investigated further in Fig. 9.

max rotation (Kaiser 1960) and oblique promax rotation (Hendrickson and White 1964). The former is perhaps the most popular orthogonal rotation method in use today, while the latter was shown by Richman (1986) to be one of the best oblique rotation methods for recovering the underlying true “simple structure” in his synthetic data tests. (Following the recommendation of Richman, the promax method was applied using a power $k = 2$.) Each method rotates the axes of a retained subset of unrotated principal components in order to achieve some degree of simple structure among variables. The resulting rotated factor loadings should be near one or near zero ideally and each variable should load heavily on one or, at most, a small number of factors only (Reyment and Jöreskog 1993). The loadings themselves can also be interpreted as simple correlations between each factor and the original variables.

In the context of this study, the variables are the PDSI grid points and the observations are the associated time series of PDSIs. The varimax rotation maintains orthogonality between the resulting factors, while promax rotation allows for intercorrelations between the factors to emerge as part of the simple structure solution. In the context of RPCA of climate data fields, it is arguable

that orthogonal factors are physically unrealistic. Therefore, an oblique solution might be preferred.

We used RPCA here to see how well the regional drought patterns in our reconstructions agree with those of KK. In their analyses, KK applied both varimax and oblique (direct quartimin) rotation to a 60-point grid of monthly instrumental PDSI data (1895–1981) across the continent. In so doing, they identified nine regional drought factors that they were able to associate with distinct, regional precipitation climatologies. We will assume this subspace dimension in our study here to simplify the analyses, but do not expect 1:1 congruence between our factors and those of KK. Unlike our summer PDSIs, the factors produced by KK were based on monthly data. The difference in grid resolution (154 vs 60) between our two studies could also affect the location of the factor boundaries. However, we should expect to see some strong similarities because the regional precipitation climatologies described by KK should contribute strongly to our summer PDSI estimates as well.

Figure 8 shows the reconstructed drought factor maps over the full 1700–1978 reconstruction period, based on the varimax rotation method. Most of the regional

Gridded Single Station PDSI Varimax Factors (1913-1978)

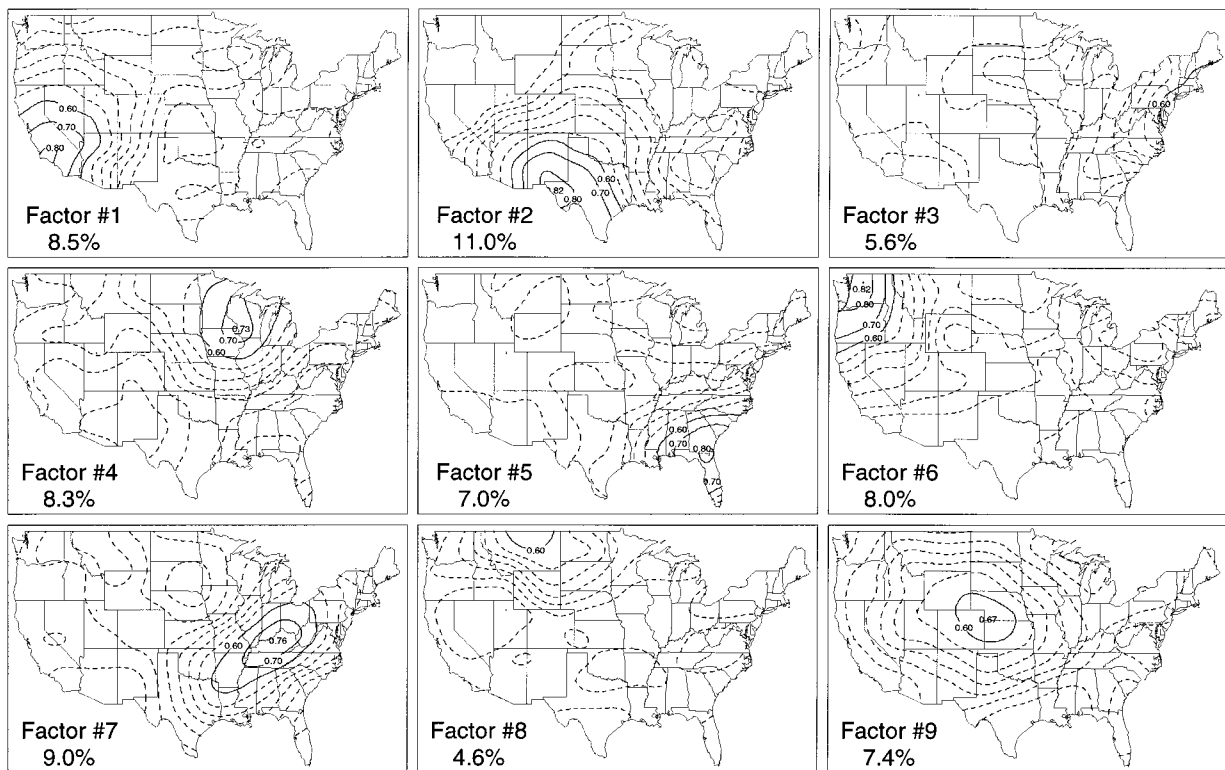


FIG. 9. Actual summer drought varimax factors for the U.S. (1913–78) based on the single-station grid. These maps agree very well with those in Fig. 8, even to the extent that the “Colorado” factor in our reconstructions is present in the actual data as well. Thus, the southwest factor of KK, calculated over the 1895–1981 period, may be more related to nonsummer PDSI variability.

drought patterns described in KK are clearly evident here. For example, factors 2–9 correspond closely to their northeast, northwest, west–north-central, southeast, central, south, east–north-central, and west factors (KK, their Fig. 4). The biggest difference between the factor analyses is between our factor 1 (located mainly over Colorado) and their southwest factor (located mainly over Arizona). To see if this difference was an artifact in our reconstructions, we performed RPCA on the single-station summer PDSI grid used for calibration and verification. In this case, the analysis period was 1913–78, common to all grid points. The nine varimax factors of the instrumental data are shown in Fig. 9. A visual comparison of the equivalent varimax factors in Figs. 8 and 9 (e.g., factor 9 with factor 1) indicates that the tree-ring estimates have indeed captured the regional summer drought climatologies in the U.S. very well. In particular, factor 9 in Fig. 9 (located equally over Colorado, Kansas, and Nebraska) is very similar to factor 1 in the reconstructions. So, it appears that the southwest factor of KK is not evident when only summer PDSI is evaluated. Rather, it is replaced by a drought factor located mainly over the eastern Colorado region.

Oblique promax rotation was applied next to the drought reconstructions. Although there were some ap-

parently significant correlations between some of the oblique factors (the four largest correlations are $r_{1,4} = 0.28$, $r_{1,7} = 0.33$, $r_{1,9} = 0.32$, and $r_{2,6} = 0.27$), the varimax and promax factors (not shown) were essentially identical. Therefore, the orthogonal varimax solution appears to be an adequate representation of the underlying regional summer drought factors in the U.S.

Figure 10 shows the factor scores estimated from the Fig. 8 varimax factors. These nine time series provide histories of relative drought and wetness for the identified regions. Some of the well-known droughts of the twentieth century are indicated in these histories. For example, the serious drought that struck the Northeast in the 1960s (Cook and Jacoby 1977) is indicated in the factor 2 scores. The drought that occurred during the “Dust Bowl” years of the 1930s (Stockton and Meko 1983) shows up in the scores of factors 3 and 4 in the Pacific Northwest and northern Great Plains. And the drought that struck the Texas region in the 1950s (Stahle and Cleveland 1988) is revealed in the scores of factor 7. In contrast, a notable wet period in the early 1900s is indicated in several of the factors. Prior to 1900, the factor scores reveal periods of drought and wetness that in some cases appear to be unprecedented in the record. The factor scores also show varying degrees of inter-

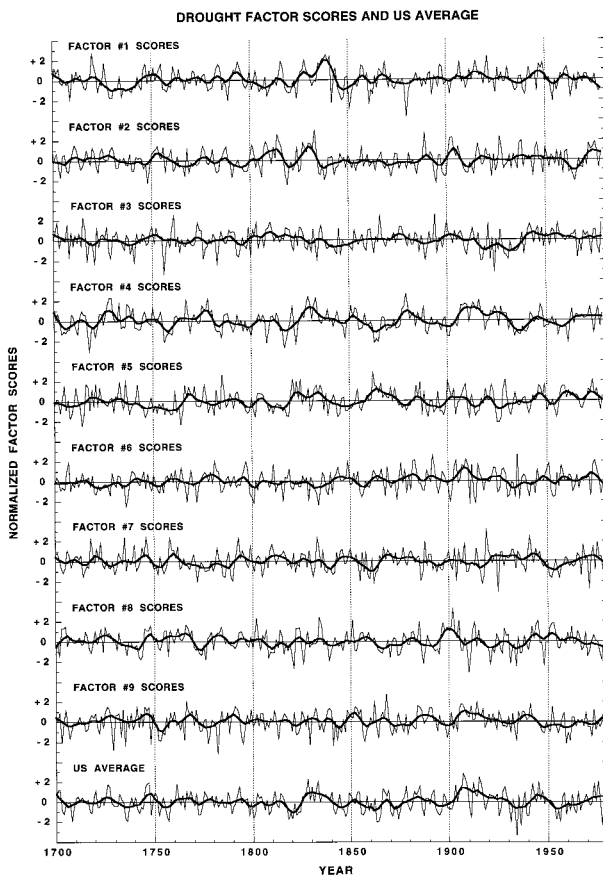


FIG. 10. The nine varimax factor scores of the loading maps shown in Fig. 8. These scores represent the regional histories of relative drought and wetness in the US since 1700. They have also been smoothed to emphasize the interdecadal (>10 yr) timescale of variability. The bottom time series is a weighted average of relative drought and wetness for the U.S. based on the scores of the first unrotated principal component of the reconstructions. It shows that the 1930s Dust Bowl drought was easily the most severe such event to hit the U.S. since 1700.

decadal variability, with factor 4 in the northern Great Plains showing the most multiyear power. Clearly, there is much to be learned about U.S. drought from the reconstructions produced here.

Also included in Fig. 10 is a plot of the scores of the first unrotated principal component of drought (U.S. average), scaled to have variance comparable to the varimax scores. This component accounts for 22% of the total PDSI variance. This series is effectively a (weakly) centrally weighted average of the actual drought reconstructions. Based on the very high correlations (~ 0.90) between the actual and estimated mean fields shown in Figs. 6b and 7b, this record is a highly accurate history of drought for the U.S. as a whole. It shows that the Dust Bowl drought of the 1930s was clearly the most severe event to strike the U.S. since 1700. Indeed, the two most extreme years in this series are 1934 and 1936. The third most severe drought year occurred in 1977. Other notable dry periods occurred around 1820, 1860,

and 1950. Two unusual wet periods also stand out in the 1820–40 and 1900–20 intervals.

c. Discussion

The results of our spatial comparisons between instrumental PDSIs and the tree-ring estimates indicate that the reconstructions have captured the inherent spatial variability of drought across the U.S. with a high degree of fidelity. This has been accomplished using PPR, which does not contain any explicit spatial component in its design, except for the selected search radius. The ability of PPR to reconstruct the spatial features of drought is undoubtedly due to the underlying regionality of climate in the U.S. that determines patterns of drought and wetness and, ultimately, patterns of tree growth (e.g., Fritts 1965; LaMarche and Fritts 1971).

7. Concluding remarks

The U.S. drought reconstruction grid produced here is a significant new application of dendroclimatic techniques to reconstruct past climate. The quality of the gridpoint reconstructions is generally quite good and spatially homogeneous. As noted earlier, the automated nature of the PPR method virtually guarantees that the gridpoint reconstructions produced here will not necessarily be the best possible at any given grid point. However, the PPR method does guarantee that each gridpoint model is developed in a consistent manner. Its specific implementation here also guarantees a near-global optimum in terms of model verification.

There is little doubt that the joint space–time methods of climate reconstruction (e.g., canonical regression or singular value decomposition) would have resulted in better calibration statistics here (e.g., a higher global R^2). These techniques are constrained to find the optimal linear association between two fields of variables. However, they would almost certainly lead to poorer verification results (see the verification surfaces shown in Appendix B, Fig. B1) because they would allow long-range, temporally unstable, tree-ring teleconnections to influence the estimation of the gridpoint PDSIs. The joint space–time methods would also be mathematically ill-conditioned if the original data were used directly here because the number of grid points (155) greatly exceeds the number of years (51) used for calibration. This problem can be ameliorated by reducing the dimensions of the problem through principal component analysis of the predictor and/or predictand fields prior to regression (Fritts 1976; Cook et al. 1994; Mann et al. 1998) but at the loss of higher-order dimensionality in the resulting field of reconstructions. The reconstructions produced by PPR do not have this limitation.

These reconstructions are freely available from the National Geophysical Data Center (NGDC), World Data Center-A for Paleoclimatology, in Boulder, Colorado.

(The Web site addresses for these data are <http://www.ngdc.noaa.gov/paleo/pdsiyear.html> for the annual PDSI maps and <http://www.ngdc.noaa.gov/paleo/us-client2.html> for the summer PDSI time series.) We hope that future analyses of these reconstructions will lead to an improved understanding of drought variability in the U.S., especially on the interdecadal timescale (e.g., Karl and Riebsame 1984), which is very difficult to investigate with instrumental climate data alone.

We expect to improve the drought reconstructions for the United States in the future through the use of improved statistical methods and, more importantly, the development of new tree-ring chronologies in areas that are now weakly modeled. In addition, efforts are now under way to extend the reconstructions back in time to enable analyses of drought variability at longer time-scales. Consequently, the PDSI reconstructions on the National Oceanic and Atmospheric Administration Web sites will be updated periodically as these improvements are made.

Acknowledgments. This research is supported by the National Oceanic and Atmospheric Administration, Office of Global Programs, Paleoclimatology Program through Grants NA36GP0139 and NA66GP0251, and is an outgrowth of previous support by the National Science Foundation, Grant ATM 88-14675 and the U.S. Geological Survey, Biological Resources Division, Agreement CA-8012-2-9001. The PDSI data were kindly obtained from Ned Guttman of NOAA. Most of the tree-ring chronologies used here came from the International Tree-Ring Data Bank (ITRDB) at the NGDC in Boulder. Others not in the ITRDB were kindly contributed by a number of scientists, including Hal Fritts, Lisa Graumlich, Tom Swetnam, Connie Woodhouse, Laura Haston, Joel Michaelsen, and Glen MacDonald.

APPENDIX A

The Point-by-Point Regression Method

Principal components regression analysis is the foundation of PPR and is described in Briffa et al. (1986) and Cook et al. (1994) for the multiple-predictor–multiple-predictand case. Here we give a brief description of this method, restricting it to the multiple-predictor–single-predictand case that is appropriate to PPR.

Let

$$\mathbf{y}_k = \mathbf{U}\mathbf{B} + \mathbf{e}_k, \quad (\text{A1})$$

where \mathbf{y}_k is the vector of standardized (i.e., zero mean, unit standard deviation) instrumental PDSIs at grid point k , \mathbf{U} is the matrix of orthogonal tree-ring principal component scores, \mathbf{B} is the matrix of regression coefficients, and \mathbf{e}_k is the vector of regression model errors. The actual tree-ring series used as predictors are related to their scores as

$$\mathbf{U} = \mathbf{X}\mathbf{F}, \quad (\text{A2})$$

where \mathbf{X} is the matrix of standardized tree-ring chronologies used as predictors and \mathbf{F} is the orthonormal matrix of column eigenvectors calculated from the correlation matrix of \mathbf{X} . Each of the k PPR regression models is developed here over the *calibration* time period 1928–78 common to the predictors and predictands, with the pre-1928 instrumental PDSI data reserved for regression model *verification* tests of the tree-ring model estimates. See Fritts (1976) and Cook et al. (1994) for more details concerning the calibration–verification procedures commonly used in dendroclimatology.

Once the regression coefficients in \mathbf{B} have been estimated for the calibration period, they can be applied to the precalibration period tree-ring scores after projecting the early tree-ring data onto the relevant eigenvectors in \mathbf{F} . The resulting augmented tree-ring scores in \mathbf{U} are then used to produce a series of standardized PDSI estimates back in time as

$$\hat{\mathbf{y}}_k = \mathbf{U}\mathbf{B}, \quad (\text{A3})$$

after which they are back-transformed into original PDSI units. Here we restrict our PDSI reconstructions to cover the period 1700–1978, which is the time interval common to all tree-ring chronologies in our network.

The description of the principal components regression model given in (A1)–(A3) is generic in that any tree-ring data can be used to form the principal component scores in \mathbf{U} . However, we have found that the reconstructions of PDSI from tree rings can be significantly improved through the careful use of autoregressive (AR) prewhitening of the both the tree rings and PDSI data prior to regression analysis. This procedure is used to correct for the sometimes large differences in short-lag autocorrelation between climate and tree rings that are believed to be due to physiological and stand dynamics effects on annual ring widths, which are unrelated to climate. In this case, low-order AR(p) models are fit to the time series used at each grid point as

$$\mathbf{z}_t = \sum_{i=1}^p \phi_i \mathbf{z}_{t-i} + a_t, \quad (\text{A4})$$

where z_t is the PDSI or tree-ring series used at grid point k , ϕ_i is the AR coefficient at lag- i yr, and a_t is the resulting series of “white noise” (i.e., serially random) residuals (Box and Jenkins 1970). The order p is objectively determined using the Akaike information criterion (AIC; Akaike 1974), with a correction for small sample bias (Hurvich and Tsai 1989). The original and corrected AICs are calculated as

$$\text{AIC} = N \ln \sigma_c^2 + 2(m + 1) \quad (\text{A5})$$

and

$$\text{AIC}_c = \text{AIC} + \frac{2(m + 1)(m + 2)}{N - m - 2}, \quad (\text{A6})$$

respectively, where N is the number of observations,

σ_e^2 is the residual variance of the model, and m is the number of explanatory variables. In the case of AR modeling, $m = p$.

The a_i of PDSI and tree rings are then used as y_k and \mathbf{X} in (A1) and (A2), respectively, instead of the original variables. The serially random property of the AR residuals simplifies tests of association between tree rings and drought because the degrees of freedom do not need to be corrected for persistence. In addition, the identification of lagged responses between tree rings and drought are also simplified by first prewhitening the time series prior to testing for lead-lag associations (Haugh and Box 1977).

After the \hat{y}_k are produced for grid point k , any autocorrelation in the PDSI that had been modeled and removed must be added back into the reconstruction. This operation usually involves adding some “redness” (i.e., positive autocorrelation) to the reconstructed PDSIs because most of the instrumental PDSI records behave as moderate “red noise” processes (sensu Gilman et al. 1963). This procedure is accomplished by substituting \hat{y} for \mathbf{z} in (A4) and using the ϕ_i of the grid point k PDSI series, with the necessary p starting values estimated by backcasting. It closely follows the “random shock model” method of Meko (1981) for reconstructing precipitation from tree rings.

The PPR method allows for precise control over which tree-ring chronologies and their principal component scores enter into the regression equation for reconstructing PDSI at each grid point. This control is exercised in four sequential stages of model development, which culminate in the selection of the final tree-ring predictors of drought. These stages result in the creation of four “pools” of tree-ring variables that seek to concentrate the common drought signal and winnow out the nondrought noise.

The level-1 pool of tree-ring variables contains those chronologies that are believed to be well related to drought at a given grid point due to their proximity to it alone. As noted earlier, the PPR method assumes that only those tree-ring chronologies proximal to a given PDSI grid point are likely to be true predictors of drought. Here we operationally define “proximal” to mean those tree-ring chronologies located within a given search radius around a PDSI grid point. This radius should be small enough to preserve the local and regional character of PDSI at each grid point but also large enough to include most or all of the “true” tree-ring predictors of drought.

The ideal search radius for this purpose would seem to be the same as that used for gridding the single-station PDSI records, that is, 150 km. However, this distance is generally impractical for many areas of the PDSI grid because the tree-ring network is much less dense and more patchy than the original single-station PDSI network. In addition, the central Great Plains is largely devoid of tree-ring chronologies, making a 150-km search radius clearly impractical there. Finally, regional

drought anomalies ought to exceed 150 km in radius on average given the size of the regional drought climatologies in the U.S. (cf. the drought factor maps in KK). This suggests that tree-ring chronologies from some greater distance (i.e., >150 km) ought to be useful predictors of PDSI at a grid point. The inherent patchiness of the tree-ring network also means that many areas of the grid will require a relatively small fixed search radius to find enough tree-ring chronologies, while other areas will require a larger search radius. This indicates the need for a dynamic search radius that will enlarge until a minimum number of tree-ring chronologies has been found for a given grid point. The minimum number used here is five, a compromise between locating a reasonable number of tree-ring chronologies per grid point versus the desire to minimize the size of the eventual search radius to preserve the meanings of proximal and true provided above. So, given a prescribed minimum search radius, the search for tree-ring chronologies is conducted as follows. If five or more series are found within the minimum radius from a PDSI grid point, the search is considered successful and terminated. If not, the search radius is expanded by 50-km increments until at least five chronologies are found.

The level-2 pool contains those tree-ring variables from the level-1 pool that are well correlated with PDSI. The level-1 search procedure only deals with finding candidate tree-ring chronologies within a given radius of each PDSI grid point. However, there is no guarantee that these candidates will be significantly correlated with PDSI at a grid point. For this reason, they are next subjected to statistical screening prior to use in regression analysis. This is accomplished by correlating the prewhitened candidate tree-ring variables with the prewhitened PDSIs over the calibration period 1928–78. The correlations are calculated using both year t and $t + 1$ tree-ring residuals as candidate predictors of year t PDSI residuals to allow for a 1-yr lag response to climate found in some tree-ring chronologies. Thus, for m candidate tree-ring chronologies found within a given search radius, there are actually $2m$ candidate predictors of PDSI at a grid point.

The screening criterion used is the two-tailed hypothesis test of the Pearson correlation coefficient (say $\alpha = 0.05$) with $n - 2$ degrees of freedom, in this case 49 for the 1928–78 calibration period. Depending on the α -level probability used for screening the level-1 candidate pool and the strength of the PDSI signal in the chronologies, the number of retained candidate predictors may be $\ll 2m$. This reduced set of m' tree-ring variables is the level-2 pool [matrix \mathbf{X} in (A2)] that is subjected to principal components analysis in the next stage of PPR.

The level-3 pool contains the tree-ring principal components that are retained as candidate predictors of PDSI in multiple regression analysis. Principal components analysis is used to reduce the size of the level-2 pool and concentrate common drought signal(s) further. Its

main virtues are the way in which it orthogonalizes the intercorrelated set of predictors and reduces the dimensions of the regression problem through the elimination of higher-order eigenvectors that account for very little variance. We use the objective Kaiser–Guttman eigenvalue-1 rule (Guttman 1954; Kaiser 1960) to eliminate those higher-order variables. This eigenvalue cutoff criterion typically reduces the dimension of the level-3 pool m'' to $<0.3m'$.

The level-4 pool of tree-ring predictor variables is the order of each gridpoint regression model, that is, the rank of \mathbf{U} in (A1). This is accomplished by first correlating the PDSIs with the orthogonal tree-ring scores over the 1928–78 calibration period. The correlations are then ranked in order of decreasing magnitude and entered into the model until the minimum AIC_c criterion is achieved. Because the entered variables are orthogonal, the square of each variable's correlation with PDSI is its partial R^2 , so the sum of those squared correlations is the final model R^2 .

APPENDIX B

Optimizing the Search Radius and Screening Probability Criteria

As implemented above, the level-3 and level-4 pooling procedures of PPR are fully automatic and objective. However, the level-1 and level-2 procedures contain somewhat ill-defined and subjective elements, these being the choice of the search radius and screening probability, respectively. There is no guarantee that a single, optimal search radius–screening probability combination exists for all points on the grid, where “optimal” means in this case the best possible reconstruction of PDSI at each location. To produce such optimal reconstructions would probably require modeling the 155 grid points as a series of completely independent regression problems, a very time-consuming and tedious option. However, one combination or narrow range of combinations of search radius–screening probability may produce on average, or *globally*, the best reconstructions across the grid. If a global optimum could be found for the search radius and screening probability, then the PPR method could be made fully objective and automatic.

To see to what degree a joint search radius–screening probability optimum exists for the PDSI grid, we conducted a number of experiments of PPR in which we varied the search radius and screening probability over a wide range of values. Specifically, we varied the search radius from 200 to 3000 km and the screening α -level probability from 0.05 to 0.40. The search radius upper limit was chosen to allow for possible transcontinental drought teleconnections to enter into the model, while the screening probability upper limit forced most variables into the principal components analysis.

To evaluate the test results, we calculated four sta-

tics as measures of goodness of fit between the actual and estimated PDSI. These tests used the actual PDSI data and the tree-ring estimates after autocorrelation had been added back into them, as described in appendix A. So, for all 155 PDSI grid points we calculated the following.

- 1) Average explained variance (R_c^2) over the 1928–78 calibration period is

$$R_c^2 = 1.0 - \left[\frac{\sum (x_i - \hat{x}_i)^2}{\sum (x_i - \bar{x}_c)^2} \right], \quad (\text{B1})$$

where x_i and \hat{x}_i are the actual and estimated data in year i of the calibration period and \bar{x}_c is the mean of the actual data. This is a direct measure of the least squares goodness of fit of the regression model that is achieved here by the minimum AIC_c criterion. However, R_c^2 is known to be a very poor, biased measure of true goodness of fit when the regression model is applied to data not used for calibration (Cramer 1987; Helland 1987), hence the need for regression model verification tests.

- 2) Average squared Pearson correlation (R_v^2) over the pre-1928 verification period is

$$R_v^2 = \frac{\left[\sum (x_i - \bar{x}_v)(\hat{x}_i - \bar{\hat{x}}_v) \right]^2}{\sum (x_i - \bar{x}_v)^2 \sum (\hat{x}_i - \bar{\hat{x}}_v)^2}, \quad (\text{B2})$$

where x_i and \hat{x}_i are the actual and estimated data in year i of the verification period and \bar{x}_v and $\bar{\hat{x}}_v$ are the means of the actual and reconstructed data in the verification period. This is a useful measure of covariance between the actual and estimated PDSIs in the verification period of withheld actual data. However, it is not sensitive to differences in mean level between the covariates. Therefore, it is the least rigorous of the three verification tests used here. The Pearson correlation itself also allows for negative relationships between variables, which would be nonsensical in the context of its application here. This never occurred in any of our PPR experiments.

- 3) Average reduction of error (RE) in the verification period is

$$\text{RE} = 1.0 - \left[\frac{\sum (x_i - \hat{x}_i)^2}{\sum (x_i - \bar{x}_c)^2} \right], \quad (\text{B3})$$

where x_i and \hat{x}_i are the actual and estimated data in year i of the verification period and \bar{x}_c is the mean of the actual data in the calibration period. This statistic was first introduced by Lorenz (1956) to meteorology as a measure of forecast skill, and has been extensively used in dendroclimatology to verify reconstructions of climate from tree rings (Fritts 1976; Kutzbach and Guetter 1980). Here RE has a theoretical range of $-\infty$ to $+1$. An $\text{RE} > 0$ indicates

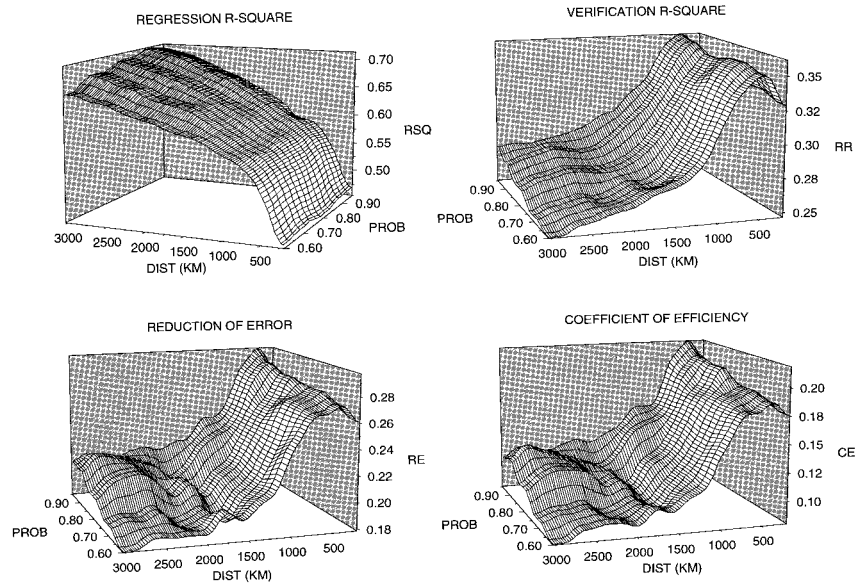


FIG. B1. The regression model calibration and verification surfaces as a function of search radius and screening probability. The screening probability is expressed as $1 - \alpha$, where α is the null hypothesis test probability. The R_c^2 surface increases without limit as the search radius enlarges, although the rate of increase diminishes beyond about 500 km. In contrast, the R_v^2 , RE, and CE surfaces all show general maxima in the form of a ridge along the 400–500-km search radius axis. Beyond that distance, the verification tests all do more poorly. The ridge of maximum verification is also not strongly dependent on screening probability.

hindcast or reconstruction skill in excess of climatology (i.e., \bar{x}_c); an RE < 0 indicates less skill than climatology.

- 4) Average coefficient of efficiency (CE) over the verification period is

$$CE = 1.0 - \frac{\sum (x_i - \hat{x}_i)^2}{\sum (x_i - \bar{x}_v)^2}, \quad (\text{B4})$$

where x_i and \hat{x}_i are the actual and estimated data in year i of the verification period and \bar{x}_v is the mean of the actual data in the verification period. This statistic was first described in the hydrology literature as an expression of the true R^2 of a regression equation when it is applied to new data (Nash and Sutcliffe 1971). Like RE, CE has a theoretical range of $-\infty$ to $+1$, but here the benchmark for determining skill is the verification period mean. Thus, a CE > 0 indicates skill in excess of the verification period climatology (i.e., \bar{x}_v); a CE < 0 indicates less skill than verification period climatology.

Among the verification statistics used here, the CE is the most rigorous. The only difference between the RE and CE lies in the denominator term. However, this difference generally makes the CE more difficult to pass (i.e., CE > 0). When $\bar{x}_v = \bar{x}_c$, CE = RE. But when $\bar{x}_v \neq \bar{x}_c$, RE will be greater than the CE by a factor related to that difference. This follows by noting that for the CE, the sum of squares in the denominator is fully corrected because \bar{x}_v is the proper mean. However for the

RE, the denominator sum of squares will not be fully corrected unless the calibration period mean is fortuitously identical to the verification period mean. When this is not the case, the denominator sum of squares of the RE will be larger than that of the CE resulting in RE > CE.

As described in section 2, the verification data available at each grid point varies in length depending on the lengths of the original station records used in gridding the PDSI. The median length of the pre-1928 data is 35 yr, with a minimum of 15, an interquartile range of 30–37, and a maximum of 90. The different lengths make verification across the network potentially inhomogeneous for comparative purposes. For this reason, we restricted the verification tests to data in the period 1893–1927. Thus, a maximum of 35 yr of data was used for verification at each grid point.

A total of 24 search radii ranging from 200 to 3000 km and five screening probability levels ranging from 0.05 to 0.40 were used, resulting in a total of 120 PPR test runs. The results of these runs are succinctly summarized in four surface plots shown in Fig. B1. For plotting purposes, the screening probabilities (i.e., α levels) are expressed as $1 - \alpha$ probabilities. The calibration R_c^2 surface shows a nearly monotonic increase in explained variance with increasing distance. This effect occurs regardless of the screening probability used. However, the R_c^2 surface does show a clear break in slope at a distance of 400–500 km. At longer distances, the rate of increase in R_c^2 noticeably declines. Thus, most

of the explained variance comes from tree-ring chronologies located within about 500 km of the PDSI grid points on average. In contrast, the R_v^2 , RE, and CE surfaces are radically different. Each of these verification statistics shows that PDSI reconstruction fidelity increases as the search radius increases from 200 to 400–500 km for each grid point on average. At greater distances there is a clear loss of fidelity. Interestingly, reconstruction fidelity rebounds somewhat at distances in excess of 2000 km, especially for the more stringent screening probabilities. This result probably reflects true synoptic-scale teleconnection patterns of drought and wetness in the continental U.S. Presumably, the stricter screening probabilities also winnowed out many spurious tree-ring chronologies, resulting in a noticeable increase in long-range verification performance. However, this rebound never regains the fidelity lost by increasing the search radius beyond ~ 500 km. Consequently, nothing is truly gained by searching for long-range tree-ring teleconnections with drought in the U.S., except excessively inflated R_c^2 .

The verification surfaces in Fig. B1 indicate the presence of a ridge of maximum reconstruction fidelity that consistently falls in the 400–500-km search radius band. This ridge is only weakly dependent on screening probability. Thus “search radius,” which determines the size of the level-1 pool of candidate tree-ring predictors, is clearly the most important free variable to select properly in the PPR method. Based on the results here, we concluded that a search radius of 450 km was the best global search radius to use. As the second free variable in this test, “screening probability” had a much weaker effect on the PPR method. Presumably, the use of principal components analysis on the level-2 pool of screened tree-ring chronologies served to protect the subsequent regression results from the inclusion of weakly correlated or spurious tree-ring predictors. Even so, there is some indication of improved verification with increasing $1 - \alpha$ probability along the 400–500-km ridge. Therefore, we chose an α -level probability of 0.10 for screening the tree-ring chronologies entering into the level-2 pool. With these two free variables fixed, the PPR method can be applied automatically for reconstructing drought across the continental U.S.

With regard to our selected 450-km search radius, the median level-1 pool size was 48 tree-ring variables, which equates to 24 tree-ring chronologies for years t and $t + 1$. This initial pool of candidate variables was reduced to a median size of 18 after screening with $\alpha = 0.10$. After principal components analysis of the 18 retained variables, a median of six eigenvectors passed the Kaiser–Guttman test. Finally, the minimum AIC_c test entered a median of three principal components into the regression model. Thus, the PPR method reduced the median predictor variable space from 48 to 3 variables, a 93.7% reduction in the variable pool size, resulting in a large conservation of degrees of freedom in the final regression model. Since the expected value

for R_c^2 increases with the number of variables in a regression model (Morrison 1990) and also increases with the number of candidate predictors available for regression (Rencher and Pun 1980), the sequential reduction of predictor variable pool size should also reduce the inflation of R_c^2 .

REFERENCES

- Akaike, H., 1974: A new look at the statistical model identification. *IEEE Trans. Autom. Control*, **AC-19**, 716–723.
- Barnston, A. G., and R. E. Livezey, 1987: Classification, seasonality, and persistence of low-frequency atmospheric circulation patterns. *Mon. Wea. Rev.*, **115**, 1083–1126.
- Bergman, K. H., C. F. Ropelewski, and M. S. Halpert, 1986: The record Southeast drought of 1986. *Weatherwise*, **39**, 262–266.
- Blasing, T. J., and D. N. Duvick, 1984: Reconstruction of precipitation history in North American corn belt using tree rings. *Nature*, **307**, 143–145.
- Box, G. E. P., and G. M. Jenkins, 1970: *Time Series Analysis: Forecasting and Control*. Holden-Day, 553 pp.
- Bretherton, C. S., C. Smith, and J. M. Wallace, 1992: An intercomparison of methods for finding coupled patterns in climate data. *J. Climate*, **5**, 541–560.
- Briffa, K. R., P. D. Jones, T. M. L. Wigley, J. R. Pilcher, and M. G. L. Baillie, 1986: Climate reconstruction from tree rings: Part 2, Spatial reconstruction of summer mean sea-level pressure patterns over Great Britain. *J. Climatol.*, **6**, 1–15.
- Broadbrooks, W. J., and P. B. Elmore, 1987: A Monte Carlo study of the sampling distribution of the congruence coefficient. *Educ. Psychol. Meas.*, **47**, 1–11.
- Cole, J. E., and E. R. Cook, 1998: The changing relationship between ENSO variability and moisture balance in the continental United States. *Geophys. Res. Lett.*, **25**, 4529–4532.
- Cook, E. R., and G. C. Jacoby Jr., 1977: Tree-ring–drought relationships in the Hudson Valley, New York. *Science*, **198**, 399–401.
- , M. A. Kablack, and G. C. Jacoby, 1988: The 1986 drought in the southeastern United States: How rare an event was it? *J. Geophys. Res.*, **93**, 14 257–14 260.
- , D. W. Stahle, and M. K. Cleaveland, 1992: Dendroclimatic evidence from eastern North America. *Climate Since AD 1500*, R. S. Bradley and P. D. Jones, Eds., Routledge, 331–348.
- , K. R. Briffa, and P. D. Jones, 1994: Spatial regression methods in dendroclimatology: A review and comparison of two techniques. *Int. J. Climatol.*, **14**, 379–402.
- , D. M. Meko, D. W. Stahle, and M. K. Cleaveland, 1996: Tree-ring reconstructions of past drought across the coterminous United States: Tests of a regression method and calibration/verification results. *Tree Rings, Environment, and Humanity*, J. S. Dean, D. M. Meko, and T. W. Swetnam, Eds., Radiocarbon, 155–169.
- , —, and C. W. Stockton, 1997: A new assessment of possible solar and lunar forcing of the bidecadal drought rhythm in the western United States. *J. Climate*, **10**, 1343–1356.
- , J. E. Cole, R. D. D’Arrigo, D. W. Stahle, and R. Villalba, 1999: Tree ring records of past ENSO variability and forcing. *El Niño and the Southern Oscillation: Multiscale Variability and its Impacts on Natural Ecosystems and Society*, H. F. Diaz and V. Markgraf, Eds., Cambridge University Press, in press.
- Cramer, J. S., 1987: Mean and variance of R^2 in small and moderate samples. *J. Econometrics*, **35**, 253–266.
- Fritts, H. C., 1965: Tree-ring evidence for climatic changes in western North America. *Mon. Wea. Rev.*, **93**, 421–443.
- , 1976: *Tree Rings and Climate*. Academic Press, 567 pp.
- , 1991: *Reconstructing Large-Scale Climate Patterns from Tree-Ring Data*. The University of Arizona Press, 286 pp.
- , T. J. Blasing, B. P. Hayden, and J. E. Kutzbach, 1971: Multivariate techniques for specifying tree-growth and climate rela-

- tionships and for reconstructing anomalies in paleoclimate. *J. Appl. Meteor.*, **10**, 845–864.
- Gilman, D. L., F. J. Fuglister, and J. M. Mitchell Jr., 1963: On the power spectrum of “red noise.” *J. Atmos. Sci.*, **20**, 182–184.
- Glahn, H. R., 1968: Canonical correlation and its relationship to discriminant analysis and multiple regression. *J. Atmos. Sci.*, **25**, 23–31.
- Graumlich, L. J., 1993: A 1000-year record of temperature and precipitation in the Sierra Nevada. *Quat. Res.*, **39**, 249–255.
- Guttman, L., 1954: Some necessary conditions for common-factor analysis. *Psychometrika*, **19**, 149–161.
- Guttman, N., 1991: Sensitivity of the Palmer hydrologic drought index to temperature and precipitation departures from average conditions. *Water Res. Bull.*, **27**, 797–807.
- Haston, L., and J. Michaelsen, 1994: Long-term central coastal California precipitation variability and relationships to El Niño–Southern Oscillation. *J. Climate*, **7**, 1373–1387.
- , and —, 1997: Spatial and temporal variability of southern California precipitation over the last 400 yr and relationships to atmospheric circulation patterns. *J. Climate*, **10**, 1836–1852.
- Haug, L. D., and G. E. P. Box, 1977: Identification of dynamic regression (distributed lag) models connecting two time series. *J. Amer. Stat. Assoc.*, **72**, 121–130.
- Helland, I. S., 1987: On the interpretation and use of R^2 in regression analysis. *Biometrics*, **43**, 61–69.
- Hendrickson, A. E., and P. O. White, 1964: Promax: A quick method for rotation to oblique simple structure. *Br. J. Stat. Psychol.*, **17**, 65–70.
- Hurvich, C. M., and C. Tsai, 1989: Regression and time series model selection in small samples. *Biometrika*, **76**, 297–307.
- Kaiser, H. F., 1960: The application of electronic computers to factor analysis. *Educ. Psychol. Meas.*, **20**, 141–151.
- Karl, T. R., and A. J. Koscielny, 1982: Drought in the United States. *J. Climatol.*, **2**, 313–329.
- , and W. E. Riebsame, 1984: The identification of 10- to 20-year temperature and precipitation fluctuations in the contiguous United States. *J. Climate Appl. Meteor.*, **23**, 950–966.
- , C. N. Williams Jr., and F. T. Quinlan, 1990: United States Historical Climatology Network (HCN) serial temperature and precipitation data. Environmental Sciences Division Publ. 3404, 371 pp. [Available from Carbon Dioxide Information Analysis Center, Oak Ridge National Laboratory, Oak Ridge, TN 37831.]
- Kutzbach, J. E., and P. J. Guetter, 1980: On the design of paleoenvironmental data networks for estimating large-scale patterns of climate. *Quat. Res.*, **14**, 169–187.
- LaMarche, V. C., Jr., and H. C. Fritts, 1971: Anomaly patterns of climate over the western United States, 1700–1930, derived from principal component analysis of tree-ring data. *Mon. Wea. Rev.*, **99**, 138–142.
- Langbein, W. B., and J. R. Slack, 1982: Yearly variations in runoff and frequency of dry years for the conterminous United States, 1911–79. U.S. Geological Survey Open-File Rep. 82-751, 85 pp. [Available from Branch of Distribution, USGS, Box 25425, Denver Federal Center, Denver, CO 80225.]
- Lorenz, E. N., 1956: Empirical orthogonal functions and statistical weather prediction. Statistical Forecasting Scientific Rep. 1, Department of Meteorology, Massachusetts Institute of Technology, Cambridge, MA, 57 pp.
- Mann, M. E., R. S. Bradley, and M. K. Hughes, 1998: Global-scale temperature patterns and climate forcing over the past six centuries. *Nature*, **392**, 779–787.
- Matthai, H. F., 1979: Hydrologic and human aspects of the 1976–77 drought. USGS Prof. Paper 1130, U.S. Government Printing Office, 84 pp. [Available from U.S. Government Printing Office, Washington, DC 20402.]
- Meko, D. M., 1981: Applications of Box-Jenkins methods of time series analysis to the reconstruction of drought from tree rings. Unpublished Ph.D. dissertation, The University of Arizona, 149 pp.
- , 1992: Dendroclimatic evidence from the Great Plains of the United States. *Climate Since A.D. 1500*, R. S. Bradley and P. D. Jones, Eds., Routledge, 312–330.
- , E. R. Cook, D. W. Stahle, C. W. Stockton, and M. K. Hughes, 1993: Spatial patterns of tree-growth anomalies in the United States and southeastern Canada. *J. Climate*, **6**, 1773–1786.
- Mitchell, J. M., Jr., C. W. Stockton, and D. M. Meko, 1979: Evidence of a 22-year rhythm of drought in the western United States related to the Hale solar cycle since the 17th century. *Solar–Terrestrial Influences on Weather and Climate*, B. M. McCormac and T. A. Seliga, Eds., D. Reidel, 125–144.
- Morrison, D. F., 1990: *Multivariate Statistical Methods*. 3d ed. McGraw-Hill, 480 pp.
- Namias, J., 1955: Some meteorological aspects of drought with special reference to the summers of 1952–54 over the United States. *Mon. Wea. Rev.*, **83**, 199–205.
- , 1966: Nature and possible causes of the northeastern United States drought during 1962–65. *Mon. Wea. Rev.*, **94**, 543–554.
- , 1978: Multiple causes of the North American abnormal winter 1976–77. *Mon. Wea. Rev.*, **106**, 279–295.
- Nash, J. E., and J. V. Sutcliffe, 1971: Riverflow forecasting through conceptual models 1, A discussion of principles. *J. Hydrol.*, **10**, 282–290.
- Palmer, W. C., 1965: Meteorological drought. Weather Bureau Res. Paper 45, U.S. Department of Commerce, Washington, DC, 58 pp.
- Rencher, A. C., and F. C. Pun, 1980: Inflation of R^2 in best subset regression. *Technometrics*, **22**, 49–53.
- Reyment, R., and K. G. Jöreskog, 1993: *Applied Factor Analysis in the Natural Sciences*. Cambridge University Press, 371 pp.
- Richman, M. B., 1986: Rotation of principal components. *J. Climatol.*, **6**, 293–335.
- Roos, M., 1994: Is the California drought over. Proceedings of the Tenth Annual Pacific Climate (PACLIM) Workshop, Interagency Ecological Studies Program for the Sacramento-San Joaquin Estuary, Tech. Rep. 36, 123–128.
- Ropelewski, C. F., and M. S. Halpert, 1986: North American precipitation and temperature patterns associated with the El Niño/Southern Oscillation (ENSO). *Mon. Wea. Rev.*, **114**, 2352–2362.
- Stahle, D. W., and M. K. Cleaveland, 1988: Texas drought history reconstructed and analyzed from 1698–1980. *J. Climate*, **1**, 59–74.
- , —, and J. G. Hehr, 1985: A 450-year drought reconstruction for Arkansas, United States. *Nature*, **316**, 530–532.
- , —, and —, 1988: North Carolina climate changes reconstructed from tree rings: A.D. 372–1985. *Science*, **240**, 1517–1519.
- Stockton, C. W., and D. M. Meko, 1975: A long-term history of drought occurrence in western United States inferred from tree rings. *Weatherwise*, **28**, 244–249.
- , and —, 1983: Drought recurrence in the Great Plains as reconstructed from long-term tree-ring records. *J. Climate Appl. Meteor.*, **22**, 17–29.
- Warrick, R. A., 1980: Drought in the Great Plains: A case study of research on climate and society in the U.S.A. *Climatic Constraints and Human Activities*, J. Ausubel and A. K. Biswas, Eds., Pergamon, 93–124.
- Woodhouse, C., and D. Meko, 1997: Number of winter precipitation days reconstructed from southwestern tree rings. *J. Climate*, **10**, 2663–2669.

North American drought: Reconstructions, causes, and consequences

Edward R. Cook^{a,*}, Richard Seager^a, Mark A. Cane^a, David W. Stahle^b

^a *Lamont-Doherty Earth Observatory, Palisades, NY 10964 USA*

^b *Department of Geosciences, University of Arkansas, Fayetteville, AR 72701 USA*

Received 29 December 2005; accepted 18 December 2006

Available online 3 January 2007

Abstract

Severe drought is the greatest recurring natural disaster to strike North America. A remarkable network of centuries-long annual tree-ring chronologies has now allowed for the reconstruction of past drought over North America covering the past 1000 or more years in most regions. These reconstructions reveal the occurrence of past “megadroughts” of unprecedented severity and duration, ones that have never been experienced by modern societies in North America. There is strong archaeological evidence for the destabilizing influence of these past droughts on advanced agricultural societies, examples that should resonate today given the increasing vulnerability of modern water-based systems to relatively short-term droughts. Understanding how these megadroughts develop and persist is a timely scientific problem. Very recently, climate models have succeeded in simulating all of the major droughts over North America from the Civil War to the severe 1998–2004 drought in the western U.S. These numerical experiments indicate the dominating importance of tropical Pacific Ocean sea surface temperatures (SSTs) in determining how much precipitation falls over large parts of North America. Of central importance to drought formation is the development of cool “La Niña-like” SSTs in the eastern tropical Pacific region. This development appears to be partially linked to changes in radiative forcing over that region, which affects the Bjerknes feedback mechanism of the ENSO cycle there. Paradoxically, warmer conditions over the tropical Pacific region lead to the development of cool La Niña-like SSTs there, which is drought inducing over North America. Whether or not this process will lead to a greater prevalence of drought in the future as the world warms due to accumulating greenhouse gases is unclear at this time.

© 2007 Elsevier B.V. All rights reserved.

Keywords: North American drought; Palmer drought index; tree rings; drought reconstructions; drought causes and consequences; ENSO variability

1. Introduction

The western United States (the ‘West’) has been in the grip of a severe drought since late 1999, which only recently (mid-2005) appears to be ending (U.S. Drought Monitor; <http://www.drought.unl.edu/dm/monitor.html>; Svoboda et al., 2002). Whether or not this change towards wetter conditions truly represents the end of this severe multi-year drought remains to be seen. However,

at its peak in July 2002, more than 50% of the contiguous U.S. was under moderate to severe drought conditions, with record or near-record precipitation deficits throughout the West (Lawrimore and Stephens, 2003). Large portions of the Canadian Prairie provinces also suffered from severe drought (Agricultural and Agri-Food Canada, 2002), as well as extensive areas of Mexico, particularly in the northern and western parts of the country (Lawrimore et al., 2002; consult the March 2003 drought map and associated report located at the North American Drought Monitor website address provided with the reference).

* Corresponding author. Tel.: +1 845 365 8618; fax: +1 845 365 8152.
E-mail address: drdendro@ldeo.columbia.edu (E.R. Cook).

The impacts of this drought on the West have been considerable. Four consecutive years of drought resulted in water supply deficits in reservoir storage, with 10 of 11 western states having below average storage by May 2004, and below 50% capacity in Arizona, New Mexico, Nevada, Utah, and Wyoming (USDA, 2004). By September 22, 2004, the elevation of Lake Powell was down 129 ft from full pool level, only 38% of *live* capacity (Upper Colorado Region Water Operations Data; <http://www.usbr.gov/uc/crsp/GetSiteInfo>). Most of this water loss from Lake Powell occurred in only three years beginning with the epic 2002 drought year, down from a lake level that was near its historic maximum in early 2000. Exacerbated by drought conditions, the 2002 fire season was the second worst in the last 50 yr, with wildfire burning over 370,000 ha, including the largest fires in the past century in Oregon, Arizona, and Colorado (NASA, 2004). Persistent drought in the American Southwest in combination with associated insect outbreaks also resulted in over three million acres of pinyon and ponderosa pine mortality in Arizona and New Mexico (Betancourt, 2003), with die-off spreading into southwestern Colorado as well. This drought highlights both the extreme vulnerability of the semi-arid West to shortfalls in precipitation and the need to better understand long-term drought variability and its causes in North America.

The impact of drought on the environment is obvious. Perhaps less obvious is its surprisingly high economic cost. Over the years 1980 to 2003, for the United States as a whole, droughts (and associated heat waves) accounted for 10 of the 58 weather-related disasters that are estimated to have cost more than one billion dollars (normalized to 2002 dollars; Ross and Lott, 2003). Those drought disasters (17.2% of the total) accounted for \$144 billion (41.2%) of the estimated \$349 billion total cost of all weather-related disasters (Ross and Lott, 2003). This is considerably more, at least until Hurricane Katrina struck the Gulf Coast, than the cost of hurricanes and tropical storms, the most frequent source of billion-dollar disasters: (16 events and 102 billion dollars over the same time period). So, in economic terms alone, droughts are the most costly natural disasters to strike the United States.

Drought maps of three notable billion-dollar drought years are shown in Fig. 1: 1980, 1988, and 2002. The estimated cost of the 2002 drought year was at \$10 billion far less than the estimated cost of droughts in 1980 (\$48.8 billion) and 1988 (\$61.6 billion). So even though the 2002 drought year was extreme, and in some areas of the West unprecedented, its overall economic impact was comparatively low. The reason for this is

probably related to where the 2002 drought happened, i.e., mostly in the inter-montane West where population density and agricultural production are relatively low. In contrast, the 1980 and 1988 droughts occurred especially over the northern and eastern Great Plains (see also Fye et al., 2004), regions of more intensive agriculture and greater population density. The number of human deaths from those droughts and associated heat waves was also high in 1980 (~10,000 deaths) and 1988 (~7500 deaths), but zero in 2002 (Ross and Lott, 2003). Location does matter for the socioeconomic impacts of drought.

Though the most recent multi-year drought to strike the West was severe, especially in terms of its impact on water resources, the two most severe droughts since 1900 remain the legendary 1930's "Dust Bowl" drought (1929–1940) and the 1950's Southwest drought (1946–1956) (Fye et al., 2003, 2004). These start and end year dates were determined by an objective method based on the duration of running sums of PDSI values (Fye et al., 2003). The two worst years of those droughts, 1934 and 1956, are shown in Fig. 2. The environmental impact of the 12-year Dust Bowl drought was certainly severe, but the great dust storms associated with it were largely a product of poor agricultural practices that exposed the subsurface soil to desiccation and wind erosion. It is hard to assign a firm economic cost to the Dust Bowl drought, which was especially severe in the northern Rocky Mountains and northern Great Plains. One indication of its economic cost comes from a paper on the effects of drought on vegetation in Montana (Ellison and Woolfolk, 1937). That report mentions that 350,000 "drought-relief" cattle were purchased by the government in 1934–35 for 38 counties in Montana at a cost of \$5 million (\$66 million in 2002 dollars; see Sahr, 2005). Viewed over the entire region affected by drought, Warrick (1980) estimates that financial assistance from the government may have been as high as \$1 billion in 1930s dollars (\$13 billion in 2002 dollars) by the end of the drought, a number that reflects only part of the total economic cost of the Dust Bowl drought. There is also no question about the immense social impact the drought had on farmers and ranchers, who were forced to flee the parched and exhausted soils of the Great Plains for better conditions elsewhere (Worster, 1979). That this upheaval occurred during the economic 'Great Depression' exacerbated the impact.

The 11-year 1950's Southwest drought was likewise extreme, with it being centered primarily over Texas and New Mexico. The environmental impact of the Southwest drought was severe, but it had less socioeconomic impact than the Dust Bowl drought because of irrigation,

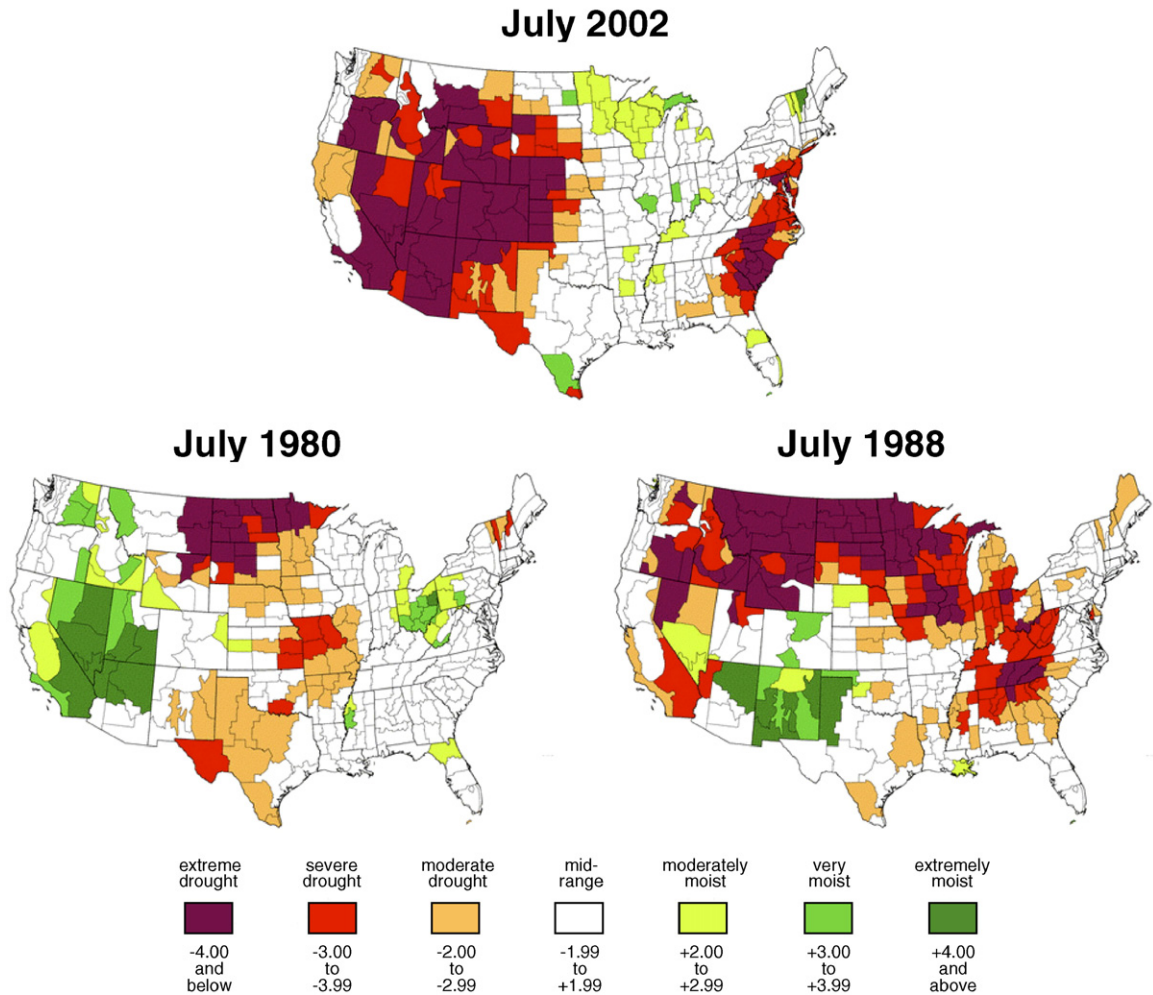


Fig. 1. Maps showing the U.S. regions most affected by drought in 1980, 1988, and 2002. The drought metric used for this purpose is the Palmer Drought Severity Index (Palmer, 1965). Note that the 2002 drought was mostly restricted to the inter-montane West, while the other two droughts were located more so in more agriculturally important regions of the Great Plains and Corn Belt. (Maps from <http://www.ncdc.noaa.gov/oa/climate/research/drought/palmer-maps/>).

improved agricultural practices, better governmental support, and a much stronger underlying economy. Regardless, the hydroclimatic severity and duration of the 12-year Dust Bowl and 11-year Southwest droughts tell us from even the relatively short 20th century climate records that things could get worse than the recent drought in the West that has lasted only 5–6 yr and, depending on locale, may not yet be ending.

The annual drought maps in Figs. 1 and 2 also illustrate that individual drought years are not necessarily good indicators of cumulative environmental and socioeconomic impacts. One dry year may be accommodated without undue environmental and economic harm providing that it is sufficiently offset by wetter conditions the following year. What really matters is *duration* because recovery from the cumulative damage

of consecutive drought years is more difficult. Thus, while the 1934 drought year clearly exceeds the overall severity of the other years shown in Figs. 1 and 2, it was also part of a much longer sequence of drier than average years (Fye et al., 2004) that resulted in the catastrophic Dust Bowl drought.

Given the enormous environmental and socioeconomic impacts of drought over the U.S., Canada, and Mexico, it is important to develop a better understanding of North American drought, especially for multi-year events. This is a propitious time to review the state of present knowledge because of striking advances in just the past two or three years:

- (1) A recent reconstruction of North American drought from AD 800 (Cook et al., 2004) creates

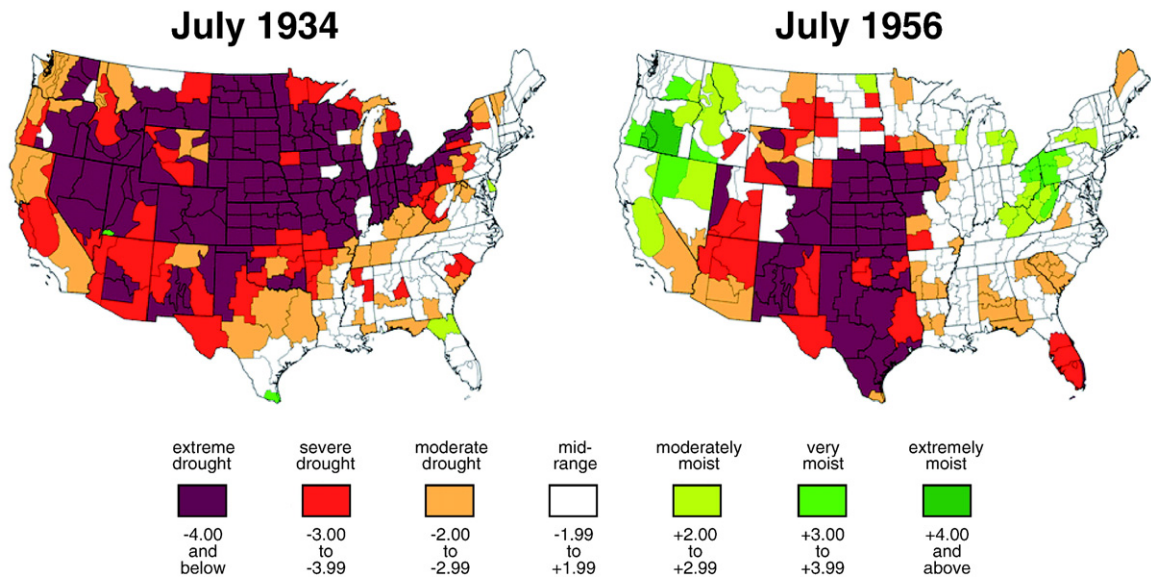


Fig. 2. Maps showing the U.S. regions most affected by drought in 1934 and 1956. These two years are part of the Dust Bowl and Southwest droughts, considered to be the worst of the 20th century. (Maps from <http://www.ncdc.noaa.gov/oa/climate/research/drought/palmer-maps/>).

the first annual, regionally resolved picture of more than a millennium of droughts and wet periods for most of the North American continent. It provides a context for the handful of droughts that we know of from the instrumental period (roughly, the 1850s onward) and a more complete picture of North American droughts of exceptional intensity and duration, “megadroughts” (Woodhouse and Overpeck, 1998; Stahle et al., 2000). For example, the 16th century megadrought identified by Stahle et al. (2000) is now seen to have affected large areas of North America, especially in the West and northern Mexico, and was much more prolonged than any of the 20th century droughts. The drought reconstructions also provide clear evidence for a much drier climate across the West and Great Plains during Medieval times, a drought that lasted with few interruptions for a few hundred years and which greatly taxed both hunter–gatherer and agriculturalist populations (Jones et al., 1999). Such “no analog” megadroughts are scary because the modern-day agricultural and hydrologic systems that depend upon adequate water supplies to produce and function may not have the resilience to survive much beyond the observed “worst case scenario” droughts of the past 100–150 yr, e.g., the Dust Bowl drought. The unprecedented growth of the West occurring now, with its increasing demand for water, makes this concern for the future even

more serious. So, understanding the causes of these past megadroughts is vitally important.

- (2) There has been rapid progress in simulating North American drought with comprehensive atmospheric general circulation models (AGCMs; Schubert et al., 2004b; Seager et al., 2005b; Herweijer et al., 2006). If global sea surface temperatures (SSTs) are specified, then important droughts such as those of the 1930s and 1950s are largely reproduced by the AGCMs. These results add important evidence about causality to the strong statistical association between certain spatial drought patterns over North America and SST anomalies over the tropical Pacific Ocean (Cole and Cook, 1998; Cook et al., 2000; Cole et al., 2002; Fye et al., 2004). An astonishing finding of this modeling work is that droughts with such major ecological and socioeconomic impacts apparently were “forced” by coherent tropical SST signals of no more than a few tenths of a degree Celsius.
- (3) The modeling results have stimulated a new understanding of the mechanisms connecting tropical SST anomalies to drought over North America. The most accepted ideas about “teleconnections” rely on Rossby wave propagation to mid-latitudes. In addition, it now appears that zonally symmetric changes in the atmospheric circulation in subtropical and middle latitudes driven by the overall warming of the tropical troposphere are a means whereby the tropics influence the mid-

latitudes throughout the year, (Seager et al., 2003, 2005a,b; Lau et al., 2006, in press). Both mechanisms imply that North American droughts should be an element of a more global pattern of drought (e.g., in southern South America, parts of Europe and Asia) (Herweijer and Seager, 2006).

- (4) To date the only part of the climate system that has proved to be predictable on seasonal and longer timescales is the tropical Pacific. That North American droughts – and their associated global hydroclimatic regimes – are linked to tropical SSTs raises the question of whether the SST patterns responsible are predictable on the time-scales of years to decades over which a serious drought develops. The importance of tropical SSTs for forcing these global hydroclimatic regimes also makes it clear that the hydrological future of many areas will be influenced by how the tropical atmosphere–ocean system responds to anthropogenic forcing. This is currently a subject of great uncertainty in model simulations and one for which theoretical understanding is limited at best.
- (5) Recent research has greatly extended our knowledge of the cultural and social impacts of past droughts (Stahle and Dean, in press). Examining these connections reveals the vulnerability of past cultures to drought, cautionary tales that especially resonate now because of the recent and perhaps ongoing drought in the West.

This paper aims to report on the current status of research into North American droughts and their consequences. It does not purport to be a comprehensive review of all work to date, much of which has been made obsolete as a result of the recent climate modeling studies. In the next section we describe the Palmer Drought Severity Index (PDSI) and explain why it is used to characterize drought. Sections 3 and 4 describe the tree-ring network that is used for drought reconstruction and the statistical methods employed. The reader who is primarily interested in the actual droughts, or is familiar with the methodology used for drought reconstruction from tree rings, may want to jump ahead to Section 5 where reconstructed drought variability since 800A.D. is discussed together with evidence for widespread medieval megadroughts. Following this, in Section 6, the social impacts of selected droughts over the last 1000 yr are discussed. This includes examples of the impacts of droughts on Indian cultures and also presents a climate background to the changing nature of European immigrants perceptions of the West through the Nineteenth Century from descriptions of the ‘Great

American Desert’ to a later ‘garden myth’ that coincided with the opening of the railroads and migration of settlers into the Plains.

Section 7 presents the results of climate modeling studies (conducted at LDEO) and makes the case for droughts being forced by cold tropical Pacific sea surface temperature (SST) anomalies. The zonal mean eddy–mean flow interaction and Rossby wave teleconnection means of transmitting the signal of cold SSTs into the mid-latitudes is discussed and it is argued that North American droughts fit into a global pattern of hydroclimate regimes with elements of zonal and hemispheric symmetry. Modeling results are illustrated through a case study of the 1890s drought, the one that created a semblance of realism in the attitudes of the Federal government to settlement of the arid regions of the West. Section 8 discusses the causes of tropical Pacific SST anomalies both on decadal timescales and over the last millennium and makes the case that the medieval megadrought was caused by a shift to a more La Nina-like state during those centuries which itself was forced by relatively high solar irradiance and weak volcanism. Section 9 considers how tropical SSTs will change in the greenhouse future and how this will impact the hydroclimatic future of the West. A summary and conclusions are offered in Section 10.

2. Measuring drought variability over North America

The environmental and socioeconomic impacts of drought over North America reveal a great need for a detailed history of drought variability and extremes for real-time drought assessment studies as new droughts develop, for modeling the causes of drought, and for improving drought prediction. As a step in that direction, Karl and Koscielny (1982) used the Palmer Drought Severity Index (PDSI; Palmer, 1965), calculated from monthly temperature and precipitation data, to describe the temporal and spatial properties of drought over the coterminous U.S. back to 1895. Prior to 1895, the available climate data used to calculate PDSI were too sparse for any earlier large-scale analyses of drought across the U.S. Shabbar and Skinner (2004) developed a similar PDSI dataset for most of Canada, but only as far back as 1940 because of short instrumental climate records in the more northerly latitudes.

Dai et al. (1998, 2004) expanded the spatial coverage of PDSI on a regular 2.5° grid to cover most of North America and other global land areas, in the process extending the PDSI records back to 1870 at some locations as well. The paucity of early climate records in northern Canada and much of Mexico limits the

usefulness of these PDSI estimates prior to the early 20th century. Another gridded PDSI dataset for North America south of 50° N has recently been produced by van der Schrier et al. (2006b). It extends back to 1901 at all locations of the grid and is based on finely interpolated monthly temperature and precipitation data (New et al., 2000; Mitchell et al., 2004; Mitchell and Jones, 2005). Again, the quality of these PDSI estimates suffers in areas like Mexico with few climate records that extend back into the early 20th century.

Based on instrumental data alone, we are largely restricted to studies of variability over the 20th century. More or less, the PDSI is a commonly used metric of drought over North America and other global land areas. Other measures of drought have also been developed for use in North America and elsewhere (Heim, 2002), such as the Standardized Precipitation Index (Guttman, 1998), but are not used to the same degree as the PDSI.

So, what exactly is the PDSI? Succinctly put, the PDSI is a reflection of how much soil moisture is currently available compared to that for normal or average conditions. The PDSI incorporates both precipitation and temperature data in a reasonably realistic water balance model that accounts for both supply (rain or snowfall water equivalent) and demand (temperature transformed into units of water lost through evapotranspiration), which affect the content of a simple 2-layer soil moisture reservoir model. A runoff term is also activated when the reservoir is full. See Palmer (1965) for details. The PDSI is most commonly calculated at monthly time steps, although there is no formal restriction on its calculation at shorter or longer intervals. The PDSI has built into its formulation a Markovian persistence term of 0.897 from one time step to the next, corresponding to an e-folding time of ~10 months. This is expressed as

$$PDSI_t = .0897 * PDSI_{t-1} + (1/3)Z_t$$

where Z_t is the moisture anomaly index for time t (Palmer, 1965; Wells et al., 2004). The Z index indicates how wet or dry it was during a single month without regard to past precipitation anomalies. Its combination with past PDSI means that the PDSI for a given month is a weighted function of current moisture conditions and an exponentially damped contribution of PDSI over previous months. This means that PDSI for the month of July integrates current and prior soil moisture conditions over several months. This point is important in understanding why only one month of PDSI is sometimes reconstructed by tree rings even though the trees are

usually sensitive to several months of changing moisture supply during a typical growing season.

Numerous reviews of the PDSI have criticized it for its complexity and empiricism (Karl, 1983; Alley, 1984; Karl, 1986; Heddington and Sabol, 1991; Guttman et al., 1992; Guttman, 1998; Heim, 2002; Keyantash and Dracup, 2002), but it remains one of the most widely used drought indices in the world and is a fundamental part of the U.S. and North American drought monitors (Svoboda et al., 2002; Lawrimore et al., 2002).

From the above brief description, it is apparent that the PDSI provides information on both relative wetness and dryness. The index itself is a dimensionless quantity that is scaled to remove, among other things, differences between regional precipitation climatologies. In principle, this allows the PDSI to be compared between, say, New York and Arizona, regions with radically different precipitation regimes. The PDSI typically falls in the range of ± 4 , which defines the extreme drought (-4) and extremely wet ($+4$) thresholds of the index (Table 1), but the range limit of the PDSI is not explicitly bounded. The frequency of events within each PDSI class in Table 1 should also be roughly comparable across regions and, therefore, independent of their regional climatologies. This means that an extreme drought (PDSI < -4) in New York should have roughly the same frequency of occurrence as an extreme drought (PDSI < -4) in Arizona. Unfortunately, this was found not to be the case using the original algorithm devised by Palmer (1965).

The spatial comparability of the PDSI across diverse climate regions has been questioned (e.g., Karl, 1983; Guttman et al., 1992) because Palmer (1965) derived coefficients used in estimating PDSI from a very geographically limited region of the central U.S. Wells et al. (2004) addressed this issue through the development of a self-calibrating PDSI (SC-PDSI) that locally adapts to the characteristics of the climate data being analyzed. This

Table 1
Classification of wet and dry conditions as defined by Palmer (1965) for the PDSI

4.00 or more	Extremely wet
3.00 to 3.99	Very wet
2.00 to 2.99	Moderately wet
1.00 to 1.99	Slightly wet
0.50 to 0.99	Incipient wet spell
0.49 to -0.49	Near normal
-0.50 to -0.99	Incipient dry spell
-1.00 to -1.99	Mild drought
-2.00 to -2.99	Moderate drought
-3.00 to -3.99	Severe drought
-4.00 or less	Extreme drought

produces better spatial comparability of PDSI over the U.S. compared to Palmer's original index, i.e., the frequency of occurrence in each PDSI class is more comparable from region to region. This improvement is especially apparent in the extreme ends of the PDSI range, a result independently validated by van der Schrier et al. (2006a,b) in Europe and North America south of 50° N. None of the other aforementioned PDSI studies (i.e., Karl and Koscielny, 1982; Dai et al., 1998, 2004), or the tree-ring reconstructions described below, is based on the SC-PDSI because it is such a new development.

3. Tree-ring reconstructions of large-scale drought variability

As indicated above (Karl and Koscielny, 1982; Dai et al., 1998, 2004; Shabbar and Skinner, 2004; Van der Schrier et al., 2006b), the climate records used to generate the large-scale PDSI datasets for North America become very sparse even in the early 20th century over significant portions of Canada and Mexico. The 100 yr of instrumental data is not enough to capture the full range of drought variability (Woodhouse and Overpeck, 1998). It is also not enough to allow drought variability to be evaluated during a time when the climate system was not heavily affected by the radiative forcing of anthropogenic greenhouse gases. Consequently, there is an urgent need to provide greatly expanded records of drought variability over North America.

The paleo-drought reconstructions needed to complement and augment the relatively short instrumental PDSI records for North America require a very special kind of climate proxy with the following properties:

1. The proxy must be highly sensitive to changes in moisture supply and evaporative stress, i.e., it must be drought-sensitive.
2. The proxy must have broad spatial coverage over North America to capture the complex spatial patterns of droughts, as revealed in Figs. 1 and 2.
3. The proxy must have well-resolved annual resolution to capture even single-year droughts.
4. The proxy must be exactly dated to allow annually resolved drought variability over North America to be compared from region to region.
5. The proxy must provide long enough records to produce estimates of past drought over the past several centuries to millennia.

Given these required properties, there is only one climate proxy that satisfies all of them: annual tree-ring

chronologies. This understanding is not new, but only over the past few decades has the power of tree-ring analysis and its well developed statistical methods been brought to bear on the reconstruction of the joint space–time properties of past climate (e.g., Fritts et al., 1971; Briffa et al., 1986; Fritts, 1991; Cook et al., 1994, 1999; Zhang et al., 2004).

The development of an extraordinary network of climate-sensitive annual tree-ring chronologies that covers much of North America has now made it possible to reconstruct the joint space–time properties of drought over much of North America. This tree-ring network is the outcome of years of effort by many dendrochronologists and tree-ring laboratories throughout North America and even Europe, often working independently of each other. Because of a willingness to collaborate, share tree-ring data, and deposit tree-ring data for public access in the International Tree-Ring Data Bank (<http://www.ncdc.noaa.gov/paleo/treering.html>), this collective dendrochronological effort has resulted in a tree-ring network that enables the reconstruction of large-scale annual patterns of drought and wetness over much of North America for the past several centuries to millennia.

3.1. Previous large-scale drought reconstructions from tree rings

One of the earliest efforts to reconstruct drought from tree rings over a large portion of the coterminous U.S. was made by Stockton and Meko (1975). Their reconstruction of July PDSI was made for 40 variable-sized climate regions located in the western two-thirds of the U.S. using a tree-ring network of 40 tree-ring chronologies that spanned most of the reconstruction domain. Recall that July PDSI is actually a reflection of July moisture supply through the Z index plus an exponentially damped function of previous monthly PDSIs, which means that July PDSI integrates the soil moisture conditions over several months. These PDSI reconstructions covered the period 1700–1962. Later, Mitchell et al. (1979) produced PDSI reconstructions for the same 40 climate regions that extended back to 1600 using the Fritts and Shatz (1975) tree-ring network of the 65 longest tree-ring chronologies located over the western portion of the domain. In each case, the method used for reconstruction was canonical regression (Fritts et al., 1971), a method that simultaneously estimates one field of variables from another field of variables. See Cook et al. (1994) for additional examples of the use of canonical regression for reconstructing climate from tree rings.

The tree-ring network in the eastern half of the U.S. was poorly developed when Stockton and Meko (1975)

made their pioneering drought reconstructions. It took several more years of intensive tree-ring network development in the eastern U.S. before a full continental reconstruction of drought for the U.S. was feasible. Experiments in that direction were conducted by Cook et al. (1992) for the eastern U.S. to test the feasibility of producing PDSI reconstructions like those produced by Stockton and Meko (1975). However, it was not until Meko et al. (1993) that a full continental examination of tree growth patterns was made using a network of 248 chronologies. That effort did not produce explicit estimates of past drought. Rather it sought to understand how best to utilize the complex mix of tree species and drought regions over the U.S. for eventual reconstruction purposes.

Meko et al. (1993) used rotated principal components analysis (RPCA; Richman, 1986) to demonstrate that the tree-ring chronologies themselves could reproduce the same nine spatial drought factors in the U.S. identified by Karl and Koscielny (1982) from their gridded instrumental PDSI data. The tree-ring factor scores were also highly correlated in most cases with the actual PDSI data in the drought factor regions. This result was highly encouraging because it demonstrated that the tree-ring network inherently contained the spatial patterns of drought variability known to exist in the instrumental records. However, Meko et al. (1993) also showed that the uneven distribution and concentration of tree-ring chronologies over the U.S., and the geographic clustering of certain tree species as well, led to geographic distortion in the RPCA spatial factors unless the tree-ring data were first gridded. This procedure itself had its own problems, however, because of the way that different tree species in the same region might respond somewhat differently to the same climate forcing. Consequently, the direct gridding of tree-ring data distributed over a large geographic region, and with a complex assemblage of tree species, will mix differences in climate response in unclear ways that are unlikely to produce the best quality drought reconstructions.

3.2. The point-by-point regression method

Building upon the results of Meko et al. (1993), Cook et al. (1996) developed and tested a reconstruction method that successfully eliminated the previously noted difficulties associated with using a complex multi-species tree-ring network for reconstructing drought across the U.S. This method is called *Point-by-Point Regression* (PPR) (Cook et al., 1996).

PPR is the sequential, automated fitting of individual principal components regression models of tree rings to

each point in a grid of instrumental climate variables, in this case PDSI. The sequential nature of PPR differentiates it from joint space–time methods used to simultaneously relate two fields of variables, such as canonical regression (Fritts et al., 1971) and orthogonal spatial regression (Briffa et al., 1986).

PPR is based on the premise that only those tree-ring chronologies proximal to a given PDSI grid point are likely to be true predictors of drought at that location, where “true” implies a causal relationship between tree rings and drought that is stable through time. The rationale behind this premise is our understanding of drought in the U.S. as a regional or mesoscale phenomenon. Consequently, synoptic-scale teleconnections between tree rings and drought, while statistically significant during any given calibration period, may not be stable through time. The local control over each regression model provided by PPR when reconstructing each grid point PDSI is not possible using the joint space–time reconstruction methods mentioned above. It also eliminates the need to grid the tree-ring data and allows each tree-ring chronology to be separately modeled as a predictor of drought.

PPR uses a *search radius* around each grid point to define the zone of local control exercised by the method in selecting candidate tree-ring predictors of PDSI. A second level of control is the *screening probability* for the correlation between tree rings and PDSI, which eliminates those chronologies from the initial candidate pool that are poorly correlated with drought. The screening is done on prewhitened tree-ring and PDSI data after the removal of short-lag autoregressive persistence (Box and Jenkins, 1976). Prewhitening effectively eliminates problems that can arise from differing levels of autocorrelation in the tree-ring and PDSI time series. It also makes statistical significance testing straightforward. The autoregressive coefficients used to prewhiten the PDSI data are also used later in PPR to add lost persistence back into the PDSI reconstructions that are initially based on the prewhitened tree-ring data. See Cook et al. (1996, 1999) for details.

Search radius and screening probability are the two primary controlling variables of PPR, but there was no *a priori* way of knowing if optimal values existed for either one. Consequently, both were tested over a broad range of values in principal components regression analysis to determine the overall best combination to use for reconstructing past drought. Each regression model was based on prewhitened instrumental PDSI and tree-ring data over a 1928–1978 *calibration period* common to all series. The pertinent statistic of interest here is the relative amount of PDSI variance explained by the

regression model, i.e., the regression R^2 . Pre-1928 PDSI data were withheld from this procedure for regression model validation tests.

For testing the level of agreement between actual PDSI and model estimates in the pre-1928 *verification period*, three statistics in order of increasing rigor were calculated: the square of the Pearson correlation (RSQ), the reduction of error (RE), and the coefficient of efficiency (CE). RSQ, RE, and CE are also measures of relative variance in common between actual and estimated PDSI. All four statistics have an upper limit of 1.0, meaning perfect agreement between the actual and estimated data. However, unlike calibration R^2 , which can never be negative, verification RSQ, RE, and CE can take on negative values if there is no verification of the estimates. As the square of Pearson correlation coefficient, RSQ is assigned a negative value if the Pearson r is negative. This places a lower limit on RSQ of -1.0 . In contrast, RE and CE have unbounded lower limits and CE can never be more positive than RE. See Cook et al. (1999) for details. After extensive testing using the calibration and verification statistics just described, Cook et al. (1999) found that a 450-km search radius and a screening probability of 0.10 (the 90% significance level) were on average the best combination to use for reconstructing PDSI over the 155-gridpoint domain.

3.3. Drought reconstructions for the coterminous U.S.

Using PPR, Cook et al. (1999) successfully reconstructed the PDSI across the coterminous U.S. from a network of 425 tree-ring chronologies and the same instrumental PDSI grid as Meko et al. (1993). The June–July–August average (summer) PDSI season was reconstructed instead of a single month like July (Stockton and Meko, 1975). This seasonal average was chosen because the northward march of the growing season in spring caused the peak response of trees to soil moisture deficits to vary with latitude. Experiments with different months and seasons indicated that the summer season PDSI was the best compromise for reconstruction. Of the 155 grid points, only the southernmost grid point in peninsular Florida (Fig. 3A) failed to reconstruct because of a lack of suitable tree-ring chronologies in that region. The PDSI reconstructions for the coterminous U.S. covered the common period 1700–1978 at 154 grid point locations.

Extensive tests of these tree-ring reconstructions revealed that they contained the large-scale features of drought variability found in the instrumental data (Cook et al., 1999). These tests included the use of RPCA,

which recovered the same nine spatial drought patterns found by Karl and Koscielny (1982) and Meko et al. (1993). This result validated the use of PPR as a method that could recover spatial information with a high degree of fidelity even though the method itself has no explicit spatial component in it. Subsequent comparisons of these drought reconstructions with those developed from the identical datasets using a completely independent method (Regularized Expectation Maximization; Zhang et al., 2004) further validated the use of PPR for reconstructing drought over the U.S.

The successful reconstruction of drought across the coterminous U.S. was a breakthrough, but it had some significant limitations. One obvious problem was that drought variability over North America does not stop at the U.S. political boundaries with Canada and Mexico. In order to study the natural patterns of drought variability over North America, those artificial constraints had to be eliminated. Another problem related to the length of these PDSI reconstructions. Although they were almost three times as long as the instrumental records, there were good reasons to believe that they were not nearly long enough to capture the full range of drought variability. Woodhouse and Overpeck (1998) and Stahle et al. (2000) each provided evidence for megadroughts in North America (i.e., droughts of exceptional intensity and duration) that predated the beginning of the reconstructions produced by Cook et al. (1999). Therefore, a concerted effort was made to eliminate the artificial political boundaries of the drought reconstructions and to extend them as far back in time as the tree-ring chronologies would allow.

4. North American drought reconstructions

In order to expand the drought reconstructions to cover most of North America, two challenges had to be overcome. First, the instrumental PDSI grid had to be greatly expanded to include parts of Canada and Mexico where the length and quality of the instrumental data was limited. The second challenge was to greatly expand the tree-ring network to enable the reconstruction of drought over as much of Canada and Mexico as possible.

4.1. Expanding the drought grid over North America

A logical choice for expanding the instrumental PDSI grid into Canada and Mexico would have been to directly use the existing 2.5° PDSI grid of Dai et al. (1998) for global land areas. This possibility was investigated, but a comparison of some of the Dai et al. (1998) grid point

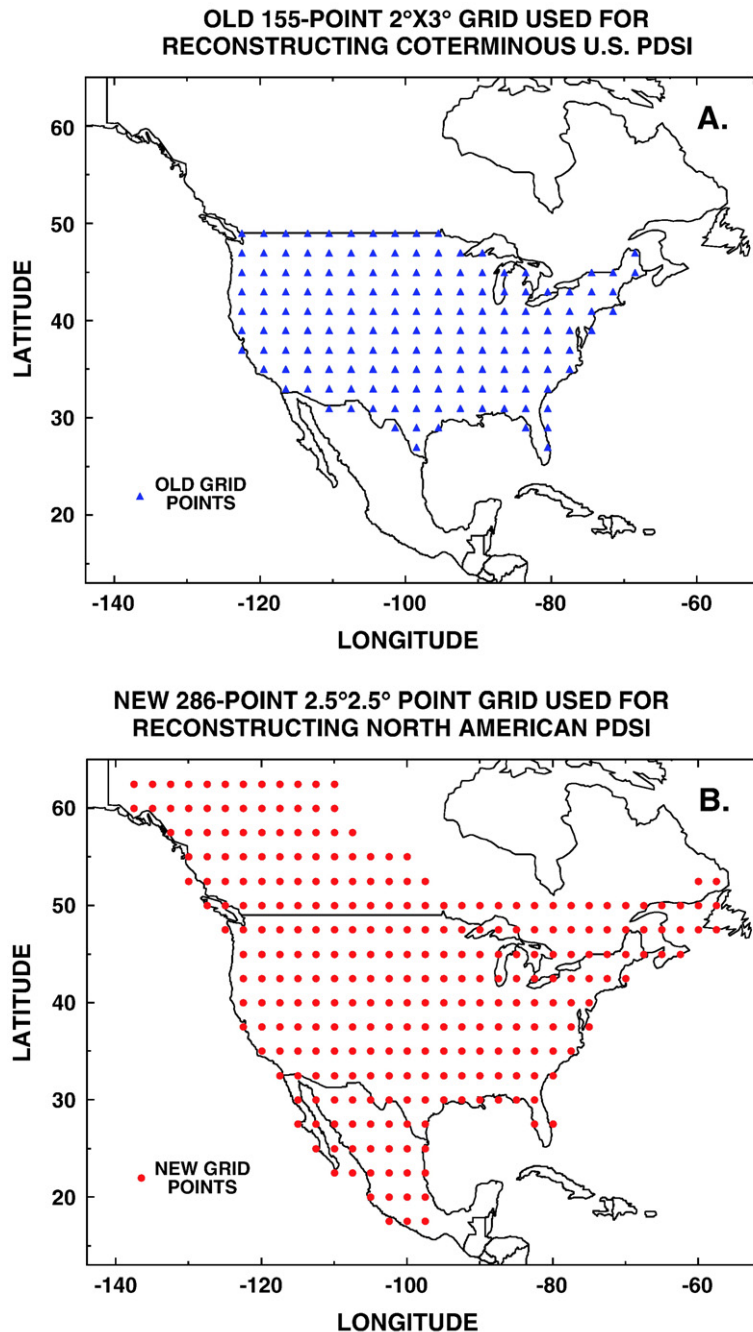


Fig. 3. The old (A) and new (B) instrumental PDSI grids used for reconstruction.

records with those closest to ones from the Cook et al. (1999) PDSI grid for the U.S. indicated somewhat weak agreement at times between the two datasets. Since the Cook et al. (1999) PDSI grid was based on the highest quality single-station USHCN monthly climate records (Karl et al., 1990), the decision was made to use these PDSI records in the expanded North American grid.

At about the same time, 131 high-quality monthly instrumental PDSI records for Canada, which all began prior to 1946, were obtained from the Meteorological Service of Canada (Skinner et al., 2001). This dataset was the basis for the interpolated PDSI records used by Shabbar and Skinner (2004) in their analyses of Canadian drought. The high-quality U.S. and Canadian

single-station PDSI records were then jointly interpolated to the same 2.5° grid as that used by Dai et al. (1998) using the same inverse distance weighted method (Cook et al., 1996). The interpolated PDSI records all began on or before 1900 in the U.S. As indicated by Shabbar and Skinner (2004), this was not possible everywhere in Canada. Therefore, areas of the Canadian grid that did not extend back to 1900 were in-filled with PDSI estimates back to 1900 using reduced-space optimal interpolation (Kaplan et al., 2000).

No similar set of high-quality single-station PDSI records existed for Mexico at the time, so the decision was made to use the Mexico portion of Dai et al. (1998) PDSI grid for that part of the North American grid. Some of the Mexican PDSI gridded records were found to be unusually erratic, with discontinuities and unrealistic extremes at some grid points, which indicated data quality problems. Those suspect PDSI grid point records were carefully edited to remove gross outliers and discontinuities. The remaining data were improved and gaps filled through the use of reduced-space optimal interpolation (Kaplan et al., 2000).

The data from the U.S., Canada, and Mexico produced a North American monthly PDSI grid composed of 286 2.5° grid points that covered most of North America (Fig. 3B). The time period common to all grid points was 1900–1990. This grid does not include Alaska, which lacks the high-quality single-station PDSI records needed for interpolation. The northern boundary of the grid in Canada was also determined by the distribution of PDSI records available for interpolation. Finally, the lack of any useful tree-ring data in the far southeastern Yucatan region of Mexico (see Fig. 3B) led to the decision not to include any PDSI grid points from that region in the new reconstructions.

4.2. Expanding the tree-ring network over North America

The second challenge was expanding the tree-ring network to cover enough of the new PDSI grid for reconstruction purposes. The tree-ring community in North America had been very active over the previous several years in developing a number of very important new tree-ring chronologies in critical areas of North America. Its willingness to share these data for large-scale drought reconstruction made it possible to rapidly expand the North American tree-ring network used here. Fig. 4A shows the tree-ring network available for reconstruction. It totals 835 annual records, many of which occupy important new regions of the grid. The new network is almost twice as large as the 425-chronology network used by Cook et al. (1999) and better fills

in important parts of the U.S. in the Great Plains and Rocky Mountains. Mexico is also now well represented by the network, but significant portions of Canada are clearly under-represented. However, the results to be presented next show that the tree-ring coverage for Canada still provides useful PDSI reconstructions in a number of regions there.

Another important feature of the expanded tree-ring network is the number of new chronologies that extend back 500 or more years in the past. Fig. 4B shows a frequency histogram of starting years of the 835 chronologies, broken down into the original 425 (blue) used by Cook et al. (1999) and the additional 410 (red) in the expanded network. There are many more now that extend back into the 16th century, a period of megadrought (Stahle et al., 2000). In addition, there are a number of new chronologies that extend back before AD 1300, another time of megadrought in some areas of the West (Woodhouse and Overpeck, 1998). This enabled the PDSI reconstructions at certain grid points to be extended much further back in time into those climatically interesting times.

4.3. Extending the PDSI reconstructions back in time

The reconstructions produced by Cook et al. (1999) were originally constrained to utilize the time interval common among all 435 annual tree-ring chronologies: AD 1700–1978. In order to utilize the full lengths of the available tree-ring records for reconstructing drought, PPR was used in a nested manner whereby the shorter chronologies already used for reconstruction were dropped out and the procedure repeated using the remaining longer series. For example, if three tree-ring chronologies passed the screening probability test and their starting years were AD 1700, 1600, and 1500, then three reconstructions were generated. The first used all three chronologies and began in AD 1700, the second used the two longer chronologies and began in AD 1600, and the third used the remaining longest chronology and began in AD 1500. Each reconstruction would also have its own calibration period R^2 and verification period RSQ, RE, and CE.

In order to put these three reconstructions together into one reasonably homogeneous record back to AD 1500, it was necessary to adjust each series to account for its different level of regression R^2 . Otherwise there might be an artificial trend or fluctuation in the reconstructed PDSI variance over time. This was accomplished by adding the lost variance due to regression back into each reconstruction, i.e., each nested reconstruction was rescaled to have the same variance over the 1928–1978 calibration period as the instrumental PDSI

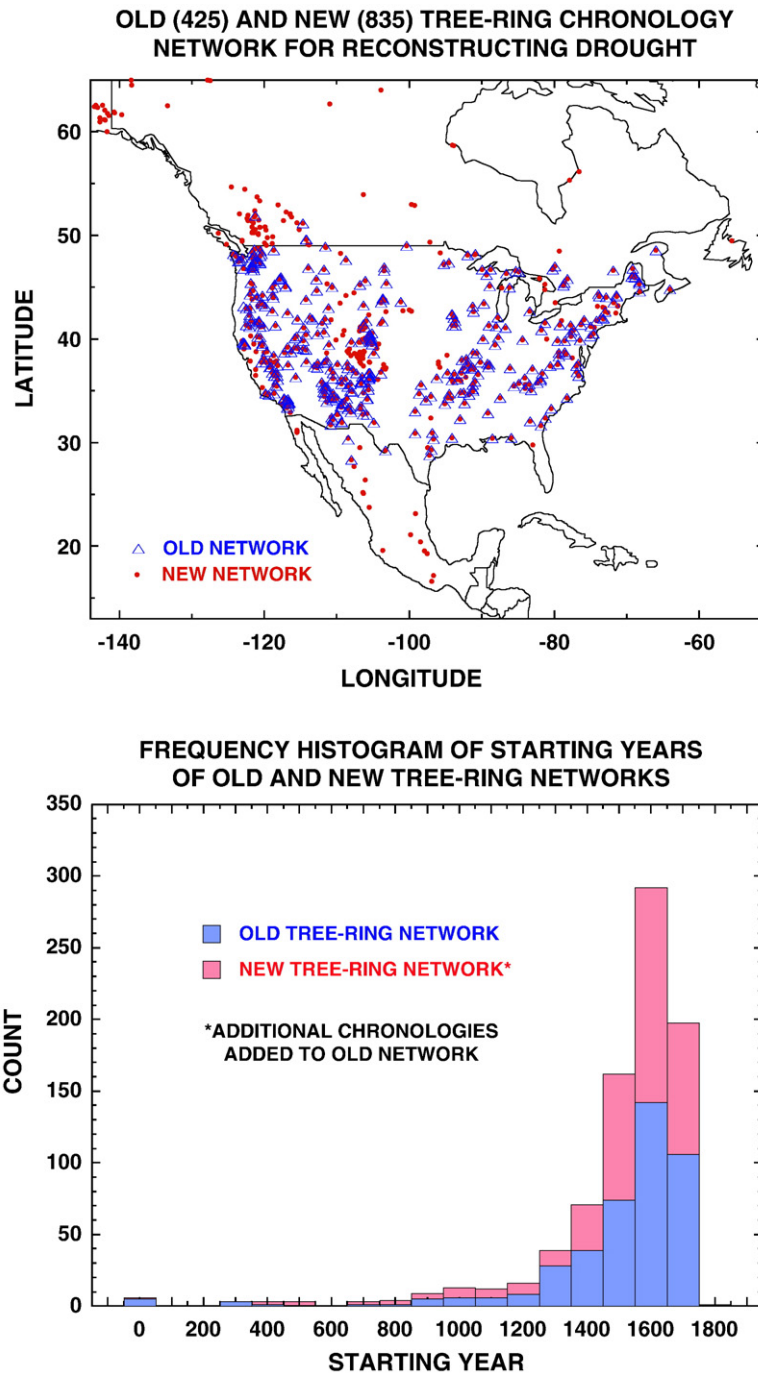


Fig. 4. The North American tree-ring network (A) used for drought reconstruction and the frequency histogram of starting years of those chronologies (B). Each shows the earlier 425-chronology network used by Cook et al. (1999) to reconstruct drought over the coterminous U.S. (blue) and the additional chronologies that make up the expanded 835-chronology North American network (red).

data. In the hypothetical example used here, this would create a PDSI reconstruction as a combination of three rescaled segments: 1500–99, 1600–99, and 1700–1978.

Fig. 5 shows an example of one reconstruction from the North American Drought Atlas that was created over

the 286 PDSI grid points (Fig. 3B). The North American Drought Atlas can be accessed online at <http://iridl.ldeo.columbia.edu/SOURCES/LDEO/TRL/NADA2004/pdsi-atlas.html> (see also <http://www.ncdc.noaa.gov/paleo/newpdsi.html> for an alternative source of these

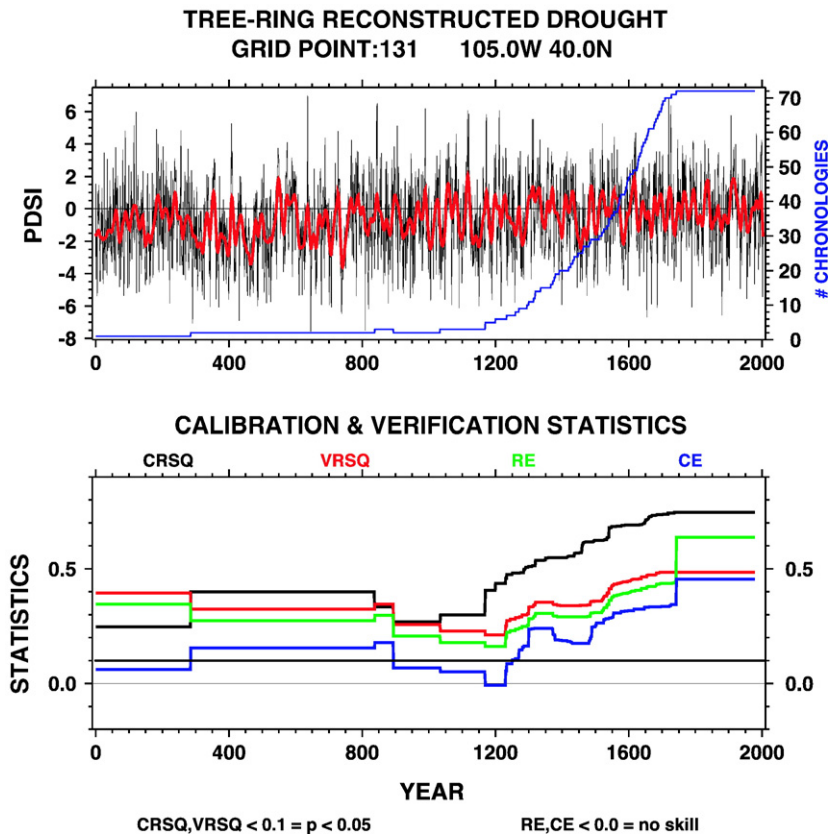


Fig. 5. An example of an extended PDSI reconstruction (upper plot in gray and red) from the North America Drought Atlas, created by using PPR in a nested manner to generate all possible length reconstructions from a suite of tree-ring chronologies with uneven starting years. The blue curve in the upper plot shows the change in the number of chronologies available back in time. As a consequence, each extension back in time has its own calibration (CRSQ, same as R^2 in the text) and verification (VRSQ, RE, and CE; VRSQ=RSQ in the text) statistics, which causes them to vary over time in the lower plot.

data). Note how the calibration and verification statistics change with time as the number of available chronologies declines. Except for one short interval centered on AD 1200 where $CE < 0$, all of these statistics remain statistically significant ($p < 0.05$) or have some detectable skill ($RE > 0$ and $CE > 0$) over the past 2000 yr, which indicates that this reconstruction located at a grid point in northern Colorado is useful for charactering past drought over the entire period of record. However, the sharp decline in the number of chronologies prior to about AD 1200 means that greater caution must be exercised in using the earlier portion.

5. The North American summer PDSI reconstructions

Using the 835 tree-ring chronologies in our network (Fig. 4A), PPR was applied sequentially over the 286 PDSI grid points (Fig. 3B) in a nested fashion to produce drought reconstructions of maximal length at

each location. The calibration period was 1928–1978 and the verification period was 1900–1927 in every case. This process produced 286 summer drought reconstructions of the kind illustrated in Fig. 5. Many of them extend back into the megadrought epochs noted by Woodhouse and Overpeck (1998) and Stahle et al. (2000). The median starting year of the reconstructions is AD 951 and 75% of the series begin on or before AD 1380. This is a remarkable improvement over the reconstructions of Cook et al. (1999) that all began on AD 1700. The reliability of the North American summer drought reconstructions will be described next through maps of the calibration and verification statistics and their overall summary statistics.

5.1. Calibration and verification results

Calibration R^2 and verification RSQ, RE, and CE statistics have been mapped over the grid to provide guidance for which areas are reconstructed well. These

maps (Fig. 6A–D) are based on the model statistics for the most highly replicated portion of the reconstruction, i.e., that interval based on the maximum number of tree-ring chronologies used in each model. Areas with significant ($p < 0.05$ or $RE > 0.1$ and $CE > 0.1$) calibration and verification are those shaded in all but the darkest blue color.

Each grid point must have a significant calibration R^2 . Otherwise, it would not have been reconstructed. Not surprisingly, the weakest areas of calibration are located in parts of northern Canada where the tree-ring network is weakly developed. Some parts of Mexico are

likewise weakly calibrated, but given the suspect quality of the PDSI data used in the Mexico part of the grid, this result may not be the fault of the tree rings alone.

The verification statistics are in general weaker than the calibration R^2 , a result that was expected based upon the well known “shrinkage” of fitted relationships when applied to withheld or independent data. In general, the areas that calibrated best also verified best. This is indicated by the correlation of R^2 with each verification statistic: 0.79 for RSQ, 0.67 for RE, and 0.50 for CE. The systematic decline in correlation from RSQ to CE reflects the increasing difficulty in achieving positive values from

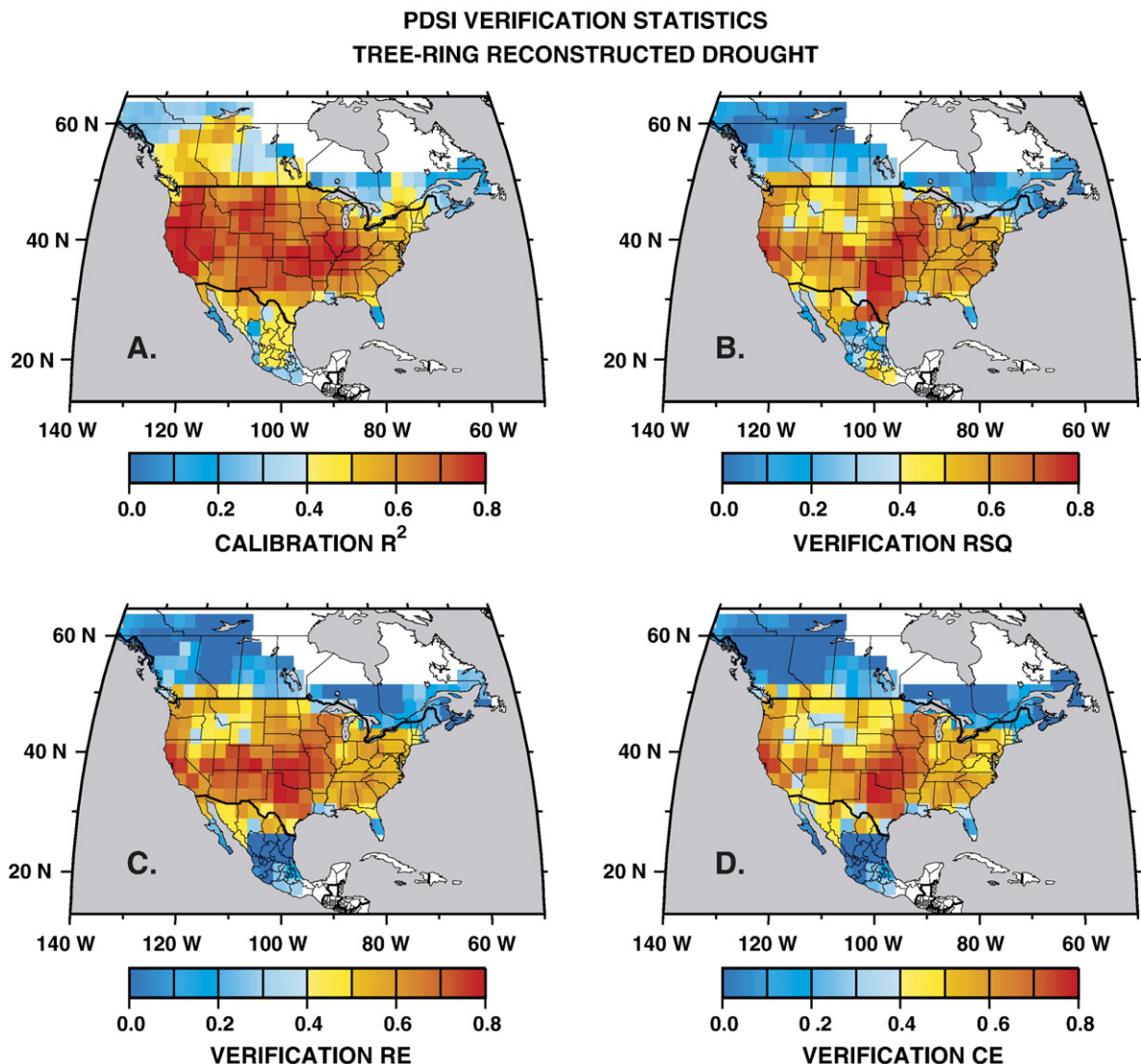


Fig. 6. Calibration and verification maps of the North America summer PDSI reconstructions. All of the grid points are significantly calibrated ($p < 0.05$). Verification $RSQ > 0.1$ ($p < 0.05$) is passed at most grid points. While RE and $CE > 0$ is often considered a sign of verification, for practical purposes, RE and $CE > 0.1$ is probably the more appropriate threshold. This being the case, parts of northern Canada and central Mexico fail to produce positive REs and CEs.

RSQ to RE and to CE. Over the domain, there are 7 negative RSQs, 58 negative REs and 77 negative CEs. Most are located in Canada, but some are also found in central Mexico. Again, the questionable quality of the gridded PDSI data in Mexico suggests that the poor verification there may not be due to the tree rings alone.

Overall, the median R^2 , RSQ, RE, and CE statistics are 0.51, 0.44, 0.42, and 0.36, respectively. These results are interesting to compare to those reported by Cook et al. (1999) for the coterminous U.S. alone: 0.55, 0.36, 0.31, and 0.22, respectively. The median R^2 in the previous study is slightly higher, but the median verification statistics are noticeably lower. Most of the improved verification in the present study probably comes about from a substantially increased tree-ring network over the coterminous U.S. (Fig. 5), which more than offsets the poor verification found in parts of Canada and Mexico.

5.2. North American drought variability since AD 951

The beginning years of the summer drought reconstructions over North America range from -1 BC to AD 1648, with most of the longer records located in the western portion of the grid. This makes a large-scale North American drought average difficult to make without introducing some geographic bias into the estimates back in time as shorter grid point reconstructions drop out. To avoid the worst of this bias, we illustrate the long-term history of North American summer drought only back to AD 951, the median starting year of the grid point reconstructions. This includes several grid points in both western and eastern North America (Fig. 7A), so there is some degree of geographic balance. The biggest missing component in the beginning is Mexico, but it is almost fully represented by AD 1380 (Fig. 7B), the year when 75% of all grid points are available.

Fig. 8 shows the average summer PDSI (MPDSI) reconstruction for all available grid points (Fig. 8A), the drought area index ($\text{DAI} < -1$) (in this case the percent of available grid points each year over the grid with $\text{PDSI} < -1$; Fig. 8B), and the percent of all grid points reconstructed for calculating these records each year (Fig. 8C). The solid black curves are the same series after applying a 60-year low-pass filter to each to highlight multi-decadal changes in drought and the upper and lower black dashed curves are 95% confidence limits based on 1000 bootstrap pseudo-samples (Efron and Tibshirani, 1986).

Not surprisingly, the MPDSI and $\text{DAI} < -1$ records are highly correlated with each other in an inverse sense

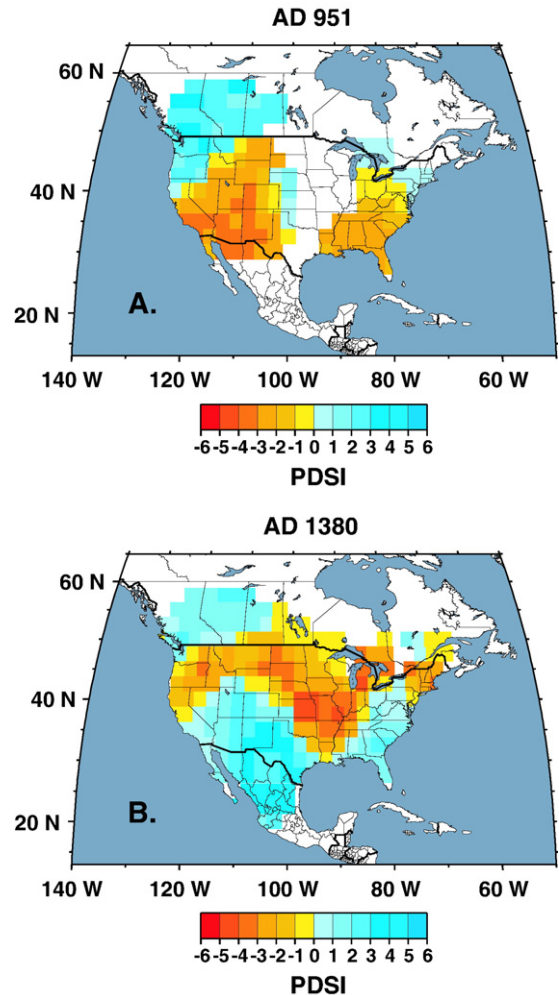


Fig. 7. Maps of reconstructed PDSI showing the geographic coverage for the years when the median (AD 951) and 75% of the grid points are reconstructed (AD 1380).

($r = -0.91$). Roughly speaking, the $\text{DAI} < -1$ over a range of 10–50% covers an MPDSI range of ± 1.0 . Interestingly, both series have long-term, nearly linear trends that collectively indicate an evolution towards wetter-than-average conditions over North America. This overall trend is punctuated by significant periods of drought and wetness that in some cases lasted for several years.

The single greatest megadrought in the record occurred over AD 1140–1162, a period of 23 consecutive years of negative MPDSI across North America. The worst decade during that period was AD 1150–59 when seven of the ten years had an average PDSI across North America below -1.0 . The spatial pattern of that decade of megadrought is shown in Fig. 9. Interestingly, this period of unusually severe aridity was mainly

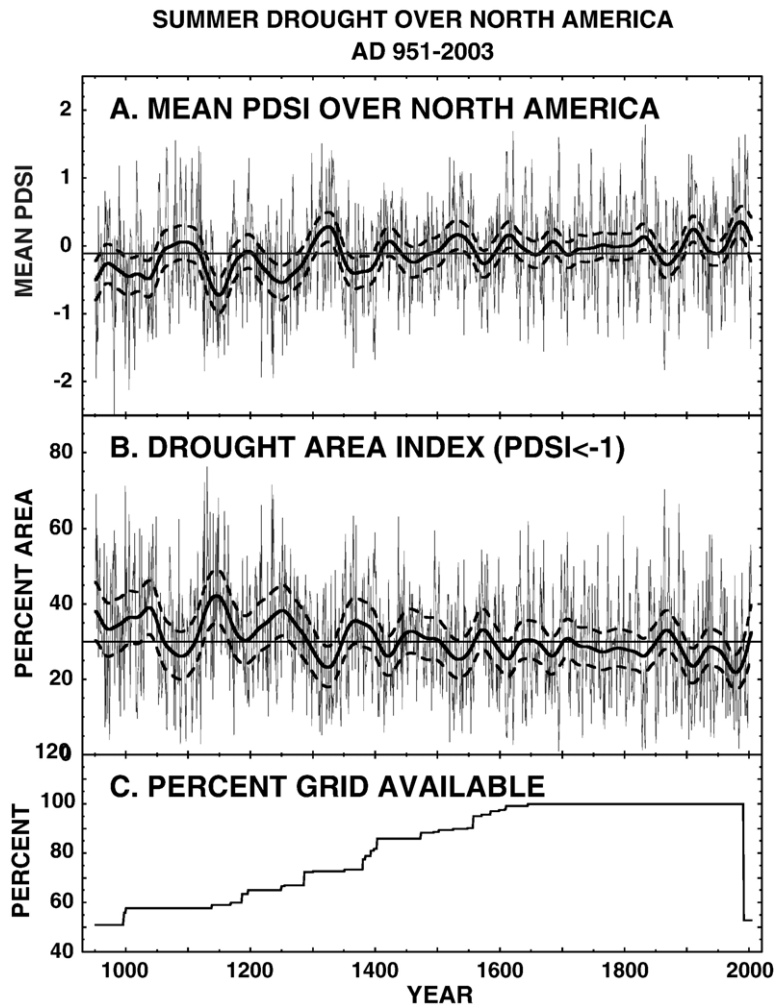


Fig. 8. Mean summer PDSI for North America (A) and percent area occupied by drought (PDSI < -1) each year (B), and the percent of the overall grid that is reconstructed each year (C). The thick solid curves are 60-year low-pass filtered versions of the annual values indicated in gray. The thick dashed curves are upper and lower 95% bootstrap confidence limits of the low-pass filtered values.

restricted to the western half of North America, with the eastern half experiencing close to normal moisture conditions on the PDSI scale (Table 1). This pattern is similar to that of the 2002 drought shown in Fig. 1, but it lasted for 10 yr. It is hard to imagine what the West would look like if the current drought with comparable severity were to last that long.

5.3. Changing aridity in the West since AD 800

Cook et al. (2004) used the North American summer PDSI reconstructions to describe long-term aridity changes in the West since AD 800 and place the current drought there in a long-term context. Fig. 10 shows the specific geographic region defined as the West (Fig. 10A) and its DAI record (Fig. 10B). On inter-

annual, 20-year, and 60-year time scales of variability, the West DAI record is similar to that for North America since AD 951 ($r=0.81$, $r=0.86$, and $r=0.93$, respectively). With 60-year smoothing, the three megadrought epochs indicated for the West, centered on AD 1034, 1150, and 1253, are all similarly pronounced in the North America average. The bigger differences appear to be found in the wetter epochs. In particular, the early 20th century “pluvial” centered on 1915, which has received much recent attention in the West (Woodhouse et al., 2005), is not as pronounced in the North America average because it was largely restricted to the West (Fye et al., 2003). This again reveals an east–west contrast in moisture supply across North America, similar in form to that during the AD 1150–1159 megadrought, but with opposite sign.

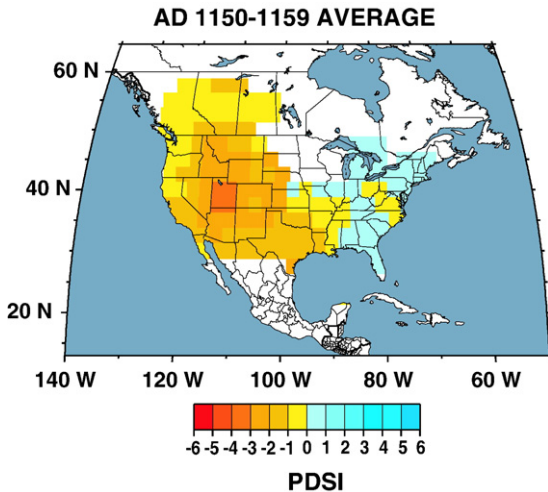


Fig. 9. Map showing the decadal mean PDSI pattern for the worst North American megadrought since AD 951. Note that it is mainly restricted to the West.

Fig. 10B also highlights the differences between 20th century drought area up through AD 2003 (boxed in yellow) and the past, especially the ~400-year period of elevated aridity from AD 900 to 1300. The mean DAI for AD 900–1300 and AD 1900–2003 are 42.3% and 30.0%, respectively, a 29% reduction in the average area affected by drought in the 20th century. This difference in average DAI is highly significant statistically ($p < 0.001$).

Further analysis of the tree-ring reconstructions (Herweijer and Seager, 2006) shows that the spatial patterns of the medieval droughts were essentially indistinct from those in the instrumental record. In addition, the PDSI extremes during the medieval droughts were no greater than for the more recent ones. While it is possible that some degree of survivorship bias in the surviving trees used to estimate severe droughts in the past has censored the magnitude of certain extreme events to some degree, it is impossible to know if this has actually occurred. Consequently, the observations made by Herweijer and Seager (2006) remain appropriate. What was so different is that, whereas the recent droughts last at most a decade, the medieval ones lasted for decades at a time and came in quick succession. The PDSI variability was, however, also similar to that of the instrumental period. The easiest way to characterize the medieval drought record is as one with variability much like today but around a mean climate that was drier. All in all this suggests that whatever currently forces intermittent droughts in the West and Plains was simply the normal state of affairs during the medieval period.

It would have immense impact on the water resources of the West in the future were modern-day conditions to

revert to the drought experienced prior to AD 1300. Understanding the causes of persistent drought, and how these will be impacted by anthropogenic climate change, should therefore be a high research priority.

6. Past historic and cultural impacts of droughts in North America

The new reconstructions of summer PDSI provide sobering examples of intense decadal droughts over the past millennium that likely had severe social consequences in both the arid West and the higher rainfall areas of the eastern United States. A well documented example from the tree-ring reconstructions is the 16th century multi-decadal megadrought over the English and Spanish colonies in North America, with the gravest impacts among the native societies of Mexico where drought interacted with conquest, forced labor, and disease to contribute to one of the most catastrophic episodes of human mortality in world history (Acuna-Soto et al., 2002). In this section, we describe three such case studies of past megadroughts over North America to provide a human impact dimension to the tree-ring reconstructions.

6.1. Drought and the Puebloan society in the American Southwest

Decadal drought seems to have also played a key role in the history of Pueblo society in the American Southwest. The “Great Drouth” from AD 1276 to 1299 was famously documented by A.E. Douglass (1929, 1935) when he developed the first archaeological tree-ring chronology for Chaco Canyon, Mesa Verde, and other major prehistoric occupations across the Colorado Plateau. Hundreds of precipitation-sensitive tree-ring chronologies have been developed following Douglass’ groundbreaking research, and they confirm the multi-decadal drought of the late 13th century. These new chronologies (e.g., those indicated in Fig. 4) have been used to estimate moderate drought (summer PDSI-2.0) or worse for the entire 22-year period from AD 1276 to 1297, concentrated over the Colorado Plateau and the ancestral Pueblo cultural area (Fig. 11).

Computational models of Anasazi farming groups in time and space (so-called multiagent models; Gumerman and Dean, 2000), using surficial geomorphology and soils, palynology, tree-ring reconstructions of climatic variability and crop yields, estimated demographic conditions, and social structures for the 11th through 14th centuries in Long Valley, Arizona, indicate that the Great Drouth would have contributed to heavy

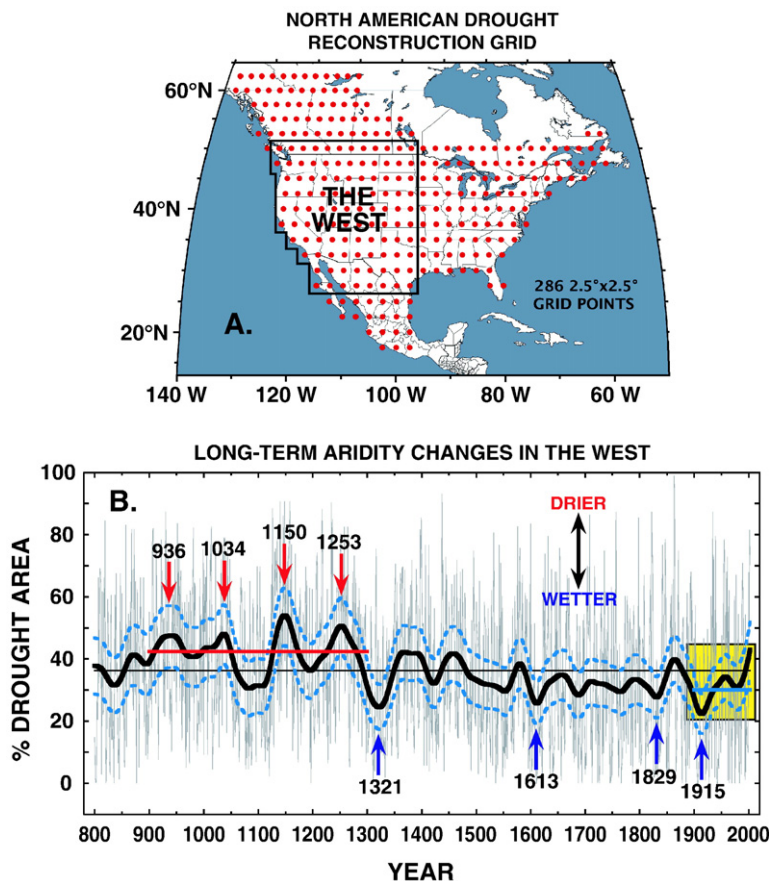


Fig. 10. Long-term aridity changes in the West (A) as measured by the percent area affected by drought ($PDSI < -1$) each year (B) (redrawn from Cook et al., 2004). The four most significant ($p < 0.05$) dry and wet epochs since AD 800 are indicated by arrows. The 20th century, up through 2003, is highlighted by the yellow box. The average drought area during that time, and that for the AD 900–1300 interval, are indicated by the thick blue and red lines, respectively. The difference between these two means is highly significant ($p < 0.001$).

population loss among the ancestral Pueblo, consistent with the archaeological evidence for abandonment of the region (Axtell et al., 2002). However, the modeling also indicates that the carrying capacity of Long Valley may not have been entirely depleted by the late 13th century drought, suggesting that social considerations must have influenced the decision to abandon the region (Axtell et al., 2002).

A six-year uninterrupted drought occurred over the Puebloan region and Great Plains during the mid-17th century (Fig. 11), and its impacts as described by the Spanish included famine, disease, mortality, and village abandonment (Sauer, 1980). The historical and dendroclimatic records for this 17th century drought may provide a useful analog for the social response of Pueblo agriculturalists to prolonged drought, including social changes associated with the Great Drought of the late-13th century.

6.2. Drought during the Mississippian Phase

Severe decadal drought was not confined to the arid west over the past millennium. The tree-ring reconstructions document prolonged drought over the central and lower Mississippi Valley during the 14th, 15th, and 16th centuries, which may have contributed to the disintegration of the large complex chiefdoms of the Mississippian period. The Mississippian Phase was characterized by platform mounds, elaborate material culture, evidence for long distance trade, and a reliance on maize and native seed cultivation, fishing, and hunting. Mississippian sites are distributed across much of the central and southeastern United States, but were most spectacularly developed at Cahokia, the largest prehistoric site in the eastern United States, located in the American Bottoms south of the confluence of the Mississippi and Missouri Rivers (Pauketat, 2004).

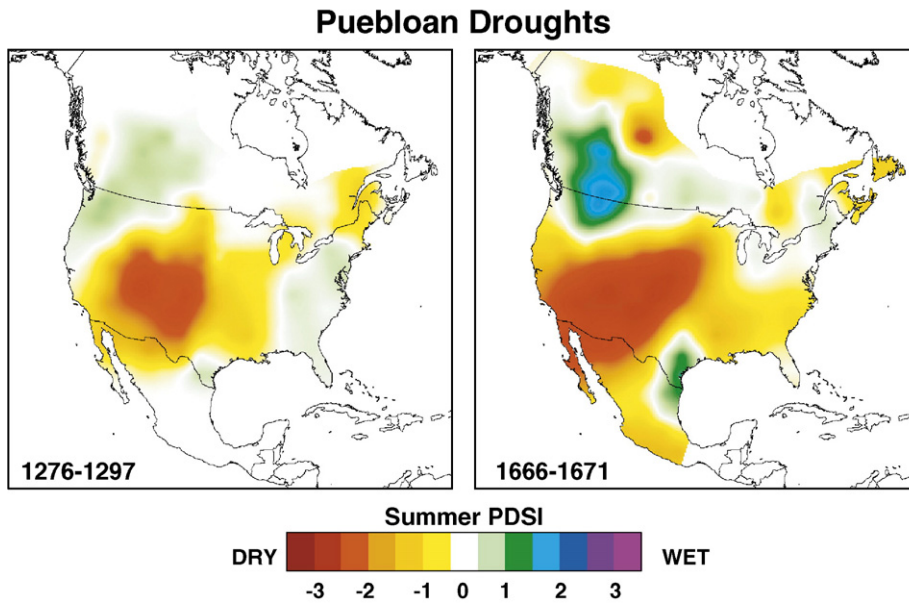


Fig. 11. Tree-ring reconstructed summer PDSI during two multi-year droughts centered over the Puebloan cultural area. The “Great Drouth” (Douglass 1929, 1935) lasted for at least 22 yr (left). The social and environmental effects of the six-year drought during the mid-17th century (right) were mentioned by Spanish archivists and may provide useful insight into the consequences of multi-year drought on prehistoric farmers in the region.

The archaeological record of development and decline at Cahokia and other major Mississippian sites has been documented with artifact analysis and radiocarbon dating (Milner, 1998). The original dating of the cultural phases at Cahokia has been shifted forward in time by a few decades in light of new results and radiocarbon calibration (Milner, 1998, p. 21). These cultural phases are believed to reflect significant changes in the human population at Cahokia, but the absolute magnitude of the population at Cahokia or in the larger American Bottoms is still very poorly known. The largest population decline at Cahokia appears to have occurred with the close of the Sterling Phase (ca. AD 1000–1200), but the final phase of occupation at Cahokia occurred during the Sand Prairie Phase, which may have persisted until ca. AD 1400 (Milner, 1998; Thomas, 2000).

Several other Mississippian mound centers were abandoned ca. 1450, including the Kincaid, Twin Mounds, and Angel sites in southern Illinois and Indiana (Cobb and Butler, 2002). The large Mississippian mound center at Spiro in eastern Oklahoma was also abandoned ca. AD 1450 (Thomas, 2000). In fact, the region from the American Bottoms south to the Ohio River and extending into central Tennessee was largely depopulated by ca. AD 1450 (Cobb and Butler, 2002). This region is centered on the confluence of the Ohio and Mississippi Rivers and is referred to as “the Vacant Quarter” (Williams, 1990; Cobb and Butler, 2002).

The abandonment of the large complex Mississippian chiefdoms by the 15th century is not well understood. Theories for chiefdom decline in the Mississippi Valley include collapse of the social organization needed to sustain the network of trade and tribute, increased warfare (which is indicated by palisade walls and skeletal evidence), deforestation and environmental degradation in the vicinity of the major population centers, flooding, and drought (Thomas, 2000; Pauketat, 2004). It is also unclear whether there was a significant population decline with the collapse of the complex chiefdoms, or whether the population was simply redistributed in smaller settlements across the region.

The summer PDSI reconstructions for the central and lower Mississippi Valley during the 14th century are based primarily on precipitation sensitive baldcypress and red cedar chronologies located in southeast Missouri, Arkansas, northern Louisiana, and east Texas (Stahle et al., 2004). These data indicate that drought prevailed in the latter half of the 14th century. Below average moisture conditions were reconstructed over the lower Mississippi Valley for 46 of 58 yr from 1344–1401 (Fig. 12). Uninterrupted moderate to severe drought was reconstructed for the two worst decades of the 14th century, AD 1344–1353 and 1379–1388 (Fig. 12). These decadal droughts were roughly contemporaneous with the decline of complex chiefdoms in

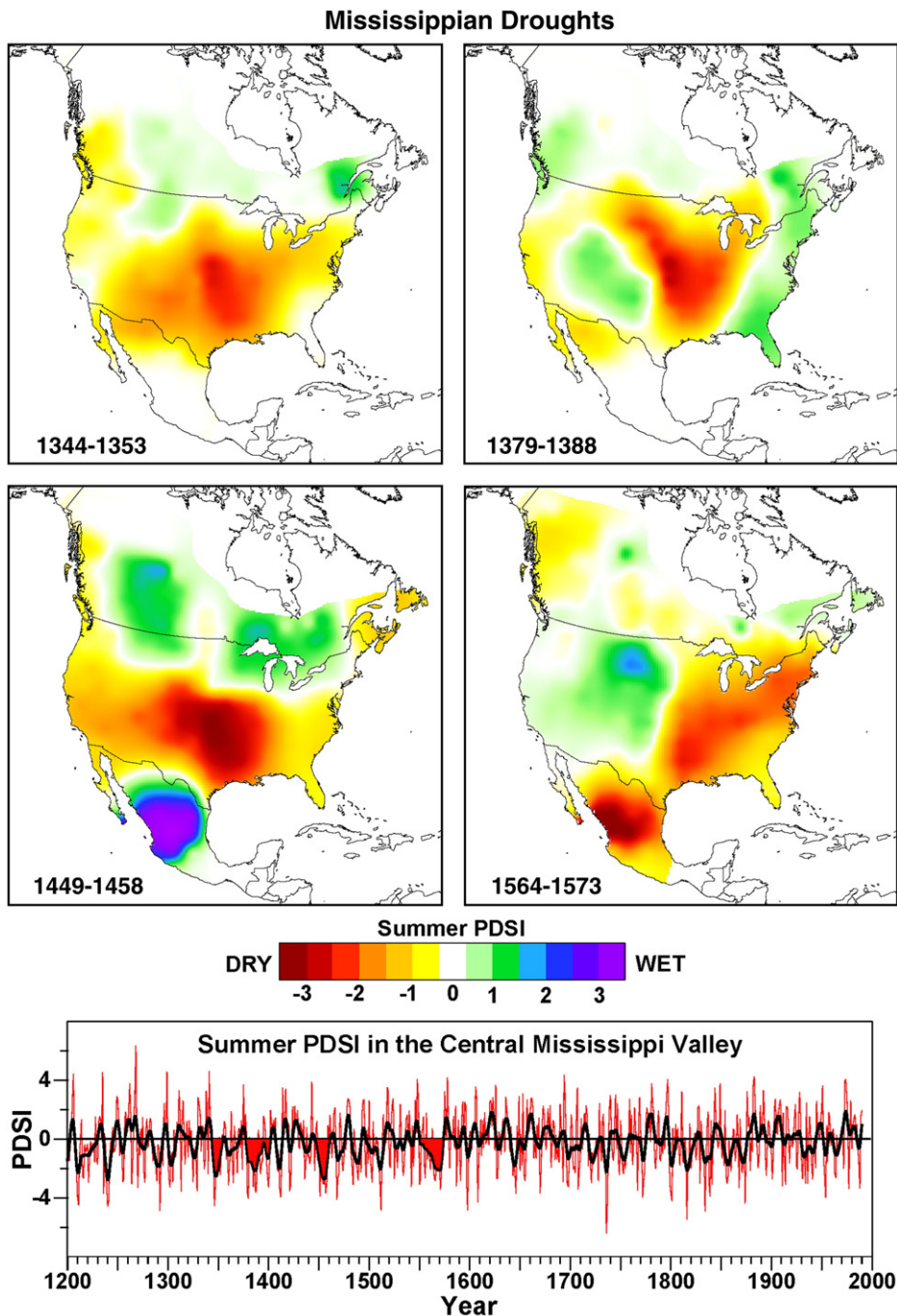


Fig. 12. Four intense decadal droughts over the central United States may have contributed to the syndrome of social and environmental change that resulted in the decline of complex Mississippian chiefdoms in the 14th and 15th centuries. The impacts of the 16th century drought (1564–1573) on native agriculturalists in South Carolina was mentioned by Spanish colonists at Santa Elena and may be relevant to earlier prehistoric drought impacts. The PDSI reconstructions for the central Mississippi Valley (time series for 37.5° N–90.0° W) indicate that the Mississippian droughts of the 14th, 15th and 16th centuries (red shading) may have been the most severe and sustained in 700 yr.

the region, possibly including the conclusion of the Sand Prairie Phase at Cahokia. Severe drought also prevailed for ten consecutive years from AD 1449–1458

(Fig. 12) and may have contributed to the depopulation of the Vacant Quarter and to the abandonment of the Spiro site.

Multi-decadal drought occurred in the Mississippi Valley and across the Southeast during the late 16th century, where it was most intense from AD 1564–1573 (Fig. 12). The agricultural impacts of this 16th century drought among the native Orista tribes of South Carolina were severe as described by the Spanish at Santa Elena colony (Anderson et al., 1995), and like the 17th century Pueblo drought (Fig. 11), the 16th century drought may provide an important historical analog to the impacts of severe decadal drought among prehistoric Mississippian agriculturalists.

The new PDSI reconstructions provide the first detailed estimates of the spatial impact of prolonged drought during this period of changing settlement patterns and increasing warfare among Mississippian chiefdoms. The widespread decadal droughts illustrated in Fig. 12 would likely have caused a sequence of poor harvests extending over a large sector of the Mississippian cultural area. The food storage capabilities of complex Mississippian chiefdoms were limited to perhaps only two years (Anderson et al., 1995), and a sequence of poor yields repeated over a few years could have been disastrous (Milner, 1998). Milner (1998) argues that widespread crop failures would have limited the ability of these chiefdoms to deploy crop surpluses from one region to another in an effort to ameliorate famine.

The time series of summer PDSI reconstructed for the confluence region of the Ohio and Mississippi Rivers (37.5° N–90.0° W) is included in Fig. 12 and indicates that the decadal droughts of the mid- to late-Mississippian period were probably the most severe and long lasting of the past 700 yr (i.e., AD 1344–1353, 1379–1388, 1449–1458, and 1564–1573; the replication and reliability of the PDSI reconstructions in the region declines before AD 1300). Climatic deterioration has been previously implicated in the decline of the Mississippian period (Thomas, 2000; Cobb and Butler, 2002), and the new PDSI reconstructions provide the first detailed temporal and spatial estimates of the most severe and sustained droughts over the central United States during the disintegration of these societies.

6.3. Perceptions of the Great Plains: The Great American Desert and the Garden Myth

The new PDSI reconstructions add interesting insight into 19th century perceptions of the American West, especially the Great Plains, and their potential for settlement and economic development. Lawson and Stockton (1981) used the earlier more limited network

of tree-ring chronologies of Stockton and Meko (1975) to document widespread drought during the explorations of Stephen Long from 1819–1820, justifying the perception of the Great American Desert that arose from the expedition. We confirm their analyses with improved estimates of the severity and geographical impact of a three-year drought (1818–1820) during and just before the Long expedition (Fig. 13). The new reconstructions also indicate a severe two-year drought (1805–1806) during and just prior to the Zebulon Pike expedition (1806–1807). These extraordinary multi-year droughts must have had a severe negative impact on the vegetation cover and wildlife population levels in the Great Plains. Weaver and Albertson (1936) documented the impact of the 1930s drought on the true prairies of western Iowa, Nebraska, and Kansas, where the death of prairie plants from drought on thin upland soils ranged from 20–50% in the east to 80–95% in the western portions of their study area. Ellison and Woolfolk (1937) documented similar damage to the grasslands and woodlands of eastern Montana during the 1930s drought. The arid conditions reported by Pike and Long seem certainly to have arisen in part from the prevailing drought conditions they observed and not simply from a naïve prejudice for the wetter climates of the eastern United States.

The Garden Myth of the Great Plains, including the notion that “rain follows the plow”, was largely propaganda promoted by boosters and land speculators after the Civil War to encourage settlement (Stegner, 1992). In fact, the tree-ring reconstructions indicate that the latter half of the 19th century was frequented by persistent, multi-year, droughts across much of the West (Fye et al., 2003; Cook et al., 2004; Herweijer et al., 2006). Nonetheless, three consecutive wet years occurred from the Southern Plains into the western United States from 1867–1869 (Fig. 13), and during this moist interval Clarence Thomas declared that “rains follows the plow” (Stegner, 1992, p. 298). The tree-ring data also indicate a three-year wet episode over the central Great Plains and West from 1877–1879 (Fig. 13), and soon after Charles Dana Wilber published his glowing impressions of Great Plains agricultural potential (Wilber, 1881). Both these wet periods, in the late 1860s and later 1870s, corresponded to El Niños and came on the heels of protracted La Niñas and droughts (see Section 7). The promising moist conditions of the late 1870s were soon followed by recurrent drought in the late 1880s and 1890s, corresponding to a return to a persistent La Niña-like state, and which followed the catastrophic blizzards of 1886–1887, leading to the collapse of many pioneer

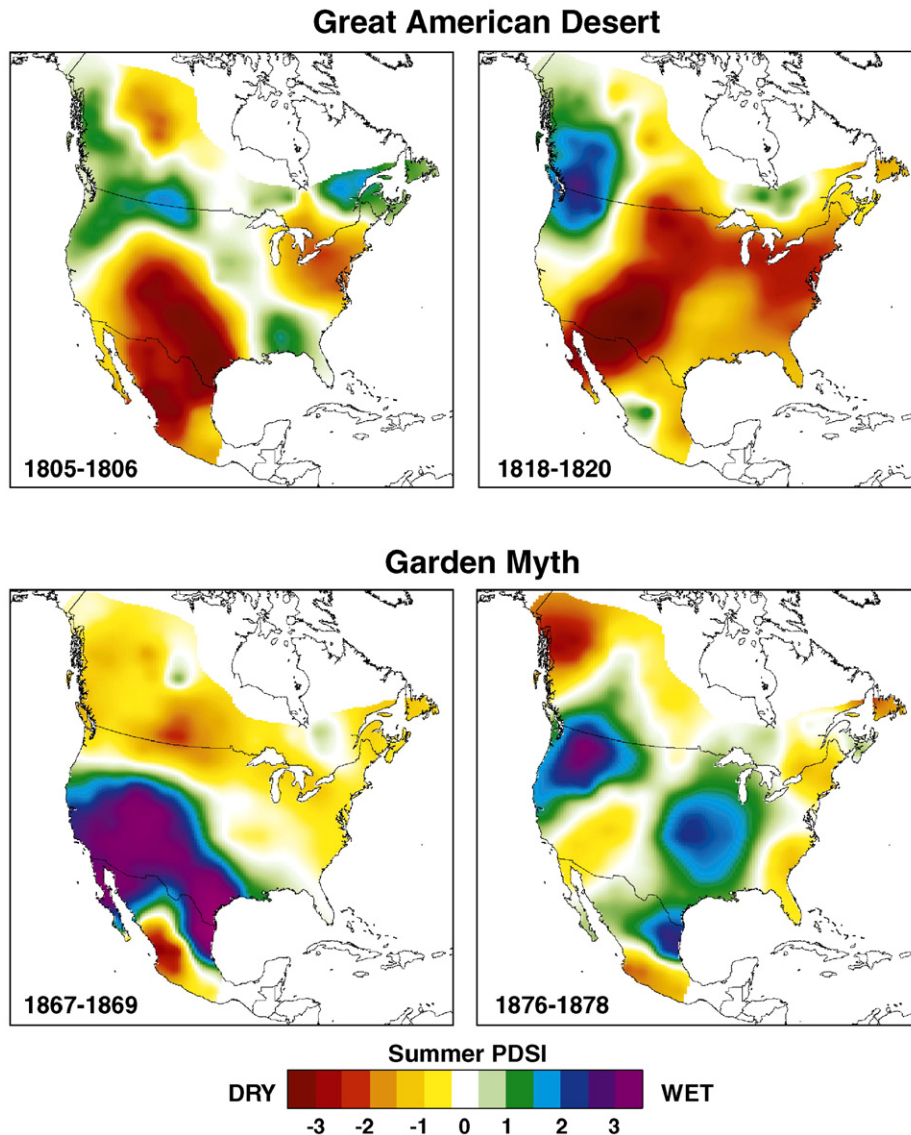


Fig. 13. Perceptions of the agricultural potential of the American West were influenced by prevailing climatic conditions (Lawson and Stockton, 1981). The Pike expedition of 1806–1807 and the Long expedition of 1819–1820 both encountered extreme drought conditions which must have contributed to their descriptions of the “Great American Desert.” Episodes of above average wetness in the 1860s and 1870s may also have helped boosters briefly promote the “Garden Myth of the Great Plains,” before the return of drought to the Plains in the 1880s and 1890s.

farms and ranches (Stegner, 1992; Wheeler, 1991, Herweijer et al., 2006).

The Great Plains climate is transitional between the humid east and the arid west. The instrumental and tree-ring reconstructed PDSI indicate that large portions of the Plains can become garden-like or desert-like, depending on the prevailing climatic regime. The proxy tree-ring data tell us that drought prevailed over much of the Plains during the 19th century. They further imply that modern industrial agriculture will become increasingly vulnerable to these decadal moisture regimes if the water resources of

the region continue to be depleted, e.g., the High Plains Aquifer (McGuire, 2004).

7. The dynamics of persistent North American droughts

It is only in the last decade, and really only in the last few years of that decade, that progress has been made in determining the causes of sustained, multi-year, droughts over North America. This work has made clear that tropical SSTs, and in particular, tropical Pacific SSTs,

are the ultimate driver. Three developments allowed this breakthrough:

1. The first was a natural development as the first persistent drought since the 1950s spread across the northern mid-latitudes in 1998 becoming the first multi-year drought event to be well captured within the Earth and space-based instrumental record.
2. The second development was a research advance that allowed the creation of global SST and sea ice datasets using sparse, ship-based, observations. These datasets extended the record of global ocean variations back until 1856 (Kaplan et al., 1998; Rayner et al., 2003). Prior to this work research on the causes of drought proceeded like the drunk looking for his keys under the lamppost — looking for causes in SST variations where there was data, that is, in the North Pacific and North Atlantic Oceans. Namias (1983) is a good place to start down this confusing route¹.
3. The third development was a change in the attitude of climate modelers. Until very recently, model simulations of SST-forced climate variations typically began in the 1950s partly because it was only over this period that upper air data was available for verification (atmospheric reanalyses were only extended back from 1960 until 1949 a few years ago). Hence model simulations tended to begin during or after the 1950s drought and, until the last few years, end before the most recent drought. Recently, enabled by the second development above, modelers have conducted simulations that begin earlier and capture the Dust Bowl drought (Schubert et al., 2004a,b) and all six multi-year droughts in the instrumental record (Herweijer and Seager, 2006; Herweijer et al., 2006; Seager, submitted for publication; Seager et al., 2005b).

The context and dynamics of North American droughts will here be illustrated using as an example the drought that began in the late 1880s and continued until 1896. The 1890s drought came after a feverous period of migration to the West, encouraged by the railroad companies and state and federal governments (Reisner, 1986). By and large the settlement had gone along with a period of wetter than usual conditions that encouraged widespread belief that ‘rain follows the

plow’. Frederick Jackson Turner had announced the closing of the frontier – defined as a region of minimal population density – in 1890 but, by the end of the drought depopulation had caused its resurrection (Worster, 1985). The 1890s drought, coming on the heels of a phenomenally cold winter in 1886 that killed vast numbers of cattle, restored some sense of realism to the difficulty of settlement in the arid regions and ended the idea that sturdy settlers, working alone, would be able to transform the West.

Libecap and Hansen (2002) demonstrate the impacts of the drought on agriculture and homesteading and the extent to which the prevalent ‘dry farming’ doctrine was inadequate to deal with the drought. To prevent further catastrophes it became recognized that the Federal government would have to be involved and the 1890s drought can take some credit for the beginning of Federally-driven irrigated agriculture with the Reclamation Act of 1902. It is of interest to examine the meteorological origins of such an important drought and historical turning point. Results presented here for the 1890s drought are very similar to those presented for twentieth century droughts by Seager et al. (2005b) and for the two other nineteenth century droughts by Herweijer et al. (2006).

7.1. *The global context of North American drought*

Determining the causes of North American droughts, like most climate phenomena, is greatly aided by taking a global perspective and recognizing that these are not geographically isolated events. Hoerling and Kumar (2003), in an influential paper entitled ‘The Perfect Ocean for Drought’, were the first to point out that the North American drought at the turn of the 21st century fitted into a zonally symmetric pattern of mid-latitude dryness that dynamically linked the droughts in North America, the Mediterranean and central Asia.

Schubert et al. (2004b) then demonstrated that within a climate model the Dust Bowl drought of the 1930s fitted into a pattern that had not just zonal symmetry but also hemispheric symmetry. This point was amplified by Seager et al. (2005b) in a climate model simulation of the 1856 to 2000 period. To ram the point home, Herweijer and Seager (2006) used station precipitation data and climate model simulations to demonstrate that each of the six multi-year mid-latitude drought events in North America that have occurred since the onset of SST observations (1856–65, the 1870s, 1890s, 1930s, 1950s and the most recent, turn-of-the-century, drought) fitted into a global

¹ It would be an interesting topic for a historian of science to determine by how many years progress in understanding global climate variations was set back by meteorologist’s habitual use of polar stereographic map projections, which inhibited the identification of tropical forcing, let alone hemispheric symmetry.

pattern with hemispheric symmetry and, in the extratropics, zonal symmetry. The drought records of the Pampas in southern South America and that of the Great Plains, in fact, share a remarkable similarity.

The global footprint of these hydroclimate regimes, and their hemispheric symmetry, suggested that the causes lay in the tropics. Indeed, Hoerling and Kumar (2003) and Schubert et al. (2004a,b) implicated tropical SSTs as the cause of the recent and Dust Bowl droughts, respectively. Going further, Seager et al. (2005b), Herweijer et al. (2006), Herweijer and Seager (2006), and Seager (submitted for publication) demonstrated that all of the six mid-latitude drought regimes were accompanied by persistent La Niña-like SSTs in the tropical Pacific, even as SST anomalies in the other oceans varied between the different events. Further, they demonstrated that this global drought history could be reproduced with remarkable fidelity in a climate model forced by the history of tropical Pacific SSTs alone.

Fig. 14 shows the observed station precipitation anomaly (from the Global Historical Climatology Network (GHCN)) and the observed SST anomaly (Kaplan et al., 1998; Rayner et al., 2003), averaged over the 1890–1896 period relative to a 1856 to 2005 climatology, together with the equivalents from the climate model ensemble of Seager et al. (2005b). The atmosphere general circulation model used is the Community Climate Model 3 (CCM3) of the National Center for Atmospheric Research. The model ensemble members were forced with observed SST anomalies in the tropical Pacific Ocean only and SST anomalies elsewhere were computed with a mixed layer ocean model — the so-called POGA-ML configuration (for Pacific Ocean–Global Atmosphere–Mixed Layer ocean). The model ensemble consists of 16 members, each integrated from 1856 to 2005 beginning with different atmospheric initial conditions on January 1, 1856. The ensemble average is shown here. The mean over such a large ensemble effectively averages over and removes the uncorrelated internal atmospheric variability in the ensemble members and isolates the part of the atmospheric circulation common to the members, that is the part that is forced by the imposed SSTs.

Station data from the 1890s is relatively sparse, and of questionable reliability, in the Americas. Nonetheless, the drought over North America can be easily seen, especially in the Plains region. The tree-ring reconstruction of the summer PDSI, which may be more accurate than the station data, is shown in the top left panel and clearly shows the drought extending into the Rockies. As described earlier, PDSI is meant to be an indicator for soil moisture anomalies. Consequently the upper right panel of Fig. 14 shows the soil moisture anomaly in the

upper 1.5 m as simulated by the POGA-ML model. The model soil moisture and tree-ring reconstructed PDSI show general agreement that most of North America except for part of the Pacific coast and New England (according to the trees) were struck by drought.

Station data is very sparse in South America but there is an indication of drought in the southern regions, an area also impacted by drought in the 1930s and 1950s. Areas of Europe were also struck by drought during this period. The observed global SST anomaly of the 1890s has a classic persistent La Niña-like pattern with a broad area of colder than usual waters in the eastern tropical Pacific, warmer waters in the central and western subtropical and mid-latitude Pacific Ocean, cool waters along the Pacific coasts of the America and a cool Indian Ocean. This pattern is very similar to that which accompanies interannual La Niña events.

The middle and lower right hand panels of Fig. 14 show the drought regime from the POGA-ML model simulations. The model reproduces the North American drought and brings into relief the drought in southern South America. The tropical Americas were wet in the model — a situation hinted at in the station data — which is also typical of La Niña conditions. The model also reproduced a drought over Europe in agreement with observations. The rough hemispheric and zonal symmetry of this drought period, like the others before and after, is clear in the model.

It is also striking that most features of the global SST field during the 1890s are reproduced by the POGA-ML model as a remote response to the tropical Pacific, La Niña-like, SST forcing. This includes the cool waters along the west coasts of the Americas and the warm waters in the mid-latitude western and central Pacific Ocean in each hemisphere, a cool Indian Ocean and cool waters across most of the Atlantic Ocean. Although the modeled SST anomalies are systematically too weak — a problem we are yet to diagnose — this amount of agreement is convincing evidence that the climate regime of the 1890s, with widespread drought throughout the mid-latitudes, was a result of the persistently cold tropical Pacific Ocean of that period. It also makes clear that the SST anomalies in regions of the ocean away from the tropical Pacific, while perhaps influencing the development of the mid-latitude droughts, are not causal but are themselves a response to the tropical Pacific SSTs.

7.2. Eddy–mean flow interaction and tropical forcing of mid-latitude drought

The anomaly during the 1890–1896 period of the zonal mean zonal winds and temperature are shown in

1890-1896 Average

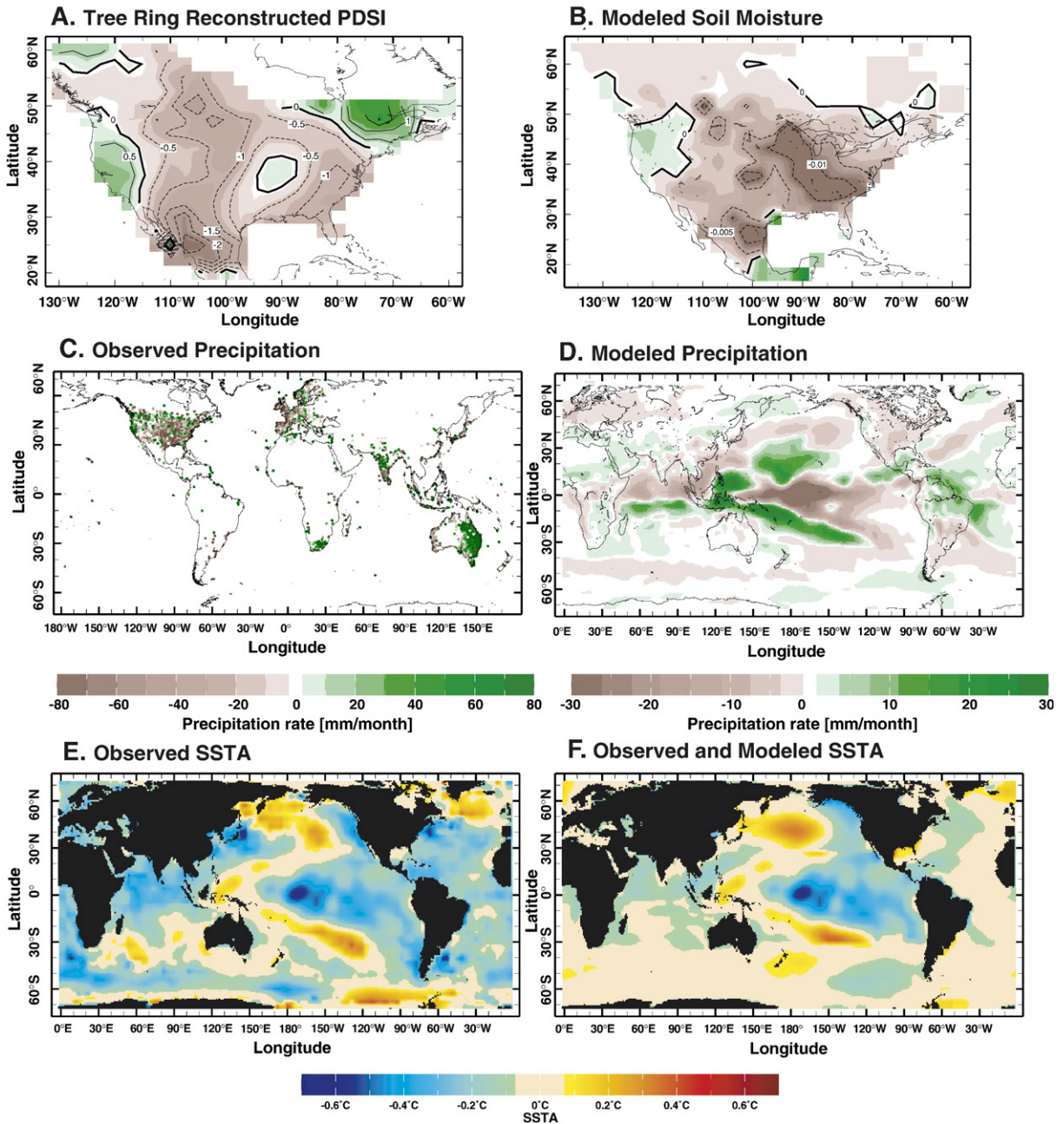


Fig. 14. Top row: the tree-ring reconstructed PDSI (left) and the modeled soil moisture anomaly within the POGA-ML ensemble (right), both non-dimensional. Middle row: the observed precipitation anomaly for 1890–1896 as derived from station data (left) and the POGA-ML simulation (right). Bottom row: the observed SST anomaly (left) and the SST anomaly from the POGA-ML model (right) which is a combination of observed SST anomaly in the tropical Pacific and computed SST anomaly elsewhere. Units are mm per month for precipitation and Kelvin for temperature.

Fig. 15, as simulated by the POGA-ML model, for both the winter and summer half years of the period. Generally the troposphere in the model was cooler

during this period, a manifestation of the overall tropical Pacific warming in the Twentieth Century, but, once more, the typical La Niña-like pattern is

POGA-ML 1890-1896 Zonal Averaged Temperature (colors), Zonal Winds (contours)

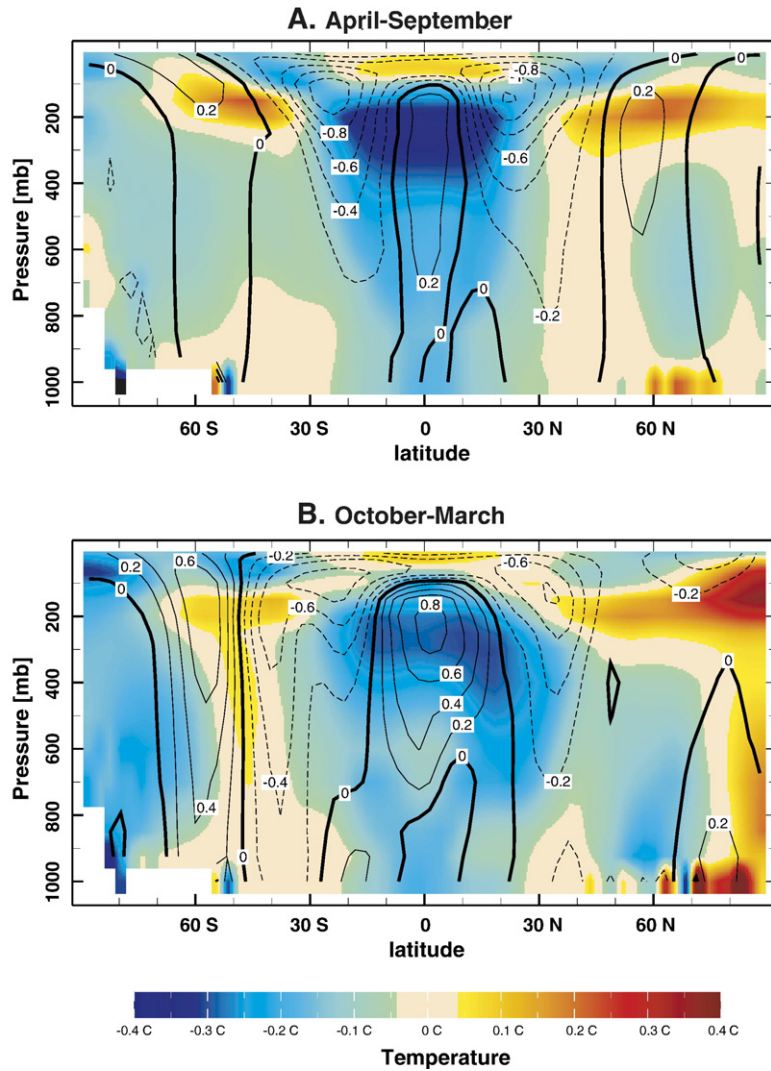


Fig. 15. Anomalies of the zonal mean temperature (colors) and zonal mean zonal wind (contours) from the POGA-ML model for the 1890–1896 period for the northern hemisphere summer seasons (above) and winter seasons (below). Units are Kelvin for temperature and meters per second for winds.

evident. There was strong cooling in the tropics with a maximum in the upper troposphere and a cooling minimum, or actual warming, in the mid-latitudes of each hemisphere. Consistent with this pattern, the subtropical jets were weaker in each hemisphere. Allowing for the overall cooler period, this is essentially the opposite of the pattern of hemispherically symmetric climate change, with tropical temperature anomalies inducing opposite signed anomalies in mid-latitudes, identified by Seager et al. (2003) as the typical response to El Niño.

How the changes in the subtropical jets impact the mid-latitude climate can be understood with reference to the zonal mean governing equations in the extratropics:

$$-f\langle\bar{v}\rangle = -\langle u\bar{v}'\rangle_y, \quad (1)$$

$$f\langle\bar{u}\rangle = -\langle\bar{\phi}\rangle_y, \quad (2)$$

$$\langle\bar{v}\rangle_y + \langle\bar{\omega}\rangle_p = 0, \quad (3)$$

$$\langle\bar{\omega}\rangle(\langle T\rangle_p - \kappa\langle T\rangle/p) = -\langle\bar{v}T'\rangle_y - \langle\bar{\omega}T'\rangle_p + \kappa\langle\bar{\omega}T'\rangle/p + R, \quad (4)$$

together with the vertically integrated moisture equation:

$$\langle \bar{P} \rangle = \langle \bar{E} \rangle - \int_0^{P_s} \left(\langle \bar{v} \rangle \langle \bar{q} \rangle_y + \langle \bar{v} \bar{q}' \rangle_y \right) dp. \quad (5)$$

In these equations the angle brackets denote a zonal mean, overbars denote the monthly time mean and primes denote the deviation from the time mean. The zonal, meridional and vertical pressure velocities are denoted by u , v and ω , T is temperature, q is specific humidity, P is precipitation, E is surface evaporation, p is pressure, ϕ is geopotential height, f is the Coriolis parameter, κ is the gas constant divided by the specific heat of air at constant pressure and R is the radiative flux convergence. Contributions to the zonal mean circulation, temperature, and precipitation by the stationary waves have been omitted for illustrative purposes but can be important.

Seager et al. (2003) detailed the way in which the changes in the subtropical jet streams impact the vertical and meridional propagation of transient eddies. The changes in subtropical jet stream and location are controlled by thermal wind balance (Eq. (2)): as the tropics cool a reduced meridional pressure gradient causes the subtropical jet to weaken. For the case of weaker jets, as during persistent La Niña conditions, transient eddies propagate less deeply into the tropical upper troposphere, instead depositing their momentum further poleward. As such, there is less poleward eddy transport of zonal momentum in the subtropical upper troposphere and more poleward transport in the mid-latitudes. The modeled anomalies of eddy momentum fluxes during the 1890s drought for the summer and winter half years are shown in Fig. 16A.

As seen in the equations, the convergence of eddy momentum flux has to be balanced by the Coriolis torque associated with the mean meridional velocity. That is, the anomalous eddy momentum fluxes induce a mean poleward flow. By continuity the induced meridional flow will force descent where there is upper tropospheric mass convergence. The subsidence is given by:

$$\langle \bar{\omega}(p) \rangle = - \int_0^p \left(\frac{1}{f} \langle \bar{u}'v' \rangle_{yy} - \frac{\beta}{f^2} \langle \bar{u}'v' \rangle_y \right) dp. \quad (6)$$

By examining the eddy momentum fluxes shown in Fig. 16A (here shown just for the October through March half year) it can be deduced from this relation that subsidence (positive ω) will occur due to the first term on the right. (The β term will move the subsidence equatorward.) The modeled subsidence anomaly during

the 1890s drought is shown in Fig. 16B: there is anomalous downward motion in the mid-latitudes of each hemisphere, just where expected if eddy momentum fluxes were the cause.

Downward motion forces warming due to compression. This is balanced in part by increased radiative cooling and in part by reduced transient eddy heat flux convergence (Seager et al., 2003). Note that, as is typical, the transient eddy heat flux acts diffusively, opposing a temperature anomaly created by the mean flow (see Robinson (2005) for a discussion of this). The subsidence will also lead to low level divergence and, as can be seen from the moisture equation, to a reduction of $P-E$ and, in general, a reduction in precipitation itself. This makes sense as a budget but also in a more fundamental way. Precipitation only occurs where there is ascending motion since that is required to convert water vapor into condensate. Any process, in this case transient eddy momentum fluxes, that forces descent will suppress precipitation. The details of how the moisture budget comes back into balance – whether there is reduced evaporation or moisture convergence by the mean flow or transient eddies – is less important than the fact that forced descent will suppress precipitation (Seager et al., 2005a). The changes in the zonal mean moisture budget are much the same as is shown for the 1930s and 1950s in Seager et al. (2005b): the precipitation anomalies most closely track the anomalous moisture convergence by the zonal mean flow, both in the tropics and the extratropics. In the zonal mean the convergences and divergences by transient eddies and stationary eddies largely cancel each other out. These results are not shown here for brevity.

7.3. Tropically-forced stationary Rossby waves and drought over North America

The zonal mean circulation anomalies are not the entire story however. In addition stationary Rossby waves are excited by the precipitation anomalies over the tropical Pacific (reduced precipitation and atmospheric heating at the Equator and increases off the Equator) and propagate poleward and eastward. Understanding of these waves goes back to Hoskins and Karoly (1981) and Trenberth et al. (1998) provide a useful review. The Rossby wave- or teleconnection-pattern associated with La Niñas creates an upper level anticyclone over the eastern North Pacific, a cyclone over western Canada, and another anticyclone over the southern United States. In winter these wave trains are essentially equivalent barotropic, that is they have the same sign throughout the troposphere, as can be seen by

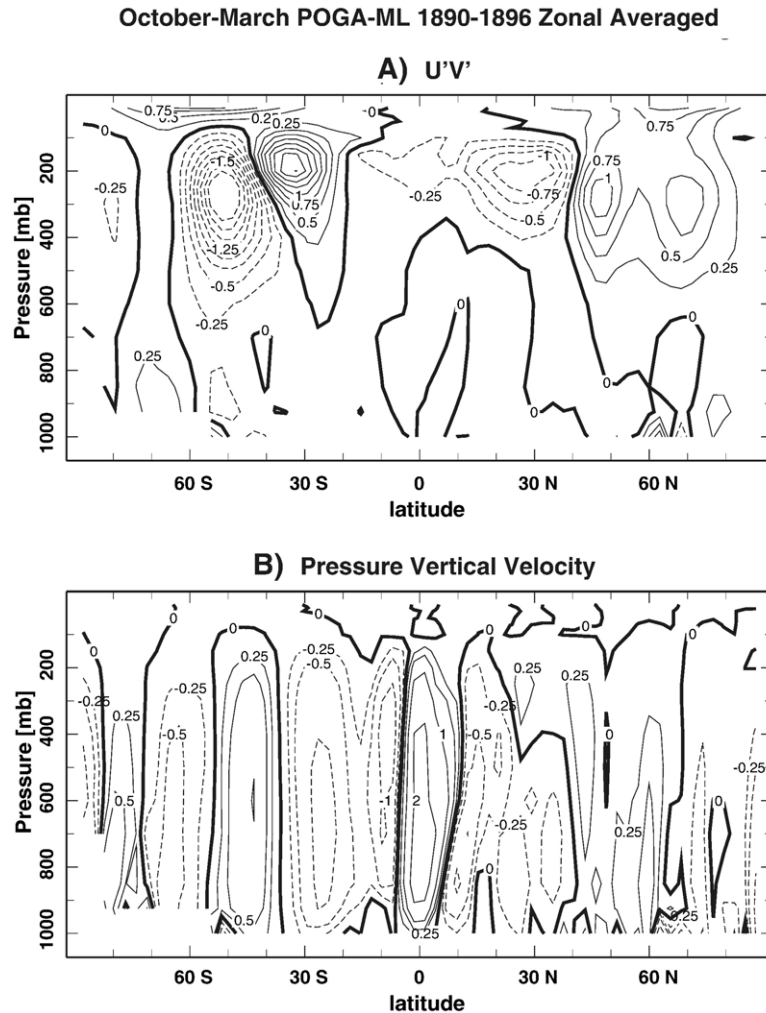


Fig. 16. The meridional flux anomalies of zonal momentum by transient eddies (top) and vertical pressure velocity (below) for the northern hemisphere winter half years as simulated by the POGA-ML model. Units are meters squared per second squared for momentum flux and Pascals per second, times one thousand, for pressure velocity.

comparing the upper level height anomalies with the lower level height anomalies in Fig. 17B.

Fig. 17A shows the upper level geopotential height anomalies over the Americas during the winters of the 1890s drought. The ridges of high pressure, expected as part of the zonal mean response to La Niña conditions, are clearly seen in the mid-latitudes of each hemisphere. In addition the Rossby wave signal over the Americas is clear with a wave train of alternating cyclones and

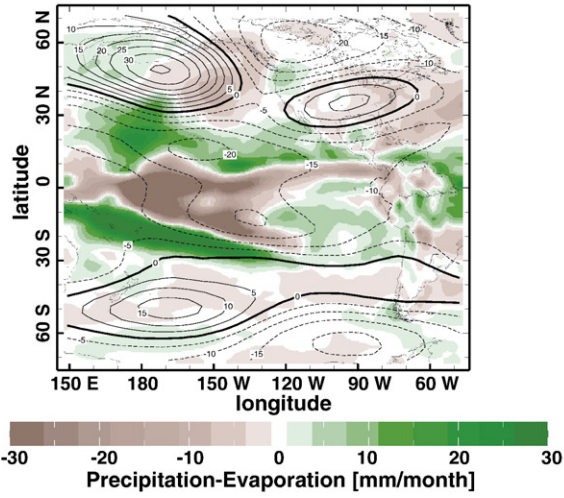
anticyclones. The southern United States lies under a high. Also shown in Fig. 17A is the $P-E$ anomaly and it is clear that this high corresponds to atmospheric moisture divergence and, hence, negative $P-E$. Thus, the zonal mean signal of mid-latitude drought is regionally intensified over North America by Rossby waves propagating from the tropical Pacific Ocean.

Fig. 17C shows that the regions of drying lie under regions of anomalous descent, just as in the zonal mean.

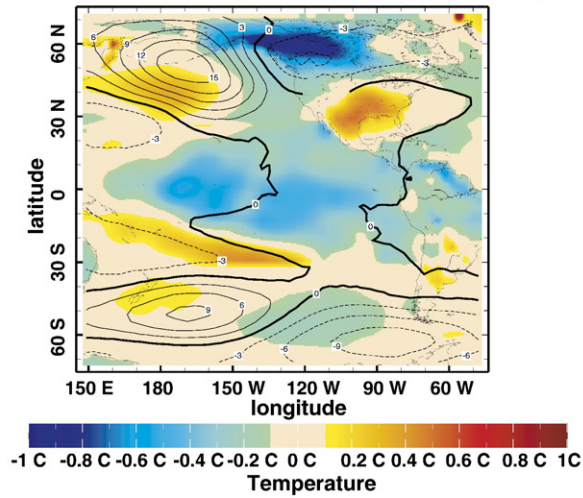
Fig. 17. The winter half years of the 1890–1896 drought as simulated with the POGA-ML model. The top panel shows the 250 mb potential height anomaly (contours) and the $P-E$ anomaly (colours). The middle panel shows anomalies of 850 mb geopotential height (contours) and surface temperature (colors). The bottom panel shows the 850 mb winds as vectors and the 500 mb vertical pressure velocity and colors and contours. Units are mm per month for $P-E$, meters for geopotential height, Kelvin for temperature, Pascals per second, times one thousand, for pressure velocity and the scale for the vectors is shown at lower right.

POGA-ML October-March 1890-1896 Average

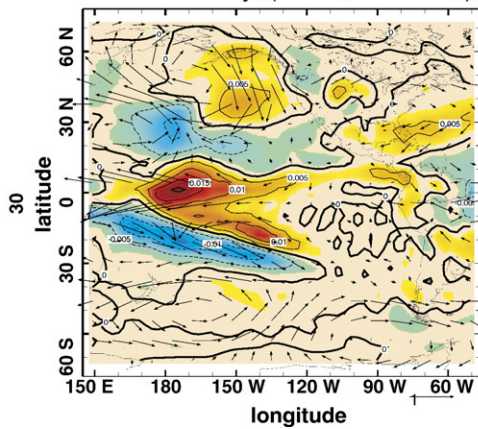
A) Precipitation-Evaporation (color), 250 mb Geopotential Height (contours)



B) Surface Temperature (colors), 850 mb Geopotential Height (contours)



C) 500 mb Vertical Pressure Velocity (colors, contours), 850 mb Winds (vectors)



In this case however the possible causes of descent are more complex than in the zonal mean and linked into the stationary wave response. As can be seen by the low level wind field anomalies in Fig. 17C, equatorward flow induces descent. This could arise from a balance between advection of planetary vorticity by the anomalous flow and vortex compression and/or between advective cooling and subsidence warming. This is quite apparent west of the west coast of North America. It is also, in general, true over the Great Plains region during summer. In this case the equatorward flow may be caused by eddy-induced subsidence and can amplify the drought by reducing the poleward flow of moisture from the Gulf of Mexico. But the situation can be made more complex by the ability of both anomalous transient eddy fluxes of heat, and anomalous mean flow advection of mean flow vorticity, to induce patterns of vertical motion.

7.4. Summertime drought and the possible role of soil moisture and land–atmosphere interaction

It has long been thought that land–atmosphere interaction can introduce persistence into droughts as reduced precipitation lowers soil moisture, reduces surface evapotranspiration and further reduces precipitation. In this sequence the length of time for soil moisture adjustment introduces a lag and a memory. Koster et al. (2004) demonstrate that, in climate models, the Great Plains and the Sahel are the two regions of the world where there is strong coupling between soil moisture and precipitation and where land surface processes can lead to persistence. Normally the timescale is thought to be on the order of seasons rather than years.

Land–atmosphere interactions are most commonly invoked during the summer season. In the models and in observations precipitation is greatly reduced during the summer (Seager et al., 2005b). During the 1930s Dust Bowl drought winter precipitation remained normal but during other droughts winter precipitation was also reduced. In general the droughts appear to be year-round phenomena.

The model simulations analyzed provide some support for a summer land–atmosphere feedback (Fig. 18). During the summers of the persistent droughts, including the 1890s one, there are positive anomalies of $P-E$ over Mexico and the southern United States.

This is despite negative P anomalies and indicates that the surface evapotranspiration is reduced by even more with anomalous atmospheric moisture convergence stepping in to provide balance. This situation would not lead to a self-sustaining drought. Instead it suggests that negative $P-E$ anomalies before the summer reduce the soil moisture and, hence, the evapotranspiration in summer leading to reduced precipitation. Since the atmospheric column becomes dry, transient eddies, acting diffusively, converge more moisture into the region. In other words soil moisture feedbacks are acting as a bridging mechanism that extends the influence of winter precipitation reductions into summer.

However this is not the only process at work in the summer. The mid-latitude ridges, related to tropical cooling, are still present in summer (Seager et al., 2005b; Herweijer et al., 2006) indicating the continued existence of atmospheric circulation anomalies forced from the tropics. It is also noticeable that, during summer, the equivalent barotropic structure of the mid-latitude circulation anomalies is interrupted over North America as surface low pressure develops over the southeast and northerlies develop to the west over the Plains. This thermal low type of pattern is suggestive of a circulation response to the change in surface and column heating as the diabatic heating by precipitation is reduced and the surface cooling by sensible heat and longwave radiation is increased. This possible circulation response, and how it feeds back into the moisture budget, is deserving of more attention.

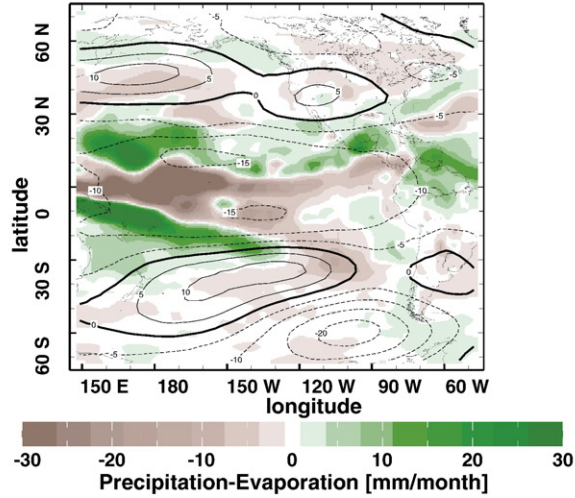
7.5. Summary of drought mechanisms

In summary, then, the persistent droughts over North America all arose as part of the response of the global climate to persistent La Niña-like conditions in the tropical Pacific Ocean. When the waters are cool so is the tropical troposphere and the subtropical jet streams weaken and move poleward. This impacts the propagation of transient eddies such that they propagate less deeply into the tropical upper troposphere. As such there is less poleward transport of zonal momentum in the subtropics and more in the mid-latitudes. The divergence of the eddy momentum transports is balanced by the Coriolis torque, resulting in poleward flow in the upper troposphere from the subtropics into the mid-latitudes.

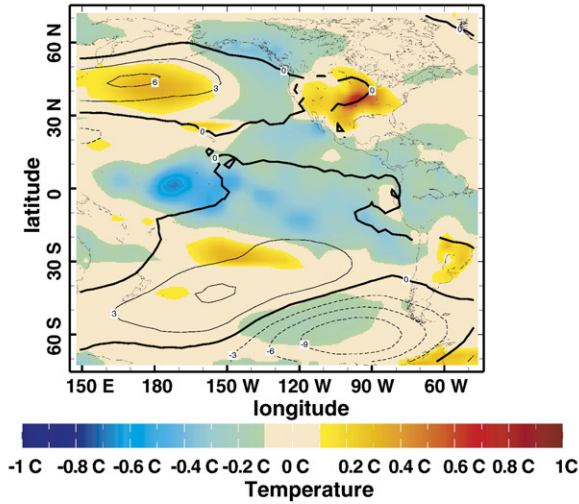
Fig. 18. The summer half years of the 1890–1896 drought as simulated with the POGA-ML model. The top panel shows the 250 mb geopotential height anomaly (contours) and the $P-E$ anomaly (colours). The middle panel shows anomalies of 850 mb geopotential height (contours) and surface temperature (colors). The bottom panel shows the 850 mb winds as vectors and the 500 mb vertical pressure velocity and colors and contours. Units are mm per month for $P-E$, meters for geopotential height, Kelvin for temperature, Pascals per second, times one thousand, for pressure velocity and the scale for the vectors is shown at lower right.

POGA-ML April-September 1890-1896 Average

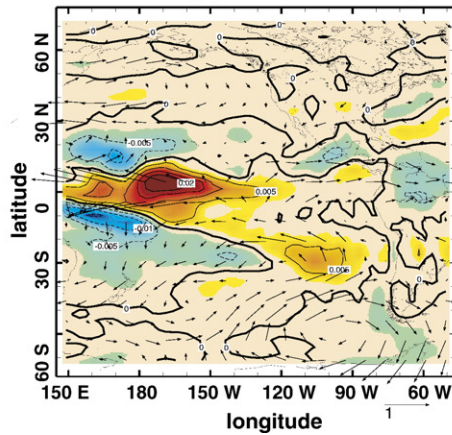
A) Precipitation-Evaporation (color), 250 mb Geopotential Height (contours)



B. Surface Temperature (color), 850 mb Geopotential Height (contours)



C. 500 mb Vertical Pressure Velocity (colors, contours), 850 mb Winds (vectors)



By continuity this induces downward motion that causes warming and suppresses precipitation — at all longitudes and in each hemisphere. This zonally symmetric mechanism of tropical forcing of mid-latitude drought regimes is interrupted by stationary Rossby wave propagation from the tropical Pacific region. These stationary waves place anomalous anticyclones over North America during extended La Niña events and enhance the droughts within this region.

7.6. Possible role of Atlantic SST anomalies

The mechanism of drought generation that we have described has only involved forcing from the tropical Pacific Ocean. This is consistent with the model results presented in which adding in global SST anomalies did not lead to clearly greater skill at simulating North American droughts. In contrast using a different climate model, Schubert et al. (2004a) claim that the Dust Bowl drought was about equally forced by the cool tropical Pacific and the warm tropical Atlantic. Sutton and Hodson (2005) have also claimed that warm tropical Atlantic SST anomalies induce drying over North America. Their results are not, however, of direct relevance to the drought problem as they examined the entire 30-year period from 1930 to 1960 and compared it to the 1960 to 1990 period, whereas it is the multi-year timescale that is of most relevance to North American droughts. Sutton and Hodson also only considered the June through August part of the year whereas, as we have already stated, the droughts in general contain significant drop-offs of precipitation in spring, fall and winter as well.

There is general agreement that it is the tropical component of Atlantic SST anomalies that are important though they arise as part of a pattern with the same sign anomalies throughout the North Atlantic. Warm Atlantic anomalies go along with drought. It is often suggested that this pattern arises as a response to changes in the Atlantic thermohaline circulation (Kushnir, 1994). However there is a significant complication in that the tropical Pacific can force remote Atlantic SST anomalies and perhaps also change the strength of the thermohaline circulation. Currently there is no proposed mechanism for how tropical Atlantic anomalies force drought. This is in contrast to the two mechanisms proposed for linking tropical Pacific anomalies and North American (and global) hydroclimate, which are well evidenced in observational analyses and models and which have clear basis in dynamical theory. It could be that, during summer, Atlantic SST anomalies influence the southerly flow on the western flank of

the North Atlantic subtropical anticyclone, but this is yet to be demonstrated.

The possibility of a role for the tropical Atlantic Ocean needs more investigation. The model results presented here and in the referenced papers clearly link the six droughts that have occurred since the mid-nineteenth century to cool tropical Pacific SSTs. Further the model results provide a consistent dynamical explanation. What is more, the observed droughts fit into as global pattern with hemispheric symmetry, a pattern that the tropical Pacific-forced model can reproduce (Herweijer and Seager, 2006). The hemispheric symmetry argues for a tropical Pacific cause, whereas the Atlantic mechanism relies on SST anomalies that have notable hemispheric *asymmetry*. It is hard to imagine how the subtropical North Atlantic SST anomalies could be responsible for the correlation between North American and South American droughts.

However it could be that the CCM3 model used here, while correctly representing the Pacific influence, misses an additional influence of the Atlantic Ocean. The other models that have been used to make the case for an Atlantic SST-drought link during the Dust Bowl need to be further investigated to see if the Atlantic also impacts the other five droughts. Further, it is imperative that the mechanisms that underlay such a link be determined.

8. Causes of tropical Pacific SST variability on decadal and centennial timescales

The last section makes a compelling case that the persistent North American droughts are “caused” by a particular pattern of decadal SST anomalies in the tropical Pacific that bears enough resemblance to the interannual La Niña SST pattern to be termed “La Niña-like”. The obvious next questions are what causes these temperature patterns and are they predictable. A clear answer has yet to emerge.

While the principal decadal pattern of Pacific SST variability does resemble the ENSO pattern, it has broader scales and relatively greater amplitude in extratropical latitudes (e.g., Fig. 14C; Zhang et al., 1997). The strength of the pattern in the North Pacific led a number of investigators to regard it as primarily a northern hemisphere extratropical phenomenon, the Pacific Decadal Variation or PDO (see especially Mantua et al., 1997). In this guise it has been shown to be linked to rainfall over western North America (Gershunov and Barnett, 1998), in the same sense as the long-established link between the ENSO cycle and rainfall (Ropelewski and Halpert, 1987). An important

finding of this work is that the relationship between the PDO and rainfall is not merely the decadal average of ENSO events. This result is confirmed by the numerical experiments of Huang et al. (2005), who show that the difference between the relatively wet period from 1976 to 1998 and the preceding dry decades is successfully simulated by an atmosphere model forced only by the mean SST anomalies in the two periods; the difference is not a rectified effect of the greater El Niño activity in the later period. Consistent with the results reported in the previous section, Huang et al. (2005) also show that the tropical SSTs are the primary reason for the rainfall difference.

These model results are in keeping with observational studies showing that there are decadal variations in the South Pacific, and that these are linked to the PDO (Garreaud and Battisti, 1999; Power et al., 1999; Deser et al., 2004). Power et al. (1999), noting that “PDO” is usually taken to be centered in the North Pacific, use “Interdecadal Pacific Oscillation” (IPO) to emphasize the basin-wide nature of Pacific variability. Having the signal appear in both hemispheres implicates the tropics as a likely source, and some of this work finds a clear tropical signature in the data (see especially Deser et al., 2004).

8.1. *Origins of tropical Pacific decadal variability*

How much of the basin wide decadal variability is driven from coupled interactions in the tropical Pacific similar to ENSO, and how much is attributable to mid-latitude sources is an area of active research. Recall that the POGA-ML experiments described in the previous section strongly suggest that the mid-latitude SST part of the IPO pattern could be forced by atmospheric anomalies driven by tropical SST anomalies. Gu and Philander (1997) proposed that mid-latitude SST anomalies generated by anomalous heat fluxes could be subducted and carried to the equator, changing temperatures in the equatorial thermocline and then upwelled to change equatorial surface temperatures. This mechanism would complete a loop from equatorial SSTs through the atmosphere to mid-latitude SSTs and then back through the ocean to equatorial SSTs. However, careful studies of Pacific SST variations in recent decades have shown that the oceanic pathway is ineffective because the mid-latitude anomalies are diluted by mixing, especially as they move along the western boundary on their way to the equator (Schneider et al., 1999; Hazeleger et al., 2001). Still, since subduction and advection of mid-latitude waters is the source for the equatorial thermocline, this oceanic mechanism must become effective at some longer timescale.

An alternate hypothesis for Pacific variability at decadal and longer periods is that it is generated solely in the tropical Pacific by ocean–atmosphere interactions similar to those driving ENSO (Karspeck and Cane, 2002; Karspeck et al., 2004). If chaotic dynamics are dominant then there might be some hope of predicting decadal variations. Karspeck et al. (2004) and Seager et al. (2004) investigated decadal predictability in idealized experiments with the intermediate Zebiak and Cane (1987) ENSO model. They found a modest degree of decadal predictability, perhaps too modest to be of practical value. Since this was in idealized experiments, it overstates the ability to predict the real world even if the dynamics of the simplified model correctly captures the dominant dynamics in nature. If the random intrusions of mid-latitude systems or the random perturbations of intraseasonal and other tropical “noise” are more important in nature than in the model, then the predictability is smaller still. At this point the issue of predictability has barely transitioned from the issue of model predictability to real world predictability with data assimilation. The origins and predictability of decadal variability of the tropical Pacific Ocean remains a fundamental research frontier. Any multi-year predictability of North American droughts will require successful multi-year predictions of tropical Pacific SSTs.

8.2. *Tropical Pacific SSTs over the last millennium*

All the hypotheses described thus far rely on interactions internal to the earth’s climate system. Another possibility is that the variations are forced externally by solar variations and changes in volcanic aerosols. The perennial problem with solar-climate connections is the very small size of the solar forcing signal, but because the amplitude of the decadal SST anomalies responsible for major droughts is so small (viz. Fig. 15), the solar option cannot be dismissed.

To explore this issue further, we begin with the millennium long record of drought in the west shown in Fig. 10. The first question to be answered is whether there is any evidence that the tropical Pacific SST–drought relation seen in the past 150 yr – the period of instrumental data – holds for the more extreme and extended droughts of this longer period. In this period we must rely on paleoproxies for SST information as well as for drought. The principal proxies able to resolve decadal variations are tree rings and isotopic analyses of corals. The tree rings relevant for tropical Pacific SSTs are primarily proxies for precipitation in places where the influence of ENSO and the IPO are strong, and so necessarily build in the modern relationship between

ENSO or IPO and drought. A true test of the SST–drought relationship can use only corals as a proxy for SSTs. Evans et al. (2002) obtained measures of tropical SSTs from corals at multiple sites, but since there is only a single coral head at each site, the records go back no more than a few hundred years. Cobb et al. (2003) overlapped shorter segments of fossil coral in a manner similar to the way tree-ring time series have been spliced together from individual trees. The result is displayed in Fig. 19. Palmyra (6° N, 162° W) is in a prime location to provide an ENSO proxy, and Cobb et al.’s $\delta^{18}\text{O}$ record from modern corals correlates with the NINO3.4 (120° W to 170° W, 5° S to 5° N) SST at $r = -0.84$ in the ENSO band. In other words, this coral proxy series correlates as well or better than any two commonly used ENSO indices (e.g. SOI, NINO3, NINO3.4) correlate with each other. It is likely that the $\delta^{18}\text{O}$ signal primarily reflects rainfall and so correlates better with NINO3.4 (and NINO3) than with local SST (see Evans et al., 2002). It also appears that the $\delta^{18}\text{O}$ signal is a good proxy for decadal SST.

The Cobb et al. record, taken together with the drought record of Fig. 10, appears to verify the modern

relationship between SST and drought. SSTs in the eastern Pacific are low (La Niña-like) in the period circa AD 1200 when severe drought prevailed in the west, and high in the 1600s, during the Little Ice Age, when the west was wetter.

Fig. 19 also displays the mean of a 100-member ensemble calculated by forcing the Zebiak–Cane model with a slightly updated version of the Crowley (2000) solar and volcanic forcing; for details see Mann et al. (2005). There is general agreement that much of the ENSO variability is generated in ways internal to the climate system, either by chaos or noise, so we cannot expect even a perfect model to agree in detail with the single realization present in the observational record. Insofar as ENSO variability is forced, then it is possible for values averaged over a number of ENSO events to have similar features in different realizations. Indeed, Fig. 19 shows, for both model and data, cold SSTs in the mean in the late 12th–early 13th centuries, moderate SSTs in the 14th–early 15th centuries, and warm SSTs in the late 17th century. In all three cases the means of the observations and the model ensemble are consistent within the ensemble sampling distribution (dashed lines

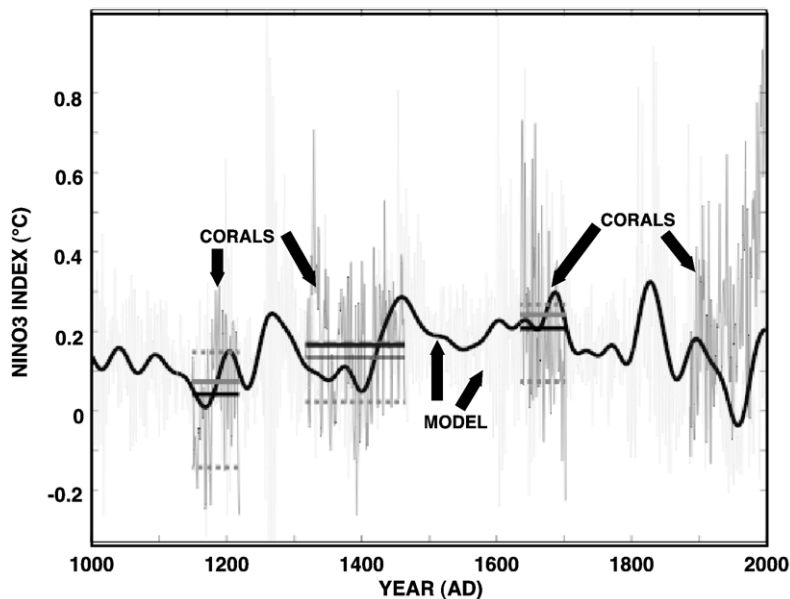


Fig. 19. After Mann et al. (2005). The annual mean NINO3 response of the Zebiak–Cane model to the combined volcanic and solar radiative forcing is compared with reconstructions of ENSO behavior from Palmyra coral oxygen isotopes. The model is run over the interval AD 1000–1999; the coral reconstruction, shown as darker grey curves, is available only for the 4 intervals shown. The continuous faint grey curve is the annual mean model NINO3 anomaly (in °C relative to the AD 1950–1980 reference period) averaged over a 100 member ensemble. Despite the averaging considerable variability remains, largely due to the influence of volcanic eruptions. The heavy black line shows 40-year smoothed values of model NINO3. The coral data (darker grey curves) are scaled so that the mean agrees with the model (see Mann et al, 2005 for details). Thick grey lines indicate averages of the scaled coral data for the three available time segments; the thick black lines are the ensemble-mean averages from the model for the corresponding time intervals. The associated inter-fourth quartile range for the model means (the interval within which the mean lies for 50% of the model realizations) is also shown (dashed grey lines). The ensemble mean is not at the center of this range, due to the skewed nature of the underlying distribution of the model NINO3 series.

on Fig. 4). Moreover, the late 17th century warmth and the 12–13th century cold are well separated within the distribution of states from the model ensemble runs: one would expect the later period to be warmer than the earlier one in roughly 7 out of every 8 realizations. Assuming these statistics, which are derived from an ensemble of model runs, apply to reality, we would expect nature's single realization to be warmer in the later period with close to a 90% probability. In both data and model there is also a systematic difference in the strength of the ENSO cycle in the two periods with more (less) ENSO variability going with a warmer (colder) mean SST in the eastern equatorial Pacific.

Due to both greater solar irradiance and fewer volcanic eruptions, the late 12th–early 13th centuries is a time of greater heating compared with the centuries since up until the last decade or two. This period is sometimes referred to as the “Medieval Warm Period”, especially in studies based on data from Europe. The late 17th century, during the Little Ice Age, is a time of reduced solar radiance and more volcanic eruptions (Crowley, 2000; Jones et al., 2001). The model and data agree on a counterintuitive result: the eastern equatorial Pacific is colder when the heating is greater and *visa versa*. This may be understood as follows (Clement et al., 1996). If there is a heating over the entire tropics then the Pacific will warm more in the west than in the east because the strong upwelling and surface divergence in the east moves some of the heat poleward. Hence the east–west temperature gradient will strengthen, so the winds will also strengthen, so the temperature gradient will increase further – the Bjerknes (1969) feedback – leading to a more La Niña-like state.

This chain of physical reasoning is certainly correct as far as it goes, but the climate system is complex and processes not considered in this argument might be important. Perhaps cloud feedbacks play a substantial role. In a time of enhanced solar heating, the oceans should generally warm everywhere, including the subduction zones of the waters, which ultimately make up the equatorial thermocline. This might mean that the upwelled waters would warm, though, as discussed above, this mechanism does not seem to have influenced the changes observed in the past few decades. In any case, the observational evidence is that times of greater heating are times when the tropical Pacific is more La Niña-like, and the agreement between the data and the simulation with the simplified Zebiak–Cane model supports the idea that the Bjerknes feedback is dominant. Future research, especially experiments with more complex models, will doubtless clarify the mechanisms.

8.3. Uncertainties in the climate forcing over the last millennium

A more problematic issue is the great uncertainties in the solar and volcanic forcing. The size of past volcanic eruptions is inferred from proxies, primarily volcanic ash in polar ice cores (e.g., Crowley, 2000). Converting the proxy records into a radiative impact requires some form of extrapolation from the few well observed volcanic eruptions in recent times, such as Pinatubo. There is no sure way to do this. The solar forcing is at least as uncertain. Reconstructions rely on sunspot observations for recent centuries, and on paleoproxy records of cosmogenic nuclides for the longer record. The latter are directly influenced by changes in magnetic flux from the sun, not changes in irradiance. A relationship between the two must be created by extrapolating from the short period of instrumental observations, a period dominated by 11-year solar cycles which have less variation than that implied by the proxies for past centuries. The values used in the model experiments fall somewhere in the middle of values appearing in the literature, but are higher than the most recent estimates (Lean et al., 2002). Since the SST response to this forcing is just at the magnitude of the drought patterns of recent times, any reduction in the estimate of irradiance forcing makes the sun an implausible cause of the drought-inducing SST anomalies. Further, Lean et al. (2002) claim that there may not be a systematic relationship between changes in irradiance and those in magnetic flux. So while there is a reasonably convincing empirical correspondence between proxies for solar output and tropical Pacific SSTs, the great uncertainties in solar irradiance forcing raise doubts about explanations of these SST variations as responses to solar forcing.

We saw that the Cobb et al. (2003) proxy data shows cooling in the eastern equatorial Pacific at times in the past when the global climate warmed due to increased solar radiation or reduced volcanism, a result reproduced in the modeling study of Mann et al. (2005) and explained by the Bjerknes feedback. However, this same relation does not appear to hold for the 20th century, when radiative forcing and global temperatures increase. (Crowley, 2000 found the greatest disagreement between global mean temperature and a model forced by solar, volcanic and greenhouse gas variations in the early 20th century.) Perhaps this change in behavior is due to the impact of atmospheric aerosol or perhaps there is something missed in our argument when the radiative increase is due to increased greenhouse gases. Another possibility is suggested by Fig. 20, which updates Cane et al. (1997) to show the temperature trend

from 1900 to 2000. There is no change in the eastern central Pacific, but the strong warming in the west means that the east–west SST gradient significantly strengthens over the century — as would be expected from the Bjerknes feedback (Fig. 20, bottom panel). It may no longer be safe to infer the basin wide tropical Pacific SST pattern from the eastern end alone.

9. Tropical Pacific SSTs and North American drought in the greenhouse future

As has been shown, precipitation over North America is highly sensitive to tropical Pacific SSTs. Consequently the hydrological future of the American

West will, at least partially, be determined by how tropical Pacific SSTs respond to rising levels of greenhouse gases. Predictions of future tropical Pacific SSTs rely on models. We would prefer that the models demonstrate the ability to simulate the defining features of the ENSO cycle with some skill. Unfortunately, most of the comprehensive Coupled General Circulation Models (CGCMs) fall short. AchutaRao and Sperber (2002) reviewed the simulations of ENSO in 17 CGCMs that were part of the Coupled Model Intercomparison Project (CMIP). Most of the model El Niños were too weak and markedly in the wrong location. Five of the models were judged to “represent well the Walker circulation anomalies, the warming and enhanced rainfall

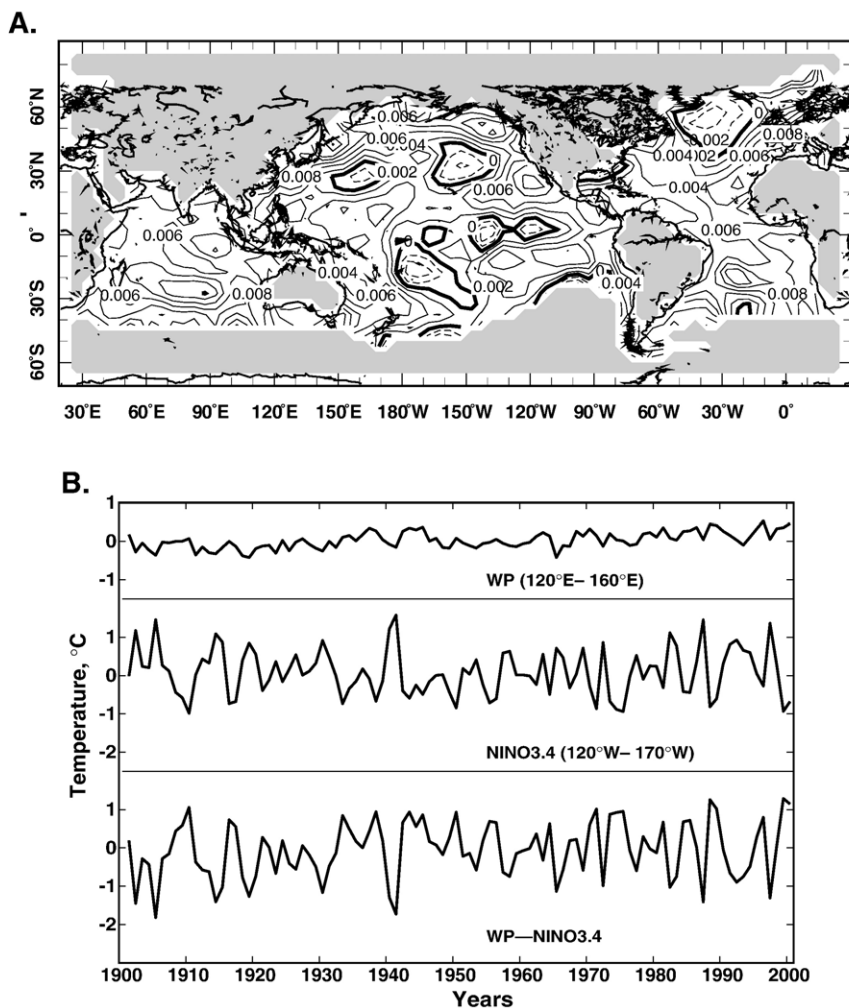


Fig. 20. (A) The trend in monthly mean SST anomalies from 1900 to 2000 in °C per century. Updated from Cane et al. (1997). Regions that cool, such as the eastern equatorial Pacific, are significantly different from the mean global SST warming of 0.4 °C per century. (B) Time series of: (top) the average SST anomaly in the WP region (120° E to 160° E; 5° N to 5° S); (middle) average SST anomaly in the NINO3.4 region (120° W to 170° W; 5° N to 5° S); (bottom) the difference WP-NINO3.4, a measure of the zonal SST gradient. The least squares estimate of the linear trends in the 3 time series (°C per century) are 0.41 ± 0.06 , -0.08 ± 0.25 , and 0.50 ± 0.25 , respectively.

in the central/east Pacific.” Some of these model ENSOs had most of their power at a higher frequency (~ 2 yr) than observed, and most did not have the correct phase with respect to the annual cycle.

Collins and the CMIP Modelling Groups (2005) examined the predictions from 20 CMIP CGCMs forced by a 1% per year increase in greenhouse gases to see whether the mean state becomes more El Niño-like or more La Niña-like. The most probable outcome is no large trend in either direction. Doherty and Hulme (2002) looked at the simulations from 12 CGCMs of changes in the SOI and tropical precipitation from 1900 to 2099. They found that changes in SOI variability are not coherent among the models, broadly consistent with Collins et al. (2005). They do find a slight overall tendency toward a more positive SOI; that is, a more La Niña-like state. Specifically, 6 of the simulations showed a statistically significant positive trend and 2 a statistically significant negative (El Niño-like) trend, while the remaining 4 showed no significant trends.

The positive trend is in keeping with expectations based on the Bjerknes feedback, but was surprising because two of the earliest studies of ENSO in the greenhouse with this generation of models reported a positive (more El Niño-like) trend in NINO3 (Timmermann et al., 1999; Cai and Whetton, 2000). Moreover, the models used in these studies, ECHAM4 and CSIRO, are among those found to have positive trends in the SOI. One possible reason for the discrepancy between the two measures of ENSO is that a trend toward more La Niña-like SSTs in the eastern Pacific is overridden by the overall global warming; as with Fig. 20, it would be revealed by looking at east–west temperature gradients instead of solely at eastern SSTs. Or, it might be that the overall pattern of the ENSO events is altered in the greenhouse world; for example, a shift to the southeast as observed in the late 20th century by Kumar et al. (1999). Doherty and Hulme (2002) found pattern changes in a minority of the 12 simulations they considered, with HADCM2 and ECHAM4 showing eastward shifts.

Recently Liu et al. (2005) have questioned the wisdom of searching for El Niño-like or La Niña-like responses to greenhouse forcing. Instead they examine a number of CGCMs subject to rising greenhouse gases and demonstrate that, instead of a change in the east–west temperature gradient, the common response is for the equatorial Pacific Ocean to warm by more than the subtropical Pacific Ocean. They relate this to changes in the Hadley Cell and surface heat fluxes. From the perspective of the zonal mean atmospheric circulation and mid-latitude drought this ‘enhanced equatorial

warming’ is likely to have impacts akin to those of El Niño. As the equator warms so will the tropical troposphere, the jets will move equatorward and strengthen and the transient eddies will drive mid-latitude ascent, increasing precipitation. Anomalous descent, and drying, would instead occur in the subtropics.

Probably the tropical ocean temperatures will respond to greenhouse forcing with some mix of a change in east–west gradient and north–south gradient and there will be attendant changes in stationary waves and the zonal mean atmospheric circulation. The hydrological future of the West will depend on what this mix is. While current models may agree on the north–south gradients they disagree on the east–west gradient and, overall, are too inconsistent to provide much guidance. Perhaps the new generation of coupled GCMs created for the fourth IPCC assessment will show more of a consensus.

Tropical SSTs are not the only influence on how precipitation will change in the greenhouse future. Globally averaged precipitation is expected to increase to balance the increase in surface evaporation, which itself is needed to balance enhanced downward longwave radiation from the atmosphere to the surface. However, the distribution of this increase in precipitation will depend on changes in surface evaporation and changes in atmospheric moisture transport to which ENSO-like changes are only one contributor. Further, a warmer atmosphere can hold more water vapor. Because the water vapor content is influenced by the exponential increase of saturation water vapor content with temperature, while the global increase in precipitation is more linear in temperature, the intensity of precipitation events is expected to increase (Trenberth et al., 2003). This has hydrological implications in that, potentially, more precipitation will go into runoff and less into recharge of soil moisture. Winter snowpack is also expected to decrease in the West reducing the spring melt and gradual recharge of streams and soil moisture at lower levels. See Stewart et al. (2004) and Mote et al. (2005) on this topic as well. These changes that can occur in the absence of circulation changes could also increase the drought risk in North America. Further, if tropical Atlantic SST anomalies really do impact precipitation over North America, the weakening of the Atlantic THC that many model project for the next century would cause cooling in the subtropical North Atlantic which, on the basis of the experiments of Sutton and Hodson (2005), would tend to increase precipitation over parts of North America. Given these complexities it is currently impossible to project what the hydrological future of the Plains and the West will be.

10. Conclusions

Recent advances in the reconstruction of past drought over North America and in modeling the causes of droughts there have provided important new insights into one of the most costly recurring natural disasters to strike North America. A grid of summer PDSI reconstructions has been developed now for most of North America from a remarkable network of long, drought-sensitive tree-ring chronologies. These reconstructions, many of which cover the past 1000 yr, have revealed the occurrence of a number of unprecedented megadroughts over the past millennium that clearly exceed any found in the instrumental records since about AD 1850, including an epoch of significantly elevated aridity that persisted for almost 400 yr over the AD 900–1300 period. In terms of duration, these past megadroughts dwarf the famous droughts of the 20th century, such as the Dust Bowl drought of the 1930s, the southern Great Plains drought of the 1950s, and the current one in the West that began in 1999 and still lingers on as of this writing in 2005.

The impact of the earlier megadroughts on Puebloan and Mississippian agricultural societies, ones based on the clever use of available water resources, is also indicated by the decline and disappearance of those cultures during prolonged drought periods. In turn, the perception of the American West as a place of settlement in the 19th century was strongly influenced by the timing of droughts and wet periods during periods of exploration there.

The extraordinary duration of past North American megadroughts is difficult to explain, but climate models strongly point to tropical Pacific Ocean SSTs as a prime player in determining how much precipitation falls over large parts of North America. Numerical experiments that successfully simulate major droughts over North America from the Civil War to the severe 1999–2004 drought in the West indicate the dominating importance of these SSTs in determining how much precipitation falls over large parts of North America. Of central importance to drought formation is the development of cool “La Niña-like” SSTs in the eastern tropical Pacific region. This development appears to be partially linked to changes in radiative forcing over that region, which affects the Bjerknes feedback mechanism of the ENSO cycle there. Paradoxically, warmer conditions over the tropical Pacific region lead to the development of cool La Niña-like SSTs there, which is drought inducing over North America. La Niña-like conditions were apparently the norm during much of the Medieval period when the West was in a protracted period of elevated aridity and solar irradiance was unusually high. Whether or not this process will lead to a greater prevalence of drought in the

future as the world warms due to accumulating greenhouse gases is unclear at this time.

It may well be that the West will luck out as rising greenhouse gases induce an equatorial warming, or an El Niño-like response, and the resulting circulation changes increase precipitation across the mid-latitudes. But we have the nagging reality that a previous time of high positive radiative forcing – the Medieval period – was associated with both colder tropical Pacific SSTs and epic drought across the West. Where the climate system to revert to that severity of drought, conflict, at least on a political level, would return to the West as cities, with relatively modest claims on available water but huge and growing populations, and water-hungry agribusiness, with great political clout, do battle over diminishing resources. The ancient Pueblo migrations may be an unfair analogy, but modern Western society, highly dependent on hydraulic engineering, is yet to be tested by the dreadful droughts we know can occur.

Acknowledgements

The drought reconstructions and their presentation in the North American Drought Atlas were supported by NOAA grant no. NA06GP0450 and NSF grant no. ATM 03-22403, respectively (to ERC). We also gratefully acknowledge the NOAA International Tree-Ring Data Bank and its many contributors for much of the tree-ring data used in this work. In addition, many tree-ring records not yet in the public domain were kindly contributed to the drought reconstruction project by a number of tree-ring scientists doing work in the United States, Canada, and Mexico. All are gratefully appreciated. Contributions of DWS were supported by the NSF Earth System History Program, grant no. ATM 04-00713. RS and MAC were funded in part under the Cooperative Institute for Climate Applications Research (CICAR) award number NA03OAR4320179 from the National Oceanic and Atmospheric Administration, U. S. Department of Commerce. The statements, findings, conclusions, and recommendations are those of the author(s) and do not necessarily reflect the views of the National Oceanic and Atmospheric Administration or the Department of Commerce. RS and MAC also received additional funding from the National Science Foundation (ATM 03-47009). This is Lamont-Doherty Earth Observatory contribution no. 6858.

References

- AchutaRao, K., Sperber, K.R., 2002. Simulation of the El Niño Southern Oscillation: results from the Coupled Model Intercomparison Project. *Climate Dynamics* 19, 191–209.

- Acuna-Soto, R., Stahle, D.W., Cleaveland, M.K., Therrell, M.D., 2002. Megadrought and megadeath in 16th century Mexico. *Emerging Infectious Diseases* 8 (4), 360–362.
- Agricultural and Agri-Food Canada, 2002. Drought Watch (for agricultural year 2002). <http://www.agr.gc.ca/pfra/drought/maps/archives/e1020830.pdf>. 2002.
- Alley, W.M., 1984. The Palmer Drought Severity Index: limitations and assumptions. *Journal of Climate and Applied Meteorology* 23, 1100–1109.
- Anderson, D.G., Stahle, D.W., Cleaveland, M.K., 1995. Paleoclimate and the potential food reserves of Mississippian societies: a case study from the Savanna River valley. *American Antiquity* 60, 258–286.
- Axtell, R.L., Epstein, J.M., Dean, J.S., Gumerman, G.J., Swedlund, A.C., Harburger, J., Chakravarty, S., Hammond, S., Parker, J., Parker, M., 2002. Population growth and collapse I a multiagent model of the Kayenta Anasazi in Long House Valley. *Proceedings of the National Academy of Sciences* 99 (suppl. 3), 7275–7279.
- Betancourt, J., 2003. The current drought (1999–2003) in historical perspective. Paper Presented at the Southwest Drought Summit, Northern Arizona University, Flagstaff, May 12–13, 2003. Available at <http://www.mpcer.nau.edu/megadrought/Betancourt%2520Abstract.pdf>.
- Bjerknes, J., 1969. Atmospheric teleconnections from the equatorial Pacific. *Monthly Weather Review* 97, 163–172.
- Box, G.E.P., Jenkins, G.M., 1976. *Time Series Analysis: Forecasting and Control*. Holden Day, San Francisco. 553 pp.
- Briffa, K.R., Jones, P.D., Wigley, T.M.L., Pilcher, J.R., Baillie, M.G.L., 1986. Climate reconstruction from tree rings: Part 2, spatial reconstruction of summer mean sea-level pressure patterns over Great Britain. *Journal of Climatology* 6, 1–15.
- Cai, W., Whetton, P.H., 2000. Evidence for a time-varying pattern of greenhouse warming in the Pacific Ocean. *Geophysical Research Letters* 27, 2577–2580.
- Cane, M.A., Clement, A.C., Kaplan, A., Kushnir, Y., Murtugudde, R., Pozdnyakov, D., Seager, R., Zebiak, S.E., 1997. 20th century sea surface temperature trends. *Science* 275, 957–960.
- Clement, A., Seager, R., Cane, M.A., Zebiak, S.E., 1996. An ocean dynamical thermostat. *Journal of Climate* 9, 2190–2196.
- Cobb, C.R., Butler, B.M., 2002. The vacant quarter revisited: late Mississippian abandonment of the Lower Ohio Valley. *American Antiquity* 67, 625–641.
- Cobb, K.M., Charles, C.D., Edwards, R.L., Cheng, H., Kastner, M., 2003. El Niño–Southern Oscillation and tropical Pacific climate during the last millennium. *Nature* 424, 271–276.
- Cole, J.E., Cook, E.R., 1998. The changing relationship between ENSO variability and moisture balance in the continental United States. *Geophysical Research Letters* 25 (24), 4529–4532.
- Cole, J.E., Overpeck, J.T., Cook, E.R., 2002. Multiyear La Niña events and persistent drought in the contiguous United States. *Geophysical Research Letters* 29 (13). doi:10.1029/2001GL013561.
- Collins, M., the CMIP Modelling Groups, 2005. El Niño or La Niña-like climate change? *Climate Dynamics* 24, 89–104.
- Cook, E.R., Stahle, D.W., Cleaveland, M.K., 1992. Dendroclimatic evidence from eastern North America. In: Bradley, R.S., Jones, P.D. (Eds.), *Climate Since 1500*. Routledge, London, pp. 331–348.
- Cook, E.R., Briffa, K.R., Jones, P.D., 1994. Spatial regression methods in dendroclimatology: a review and comparison of two techniques. *International Journal of Climatology* 14, 379–402.
- Cook, E.R., Meko, D.M., Stahle, D.W., Cleaveland, M.K., 1996. Tree-ring reconstructions of past drought across the coterminous United States: tests of a regression method and calibration/verification results. In: Dean, J.S., Meko, D.M., Swetnam, T.W. (Eds.), *Tree Rings, Environment, and Humanity*. Radiocarbon, Tucson, pp. 155–169.
- Cook, E.R., Meko, D.M., Stahle, D.W., Cleaveland, M.K., 1999. Drought reconstructions for the continental United States. *Journal of Climate* 12, 1145–1162.
- Cook, E.R., D'Arrigo, R.D., Cole, J.E., Stahle, D.W., Villalba, R., 2000. Tree-ring records of past ENSO variability and forcing. In: Diaz, H.F., Markgraf, V. (Eds.), *El Niño and the Southern Oscillation: Multiscale Variability and its Impacts on Natural Ecosystems and Society*. Cambridge University Press, Cambridge, pp. 297–323.
- Cook, E.R., Woodhouse, C.A., Eakin, C.M., Meko, D.M., Stahle, D.W., 2004. Long-term aridity changes in the western United States. *Science* 306, 1015–1018.
- Crowley, T.J., 2000. Causes of climate change over the past 1000 years. *Science* 289, 270–277.
- Dai, A., Trenberth, K.E., Karl, T.R., 1998. Global variations in droughts and wet spells: 1900–1995. *Geophysical Research Letters* 25 (17), 3367–3370.
- Dai, A., Trenberth, K.E., Qian, T., 2004. A global dataset of Palmer Drought Severity Index for 1870–2002: relationship with soil moisture and effects of surface warming. *Journal of Hydrometeorology* 5, 1117–1130.
- Deser, C., Phillips, A.S., Hurrell, J.W., 2004. Pacific interdecadal climate variability, linkages between the tropics and north Pacific during boreal winter since 1900. *Journal of Climate* 17 (16), 3109–3124.
- Doherty, R., Hulme, M., 2002. The relationship between the SOI and the extended tropical precipitation in simulations of future climate change. *Geophysical Research Letters* 29 (10), 1475. doi:10.1029/2001GLO14601.
- Douglass, A.E., 1929. The secret of the Southwest solved with talkative tree rings. *National Geographic* 736–770. December.
- Douglass, A.E., 1935. Dating Pueblo Bonito and other ruins of the Southwest. National Geographic Society Contributed Technical Papers. Pueblo Bonito Series, 1, pp. 1–74.
- Efron, B., Tibshirani, R., 1986. Bootstrap methods for standard errors, confidence intervals, and other measures of statistical accuracy. *Statistical Science* 1, 54–77.
- Ellison, L., Woolfolk, E.J., 1937. Effects of drought on vegetation near Miles City, Montana. *Ecology* 18 (3), 329–336.
- Evans, M.N., Kaplan, A., Cane, M.A., 2002. Pacific sea surface temperature field reconstruction from coral $\delta^{18}\text{O}$ data using reduced space objective analysis. *Paleoceanography* 17 (1). doi:10.1029/2000PA000590.
- Fritts, H.C., 1991. *Reconstructing Large-Scale Climatic Patterns from Tree-Ring Data*. University of Arizona Press, Tucson, AZ. 286 pp.
- Fritts, H.C., Shatz, D.J., 1975. Selecting and characterizing tree-ring chronologies for dendroclimatic analysis. *Tree-Ring Bulletin* 35, 31–40.
- Fritts, H.C., Blasing, T.J., Hayden, B.P., Kutzbach, J.E., 1971. Multivariate techniques for specifying tree-growth and climate relationships and for reconstructing anomalies in paleoclimate. *Journal of Applied Meteorology* 10, 845–864.
- Fye, F., Stahle, D.W., Cook, E.R., 2003. Paleoclimatic analogs to 20th century moisture regimes across the USA. *Bulletin of the American Meteorological Society* 84 (7), 901–909.
- Fye, F., Stahle, D.W., Cook, E.R., 2004. Twentieth-century sea surface temperature patterns in the Pacific during decadal moisture regimes over the United States. *Earth Interactions* 8, 22 Paper.
- Garreaud, R.D., Battisti, D.S., 1999. Interannual and interdecadal variability of the tropospheric circulation in the Southern Hemisphere. *Journal of Climate* 12, 2113–2123.

- Gershunov, A., Barnett, T.P., 1998. Interdecadal modulation of ENSO teleconnections. *Bulletin of the American Meteorological Society* 79, 2715–2725.
- Gu, D., Philander, S.G.H., 1997. Interdecadal climate fluctuations that depend on exchanges between the tropics and extratropics. *Science* 275, 805–807.
- Gumerman, G.J., Dean, J., 2000. Artificial Anasazi. *Discovering Archaeology* 2, 44–51.
- Guttman, N.B., 1998. Comparing the Palmer Drought Index and the Standardized Precipitation Index. *Journal of the American Water Resources Association* 34, 113–121.
- Guttman, N.B., Wallis, J.R., Hosking, J.R.M., 1992. Spatial comparability of the Palmer Drought Severity Index. *Water Resources Bulletin* 28, 1111–1119.
- Hazeleger, W., Visbeck, M., Cane, M.A., Karspeck, A.R., Naik, N.H., 2001. Decadal upper ocean temperature variability in the tropical Pacific. *Journal of Geophysical Research* 106, 8971–8988.
- Heddinghaus, T.R., Sabol, P., 1991. A review of the Palmer Drought Severity Index and where do we go from here? Preprints, Seventh Conference on Applied Climatology, Dallas, TX. American Meteorological Society 242–246.
- Heim Jr., R.R., 2002. A review of Twentieth-Century drought indices used in the United States. *Bulletin of the American Meteorological Society* 83, 1149–1165.
- Herweijer, C., Seager, R., 2006. The global footprint of persistent extra-tropical drought in the instrumental era. *International Journal of Climatology* (in review).
- Herweijer, C., Seager, R., Cook, E.R., 2006. North American droughts of the mid to late nineteenth century: a history, simulation and implication for Medieval drought. *The Holocene* 16, 159–171.
- Hoerling, M., Kumar, A., 2003. The perfect ocean for drought. *Science* 299, 691–694.
- Hoskins, B.J., Karoly, K., 1981. The steady response of a spherical atmosphere to thermal and orographic forcing. *Journal of the Atmospheric Sciences* 38, 1179–1196.
- Huang, H.-P., Seager, R., Kushnir, Y., 2005. The 1976/77 transition in precipitation over the Americas and the influence of tropical sea surface temperature. *Climate Dynamics* 24, 721–740.
- Jones, T.L., Brown, G.M., Raab, L.M., McVicker, J.L., Spaulding, W.G., Kennet, D.J., York, A., Walker, P.L., 1999. Environmental imperatives reconsidered: demographic crises in western North America during the medieval climate anomaly. *Current Anthropology* 40, 137–169.
- Jones, P.D., Osborn, T.J., Briffa, K.R., 2001. The evolution of climate over the last millennium. *Science* 292, 662–667.
- Kaplan, A., Cane, M.A., Kushnir, Y., Clement, A.C., Blumenthal, M.B., Rajagopalan, B., 1998. Analyses of global sea surface temperature: 1856–1991. *Journal of Geophysical Research* 103, 18567–18589.
- Kaplan, A., Kushnir, Y., Cane, M.A., 2000. Reduced space optimal interpolation of historical marine sea level pressure: 1854–1992. *Journal of Climate* 13, 2987–3002.
- Karl, T.R., 1983. Some spatial characteristics of drought duration in the United States. *Journal of Climate and Applied Meteorology* 22, 1356–1366.
- Karl, T.R., 1986. The sensitivity of the Palmer Drought Severity Index and Palmer's Z-index to their calibration coefficients including potential evapotranspiration. *Journal of Climate and Applied Meteorology* 25, 77–86.
- Karl, T.R., Koscielny, A.J., 1982. Drought in the United States. *Journal of Climatology* 2, 313–329.
- Karl, T.R., Williams Jr., C.N., Quinlan, F.T., 1990. United States Historical Climatology Network (HCN) serial temperature and precipitation data. Environmental Sciences Division Publication, vol. 3404, p. 371. Available from Carbon Dioxide Information Analysis Center, Oak Ridge National Laboratory, Oak Ridge, TN 37831.
- Karspeck, A., Cane, M.A., 2002. Tropical pacific 1976–77 climate shift in a linear, wind driven model. *Journal of Physical Oceanography* 32, 2350–2360.
- Karspeck, A., Seager, R., Cane, M.A., 2004. Predictability of tropical Pacific decadal variability in an intermediate model. *Journal of Climate* 17, 2842–2850.
- Keyantash, J., Dracup, J.A., 2002. The quantification of drought: an evaluation of drought indices. *Bulletin of the American Meteorological Society* 83, 1167–1180.
- Koster, R.D., Dirmeyer, P.A., Guo, Z., Bonan, G., Chan, E., Cox, P., Gordon, C.T., Kanae, S., Kowalczyk, E., Lawrence, D., et al., 2004. Regions of strong coupling between soil moisture and precipitation. *Science* 305, 1138–1140.
- Kumar, K., Rajagopalan, B., Cane, M.A., 1999. On the weakening relationship between the Indian Monsoon and ENSO. *Science* 284, 2156–2159.
- Kushnir, Y., 1994. Interdecadal variations in north-Atlantic sea-surface temperature and associated atmospheric conditions. *Journal of Climate* 7, 141–157.
- Lau, N.-C., A. Leetmaa, A., Nath, M.J., 2006. Attribution of atmospheric variations in the 1997–2003 period to SST anomalies in the Pacific and Indian Ocean basins. *Journal of Climate* 19, 3607–3628.
- Lau, N.-C., Leetmaa, A., Nath, M.J., Wang, H.-L., in press. Influences of ENSO-induced Indo-West Pacific SST anomalies on extratropical atmospheric variability during the boreal summer. *Journal of Climate*.
- Lawrimore, J., Stephens, S., 2003. Climate of 2002 Annual Review. NOAA National Climatic Data Center. <http://lwf.ncdc.noaa.gov/oa/climate/research/2002/ann/drought-summary.html>.
- Lawrimore, J., Heim Jr., R.R., Svoboda, M., Swail, V., Englehart, P.J., 2002. Beginning a new era of drought monitoring across North America. *Bulletin of the American Meteorological Society* 83, 1191–1192. Available at <http://www.ncdc.noaa.gov/oa/climate/monitoring/drought/nadm/nadm-map.html>.
- Lawson, M.P., Stockton, C.W., 1981. Desert myth and climatic reality. *Annals, Association of American Geographers* 71, 527–535.
- Lean, J.L., Wang, Y.-M., Sheeley Jr., N.R., 2002. The effect of increasing solar activity on the Sun's total and open magnetic flux during multiple cycles: implications for solar forcing of climate. *Geophysical Research Letters* 29 (24), 2224. doi:10.1029/2002GL015880.
- Libecap, G.D., Hansen, Z.K., 2002. 'Rain follows the plow' and dry farming doctrine: the climate information problem and homestead failure in the upper Great Plains, 1890–1925. *Journal of Economic History* 62, 86–120.
- Liu, Z., Vavrus, S., He, F., Weng, N., Zhong, Y., 2005. Rethink tropical ocean response to global warming: the enhanced equatorial warming. *Journal of Climate* 18, 4684–4700.
- Mann, M.E., Cane, M.A., Zebiak, S.E., Clement, A., 2005. Volcanic and solar forcing of El Niño over the past 1000 years. *Journal of Climate* 18, 447–456.
- Mantua, N.J., Hare, S.R., Zhang, Y., Wallace, J.M., Francis, R.C., 1997. A Pacific interdecadal oscillation with impacts on salmon production. *Bulletin of the American Meteorological Society* 78, 1069–1079.
- McGuire, V.L., 2004. Water-level changes in the high plains aquifer, predevelopment to 2003 and 2002 to 2003 (Fact Sheet 2004–3097). Washington, DC, US Geological Survey. Available at <http://pubs.usgs.gov/fs/2004/3097/>.

- Meko, D.M., Cook, E.R., Stahle, D.W., Stockton, C.W., Hughes, M.K., 1993. Spatial patterns of tree-growth anomalies in the United States and southeastern Canada. *Journal of Climate* 6, 1773–1786.
- Milner, G.R., 1998. *The Cahokia Chiefdom*. Smithsonian Institution Press, Washington. 216 pp.
- Mitchell, T.D., Jones, P.D., 2005. An improved method of constructing a database of monthly climate observations and associated high-resolution grids. *International Journal of Climatology* 25, 693–712.
- Mitchell Jr., J.M., Stockton, C.W., Meko, D.M., 1979. Evidence of a 22-year rhythm of drought in the western United States related to the Hale solar cycle since the 17th century. *Solar-Terrestrial Influences on Weather and Climate*. In: McCormac, B.M., Seliga, T.A. (Eds.), D. Reidel, pp. 125–144.
- Mitchell, T.D., Carter, T.R., Jones, P.D., Hulme, M., New, M., 2004. A comprehensive set of high-resolution grids of monthly climate for Europe and the globe: the observed record (1901–2000) and 16 scenarios (2001–2100). Tyndall Working Paper, 55. Tyndall Centre, UEA, Norwich, UK.
- Mote, P.W., Hamlet, A.F., Clark, M.P., Lettenmaier, D.P., 2005. Declining mountain snowpack in western North America. *Bulletin of the American Meteorological Society* 86, 39–49.
- Namias, J., 1983. Some causes of United States drought. *Journal of Applied Meteorology* 22, 30–39.
- NASA, 2004. Looking at Earth, “Drought Signals Sever Fire Season in the U.S.” Available at http://www1.nasa.gov/vision/earth/lookingatearth/Western_Drought.html.
- New, M., Hulme, M., Jones, P.D., 2000. Representing twentieth century space–time climate variability. Part 2: development of 1901–96 monthly grids of terrestrial surface climate. *Journal of Climate* 13, 2217–2238.
- Palmer, W.C., 1965. Meteorological drought. Research Paper, vol. 45. U.S. Weather Bureau.
- Pauketat, T.R., 2004. *Ancient Cahokia and the Mississippians*. Cambridge University Press. 218 pp.
- Power, S., Casey, T., Folland, C., Colman, A., Mehta, V., 1999. Interdecadal modulation of the impact of ENSO on Australia. *Climate Dynamics* 15 (5), 319–324.
- Rayner, N.A., Parker, D.E., Horton, E.B., Folland, C.K., Alexander, L.V., Rowell, D.P., Kent, E.C., Kaplan, A., 2003. Global analyses of sea surface temperature, sea ice, and night marine air temperature since the late nineteenth century. *Journal of Geophysical Research* 108. doi:10.1029/2002JD002670.
- Reisner, M., 1986. *Cadillac Desert: the American West and its Disappearing Water*. Penguin Books, New York. 582 pp.
- Richman, M.B., 1986. Rotation of principal components. *International Journal of Climatology* 6, 293–335.
- Robinson, W.A., 2005. Eddy-mediated interactions between low latitudes and the extratropics. In: Schneider, T., Sobel, A.S. (Eds.), *The Global Circulation*. Princeton University Press, Princeton, NJ.
- Ropelewski, C., Halpert, M., 1987. Global and regional scale precipitation patterns associated with the El Niño/Southern Oscillation. *Monthly Weather Review* 115, 1606–1626.
- Ross, T., Lott, N., 2003. A climatology of 1980–2003 extreme weather and climate events. National Climatic Data Center Technical Report No. 2003-01. NOAA/NESDIS. National Climatic Data Center, Asheville, NC. Available at <http://www.ncdc.noaa.gov/ol/reports/billionz.html>.
- Sahr, R.C., 2005. Inflation conversion factors for dollars 1665 to estimated 2015. Political Science Department, Oregon State University, Corvallis, OR. Available at http://oregonstate.edu/dept/pol_sci/fac/sahr/sahr.htm.
- Sauer, C.O., 1980. *Seventeenth Century North America*. Turtle Island, Berkeley, CA. 295 pp.
- Schneider, N., Venzke, S., Miller, A.J., Pierce, D.W., Barnett, T.O., Deser, C., Latif, M., 1999. Pacific thermocline bridge revisited. *Geophysical Research Letters* 26, 1329–1332.
- Schubert, S.D., Suarez, M.J., Region, P.J., Koster, R.D., Bacmeister, J.T., 2004a. On the cause of the 1930s Dust Bowl. *Science* 303, 1855–1859.
- Schubert, S.D., Suarez, M.J., Region, P.J., Koster, R.D., Bacmeister, J.T., 2004b. Causes of long-term drought in the United States Great Plains. *Journal of Climate* 17, 485–503.
- Seager, R., submitted for publication. The turn-of-the-century drought over North America: global context, dynamics and past analogues. *Journal of Climate*.
- Seager, R., Harnik, N., Kushnir, Y., Robinson, W.A., Miller, J., 2003. Mechanisms of hemispherically symmetric precipitation variability. *Journal of Climate* 16, 2960–2978.
- Seager, R., Karspeck, A., Cane, M.A., Kushnir, Y., Giannini, A., Kaplan, A., Kerman, B., Velez, J., 2004. Predicting Pacific decadal variability. In: Wang, C., Xie, S.-P., Carton, J.A. (Eds.), *In the Ocean–Atmosphere Interaction*. American Geophysical Union, Washington DC, pp. 115–130.
- Seager, R., Harnik, N., Robinson, W.A., Kushnir, Y., Ting, M., Huang, H.-P., Velez, J., 2005a. Mechanisms of ENSO-forcing of hemispherically symmetric precipitation variability. *Quarterly Journal of the Royal Meteorological Society* 131, 1501–1527.
- Seager, R., Kushnir, Y., Herweijer, C., Naik, N., Miller, J., 2005b. Modeling of tropical forcing of persistent droughts and pluvials over western North America: 1856–2000. *Journal of Climate* 18, 4065–4088.
- Shabbar, A., Skinner, W., 2004. Summer drought patterns in Canada and the relationship to global sea surface temperatures. *Journal of Climate* 17 (14), 2866–2880.
- Skinner, W.R., Heinze, K., Vincent, L.A., Mekis, E., 2001. The Palmer Drought Severity Index as calculated from the rehabilitated Canadian historical climate database over the 20th Century. *Climate Changes: Proceedings of the 2001 Annual Meeting of the Canadian Association of Geographers*, Montreal, May 30–June 3, 2001.
- Stahle, D.W., Dean, J.S., in press. Tree ring evidence for North American climatic extremes and social disasters. In: Hughes, M.K., Swetnam, T.W., Diaz, H.F. (Eds.), *Dendroclimatology: Progress and Prospects*. Springer Series “Developments in Paleocological Research”.
- Stahle, D.W., Cook, E.R., Cleaveland, M.K., Therrell, M.D., Meko, D.M., Grissino-Mayer, H.D., Watson, E., Luckman, B.H., 2000. Tree-ring data document 16th century megadrought over North America. *Eos* 81 (12), 121.
- Stahle, D.W., Fye, F.K., Therrell, M.D., 2004. Interannual to decadal climate and streamflow variability estimated from tree rings. In: Gillespie, A.R., Porter, S.C., Atwater, B.F. (Eds.), *In the Quaternary Period in the United States*. Elsevier, Amsterdam, pp. 491–504.
- Stegner, W., 1992. *Beyond the Hundredth Meridian*. Penguin Books, New York. 438 pp.
- Stewart, I.T., Cayan, D.R., Dettinger, M.D., 2004. Changes in snowmelt runoff timing in western North America under a ‘business as usual’ climate change scenario. *Climatic Change* 62, 217–232.
- Stockton, C.W., Meko, D.M., 1975. A long-term history of drought occurrence in western United States as inferred from tree rings. *Weatherwise* 28, 244–249.
- Sutton, R.T., Hodson, D.L.R., 2005. Atlantic Ocean forcing of North American and European summer climate. *Science* 309, 115–118.

- Svoboda, M., LeCompte, D., Hayes, M., Heim, R., Gleason, K., Angel, J., Rippey, B., Tinker, R., Palecki, M., Stooksbury, D., Miskus, D., Stephens, S., 2002. The drought monitor. *Bulletin of the American Meteorological Society* 83 (8), 1181–1190. Available at <http://www.drought.unl.edu/dm/monitor.html>.
- Thomas, D.H., 2000. *Exploring Native North America*. Oxford University Press. 227 pp.
- Timmermann, A., Oberhuber, J., Bacher, A., Esch, M., Latif, M., Roeckner, E., 1999. Increased El Niño frequency in a climate model forced by future greenhouse gas warming. *Nature* 398, 694–696.
- Trenberth, K.E., Branstator, G.W., Karoly, D., Kumar, A., Lau, N.-C., Ropelewski, C., 1998. Progress during TOGA in understanding and modeling global teleconnections associated with tropical sea surface temperature. *Journal of Geophysical Research* 103, 14291–14324.
- Trenberth, K.E., Dai, A., Rasmusson, E.M., Parsons, D.B., 2003. The changing character of precipitation. *Bulletin of the American Meteorological Society* 37, 129–148.
- USDA, 2004. Natural resources conservation service. National Water and Climate Center. Reservoir Storage as of May 1, 2004. Available at <http://www.wcc.nrcs.usda.gov/cgibin/resvgrph2.pl?area%=west&year=2004&month=05>.
- van der Schrier, G., Briffa, K.R., Jones, P.D., Osborn, T.J., 2006a. Summer moisture availability across Europe. *Journal of Climate* 19, 2818–2834.
- van der Schrier, G., Briffa, K.R., Osborn, T.J., Cook, E.R., 2006b. Summer moisture availability across North America. *Journal of Geophysical Research* 111, D11102. doi:10.1029/2005JD006745.
- Warrick, R.A., 1980. Drought in the Great Plains: a case study of Research on Climate and Society in the USA. In: Ausubel, J., Biswas, A.K. (Eds.), *Climatic Constraints and Human Activities*, pp. 93–123. IIASA Proceedings Series, vol. 10. Pergamon Press, New York.
- Weaver, J.E., Albertson, F.W., 1936. Effects of the Great Drought on the prairies of Iowa, Nebraska, and Kansas. *Ecology* 17, 567–639.
- Wells, N., Goddard, S., Hayes, M.J., 2004. A self-calibrating Palmer Drought Severity Index. *Journal of Climate* 17, 2335–2351.
- Wheeler, D.L., 1991. The blizzard of 1886 and its effect on the range cattle industry in the southern Plains. *Southwestern Historical Quarterly* 94.
- Wilber, C.D., 1881. *The Great Valley and Prairies of Nebraska and the Northwest*. Daily Republican Print, Omaha, NB. 382 pp.
- Williams, S., 1990. The Vacant Quarter and other late events in the Lower Valley. In: Dye, D.H., Cox, C.A. (Eds.), *Towns and Temples Along the Mississippi*. University of Alabama Press, Tuscaloosa, pp. 170–180.
- Woodhouse, C.A., Overpeck, J.T., 1998. 2000 years of drought variability in the central United States. *Bulletin of the American Meteorological Society* 79, 2693–2714.
- Woodhouse, C.A., Kunkel, K.E., Easterling, D.R., Cook, E.R., 2005. The twentieth-century pluvial in the western United States. *Geophysical Research Letters* 32, L07701. doi:10.1029/2005GL022413.
- Worster, D., 1979. *Dust Bowl: the southern plains in the 1930s*. Oxford University Press, New York. 227 pp.
- Worster, D., 1985. *Rivers of Empire: Water, Aridity and the Growth of the American West*. Pantheon Books, New York, p. 402.
- Zebiak, S.E., Cane, M.A., 1987. A model El Niño–Southern Oscillation. *Monthly Weather Review* 115, 2262–2278.
- Zhang, Y., Wallace, J.M., Battisti, D.S., 1997. ENSO-like decade-to-century scale variability. 1900–93. *Journal of Climate* 10, 1004–1020.
- Zhang, Z., Mann, M.E., Cook, E.R., 2004. Alternative methods of proxy-based climate field reconstruction: application to summer drought over the conterminous United States back to AD 1700 from tree-ring data. *The Holocene* 14 (4), 502–516.

DRAFT

ATTACHMENT C
HCH 1% Drought Reconstruction Technical Memorandum



Technical Memorandum

Date: March 14, 2013

To: Paul Johnson, SAIC

Cc: Nathan Winkley, Mike Jacobs, John Christopher, Lynn Moore

From: John Winchester, High Country Hydrology, Inc.

Re: Extended drought reconstruction from PDSI

This memo summarizes the development of long-term reconstructed streamflows.

Background

Stream gauge records in south-central Kansas generally start in the 1920s. These cover the droughts of the 1930s, 1950s and 1990s, but do not necessarily reflect the long-term hydrologic variability.

Our research found that the only long-term surrogate data for south-central Kansas is approximately 1000 years of summer Palmer Drought Severity Index (PDSI) data developed by Dr. Edward Cook at the Lamont-Doherty Earth Observatory of Columbia University.¹ The Palmer soil moisture algorithm is calibrated for relatively homogeneous regions. The Palmer Index varies roughly between -6.0 and +6.0, which Palmer arbitrarily selected based on his original study areas in central Iowa and western Kansas.² The PDSI is a meteorological drought index, and it responds to abnormally wet or dry weather conditions. For example, when precipitation increases from below average to above average, the PDSI shows an end to the drought without considering streamflow, lake and reservoir levels, and other longer-term hydrologic impacts.

The Available PDSI Data

Cook originally produced a gridded network for the continental United States in 1999, based on 388 tree ring chronologies. In 2004 he expanded the spatial and temporal coverage to include 286 points in a 2.5 degree grid covering most of North America, as shown in Figure 1. The 2004 PDSI reconstructions are based on 835 tree-ring chronologies. Figure 2 shows the tree ring sites used for the 1999 network (there was no comparable map for the 2004 chronologies on the NOAA web site). As shown in the figure, in 1999 there are no tree ring sites located in Kansas, so PDSI values for the six locations in Kansas are interpolated from sites in other states.

¹ <http://www.ncdc.noaa.gov/paleo/pdsi.html>

² Palmer, Wayne C., Meteorological Drought – Research Paper No. 45. Office of Climatology, Washington DC. 1965.

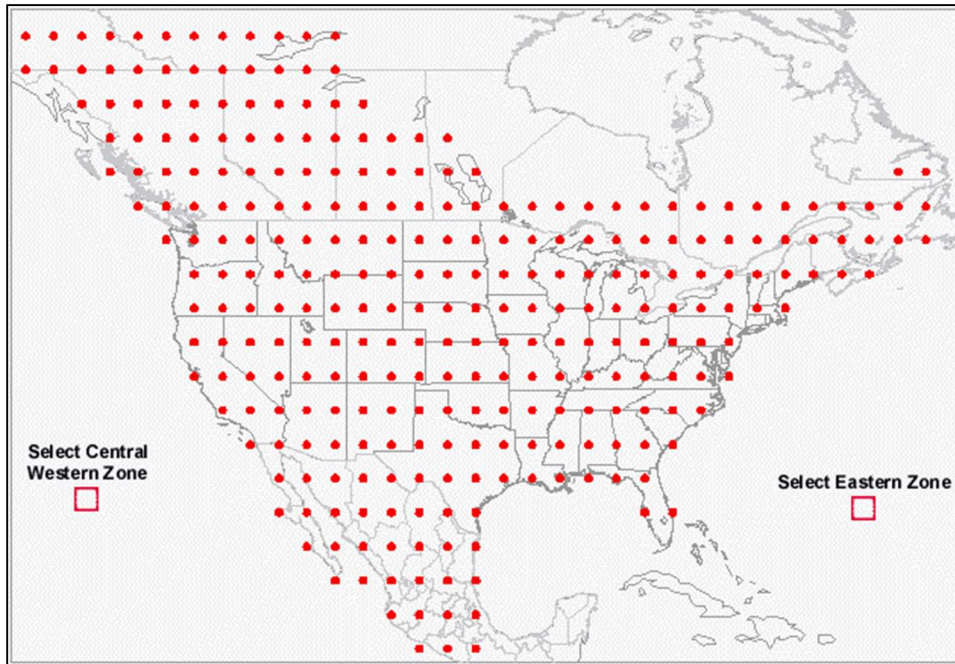


Figure 1. Grid locations where PDSI has been generated (Cook, 2004).

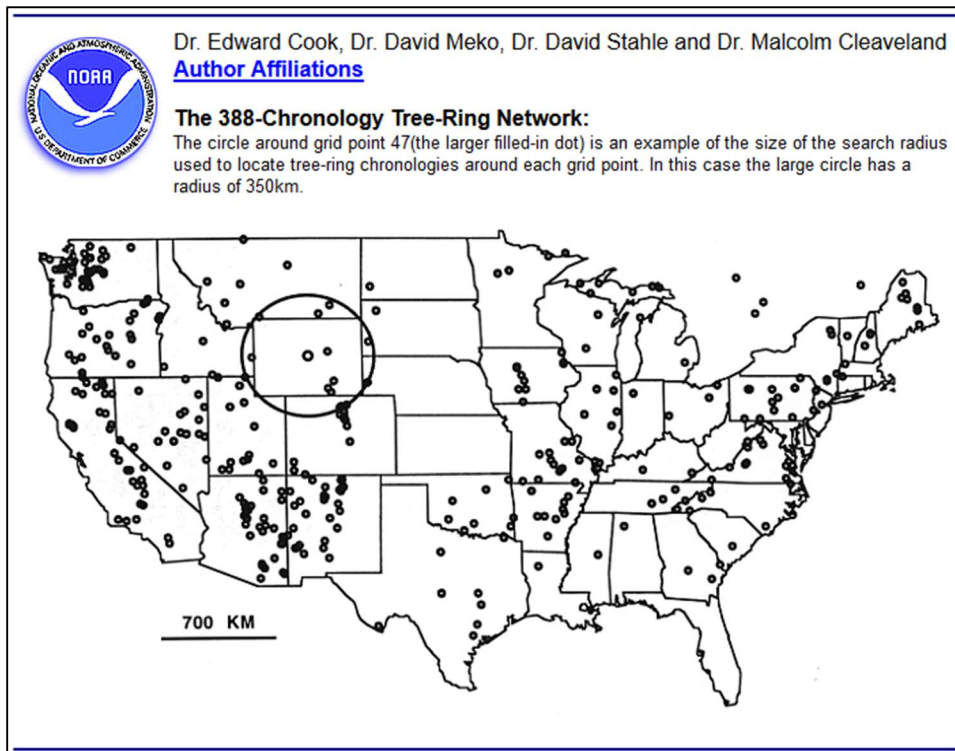


Figure 2. Locations of tree ring chronologies used by Cook in 1999.

The PDSI values generated in 2004 represent the average summer (June-August) PDSI.³ Six of the grid locations published in 2004 fall within Kansas. Comparing the summer PDSI with annual flows for the Little Arkansas River at Valley Center, we found that the best correlation between streamflow and PDSI was obtained when we used the PDSI for southwestern Kansas.

The PDSI data for southwestern Kansas has a period of record from 887 AD – 2003 AD. Figure 3 shows a time series of the PDSI and the number of tree ring sites used to reconstruct the PDSI for the period of record.

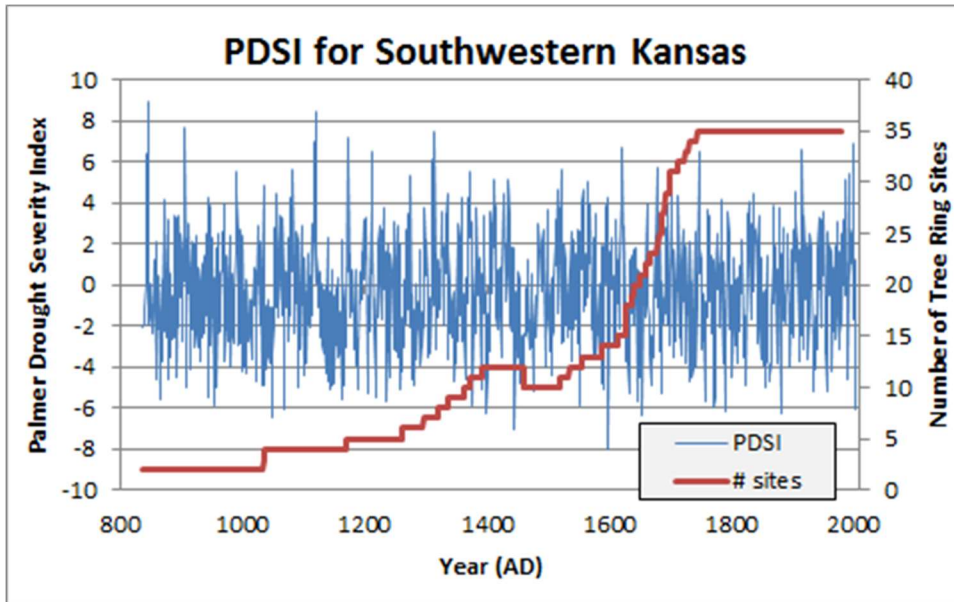


Figure 3. PDSI and number of tree sites.

The Cook data set included both the PDSI calculated from historical records for 1900-2003, and the reconstructed PDSI for 887-2003. The correlation between these two data sets had an r^2 of 0.82. For the following analyses, we used a composite PDSI that was made up of the reconstructed values for the years 887-1899, and actual values for 1900-2003.

Drought Return Period

Using the PDSI data, we calculated the return period for various droughts. While the method for calculating the return period for a single year is well documented, there is no standard method for calculating the return period for multi-year droughts.

We calculated and compared the return period for droughts in three ways: using single years, using the number of consecutive years in a drought, and using the cumulative PDSI.

³ <http://www.ncdc.noaa.gov/paleo/pdsi.html>

Single Year Severity

To calculate the return period of single years, we sorted the annual PDSI values into ascending order, so the most negative values were first. We ranked the data, with 1 being the most negative value.

We applied the equation for recurrence intervals to this data,

$$T = (n+1)/m$$

where

T = recurrence interval in years

n = number of years in the time series

m = rank of the individual year (1, 2, 3...)⁴

While there were drier years before 1900, during the gauged period of record covered by the PDSI (1923-2003), defining droughts based on single years showed that 2002 was the driest single year in the 1900-2003 period of record, followed by 1956 and 1934.

While individual years are interesting, they do not adequately describe the droughts experienced in Kansas.

Number of Drought Years

Counting the number of years with below average precipitation and runoff can be used to determine the duration of a drought.

Rather than simply count the number of sequential years with a PDSI below zero, we modified our calculation of duration to account for variation of average years, and to allow for single years with average conditions that occur in a string of drought years.

Based on Palmer's original paper, the range of -0.49 to 0.49 is considered "near normal." Because there are years with a negative PDSI that are still considered within the normal range, we did not consider a year a drought year until the PDSI was less than -0.5. This assumption eliminated 82 of the 1167 years from the drought classification.⁵

In recognition that droughts can last through a single near-average year, series of drought years were considered unbroken if it contained a single year with a positive PDSI less than 0.5. While there were individual positive years in strings of drought years, this assumption did not change any of the calculated drought durations because all the individual years had a PDSI of greater than 0.5.

⁴ Dunne, Thomas, and Leopold, Luna. Water in Environmental Planning, 1978.

⁵ PDSI drought durations.xlsx

Drought Duration and Severity

City staff at Wichita asked us to analyze surrogate hydrologic data to determine long-term drought durations and severities. This memo discusses long-term droughts and potential data sets that could be used for planning purposes.

Drought Duration and Severity

There are no long-term streamflow reconstructions for south-central Kansas, however Ed Cook and John Krusic have reconstructed annual values of the Palmer Drought Severity Index (PDSI) across North America, including six points in Kansas. We compared the annual values of PDSI with gauged streamflows for 1923-2003, and found that the PDSI for southwest Kansas was the best match for streamflows near Wichita. The PDSI reconstruction for southwest Kansas covers 1166 years, from 837 to 2003.

The PDSI reconstruction for southeast Kansas is based on tree ring chronologies. The number of sites used to develop the PDSI for southwest Kansas ranges from 2 to 35. Statistically comparing different periods of the reconstructed PDSI, we determined that years with more than 15 tree ring sites produced statistics more comparable with the historical record, whereas earlier values based on fewer sites tended to be biased toward drought. Consequently we have limited our use of reconstructed PDSI to the years 1640-2003, which are based on 15 or more tree ring sites.

To determine drought duration, we counted the number of below-average years that occurred in a row, and then calculated the exceedance probability for the different durations using the standard equation,

$$\text{Exceedance} = \text{Rank} / (\text{Sample Size} + 1)$$

Using the same PDSI data, we calculated the total cumulative PDSI for each drought. Because annual PDSI data does not correlate well with historical daily stream gauge data, we suggest that the simplest strategy to generate model input for drought sequences is to use historical streamflow data from years with similar PDSI values. Based on historical PDSI data, we have assembled combinations of gauge data to represent the historical droughts portrayed in the PDSI data. Drought duration, severity and representative years from the historical gauge record are shown in Table 1 for various droughts.

Table 1. Drought Durations and Severity from PDSI Data

Suggested Drought Intervals based on reconstructed PDSI (1640-2003)				Representative Historical Years	
Exceedence Probability	Duration (yrs)	Cumulative PDSI	Mean pdsi	Years	Actual Cum. PDSI
10%	2	-4.4	-2.20	1925-1926	-4.9
4.0%	4	-8.8	-2.21	1925-1926, 1981 x 2	-8.8
2.0%	6	-15.6	-2.60	1952-1956, 1959	-16.1
1.3%	7	-19.6	-2.80	1946, 1952-1956, 1981	-19.6
1.0%	8	-22.4	-2.80	1933-1940	-24.4
0.40%	10	-31.4	-3.14	1952-1956 x 2	-31.1
0.20%	12	-38.2	-3.18	1952-1956 x 2, 1963-1964	-38.4
0.10%	14	-45.0	-3.21	1925, 1933-1940, 1936-1937, 1937, 1940, 1976	-45.0

Design Drought

City staff requested that we fit the drought-duration data to a distribution so they can see how much of the data is included in various multiples of the standard deviation.

The annual PDSI data were classified into wet and dry years, with wet years having a PDSI greater than 1, dry years less than a PDSI of -1, and normal years between 1 and -1. If two dry years were separated by a single wet year with a PDSI of 0.5 or less, the dry streak was considered to be continuous.

Assuming the year counts were divided into 9 bins, the Johnson’s Special Unbounded (SU) distribution best matched the number of consecutive drought years. The analysis of fit was made using sequential years for both wet and dry years (both positive and negative values of PDSI). The red data points show the number of droughts that occurred for each drought duration on the x-axis. Note that the secondary axis only approximately matches the function because it is not possible to mix x-y and bar graph types in Excel.

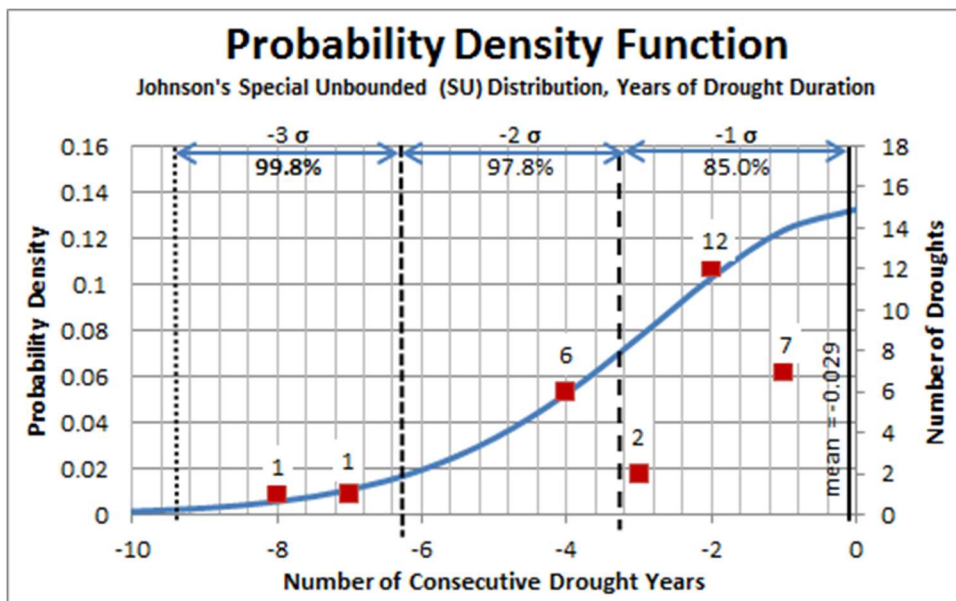


Figure 4. Fitted distribution and actual number of droughts

The graph shows the actual number of droughts for durations of 1, 2, 3... years. The analysis was done using an odd number of bins (9 bins for 16 years), which eliminated the outliers for droughts of 1- and 3-years.

Assuming the distribution represents the data, this graph shows that droughts with durations within 2 standard deviations would represent 97.8 percent of the droughts, including the drought with a 2-percent chance of occurring.

A thousand years of drought and climatic variability in Kansas: Implications for water resources management

Anthony L. Layzell
Kansas Geological Survey
2012

Table of Contents

1. Introduction
2. Types and Measures of Data
 - 2.1. Drought Indices
 - 2.2. Paleoclimatic Data
 - 2.2.1. Long-term PDSI Reconstructions
3. Analyses
 - 3.1. Drought Severity
 - 3.2. Drought Duration
 - 3.2.1. Megadroughts
 - 3.2.2. Megadroughts from 1500-2011 AD
 - 3.2.3. Megadroughts from 850-1500 AD
 - 3.3. The Medieval Warm Period
 - 3.4. Risk Analysis
4. Policy and Management Implications
5. References
6. Appendix: Calibration and Verification Statistics

1. Introduction

Periods of severe drought are one of the greatest recurring natural disasters in North America. In any given year, droughts occur all across North America resulting in significant impacts on local economies, societies, and the natural environment. Drought conditions in the United States cost on average \$6-8 billion every year, but have ranged as high as \$39 billion during the three-year drought of 1987-89 (Riebsame et al., 1991). In Kansas alone, the recent 2011 drought resulted in losses in excess of \$1.7 billion (Kansas Department of Agriculture, 2011).

Droughts impact both surface- and ground-water resources and often result in reductions in water supply and crop failure particularly in agriculturally sensitive areas such as the High Plains of western Kansas. This region is becoming increasingly vulnerable to drought due to a variety of factors including the increased cultivation of marginal lands and the increased use of ground-water resources from the High Plains aquifer (Woodhouse and Overpeck, 1998), where water withdrawal has exceeded recharge for many years (e.g. McGuire, 2009).

The droughts of the 1930s and the 1950s remain the benchmarks in terms of duration, severity, and spatial extent for Kansas in the 20th century. Therefore, determining how representative these historic droughts have been in terms of drought occurrence is vitally important. The key question is how unusual are severe droughts, such as the Dust Bowl? Was this drought a rare event or should we expect droughts of similar or even greater magnitude in the future?

Direct observations of temperature and precipitation from instrumental records are largely restricted to the past 100 years and are therefore too short to adequately answer these questions. Therefore, in order to assess the full range of drought variability, it is important to place historic droughts in a longer-term context by utilizing paleoclimate proxy records.

This report investigates past drought occurrences from paleoclimate records over the last 1000 years. In particular, we focus on Palmer Drought Severity Index (PDSI) reconstructions calculated from annual tree-ring chronologies. Additional paleoclimate proxies and historical records are also examined to lend further support to reported past drought variability.

2. Types and Measures of Data

2.1 Drought Indices

The Palmer Drought Severity Index (PDSI) is one of the most widely used indices to measure drought in North America. The PDSI was developed by Palmer (1965) to measure the intensity and duration of long-term drought. It uses precipitation and temperature data to determine how much soil moisture is available compared to average conditions. PDSI values therefore provide data on both relative wetness and dryness over a given period. The index typically ranges between -4 (extremely dry) and 4 (extremely wet) but the range limit is not explicitly bound. As the index is standardized to local climate, it may be applied to any part of the country to demonstrate relative wetness and dryness.

2.2 Paleoclimate Data

PDSI values calculated from instrumental data provide a valuable means to assess drought variability over the instrumental record (i.e. the past 100 years). Recently, the Kansas Geological Survey has published historic climate and PDSI data (1895 to 2011) online in the form of the Kansas High Plains Aquifer Atlas (http://www.kgs.ku.edu/HighPlains/HPA_Atlas/Climate%20and%20Climate%20Trends/index.html#). Based on these data alone, the droughts of the 1930s and 1950s appear to be anomalous in terms of their severity and duration (Fig. 1).

Palmer Drought Severity Index (PDSI) Trends from 1895 to 2011

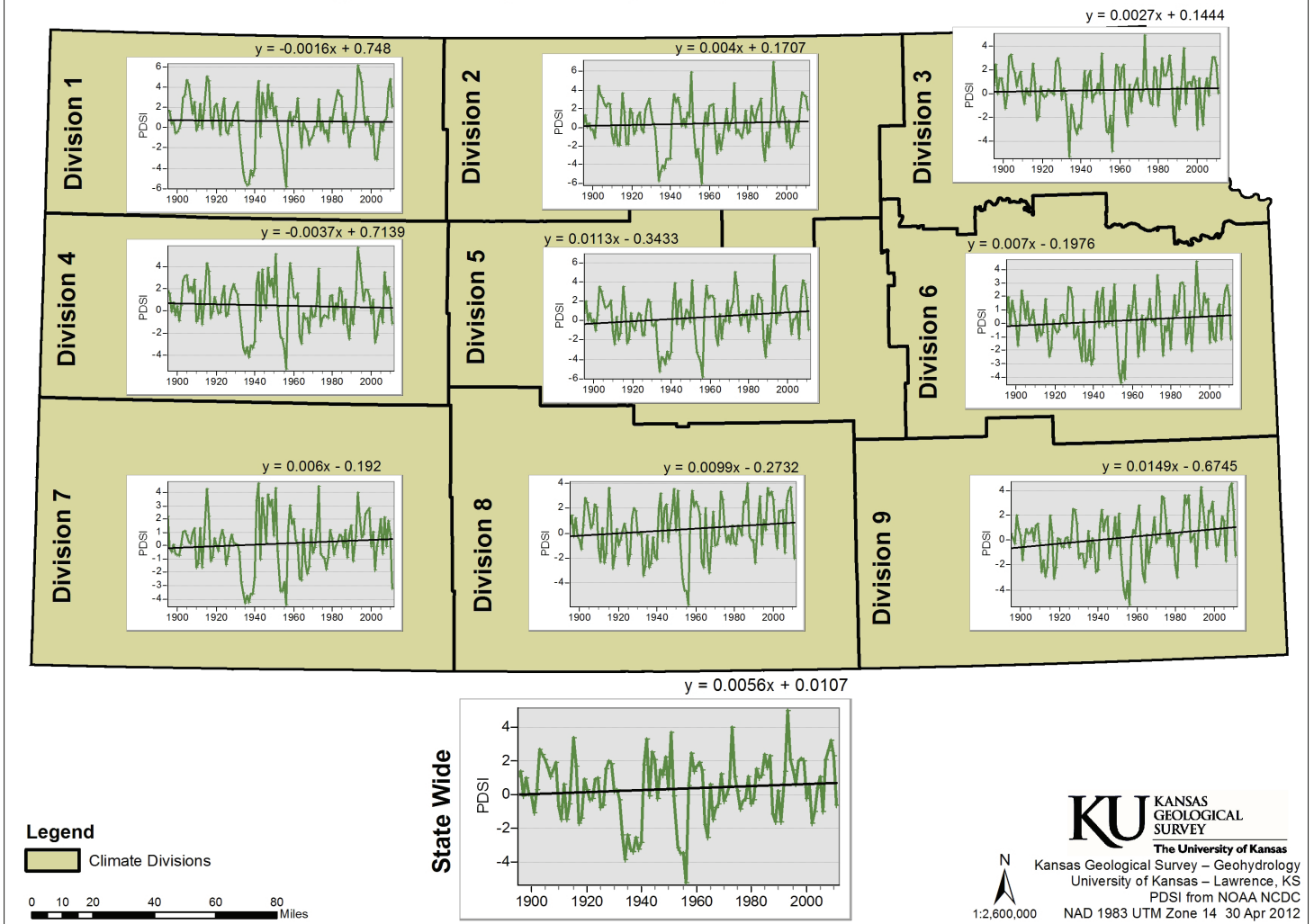


Figure 1. Instrumental PDSI trends for Kansas from 1895 to 2011. Image from the High Plains Aquifer Atlas (www.kgs.ku.edu/HighPlains/HPA_Atlas/index.html).

However, paleoclimatic records allow one to assess the full range of drought variability by utilizing data that span longer periods of time. Long-term records have been developed from a variety of different proxies that span a range of time periods from hundreds to thousands of years. Proxies include tree-rings, sediments from lakes, sand dunes, and rivers, as well as historical and archeological records. These proxies record natural variability in drought occurrence and allow us to compare historic droughts of the 20th century with those of the past.

This report will focus on the paleoclimatic record developed from tree-ring studies. However, it is important to note that when used together, multiple proxy records provide a more complete picture of past change than that offered by any one proxy or instrumental data alone. Therefore, this report will supplement tree-ring reconstructions with data from historical, archeological, and geomorphic records in order to more fully investigate past drought variability.

2.2.1 Long-term PDSI Reconstructions

Tree-rings chronologies are based on the actual growth rate of highly drought-sensitive trees and therefore function as an important indicator of past droughts. Adequate moisture and a long growing season result in wide tree rings while drought years create very narrow rings. Importantly, individual tree-rings can be dated to the exact calendar year using cross-matching techniques.

Recently, an extensive network of annual tree-ring chronologies has been developed and made publically available through the International Tree-Ring Data Bank (<http://www.ncdc.noaa.gov/paleo/treering.html>). Utilizing these data, annual PDSI reconstructions have been developed for 286 grid points across most of North America (Cook and Krusic, 2004). Reconstructions utilized the nearest available tree-ring chronologies to each grid point and were produced with a well-tested point-by-point principal-components regression procedure. See Cook et al. (1999) for detailed methodology used to develop PDSI reconstructions. PDSI reconstructions are evaluated using four statistics, which indicate high overall calibration and verification (see appendix for more details).

Regression based tree-ring PDSI reconstructions tend to underestimate extreme values, although dry extremes are better represented than wet extremes, but are reasonably accurate in terms of extent and duration (Woodhouse and Overpeck, 1998). Therefore, such reconstructions facilitate accurate assessment of the relative severity of 20th-century droughts compared to droughts in the more distant past.

A previous paleoclimate report for the Ogallala region by Young and Buddemeier (2002) utilized PDSI reconstructions by Cook et al. (1999), which were developed from 425 tree-ring chronologies and extended from ~1170 to 1978 AD for western Kansas. Since the publication of this report, new PDSI reconstructions have been produced that represent a substantial spatial and temporal improvement and enable us to better assess the nature of past drought variability. New reconstructions are now based on almost twice as many tree-ring chronologies (835 in total) and extend over longer time periods (from 837 to 2003 AD for western Kansas). PDSI estimates are based on instrumental data after 1978. PDSI data are available publically in the form of the North American Drought Atlas (<http://iridl.ldeo.columbia.edu/SOURCES/.LDEO/.TRL/.NADA2004/.pdsi-atlas.html>). Data were obtained for six grid points in Kansas, thereby dividing the state into six regions (Northwest, Southwest, North-central, South-central, Northeast, Southeast) for analysis in this report.

3. Analyses

3.1 Drought Severity

Figure 2 contains plots of annually resolved PDSI tree-ring reconstructions for six regions in Kansas. *These plots highlight numerous years in the past where drought conditions exceeded the severity of the 1930s and 1950s droughts in each region.* The peak individual drought years during the 1930s and 1950s droughts were determined to be 1934 and 1956 respectively. PDSI values for these years are highlighted with dashed lines on figure 2 and provide a benchmark by which to assess drought occurrence within each region. This type of analysis, however, does not favor regional comparisons as different PDSI thresholds are used in each region.

In order to facilitate regional comparison, we averaged the six regional PDSI values for 1934 and 1956 respectively, generating two thresholds by which to compare the different regions. These thresholds enable us to determine the number of years where droughts of a similar or greater magnitude occurred (i.e. years where PDSI is less than the threshold values). The averaged PDSI values for 1934 and 1956 are -4.9 and -5.9 respectively. Figure 3 highlights the total number of drought years in each region where PDSI values were less than or equal to the threshold values. Note that data were unavailable for some regions between 837-1000 AD and therefore, in order to facilitate fair comparison between regions, this analysis was restricted to data post 1000 AD.

The PDSI data indicate that western Kansas has experienced more severe droughts than eastern Kansas over the past 1000 years. Furthermore, the data also indicate that northern Kansas has typically experienced more severe droughts than southern Kansas. The west to east trend is not surprising given the strong latitudinal

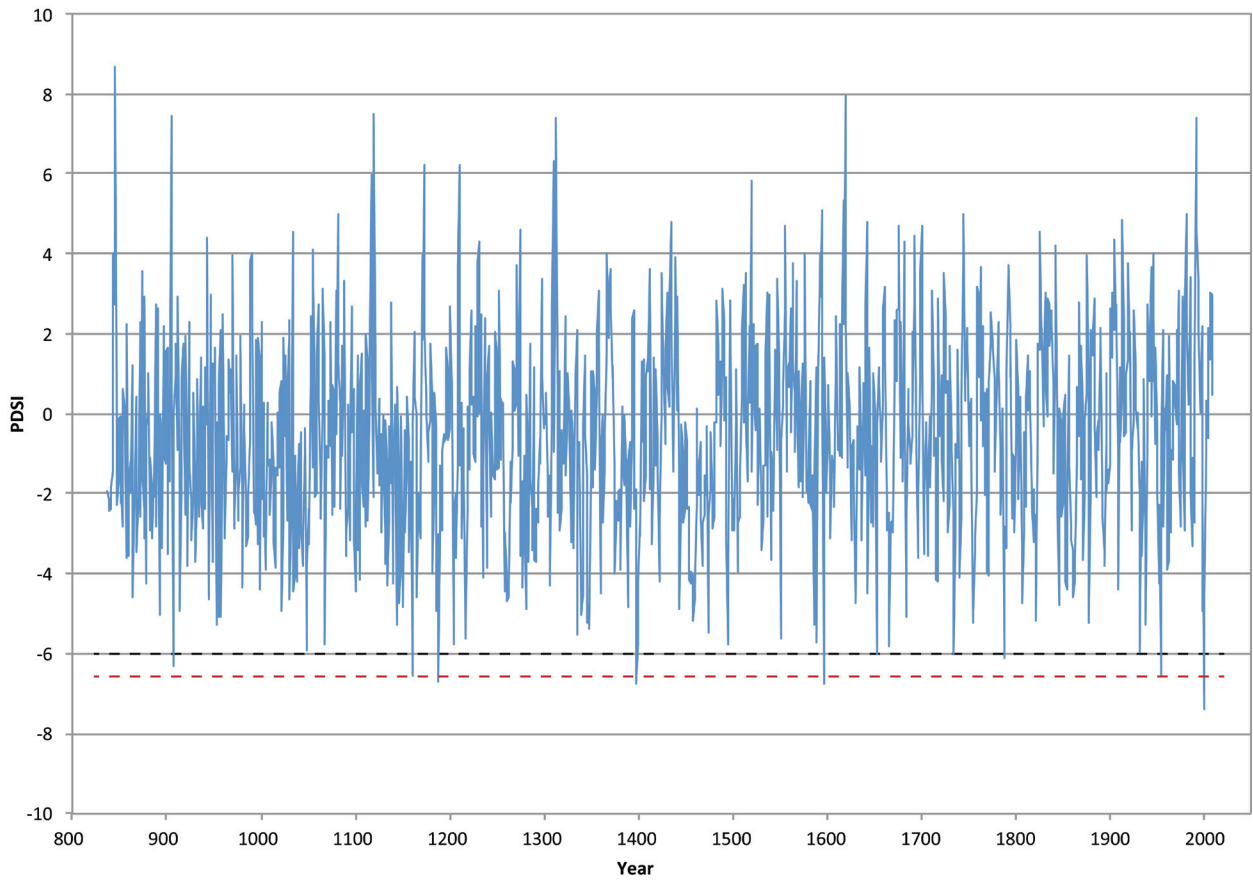


Figure 2a. Annual PDSI reconstructions from tree rings for northwestern Kansas. Dashed lines indicate the 1934 (black) and 1956 (red) PDSI values.

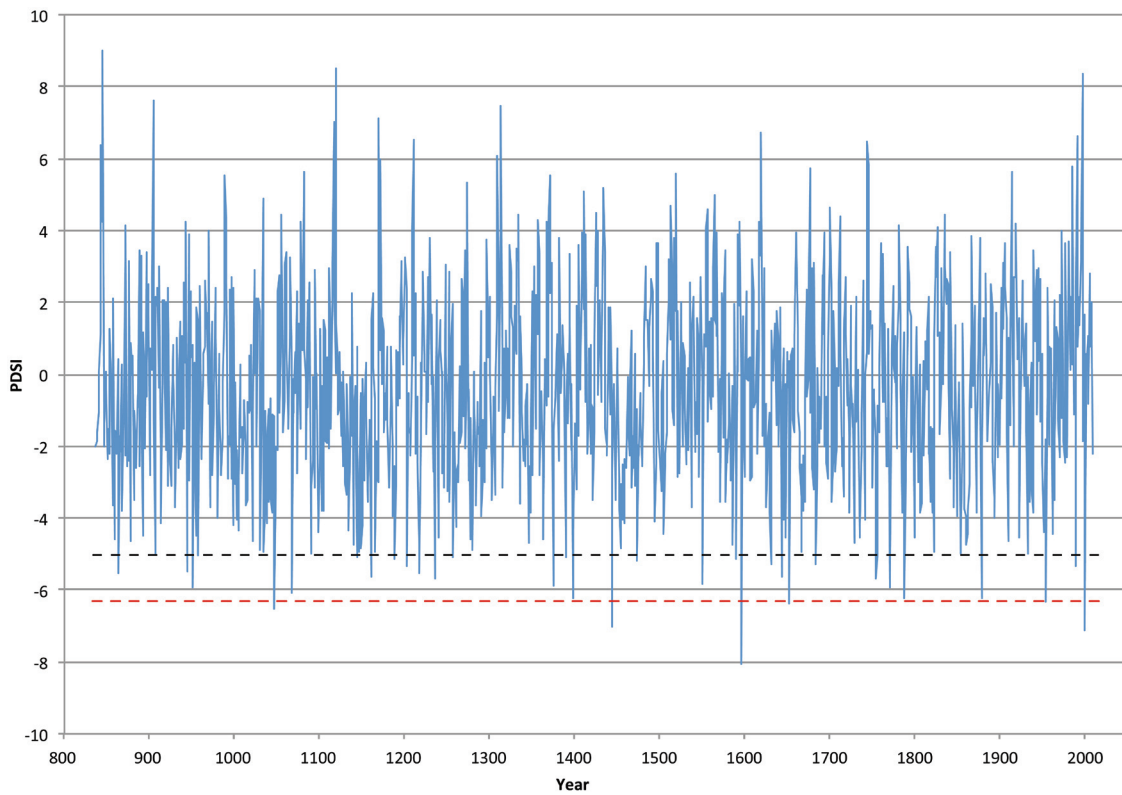


Figure 2b. Annual PDSI reconstructions from tree rings for southwestern Kansas. Dashed lines indicate the 1934 (black) and 1956 (red) PDSI values.

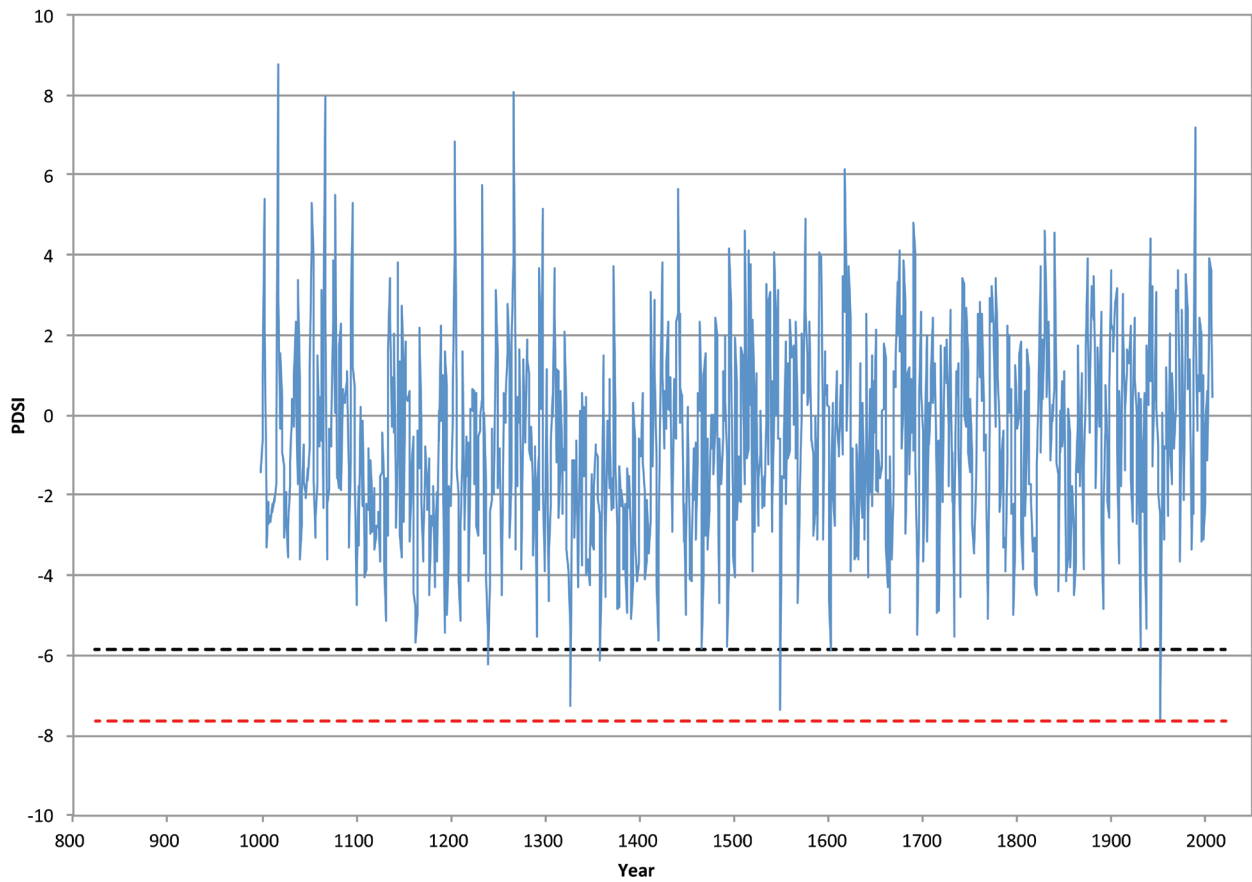


Figure 2c. Annual PDSI reconstructions from tree rings for north-central Kansas. Dashed lines indicate the 1934 (black) and 1956 (red) PDSI values.

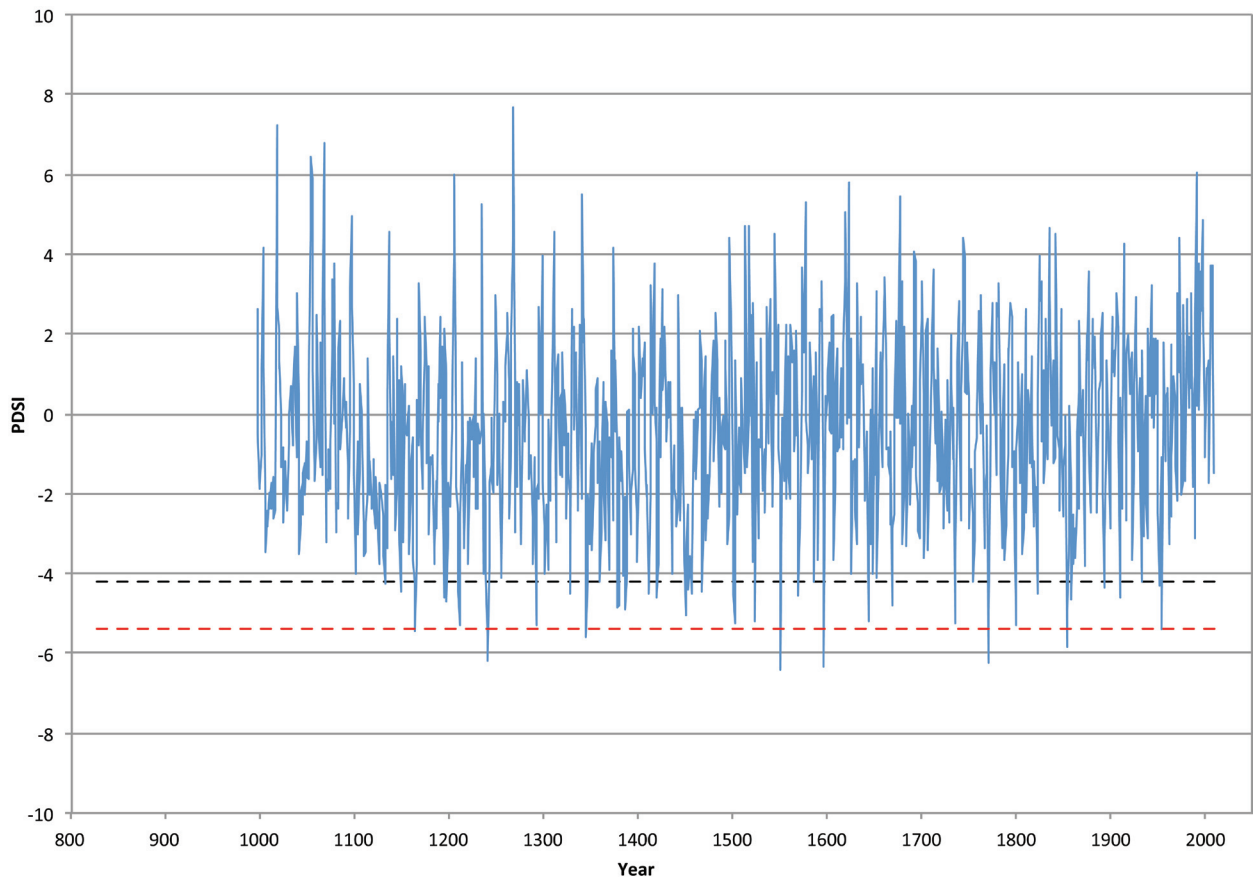


Figure 2d. Annual PDSI reconstructions from tree rings for south-central Kansas. Dashed lines indicate the 1934 (black) and 1956 (red) PDSI values.

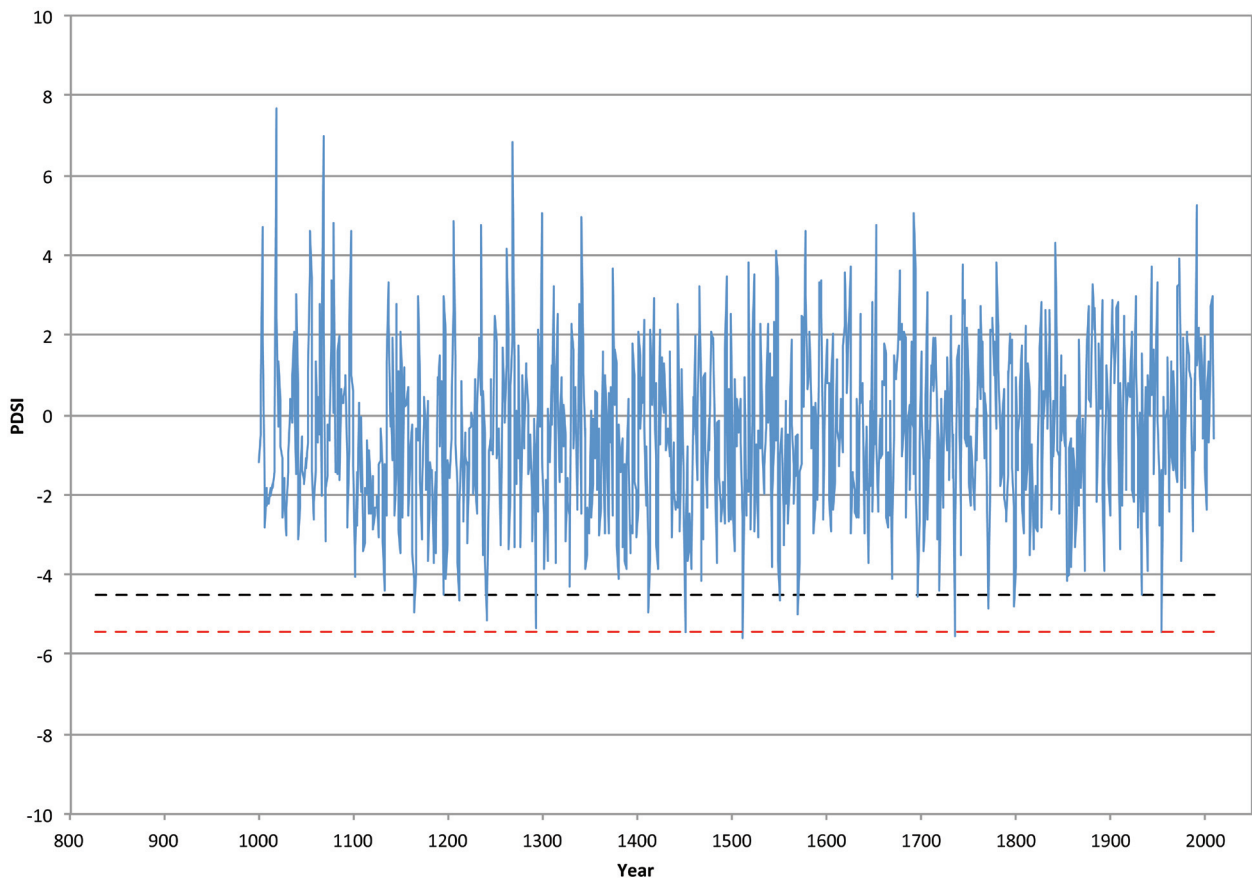


Figure 2e. Annual PDSI reconstructions from tree rings for northeastern Kansas. Dashed lines indicate the 1934 (black) and 1956 (red) PDSI values.

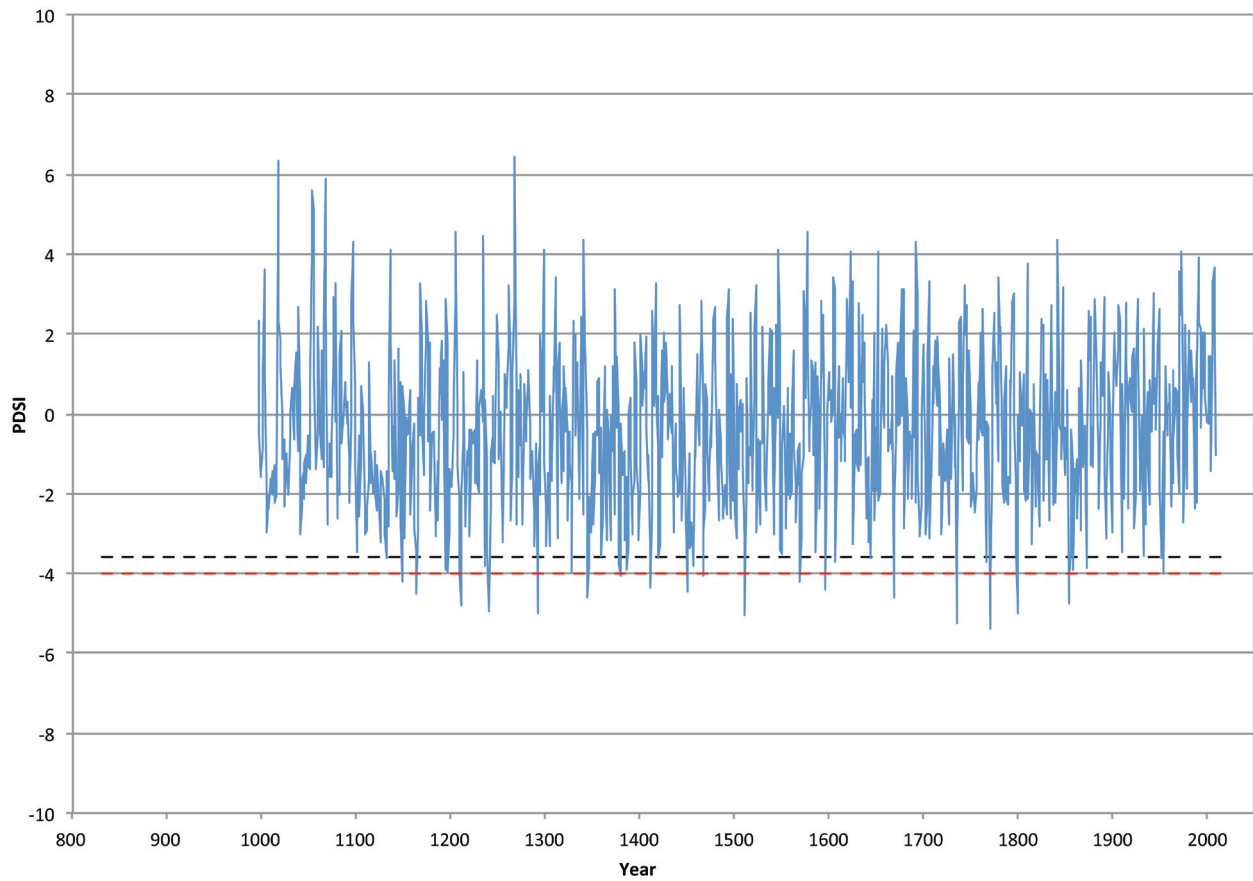


Figure 2f. Annual PDSI reconstructions from tree rings for southeastern Kansas. Dashed lines indicate the 1934 (black) and 1956 (red) PDSI values.

climate gradient in Kansas. The north to south trend can be explained by investigating the spatial patterns of historic 20th-century droughts. For example, the Dust Bowl drought was spatially centered over the Pacific Northwest and later over the northern Plains while the 1950s drought, in contrast, was centered over the southern Great Plains and later shifted into the southwest US (e.g. Stahle et al., 2007; Fig. 4). Hoerling et al. (2009) suggest that the 1950s drought was driven by changes in sea-surface temperatures, more specifically the El Niño-Southern Oscillation. They found that during La Niña years, characterized by cold sea-surface temperatures in the equatorial Pacific, droughts are common in the southern Plains. In contrast, they suggest that the Dust Bowl drought was caused by random atmospheric variation rather than changes in ocean temperatures. Therefore, the PDSI data appear to suggest that the random forcing mechanisms of the Dust Bowl drought have been more common over the past 1000 years than those that resulted in the 1950s drought.

Another way to analyze the PDSI data is to determine how many years exceed the threshold in a given century. By this method *we should expect individual drought years at least as severe as 1934 on average 3-4 times a century in western Kansas, 2-3 times in central Kansas, and about once a century in eastern Kansas.*

However, this analytical method (i.e. using averaged PDSI thresholds) can be misleading. For example, figure 3 indicates that there are no droughts in the paleorecord that exceed the 1956 threshold in eastern Kansas. This is misleading because of the strong regional expression of drought in the state. For example, in southeastern Kansas the 1956 PDSI was -4.0, which indicates extreme drought. However, because drought conditions were more severe elsewhere in the state, the regionally averaged threshold for 1956 is skewed to -5.9. While there are no past drought years with PDSI values less than -5.9 in southeastern Kansas, there are at least 22 past drought years with PDSI values less than -4.0 (see Fig. 2f). We therefore suggest that both methods of analysis (i.e. assessing drought severity *within* and *between* regions) should be used in conjunction when assessing the variability of drought severity across Kansas.

3.2 Drought Duration

One of the key characteristics of the 1930s and 1950s droughts was not only their severity in a given year but their *duration*. Individual drought years are therefore not necessarily good indicators of cumulative socio-economic or environmental impacts as one dry year may be accommodated if it is sufficiently offset by wetter conditions the following year (Cook et al., 2007). For example, the 2002 drought year in southwestern Kansas was more severe than the peak year of the Dust Bowl (PDSI values of -7.1 and -5.0 respectively). However, 2002 was bounded by years of positive PDSI values whereas the Dust Bowl drought consisted of several consecutive years of drought conditions. It is therefore important to assess the duration of past periods of drought.

The duration of droughts is more difficult to estimate because climatic variability tends to punctuate dry multi-year intervals with occasional wet years (Cook et al., 2009). Furthermore, there is no unique solution for calculating drought duration. For example, the 1930s and 1950s droughts have been estimated to have lasted 12 and 14 years (Stahle et al., 2007) or 7 and 8 years (Andreadis et al., 2005) respectively. One method to determine drought duration is to utilize a low-pass filter, such as a moving-average, which allows for analysis of decadal to multi-decadal changes in aridity.

Figure 5 contains plots of PDSI values smoothed over 10- and 50-year periods. For this analysis we determine the beginning and end of a drought period from the smoothed data by identifying when it is preceded or followed by more than two consecutive years of positive PDSI values. Using this technique we identify the duration of the 1930s and 1950s droughts in Kansas as lasting 13 and 18 years respectively.

Using these durations we are able to identify several periods of past drought with durations similar (i.e. 10-20 years) to the severe historic droughts of the 20th century. These droughts are highlighted in figure 5 by light gray bars. Figure 6 shows the number of droughts of similar duration to the historic 20th century droughts over the past 500 years. We limit this analysis to the past 500 years because the majority of droughts prior to this appear to be of much greater duration. Drought duration over the past 500 years illustrates a similar pattern to

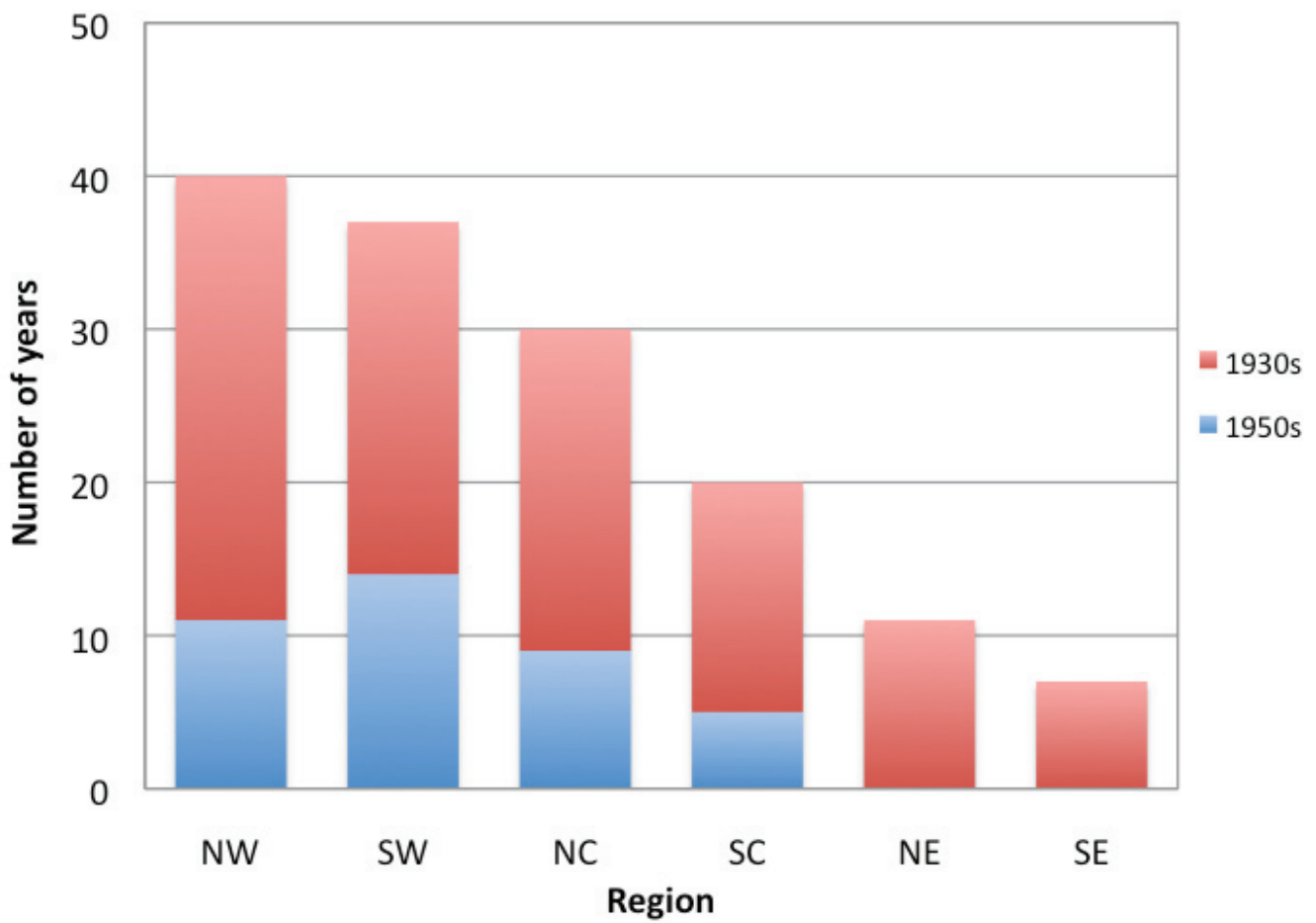


Figure 3. Number of drought years more severe than the peak years of the 1930s and 1950s droughts. Note that this analysis uses threshold PDSI values averaged across all six regions.

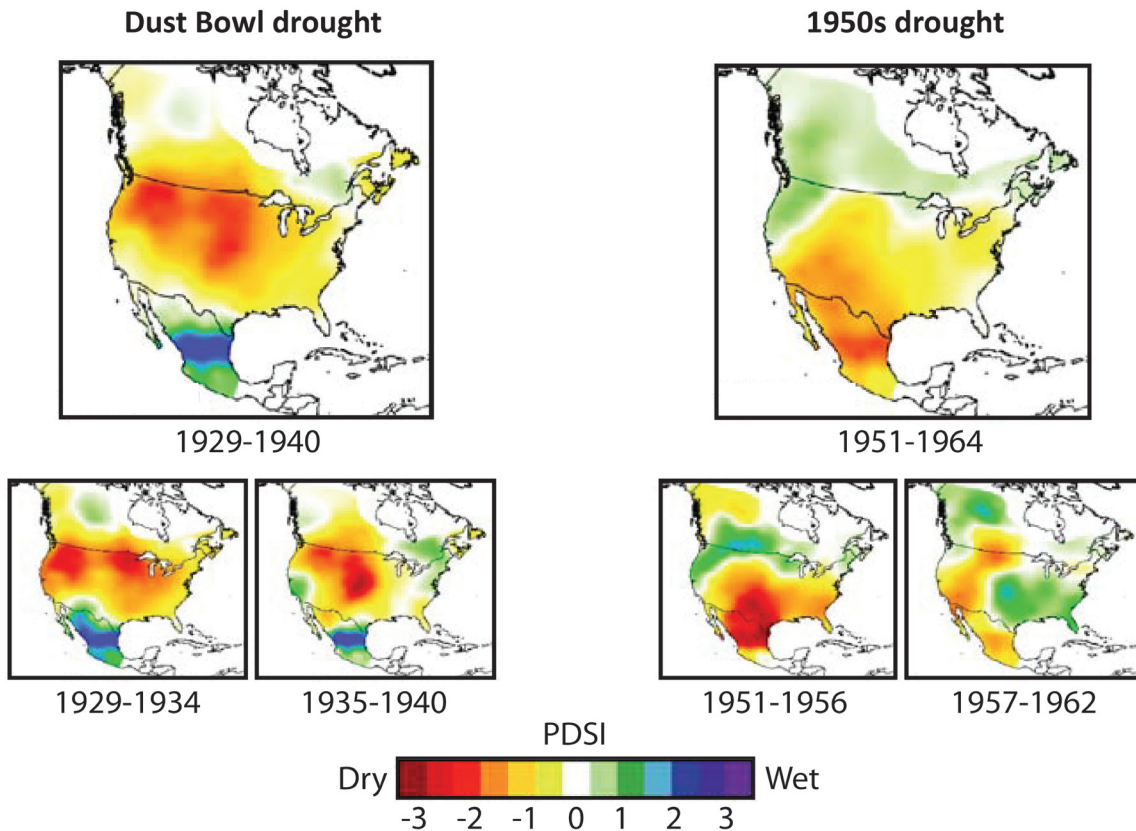


Figure 4. Mapped spatial patterns of the 1930s and 1950s droughts using instrumental PDSI data. Figure modified from Stahle et al. (2007).

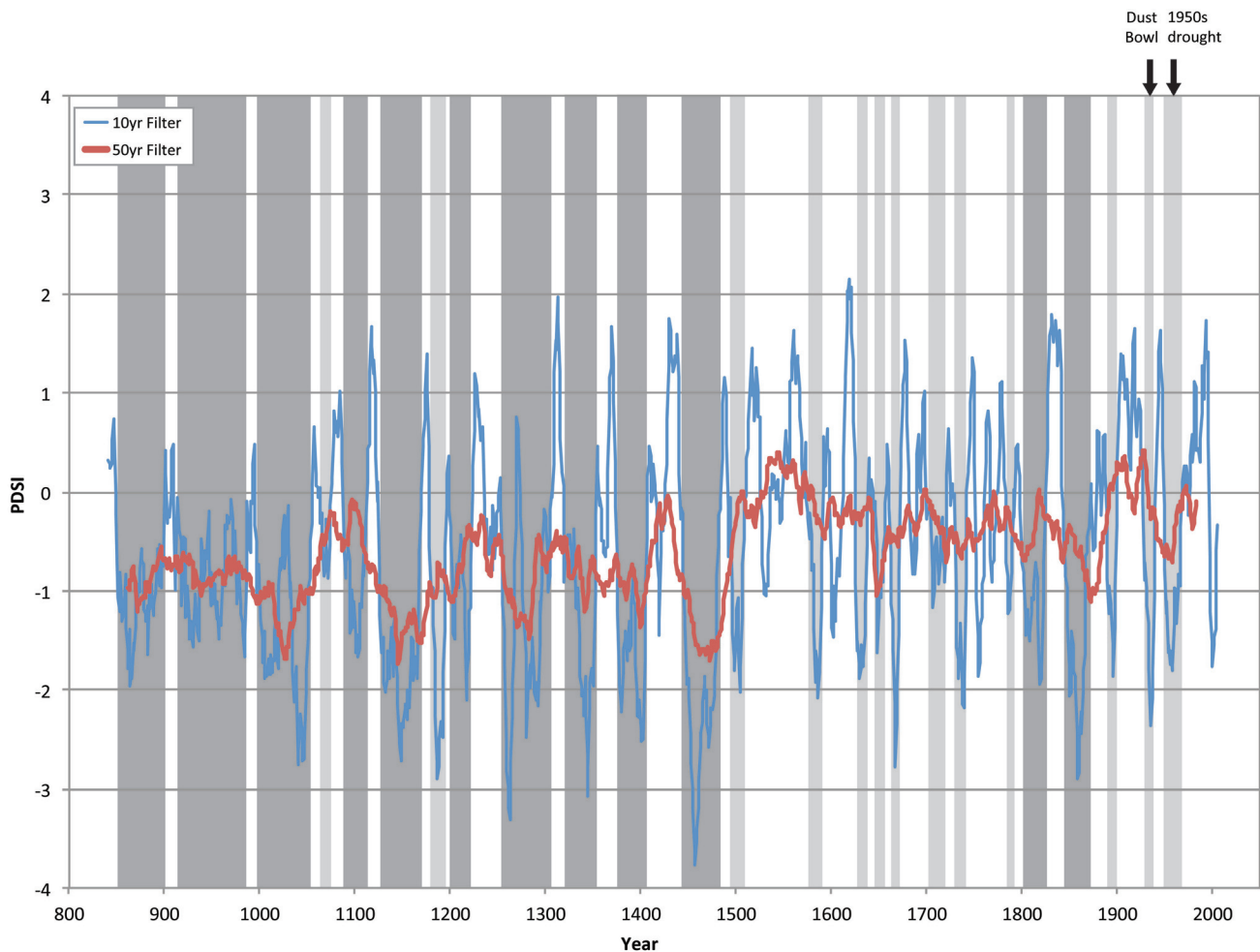


Figure 5a. Smoothed PDSI reconstructions for northwestern Kansas. Light-gray bars indicate droughts of similar duration to the 1930s and 1950s droughts while dark-gray bars indicate droughts of greater duration.

drought severity with western and northern Kansas experiencing more decadal drought periods than eastern Kansas. From these data *we should expect decadal droughts on average two times a century in western Kansas and about once a century in eastern Kansas.*

3.2.1 Megadroughts

Droughts of unusually long duration compared to those observed in the instrumental record are often called ‘megadroughts.’ In order to constitute a megadrought, a past multi-year drought must exceed the duration of the most extreme droughts in the 20th century. Therefore, for this study, a megadrought is defined as a drought lasting more than 20 years in duration.

PDSI reconstructions highlight several periods of extreme drought in the past with much longer durations compared to those of the 20th century, particular prior to 1500 AD. These multi-decadal droughts are highlighted in figure 5 by dark gray bars. Additionally, documented megadroughts are typically at least as severe as the 1930s and 1950s droughts.

It is important to validate the occurrence of past megadroughts by utilizing other proxy records. Figure 7 synthesizes the records of drought variability shown in figure 5 and in addition highlights different lines of environmental and societal evidence that support drought conditions during documented megadroughts.

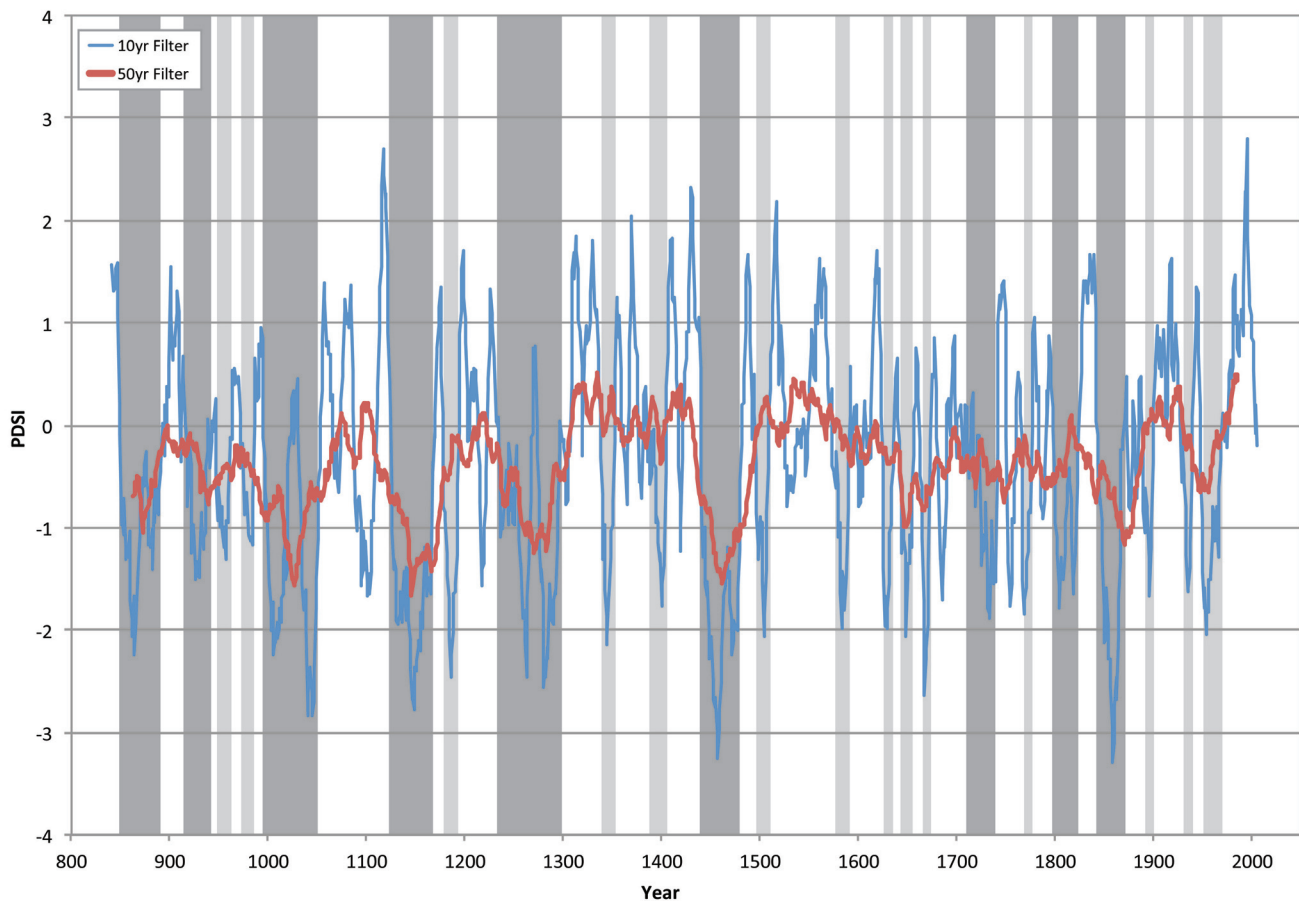


Figure 5b. Smoothed PDSI reconstructions for southwestern Kansas. Light-gray bars indicate droughts of similar duration to the 1930s and 1950s droughts while dark-gray bars indicate droughts of greater duration.

3.2.2. Megadroughts from 1500 to 2011 AD

PDSI reconstructions indicate the likely occurrence of megadroughts in the beginning and middle part of the 19th century, which persisted on average for 30 years (Figs. 5 and 7). Drought conditions around 1850 are noted in a variety of historical data, including early meteorological records (Ludlum, 1971). Stahle et al. (2007) cite evidence from the Kiowa of the southern Great Plains that cites 1855, known among the Kiowa as the “sitting summer,” as a year of severe drought. Woodhouse and Overpeck (1998) note that drought conditions were also documented in Kansas newspapers in 1860. Woodhouse et al. (2002) used streamflow reconstructions from eastern Colorado to document a period of remarkable sustained drought from approximately 1845 to 1856. This period of drought, together with human impacts, may have also resulted in a severe decline in the populations of the Great Plains bison (Woodhouse et al., 2002). Historical accounts from early explorers in the region during the 19th century report periods of blowing sand indicative of eolian activity and sand-dune activation for an area extending from northern Nebraska to southern Texas (Muhs and Holiday, 1995). Eolian activity is primarily driven by droughts severe enough to remove the stabilizing effects of vegetation. Forman et al. (2008) observed discrete episodes of sand deposition in the Arkansas River valley of southwestern Kansas between 1620-1680 and 1800-1820 AD (Fig. 6).

3.2.3 Megadroughts from 850 to 1500 AD

PDSI data highlight several likely past megadroughts from 850 to 1500 AD (Figs 5 and 7). Although these megadroughts were punctuated with wet intervals, overall they suggest protracted aridity lasting on average 40-50 years in duration. The longest megadrought on record occurred in north-central Kansas and lasted 110 years

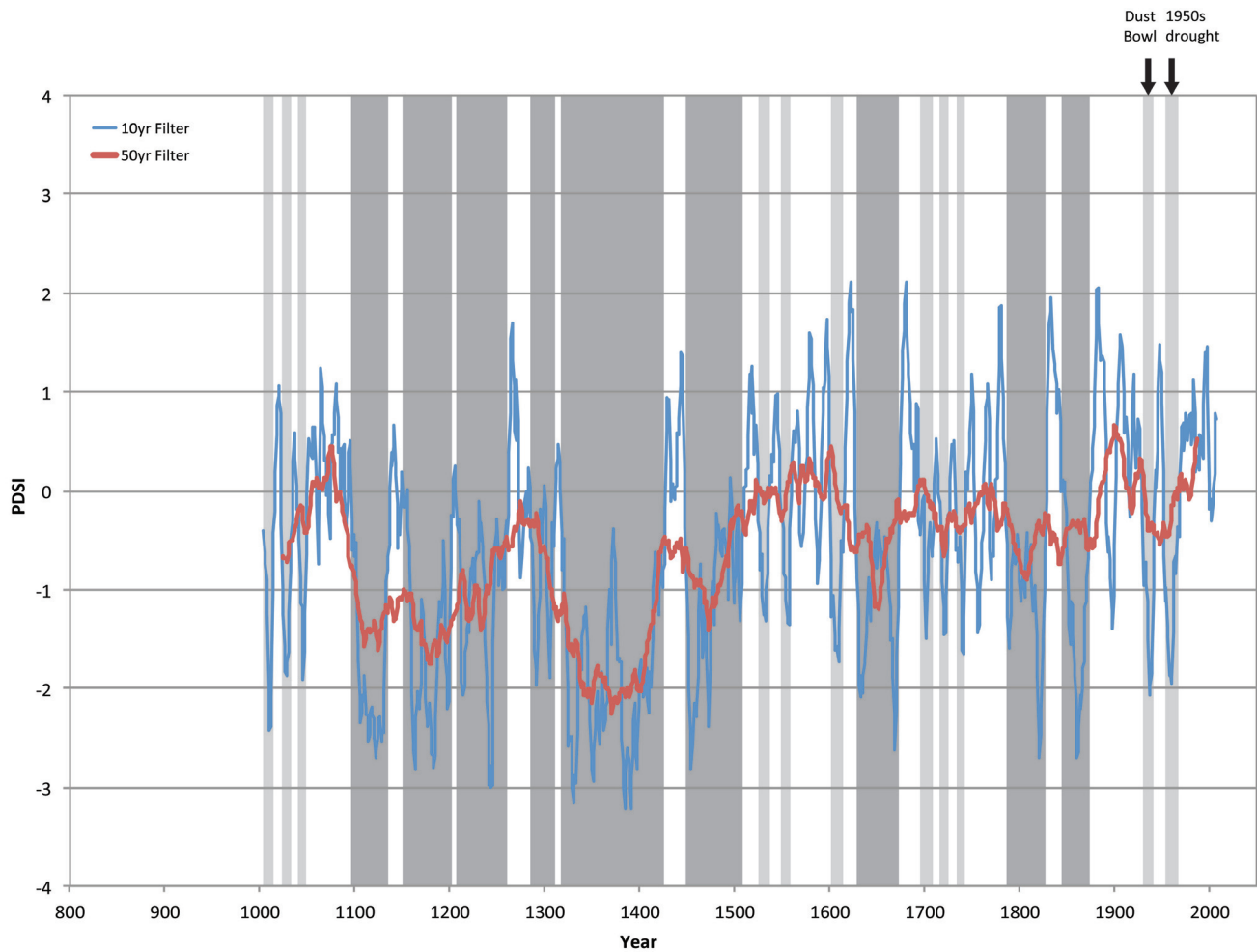


Figure 5c. Smoothed PDSI reconstructions for north-central Kansas. Light-gray bars indicate droughts of similar duration to the 1930s and 1950s droughts while dark-gray bars indicate droughts of greater duration.

from 1317 to 1427 AD. This megadrought was also much more severe than historic 20th-century droughts. Figure 7 highlights the spatial variability of megadroughts across the state. For example, the protracted 110-year megadrought in north-central Kansas was separated into two separate decadal droughts in western Kansas.

Most dune records from the central Great Plains show significant sand-dune activation due to increasing aridity and reductions in vegetation cover between 950-1350 AD. Evidence of sand-dune mobilization from the Great Bend Sand Prairie in south-central Kansas – the largest dune field in Kansas – has been documented between 1050-1250 and 1450-1650 AD (Arbogast, 1996). Halfen et al. (2011) also identified active dune migration in south-central Kansas between 1000-1100 AD. Dunes in the Cimarron River valley of southwestern Kansas were active between 1050 and 1250 AD (Lepper and Scott, 2005) while dunes in the Abilene dune field of north-central Kansas were active more broadly between 890-1490 AD (Hanson et al., 2010). The time intervals for dune activation overlap periods of megadroughts identified from PDSI reconstructions.

Support for the occurrence of megadroughts between 850 and 1500 AD can also be gleaned from the archeological record, which highlights the destabilizing effects of past severe droughts. Benson et al. (2007) suggest that multi-decadal droughts between 990-1060, 1135-1170, and 1276-1297 AD had significant impacts on a variety of prehistoric populations in the Southwest, including Anasazi and Fremont cultures, and the Midwest, such as the Mississippian society.

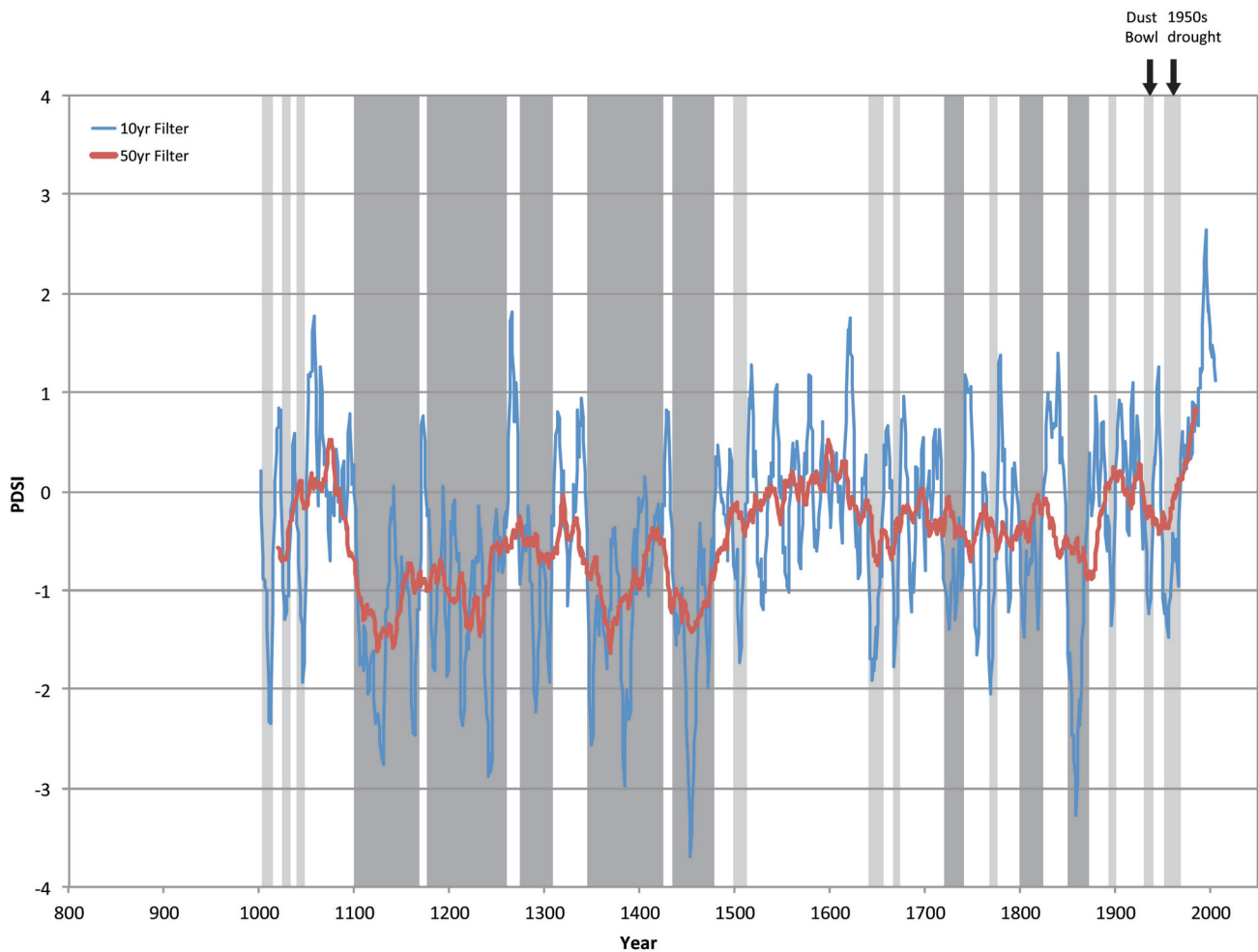


Figure 5d. Smoothed PDSI reconstructions for south-central Kansas. Light-gray bars indicate droughts of similar duration to the 1930s and 1950s droughts while dark-gray bars indicate droughts of greater duration.

The 13th century drought is commonly referred to as the “Great Drought” in the southwest and contributed to significant social change in the Four Corners region through severe population loss and the abandonment of Anasazi settlements. This megadrought would have strongly impacted maize agriculture, which had become the dietary staple of the Anasazi (Benson et al., 2007). Rapid population declines have been documented from archeological sites starting at 1130 and 1280 AD. Studies have also reported population declines in the Fremont cultures located in the Four Corners region around 1000 AD, which may be attributable to the 990-1060 drought.

Severe multi-decadal droughts during the 14th and 15th centuries likely contributed to the decline of Mississippian agricultural societies (e.g. Cobb and Butler, 2002; Cook et al., 2007). Cook et al. (2007) suggest that widespread droughts at this time would likely have caused a sequence of poor harvests that would have proved disastrous. Several Mississippian settlements were abandoned by 1450 including Cahokia, located near the confluence of the Mississippi and Missouri rivers, and Spiro, situated in eastern Oklahoma. Evidence also suggests that the late 13th century megadrought also impacted the Cahokia region (e.g. Benson et al., 2007).

Overall the paleoclimate record suggests that Kansas has experienced droughts of far greater duration in the past than any experienced in the 20th century. This conclusion is supported by several historic, geomorphic, and archeological studies.

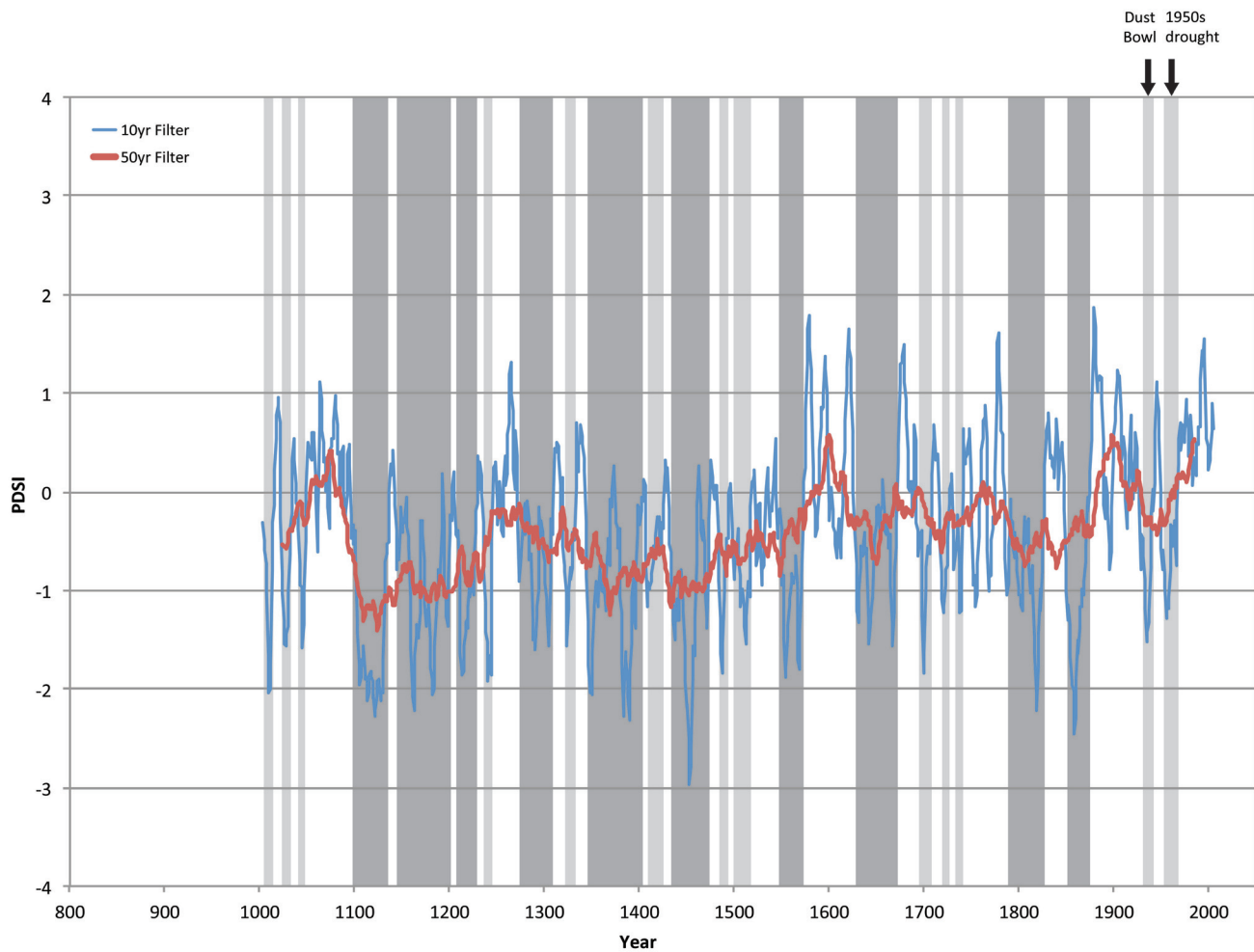


Figure 5e. Smoothed PDSI reconstructions for northeastern Kansas. Light-gray bars indicate droughts of similar duration to the 1930s and 1950s droughts while dark-gray bars indicate droughts of greater duration.

3.3 The Medieval Warm Period

Many of the past megadroughts documented in the paleoclimate record occurred during an era known as the Medieval Warm Period (MWP). The occurrence of several megadroughts during the MWP is troubling as it suggests that the climate system has the capacity to get ‘stuck’ in drought-inducing modes over the Great Plains that can last several decades to a century or more (Cook et al., 2009).

The MWP has been suggested as an approximate analog for likely future warming and drought conditions (e.g. Woodhouse et al., 2010) and thus serves as an important period to investigate. The MWP lasted from approximately 900 to 1300 AD and was characterized by significant climatic variability compared to the modern period. This period was identified by Lamb (1965) as a period of unusual warm temperatures in northern Europe but has since been documented in proxy records from across the globe (e.g. Graham et al., 2011). Other paleoclimate studies record a series of severe droughts across western North America (Cook et al., 2004) during this period, extending eastward into the central Great Plains (e.g. Daniels and Knox, 2005). In addition, the paleoclimatic data suggest a drought-regime change about 500 years ago (Fig. 7). The shift around 1500 AD to droughts of shorter duration may coincide with the onset of cooler climatic conditions during the Little Ice Age.

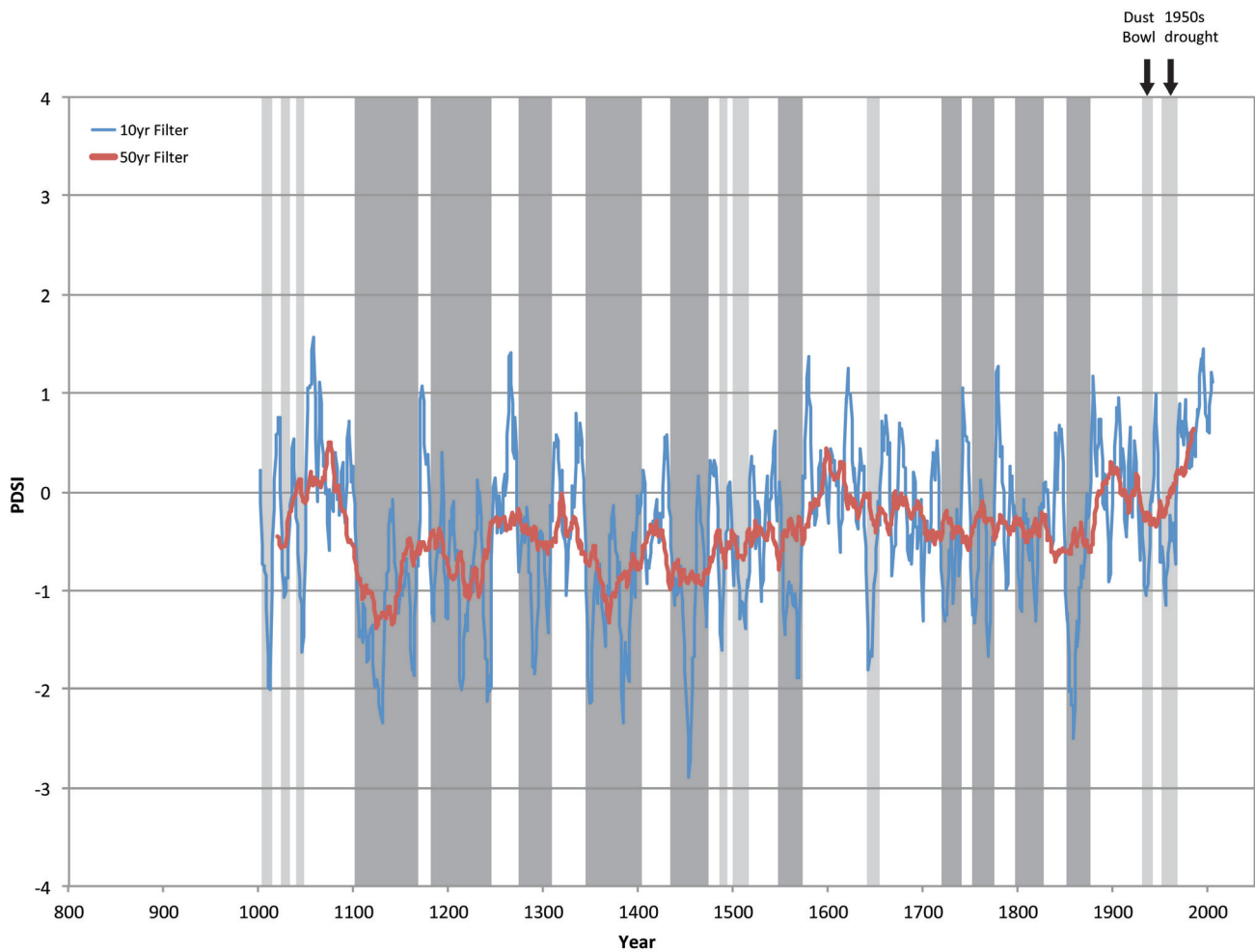


Figure 5f. Smoothed PDSI reconstructions for southeastern Kansas. Light-gray bars indicate droughts of similar duration to the 1930s and 1950s droughts while dark-gray bars indicate droughts of greater duration.

3.4 Risk analysis

Utilizing a similar approach to a previous paleoclimate report published by the Kansas Geological Survey (Young and Buddemeier, 2002), we can provide a quantitative analysis for assessing the risk of drought in Kansas. The paleoclimate data indicate that for western Kansas a drought as severe as the Dust Bowl has occurred on average 3 to 4 times a century. If “3 to 4 times a century” means that there has been on average 3.5 droughts more severe than the Dust Bowl per 100 years, then there is a 3.5% chance that any given year within a 100-year period will have such a severe drought. We can further estimate probabilities for shorter periods using simple arithmetic. For example, there is a 35% chance of a severe drought year in any decade, a 70% chance over a 20-year planning horizon and, in terms of probability, a 100% chance over the estimated 40-year working lifetime of an individual farmer in western Kansas. In eastern Kansas the probabilities are lower as droughts as severe as the Dust Bowl have only occurred about once every century.

We can do a similar analysis for drought duration. For western Kansas, decadal-length droughts have occurred on average twice a century. Therefore, there is a 20% chance of a Dust Bowl length drought in a given decade, a 40% chance over a 20-year period, and an 80% chance over a 40-year period in western Kansas.

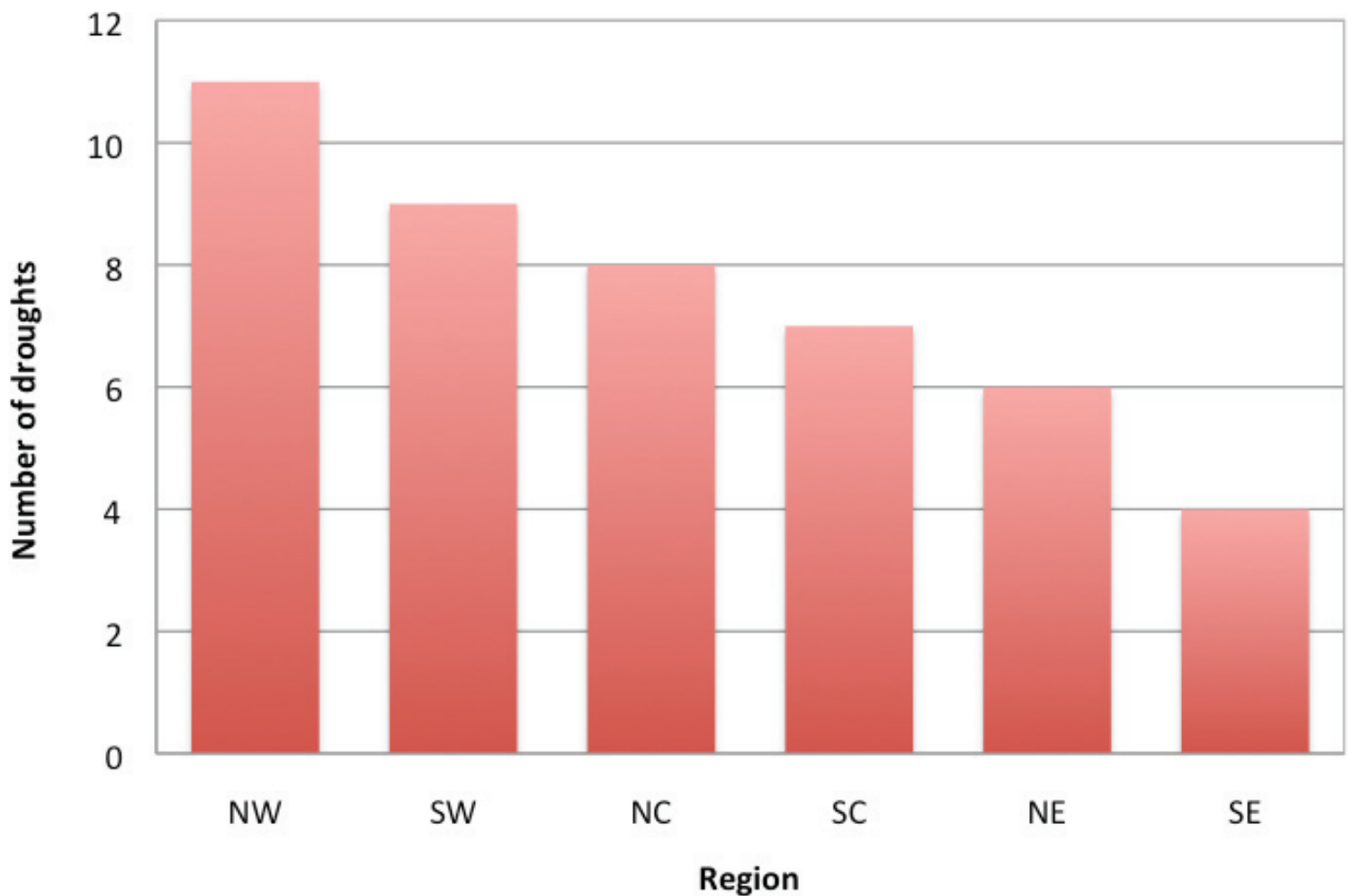


Figure 6. Number of drought periods from 1500 to 2011 AD of similar duration to the 1930s and 1950s droughts (i.e. lasting 10-20 years) by region.

4. Policy and Management Implications

Drought conditions have a significant impact on surface- and ground-water resources through heightened demand and reductions in water supply. Water systems are commonly designed to handle the “drought of record,” identified as the most severe hydrological event from the instrumental record. For the state of Kansas, the 1950s drought (1952-57) remains the planning benchmark and is used to calculate reservoir yield through droughts with a 2% chance of occurrence in any one year (K.A.R. 98-5-8). However, this report provides multiple lines of evidence to support the conclusion that drought variability in the 20th century is just a subset of the full range of variability that one should expect under naturally occurring climatic conditions. In other words, in terms of the long-term record of drought variability, the 1930s and 1950s droughts are not unusual. In fact, the paleoclimatic record indicates that droughts of greater severity and longer duration have occurred in the past. Furthermore, it is possible that the conditions that led to past megadroughts, such as those that occurred during the MWP, could occur in the future. Such severe drought conditions are of great concern because modern-day agricultural and water systems may not have the resilience to survive droughts beyond the “worst case scenario” droughts of the past 100 years (Cook et al., 2007).

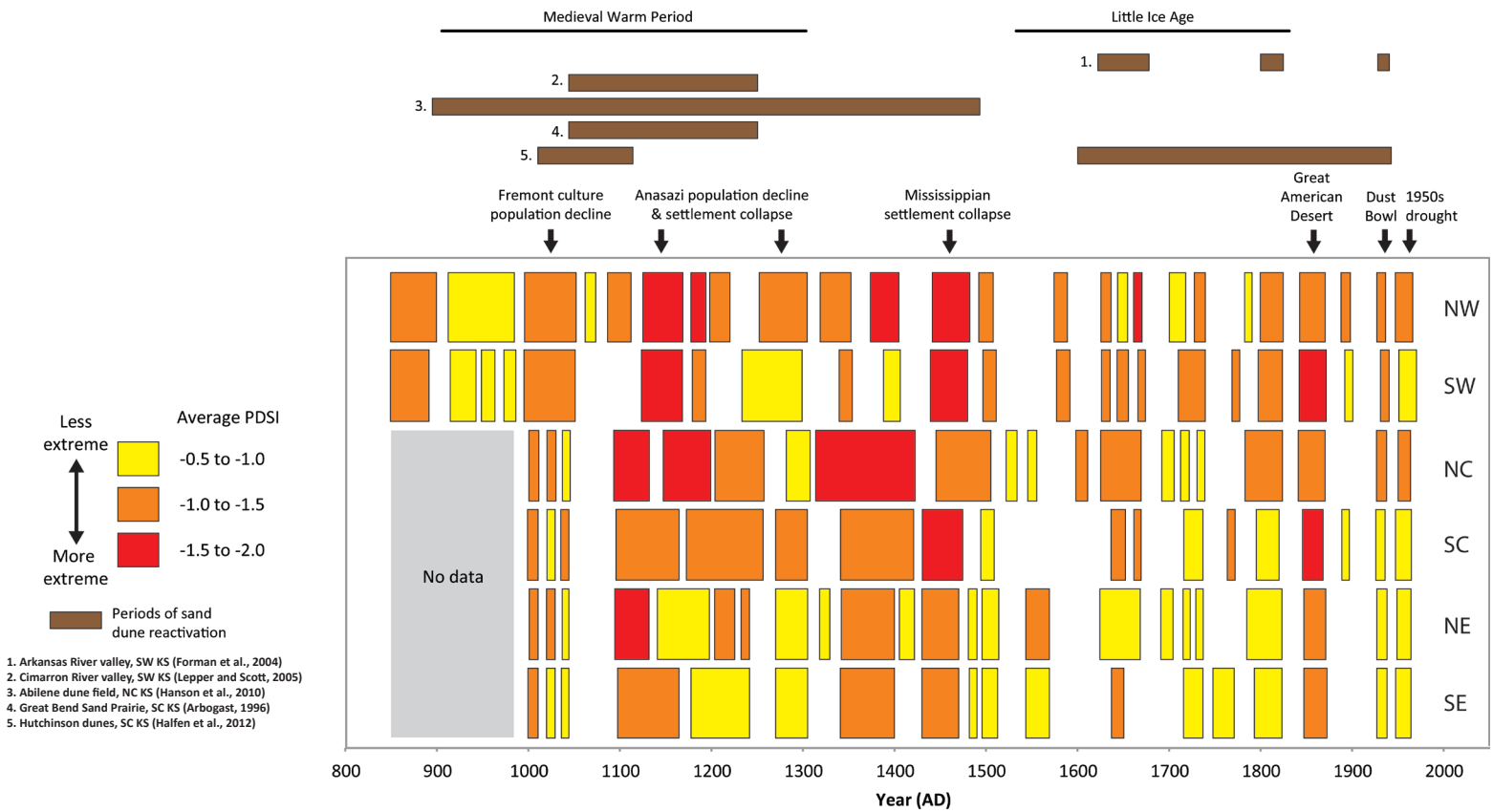


Figure 7. Synthesis of regional reconstructed PDSI data with additional paleoenvironmental proxy data from geomorphic and archeological sources.

In terms of water-resource management, paleoclimatic data have important implications. For example, reservoirs are typically designed with conservation pools to specifically meet water demand during drought conditions. However, would these designs be adequate under megadrought conditions? Additionally, management of aquifer resources must be designed to accommodate high demand during protracted droughts while sustaining or extending the usable lifetime of the resource.

Woodhouse and Overpeck (1998) highlight two factors that may compound the susceptibility of the Great Plains to future drought: 1) increased vulnerability due to land-use practices, specifically the use of irrigation to bring marginal lands into agricultural production, and 2) the enhanced likelihood of drought due to global warming. Furthermore, certain factors present challenges to effective water-resource management including 1) current levels of uncertainty in predicting future drought occurrence, 2) the assumption of climatic stationarity by water-resource planners, and 3) competing management interests (e.g. Lins and Stakhiv, 1998; Hartmann, 2005).

Given these challenges, it would be wise to adopt a probabilistic approach to drought forecasting and planning that incorporates the full range of drought variability indicated in the paleoclimatic record.

5. References

- Andreadis, K. M., Clark, E. A., Wood, A. W., Hamlet, A. F., and Lettenmaier, D. P., 2005, Twentieth-century drought in the conterminous United States: *Journal of Hydrometeorology*, v. 6, p. 985-1001.
- Arbogast, A. F., 1996, Stratigraphic evidence for late-Holocene aeolian sand mobilization and soil formation in south-central Kansas, USA: *Journal of Arid Environments*, v. 34, p. 403-414.
- Benson, L. V., Berry, M. S., Jolie, E. A., Spangler, J. D., Stahle, D. W., and Hattori, E. M., 2007, Possible impacts of early-11th-, middle-12th-, and late-13th-century droughts on western native Americans and the Mississippian Cahokians: *Quaternary Science Reviews*, v. 26, p. 336-350.
- Cobb, C. R., and Butler, B. M., 2002, The vacant quarter revisited: late Mississippian abandonment of the Lower Ohio Valley: *American Antiquity*, v. 67, p. 625-641.
- Cook, E. R., Meko, D. M., Stahle, D. W., and Cleaveland, M. K., 1999, Drought reconstructions for the continental United States: *Journal of Climate*, v. 12, p. 1145-1162.
- Cook, E., and Krusic, P., 2004, North American summer PDSI reconstructions. IGBP PAGES/World Data Center for Paleoclimatology 2004-045: Paleoclimatology Program, National Geophysical Data Center Boulder, CO.
- Cook, E. R., Woodhouse, C., Eakin, C. M., Meko, D. M., and Stahle, D. W., 2004, Long-term aridity changes in the western United States: *Science*, v. 306, p. 1015-1018.
- Cook, E. R., Seager, R., Cane, M. A., and Stahle, D. W., 2007, North American drought: reconstructions, causes and consequences: *Earth Science Reviews*, v. 81, p. 93-134.
- Cook, E. R., Seager, R., Heim, R. R., Vose, R. S., Herweijer, C., and Woodhouse, C., 2009, Megadroughts in North America: placing IPCC projections of hydroclimatic change in a long-term palaeoclimate context: *Journal of Quaternary Science*, v. 25, p. 48-61.
- Daniels, J. M., and Knox, J. C., 2005, Alluvial stratigraphic evidence for channel incision during the Mediaeval Warm Period on the central Great Plains, USA: *The Holocene*, v. 15, p. 736-747.
- Forman, S. L., Marin, L., Gomez, J., and Pierson, J., 2008, Late Quaternary sand depositional record for south-western Kansas: landscape sensitivity to droughts: *Paleogeography, Paleoclimatology, Paleoecology*, v. 265, p. 107-120.
- Graham, N. E., Ammann, C. M., Fleitmann, D., Cobb, K. M., and Lutervacher, J., 2011, Support for global climate reorganization during the "Medieval Climate Anomaly": *Climate Dynamics*, v. 37, p. 1217-1245.
- Halfen, A. F., Johnson, W. C., Hanson, P. R., Woodburn, T. L., Young, A. R., and Ludvigson, G. A., 2012, Activation history of the Hutchinson dunes in east-central Kansas, USA, during the past 2200 years: *Aeolian Research*, v. 5, p. 9-20.
- Hartmann, H. C., 2005, Use of climate information in water resources management; *in*, *Encyclopedia of Hydrological Sciences*, M. G. Anderson, ed.: John Wiley and Sons, Ltd: Malden, MA, 202 p.
- Hanson, P. R., Arbogast, A. F., Johnson, W. C., Joeckel, R. M., and Young, A. R., 2010, Megadroughts and late Holocene dune activation at the eastern margin of the Great Plains, north-central Kansas, USA. *Aeolian Research*, v. 1, p. 101-110.
- Hoerling, M., Quan, X., and Eischeid, J., 2009, Distinct causes for two principal U.S. droughts of the 20th century: *Geophysical Research Letters*, v. 36, p. L19708 doi:10.1029/2009GL039860
- Kansas Department of Agriculture, 2011: <http://www.ksda.gov/news/id/405>
- Lamb, H. H., 1965, The early medieval warm epoch and its sequel: *Paleogeography, Paleoclimatology, Paleoecology*, v. 1, p. 13-37.
- Lepper, K., and Scott, G. F., 2005, Late Holocene eolian activity in the Cimarron River valley of west-central Oklahoma: *Geomorphology*, v. 70, p. 42-52.
- Lins, H. F. and Stakhiv, E. Z., 1998, Managing the nation's water in a changing climate: *Journal of the American Water Resources Association*, v. 34, p. 125-126.
- Ludlum, D. M., 1971, *Weather record book: Weatherwise*, 98 p.
- McGuire, V. L., 2009, Water-level changes in the High Plains aquifer, predevelopment to 2007, 2005-06, and 2006-07: U.S. Geological Survey, Circular 2009-5019, 9 p.

- Muhs, D. R., and Holliday, V. T., 1995, Evidence of active dune sand on the Great Plains in the 19th century from accounts of early explorers: *Quaternary Research*, v. 43, p. 198–208.
- Palmer, W. C., 1965, *Meteorological drought*: U.S. Weather Bureau, Research Paper, vol. 45.
- Riebsame, W. E., Changnon, S. A., and Karl, T. R., 1991, *Drought and natural resources management in the United States: impacts and implications of the 1987-89 drought*: Westview Press, Boulder, 174 p.
- Stahle, D. W., Fye, F. K., Cook, E. R., and Griffin, R. D., 2007, Tree-ring reconstructed megadroughts over North America since A.D. 1300: *Climate Change*, v. 83, p. 133–149.
- Woodhouse, C. A., and Overpeck, J. A., 1998, 2000 years of drought variability in the central United States: *Bulletin of the American Meteorological Society*, v. 79, p. 2643–2714.
- Woodhouse, C. A., Lukas, J. J., and Brown, P. M., 2002, Drought in the western Great Plains, 1845-56: *Bulletin of the American Meteorological Society*, v. 83, p. 1485-1493.
- Woodhouse, C. A., Meko, D. N., MacDonald, G. M., Stahle, D. W., and Cook, E. R., 2010, A 1,200-year perspective of 21st century drought in southwestern North America: *Proceedings of the National Academy of Science*, v. 107, no. 50, p. 21283-21288.
- Young, D. P., and Buddemeier, R. W., 2002, *Climate variation: Implications of long-term records and recent observations*: Kansas Geological Survey, Open-file Report 2002-25E.

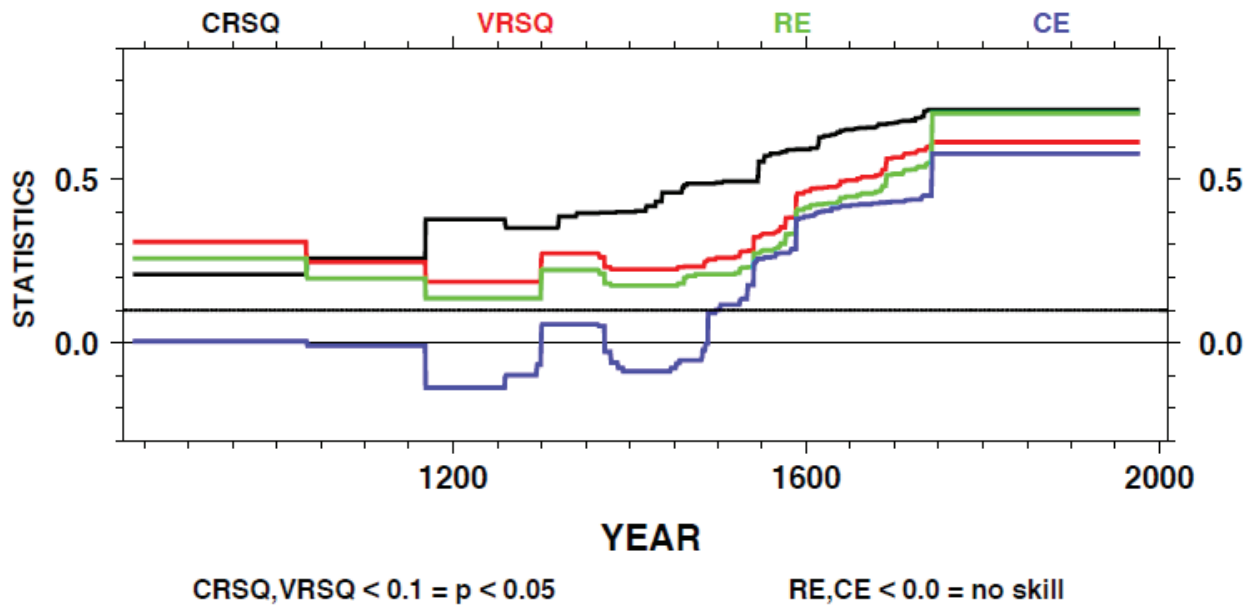
Appendix: Calibration and Verification Statistics

The data used in this report were obtained from the North American Drought Atlas (Cook and Krusic, 2004). Cook and Krusic used four statistics as measures of association between the actual and estimated PDSI in order to test the fidelity of PDSI reconstructions.

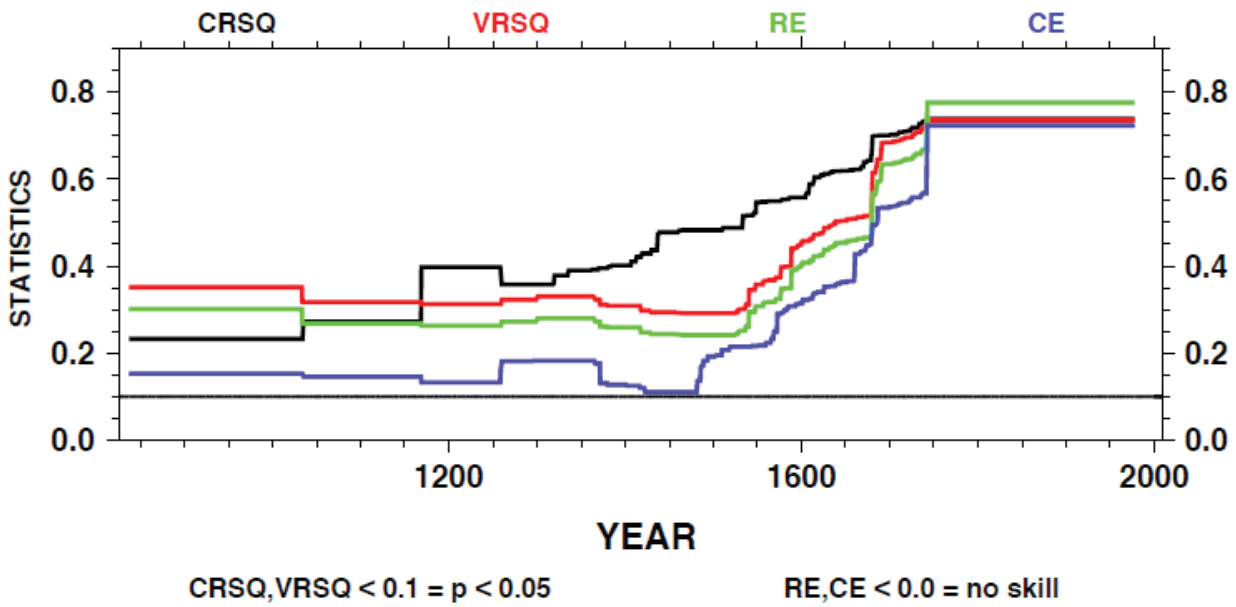
- 1) Calibration R-Square (CRSQ). This statistic measures the percent PDSI variance explained by the tree-ring chronologies at each grid point over the 1928-1978 calibration period, based on a regression modeling procedure described in Cook et al. (1999). As defined here, CRSQ is equivalent to the “coefficient of multiple determination” found in standard statistic texts. It ranges from 0 (no calibrated variance) to 1.0 (perfect agreement between instrumental PDSI and the tree-ring estimates). The former represents complete failure to estimate PDSI from tree rings and the latter is not plausible if the model is not seriously over-fit.
- 2) Verification R-Square (VRSQ). This statistic measures the percent PDSI variance in common between actual and estimated PDSI in the 1900-1927 verification period. It is calculated as the square of the Pearson correlation coefficient, which is a well known measure of association between two variables. VRSQ also ranges from 0 to 1.0 (VRSQ is assigned a 0 value if the correlation is negative). Roughly speaking, $VRSQ > 0.11$ is statistically significant at the 1-tailed 95% level using our 28-year verification period data.
- 3) Verification reduction of error (RE). This statistic was originally derived by Edward Lorenz as a test of meteorological forecast skill. Unlike CRSQ and VRSQ, RE has a theoretical range of -infinity to 1.0. Over the range 0-1.0, RE expresses the degree to which the estimates over the verification period are better than “climatology,” i.e. the calibration period mean of the actual data. So, a positive RE means that the PDSI estimates are better than just using the calibration period mean as a reconstruction of past PDSI behavior. A negative RE is generally interpreted as meaning that the estimates are worse than the calibration period mean and, therefore, have no skill. The use of the calibration period mean as the “yardstick” for assessing reconstruction skill makes this statistic more difficult to pass than VRSQ. However, it is also less robust, meaning that it is very sensitive to even a few bad estimates in the verification period. Therefore, $RE > 0$ is interpreted as evidence for a reconstruction that contains some skill over that of climatology.
- 4) Verification coefficient of efficiency (CE). This statistic comes from the hydrology literature and is very similar to the RE. It too has a theoretical range of -infinity to 1.0. The crucial difference is that the CE uses the verification period mean of the withheld actual data as the “yardstick” for assessing the skill of the estimates. This seemingly minor difference is important because it results in the CE being even more difficult than the RE to pass (i.e., a $CE > 0$).

Here we include the calibration and verification statistics for the six gridpoints utilized in this report. Note that all data are statistically significant for the period of record with the exception of northwestern Kansas, which fails the notoriously hard-to-pass CE test before 1500 AD. Overall the PDSI data are well calibrated and verified.

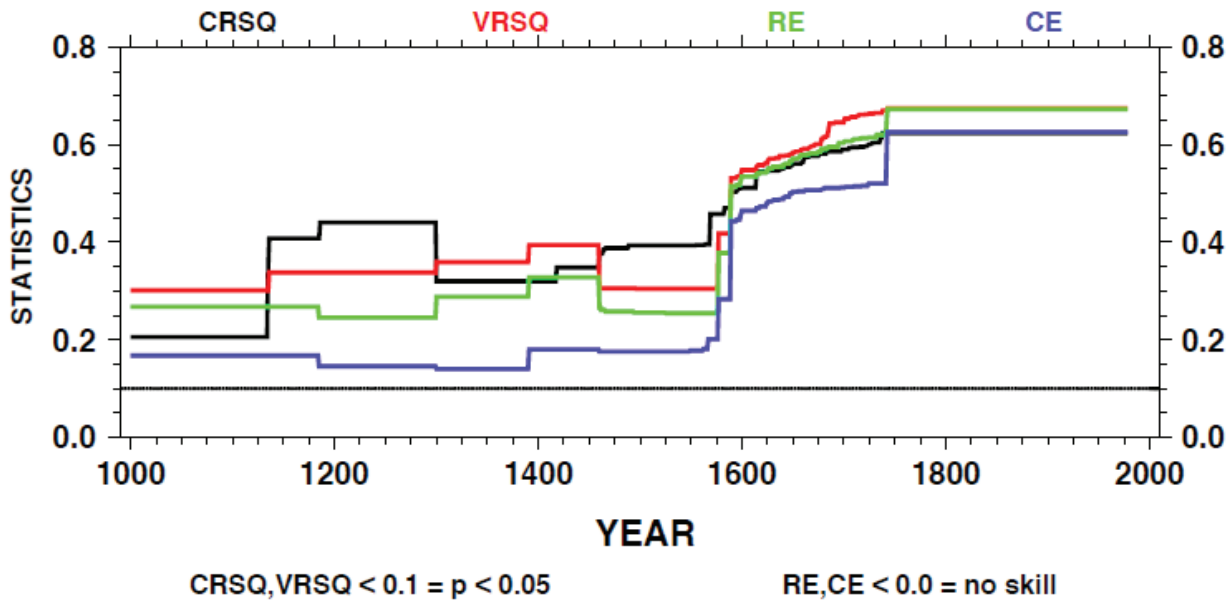
Northwestern Kansas



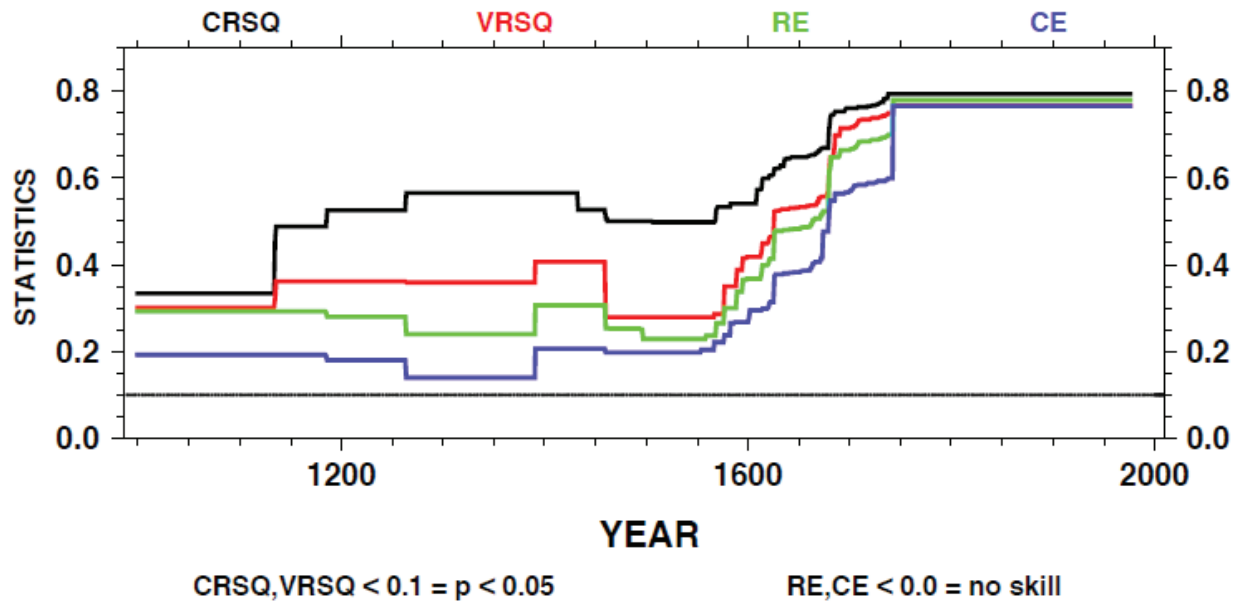
Southwestern Kansas



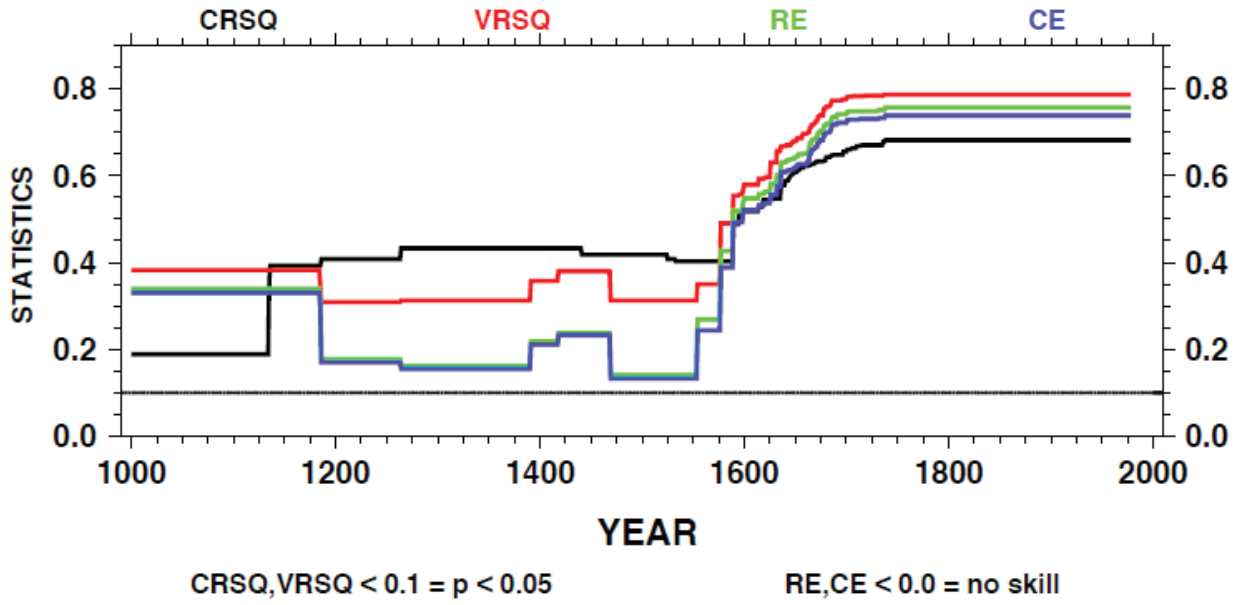
North-central Kansas



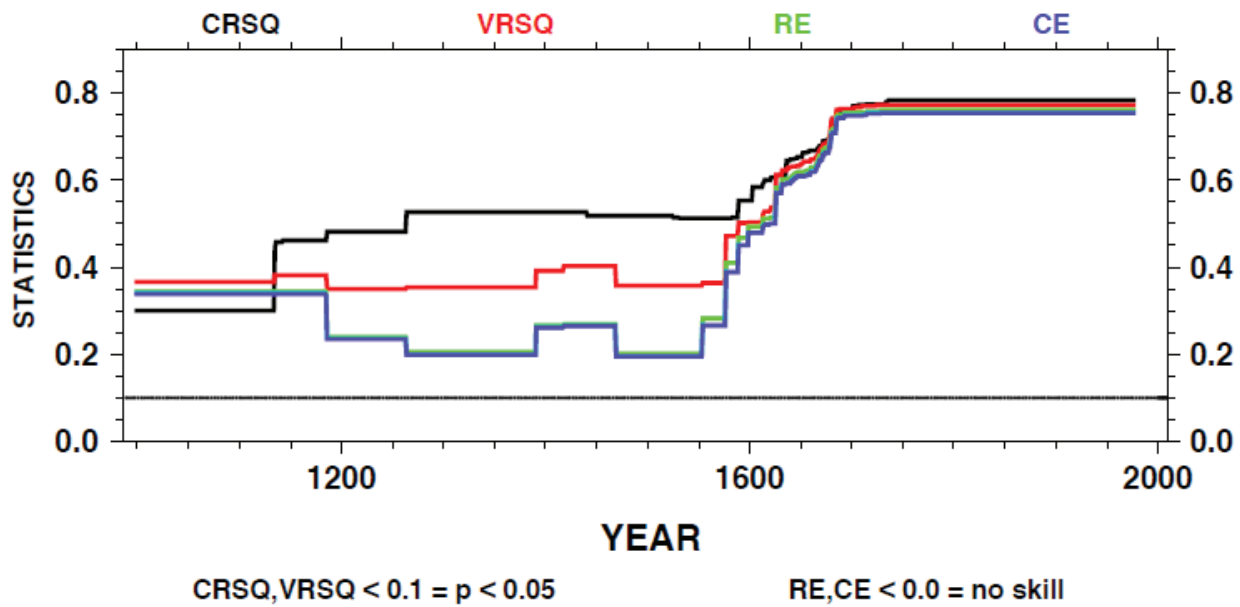
South-central Kansas



Northeastern Kansas



Southeastern Kansas



2000 Years of Drought Variability in the Central United States



Connie A. Woodhouse*⁺ and Jonathan T. Overpeck*^{+,#}

ABSTRACT

Droughts are one of the most devastating natural hazards faced by the United States today. Severe droughts of the twentieth century have had large impacts on economies, society, and the environment, especially in the Great Plains. However, the instrumental record of the last 100 years contains only a limited subset of drought realizations. One must turn to the paleoclimatic record to examine the full range of past drought variability, including the range of magnitude and duration, and thus gain the improved understanding needed for society to anticipate and plan for droughts of the future. Historical documents, tree rings, archaeological remains, lake sediment, and geomorphic data make it clear that the droughts of the twentieth century, including those of the 1930s and 1950s, were eclipsed several times by droughts earlier in the last 2000 years, and as recently as the late sixteenth century. In general, some droughts prior to 1600 appear to be characterized by longer duration (i.e., multidecadal) and greater spatial extent than those of the twentieth century. The authors' assessment of the full range of past natural drought variability, deduced from a comprehensive review of the paleoclimatic literature, suggests that droughts more severe than those of the 1930s and 1950s are likely to occur in the future, a likelihood that might be exacerbated by greenhouse warming in the next century. Persistence conditions that lead to decadal-scale drought may be related to low-frequency variations, or base-state shifts, in both the Pacific and Atlantic Oceans, although more research is needed to understand the mechanisms of severe drought.

1. Introduction

Drought is one of the most damaging climate-related hazards to impact societies. Although drought is a naturally occurring phenomenon throughout most parts of the world, its effects have tremendous consequences for the physical, economic, social, and political elements of our environment. Droughts impact both surface and groundwater resources and can lead to reductions in water supply, diminished water quality, crop failure, reduced range productivity, diminished power generation, disturbed riparian habitats, and suspended recreation activities, as well as a host

of other associated economic and social activities (Riebsame et al. 1991).

The droughts of the 1930s, 1950s, and 1980s caused great economic and societal losses in the Great Plains of the United States, a region particularly prone to drought (Karl and Koscielny 1982; Diaz 1983; Karl 1983) (Fig. 1). This area shows signs of becoming increasingly vulnerable to drought because of factors such as the increase in cultivation of marginal lands and the escalated use of groundwater from the Ogallala Aquifer, where water withdrawal has exceeded recharge for many years (Glantz 1989; White and Kromm 1987). Estimates for the return intervals for a Great Plains drought of 1930s duration and intensity, based on the properties of the twentieth-century record, vary from 75 to 3000 years (Bowden et al. 1981; Yevjevich 1967). Estimates of this type do not provide a very clear understanding of how rare the severe droughts of the twentieth century were in the context of the last 2000 years, nor whether drought of even greater magnitude is possible.

Paleoclimatic data offer a way to evaluate the severity, duration, and extent of twentieth-century

*NOAA Paleoclimatology Program, NGDC, Boulder, Colorado.

⁺INSTAAR, University of Colorado, Boulder, Colorado.

[#]Department of Geological Sciences, University of Colorado, Boulder, Colorado.

Corresponding author address: Dr. Connie A. Woodhouse, World Data Center for Paleoclimatology, NOAA/NGDC, 325 Broadway, Boulder, CO 80303.

E-mail: woodhouse@ngdc.noaa.gov

In final form 11 September 1998.

©1998 American Meteorological Society

2. Paleoclimatic evidence for Great Plains drought, A.D. 1–1900

A variety of paleoclimatic data sources can each be tapped to provide key insights into Great Plains drought. Taken together, these proxy data offer a much more complete picture of natural drought variability than offered by instrumental data or any one proxy source alone. A summary of proxy paleodrought data sources and their characteristics is given in Table 1.

a. Seventeenth–nineteenth century drought in the Great Plains

Temperature and precipitation records, extending from 1851 to 1890, exist for early meteorological stations and forts in the Great Plains but are quite fragmented and patchy. Data (locations are shown in green on map in Fig. 2) have been analyzed by Mock (1991), who determined that no drought since 1868 has been as severe as that of the 1930s. However, due to

the scarcity of records, he was unable to make a full assessment of a drought in 1860, which may have exceeded the severity of the 1930s drought. Historical accounts from newspapers and diaries provide additional documentation of nineteenth-century drought events. The 1860 drought was reported in Kansas newspapers, which continued to mention the severity of this drought for several decades after the event (Bark 1978). Less severe droughts were also reported in historical documents and early meteorological records for several years around 1860, in the late 1880s, and in the early 1890s (Ludlum 1971; Bradley 1976; Bark 1978). The map in Fig. 2 shows general locations of data sources and drought years documented in historical data, while Fig. 3 (top) shows a time line of these droughts. Accounts of early explorers document periods of blowing sand (an indication of drought conditions) for an area extending from northern Nebraska to southern Texas (Muhs and Holliday 1995). These areas are shown in brown in the map in Fig. 2, along with dates of documented

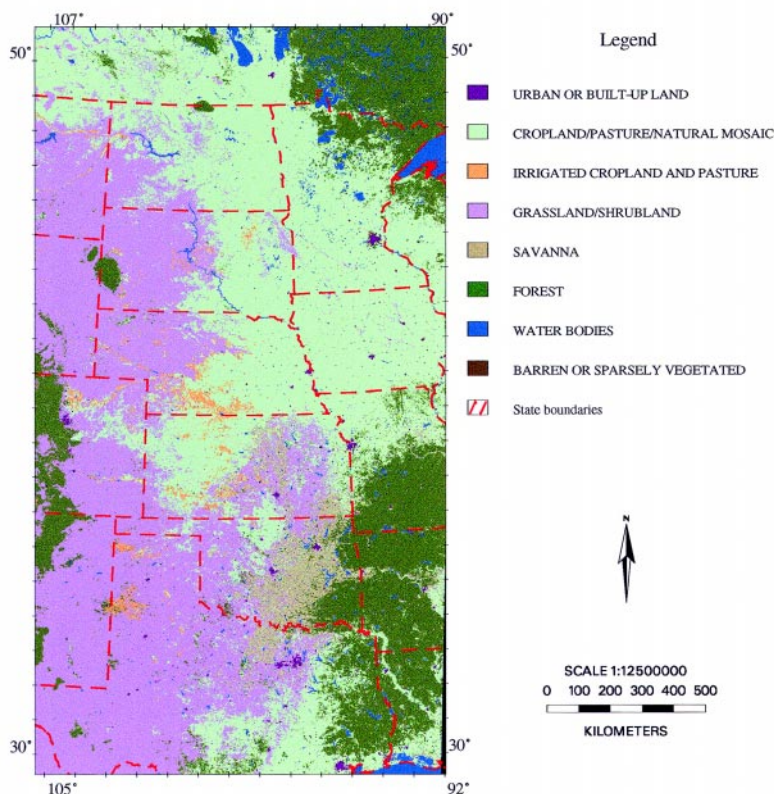


FIG. 1. Advanced Very High Resolution Radiometer Data (AVHRR)-derived 1-km land cover map of the Great Plains (Townshend et al. 1994). Large portions of this area, used for both agriculture and livestock grazing, are highly susceptible to drought.

droughts in the context of the past two millennia (e.g., Overpeck 1996). In this review paper, we bring together evidence of a greater range of drought variability than found in the instrumental record, from all available sources of paleoclimatic data, including historical documents, tree rings, archaeological remains, lake sediment, and geomorphic data, to evaluate the representativeness of twentieth-century droughts in terms of those that have occurred under naturally varying climate conditions of the past several thousand years. The persistence of drought-causing atmospheric conditions is examined through a review of the current literature on twentieth-century droughts, as well as through an examination of whether base-state shifts and low-frequency variation in oceanic/atmospheric systems can yield the persistence needed for the multidecadal- to century-scale droughts of the past. Finally, the prospects of future drought are considered, both in view of the full range of past natural drought variability, and in terms of land use practice and human greenhouse gas-induced climate change.

TABLE 1. Paleodrought data sources and characteristics.

Proxy data source	Continuous record?	Length of records	Resolution	Dating accuracy	Spatial coverage*	Limitations and potential biases
Early instrumental	Not always	Years–decades	Daily–monthly	Day–month	Local	Quality of instruments and collection of data inconsistent
Historical accounts	No	Decades–centuries	Daily–seasonal	Day–season	Local–regional	Observations subject to human perspective
Tree rings	Yes	Centuries–millennia	Seasonal–annual	Year	Local to ~300 km	(a) Dry extremes more reliably represented than wet, (b) quantitative reconstructions limited to “analog” conditions within range of instrumental variations
Lake sediments	Usually	Millennia	Seasonal (varves)–decadal	$\pm 2\%$ – 4% (^{14}C)** $\pm 2\%$ (varves)	Local–regional	(a) Suitable lakes not abundant, (b) analog problem as with tree rings
Alluvial sediments	No	Millennia	Century	$\pm 2\%$ – 5% (^{14}C)	Local	Fluvial response to climate change not well constrained
Eolian sediments	No	Millennia	Century	$\pm 2\%$ – 6% (^{14}C)	Local–regional	Eolian/soil response to climate not well constrained
Flooded trees	No	Millennia	Annual–century	2%–10% (^{14}C) year (dendrochronologically dated)	Local	(a) Little of this type of data available, (b) rising lake levels inferred from tree deaths, (c) timing of lake level drop difficult to estimate
Archaeological data	No	Centuries–millennia	Annual–century	Decade–century (^{14}C) year (dendrochronologically dated)	Local	Climate inferred from human activity

*Spatial coverages listed refer to general spatial representativeness of a single site. Some proxy sources (e.g., tree rings) have been used to reconstruct much broader-scale climatic variability when sufficient networks of sites are available.

**The age models of the original peer-reviewed papers were used, after checking to make sure they were internally and regionally consistent, based on common ^{14}C half-life and converted to calendar years (i.e., Stuiver and Polach 1977; Stuiver and Becker 1986)

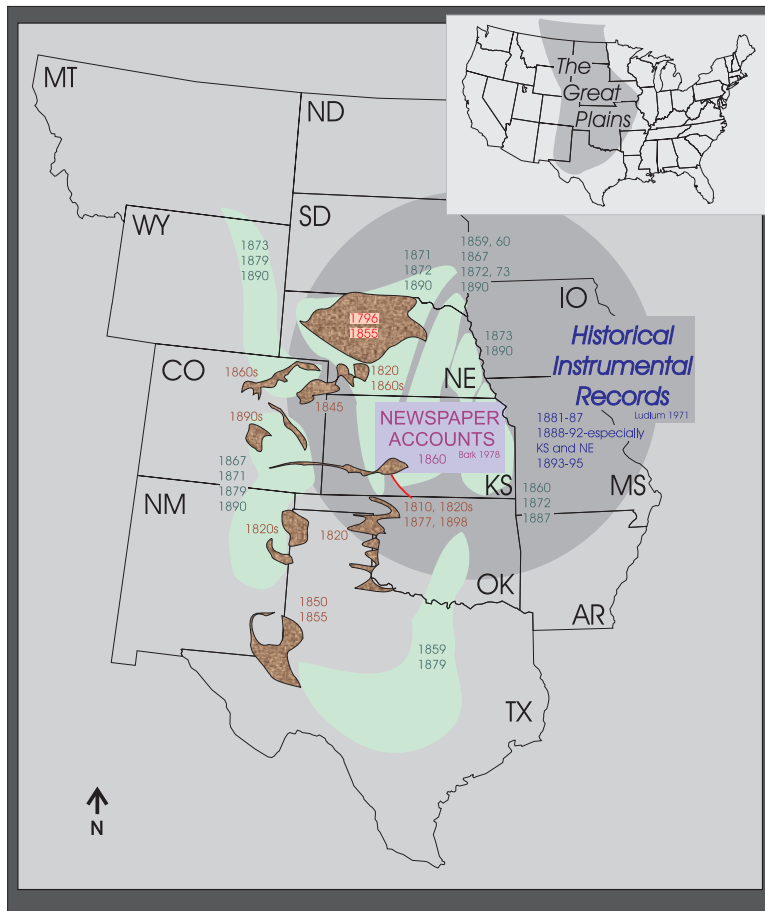


FIG. 2. Locations of sources of historical drought data for the Great Plains, 1795–1895. Green shaded areas represent climate regions based on cluster analysis from Mock’s (1991) analysis of nineteenth-century climate records. The dates (dark green) represent years in which droughts were reported in more than one region for two or more consecutive seasons. Brown areas are regions of sand dunes and eolian activity, accompanied by the years (in red) in which active sand movement was reported (Muhs and Holliday 1995). The gray region represents the general region of early meteorological stations from which Ludlum (1971) derived drought years (in blue). Newspaper accounts are from a variety of newspapers in eastern and central Kansas (Bark 1978).

eolian activity, and on the time line in Fig. 3. Several periods of eolian activity were reported in many areas between 1840 and 1865, with other intervals in the late 1700s and early 1800s, as well as at the end of the nineteenth century (Muhs and Holliday 1995). Interestingly, although some eolian activity was reported in the 1930s and 1950s, these twentieth-century droughts were not severe or long enough to cause regional mobilization of dunes (Muhs and Maat 1993; Madole 1994; Muhs and Holliday 1995).

Numerous reconstructions of precipitation and summer drought have been generated for the Great Plains from tree-ring chronologies located in regions proximal to the Great Plains, shown on the map in

Fig. 4a (Table 2 contains the key for the symbols in this figure). Regression-based tree-ring reconstructions of climate tend to underestimate extreme values, a consequence of the regression techniques used in producing the reconstructions. However, dry extremes are better replicated than wet extremes, and reconstructions of drought extent and duration are reasonably accurate. For example, in Fig. 5, a comparison of observed and reconstructed mapped Palmer Drought Severity Index (PDSI) (Palmer 1965) values for the severe drought years of 1934 and 1956 shows that drought severity is generally about one PDSI value lower (less severe) for the reconstructed values than for the observed values (Cook et al. 1998). However, the spatial extents of the droughts are well replicated by the reconstructed values, as are drought durations of the 1930s and 1950s events. Although the absolute severity is not duplicated in the tree-ring reconstructions, assessments of the relative severity of twentieth-century droughts compared to droughts in previous centuries can still be made. The amount of variance in the observed drought and precipitation series explained by tree-ring chronologies varies, with average values of about 55%, ranging up to 67% (Table 3). These values are good compared to those obtained in dendroclimatic studies in the semiarid to arid western United States, where trees are notably sensitive to climate. The tree-ring records, of course, are unable to explain all of the drought or precipitation variability because tree growth is usually not solely affected by precipitation or drought conditions (Douglass 1914, 1929).

Many of the tree-ring reconstructions suggest that the droughts of the 1930s and 1950s have been equaled or, in some regions, surpassed by droughts in the past several centuries. This is illustrated in the graphs of PDSI reconstructions from Cook et al. (1996) and Cook et al. (1998) for grid points in eastern Montana, central Kansas, and north-central Texas in Fig. 6. Other studies support this finding. Stockton and Meko (1983) reconstructed annual precipitation for four regions flanking the Great Plains (centered in

Iowa, Oklahoma, eastern Wyoming, and eastern Montana). Although they found the individual years of 1934, 1936, and 1939 to be among the driest 10 of 278 years investigated (1700–1977), they found several periods of widespread prolonged drought (3–10 years) that equaled or surpassed the 1930s drought in intensity and duration: the late 1750s, early 1820s, early 1860s and 1890s. Periods of extreme drought revealed by other dendrochronological assessments for the west-central Great Plains coincide with these periods (Weakly 1965; Wedel 1986; Lawson 1970; Lawson and Stockton 1981). Stahle and Cleaveland's (1988) reconstructions of June PSDI in Texas showed the most severe and uninterrupted drought since 1698 was the 1950s drought, but the three driest decades (with some interspersed years of nondrought conditions), by decreasing severity, were 1855–64, 1950–59, and 1772–81. Another dendroclimatic study from the southern plains found prolonged (10 years or more) droughts in Arkansas around 1670, 1765, 1835, 1850, and 1875 that were comparable to twentieth-century events (Stahle et al. 1985), whereas a study in the Texas–Oklahoma–Arkansas region found the drought of the 1950s was exceeded only in 1860 in the last 231 years (Blasing et al. 1988), a particularly noteworthy year in the historical data, as mentioned above. In a reconstruction of precipitation for the corn belt of Iowa and Illinois, no droughts in the past 300 years were found to be appreciably worse than the 1930s drought, but two were of about the same magnitude (late 1880s–1890s and around 1820) (Blasing and Duvick 1984). Reconstructions of precipitation in Iowa (1640–1982) indicated that four 10-yr periods were drier than the period 1931–1940, and in order of decreasing dryness, these were 1816–25, 1696–1705, 1664–73, and 1735–44 (Cleaveland and Duvick 1992). Figure 3 summarizes the timing of droughts in these dendroclimatic studies and illustrates the regional impacts of some of these periods of drought.

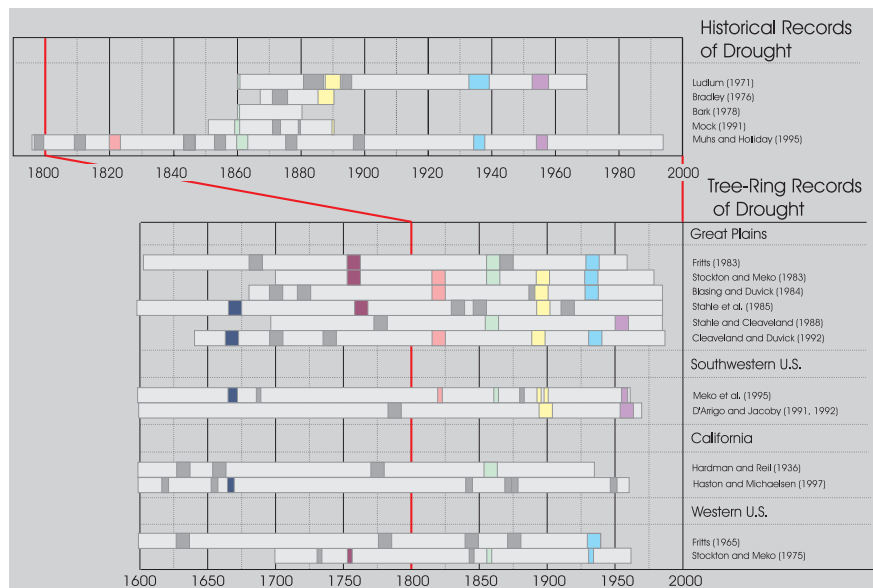


FIG. 3. Paleoclimatic records of Great Plains and western U.S. drought (1600–present) based on historical and tree-ring data. The pale gray horizontal bars reflect the length of the series, and the dark gray and colored bars indicate periods of drought in 3–10-yr increments. Colors mark more widespread droughts that occurred over the same time period in a number of records. The historical droughts are all those reported in the literature. The droughts recorded by tree-ring data are those listed in the literature as the most extreme (e.g., the five most severe 10-yr drought periods in a record). For the few reconstructions that were not accompanied by specific lists of droughts, periods of drought that equaled or exceeded twentieth-century droughts are shown.

The widespread and persistent nature of some of the severe Great Plains droughts of the past three centuries can be compared to twentieth-century droughts using the maps of tree-ring reconstructions of gridded PDSI for the United States (Cook et al. 1996; see maps of other droughts in the past three centuries at the NOAA/NESDIS Web site at <http://www.ngdc.noaa.gov/paleo/drought.html>). For example, Fig. 7 shows that the prolonged drought that centered around 1820 appears to be at least equivalent in extent and duration to the 1950s drought (Cook et al. 1998). The latter part of the 1750s was also a period of prolonged and widespread drought, comparable to those of the twentieth century.

Multiple sources of proxy data, including tree-ring reconstructions and historical records and accounts, work together to confirm the occurrence of several nineteenth-century droughts, as shown in Fig. 6. The 1820s drought is one of several that is documented in the historical accounts of eolian activity (Muhs and Holliday 1995), as well as in tree-ring reconstructions (Lawson and Stockton 1981; Stockton and Meko 1983; Blasing and Duvick 1984; Cleaveland and Duvick 1992; Cook et al. 1998). The drought that oc-

curred about 1860 is notable in much of the historical data [eolian activity, newspapers, and early meteorological records (Ludlum 1971; Bark 1978; Mock 1991;

Muhs and Holliday 1995)] and in drought reconstructions for the central and northern Great Plains (Fritts 1983; Stockton and Meko 1983), as well as in eastern California (Hardman and Reil 1936) and throughout the southwestern and western United States (Stockton and Meko 1975; Meko et al. 1995). While the historical evidence of eolian activity suggests these two nineteenth-century droughts were more severe than twentieth-century droughts, it is not clear from the dendrochronological records that nineteenth-century droughts were indisputably more extreme. Rapid increases in Native American and Euro-American populations as well as bison populations may have led to severe land cover degradation and increased eolian activity between 1820 and 1850 (West 1997). In any case, it is clear that major multiyear Great Plains drought has occurred naturally once or twice a century over the last 400 years.

b. Thirteenth-to-sixteenth-century megadroughts

Prior to the seventeenth century, the availability of high-resolution proxy data for Great Plains drought is reduced, but useful information can still be gleaned from a wide variety of proxy data, including data from other areas of the western United States (Table 1). We include these more distant records because they provide corroborative information for droughts documented in the few available Great Plains records and allow an assessment of the extent of some of these great droughts. Instrumental records indicate that the major droughts impacting the Great Plains in the twentieth century also affected areas of the western United States (see Fig. 5); thus we feel that our use of proxy data from the western United States to support evidence of drought in the Great Plains is justified. There are few tree-ring chronologies for the Great Plains that extend prior to the 1600s, but there are long chronologies for other areas in the western United States that reflect spatially extensive droughts. Other proxy data with a coarser temporal resolution or less accurate temporal control than tree-ring data include those from lake sediment, alluvial, eolian, and archaeological

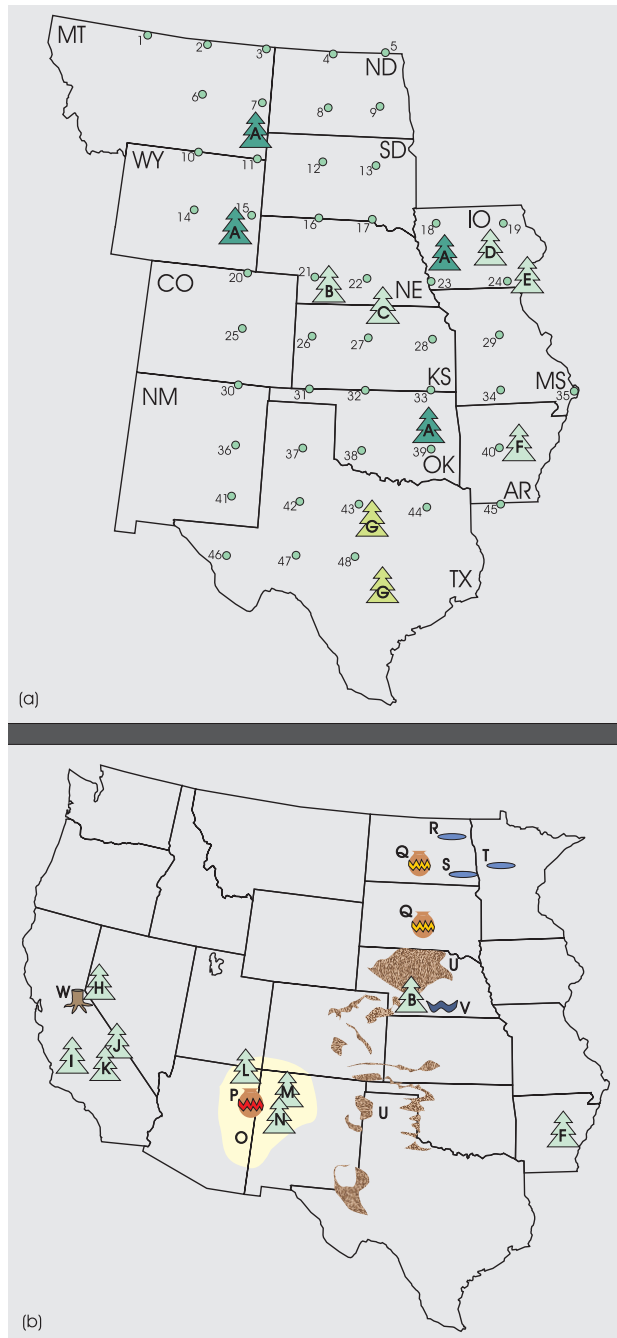


FIG. 4. (a) Locations of drought-sensitive tree-ring chronologies and reconstructions of precipitation or drought in the Great Plains. Numbered dots are locations of Cook et al.'s (1996) gridded PDSI reconstructions. The key for lettered symbols is in Table 2. Statistical relationships (explained variance) between observed and reconstructed series of tree-ring chronologies are listed by author and/or grid number in Table 3. Note that while reconstructions are for regions within the Great Plains, the reconstructions are generated from trees located in areas flanking the Great Plains reconstructions (the exception is Weakly's southwestern Nebraska chronology). Tree growth reflects large-scale climate variations, and thus trees proximal to the Great Plains have been used successfully to reconstruct climate variations in this region. (b) Locations of many of the paleoclimatic records documenting drought in the Great Plains and western United States for the period A.D. 1-1600. The key for lettered symbols is in Table 2.

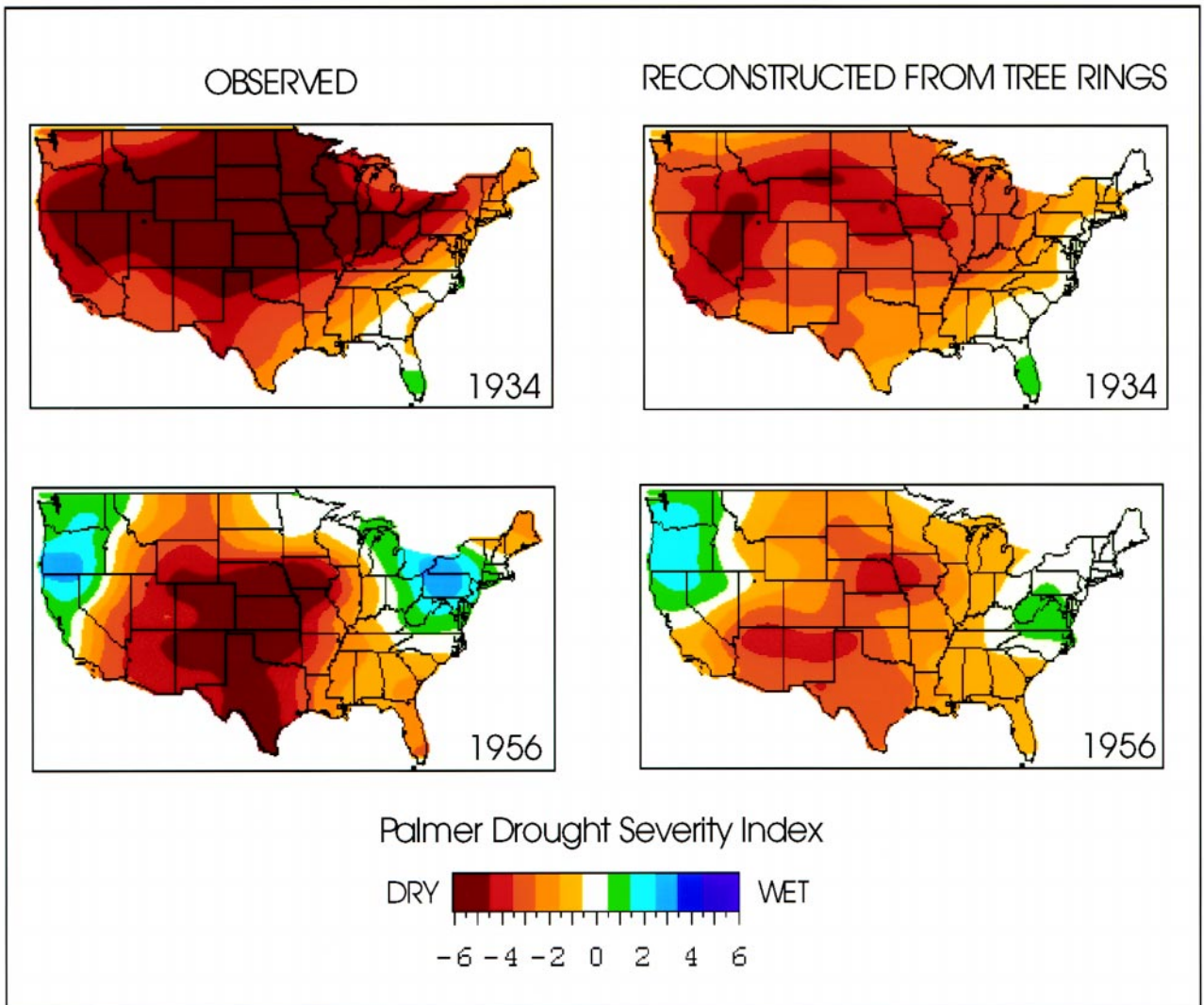


FIG. 5. Comparison of observed and tree-ring reconstructed PDSI values for two of the most extreme drought years in the twentieth century, 1934 and 1956. Although the severity of these droughts is not fully captured by the tree-ring reconstructions, the reconstructions duplicate the spatial extent and duration (see Fig. 6) of these droughts. Images are from the NOAA/NESDIS Web site (see text) (Karl et al. 1990; Guttman 1991; Cook et al. 1996).

sources. These data provide evidence to support the droughts documented in the few available extralong Great Plains tree-ring records, as well as for the period prior to that covered by tree-ring reconstructions. Locations of these proxy records are shown in Fig. 4b and described in Table 2. Thus, although the rapid decline in the number of annually resolved drought records prior to about 1600 makes it difficult to resolve interannual variations in drought frequency and magnitude, paleoclimatic records can provide key constraints on the full range of natural decadal to interdecadal drought variability.

During the thirteenth to sixteenth centuries, there is evidence for two major droughts that likely significantly exceeded the severity, length, and spatial extent

of twentieth-century droughts. The most recent of these “megadroughts” occurred throughout the western United States in the second part of the sixteenth century. The dendrochronological records that reflect this drought and their locations are indicated in Figs. 8 (time line) and 9a (map, key in Table 2). This drought is indicated in a southwestern Nebraska chronology (Weakly 1965) as well as in a reconstruction of Arkansas drought (Stahle et al. 1985). Weakly (Wedel 1986) notes two periods of what he terms “very severe” drought, from 1539 to 1564 and from 1587 to 1605. Stahle et al. (1985) suggest that the period 1549–77 was likely the worst drought in Arkansas in the past 450 years. Other tree-ring reconstructions for the broader western United States reflect this drought,

TABLE 2. Key for map symbols in Figs. 4a, 4b, 9a, and 9b.

Map letter	Reference	Proxy data source	Proxy variable	Location
A	Stockton and Meko (1983)	Tree rings	Precipitation	Four regions flanking Great Plains
B	Weakly (1965)	Tree rings	Precipitation	Southwest NE
C	Fritts (1983)	Tree rings	Precipitation	Central plains
D	Cleaveland and Duvick (1992)	Tree rings	Drought	IA
E	Blasing and Duvick (1984)	Tree rings	Precipitation	Western corn belt
F	Stahle et al. (1985)	Tree rings	Drought	AR
G	Stahle and Cleaveland (1988)	Tree rings	Drought	North and south TX
H	Hardman and Reil (1936)	Tree rings	Flow	Truckee River, CA
I	Haston and Michaelsen (1997)	Tree rings	Precipitation	South CA
J	Hughes and Graumlich (1996)	Tree rings	Precipitation	White Mts./south Great Basin
K	Hughes and Brown (1992)	Tree rings	Drought	Central CA
L	Stockton and Jacoby (1976), Meko et al. 1995	Tree rings	Flow, precipitation	Colorado River, AZ, NM, CO, UT
M	D'Arrigo and Jacoby (1991, 1992)	Tree rings	Precipitation	Northwest NM
N	Grissino-Mayer (1996)	Tree rings	Precipitation	Northwest NM
O	see Dean (1994)	Tree rings	Precipitation	South CO Plateau
P	Euler et al. (1979), Dean et al. (1985), Peterson (1994)	Archaeological remains	Drought	Four Corners area
Q	Lehmer (1970), Wendland (1978)	Archaeological remains	Drought	Missouri Valley
R	Fritz et al. (1991)	Lake sediments	Salinity	Devil's Lake, ND
S	Laird et al. (1996), Laird et al. (1998)	Lake sediments	Salinity	Moon Lake, ND
T	Dean et al. (1994), Dean (1997)	Lake sediments	Aridity	Elk Lake, western MN
U	Muhs and Holliday (1995) and others	Eolian sediments	Drought	Western Great Plains
V	Brice (1966), May (1989), Martin (1992)	Fluvial sediments	Xeric conditions	Southwest NE, north KS
W	Stine (1994)	Flooded stumps	Lake levels	Sierra Nevada, CA

including a number of reconstructions from the Four Corners region (the junction of Arizona, New Mexico, Utah, and Colorado) (Rose et al. 1982; D'Arrigo and Jacoby 1991, 1992; Grissino-Mayer 1996). In their 1000-yr-long reconstruction of winter precipitation D'Arrigo and Jacoby (1991, 1992) found the 1950s drought was surpassed only by a 22-yr drought in the

late 1500s. The reconstruction of Colorado River flow for 1520–1961 shows the period 1579–98 to reflect the longest and most severe drought in this record (Stockton and Jacoby 1976; Meko et al. 1995). In the White Mountains of eastern California, precipitation reconstructed from bristlecone pine shows a moderate drought in the late sixteenth century (Hughes and

TABLE 3. Variance in observed precipitation and drought series explained (r^2) or shared (r) by tree-ring chronologies.

Study	Region	Variable*	Years	Variance explained (r^2) or shared (r)**
Weakly (1965)	Western NE	Annual precipitation at North Platte	1210–1965	$r = 0.63$ (ring widths) $r = 0.75$ (ring area)
Fritts (1983)	Central Great Plains	Annual regional precipitation	1600–1963	$0.20 \leq r^2 < 0.40$
Stockton and Meko (1983)	Eastern MT Eastern WY IA OK	Annual regional precipitation	1700–1977	$r^2 = 0.52$ $r^2_{adj} = 0.54$ $r^2_{adj} = 0.44$ $r^2_{adj} = 0.40$
Blasing and Duvick (1984)	IA, IL	Annual regional precipitation	1680–1980	$r^2 = 0.62$
Stahle et al. (1985)	AK	June PDSI	1531–1980	$r^2_{adj} = 0.40$
Stahle and Cleaveland (1988)	North TX South TX	June PDSI	1698–1980	$r^2_{adj} = 0.59$ $r^2_{adj} = 0.60$
Cleaveland and Duvick (1992)	IA	July PDHI	1640–1982	$r^2_{adj} = 0.67$
Cook et al. (1996)	United States (Great Plains gridpoint results reported here; see Fig. 5a for locations)	Summer PDSI	1700–1979	
	Grid points 34, 35, 47		$r^2 \geq 0.60$	
	6, 7, 10, 11, 19, 24, 25, 29, 33, 39, 40, 42, 43, 44, 46, 48			$0.50 \leq r < 0.60$
	1, 2, 3, 14, 15, 18, 20, 22, 23, 26, 27, 28, 30, 32, 36, 38, 41			$0.40 \leq r^2 < 0.60$
	8, 9, 12, 13, 16, 17, 21, 31, 37, 45			$0.30 \leq r^2 < 0.40$
	4,5		$r^2 < 0.30$	

*PDSI: Palmer Drought Severity Index; PHDI: Palmer Hydrological Drought Index (Palmer 1965),

**The use of r^2 or r^2_{adj} depends on how results were reported in specified studies.

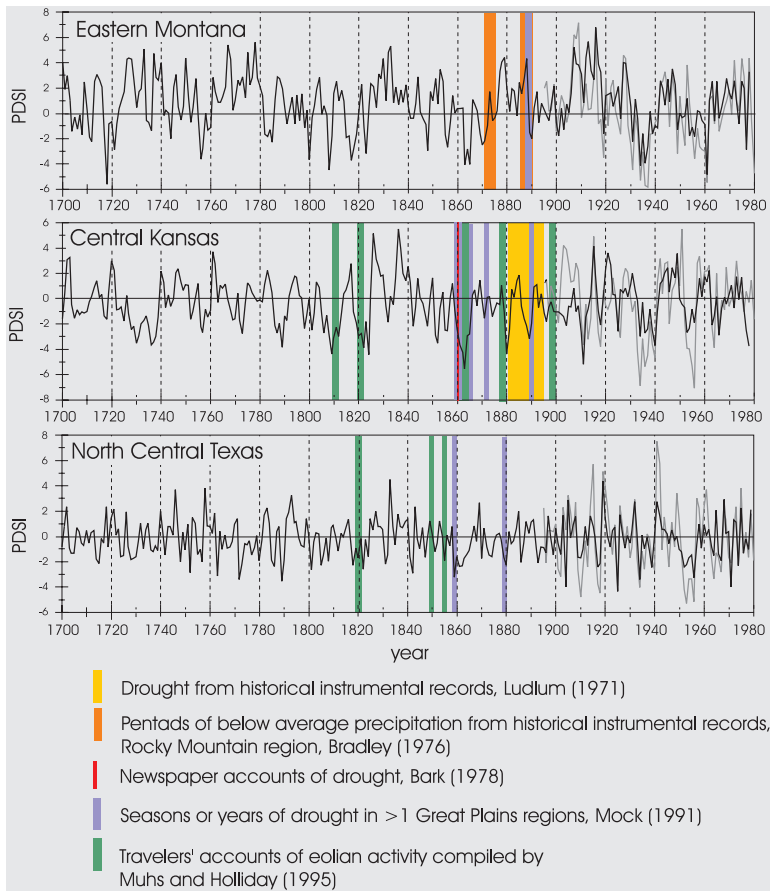


FIG. 6. Palmer Drought Severity Index records (1700–1979) for eastern Montana (grid point 7 in Fig. 4a) (top), central Kansas (grid point 27) (middle), and north-central Texas (grid point 42) (bottom), as reconstructed using tree-ring data [Cook et al. 1996; see also the NOAA/NESDIS Web site (see text)]. Also shown are the observed PDSI values for grid points (light gray lines). The colored vertical bars indicate years of drought from historical accounts.

Graumlich 1996). A flow reconstruction for the Truckee River in eastern California reflects this sixteenth-century drought (Hardman and Reil 1936), as do reconstructions of precipitation for northern and southern regions of California west of the Sierra Nevada (Haston and Michaelsen 1997). Additionally, reconstructions of western U.S. regional precipitation indicate a drought beginning in the southwest around 1565 and spreading to the entire western United States by 1585 (Fritts 1965), corresponding to drought evidence in both lake sediment data from western Minnesota (Dean et al. 1994) and scarcity of old, living conifers established before about 1600 in the southwest (Swetnam and Betancourt 1998). Recent analysis of eolian sedimentation dates in the Wray dune field of eastern Colorado by Muhs et al. (1997) estimate the most recent period of eolian activity to have occurred in the past ~400 years (^{14}C yr before present),

while Stokes and Swinehart (1997) document an optically dated period of eolian activity in the Nebraska Sand Hills that also coincides with the late sixteenth-century drought. Eolian activity is primarily due to drought severe enough to remove vegetation (Muhs and Holliday 1995), and the late 1500s drought was likely severe and long enough to have cleared sand deposits of live vegetation.

The other megadrought of the thirteenth to sixteenth centuries occurred in the last quarter of the thirteenth century. The time line in Fig. 8 shows the tree-ring records that reflect this drought, while Fig. 10 shows the proxy records that reflect this drought in a coarser temporal context (locations of the proxy records are shown in Fig. 9b, key in Table 2). Most of the proxy records mentioned for the sixteenth-century drought that extend back to the thirteenth century also record this severe multi-decadal drought, including tree-ring chronologies and/or reconstructions for southwestern Nebraska (Weakly 1965), northern New Mexico (Grissino-Mayer 1996), the Four Corners area (Rose et al. 1982), and the White Mountains (Hughes and Graumlich 1996). Weakly (1965) reported a 38-yr drought from 1276 to 1313 in his southwestern Nebraska tree-ring chronology, the

longest drought in the past 750 years. Other less finely resolved proxy data also testify to the occurrence of this drought, which in some areas appears to have rivaled or exceeded even the sixteenth-century drought and was almost certainly of much greater intensity and duration than any drought of the twentieth century. Recent analysis of eolian sediments in the Nebraska Sand Hills suggests an onset of eolian activity beginning within the past 800 ^{14}C years (Muhs et al. 1997). A period of drought at this time is documented in the varve record of western Minnesota (Dean et al. 1994). Archaeological data from the Great Plains and Four Corners areas also provide documentation of this drought (Bryson et al. 1970; Lehmer 1970; Wendland 1978; Euler et al. 1979; Dean et al. 1985; Dean 1994; Peterson 1994). In the Southwest this drought, sometimes referred to as the “Great Drought,” coincided with the abandonment of Anasazi settlements, redis-

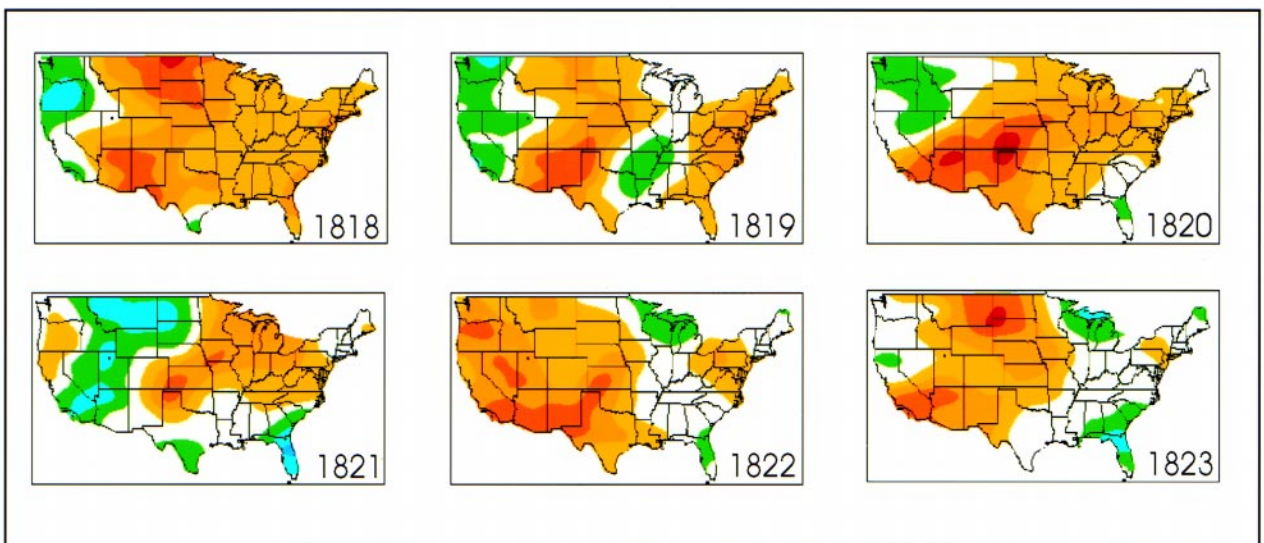
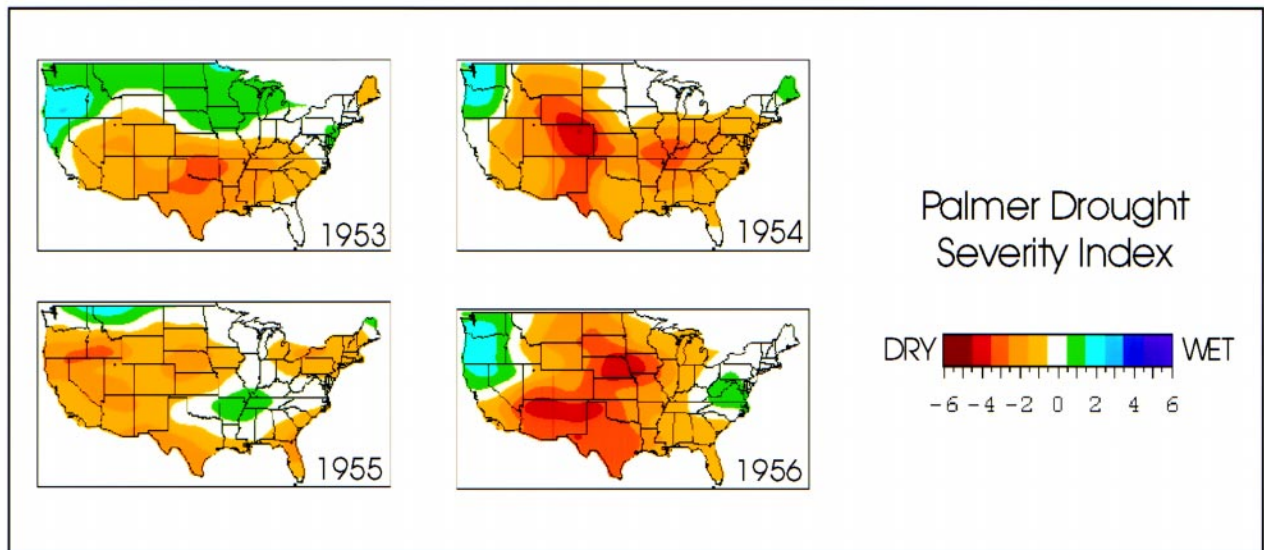


Fig. 7. Comparison of duration and extent of two severe droughts, the 1950s drought (top) and the drought centered on 1820 (bottom), both reconstructed from tree-ring chronologies (Cook et al. 1996; Cook et al. 1998).

tribution of populations, and widespread societal reorganization (Douglass 1935; Dean 1994). This period of drought is also reflected in unprecedentedly low lake levels as reconstructed through the dating of tree stumps rooted in what are today bottoms of several streams and lakes in the Sierra Nevada of eastern California (Stine 1994).

Several tree-ring reconstructions allow a temporal evaluation of the thirteenth and sixteenth-century megadroughts relative to more recent droughts (Dean 1994; Grissino-Mayer 1996; Hughes and Graumlich 1996). Of the reconstructions that reflect both sixteenth- and thirteenth-century droughts, the sixteenth-century drought appears to have been the most severe and per-

sistent drought in the Southwest in the past 1000–2000 years, whereas the thirteenth-century drought was the most persistent and severe drought in the California mountain ranges and, likely, the Great Plains (Weakly 1965). It is more difficult to evaluate the spatial extent of the two major paleodroughts. At a minimum, both droughts appear to have impacted the Great Plains, Southwest, southern and western Great Basin, and Sierra Nevada (Figs. 9a,b). A survey of other tree-ring chronologies for the northwestern Great Basin and northeastern Utah (from the International Tree-Ring Data Base, World Data Center-A, Paleoclimatology, Boulder, Colorado) shows marked periods of low growth in the latter part of the thirteenth century in

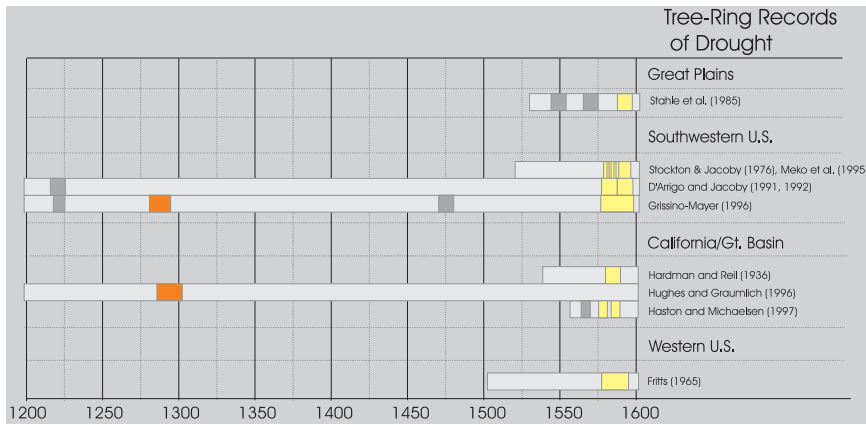


FIG. 8. Paleoclimatic records of Great Plains and western U.S. drought (thirteenth century through the sixteenth century) based on tree-ring data. As in Fig. 3, the pale gray horizontal bars reflect the length of the series, and the dark gray and colored bars indicate periods of drought. Yellow bars mark records that reflect the late fifteenth-century drought, while orange bars mark records that reflect the late thirteenth-century drought.

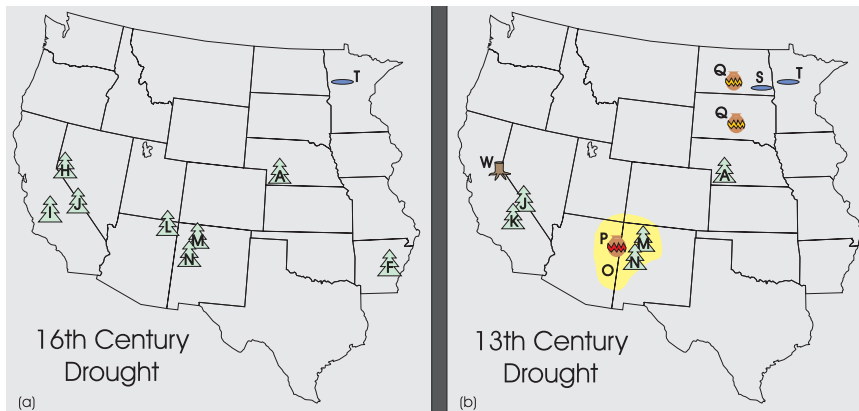


FIG. 9. (a) Location of paleoclimatic records that document the late sixteenth-century drought. Proxy data reflect the widespread nature of this drought, which was especially notable in the Southwest but also detected in records from areas ranging from the northeastern and southeastern Great Plains to the California coast. Most proxy records indicate the duration of this drought was close to 20 yr. (b) Location of paleoclimatic records that document the late thirteenth-century drought. Fewer proxy records are available for this drought, but most that do exist for this period reflect drought that was at least 25 yr in duration and that appears to have ranged from the northern Great Plains, through the Southwest, and to the southern end of the Sierra Nevada. The key for the lettered symbols is in Table 2.

these areas as well. For comparison, severe drought conditions in 1934 (see Fig. 5) also covered most of these areas, but the 1934 conditions were part of a drought that lasted only several years, as opposed to decades (Karl et al. 1990; Guttman 1991; Cook et al. 1996).

c. Evidence for drought, A.D. 1–1200

The temporal resolution and interpretation of most proxy data for the period A.D. 1–1200 make it difficult

to assess droughts of this period in the same way as more recent droughts. Many of the proxy records that exist for this period extend back several millennia or more. Because of their great length, even proxy records with annual resolution are typically analyzed in terms of multidecadal- to century-scale variations. Consequently, our assessment of drought within this time frame focuses on low-frequency (decade to century scale) drought variability relative to the twentieth century. However, even given this low-frequency perspective, proxy records suggest that droughts of the period A.D. 1–1200 occurred on a scale that has not been duplicated since Europeans came to the Great Plains.

At least four periods of widespread drought between A.D. 1 and 1200 are found in a variety of proxy data from the Great Plains and the western United States as illustrated in Fig. 10. Of these four, the most recent is the least well documented. A limited number of proxy records suggest that a drought began around mid A.D. 1100, although it is difficult to separate this drought from the late thirteenth-century drought in some of the less finely resolved records. This drought is suggested in the Southwestern archaeological data as a forerunner to the more severe late 1200s drought (Euler

et al. 1979; Dean et al. 1985) and is also documented in White Mountains and Four Corners tree-ring records (LaMarche 1974; Rose et al. 1982), in a preliminary Colorado Front Range tree-ring chronology (P. Brown 1997, personal communication), and in western Minnesota lake sediments (Dean et al. 1994; Dean 1997). Archeological and pollen data have also been cited as evidence for an onset of markedly drier conditions in the northern Great Plains about this time

(Lehmer 1970; Wendland 1978), and in northwestern Iowa after about A.D. 1100 and intensifying by A.D. 1200 (Bryson and Murray 1977). The next major drought is characterized primarily by an onset of eolian activity in the western Great Plains. It is difficult to determine the exact date of onset, but activity began sometime after ~A.D. 950 (Forman et al. 1992; Forman et al. 1995; Madole 1994, 1995; Muhs et al. 1996). Other proxy data that help confirm this period of drought are those from North Dakota lake sediments (Laird et al. 1996; Laird et al. 1998) and alluvial sediment records from western Nebraska and Kansas (Brice 1966; May 1989; Martin 1992). Although there is dendroclimatic and lake-level evidence of drought in the Sierra Nevada and White Mountains between ~A.D. 900 and 1100, (LaMarche 1974; Stine 1994; Hughes and Graumlich 1996), there is no evidence of an onset of drought conditions occurring in the Southwest at this time.

The third major drought episode of the A.D. 1–1200 period occurred roughly between A.D. 700 and 900. In archaeological evidence in the Four Corners area, A.D. 750 was the starting date for a drought that lasted several centuries (Euler et al. 1979; Dean et al. 1985; Peterson 1994), and a tree-ring reconstruction of drought for New Mexico also reflects this drought (Grissino-Mayer 1996). Drought is recorded in western Minnesota lake varves at this time (Dean et al. 1994; Dean 1997) while North Dakota lake sediments indicate drought conditions typified the period A.D. 700–850 (Fig. 11; Laird et al. 1996; Laird et al. 1998). In another more coarsely resolved record of lake sediments in North Dakota, high salinity conditions are indicated to have begun about this time and continued through the fifteenth century, a period containing the droughts of the tenth, twelfth, and late thirteenth centuries (Fritz et al. 1991). In the central California drought record from giant sequoia, the

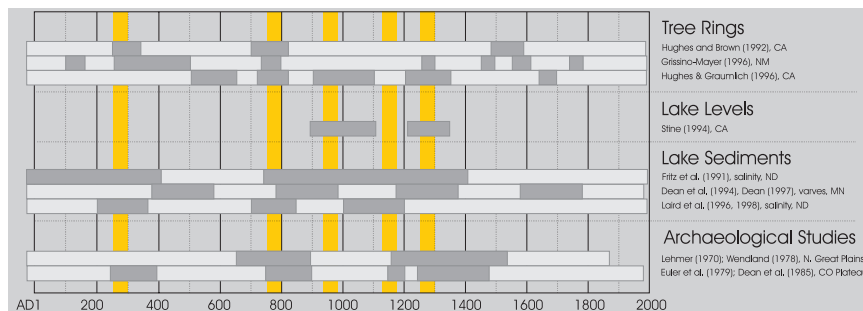


FIG. 10. Paleoclimatic records of Great Plains and western U.S. century-scale drought, A.D. 1–present, as recorded in a variety of paleoclimatic data. The pale gray horizontal bars reflect the length of the series, and the dark gray indicate periods of drought. Orange vertical bars represent multidecadal droughts that appear to have been widespread.

period A.D. 699–823 had the highest drought frequency in the past 2000 years (Hughes and Brown 1992). Drought appears to have occurred in the White Mountains about this time as well (Hughes and Graumlich 1996). The onset of the earliest of these four droughts occurred about the middle of the third century and appears to have lasted up to three centuries. A dendroclimatic reconstruction of precipitation for northern New Mexico (Grissino-Mayer 1996) shows this to be a period of consistently average to below-average precipitation until about A.D. 500. Drought-sensitive giant sequoia in central California suggest that the period A.D. 236–377 was one of the three periods with the highest frequency of drought within the past two millennia (Hughes and Brown 1992). During the closely corresponding period, A.D. 200–370, more frequent drought conditions were indicated by high lake salinity in North Dakota lake sediments (Laird et al. 1996; Laird et al. 1998). Archaeological remains in

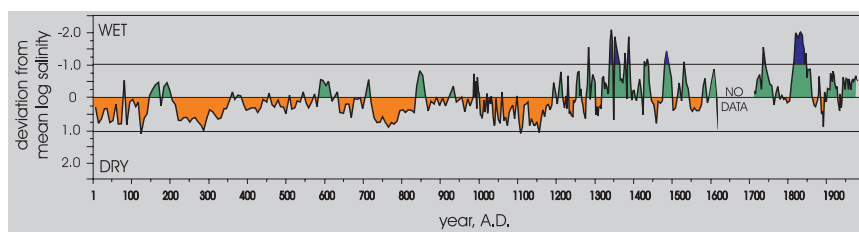


FIG. 11. North Dakota Moon Lake salinity record, here spanning A.D. 1–1980 (Laird et al. 1996). Deviations from the mean (based on past 2300 yr) log salinity values are shown with negative values indicating low salinity and wet conditions and positive values indicating high salinity and dry conditions. Note the shift in salinity values around A.D. 1200, likely reflecting a change in drought regime from more frequent, intense droughts prior to A.D. 1200 to relatively wetter conditions in the last 750 yr. The average temporal resolution of the chronology is about one sample per five years, with an estimated error in the absolute chronology of ± 50 –60 yr. The 92-yr gap in the data from 1618 to 1710 is due to desiccation in this section of the core.

the Four Corners (Euler et al. 1979; Dean et al. 1985) indicate drought conditions from A.D. 250 to 400.

3. The paleoclimatic perspective: A summary

Paleoclimatic data provide evidence that twentieth-century droughts are not representative of the full range of drought variability that has occurred over the last 2000 years. The collection of dendroclimatic reconstructions for the Great Plains region suggests that the severe droughts of the twentieth century, although certainly major in terms of their societal and economic impacts, are by no means unprecedented in the past four centuries. Moreover, when all proxy data, including historical accounts of eolian activity, are considered, it is likely that droughts of a magnitude at least equal to those of the 1930s and 1950s have occurred with some regularity over the past 400 years. A look farther back in time reveals evidence that the multidecadal drought events of the late thirteenth and/or sixteenth centuries were of a much greater duration and severity than twentieth-century droughts. Interestingly, in the interval between these two big droughts, there is little evidence of severe and/or widespread drought.

Laird et al. (1996) and Laird et al. (1998) suggest that their North Dakota lake sediment data reflect a drought regime shift occurring around A.D. 1200, with droughts prior to this time characterized by much greater intensity and frequency (Fig. 11). Although the type of proxy data that extend back several thousand years tend to have a decadal- to century-scale temporal resolution and dating accuracy that confounds close comparisons, the few annually resolved paleoclimatic records that do exist for this period provide some evidence for longer periods of drought or periods of more frequent drought prior to the thirteenth century (LaMarche 1974; Dean 1994; Grissino-Mayer 1996; Hughes and Graumlich 1996). Several tree-ring records and reconstructions for the Southwest and the White Mountains/Great Basin region support the idea of a major drought regime shift after the late thirteenth-century drought. The timing is somewhat later than suggested by Laird et al. (1996) and Laird et al. (1998), but the difference may be due to the greater precision in dendrochronological dating compared to radiocarbon dating. For the most part, these longer records have been analyzed in terms of low-frequency variations, but twentieth-century variations can still be

evaluated in the context of the previous 2000 years. Dendroclimatic evidence suggests that many droughts prior to the late thirteenth-century drought were at least decades in duration. In contrast, the droughts since the thirteenth-century event apparently have tended to be a decade or less in duration, with the exception of the late sixteenth-century multidecadal drought in the Southwest. The North Dakota lake sediment record along with these tree-ring records from the Southwest, the Great Basin, and the White Mountains suggest that a drought regime shift may have occurred not only in the Great Plains, but over much of the western United States as well. The evidence for a drought regime shift around 700 years ago is intriguing, but more investigations incorporating millennium-length records of highly resolved, precisely dated paleoclimatic data are needed to confirm and understand the full nature and extent of this event.

An assessment of the available proxy data suggests that droughts of the twentieth century have been characterized by moderate severity and comparatively short duration, relative to the full range of past drought variability. This indicates the possibility that future droughts may be of a much greater severity and duration than what we have yet experienced. It is imperative to understand what caused the great droughts of the past 2000 years and if similar droughts are likely to occur in the future.

4. The causes of Great Plains drought

An inquiry into the mechanisms behind Great Plains drought begins with an examination of precipitation climatology and the atmospheric conditions associated with twentieth-century drought. The semiarid to subhumid climate of the Great Plains is influenced by several different air masses, each with spatially and seasonally varying impacts on the region: dry westerly flow of air from the Pacific; the cold, dry arctic air masses from the north; and the warm, moist tropical air masses from the south (Bryson 1966; Bryson and Hare 1974). The polar jet stream brings Pacific moisture to the area in the cool season, but the region is generally quite dry in winter (Doesken and Stanton 1992). In summer, although the central Great Plains is under the drying influence of a strong subtropical ridge, moisture is drawn into the area from the Gulf of Mexico by the Great Plains nocturnal low-level jet (LLJ). The LLJ is a synoptic-scale feature associated with convective storm activity and represents the in-

trusion of the Atlantic anticyclonic subtropical gyre (associated with the Bermuda high) into the interior United States (Tang and Reiter 1984; Helfand and Schubert 1995; Higgins et al. 1997). Another source of summer precipitation is mesoscale convective complexes (MCCs), which can contribute between 30% and 70% of the total warm season precipitation over much of the Great Plains (Fritsch et al. 1986). Less consistently, synoptic-scale upper-level disturbances also contribute summertime moisture (Helfand and Schubert 1995; Mock 1996). In spring, the mixing of cold air masses from the Arctic with warm, moist air tropical masses from the Gulf of Mexico causes an increase in precipitation (Bryson 1966). During this season, meridional troughs and cutoff lows in midlatitude frontal systems draw moisture from the Gulf of Mexico into the western Great Plains (Hirschboeck 1991). Fall is a relatively dry season as Pacific air dominates most of the region (Bryson 1966; Mock 1996).

Drought in the Great Plains can occur during any season, but since late spring and summer are the seasons when most of the precipitation falls, these are the most important drought seasons. In general, Great Plains drought is characterized by a semipermanent mid- to upper-tropospheric anticyclone over the plains, sustained by anticyclones in both the eastern central Pacific and eastern central Atlantic and accompanied by intervening troughs (Namias 1955, 1983) that can persist throughout the summer. Under this configuration, the jet stream is diverted to the north and the plains anticyclone blocks moisture from the Gulf (Borchert 1950). The Great Plains region is commonly not homogeneous with respect to drought because of the spatially variable influence of the circulation features related to seasonal precipitation (Karl and Koscielny 1982). Figure 12 illustrates this by showing the spatial distribution of PDSI values for three different twentieth-century drought years and accompanying PDSI time series for three

different regions. The position of the semipermanent ridge of high pressure appears to be particularly important. At times when the ridge is displaced east of its usual position over the west-central United States, Gulf of Mexico moisture is unable to penetrate into the central United States (Oglesby 1991), but there appear to be varying degrees of displacement. The 1950s drought was most severe in the southern Great Plains, suggesting a complete failure of Gulf of Mexico moisture to enter the central United States (Borchert 1971). In contrast, the 1988 drought was characterized by an inverted U shape, in which drought was largely restricted to the northern Plains as well as the west coast and southeastern United States, while Gulf moisture was able to find a way into the south-central United States (Oglesby 1991) (Fig. 12). Once a drought-inducing circulation pattern is set up, dry conditions can be perpetuated or amplified by persistent recurrent subsidence leading to heat waves, clear skies, and soil moisture deficits (Charney 1975; Namias 1983; Oglesby and Erickson 1989).

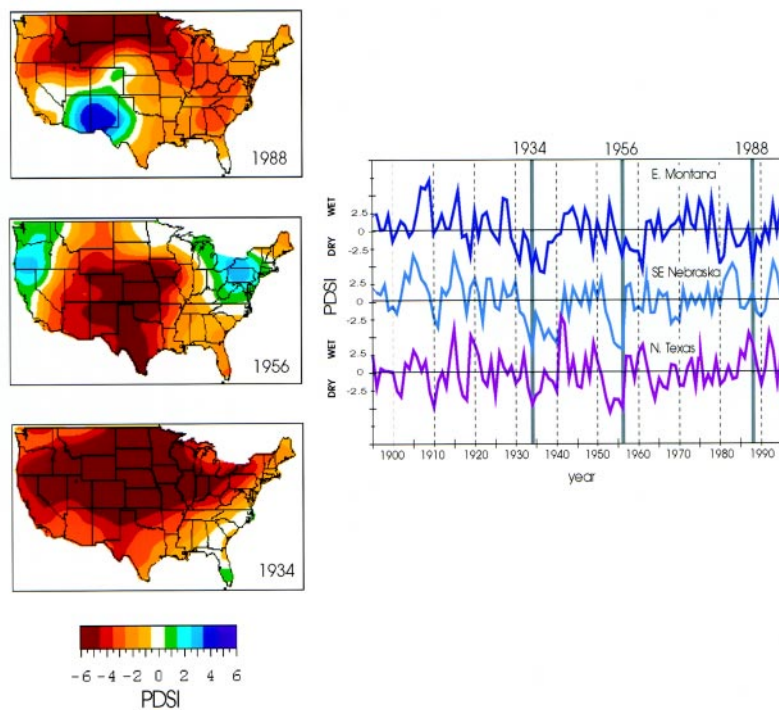


FIG. 12. Spatial distribution of observed PDSI values for three severe twentieth-century drought years (1988, 1956, 1934) (left) and time series of observed PDSI for three grid points in the Great Plains, 1900–94 (right). Gray vertical bars in the time series mark the drought years mapped. This set of maps shows that although PDSI values are low for all three grid points in 1934, in 1956 drought was more severe in the central and southern Great Plains, whereas in 1988, drought is only reflected in the Montana time series, and on the map, across the northern Great Plains [Karl et al. 1990; Guttman 1991; Cook et al. 1996; see also the NOAA/NESDIS Web site (URL given in text)].

What sets up these drought-producing atmospheric circulation patterns, and what drives the variability that leads to the spatial distribution of drought in the Great Plains? There is strong evidence that the state of the oceans, both Pacific and Atlantic, can lead to drought conditions in the Great Plains, directly or indirectly, by inducing perturbations in patterns of atmospheric circulation and the transport of moisture (Trenberth et al. 1988; Palmer and Branković 1989; Trenberth and Guillemot 1996; Ting and Wang 1997). The position of the ridge of high pressure over the plains has been found to be associated with the strength and position of the surface Bermuda high (also called the Atlantic subtropical high) over the Atlantic, which is also linked to the strength of the LLJ (Helfand and Schubert 1995). When this Bermuda high is in a position farther east and north than normal, moist air flows around the high and into the eastern coast, while the Great Plains remains dry. In its usual position, farther south and west, the moist Gulf of Mexico air moves around the high and into the central United States (Forman et al. 1995). The position of this high is likely related to sea surface temperatures (SSTs) in the Gulf of Mexico (Oglesby 1991).

Conditions in the Pacific also influence Great Plains drought-associated circulation patterns. A number of studies have linked conditions in both the equatorial Pacific [El Niño–Southern Oscillation (ENSO)-related conditions] and the northern Pacific to spring and summer precipitation variability in the Great Plains (Trenberth et al. 1988; Kiladis and Diaz 1989; Palmer and Branković 1989; Bunkers et al. 1996; Phillips et al. 1996; Ting and Wang 1997). SSTs in the equatorial Pacific appear to have more influence on summer drought conditions in the northern Great Plains, whereas northern Pacific SSTs are more closely linked to conditions in the central and southern Great Plains (Ting and Wang 1997). The two modes of SST (i.e., the patterns of covariance between SST and precipitation in the two regions) operate independently for the most part and can compound or cancel out one another's impacts on precipitation in the Great Plains. For instance, in 1988, SSTs from both areas contributed to drought conditions, whereas in 1987, modes were in opposition, and precipitation was near normal throughout the Great Plains. The interplay between conditions in the tropical and northern Pacific have been linked to decadal-scale PDSI variability in areas of the United States that include the Great Plains (Cole and Cook 1998). Although Pacific SSTs are not directly linked to the transport

of Pacific moisture into the Great Plains, they apparently cause changes in circulation patterns, which, in turn, influence the transport of Gulf of Mexico moisture into the region and the position of the jet stream (Ting and Wang 1997). The position of the jet is associated with the locations of surface fronts and cyclogenesis (Barry and Chorley 1987).

Persistence of drought-producing conditions is a key feature of drought (Namias 1983). The causes of persistent drought-producing conditions on the timescales of months to a season are fairly well understood, but the causes of droughts with durations of years (e.g., 1930s) to decades or centuries (i.e., paleodroughts) are not well understood. Twentieth-century droughts have occurred on subdecadal timescales and persistence related to these droughts has been attributed to anomalous circulation patterns supported by low soil moisture, strong surface heating, and large-scale subsidence (Namias 1983). These synoptic-scale to mesoscale patterns are also maintained by variability in modes of seasonally related large-scale atmospheric circulation (Diaz 1986; Barnston and Livezey 1987; Diaz 1991).

A principal difference between major droughts of the twentieth century and major droughts of the more distant past is the duration, which is on the order of seasons to years compared to decades to centuries. What caused persistence of drought conditions on these timescales? A number of mechanisms may be influencing persistence on decadal timescales. One possible cause of long-term persistence may be related to persistent anomalous boundary conditions influenced by low-frequency variations in the thermal characteristics of oceans (Namias 1983). There is evidence that variations in large-scale patterns of atmospheric circulation and atmosphere–ocean interactions that impact regional precipitation occur on the order of decades to centuries. A recent example of decadal-scale variation is the change in conditions in the North Pacific atmosphere and ocean beginning in the mid-1970s, which impacted climate conditions across the United States (Miller et al. 1994; Trenberth and Hurrell 1994). In the Atlantic Ocean, decadal-scale variations in the Northern Atlantic oscillation (NAO) have been detected and linked to climatic conditions in Europe and the Mediterranean (Hurrell 1995). Other less well investigated twentieth-century decadal shifts in atmospheric circulation patterns have been characterized by changes in zonal versus meridional circulation over North America (Dzerdzeevskii 1969; Granger 1984). Another possibly important source of

decadal-scale precipitation variability is the ~20 yr solar–lunar cycle. This cycle has been investigated for years by many researchers (e.g., Mitchell et al. 1979; Stockton et al. 1983; Currie 1981, 1984a,b; Cook et al. 1997) and is a feature that is increasingly being discussed as a control on drought occurrence in the western United States, although the physical link between these cycles, atmospheric circulation, and solar–lunar variability has not yet been determined. A number of proxy records reflect oscillations at the wavelength of these cycles, including tree-ring width chronologies for the western United States (Cook et al. 1997), salinity in North Dakota lake sediments (Laird et al. 1998), and varve thickness records in western Minnesota (Anderson 1992).

At longer timescales, low-frequency variability in ocean SSTs and ocean–atmosphere interactions is a likely source of persistent Great Plains drought conditions in the past. Research has shown changes in the conditions in oceans, such as occurred recently in the North Pacific Ocean, are manifested in long-term climate and proxy records that suggest low-frequency variations have occurred in both Pacific and Atlantic Oceans (e.g., Michaelsen 1989; Duplessey et al. 1992; Rasmussen et al. 1995; Jennings and Weiner 1996; Keigwin 1996). Tree-ring chronologies from the southwestern United States that are sensitive to variations in ENSO reveal a tendency toward low-frequency variations in ENSO events on century scales (Michaelsen 1989). It is known that ENSO events are linked to precipitation in the Great Plains on an event basis (Trenberth et al. 1988; Kiladis and Diaz 1989; Palmer and Branković 1989; Bunkers et al. 1996; Phillips et al. 1996; Ting and Wang 1997), and Rasmussen et al. (1995) suggest that variations in ENSO intensity at the century timescale may broadly correspond to a modulation of interdecadal variations in drought in the Great Plains, with more severe drought epochs (i.e., 1930s–1950s) coinciding with intervals of low ENSO variability. At present, it is not known whether decadal- to century-scale ENSO variability is due to internal variability or external mechanisms, or a combination of both. Currently, there are no good long centuries-long records of North Pacific variability.

Variations in the base state of the Atlantic Ocean may be an important influence on Great Plains precipitation if these variations change the position of the Bermuda high/Atlantic gyre or affect in other ways the ability of Gulf of Mexico moisture to penetrate into the interior United States. For example, Forman et al.

(1995) suggested that dune reactivation about 1000 years before present was due to a small easterly shift of the Bermuda high from its usual position in combination with a slight eastward shift of a western-central U.S. ridge aloft, a set of conditions that leads to drought today. There are several sources of proxy data in the North Atlantic Ocean that suggest low-frequency changes in the conditions of this ocean have occurred. A 1300-yr-long record of changes in the East Greenland Current from sediment cores on the coast of eastern Greenland shows a cold interval beginning around A.D. 1270 and peaking around 1370 (Jennings and Weiner 1996), which roughly coincides with the western U.S. drought of the late thirteenth century. However, another cold period in this North Atlantic record spanned the mid–sixteenth century to the early twentieth century, a period not notable for drought in the Great Plains (in fact, the early part of this period was characterized by a lack of drought). In the Sargasso Sea, century-scale variations in SSTs are reflected in $\delta^{18}\text{O}$ changes in planktonic foraminifera from marine sediments (Keigwin 1996). Temperatures yielded from this record indicate oscillations from a minimum in A.D. 250–450, to a maximum in A.D. 950–1050, to another minimum in A.D. 1500–1650. All three of these periods correspond to periods of Great Plains drought. Although periods of major Great Plains drought appear to correspond to extremes in the SST record of either sign, perhaps an Atlantic–drought link is related to periods of anomalous conditions or periods of significant change in SST. It is also likely that the effects of anomalous conditions in the Atlantic on Great Plains drought may interact with the impacts of conditions in the Pacific in ways that may enhance or diminish drought conditions.

5. Droughts of the future

A review of the available paleoclimatic data indicates that twentieth-century droughts do not represent the full range of potential drought variability given a climate like that of today. In assessing the possible magnitude of future drought, it is necessary to consider this full range of drought. It is possible that the conditions that lead to severe droughts, such as those of the late sixteenth century, could recur in the future, leading to a natural disaster of a dimension unprecedented in the twentieth century. Two factors may further compound the susceptibility of the Great Plains to drought in the future: 1) increased vulnerability due to human

land use practices, and 2) enhanced likelihood of drought due to global warming.

As the limits of productive agricultural lands have been reached, more marginally arable lands have been put into agricultural production in times of favorable climatic conditions and through the use of irrigation. This practice has resulted in an increasing vulnerability to drought in many areas of the Great Plains (Lockeretz 1978; Barr 1981; Hecht 1983). Although the total acreage of irrigated land is not great, irrigation has been an important factor in the increase in cultivated acreage. The High Plains (Ogallala) Aquifer supplies 30% of the ground water used for irrigation in the United States (United States Geological Survey 1997) and is the primary source of water for irrigation in the Great Plains. Since the time of development, pumping of this ground water resource has resulted in water-level drops of more than 15 m in parts of the central and southern plains, with drops that exceed 30 m in several locations, and is already depleted in some areas (Glantz 1989; White and Kromm 1987; United States Geological Survey 1997).

The impacts of drought in these marginal areas have been tempered through social support, but these mitigation measures have been costly. Federal aid costs (disaster assistance, crop insurance, and emergency feed assistance) for the 1988 drought amounted to \$7 billion with additional aid supplied by individual states (Riebsame et al. 1991). Total costs associated with this most recent severe drought amounted to over \$39 billion (Riebsame et al. 1991). The duration of this drought was about 3 years and the percent of the contiguous United States in severe or extreme drought (Palmer Drought Hydrologic Index ≤ -3.0) peaked at 37% in 1988 (Riebsame et al. 1991). In contrast, the 1930s drought lasted about 7 years, and at its peak almost 70% of the contiguous United States experienced severe or extreme drought (Riebsame et al. 1991). It is difficult to calculate and compare the costs and losses associated with drought, but the costs of mitigating impacts of a 1930s-magnitude drought today would surely be considerable.

General circulation models (GCMs) have been used to estimate the climate change that will accompany increases in tropospheric greenhouse gases leading to a doubling of atmospheric CO_2 , calculated to occur in the mid- to late twenty-first century. Most state-of-the-art simulations suggest drier summers will prevail in the central United States under a $2 \times \text{CO}_2$ climate scenario (Manabe and Wetherald 1987; Rind et al. 1990; Wetherald and Manabe 1995; Gregory

et al. 1997). Model simulations show an earlier drying of soils in spring due to the coincidence of less winter precipitation in the form of snow and warmer temperatures, conditions leading to greater evapotranspiration relative to precipitation in late spring and summer (United States Global Change Research Program 1995; Gregory et al. 1997). Dry conditions may be further enhanced by a decrease in summer precipitation and relative humidity (Wetherald and Manabe 1995; Gregory et al. 1997). In addition, some GCM studies have suggested an increase in the occurrence of extreme events with global warming (Overpeck et al. 1990; Rind et al. 1990), and although recent modeling results report modest decreases in mean values of summer precipitation and soil moisture in the central United States, a marked increase in the frequency and duration of extreme droughts under $2 \times \text{CO}_2$ conditions is also reported (Gregory et al. 1997).

Paleoclimatic data strongly support evidence for Great Plains droughts of a magnitude greater than those of the twentieth century, while current land use practices and GCM predictions point to an increased vulnerability to Great Plains droughts in the next century. Given the likelihood that we are not able to predict the exact extent and duration of the next major drought, it would be wise to adopt a probabilistic approach to drought forecasting and planning that incorporates the range of variability suggested by the proxy data. The paleoclimatic data suggest a 1930s-magnitude Dust Bowl drought occurred once or twice a century over the past 300–400 years, and a decadal-length drought once every 500 years. In addition, paleoclimatic data suggest a drought regime change about 800 years ago, which was likely due to some change in the base state of the climate. An increase in global temperatures is one mechanism that could possibly induce such a base-state change in climate and thus confront society with some costly surprises in the form of multidecadal drought. The prospect of great drought in the future highlights the need to place higher priority on narrowing the uncertainty about future drought by improving our understanding of the causes of drought and our ability to predict great droughts in the future.

Assessments of future drought variability must tap paleoclimatic data, in combination with climate models, to understand the full range of natural interannual to interdecadal drought variability, and to estimate the human-induced climate changes that might occur, superimposed on natural variability. Our current understanding of drought and drought prediction is based

on twentieth-century climate variability. This review of the paleoclimatic data for Great Plains drought over the past 2000 years provides a number of lines of evidence that support our conclusion that twentieth-century variability is just a subset of the total climatic variability that can be expected to occur under naturally occurring climatic conditions. We need to gain an understanding of the processes behind the bigger, longer droughts of the last 2000 years. Equally important, we have to make sure our predictive models are capable of simulating these processes and the full range of drought variability. This will require additional paleoclimatic data to map out the exact time-space character of past droughts and associated Pacific and Atlantic influences, and to test the ability of models to simulate the full range of potential drought.

Acknowledgments. We thank H. Diaz, C. Mock, R. Pulwarty, and two anonymous reviewers for their insightful comments; J. Mangan for graphics; and K. Laird, P. Brown, and H. Grissino-Mayer for data contributions. Funding was provided by the NOAA Office of Global Programs, the National Research Council, and NASA.

References

- Anderson, R. Y., 1992: Possible connection between surface winds, solar activity, and the Earth's magnetic field. *Nature*, **358**, 51–53.
- Bark, L. D., 1978: History of American drought. *North American Droughts*, N. J. Rosenberg, Ed., Westview Press, 9–23.
- Barnston, A. G., and R. E. Livesey, 1987: Classification, seasonality, and persistence of low-frequency atmospheric circulation patterns. *Mon. Wea. Rev.*, **115**, 1083–1126.
- Barr, T. N., 1981: The work food situation and global grain prospects. *Science*, **214**, 1087–1095.
- Barry, R. G., and R. J. Chorley, 1987: *Atmosphere, Weather, and Climate*. 5th ed. Methuen, 460 pp.
- Blasing, T. J., and D. N. Duvick, 1984: Reconstruction of precipitation history in North American corn belt using tree rings. *Nature*, **307**, 143–145.
- , D. W. Stahle, and D. N. Duvick, 1988: Tree ring-based reconstruction of annual precipitation in the south-central U.S. from 1750–1980. *Water Resour. Bull.*, **24**, 163–171.
- Borchert, J. R., 1950: The climate of the central North American grassland. *Ann. Assoc. Amer. Geogr.*, **40**, 1–39.
- , 1971: The dust bowl in the 1970s. *Ann. Assoc. Amer. Geogr.*, **61**, 1–22.
- Bowden, M. J., R. W. Kates, P. A. Kay, W. E. Riebsame, R. A. Warrick, D. L. Johnson, H. A. Gould, and D. Weiner, 1981: The effect of climate fluctuations on human populations: Two hypotheses. *Climate and History: Studies in Past Climates and Their Impacts on Man*, T. M. L. Wrigley, M. J. Ingram, and G. Farmer, Eds., Cambridge University Press, 479–513.
- Bradley, R. S., 1976: *Precipitation History of the Rocky Mountain States*. Westview Press, 334 pp.
- Brice, J. C., 1966: Erosion and deposition in the loess-mantled Great Plains, Medicine Creek drainage basin, Nebraska. U.S. Geological Survey Professional Paper 352-H, 339 pp. [Available from USGS Information Services, Box 25286, Denver Federal Center, Denver, CO 80225.]
- Bryson, R. A., 1966: Air masses, streamlines, and the boreal forest. *Geogr. Bull.*, **8**, 228–269.
- , and F. K. Hare, 1974: *The Climates of North America*. Vol. II, *World Survey of Climate*, Elsevier, 420 pp.
- , and T. J. Murray, 1977: *Climates of Hunger*. University of Wisconsin Press, 171 pp.
- , D. A. Baerreis, and W. M. Wendland, 1970: The character of late-glacial and post-glacial climatic changes. *Pleistocene and Recent Environments of the Central Great Plains*, W. Dort and J. K. Jones, Eds., University Press of Kansas, 53–74.
- Bunkers, M. J., J. R. Miller Jr., and A. T. DeGaetano, 1996: An examination of El Niño–La Niña-related precipitation and temperature anomalies across the northern plains. *J. Climate*, **9**, 147–160.
- Charney, J. G., 1975: Dynamics of deserts and drought in the Sahel. *Quart. J. Roy. Meteor. Soc.*, **101**, 193–202.
- Cleaveland, M. K., and D. N. Duvick, 1992: Iowa climate reconstructed from tree rings, 1640–1982. *Water Resour. Res.*, **28**, 2607–2615.
- Cole, J. E., and E. R. Cook, 1998: Decadal changes in the relationship between El Niño/Southern Oscillation variability and moisture balance in the continental United States. *Geophys. Res. Lett.*, in press.
- Cook, E. R., D. M. Meko, D. W. Stahle, and M. K. Cleaveland, 1996: Tree-ring reconstructions of past drought across the conterminous United States: Tests of a regression method and calibration/verification results. *Tree Rings, Environment, and Humanity*, J. S. Dean, D. M. Meko, and T. W. Swetnam, Eds., Radiocarbon, 155–169.
- , —, and C. W. Stockton, 1997: A new assessment of possible solar and lunar forcing of the bidecadal drought rhythm in the western United States. *J. Climate*, **10**, 1343–1356.
- , —, D. W. Stahle, and M. K. Cleaveland, cited 1998: NOAA NESDIS drought variability. [Available online at <http://www.ngdc.noaa.gov/paleo/drought.html>.]
- Currie, R. G., 1981: Evidence for 18.6 year MN signal in temperature and drought conditions in North America since A.D. 1800. *J. Geophys. Res.*, **86**, 11 055–11 064.
- , 1984a: Evidence for 18.6 year lunar nodal drought in western North American during the past millennium. *J. Geophys. Res.*, **89**, 1295–1308.
- , 1984b: Periodic (18.6-year) and cyclic (11-year) induced drought and flood in western North America. *J. Geophys. Res.*, **89**, 7215–7230.
- D'Arrigo, R. D., and G. C. Jacoby, 1991: A 1000-year record of winter precipitation from northwestern New Mexico, USA: A reconstruction from tree-rings and its relationship to El Niño and the Southern Oscillation. *Holocene*, **1**, 95–101.
- , and —, 1992: A tree-ring reconstruction of New Mexico winter precipitation and its relation to El Niño/Southern Oscillation events. *El Niño: Historical and Paleoclimatic Aspects of the Southern Oscillation*, H. F. Diaz and V. Markgraf, Eds., Cambridge University Press, 243–257.

- Dean, J. S., 1994: The Medieval Warm Period on the southern Colorado Plateau. *Climate Change*, **26**, 225–241.
- , R. C. Euler, G. J. Gumerman, F. R. Plog, R. H. Hevly, and T. N. V. Karlstrom, 1985: Human behavior, demography, and paleoenvironment on the Colorado Plateau. *Amer. Antiquity*, **50**, 537–554.
- Dean, W. E., 1997: Rates, timing, and cyclicity of Holocene eolian activity in north-central U.S.: Evidence from varved lake sediments. *Geology*, **25**, 331–334.
- , J. P. Bradbury, R. Y. Anderson, L. R. Bader, and K. Dieterich-Rurup, 1994: A high-resolution record of climatic change in Elk Lake, Minnesota for the last 1500 years. U.S. Department of the Interior, USGS Open File Rep. 94-578, 127 pp. [Available from USGS Information Services, Box 25286, Denver Federal Center, Denver, CO 80225.]
- Diaz, H. F., 1983: Drought in the United States: Some aspects of major dry and wet periods in the contiguous United States, 1895–1981. *J. Climate Appl. Meteor.*, **22**, 3–16.
- , 1986: An analysis of twentieth century climate fluctuations in northern North America. *J. Climate Appl. Meteor.*, **25**, 1625–1657.
- , 1991: Some characteristics of wet and dry regimes in the contiguous United States: Implications for climate change detection efforts. *Greenhouse-Gas-Induced Climatic Change: A Critical Appraisal of Simulations and Observations*, M. E. Schlesinger, Ed., Elsevier, 269–296.
- Doesken, N. J., and W. P. Stanton, 1991: Colorado: Floods and droughts. National Water Summary, 1988–89—Floods and droughts: Hydrologic perspectives on water issues. USGS Water-Supply Paper 2375, 591 pp. [Available from USGS Information Services, Box 25286, Denver Federal Center, Denver, CO 80225.]
- Douglass, A. E., 1914: A method of estimating rainfall by the growth of trees. *The Climatic Factor*, E. Huntington, Ed., Carnegie Institute, 101–122.
- , 1929: The secret of the Southwest solved by talkative trees. *Natl. Geogr. Mag.*, **56**, 736–770.
- , 1935: Dating Puebli Bonito and other ruins of the Southwest. Natl. Geogr. Soc. Pueblo Bonito Series 1, 74 pp. [Available from National Geographic Society, P.O. Box 98199, Washington, DC 20090-8199.]
- Duplessy, J. C., L. D. Labeyrie, M. Arnold, M. Paterne, J. Duprat, and T. C. E. van Weering, 1992: Changes in surface salinity of the North Atlantic Ocean during the last deglaciation. *Nature*, **358**, 485–488.
- Dzerdzeevskii, B. L., 1969: Climatic epochs in the twentieth century and some comments on the analysis of past climate. *Quaternary Geology and Climate*, H. E. Wright, Eds., Proceedings of the VII Congress of the International Association of Quaternary Research, Vol. 16, National Academy of Sciences, 49–60.
- Euler, R. C., G. J. Gumerman, T. N. V. Karlstrom, J. S. Dean, and R. H. Hevly, 1979: The Colorado Plateaus: Cultural dynamics and paleoenvironments. *Science*, **205**, 1089–1100.
- Forman, S. L., A. F. H. Goetz, and R. H. Yuhas, 1992: Large-scale stabilized dunes on the High Plains of Colorado: Understanding the landscape response to Holocene climates with the aid of images from space. *Geology*, **20**, 145–148.
- , R. Olgesby, V. Markgraf, and T. Stafford, 1995: Paleoclimatic significance of late Quaternary eolian deposition on the piedmont and high plains, central United States. *Global Planet. Change*, **11**, 35–55.
- Fritsch, J. M., R. J. Kane, and C. R. Chelius, 1986: The contribution of mesoscale convective weather systems to the warm season precipitation in the United States. *J. Climate Appl. Meteor.*, **25**, 1333–1345.
- Fritts, H. C., 1965: Tree-ring evidences for climatic changes in western North America. *Mon. Wea. Rev.*, **93**, 421–443.
- , 1983: Tree-ring dating and reconstructed variations in central Plains climate. *Trans. Nebraska Acad. Sci.*, **11**, 37–41.
- Fritz, S. C., S. Juggins, R. W. Battarbee, and D. R. Engstrom, 1991: Reconstruction of past changes in salinity and climate using a diatom-based transfer function. *Nature*, **352**, 706–708.
- Glantz, M., Ed., 1989: Forecasting by analogy: Societal responses to regional climatic change. Summary Report, Environmental and Societal Impacts Group, NCAR, 77 pp. [Available from NCAR Library, P.O. Box 3000, Boulder, CO 80307-3000.]
- Granger, O. E., 1984: Twentieth-century climate anomaly patterns over the southwestern United States. *Phys. Geogr.*, **5**, 164–185.
- Gregory, J. M., J. F. B. Mitchell, and A. J. Brady, 1997: Summer drought in northern midlatitudes in a time-dependent CO₂ climate experiment. *J. Climate*, **10**, 662–686.
- Grissino-Mayer, H. D., 1996: A 2129-year reconstruction of precipitation for northwestern New Mexico, U.S.A. *Tree Rings, Environment, and Humanity*, J. S. Dean, D. M. Meko, and T. W. Swetnam, Eds., Radiocarbon, 191–204.
- Guttman, N., 1991: Sensitivity of the Palmer Hydrologic Drought Index to temperature and precipitation departures from average conditions. *Water Resour. Res.*, **27**, 797–807.
- Hardman, G., and O. E. Reil, 1936: The relationship between tree-growth and stream runoff in the Truckee River basin, California–Nevada. University of Nevada Agricultural Experiment Station Bull. 141, 38 pp. [Available from Nevada Agricultural Experiment Station, University of Nevada, Reno, NV 89557-0107.]
- Haston, L., and J. Michaelsen, 1997: Spatial and temporal variability of southern California precipitation over the last 400 years and relationships to atmospheric circulation patterns. *J. Climate*, **10**, 1836–1852.
- Hecht, A. D., 1983: Drought in the Great Plains: History of societal response. *J. Climate Appl. Meteor.*, **22**, 51–56.
- Helfand, H. M., and S. D. Schubert, 1995: Climatology of the simulated Great Plains low-level jet and its contribution to the moisture budget of the United States. *J. Climate*, **8**, 784–806.
- Higgins, R. W., Y. Yao, E. S. Yarosh, J. E. Janowiak, and K. C. Mo, 1997: Influence of the Great Plains low-level jet on summertime precipitation and moisture transport over the central United States. *J. Climate*, **10**, 481–507.
- Hirschboeck, K. K., 1991: Climate and floods. National Water Summary, 1988–89—Floods and droughts: Hydrologic perspectives on water issues. USGS Water-Supply Paper 2375, 591 pp. [Available from USGS Information Services, Box 25286, Denver Federal Center, Denver, CO 80225.]
- Hughes, M. K., and P. M. Brown, 1992: Drought frequency in central California since 101 B.C. recorded in giant sequoia tree rings. *Climate Dyn.*, **6**, 161–167.
- , and L. J. Graumlich, 1996: Multimillennial dendroclimatic studies from the western United States. *Climate Variations and Forcing Mechanisms of the Last 2000 Years*, P. D. Jones, R. S. Bradley, and J. Jouzel, Eds., Springer-Verlag, 109–124.

- Hurrell, J. W., 1995: Decadal trends in the North Atlantic oscillation: Regional temperatures and precipitation. *Science*, **269**, 676–679.
- Jennings, A. E., and N. J. Weiner, 1996: Environmental change in eastern Greenland during the last 1300 years: Evidence from foraminifera and lithofacies in Nansen Fjord, 68°N. *Holocene*, **6**, 179–191.
- Karl, T. R., 1983: Some spatial characteristics of drought duration in the United States. *J. Climate Appl. Meteor.*, **22**, 1356–1366.
- , and A. J. Koscielny, 1982: Drought in the United States: 1895–1981. *J. Climatol.*, **2**, 313–329.
- , C. N. Williams Jr., F. T. Quinlan, and T. A. Boden, 1990: United States Historical Climatology Network (HCN) serial temperature and precipitation data. ORNL/CDIAC-30, NDP-019/R1, 377 pp. [Available from Carbon Dioxide Information Analysis Center, Oak Ridge National Laboratory, Building 1000, P.O. Box 2008, MS-6335, Oak Ridge, TN 37831-6266.]
- Keigwin, L. D., 1996: The Little Ice Age and Medieval Warm Period in the Sargasso Sea. *Science*, **274**, 1504–1508.
- Kiladis, G. N., and H. F. Diaz, 1989: Global climatic anomalies associated with extremes in the Southern Oscillation. *J. Climate*, **2**, 1069–1090.
- Laird, K. R., S. C. Fritz, K. A. Maasch, and B. F. Cumming, 1996: Greater drought intensity and frequency before A.D. 1200 in the northern Great Plains, U.S.A. *Nature*, **384**, 552–554.
- , —, and B. F. Cumming, 1998: A diatom-based reconstruction of drought intensity, duration, and frequency from Moon Lake, North Dakota: A sub-decadal record of the last 2300 years. *J. Paleolimnol.*, **19**, 161–179.
- LaMarche, V. C., Jr., 1974: Paleoclimatic inferences from long tree-ring records. *Science*, **183**, 1043–1048.
- Lawson, M. P., 1970: A dendroclimatological interpretation of the Great American Desert. *Proc. Assoc. Amer. Geogr.*, **3**, 109–114.
- , and C. W. Stockton, 1981: Desert myth and climatic reality. *Ann. Assoc. Amer. Geogr.*, **71**, 527–535.
- Lehmer, D. J., 1970: Climate and culture history in the Middle Missouri Valley. *Pleistocene and Recent Environments of the Central Great Plains*, W. Dort and J. K. Jones, Eds., University Press of Kansas, 117–129.
- Lockeretz, W., 1978: The lessons of the Dust Bowl. *Amer. Sci.*, **66**, 560–569.
- Ludlum, D. M., 1971: *Weather Record Book*. Weatherwise, 98 pp.
- Madole, R., 1994: Stratigraphic evidence of desertification in the west-central Great Plains within the past 1000 years. *Geology*, **22**, 483–486.
- , 1995: Spatial and temporal patterns of late Quaternary eolian deposits, eastern Colorado, U.S.A. *Quat. Sci. Rev.*, **14**, 155–177.
- Manabe, S., and R. T. Wetherald, 1987: Large-scale changes of soil wetness induced by an increase in atmospheric carbon dioxide. *J. Atmos. Sci.*, **44**, 1211–1235.
- Martin, C. W., 1992: The response of fluvial systems to climate change: An example from the central Great Plains. *Phys. Geogr.*, **13**, 101–114.
- May, D. W., 1989: Holocene alluvial fills in the South Loup River valley, Nebraska. *Quat. Res.*, **32**, 117–120.
- Meko, D., C. W. Stockton, and W. R. Boggess, 1995: The tree-ring record of severe sustained drought. *Water Resour. Bull.*, **31**, 789–801.
- Michaelsen, J., 1989: Long-period fluctuations in El Niño amplitude and frequency reconstructed from tree rings. *Aspects of Climate Variability in the Pacific and Western Americas*, *Geophys. Monogr.*, No. 55, Amer. Geophys. Union, 69–74.
- Miller, A. J., D. R. Cayan, T. P. Barnett, N. E. Graham, and J. M. Oberhuber, 1994: The 1976–77 climate shift of the Pacific Ocean. *Oceanography*, **7**, 21–26.
- Mitchell, J. M., Jr., C. W. Stockton, and D. M. Meko, 1979: Evidence of a 22-year rhythm of drought in the western United States related to the Hale solar cycle since the 17th century. *Solar-Terrestrial Influences in Weather and Climate*, B. M. McCormac and T. A. Seliga, Eds., D. Reidel, 125–144.
- Mock, C. J., 1991: Drought and precipitation fluctuations in the Great Plains during the late nineteenth century. *Great Plains Res.*, **1**, 26–56.
- , 1996: Climatic controls and spatial variations of precipitation in the western United States. *J. Climate*, **9**, 1111–1125.
- Muhs, D. R., and P. B. Maat, 1993: The potential response of eolian sands to greenhouse warming and precipitation reduction on the Great Plains of the U.S.A. *J. Arid. Environ.*, **25**, 351–361.
- , and V. T. Holliday, 1995: Evidence of active dune sand on the Great Plains in the 19th century from accounts of early explorers. *Quat. Res.*, **43**, 198–208.
- , T. W. Stafford, S. D. Cowherd, S. A. Mahan, R. Kihl, P. B. Maat, C. A. Bush, and J. Nehring, 1996: Origin of the late Quaternary dune fields of northeastern Colorado. *Geomorphology*, **17**, 129–149.
- , —, J. B. Swinehart, S. D. Cowherd, S. A. Mahan, C. A. Bush, R. F. Madole, and P. B. Maat, 1997: Late Holocene eolian activity in the mineralogically mature Nebraska Sand Hills. *Quat. Res.*, **48**, 162–176.
- Namias, J., 1955: Some meteorological aspects of drought with special reference to the summers of 1952–54 over the United States. *Mon. Wea. Rev.*, **83**, 199–205.
- , 1983: Some causes of United States drought. *J. Climate Appl. Meteor.*, **22**, 30–39.
- Oglesby, R. J., 1991: Springtime soil moisture, natural climatic variability, and North American drought as simulated by the NCAR Community Climate Model 1. *J. Climate*, **4**, 890–897.
- , and D. J. Erickson III, 1989: Soil moisture and persistence of North American drought. *J. Climate*, **2**, 1362–1380.
- Overpeck, J. T., 1996: Warm climate surprises. *Science*, **271**, 1820–1821.
- , D. Rind, and R. Goldberg, 1990: Climate-induced changes in forest disturbance and vegetation. *Nature*, **343**, 51–53.
- Palmer, T. N., and C. Branković, 1989: The 1988 U.S. drought linked to anomalous sea surface temperature. *Nature*, **338**, 54–57.
- Palmer, W. C., 1965: Meteorological drought. U.S. Weather Bureau Research Paper 45, National Weather Service, 58 pp. [Available from NOAA, 1325 East-West Highway, Silver Spring, MD 20910.]
- Peterson, K. L., 1994: A warm and wet Little Climatic Optimum and a cold and dry Little Ice Age in the southern Rocky Mountains, U.S.A. *Climate Change*, **26**, 243–269.
- Phillips, J. G., C. Rosenzweig, and M. Cane, 1996: Exploring the potential for using ENSO forecasts in the U.S. corn belt. *Drought Network News*, **8**, 6–10.

- Rasmussen, E. M., X. Wang, and C. F. Ropelewski, 1995: Secular variability of the ENSO cycle. *Natural Climate Variability on Decade-to-Century Time Scales*, D. G. Martinson, K. Bryan, M. Ghil, M. M. Hall, T. R. Karl, E. S. Sarachik, S. Sorooshian, and L. D. Talley, Eds., National Academy Press, 458–469.
- Riebsame, W. E., S. A. Changnon, and T. R. Karl, 1991: *Drought and Natural Resources Management in the United States: Impacts and Implications of the 1987–89 Drought*. Westview Press, 174 pp.
- Rind, D., R. Goldberg, J. Hansen, C. Rosenzweig, and R. Ruedy, 1990: Potential evapotranspiration and the likelihood of future drought. *J. Geophys. Res.*, **95**, 9983–10 004.
- Rose, M. R., J. S. Dean, and W. B. Robinson, 1982: Dendroclimatic reconstruction for the southeastern Colorado Plateau. Final Report to Dolores Archaeological Program, University of Colorado, 425 pp. [Available from National Technical Information Service, Bureau of Reclamation, Engineering and Research Center, Denver Federal Center, Denver, CO 80225.]
- Stahle, D. W., and M. K. Cleaveland, 1988: Texas drought history reconstructed and analyzed from 1698 to 1980. *J. Climate*, **1**, 59–74.
- , —, and J. G. Hehr, 1985: A 450-year drought reconstruction for Arkansas, United States. *Nature*, **316**, 530–532.
- Stine, S., 1994: Extreme and persistent drought in California and Patagonia during mediaeval time. *Nature*, **369**, 546–549.
- Stockton, C. W., and D. M. Meko, 1975: A long-term history of drought occurrence in western United States as inferred from tree rings. *Weatherwise*, **28** (6), 244–249.
- , and G. C. Jacoby, 1976: Long-term surface water supply and streamflow levels in the upper Colorado River basin. Lake Powell Research Project Bull. 18, Inst. of Geophysics and Planetary Physics, University of California, Los Angeles, 70 pp. [Available from University of California, Los Angeles, 3845 Slichter Hall, Mail Code 156704, Los Angeles, CA 90095-1567.]
- , and D. M. Meko, 1983: Drought recurrence in the Great Plains as reconstructed from long-term tree-ring records. *J. Climate Appl. Meteor.*, **22**, 17–29.
- , J. M. Mitchell Jr., and D. M. Meko, 1983: A reappraisal of the 22-year drought cycle. *Solar-Terrestrial Influences in Weather and Climate*, B. M. McCormac, Ed., Colorado Associated University Press, 507–515.
- Stokes, S., and J. B. Swinehart, 1997: Middle- and late-Holocene dune reactivation in the Nebraska Sand Hills, U.S.A. *Holocene*, **7**, 263–272.
- Stuiver, M., and H. A. Polach, 1977: Reporting of ¹⁴C data. *Radiocarbon*, **19**, 355–363.
- , and B. Becker, 1986: High-precision decadal calibration of the radiocarbon time scale, AD 1950–2500 BC. *Radiocarbon*, **28**, 863–910.
- Swetnam, T. W., and J. L. Betancourt, 1998: Mesoscale disturbance and ecological response to decadal climatic variability in the American southwest. *J. Climate*, **11**, 3128–3147
- Tang, M., and E. R. Reiter, 1984: Plateau monsoons of the Northern Hemisphere: A comparison between North America and Tibet. *Mon. Wea. Rev.*, **112**, 617–637.
- Ting, M., and H. Wang, 1997: Summertime U.S. precipitation variability and its relation to Pacific sea surface temperature. *J. Climate*, **10**, 1853–1873.
- Townshend, J. R. G., C. O. Justice, D. Skole, J.-P. Malingreau, J. Cihlar, P. M. Teillet, F. Sadowski, and S. Ruttenberg, 1994: The 1-km AVHRR global data set: Needs of the International Geosphere Biosphere Program. *Int. J. Remote Sens.*, **15**, 3319–3332.
- Trenberth, K. E., and J. W. Hurrell, 1994: Decadal atmospheric-ocean variations in the Pacific. *Climate Dyn.*, **9**, 303–319.
- , and C. J. Guillemot, 1996: Physical processes involved in the 1988 drought and 1993 floods in North America. *J. Climate*, **9**, 1288–1298.
- , G. W. Branstrator, and P. A. Arkin, 1988: Origins of the 1988 North American drought. *Science*, **242**, 1640–1645.
- United States Geological Survey, cited 1997: Water levels in the High Plains Aquifer. [Available online at <http://water.usgs.gov/public/wid/html/GW.html#HDR6>.]
- United States Global Change Research Program, 1995: Forum of global change modeling. USGCRP-95-02, National Science Foundation, 26 pp.
- Weakly, H. E., 1965: Recurrence of drought in the Great Plains during the last 700 years. *Agric. Engin.*, **46**, 85.
- Wedel, W. R., 1986: *Central Plains Prehistory: Holocene Environments and Culture Change in the Republican River Basin*. University of Nebraska Press, 280 pp.
- Wendland, W. M., 1978: Holocene man in North America: The ecological setting and climate background. *Plains Anthropol.*, **23**, 273–287.
- West, E., 1997: *The Way to the West: Essays on the Central Plains*. University of New Mexico Press, 244 pp.
- Wetherald, R. T., and S. Manabe, 1995: The mechanisms of summer dryness induced by greenhouse warming. *J. Climate*, **8**, 3096–3108.
- White, S. E., and D. E. Kromm, 1987: Local groundwater management effectiveness in the Colorado and Kansas Ogallala region. *Natural Resour. J.*, **35**, 275–307.
- Yevjevich, V., 1967: A objective approach to definitions and investigations of continental drought. Hydrology Papers, No. 23, Colorado State University, 19 pp. [Available from University Archives, Colorado State University, Fort Collins, CO 80523.]



conditions for a given area. Negative PDSI values represent time periods drier than normal, while positive PDSI values represent periods wetter than normal. The lower PDSI value the drier the period of consideration. For example, a drought year of with a PDSI value of -4.0 would be drier and considered more extreme than a drought year with a value of -3.0.

The City contracted High Country Hydrology, Inc. (HCH) to examine hydrologic data to quantify the duration and intensity of a drought with a 1% exceedance probability. During their review of hydrologic data, HCH found that estimates of the Palmer Drought Severity Index (PDSI) generated from tree ring chronology could be used to review historic droughts of record for their intensity and duration (Attachment C). HCH calculated that a 1% drought can be approximated by the drought of 1933 through 1940, as illustrated in Table 2 below.

Table 2-2: 1% Drought Reconstruction from PDSI

Suggested Drought Intervals based on Reconstructed PDSI (1640-2003)				Representative Historical Years	
Exceedance Probability %	Duration (Years)	Cumulative PDSI	Mean PDSI	Years	Actual Cumulative PDSI
10%	2	-4.4	-2.20	1925-1926	-4.9
4%	4	-8.8	-2.21	1925-1926, 1981 x 2	-8.8
2.0%	6	-15.6	-2.60	1952-1956, 1959	-16.1
1.3%	7	-19.6	-2.80	1946, 1952-1956, 1981	-19.6
1.0%	8	-22.4	-2.80	1933-1940	-24.4
0.40%	10	-31.4	-3.14	1952-1956 x 2	-31.1
0.20%	12	-38.2	-3.18	1952-1956 x 2, 1963-1964	-38.4
0.10%	14	-45.0	-3.21	1925, 1933-1940, 1936-1937, 1937, 1940, 1976	-45.0

Source: Attachment C, HCH Technical Memorandum 4, March 14, 2013, Table 1

2.2 City of Wichita - Future Raw Water Demand Assessment

The City's projected water demands were recently examined in a study completed by Science Applications International (SAIC) and Professional Engineering Consultants (PEC) in August of 2013 (Attachment D). This study indicates that by the year 2060 the City's normal annual water demands will be in the range of 71,370 acre-feet (AF) to 105,858 AF. Three growth scenarios were included within the study (low, medium, and high growth) to generate a band of likely forecasted populations. The medium growth forecast with a projected demand of 87,597 AF by the year 2060 was selected for modeling future demands to simulate future demands between the confines of the low and high bands of forecasted

Appendix A - Hydrology

Hydrologic Operations Model

Burns & McDonnell's (B&M) Reservoir Network (RESNET) computer simulation model was used to evaluate potential hydrologic impacts for the Integrated Local Water Supply (ILWS) system. The model performs a daily simulation of reservoirs and streams as a circulating network and uses least-cost optimizing procedures to arrive at an optimized solution. The model is based on the Microsoft ACCESS database application and utilizes the database to contain the model input data, output data, and other modeling and solution control parameters and functions.

The operations model calculates a daily water balance for the ILWS system during the 85-year model simulation period (water years [WY] 1923–2007). The model requires the following general data sets for operation:

- Historical mean daily stream discharge at selected points within the project area
- Historical monthly reservoir evaporation rates
- Available storage and other physical data for Cheney Reservoir
- Available storage, natural recharge and other parameters for the Equus Beds aquifer
- City's current and projected water demands
- Irrigation demands for agriculture in the Equus Beds Well Field area
- Minimum desirable streamflow requirements
- Supply capability and other operating parameters for all current and potential water supply sources
- Preferred allocation order for each water supply source

B&M previously utilized the model (based on WY 1923-1996) to evaluate impacts by the ILWS system alternatives for Wichita's 2003 Environmental Impact Statement (EIS)¹. Appendix C from the 2003 EIS describes the general construct and operations of the model. Reclamation reviewed the 2003 EIS and requested additional documentation from B&M regarding key components of the model. The request for additional information included:

- Details regarding the structure, operations, and data comprising the RESNET database model, and development of executable version of the model for Reclamation (included as Attachment A).
- Supporting documentation for the development of the aquifer-stream gain-loss table (included as Attachment B).
- Details on the development of historic streamflow discharge for RESNET model nodes (included as Attachment C).
- Details on the development of historic evaporation from Cheney Reservoir (included as Attachment D).

This additional requested information is presented as Attachments A-D of this Hydrology Appendix.

Scenarios Evaluated

Three alternatives were simulated by the model for the purposes of the current EIS:

¹ Final Environmental Impact Statement for Integrated Local Water Supply Plan, Wichita, Kansas; prepared by City of Wichita, Department of Water and Sewer; 2003

-
- Current – This alternative simulates what might be considered the current level-of-development on the supply system. It utilizes the year 2000 raw water demands for the City of Wichita and assumes no components of the ILWS project are in place (including those of phase 1 already built).
 - No-Project – This alternative is same as Current above, except the City of Wichita raw water demands are projected to year 2050.
 - ILWSP100 – This alternative includes the following proposed components of the ILWS and uses City of Wichita raw water demands projected to year 2050:
 - Aquifer storage and recovery (ASR) project features to capture 60 MGD (million gallons per day) of induced infiltration groundwater and 40 MGD of direct diversion of surface water from Little Arkansas River (ASR)
 - Redevelopment of the Bentley Reserve Well Field
 - Expansion of the Local Well Field

Model Operational Period-of-Record -

A product of the above review process of the 2003 version of the model was the extension of the modeling period by 11 years by B&M to include more current information. The current modeling period now covers an 85-year period and extends from water years 1923 through 2007. The model utilizes historic recorded and estimated daily streamflows and climatological data for that period. The use of this historic sequence for evaluating the proposed system is premised on the assumption that the past historic climatologic sequence will repeat itself in the future. This period includes significant drought events occurring during the 1930's and 1950's.

Model System Network -

A diagram displaying the model network is shown in Figure 1 of Attachment A. The model is comprised of 20 nodes at which daily demands and flows are calculated. Two of the nodes represent system storage: Cheney Reservoir and the Equus Beds Aquifer. Model nodes are connected together by various links representing stream connections, aquifer-stream interactions (accretions and infiltration to and from stream and aquifer), or diversion delivery pipelines. More detailed information on model structure, node connectivity, and decision parameters can be found in Attachment D.

Model Inflows -

Inflows to model stream nodes, and flow gains (unregulated flow) between stream nodes were derived from historic U.S. Geological Survey (USGS) recorded flows at various stations in the basin. Results from the groundwater/surface water interaction analyses in Attachment B were used to adjust unregulated flow in the model to eliminate 'double accounting' of model calculated return flows (see Section 6 – Attachment C).

For nodes where recorded discharge data were incomplete for the entire modeling period, regression analyses and drainage area ratios were used to estimate missing data. See Attachment C for further details on generation of model flow data.

Model Demands –

The model utilizes two primary demands to be applied to the water supply system:

- City of Wichita raw water demands.
- Agricultural diversions from Equus Beds Aquifer.

For the 'Current' modeling scenario, City of Wichita's demands are based on year 2000 average-day demand. For the 'No Project' and 'ILWSP100' alternatives, the demand is based on Wichita's year 2050

average day demand. More details on the development of demands can be found in section 1.5.1 of Attachment A of this Appendix, and in Appendix C of the 2003 EIS.

The agricultural demand from the aquifer is based on an average annual value of 26,500 acre-feet which is distributed evenly over the growing season of mid-May through mid-September (Sect. 1.5.6, Attachment A).

Cheney Reservoir -

Current area-capacity-elevation data are used by the model to calculate pool elevation and reservoir surface area for a given storage volume in Cheney Reservoir. Section 1.3.1 and Table 8 of Attachment A displays the various reservoir allocations used.

The model calculates a daily reservoir evaporation volume based on the simulated surface area and the historic daily evaporation rate. The daily evaporation rate was derived from recorded monthly pan evaporation at Cheney, when that data were available. For months when actual pan evaporation data were not recorded, the evaporation rate was estimated by B&M using their ETCALC model. Monthly evaporation was evenly distributed over month into daily evaporation. See Attachment D for additional details on calculation of reservoir evaporation rates.

Equus Beds Aquifer -

The model operates the Equus Beds Aquifer similar to how a surface-water reservoir is operated. The USGS MODFLOW groundwater flow model was utilized by B&M to define a table that relates aquifer elevation, aquifer storage deficit, and aquifer gains and losses to the Arkansas and Little Arkansas Rivers (see Table A-1 in Attachment B). With additional model evaluation, the distribution of MODFLOW derived gain/losses to model nodes were modified as indicated in Table 9, Attachment A. The model simulates aquifer gains/losses to the following river nodes: Arkansas River near Maize, Little Arkansas River near Halstead, and Little Arkansas River near Sedgwick.

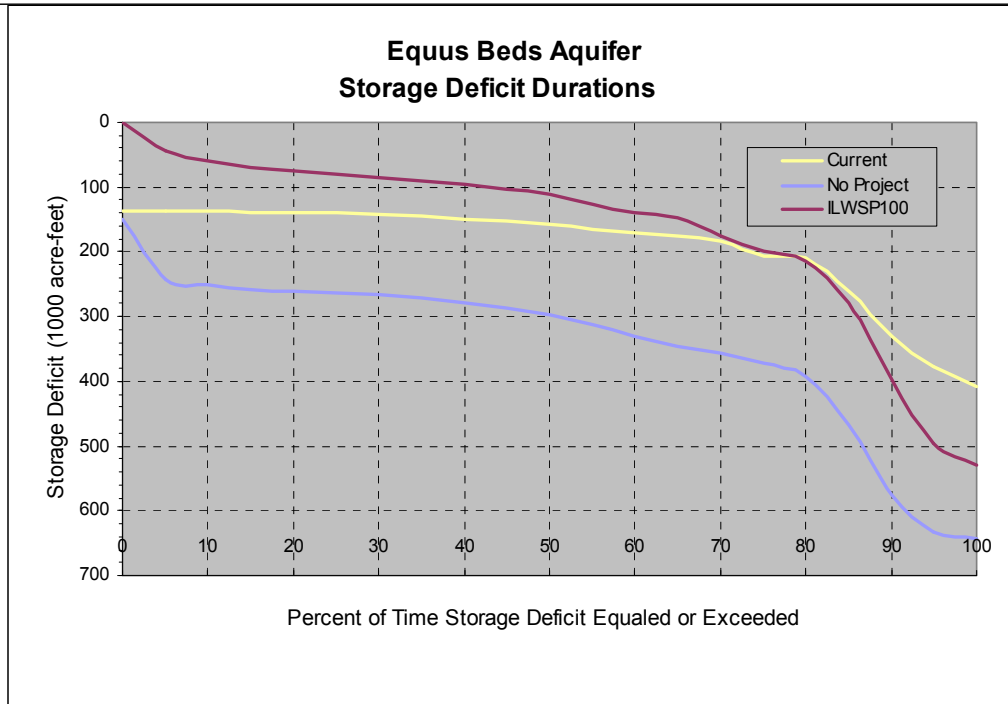
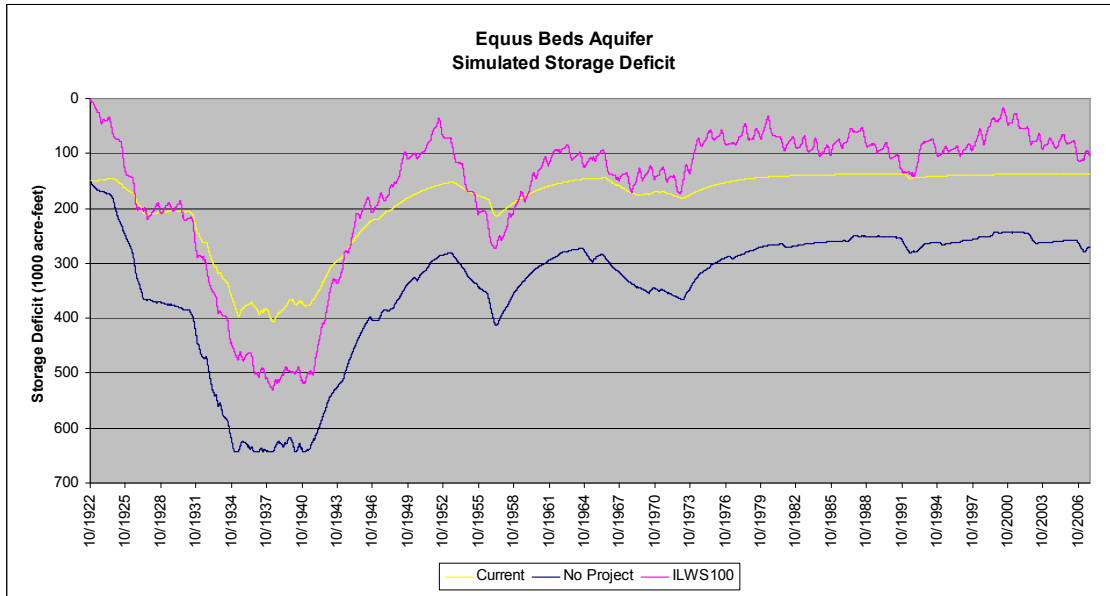
Model Simulation Results

Following is a discussion of simulation results for the three scenarios defined above. It primarily focuses on quantifying the impact differences between the future (year 2050 demands) with and without the preferred ASR 100 MGD project scenario. The inclusion of the 'current' scenario (no project implemented and year 2000 Wichita demands) in various charts is to illustrate the differences that will occur between now and the future planning horizon of year 2050, whether or not the project is implemented. The discussion is categorized by the hydrologic system potentially being impacted.

Equus Beds Aquifer -

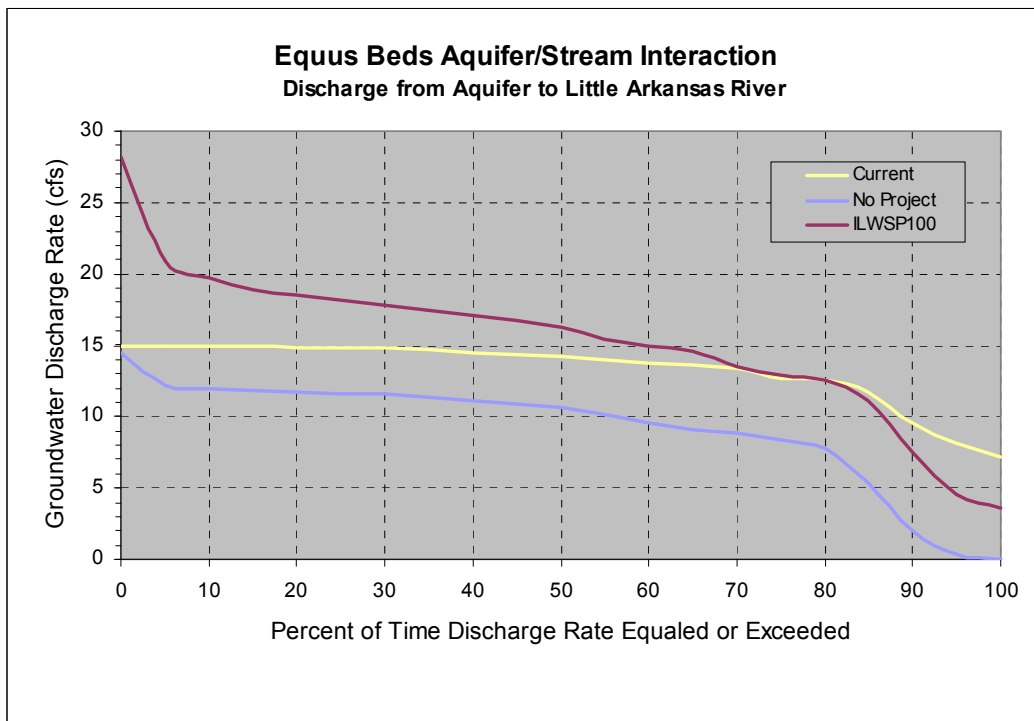
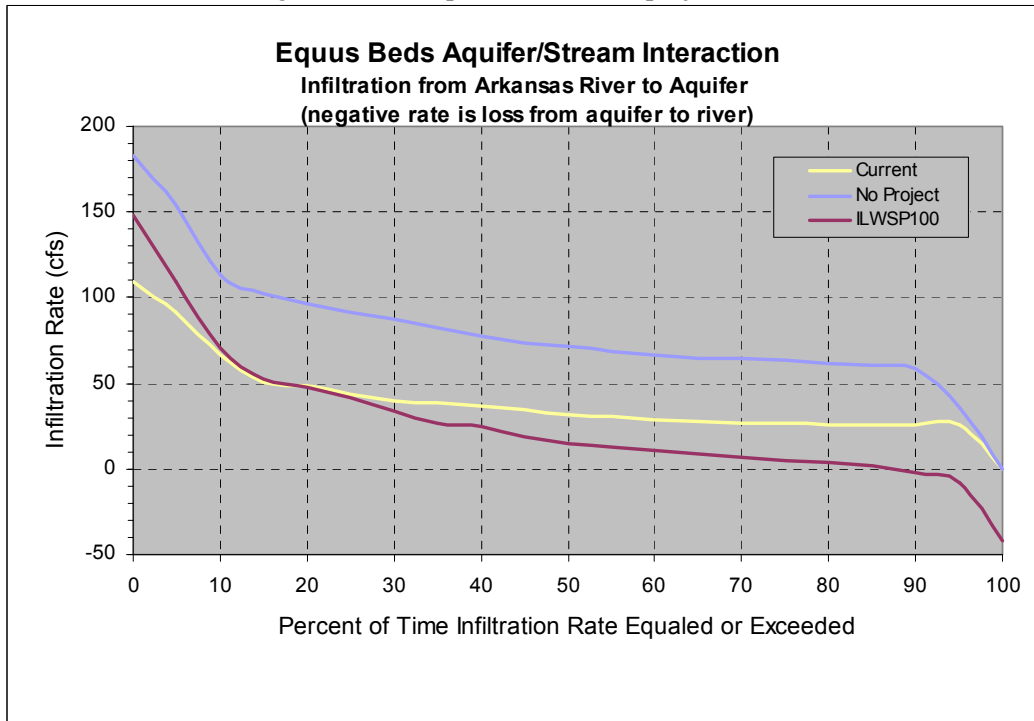
In general, the ASR component of this project will increase the volume of water in storage within the Equus Beds aquifer available for later withdrawal. Increasing the aquifer storage volume will result in a corresponding increase in the elevation of the aquifer water table. This increases the hydraulic gradients from the aquifer to the Little Arkansas River, resulting in a potential increase in base-flow accretions to that river. It also results in a general reduction of hydraulic gradients from the Arkansas River into the aquifer, resulting in decreased infiltration from the Arkansas River to the aquifer.

The following chart shows simulated aquifer storage deficit and monthly median water table elevations. Without implementation of the project, increasing demands will decrease aquifer storage from current conditions. With the project, aquifer storage will generally increase to levels above current conditions, with the exception of drought periods. It is estimated that for 70 percent of the time, aquifer levels will be greater than current conditions with the project in place.



With an increase in aquifer storage, there is an associated decrease in infiltration from the Arkansas River to the aquifer, and an increase in discharge from the aquifer to the Little Arkansas River. Infiltration from the Arkansas River to the aquifer will generally decrease by about 50 cubic feet per second (cfs) for a majority of the time, as compared to without project. This will help reduce the influx of higher saline

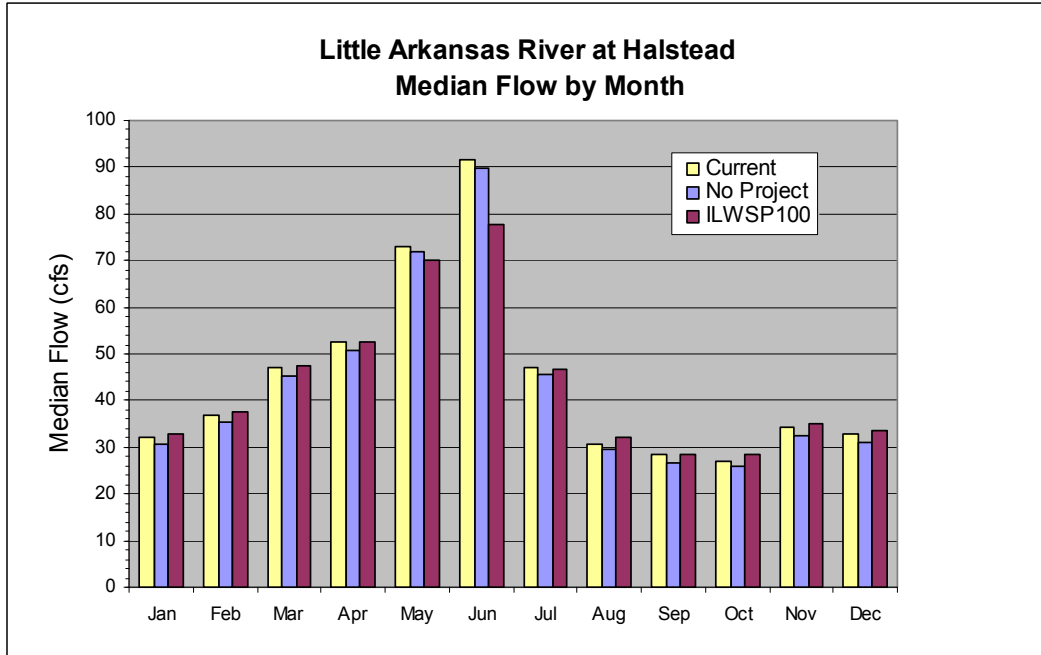
water from the Arkansas River to the aquifer. Discharge from the aquifer to the Little Arkansas River is anticipated to increase 4 cfs or greater as compared to without project conditions.



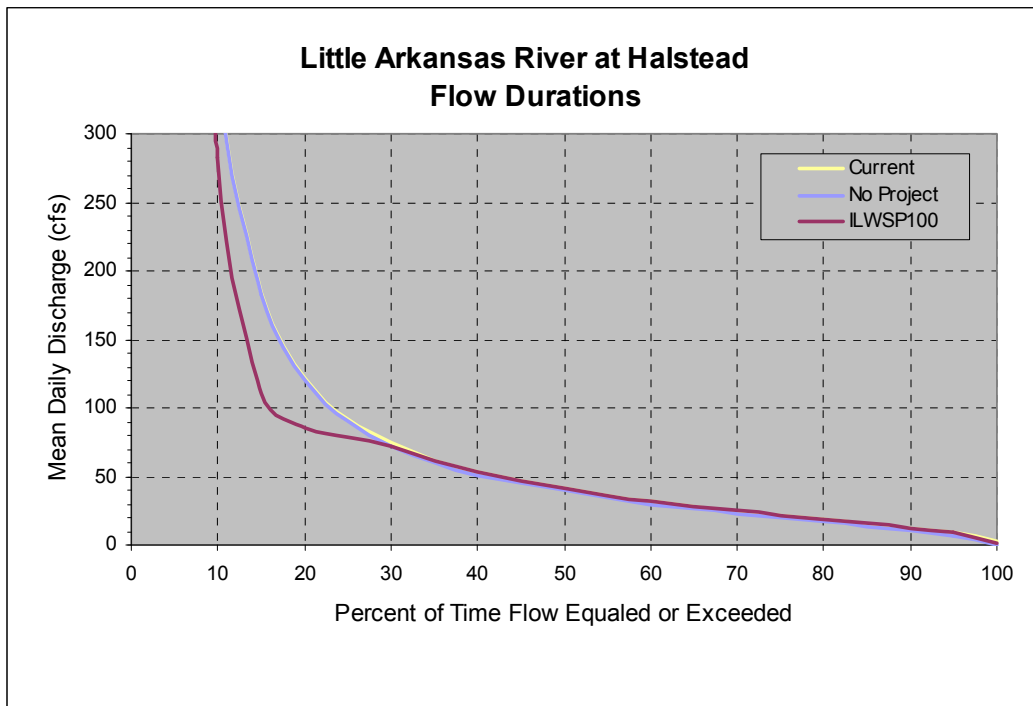
Little Arkansas River at Halstead –

Project features impacting this site are the ASR induced infiltration wells installed above this location. These wells will provide approximately half of the total ASR project diversion capacity. Recharge to the aquifer in the area above Halstead by the ASR component will result in a general increase in the aquifer

water table and a corresponding increase in baseflow accretions to the stream above this location. With the project, median discharge at Halstead is anticipated to increase from 1 to 3 cfs for all months, except May and June, when there will be declines up to 12 cfs. May and June are generally the highest flow periods and it will be during these times that the greatest diversions to the infiltration wells will occur.

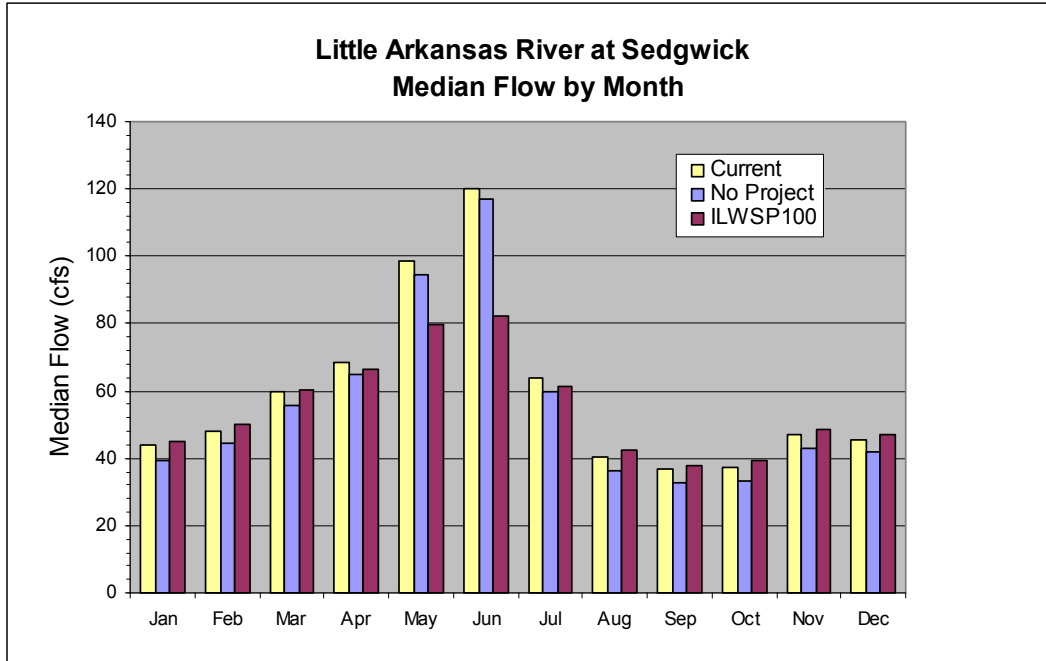


Little Arkansas River at Halstead Median Flow by Month (cfs)												
	Jan	Feb	Mar	Apr	May	Jun	Jul	Aug	Sep	Oct	Nov	Dec
No Project	30.5	35.3	45.1	50.6	71.8	89.7	45.6	29.6	26.7	25.9	32.6	31.1
ILWSP100	33.0	37.7	47.4	52.6	70.0	77.8	46.6	32.1	28.5	28.4	35.0	33.4
Difference	2.5	2.3	2.3	2.0	-1.8	-11.8	1.0	2.4	1.8	2.5	2.3	2.3

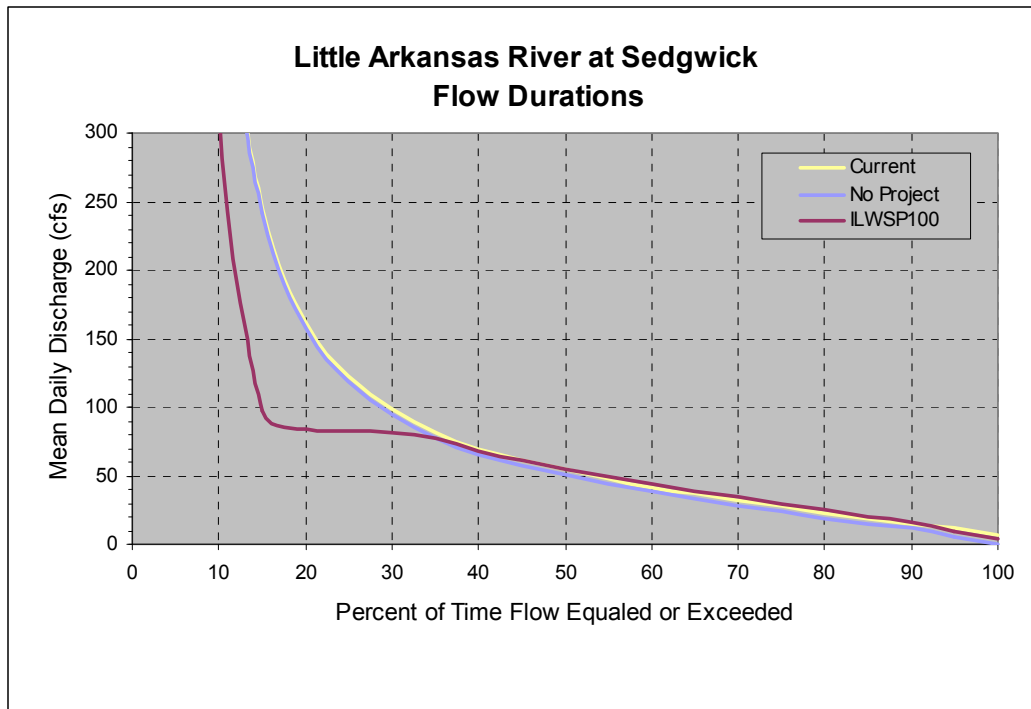


Little Arkansas River at Sedgwick -

The other half of the ASR infiltration well diversion capacity is to be installed between the Halstead and Sedgwick nodes. Sedgwick is also the location for the ASR surface water diversion site. Similar to impacts at the Halstead node, the increased recharge to the aquifer above Sedgwick will generally result in slightly higher aquifer discharge to the Little Arkansas. Median flow in the stream is expected to increase 2 to 6 cfs for all months, except May and June, when greater diversions will result in median flow declines of 15 to 35 cfs.



Little Arkansas River at Sedgwick												
Median Flow by Month (cfs)												
	Jan	Feb	Mar	Apr	May	Jun	Jul	Aug	Sep	Oct	Nov	Dec
No Project	39.3	44.2	55.8	64.7	94.4	116.9	59.7	36.4	32.5	33.4	43.0	41.7
ILWSP100	45.2	49.9	60.0	66.5	79.7	82.1	61.4	42.2	37.6	39.4	48.3	47.1
Difference	5.8	5.6	4.3	1.8	-14.7	-34.8	1.7	5.8	5.1	6.0	5.3	5.3



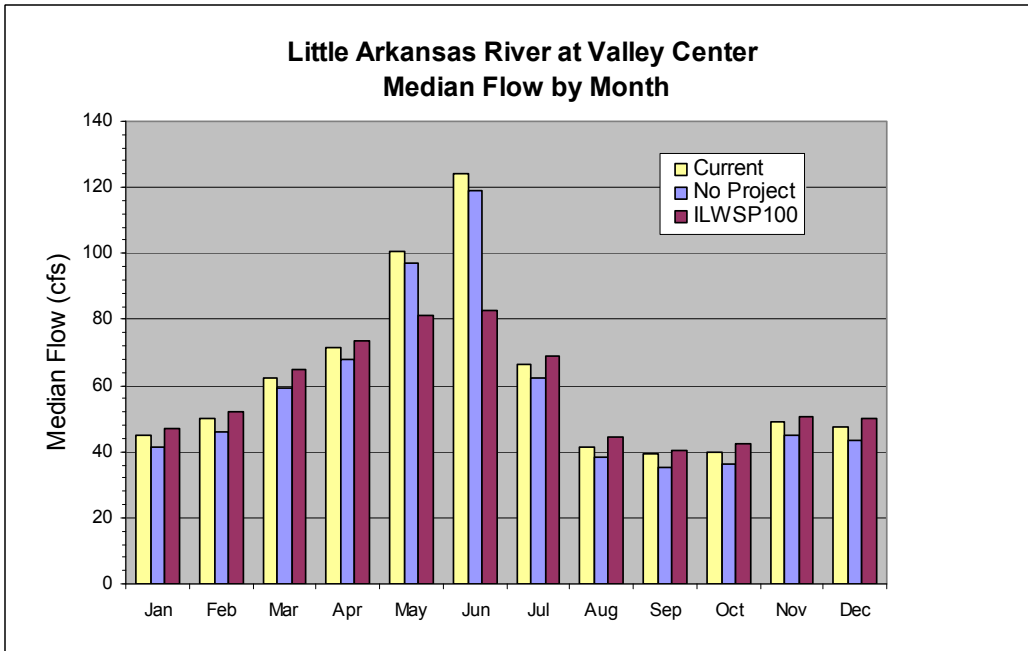
Little Arkansas River at Valley Center –

For all months except May and June, median flows at this location will increase 6 to 7 cfs with implementation of the project. This reflects the increased groundwater contributions to the Little Arkansas River above this location from increased aquifer storage. May and June exhibit a lower median flow than without project due to greater diversions occurring during those months. The simulated flow frequency curves indicate that, at lower flows, streamflow discharge will be generally slightly higher with the project than without.

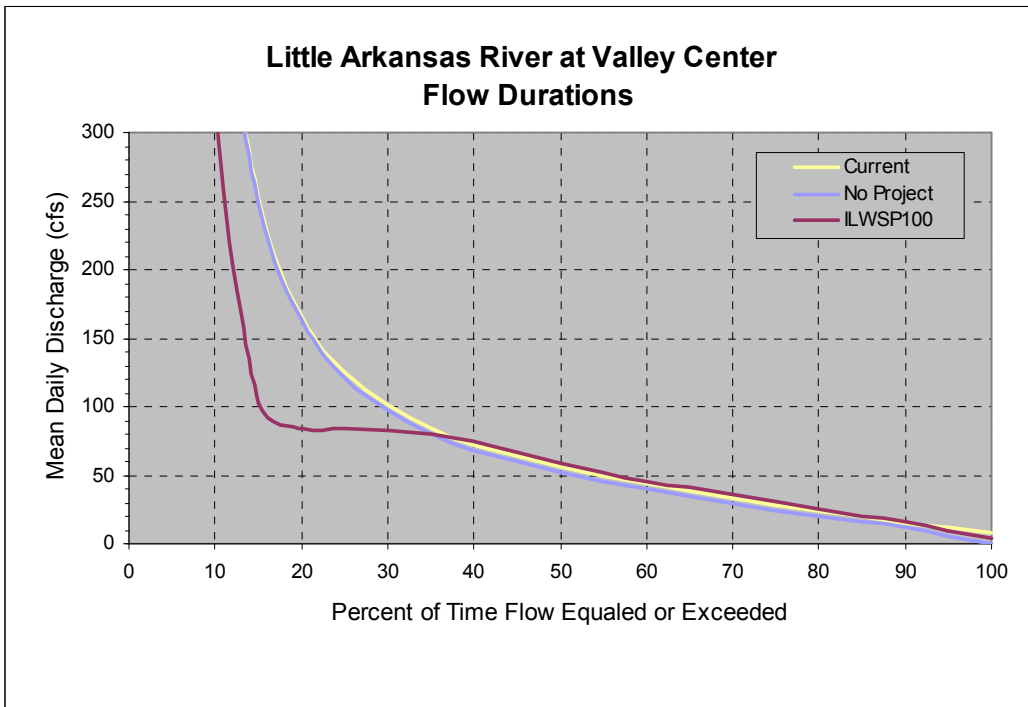
Median water surface elevations are anticipated to be about the same with project as compared to without project for all months, except May and June, when there will be declines of about 0.1 - 0.2 feet.

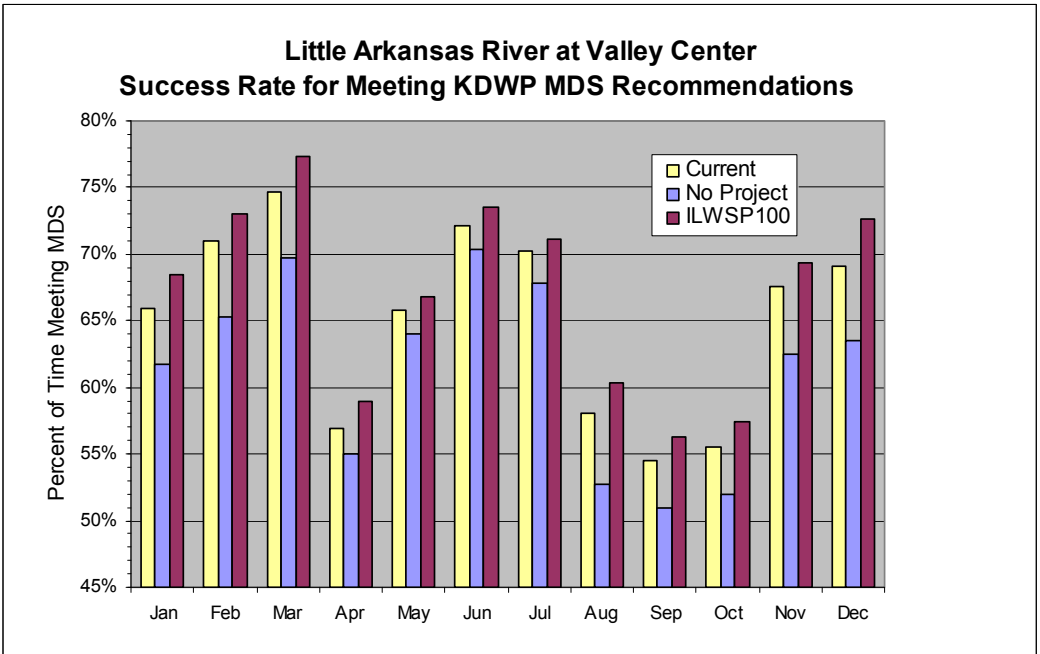
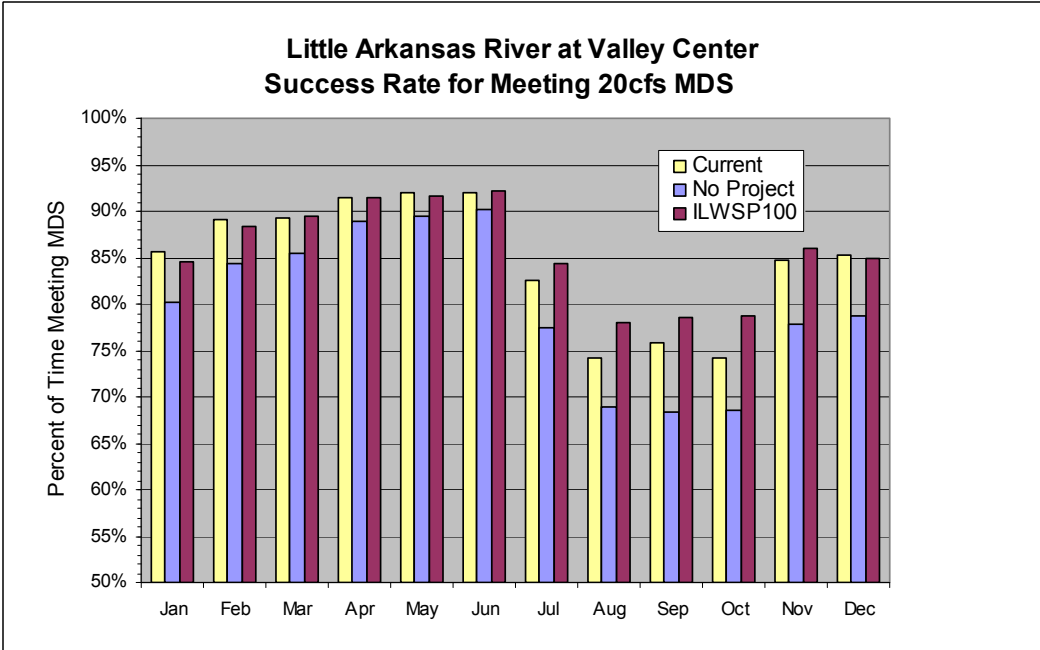
Kansas has established a minimum desirable streamflow (MDS) of 20 cfs for all months at this location. Simulated median monthly flows with the project in place are greater than the MDS. Simulated daily discharge with the project is anticipated to exceed this MDS 74 percent to 92 percent of the time, depending on month. Implementation of the project will increase the probability of streamflows meeting or exceeding the MDS as compared to without project.

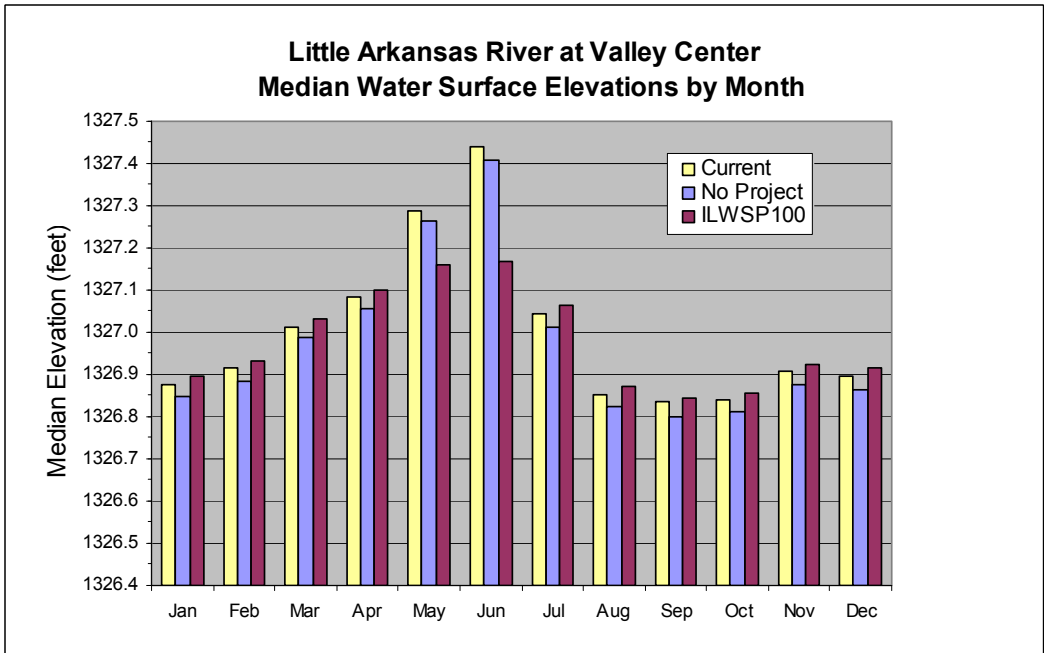
The Kansas Department of Wildlife and Parks (KDWP) has recommended higher minimum flow values of 60 cfs in April, May, and June; and 34 cfs for the remaining months. The success rates for meeting those flows with the project in place will be greater than those without the project, varying from 51 percent in December to 74 percent in June.



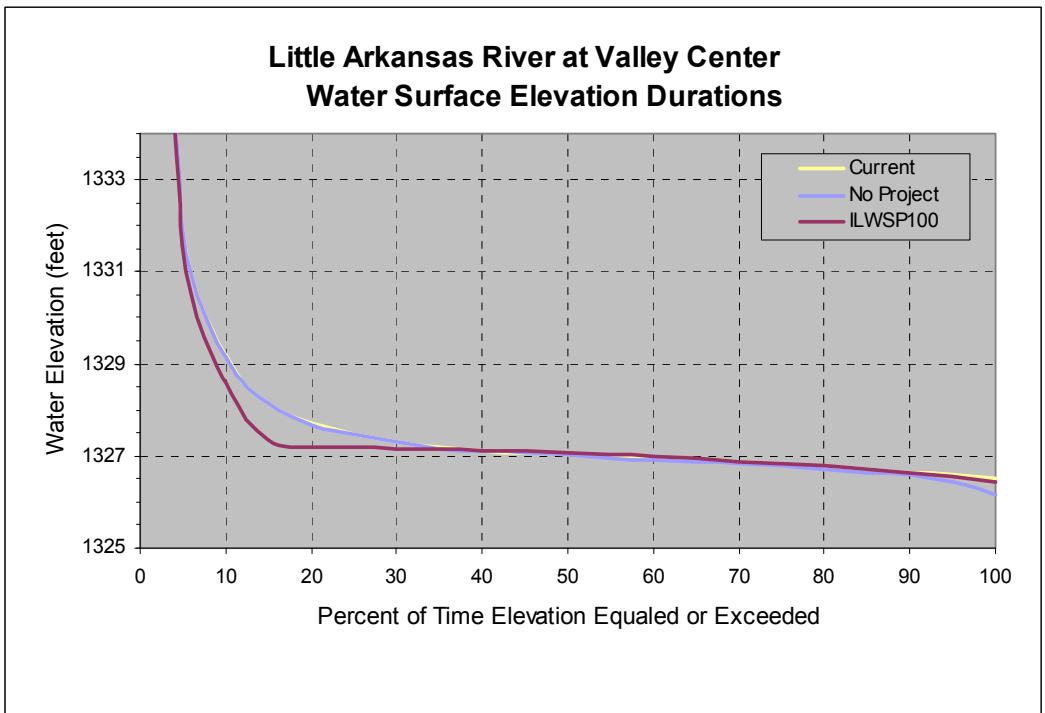
Little Arkansas River at Valley Center Median Flow by Month (cfs)													
	Jan	Feb	Mar	Apr	May	Jun	Jul	Aug	Sep	Oct	Nov	Dec	
No Project	41.2	45.9	59.0	67.8	97.0	119.0	62.4	38.2	35.1	36.5	44.9	43.5	
ILWSP100	47.2	52.2	64.8	73.7	81.3	82.7	68.8	44.2	40.6	42.3	50.8	50.1	
Difference	6.0	6.3	5.7	5.9	-15.6	-36.3	6.4	6.0	5.5	5.8	5.9	6.6	





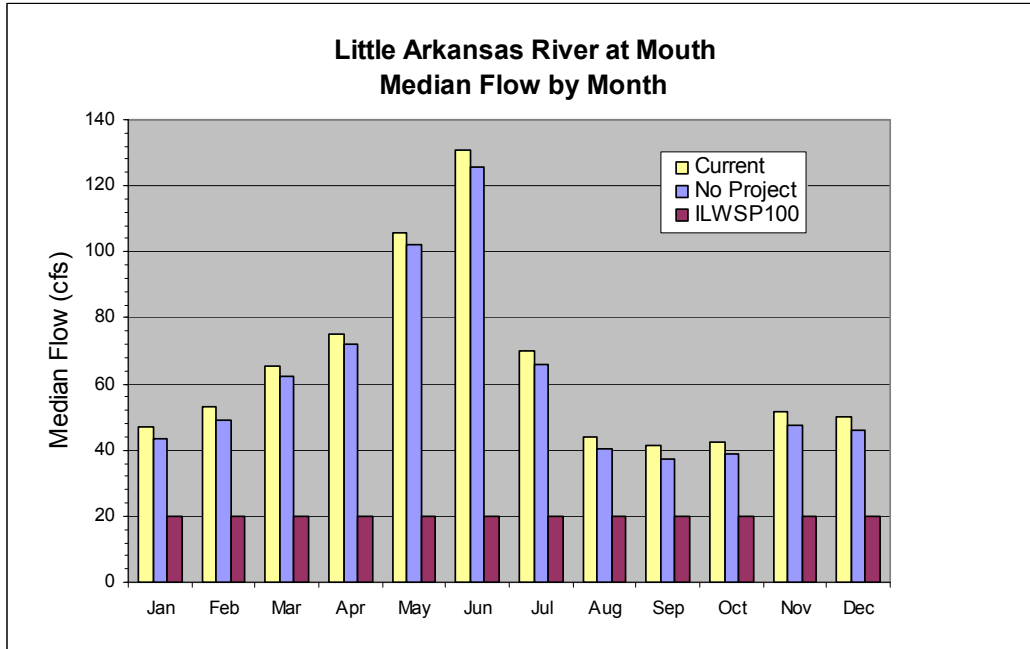


Little Arkansas River at Valley Center Median Water Surface Elevation by Month (feet)													
	Jan	Feb	Mar	Apr	May	Jun	Jul	Aug	Sep	Oct	Nov	Dec	
No Project	1326.8	1326.9	1327.0	1327.1	1327.3	1327.4	1327.0	1326.8	1326.8	1326.8	1326.9	1326.9	1326.9
ILWSP100	1326.9	1326.9	1327.0	1327.1	1327.2	1327.2	1327.1	1326.9	1326.8	1326.9	1326.9	1326.9	1326.9
Difference	0.0	0.0	0.0	0.0	-0.1	-0.2	0.0	0.0	0.0	0.0	0.0	0.0	0.1

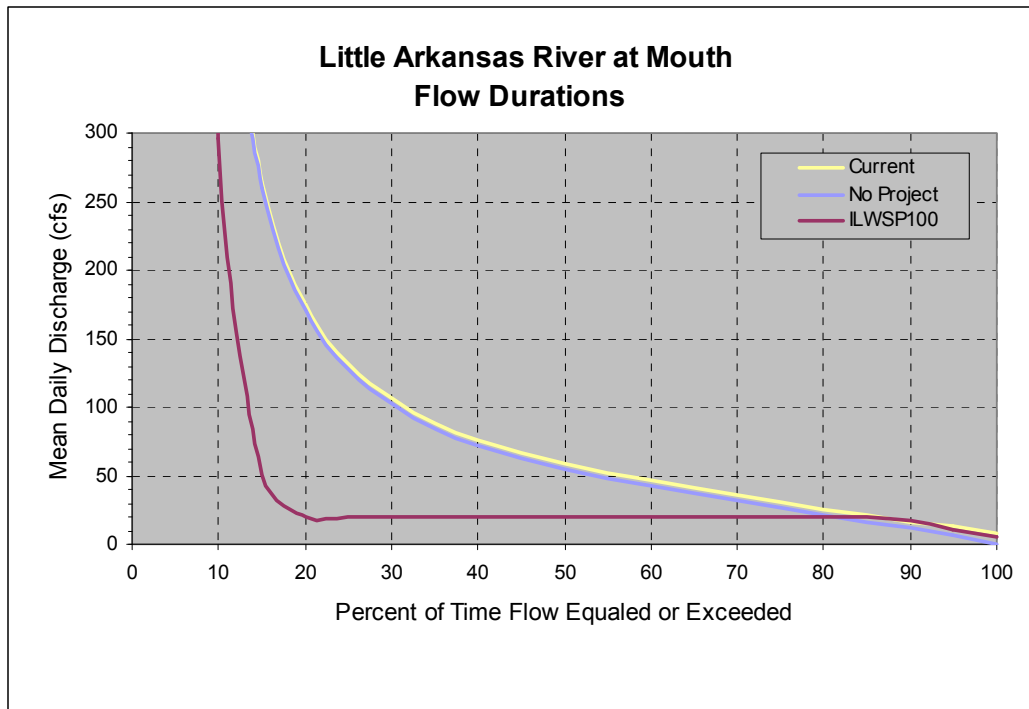


Little Arkansas River at Mouth –

The most significant changes to flows affected by the ILWSP are those occurring at the mouth of the Little Arkansas River. In addition to ASR diversion impacts occurring further upstream, the expansion of the Local Well Field will have the most significant impact on streamflow at this location. The expansion is proposed to divert up to 45 MGD (about 70 cfs) from the Little Arkansas River. Those diversions will be limited to those periods when flow in the river at this location is above 20 cfs. Therefore, with the project in place, the median monthly discharge for all months is anticipated to be 20 cfs. This results in reductions of monthly median discharge ranging from 17 to 106 cfs versus no-project conditions. Simulated daily flow durations indicate that for 80 percent of the time, discharge at this location will be significantly less than without project.



Little Arkansas River at Mouth												
Median Flow by Month (cfs)												
	Jan	Feb	Mar	Apr	May	Jun	Jul	Aug	Sep	Oct	Nov	Dec
No Project	43.5	48.9	62.4	71.9	102.1	125.9	65.8	40.3	37.1	38.8	47.5	46.0
ILWSP100	20.0	20.0	20.0	20.0	20.0	20.1	20.0	20.0	20.0	20.0	20.0	20.0
Difference	-23.5	-28.8	-42.4	-51.9	-82.1	-105.8	-45.8	-20.3	-17.1	-18.8	-27.5	-26.0

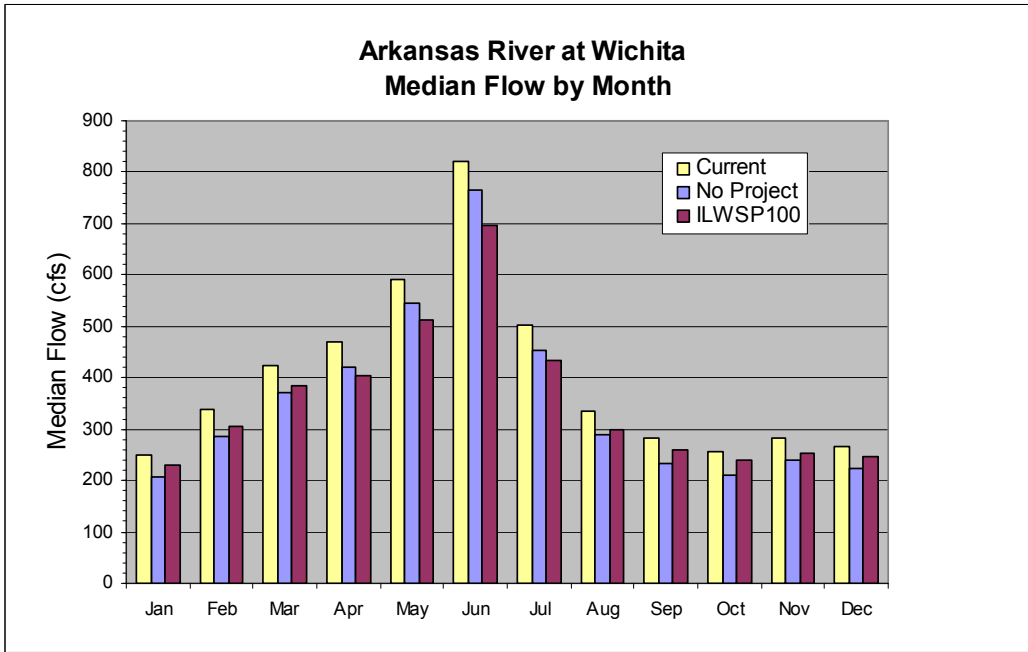


Arkansas River at Wichita -

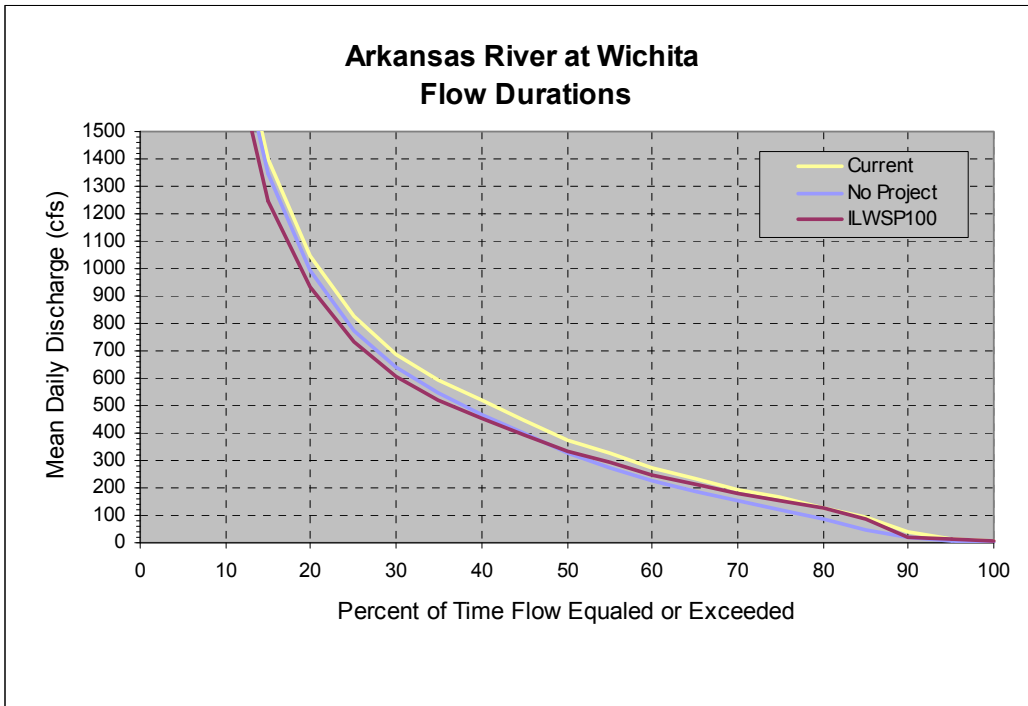
This location represents the USGS streamflow gauging station located just downstream from the confluence of the Arkansas and Little Arkansas Rivers. Therefore, impacts to stream discharge at this location are a culmination of several ILWSP impacts to the Little Arkansas and Arkansas Rivers. These impacts include:

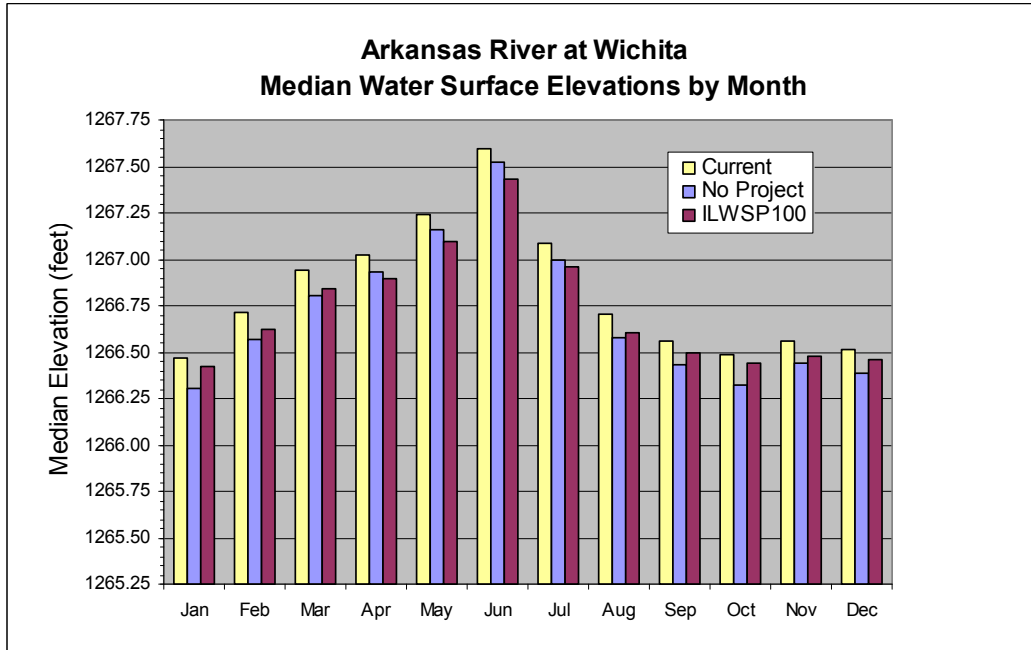
- Induced infiltration from the Arkansas River resulting from redevelopment of the Bentley Reserve Well Field.
- Changes in stream/aquifer interaction rates between the Equus Beds Aquifer and the Little Arkansas and Arkansas Rivers.
- Induced infiltration from the Arkansas River resulting from operation of the existing Local Well Field.
- Diversions from the Little Arkansas River for recharge of Equus Beds Aquifer.
- Induced infiltration from the Little Arkansas due to operation of the expanded Local Well Field.

With relatively greater discharge at this location, the impacts from diversions are a smaller percentage of overall discharge. Simulated flow duration curves indicate that during lower flow periods, flows with the project will be generally higher than without project. Conversely, during higher discharge periods, flows with the project will be generally lower than without project. Water surface elevations are anticipated to only vary within approximately 0.1 feet from without project conditions to with project.

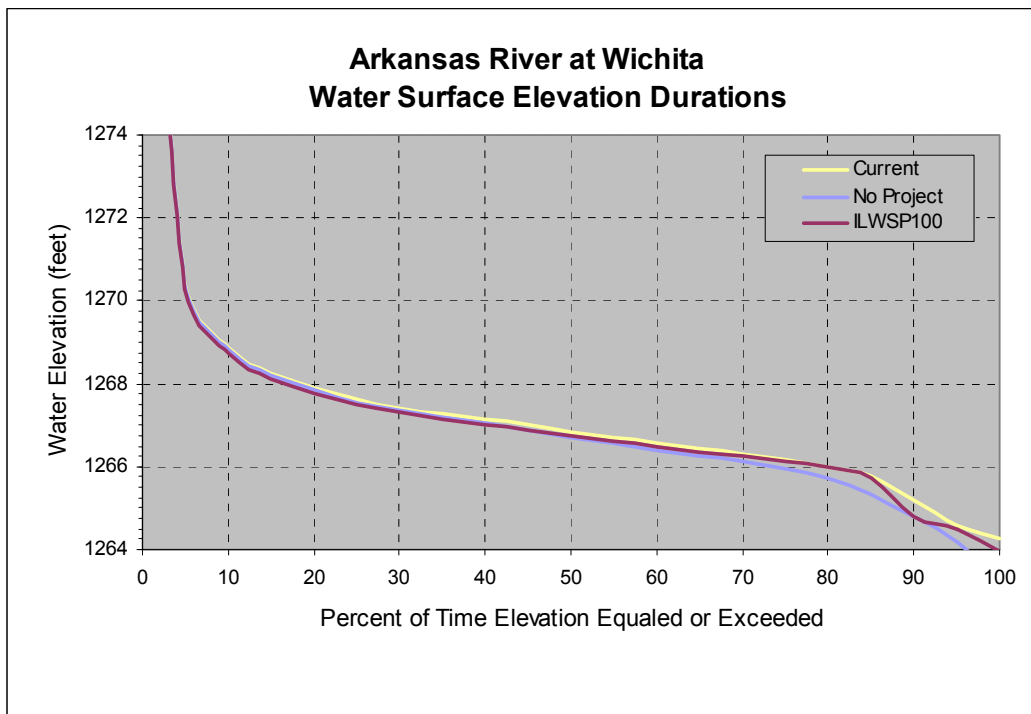


Arkansas River at Wichita Median Flow by Month (cfs)												
	Jan	Feb	Mar	Apr	May	Jun	Jul	Aug	Sep	Oct	Nov	Dec
No Project	205.5	286.8	372.0	419.5	544.2	764.7	454.5	288.9	234.6	209.8	238.1	223.4
ILWSP100	231.4	306.8	385.9	405.1	511.0	697.0	434.9	299.7	258.8	240.0	252.6	247.5
Difference	25.9	20.0	13.9	-14.3	-33.2	-67.7	-19.6	10.8	24.1	30.2	14.4	24.1





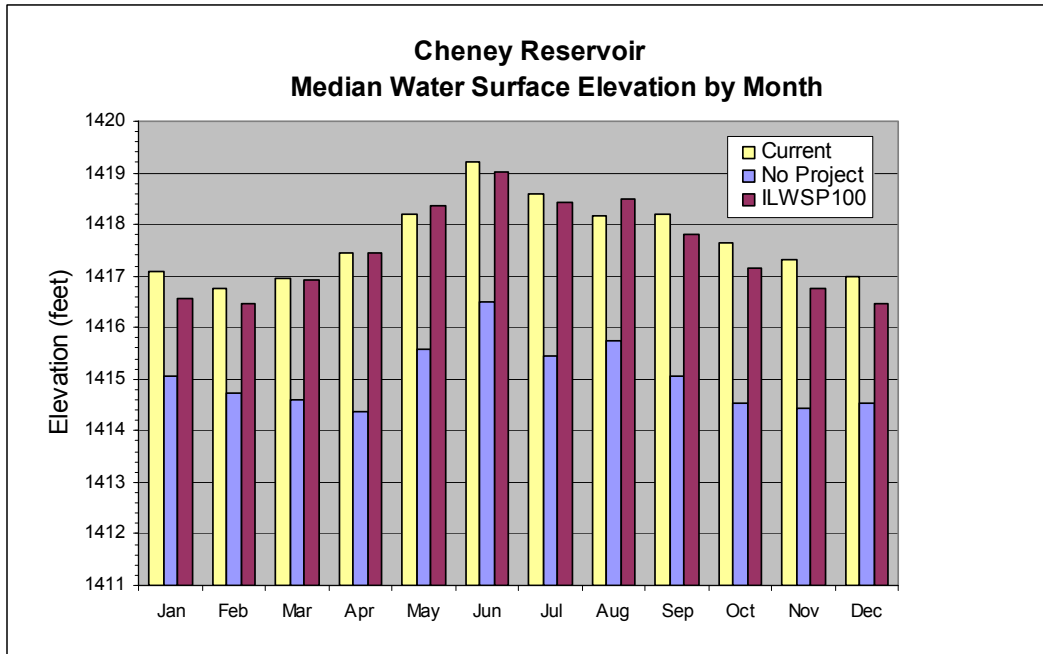
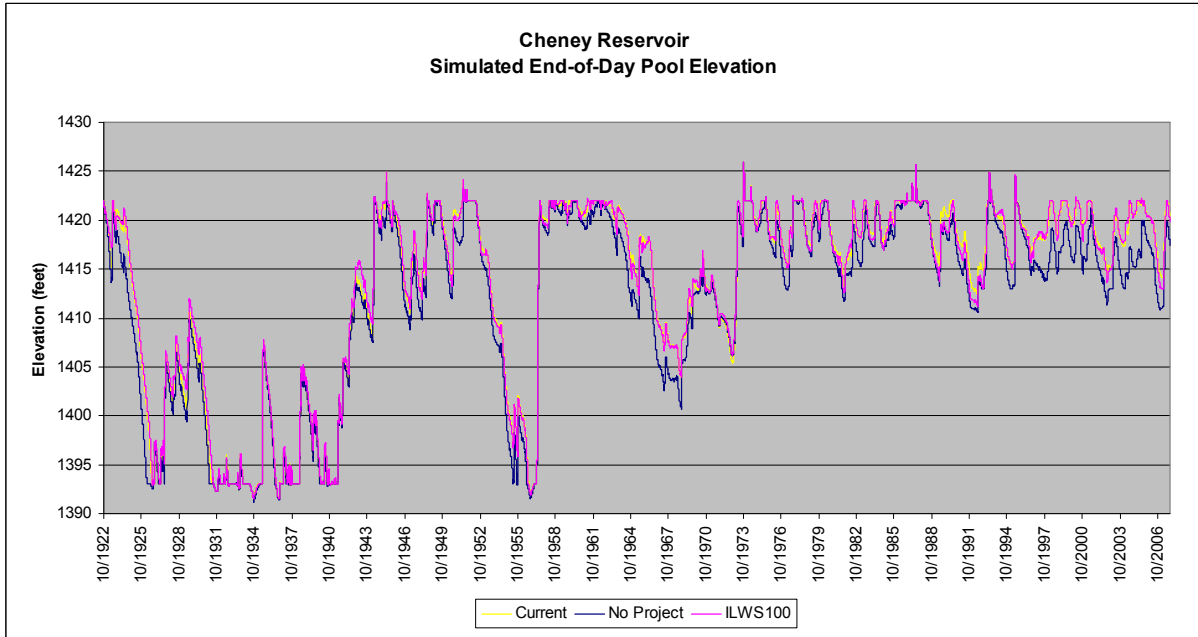
Arkansas River at Wichita												
Median Water Surface Elevation by Month (feet)												
	Jan	Feb	Mar	Apr	May	Jun	Jul	Aug	Sep	Oct	Nov	Dec
No Project	1266.3	1266.6	1266.8	1266.9	1267.2	1267.5	1267.0	1266.6	1266.4	1266.3	1266.4	1266.4
ILWSP100	1266.4	1266.6	1266.8	1266.9	1267.1	1267.4	1267.0	1266.6	1266.5	1266.4	1266.5	1266.5
Difference	0.1	0.1	0.0	0.0	-0.1	-0.1	0.0	0.0	0.1	0.1	0.0	0.1



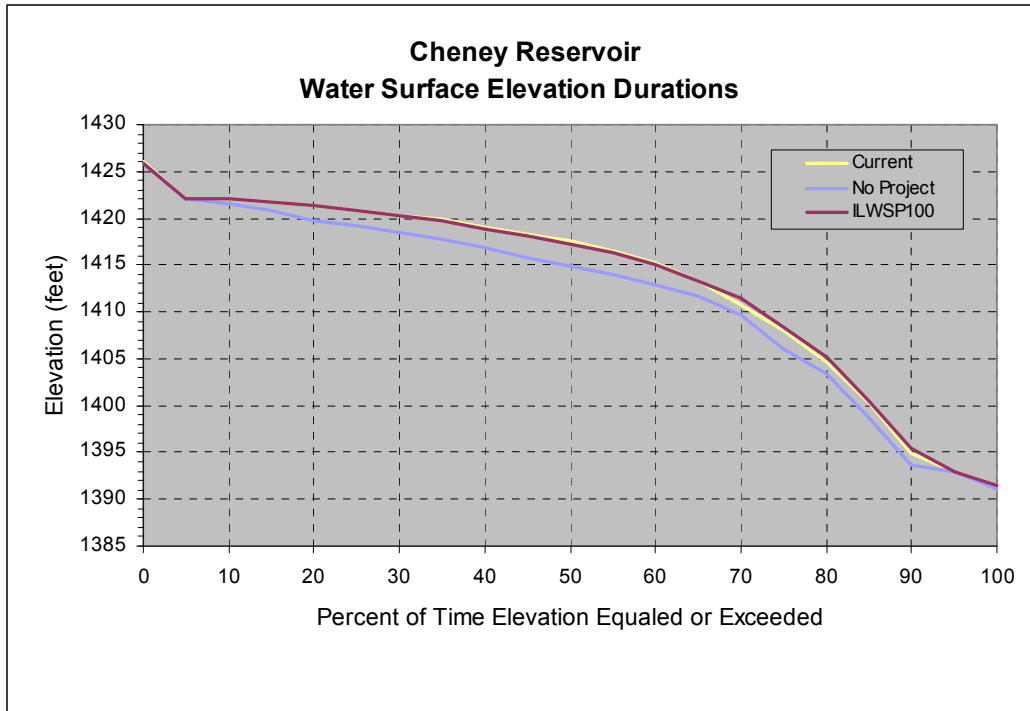
Cheney Reservoir -

The primary purpose of Cheney Reservoir is to provide a supply of water to Wichita. Without the project, increasing future demands will incur the operation of the reservoir at lower elevations. During drought

periods, the demands on the reservoir will deplete the usable supply. With project implementation, there will be, generally, less of a demand on the reservoir as more of the demand can be shifted to aquifer storage. This will result in higher pool elevations of 1.5 to 3 feet over no-project conditions.

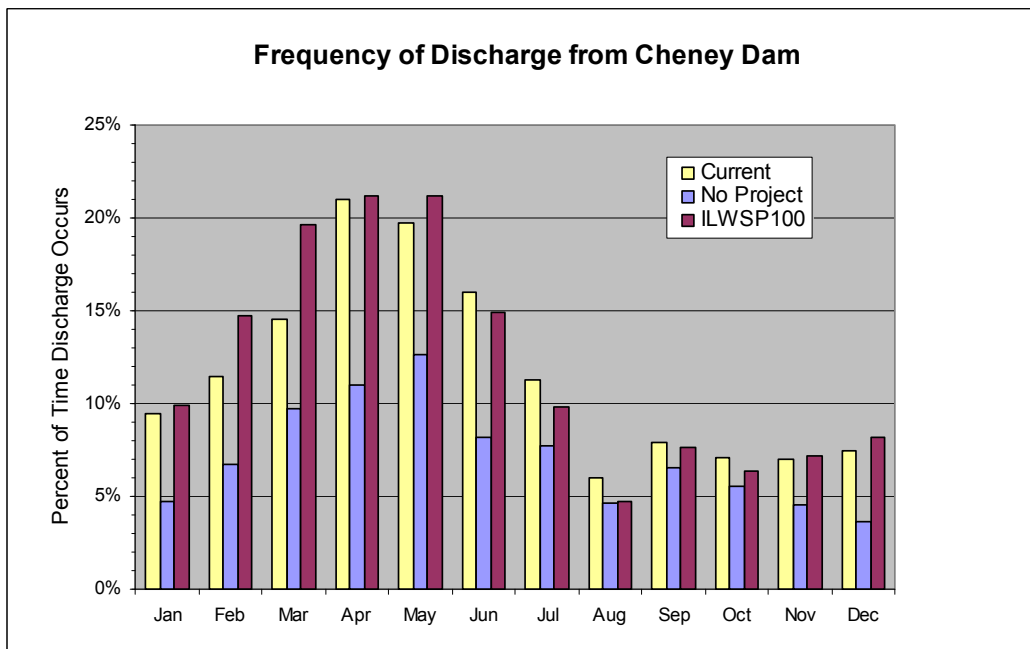


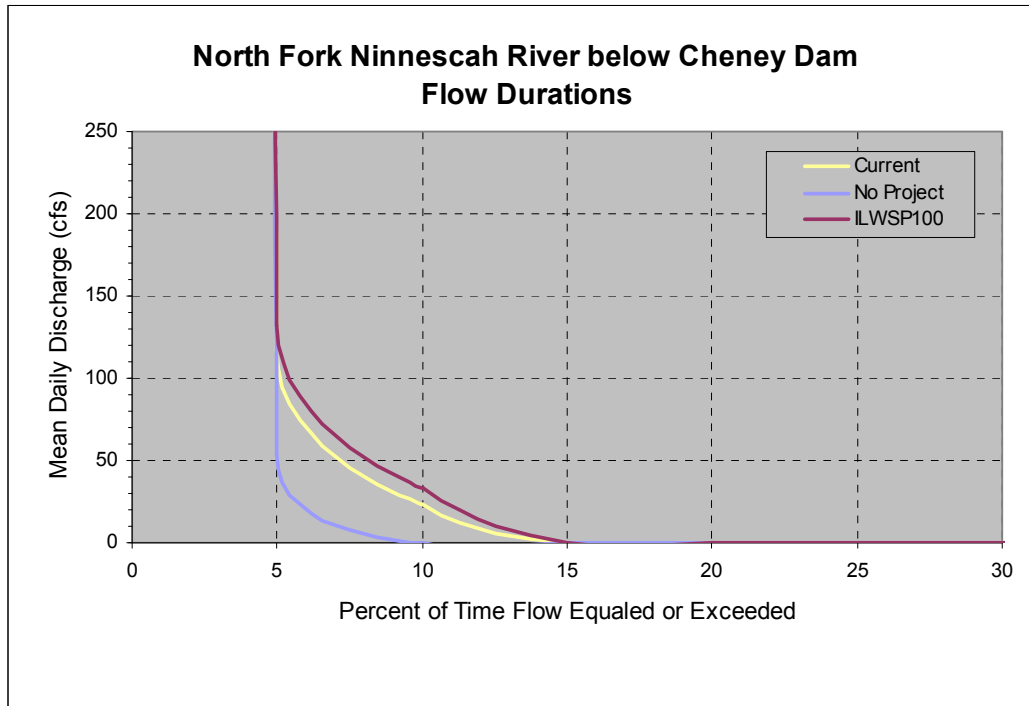
Cheney Reservoir												
Median Pool Elevation by Month (feet)												
	Jan	Feb	Mar	Apr	May	Jun	Jul	Aug	Sep	Oct	Nov	Dec
No Project	1415.1	1414.7	1414.6	1414.4	1415.6	1416.5	1415.5	1415.8	1415.1	1414.5	1414.4	1414.5
ILWSP100	1416.6	1416.5	1416.9	1417.4	1418.4	1419.0	1418.4	1418.5	1417.8	1417.1	1416.8	1416.5
Difference	1.5	1.8	2.3	3.1	2.8	2.5	3.0	2.7	2.8	2.6	2.3	1.9



North Fork Ninescah River below Cheney Reservoir -

There are no minimum release requirements from Cheney Reservoir. Therefore, releases generally only occur after significant runoff events and when the conservation pool in the reservoir is full (elevation 1421.6 feet). Without the implementation of the project, releases and spills from Cheney Reservoir will occur less frequently since Wichita will be utilizing more of the conservation storage in the reservoir. Will the project in place, there will be less demand on Cheney, resulting in greater storage in the reservoir and more frequent release events to the North Fork Ninescah River.





Ninescah River near Peck -

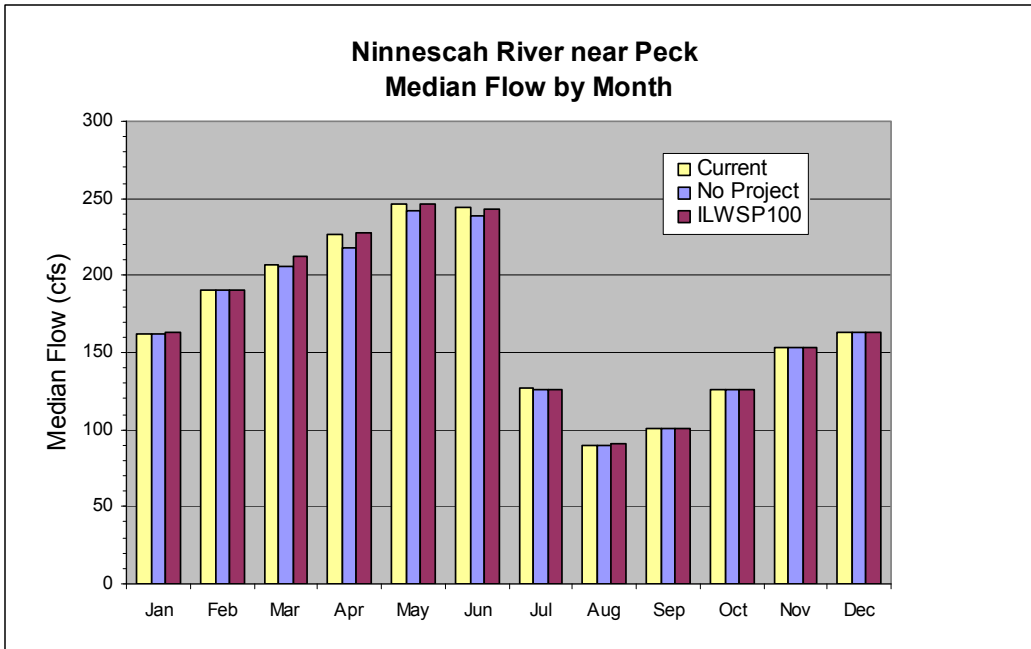
Project impacts to stream discharge at this location are those produced by changes in releases from Cheney Reservoir. The releases from Cheney make up only a small portion of the total stream discharge at this location. Therefore, project impacts are relatively small compared to total discharge.

Implementation of the project may result in increases in discharge of up to 9 cfs created by increasing spills from the reservoir over no-project conditions. But for a majority of the time, discharge would be about the same as without project.

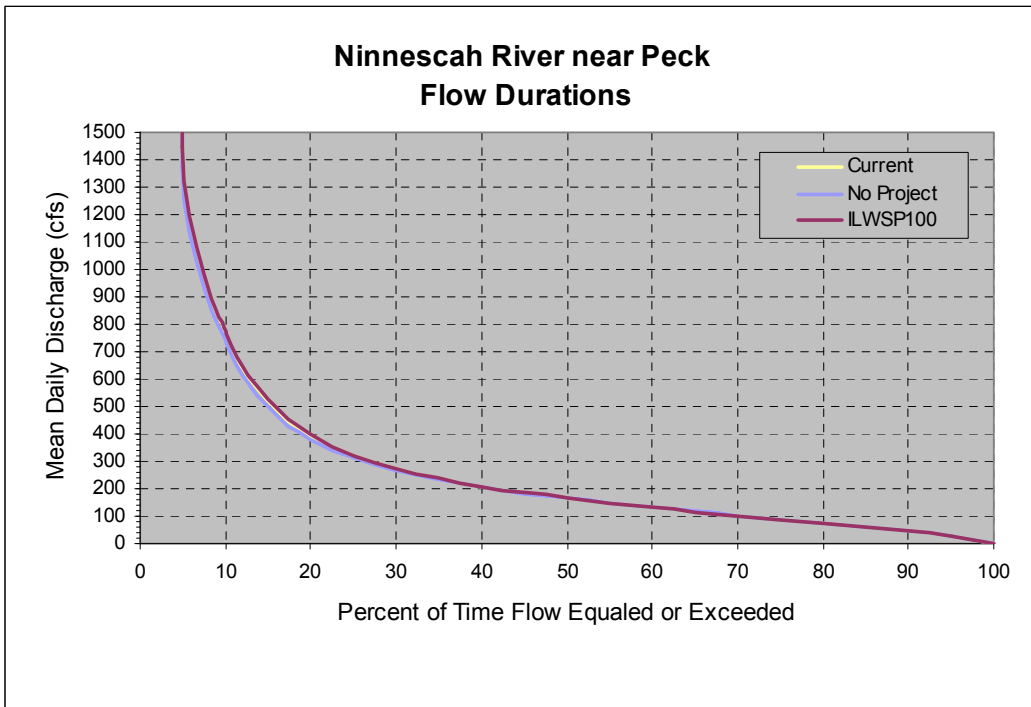
The KWO has established the MDS at this location to be:

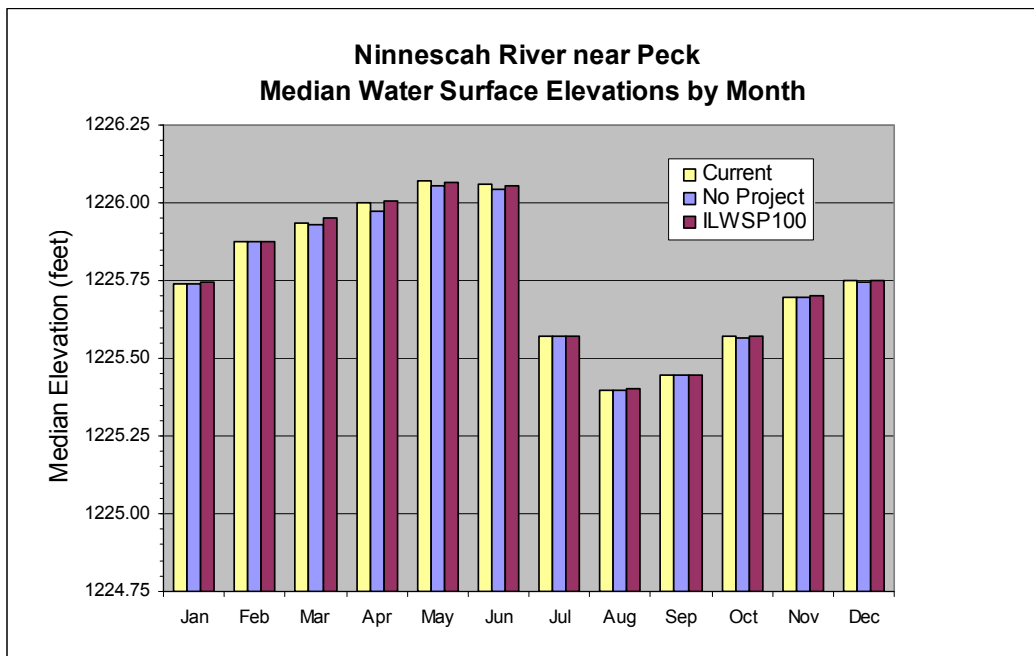
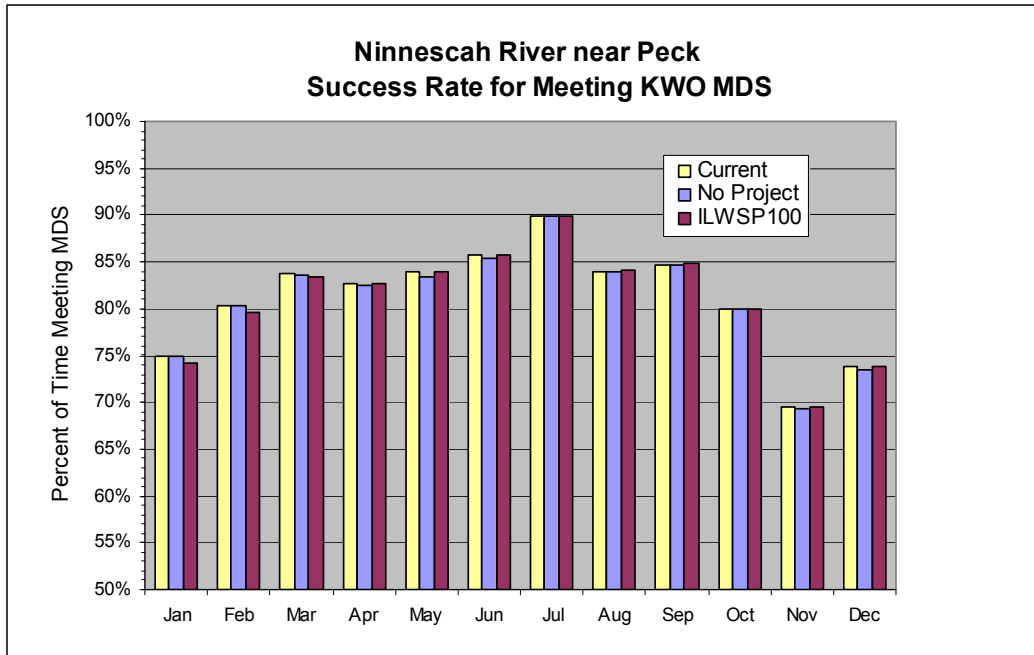
- 100 cfs in November through May
- 70 cfs in June
- 30 cfs in July through September
- 50 cfs in October

The percentage of time that these MDS values will be met will vary little between with or without project conditions.



Ninnescah River near Peck Median Flow by Month (cfs)												
	Jan	Feb	Mar	Apr	May	Jun	Jul	Aug	Sep	Oct	Nov	Dec
No Project	161.7	190.0	206.1	218.4	241.5	238.5	126.2	90.1	100.4	125.7	153.2	163.4
ILWSP100	162.6	190.8	212.3	227.2	245.9	242.7	126.4	90.7	100.5	126.1	153.7	163.7
Difference	0.9	0.9	6.2	8.8	4.4	4.2	0.2	0.6	0.2	0.4	0.5	0.3

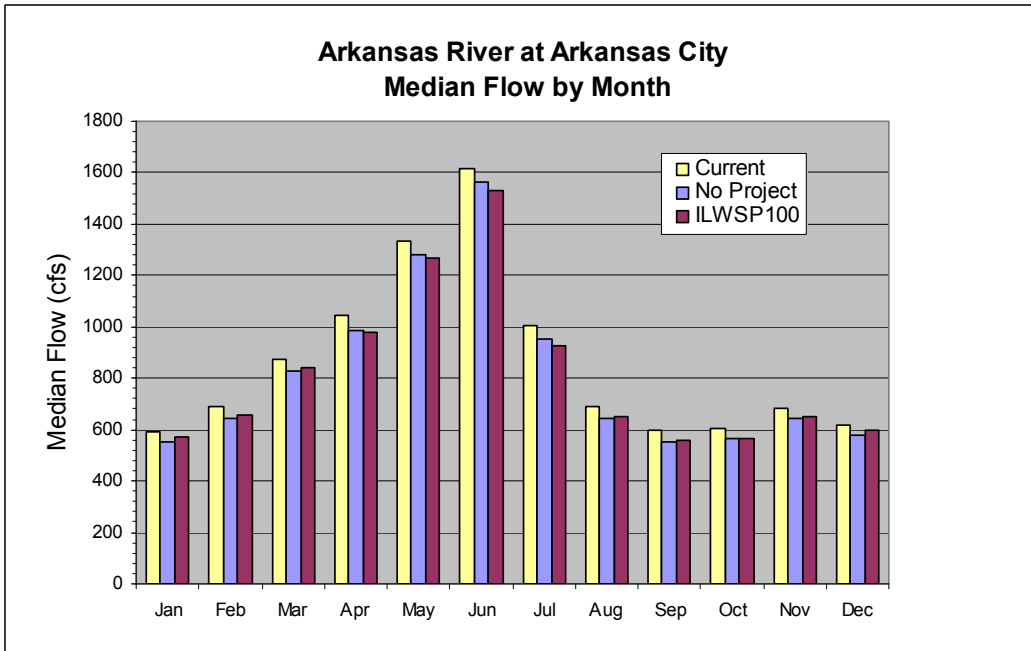




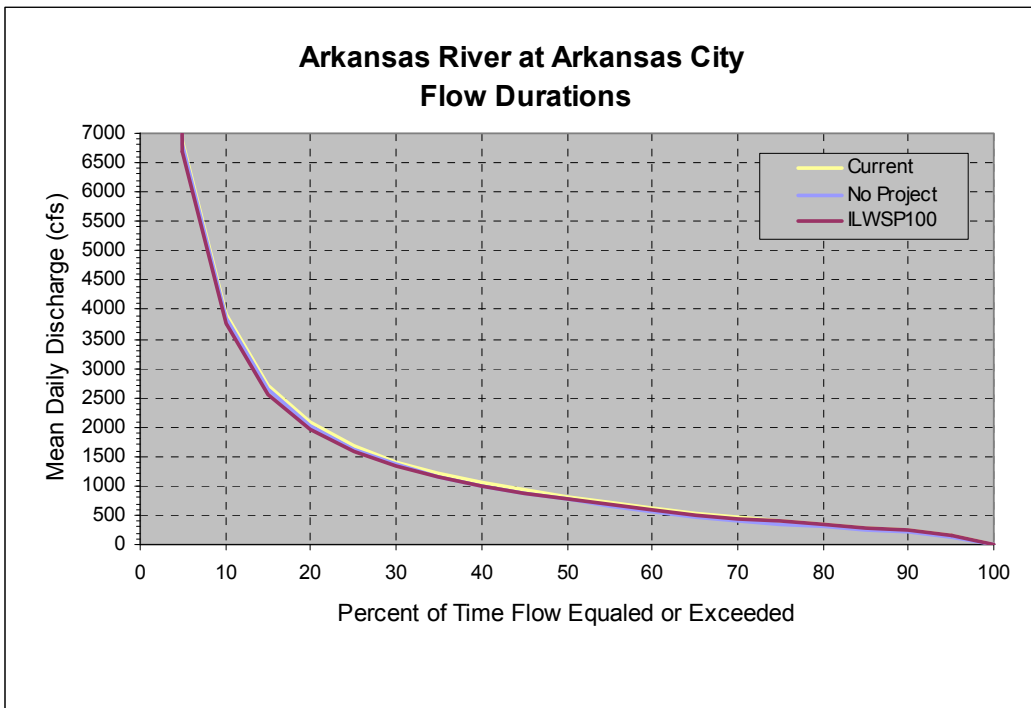
Arkansas River at Arkansas City -

This station is located near the Kansas- Oklahoma state line, approximately 24 miles downstream from the confluence of the Ninnescah and Arkansas Rivers. Discharge at this location would reflect the net impacts from the total ILWS project.

Due to its distance from the project area, and the intervening streamflow gains, the effects of the project on total discharge at this location are relatively small. Simulated median monthly flows suggest that during the peak flow month of June, discharge at this location could be 36 cfs less with implementation of project versus without project. This is approximately 2 percent of the median discharge for that month.



Arkansas River at Arkansas City Median Flow by Month (cfs)														
	Jan	Feb	Mar	Apr	May	Jun	Jul	Aug	Sep	Oct	Nov	Dec		
No Project	551.8	646.4	827.1	986.2	1284.1	1564.2	952.1	642.9	552.3	562.3	641.0	577.1		
ILWSP100	572.6	659.6	841.6	978.9	1267.3	1528.5	927.1	650.0	561.0	567.8	648.7	598.3		
Difference	20.8	13.2	14.5	-7.3	-16.7	-35.7	-25.1	7.2	8.7	5.5	7.7	21.2		



Attachment A

Supplemental Information on RESNET Operations Model

OPERATIONS MODEL

This appendix documents the computer model that has been developed to simulate operation of the City of Wichita’s Integrated Local Water Supply (ILWS) Plan. This operations model was used initially to help with the conceptual design of the ILWS system; it was later used to quantify potential hydrologic impacts for the project’s environmental impact statement (EIS).

The operations model for the ILWS system was developed using Burns & McDonnell’s Reservoir Network (RESNET) simulation model (Foster, 1989). This computer model represents the stream/reservoir system being simulated as a circulating network. This network representation allows the RESNET model to efficiently determine an optimum solution for each daily time step using least-cost network optimization techniques. This architecture makes it possible for RESNET to simulate systems of virtually unlimited complexity. The optimum network solution determined by the model each day represents a water balance for the ILWS system. This process is repeated for each day during the 85-year model simulation period (water years [WY] 1923–2007). Discussed below are the model’s setup and input data, operating assumptions, and output data.

1 Model Setup and Input Data

The ILWS operations model uses the following types of hydrologic data:

- Historical mean daily stream discharge estimates at selected points within the project area
- Historical monthly reservoir evaporation rates
- Available storage and other physical data for Cheney Reservoir and the Equus Beds Aquifer
- City’s current and projected water demands
- Irrigation demands for agriculture in the Equus Beds Well Field area
- Minimum desirable streamflow requirements
- Supply capability, operating parameters, and preferred allocation order for all current and potential water supply sources

These input data and operating assumptions are discussed in later sections. The ILWS system is represented in the operations model as a network of nodes with connecting links. A schematic of the overall operations model network is shown in Figure 1. Each of the components of the ILWS model is described further below.

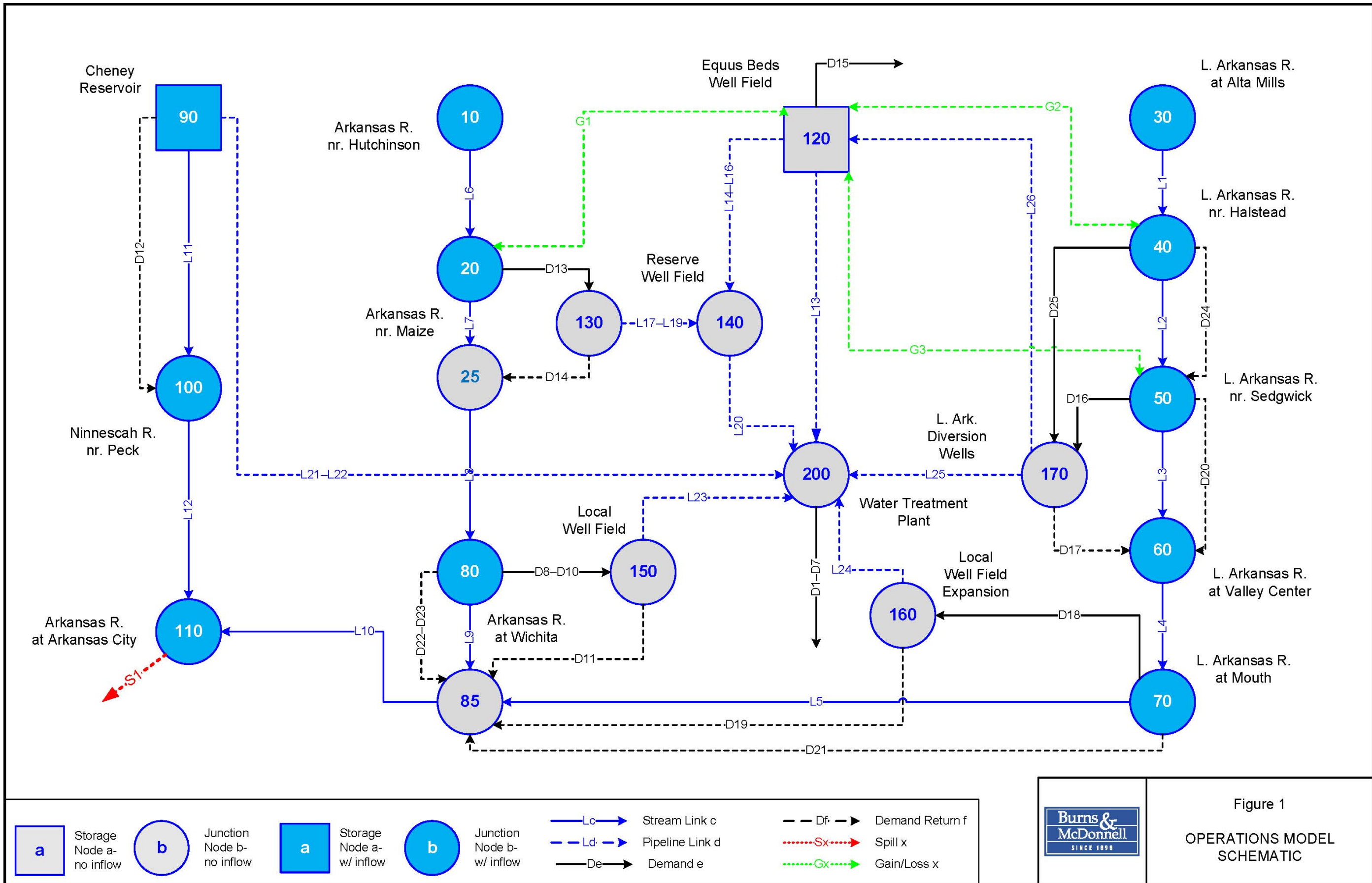


Figure 1
OPERATIONS MODEL
SCHEMATIC

The RESNET model utilizes a Microsoft Access database file for storage of all model input and output data. The individual data tables used by the model are listed below in alphabetical order along with a brief description of their contents.

- tblRnAreaCapacity — Elevation-area-storage-leakage rate data for each model reservoir
- tblRnDemand — Input data for each model demand
- tblRnDemandData — Annual distribution data for applicable demands
- tblRnDemandOperations — Daily demand volumes and other related output data
- tblRnDischargeSummary — Daily discharge below selected stream nodes
- tblRnError — RESNET error messages
- tblRnEvapData — Daily net evaporation data for applicable reservoirs
- tblRnEvapStation — Station identification for evaporation data in tblRnEvapData table
- tblRnFlowData — Daily unregulated inflow data for applicable model nodes
- tblRnFlowStation — Station identification for flow data in tblRnFlowData
- tblRnGageRating — Rating table data for stream nodes located at USGS gages
- tblRnImport — Data for each model import
- tblRnImportData — Annual distribution data for applicable imports
- tblRnLink — Input data for each model link
- tblRnLinkOperations — Daily link flow rates and other related output data
- tblRnModel — Base data that identifies each unique model alternative
- tblRnNetworkArcDump — Dump of network arc data when RESNET cannot find a feasible solution
- tblRnNetworkNodeDump — Dump of network node data when RESNET cannot find a feasible solution
- tblRnNode — Input data for each model node
- tblRnNodeOperations — Daily water balance for each node
- tblRnReservoir — Input data for each model reservoir
- tblRnReservoirLevel — Level/priority data for each model reservoir
- tblRnReservoirOperations — Daily storage and related output data for each reservoir
- tblRnSpill — Input data for each model spill node
- tblRnStorageSummary — Daily end-of-day storage in Cheney Reservoir and Equus Beds aquifer
- tblRnSupplySummary — Daily summary of each supply source’s contribution toward meeting City’s raw water demand
- tblRnWSElevSummary — Estimates of mean daily water surface elevations at four stream nodes plus daily end-of-day pool elevation and area for Cheney Reservoir

1.1 Model Data

Each unique ILWS alternative is represented by a single record in the model table (tblRnModel). The fields in this table are described below. In Table 1 and similar tables that follow, spaces have been added to the field names to improve readability.

Table 1: Data Fields in Model Table (tblRnModel)

Field Name	Description
ID	Unique record identifier assigned by system. This field contains the model ID that is used to identify each alternative model run.
Name	Short descriptive name for each alternative model run

Description	Description of model run
Start Date	Start date for model run (mm/dd/yyyy)
End Date	End date for model run (mm/dd/yyyy)
No Decimals	Requested precision for model results. The RESNET model uses acre-feet as its base volumetric unit so if this value is one the model will estimate volumes to nearest one tenth of an acre-foot.
Save Operations	True/false flag that indicates if detailed daily output data should be stored
No Zones	Should be zero for all ILWS model runs
Failure Probability	Not used by ILWS model
Primary Dmd Shortages	Number of days during simulation period with shortage in any primary demand
Source Model ID	Used for model cloning only

1.2 Model Nodes

The majority of the model nodes used in the operations model represent locations on project area streams, which include the Arkansas, Little Arkansas, North Fork Ninnescah and Ninnescah rivers. The remainder of the model nodes represent off-stream features, such as well fields, treatment plants and pipeline junctions. Each of these nodes is listed in Table 2.

Table 2: ILWS Model Nodes

Node Nos.	Name	Description	Unregulated Inflow?
10	Arkansas R. near Hutchinson	Located at USGS stream gage of same name. In model domain, most upstream node on Arkansas River.	Yes
20	Arkansas R. near Maize	Located at USGS stream gage of same name. Assumed supply source for Reserve Well Field and gains/losses to Equus Beds aquifer.	Yes
25	Arkansas R. below Maize	Located immediately downstream of Node No. 20	No
30	L. Arkansas R. at Alta Mills	Located at USGS stream gage of same name. In model domain, most upstream node on Little Arkansas River.	Yes
40	L. Arkansas R. near Halstead	Located at approximate position of Phase 1 intake. Assumed supply source for half of recharge diversion wells.	Yes
50	L. Arkansas R. near Sedgwick	Located at USGS stream gage of same name. Assumed supply source of surface water intake and balance of recharge diversion wells.	Yes
60	L. Arkansas R. at Valley Center	Located at USGS stream gage of same name.	Yes
70	L. Arkansas R. at Mouth	Located at mouth of Little Arkansas River.	Yes

80	Arkansas R. at Wichita	Located at USGS stream gage of same name. Assumed supply source for existing Local (E&S) Well Field.	Yes
85	Arkansas R. below Wichita	Located immediately downstream of Node No. 80	No
90	Cheney Reservoir	A storage node located on the North Fork Ninescah River at Cheney Dam.	Yes
100	Ninescah R. near Peck	Located at USGS stream gage of same name.	Yes
110	Arkansas R. at Arkansas City	Located at USGS stream gage of same name. Most downstream node in model domain.	Yes
120	Equus Beds Aquifer/Well Field	Storage node that represents Equus Beds Aquifer.	No
130	Reserve Well Field	Node that represents the total supply available from the Bentley Reserve Well Field. This well field is modeled as a direct surface water diversion (that is, aquifer storage is ignored and pumping is assumed to induce immediate and equal infiltration from the Arkansas River).	No
140	Reserve Well Field Junction	Junction node for supplies from Equus and Reserve Well Fields.	No
150	Local Well Field	Located along Arkansas River in downtown Wichita. This node represents the combined supply available from the existing Local (E&S) Well Fields. This well field is modeled like a direct, surface water diversion from the Arkansas River.	No
160	Local Well Field Expansion	Located along the Little Arkansas River in downtown Wichita. This node represents the combined supply available from the proposed Local Well Field Expansion. This well field is modeled as a direct, surface water diversion from the Little Arkansas River.	No
170	L. Arkansas R. Intake/Diversion Wells	Located along the Little Arkansas River. This node represents the combined supply available for aquifer recharge from the proposed surface intake and alluvial diversion wells. Pumping at the diversion wells is assumed to induce immediate infiltration from the Little Arkansas River.	No
200	Water Treatment Plant	Located at Wichita's main water treatment plant near the confluence of the Arkansas and Little Arkansas rivers. All raw water supplied to the City is assumed to flow through this node.	No

As noted in Table 2, slightly more than half of these nodes have unregulated inflow. These nodes are shown in blue in Figure 1. Unregulated inflow is surface runoff that enters tributary stream(s) above a node but below any upstream nodes. The methodology used to estimate unregulated inflow is described in a separate appendix (Burns & McDonnell, 2008c).

The node data for each model run is stored in an Access table named tblRnNode. The data fields in this table are listed in Table 3.

1.3 Model Storage Nodes

Two of the nodes in the operations model are storage nodes, or reservoirs: Cheney Reservoir (Node No. 90) and Equus Beds Aquifer (Node No. 120). Unlike non-storage nodes, these nodes have the ability to retain water from one time step to the next. In RESNET, a reservoir’s storage is divided into levels with each level having a defined storage priority. Levels with the highest priority are filled first when water is

Table 3: Data Fields in Node Table (tblRnNode)

Field Name	Description
ID	Unique record identifier assigned by system. This field contains the node IDs that are used to identify the nodes in each alternative model run.
Model ID	Identifier (ID) for corresponding model in Model table (tblRnModel)
Number	Node number. Used as shorthand identifier for each node only.
Name	Short node name
Description	Description of node
Flow Station ID	If this node has unregulated inflow, the applicable flow station ID. Otherwise, this field will be null.
Source Node ID	Used for cloning only

available and used last when water from storage is required to meet demands. These priorities define the unit benefit of having water stored in each level. The defined reservoir levels for Cheney Reservoir and the Equus Beds Aquifer are listed in Table 4.

Table 4: ILWS Reservoir Storage Levels

Level No.	Cheney Reservoir		Equus Beds Aquifer	
	Storage (acre-feet)	Storage Priority	Storage Deficit (acre-feet)	Storage Priority
1	1,140	999	-643,000	999
2	2,000	990	-200,000	770
3	4,000	980	-114,000	760
4	8,000	960	-103,200	750
5	10,000	950	-92,400	740
6	15,476	900	-81,600	730
7	24,817	750	-70,800	720
8	37,170	725	-60,000	710
9	53,265	700	-50,000	700
10	73,356	675	-41667	675
11	97,645	650	-33,333	650
12	125,842	350	-25,000	625

13	152,222	300	-16,667	500
14	170,575	100	-8,333	575
15	247,931	1	0	550

When both reservoirs are relatively full, water will be withdrawn from Cheney Reservoir first because it has a lower storage priority (for example, level 12 has a priority of only 350 for Cheney Reservoir but 625 for the Equus Beds Aquifer). This bias attempts to preserve the water stored in the Equus Beds because this water is relatively more expensive. However, once both reservoirs are drawn down further during a prolonged dry period, the storage priorities are coordinated so that both are drawn down at about the same rate.

There are three Access tables that apply to each model reservoir. The data fields for these tables are described in Tables 5, 6 and 7.

Table 5: Data Fields in Reservoir Table (tblRnReservoir)

Field Name	Description
ID	Unique record identifier assigned by system. This field contains the reservoir IDs that are used to identify the reservoirs in each alternative model run.
Node ID	ID for corresponding node in Node table (tblRnNode)
Initial Storage	Initial storage in the reservoir at start of model run (acre-feet)
Evap Station ID	If this reservoir has evaporation losses, the corresponding evaporation station ID in tblRnEvapStation
Loss Node ID 1	For leaky reservoir, the first loss node ID. Null if not applicable.
Loss Node ID 2	For leaky reservoir, the second loss node ID. Null if not applicable
Loss Node ID 3	For leaky reservoir, the third loss node ID. Null if not applicable
BOC Storage	Reservoir storage at bottom of conservation pool (acre-feet). Not used for ILWS operations model
TOC Storage	Reservoir storage at top of conservation pool (acre-feet). Not used for ILWS operations model
Base Water Right	Base annual water right (acre-feet). Applicable for Equus Beds only.
Max Recharge	Maximum value for recharge credit account (acre-feet). Applicable for Equus Beds only.
Initial Recharge	Initial value of recharge credit account (acre-feet). Applicable for Equus Beds only.
Min Storage	Output field that reports minimum reservoir storage during model run (acre-feet)
Source Reservoir ID	Used for model cloning only.

Table 6: Data Fields in Reservoir Area-Capacity Table (tblRnAreaCapacity)

Field Name	Description
------------	-------------

ID	Unique record identifier assigned by system.
Reservoir ID	ID for corresponding reservoir in Reservoir table (tblRnReservoir)
Elevation	Reference pool or aquifer elevation for current reservoir (feet NGVD)
Area	Reservoir pool area for current reservoir at specified elevation (acres)
Storage	Reservoir storage for current reservoir at specified elevation (acre-feet)
Loss Rate 1	Reservoir loss rate to loss node 1 (acre-feet/day)
Loss Rate 2	Reservoir loss rate to loss node 2 (acre-feet/day)
Loss Rate 3	Reservoir loss rate to loss node 3 (acre-feet/day)

Table 7: Data Fields in Reservoir Level Table (tblRnReservoirLevel)

Field Name	Description
ID	Unique record identifier assigned by system.
Reservoir ID	ID for corresponding reservoir in Reservoir table (tblRnReservoir)
Level Num	Sequential level number. Used only for more convenient reference
Level Volume	Storage volume for current reservoir at top of specified level (acre-feet)
Priority	Storage priority for specified level

Additional data for the two system reservoirs are described in the following sections.

1.3.1 Cheney Reservoir

Cheney Reservoir is located on the North Fork Ninescah River near Cheney, Kansas. This reservoir has the following defined storage pools:

- Dead pool: 979 acre-feet between elevation 1,367 and 1,378.5 feet NGVD
- Fish & wildlife pool: 14,310 acre-feet between elevation 1,378.5 and 1,392.9 feet NGVD
- Conservation pool: 151,800 acre-feet between elevation 1,392.9 and 1,421.6 feet NGVD
- Flood pool: 80,860 acre-feet between elevation 1,421.6 and 1,429 feet
- Surcharge pool: 451,347 acre-feet between elevation 1,429 and 1,453.4 feet NGVD

Table 8 lists the elevation-area-storage data for Cheney Reservoir.

Table 8: Cheney Reservoir Elevation-Area-Storage Data

Pool Elevation (feet NGVD)	Pool Area (acres)	Pool Storage (acre-feet)
1,367	0	0
1,370	14	13
1,375	107	272
1,380	445	1,545
1,385	808	4,535

1,390	1,504	10,241
1,395	2,333	19,793
1,400	3,291	33,761
1,405	4,530	53,265
1,410	5,785	78,987
1,415	7,293	111,602
1,420	8,976	152,222
1,425	10,788	201,557
1,430	12,835	260,557
1,435	14,949	330,019
1,440	17,466	411,058
1,445	20,631	506,303
1,450	23,387	616,350

As a conventional surface reservoir, Cheney Reservoir is also subject to evaporation losses. The estimated net evaporation rates from Cheney Reservoir are described in a separate appendix (Burns & McDonnell, 2008a). These rates account for the net evaporation losses each day (gross evaporation loss less direct precipitation gain).

1.3.2 Equus Beds Aquifer

The Equus Beds aquifer is modeled similar to a surface water reservoir except it does not have evaporation losses. Natural aquifer recharge was estimated to be 3.2 inches per year by the U.S. Geological Survey. This natural recharge is represented in the operations model as an import to this node (No. 120) of 18,800 acre-feet/year.

The interaction between the Equus Beds aquifer and local streams was evaluated in the MODFLOW groundwater model. Generally, aquifers receive their recharge from precipitation and streams serve as aquifer drains. The outflow from aquifers supports the baseflow in these streams. The Equus Beds aquifer has two streams that are major components of the hydrogeological system. The Arkansas River is generally parallel to the pre-development groundwater flow gradient so the interaction between the aquifer and this river was relatively minor. In contrast, the Little Arkansas River is at the down-gradient edge of the Equus Beds aquifer and generally perpendicular to the predominant groundwater flow direction. Changes in the aquifer groundwater level impact the differential head between the aquifer and streams and can result in significant changes in the volume of flow between the aquifer and streams.

The water budget summary feature in MODFLOW provides an accounting of the total water flow from aquifer to stream and stream to aquifer. These total aquifer-stream interaction flows are discussed in the accompanying groundwater appendix (Burns & McDonnell, 2008b) and repeated in Table 9.

Table 9: Equus Beds Storage Deficit-Gain-Loss Data

Index Well 886 Elevation (feet NGVD)	Storage Deficit (acre-feet)	Total Gain from Rivers (cfs)	Total Loss to Rivers (cfs)	Net Equus Beds Loss Rates (cfs)	
				To Arkansas River	To Little Arkansas River
1,342	429,700	133	23	-116.6	6.6
1,360	289,400	100	38	-72.8	10.8
1,366	242,700	89	43	-58.3	12.3
1,370	211,500	82	44	-50.5	12.5
1,375	172,600	73	48	-38.7	13.7
1,380	133,600	62	53	-24.1	15.1
1,385	94,700	54	60	-11.1	17.1
1,389	63,500	48	68	0.6	19.4
1,390	55,700	46	70	4.1	20.0
1,395	16,800	38	82	20.6	23.4
1,396	9,000	36	85	24.8	24.2
1,402	0	29	99	41.8	28.2

Table 9 lists the total gain and loss data for the Equus Beds aquifer as a function of water level. Initially, it was assumed that all aquifer gains come from the Arkansas River and all losses accrue to the Little Arkansas River but subsequent analyses proved this assumption to be too simplistic. In the ILWS plan and operations model the Arkansas and Little Arkansas rivers are treated as two distinct sources. Therefore, the flow between the aquifer and Arkansas River must be differentiated from the flow between the aquifer and Little Arkansas River. These flows were differentiated through an analysis that is described in the Streamflow Appendix (Burns & McDonnell, 2008c). The last two columns in Table 9 show the resulting distribution of these aquifer losses.

With recognition of this aquifer interaction, the RESNET model was customized for development of the ILWS system operations model by adding the ability to model a leaky reservoir. Leakage rates are entered into the model for each destination node as a function of reservoir storage. These reservoir leakage or loss rates can be negative, indicating an actual gain.

1.4 Model Links

The nodes described above are interconnected in the operations model by a series of model links. These links, which are listed in Table 10, represent both natural stream reaches, and pipelines and other man-made conveyance facilities. These stream and pipeline links are shown respectively as solid or dashed blue lines in Figure 1. Each model link has only one origin node and one terminal node. The flow in these links can travel in only one direction from their origin node to their terminal node. Each link also has a specified minimum and maximum flow rate, expressed in acre-feet/day. Generally, the minimum flow rate for these links is zero but the maximum flow rate is dependent on the link type; natural streams are assigned an arbitrarily large flow rate and pipelines are assigned maximum flow rates based on their flow capacity. The RESNET model uses a least-cost algorithm to find the best solution in each time step. Therefore, each link also has an assigned unit flow cost, which is expressed in arbitrary cost units per acre-foot.

Table 10: ILWS Model Links

Link No.	Origin→ Terminal Node Nos.	Description	Minimum Flow Rate (ac-ft/day)	Maximum Flow Rate (ac-ft/day)	Unit Cost/ ac-ft
L1	30→40	L Arkansas R: Alta Mills–Halstead	0	1,000,000	0
L2	40→50	L Arkansas R: Halstead–Sedgwick	0	1,000,000	0
L3	50→60	L Arkansas R: Sedgwick–Valley Center	0	1,000,000	0
L4	60→70	L Arkansas R: Valley Center–Mouth	0	1,000,000	0
L5	70→80	L. Arkansas R: Mouth–Arkansas R	0	1,000,000	0
L6	10→20	Arkansas R: Hutchinson–Maize	0	1,000,000	0
L7	20→25	Arkansas R: Maize–below Maize	0	1,000,000	0
L8	25→80	Arkansas R, below Maize–Wichita	0	1,000,000	0
L9	80→85	Arkansas R: Wichita–below Wichita	0	1,000,000	0
L10	85→110	Arkansas R: below Wichita–Arkansas City	0	1,000,000	0
L11	90→100	North Fork/Ninnescah R: Cheney Reservoir–Peck	0	1,000,000	0
L12	100→110	Ninnescah/Arkansas R: Peck–Arkansas City	0	1,000,000	0
L13	120→200	Pipeline: Equus Beds WF–WTP	0	349	10
L14	120→140	Pipeline: Equus Beds WF–RWF Junction	0	33	-75
L15	120→140	Pipeline: Equus Beds WF–RWF Junction	0	33	-50
L16	120→140	Pipeline: Equus Beds WF–RWF Junction	0	33	-25
L17	130→140	Pipeline: Reserve WF–RWF Junction	0	11	510
L18	130→140	Pipeline: Reserve WF–RWF Junction	0	11	535
L19	130→140	Pipeline: Reserve WF–RWF Junction	0	11	560
L20	140→200	Pipeline: RWF Junction–WTP	0	132	10
L21	90→200	Pipeline: Cheney Reservoir–WTP	0	144	10
L22	90→200	Pipeline: Cheney Reservoir–WTP	0	101	10
L23	150→200	Pipeline: Local WF–WTP	0	113	30
L24	160→200	Pipeline: Local WF Expansion–WTP	0	138	10
L25	170→200	Pipeline: Intake–WTP	0	0	20
L26	170→120	Pipeline: Intake/Diversion Wells–Equus Beds	0	306.9	30

The data for these model links is stored in an Access table named tblRnLink. The fields in this table are described in Table 11. For most model links, their intended purpose is self explanatory; however, there are a few exceptions that warrant additional explanation. These special cases are discussed below.

1.4.1 Bentley Reserve Well Field

The Bentley Reserve Well Field is located in the alluvium of the Arkansas River so pumping from this well field will induce infiltration of relatively saline water from the Arkansas River. To avoid excessive quality impacts to the City’s water supply, the operations model is configured to provide mandatory blending of this Reserve Well Field water with better-quality water from the Equus Beds Well Field at a ratio of three to one (that is, three parts Equus Beds water for each one part Reserve Well Field water). The RESNET model does not have the direct capability to regulate the flow in one link based on the flow in a parallel link; therefore, this blending process is approximated by using three links each from the Equus Beds to RWF Junction (L14, L15 and L16) and three links from the Reserve Well Field to the RWF Junction (L17, L18 and L19).

Table 11: Data Fields in Link Table (tblRnLink)

Field Name	Description
ID	Unique record identifier assigned by system. This field contains the link IDs that are used to identify the links in each model run.
Number	Sequential link number. Used for more convenient reference only.
Name	Short link name
Origin Node ID	Identifier corresponding to origin node in tblRnNode
Terminal Node Id	Identifier corresponding to terminal node in tblRnNode
Minimum Flow	Minimum allowable flow in this link (acre-feet/day)
Maximum Flow	Maximum allowable flow in this link (acre-feet/day)
Cost	Unit cost of flow in this link (per acre-foot)
Loss Node ID	For leaky stream segment, ID for node where losses accrue. Not utilized in ILWS model.
Link Loss Percent	For leaky stream segments, percent of flow loss in link (percent). Not used in ILWS model.
Link Loss Max	Maximum loss in link (acre-feet/day). Not used in ILWS model.
Limit Link ID	Link ID used to limiting flow for this link. Not used in ILWS model.
Limit Demand ID	Demand ID used to limit flow in this link. Not used in ILWS model.
Source Link ID	Used for cloning only

When water is available from the Reserve Well Field and there is sufficient water supply demand to utilize this water, the operations model will first use up to 33 acre-feet/day of water from the Equus Beds Well Field via link L14 before then using up to 11 acre-feet/day of water from the Reserve Well Field through link L17. If there is additional water available from the Reserve Well Field, this process will continue with the model using in order links L15, L18, L16 and finally L19.

1.4.2 Cheney Reservoir Supply Pipeline

Deliveries from Cheney Reservoir to the City’s water treatment plant are modeled using two parallel links even though there is only one physical supply pipeline. The first link (L21) has a maximum flow based on the City’s original water right for Cheney Reservoir (47 million gallons per day [MGD] or 144 acre-feet/day). Water can be supplied to the City through this link whenever there is water available in the reservoir’s conservation pool. The second link from Cheney Reservoir (L22) represents the balance of the

capacity in this supply pipeline (80 MGD less 47 MGD = 33 MGD or 101 acre-feet/day). This additional supply capability is available only when the reservoir’s conservation pool is full or near full.

1.5 Model Demands

In the ILWS operations model, system demands are used to accomplish a variety of purposes. The most obvious purpose is to satisfy actual water demands, such as the required raw water supply to the City’s water treatment plant. The water extracted from the Equus Beds aquifer by farmers for irrigation is a similar consumptive water demand. All other model demands are termed flow-through demands because all of the water withdrawn at the given node is returned to the system at another node. These flow-through demands are used to represent minimum streamflow requirements and also the available supplies to pump stations.

In the RESNET model, each demand has a source node, annual demand volume and demand priority. Optionally, these demands can also have a return node and return percentage, and a specified annual demand distribution. If no demand distribution is provided, the annual demand volume is distributed evenly across each day of the year.

Demands with the highest priority yield the highest benefit per unit when satisfied. For example, a demand for 10 acre-feet/day with a priority of 500 will yield 5,000 benefit units when satisfied. Benefits are treated as negative costs (with the same units) in the RESNET model. Therefore, in order to minimize costs the model will try to satisfy the demands with the highest priorities first.

The model demands included in the ILWS operations model are described in Table 12.

Table 12: ILWS Model Demands

Demand No.	Origin Node No.	Annual Demand (ac-ft/yr)	Dmd Dist?	Priority	Return		Description
					Node No.	Per-cent	
D1	200	87,563.1	Yes	806	---	---	Wichita: 0-70%
D2	200	6,254.5	Yes	805	---	---	Wichita: 70-75%
D3	200	6,254.5	Yes	804	---	---	Wichita: 75-80%
D4	200	6,254.5	Yes	803	---	---	Wichita: 80-85%
D5	200	6,254.5	Yes	802	---	---	Wichita: 85-90%
D6	200	6,254.5	Yes	801	---	---	Wichita: 90-95%
D7	200	6,254.5	Yes	800	---	---	Wichita: 95-1000%
D8	80	5,604	No	850	150	100	E Wells: 0-5MGD
D9	80	5,604	No	800	150	100	E Wells: 5-10MGD
D10	80	22,418	No	750	150	100	S Wells: 20MGD
D11	150	33,627	No	10	85	100	Local WF Excess Return
D12	90	1,448,000	No	10	100	100	Cheney spillway drawdown
D13	20	5,000	No	875	130	100	Reserve WF supply
D14	130	11,209	No	10	25	100	RWF excess return

D15	120	26,500	Yes	900	---	---	Equus Beds irrigation
D16	50	56,044	No	825	170	100	Sedgwick recharge supply
D17	170	112,088	No	10	60	100	Excess recharge return
D18	70	50,440	No	825	160	100	Local WF Expansion supply
D19	160	50,440	No	10	85	100	Local WF Expansion excess return
D20	50	28,960	No	850	60	100	L Arkansas R minimum flow at Sedgwick
D21	70	14,480	No	850	85	100	L Arkansas R minimum flow at mouth
D22	80	362,000	No	825	85	100	Arkansas R minimum flow: 500 cfs
D23	80	724,000	No	775	85	100	Arkansas R minimum flow: 500-1500 cfs
D24	40	28,960	No	850	50	100	L Arkansas R minimum flow at Halstead
D25	40	56,044	No	825	170	100	Halstead recharge supply

The data for these model demands is stored in two Access tables: tblRnDemand and tblRnDemandData. The data fields in these tables are described in Tables 13 and 14.

Table 13: Data Fields in Demand Table (tblRnDemand)

Field Name	Description
ID	Unique record identifier assigned by system. This field contains the demand IDs that are used to identify the demands in each model run.
Node ID	Identifier for node where this demand originates
Number	Sequential demand number. Used for more convenient reference only.
Name	Short demand name
Description	Description of demand
Demand	Desired annual quantity for the current demand (acre-feet/year)
Priority	Priority for current demand
Return Node ID	Node ID for return node. Null if not applicable
Return Percent	Percentage of volume in this demand that is returned to system at specified node
Primary Demand	True/false flag that indicates if current demand is considered to be a primary demand.
Shortage Days	Output field that accumulates number of days during simulation period with shortages at current demand
Source Demand Id	Used for cloning only.

Table 14: Data Fields in Demand Distribution Table (tblRnDemandData)

Field Name	Description
ID	Unique record identifier assigned by system.
Demand ID	Identifier for corresponding demand in tblRnDemand
Month	Month number (1=Jan, 2=Feb, etc.)
Day	Day of month
Demand Percent	Portion of the annual demand volume that is desired on this day of year (percent of annual)

The model demands listed in Table 12 are discussed further below.

1.5.1 Wichita Raw Water Demands

The total raw water demand for the City of Wichita was segregated into seven parts for modeling purposes. These seven individual demands (D1-D7) were included to show the potential impact of additional water conservation measures on system reliability. The demand quantities listed in Table 3 for these demands total to 125,090 acre-feet/year, which is equivalent to an average of 111.8 MGD. This is the City’s estimated average-day demand in 2050. For current conditions, a total City water demand of 78,768 acre-feet, or 70.4 MGD, was used. These demand estimates include the impact of typical conservation measures, such as existing City ordinances that require use of low-flow showerheads and toilets in new construction, but not additional conservation measures during dry periods, such as restrictions on lawn watering and vehicle washing. None of these additional conservation measures were implemented in the model runs used in the EIS, but they can be simulated by progressively reducing the demand priorities of demands D7, D6, etc. The distribution of the City’s water demand was derived from actual usage data for calendar year 1991 (Burns & McDonnell, 2003).

1.5.2 Local Well Field

Demands D8–D11 and D22–D23 are used to model the City’s existing Local Well Field, which is a combination of the Emergency and Sims well fields and, therefore, often referred to as the E&S well fields. The “E” wells have a total capacity of 10 MGD and the “S” wells a total capacity of 20 MGD. Demand D8 represents the first 5 MGD of supply from the “E” wells, with D9 the second half. Demand D10 represents the 20 MGD available from the “S” wells. Demand D11 is a low-priority demand that returns “excess” diversions to the Local Well Field back to the Arkansas River when not needed to satisfy the City’s water demands. Demands D22 and D23 are flow-through demands (that is, in-stream flow requirements) that restrict when the Local Well Field can operate because of the lower-quality water available from the Arkansas River.

Among these five demands, D8 has the highest priority (850) so up to 5 MGD is assumed to be available from the “E” wells whenever there is flow in the Arkansas River at Node No. 80. The demand with the next lower priority is D22 (825) so the model will attempt to satisfy this demand next. This demand represents an in-stream flow requirement of 500 cfs. The water quality of the Arkansas River tends to improve at higher flow rates so demand D22 prevents the balance of the “E” wells (demand D9 with priority 800) from operating unless the flow in the Arkansas River is greater than 500 cfs. In a similar manner, demand D23, which has an average rate of 1,000 cfs, prevents the “S” wells from operating unless the flow in the Arkansas River totals over 1,500 cfs.

1.5.3 Local Well Field Expansion

In the model runs completed for the EIS, the Local Well Field was assumed to be expanded by 45 MGD with a series of alluvial wells along the Little Arkansas River. The supply and excess return from this new source is represented by demands D18 and D19. Demand D21 is a flow-through demand that also originates at Node No. 70. This demand, with a priority of 850, prevents the local well field expansion (demand D18 with priority 825) from operating unless the flow in the Little Arkansas River exceeds 20 cfs at its mouth.

1.5.4 Cheney Drawdown

The RESNET model attempts to put all available water to beneficial use. That is, it attempts to minimize spills (Section 1.5). In Cheney Reservoir, the elevation-storage data includes the flood control and surcharge pools. Without some means to evacuate these upper pools, the model would try to keep this water in storage if its release would contribute to a spill. Demand D12 mimics the reservoir's spillway to provide a means to draw the reservoir back down to the top of its conservation pool.

1.5.5 Reserve Well Field

The Bentley Reserve Well Field has a planned capacity of 10.8 MGD. This water source is represented in the operations model by a supply demand (D13) and an excess return demand (D14). Pumping at this well field is assumed to induce infiltration from the Arkansas River so this source is assumed available whenever there is sufficient flow in the Arkansas River. As discuss above (Section 1.3.1), the water withdrawn from this source must be blended with three times as much better-quality water from the Equus Beds Well Field.

1.5.6 Equus Beds Irrigation Demand

Within the Equus Beds Well Field area, agriculture is the dominate land use. Many of the farmers in this area irrigate with groundwater withdrawn from the Equus Beds aquifer. The demand for irrigation withdrawals from the aquifer is represented in the operations model by demand D15. This demand has an annual quantity of 26,500 acre-feet, which was derived from review of reported water usage records for the entire aquifer. These records are collected by the Kansas Division of Water Resources. Generally, only annual water usage data are available so these irrigation withdrawals are assumed to occur at a constant rate over the entire growing season (mid-May through mid-September).

1.5.7 Equus Beds Recharge

Recharge to the Equus Beds aquifer is represented in the operations model by demands D16, D17, D25, D20 and D24. Demands D20 and D24 are flow-through demands that restrict withdrawals from the Little Arkansas River to periods when the flow exceeds 40 cfs. The potential recharge supply is represented by demands D16 and D25, which total to either 100 or 150 MGD, depending on alternative. Fifty percent of these withdrawals are assumed to occur above Halstead (D25) and the balance between Halstead and Sedgwick. The operations model makes no distinction between withdrawals via a surface water intake or through alluvial wells. The supply demands (D16 and D25) will withdraw water from the Little Arkansas River whenever conditions permit. If the Equus Beds aquifer is fully recharged, demand D17 provides a means to return this water back to the river.

1.6 Model Imports

In RESNET an import is a fixed quantity of water that accrues at a specified node each year. Only one import is used in the ILWS operations model. This import represents the average annual natural recharge

to the Equus Beds aquifer. Imports and their corresponding annual distribution data are stored in two Access tables: tblRnImport and tblRnImportData. The data fields for these two tables are listed in Tables 15 and 16.

Table 15: Data Fields in Import Table (tblRnImport)

Field Name	Description
ID	Unique record identifier assigned by system. This field contains the import IDs that are used to identify the imports in each model run.
Node ID	Identifier for node where this import accrues
Import	Annual quantity for the current import (acre-feet/year)
Source Import ID	Used for cloning only.

Table 16: Data Fields in Import Distribution Table (tblRnImportData)

Field Name	Description
ID	Unique record identifier assigned by system.
Import ID	Identifier for corresponding import in tblRnImport
Month	Month number (1=Jan, 2=Feb, etc.)
Day	Day of month
Import Percent	Portion of the annual import volume that is received on this day of year (percent of annual)

1.7 Model Spills

A spill is a final sink for any water in the system that is left over after all possible demands are met and reservoirs filled. In the ILWS model, there is only one designated spill (S1), which is located at the most downstream node in the system, the Arkansas River at Arkansas City (Node No. 110). This spill is assigned a very high unit cost (15,000 per acre-foot) so the model will minimize spill quantities to the extent practicable in finding the least-cost network solution for each time step.

In RESNET, spill data is stored in an Access table named tblRnSpill. The data fields in this table are described in Table 17.

Table 17: Data Fields in Spill Table (tblRnSpill)

Field Name	Description
ID	Unique record identifier assigned by system. This field contains the spill IDs that are used to identify the spills in each model run.
Node ID	Identifier for node where this spill originates
Cost	Unit cost of water lost to system through this spill (per acre-foot). Spill costs are usually relatively high such a 10,000 or more.
Source Import ID	Used for cloning only.

2 Operations Model Output Data

Execution of the operations model generates data that depicts the daily water balance calculated for each day during the 85-year simulation period. These data are stored as four separate data streams, with one stream each for nodes, reservoirs, links and demands. These four data streams are described below.

2.1 Node Operations Data

The ILWS operations model will output a water balance for each node in the model for each day. These data are stored in an Access table named tblRnNodeOperations. The individual fields in this table are described in Table 18.

Table 18: Data Fields in Node Operations Table (tblRnNodeOperations)

Field Name	Description
ID	Unique record identifier assigned by system
Node ID	Identifier for corresponding node from tblRnNode table. These node IDs are unique to each alternative model run.
Date	Date for these data (mm/dd/yyyy)
Inflow	The unregulated inflow (if any) to this node on specified date (acre-feet).
Upstream Release	The total flow on specified date in all links that terminate at this node (acre-feet). For example, at Node No. 110, this field would include the total flow in links L10 and L12.
Import	The import to this node on specified date (acre-feet). This field will be zero for all nodes except Node No. 120.
Demand Return	If the current node is a return node for any flow-through demand, this field will contain the total return flow at this node (acre-feet). If this node is the return node for multiple demands (for example, Node No. 85 is the return node for demands D11, D19, D21, D22 and D23), this field will contain the total for all return flows.
Downstream Release	The total flow on specified date in all links that originate at the current node (acre-feet).
Demand	The total for all demands that originate at the current node satisfied on specified date (acre-feet).
Spill	Total spills on specified date from this node (acre-feet). This field will be zero except at Node No. 110.
Losses	Total reservoir losses on specified date from this node (acre-feet). This field will be zero for all nodes except Node No. 120.

2.2 Reservoir Operations Data

The data included in the node operations table shows a complete water balance at each node except for storage nodes. At these storage nodes or reservoirs, the additional data needed to complete the water balance are listed in the reservoir operations data table. These data are stored in an Access table named tblRnReservoirOperations. The individual fields in this table are described in Table 19.

Table 19: Data Fields in Reservoir Operations Table (tblRnReservoirOperations)

Field Name	Description
ID	Unique record identifier assigned by system
Reservoir ID	Identifier for corresponding reservoir from tblRnReservoir table. These reservoir IDs are unique to each alternative model run.
Date	Date for these data (mm/dd/yyyy)
Evap Rate	The net evaporation loss rate from this reservoir on specified date (inches). On date with net gain from precipitation, this rate will be negative.
Evap Volume	The net evaporation volume from the current reservoir on specified date (acre-feet). Evaporation volumes are calculated as the product of the evaporation rate and average reservoir surface area $[(BOPArea+EOPArea)/2]$.
BOP Area	Estimated pool area for current reservoir at start of specified day (acres).
BOP Storage	Storage contents of current reservoir at start of specified day (acre-feet).
EOP Area	Estimated pool area for current reservoir at end of specified day (acres).
EOP Storage	Storage contents of current reservoir at end of specified day (acre-feet).
EOP Pool Elev	Pool elevation of current reservoir at end of specified day (feet).
Loss 1	Net losses from current reservoir to first loss node on specified date (acre-feet).
Loss 2	Net losses from current reservoir to second loss node on specified date (acre-feet).
Loss 3	Net losses from current reservoir to third loss node on specified date (acre-feet).
BOP Recharge	Balance in recharge credit account for current reservoir at start of specified day (acre-feet). Applies only to Node No. 120.
EOP Recharge	Balance in recharge credit account for current reservoir at end of specified day (acre-feet). Applies only to Node No. 120.
BOP Water Right	Balance in annual water right account for current reservoir at start of specified day (acre-feet). Applies only to Node No. 120.
EOP Water Right	Balance in annual water right account for current reservoir at end of specified day (acre-feet). Applies only to Node No. 120.

2.3 Link Operations Data

The flow in each model link on each day is summarized in the link operations table, which is named tblLinkOperations in the Access database. The individual fields in this table are described in Table 20.

Table 20: Data Fields in Link Operations Table (tblRnLinkOperations)

Field Name	Description
ID	Unique record identifier assigned by system
Link ID	Identifier for corresponding link from tblRnLink table. These link IDs are unique to each alternative model run.
Date	Date for these data (mm/dd/yyyy)
Flow	The flow in the current link on specified date (acre-feet).
Loss	Flow loss from current link on specified date (acre-feet). This model option is not used for the ILWS model so this field will always be zero.

2.4 Demand Operations Data

The final operation table used in the RESNET model is the demand operations data table (tblRnDemandOperations). The individual fields in this table are described in Table 21.

Table 21: Data Fields in Demand Operations Table (tblRnDemandOperations)

Field Name	Description
ID	Unique record identifier assigned by system
Demand ID	Identifier for corresponding demand from tblRnDemand table. These demand IDs are unique to each alternative model run.
Date	Date for these data (mm/dd/yyyy)
Demand	Actual volume for current demand satisfied on specified date (acre-feet).
Demand Shortage	Difference between desired and actual volume for current demand on specified date (acre-feet).
Return Flow	Portion of current demand that is returned to system on specified date (acre-feet).

2.5 Post-processing Data

Execution of the RESNET model generates the four output tables described above. To aid in subsequent analysis, several Access routines have been developed that generate auxiliary data tables from the data contained in the four primary output tables. These routines are available in the main RESNET model database file and will generate the following summary tables:

2.5.1 Discharge Summary Data

In the RESNET model, minimum required streamflow and deliveries to pump stations are modeled as flow-through demands. For this reason, the flow in a stream below a given model node is often a combination of terms at some locations. The process for calculating these flows is outlined below.

- Arkansas River near Hutchinson (Node No. 10): Flow in Link L6 only
- Arkansas River near Maize (Node No. 25): Flow in Link L8 only
- Arkansas River below Wichita (Node No. 85): Flow in Link L10 only
- Little Arkansas River at Alta Mills (Node No. 30): Flow in Link L1 only
- Little Arkansas River at Halstead (Node No. 40): Flow in Link L2 plus Demand D24 plus lesser of Demands D17 and D24
- Little Arkansas River at Sedgwick (Node No. 50): Flow in Link L3 plus Demands D20 and D17
- Little Arkansas River at Valley Center (Node No. 60): Flow in Link L4 only
- Little Arkansas River at Mouth (Node No. 70): Flow in Link L5 plus Demands D19 and D21
- North Fork Ninnescah River (Node No. 90): Flow in Link L11 plus Demand D12
- Ninnescah River near Peck (Node No. 100): Flow in Link L12 only
- Arkansas River at Arkansas City (Node No. 110): Spill at Node 110 (sum of flows in Links L10 and L12)

A post-processing routine has been developed that generates a discharge summary table (tblRnDischargeSummary) that combines the various link and demand flows listed above for each day during the model simulation period. The individual fields in this table are listed in Table 22.

Table 22: Data Fields in Discharge Summary Table (tblRnDischargeSummary)

Field Name	Description
ID	Unique record identifier assigned by system
Model ID	Identifier for corresponding model run in tblRnModel table.
Date	Date for these data (mm/dd/yyyy)
Halstead	Mean daily flow in Little Arkansas River near Halstead (cfs).
Sedgwick	Mean daily flow in Little Arkansas River near Sedgwick (cfs).
Valley Center	Mean daily flow in Little Arkansas River at Valley Center (cfs).
L Ark Mouth	Mean daily flow in Little Arkansas River at it mouth in Wichita (cfs)
Wichita	Mean daily flow in Arkansas River at Wichita (cfs)
Below Cheney	Mean daily flow in North Fork Ninnescah River below Cheney Reservoir (cfs)
Peck	Mean daily flow in Ninnescah River near Peck (cfs)
Ark City	Mean daily flow in Arkansas River at Arkansas City (cfs)

2.5.2 Storage Summary Data

The daily end-of-day storage in Cheney Reservoir and storage deficits in the Equus Beds aquifer are available in the storage summary table (tblRnStorageSummary). The fields in this table are described in Table 23.

Table 23: Data Fields in Storage Summary Table (tblRnStorageSummary)

Field Name	Description
ID	Unique record identifier assigned by system
Model ID	Identifier for corresponding model run in tblRnModel table.
Date	Date for these data (mm/dd/yyyy)
Cheney	End-of-day storage in Cheney Reservoir on this date (acre-feet).
Equus Beds	End-of-day storage deficit in Equus Beds aquifer (acre-feet).

2.5.3 Water Supply Summary Data

The City’s total raw water demand each day is determined by the related demand and demand distribution data described above (Section 1.5.1). The supply summary table (tblRnSupplySummary) shows where the water to meet this demand comes from each day. This table also summaries the water delivered to the Equus Beds for recharge and aquifer gains and losses from the Arkansas and Little Arkansas rivers. The fields in the supply summary table are listed in Table 24

Table 24: Data Fields in Supply Summary Table (tblRnSupplySummary)

Field Name	Description
ID	Unique record identifier assigned by system
Model ID	Identifier for corresponding model run in tblRnModel table.
Date	Date for these data (mm/dd/yyyy)
Cheney	Water supplied from Cheney Reservoir on this date (acre-feet).
Equus Beds	Water supplied from Equus Beds well field on this date (acre-feet).
Bentley Reserve	Water supplied from the Bentley Reserve well field (acre-feet).
Local WF	Water supplied from the existing local (E&S) well fields (acre-feet)
Local Expansion	Water supplied from the planned expansion of the local well field (acre-feet).
L Ark Diversion	Water supplied by direct diversion from the Little Arkansas River (acre-feet)
Equus Beds Recharge	Water diverted from the Little Arkansas River for recharge of the Equus Beds aquifer (acre-feet)
Ark Losses	Net losses from Equus Beds aquifer to Arkansas River (acre-feet)
L Ark Gains	Net losses from Equus Beds aquifer to Little Arkansas River (acre-feet)

2.5.4 Water Surface Elevation Summary Data

The water surface elevations at four locations in the model area are estimated from the modeled daily discharges at these locations. These locations are as follows:

- Little Arkansas River at Valley Center
- Arkansas River at Wichita
- Ninnescah River near Peck
- Arkansas River at Arkansas City

These four locations are all located at active USGS stream gages. The water surface elevations at these locations are calculated using rating tables obtained from the USGS. The rating table data for these gages are stored in a database table named tblRnGageRating. The fields in the gage rating table are described in Table 25.

Table 25: Data Fields in Gage Rating Table (tblRnGageRating)

Field Name	Description
ID	Unique record identifier assigned by system
Number	Station number for USGS stream gage
Gage Height	Gage height reading (feet)
WS Elev	Water surface elevation corresponding to this gage height (feet NGVD). Equivalent to gage height plus gage datum elevation.
Discharge	Estimate stream discharge at this gage height (cfs)

The estimated water surface elevations at the four stream nodes are written to a summary table named tblRnWSElevSummary. This table also contains the end-of-day pool elevation and pool area for Cheney Reservoir. The fields in the water surface elevation summary table are listed in Table 26.

Table 26: Data Fields in Water Surface ElevationSupply Summary Table (tblRnSupplySummary)

Field Name	Description
ID	Unique record identifier assigned by system
Model ID	Identifier for corresponding model run in tblRnModel table.
Date	Date for these data (mm/dd/yyyy)
Valley Center	Estimated water surface elevation in Little Arkansas River at Valley Center (feet NGVD).
Wichita	Estimated water surface elevation in Arkansas River at Wichita (feet NGVD).
Cheney	End-of-day pool elevation in Cheney Reservoir (feet NGVD).
Peck	Estimated water surface elevation in Ninnescah River near Peck (feet NGVD)
Ark City	Estimated water surface elevation in Arkansas River at Arkansas City (feet NGVD).
Cheney Area	End-of-day pool area for Cheney Reservoir (acres)

3 References

Complete citations for the references cited in this document are listed below:

Burns & McDonnell. (2003). *Final Environmental Impact Statement for Integrated Local Water Supply Plan, Wichita, Kansas*. Prepared from City of Wichita, Department of Water and Sewer. Kansas City: Published by author.

Burns & McDonnell. (2008a, July). *Reservoir Evaporation*. Prepared from City of Wichita, Department of Water and Sewer. Kansas City: Published by author.

Burns & McDonnell. (2008b, October). *Equus Beds Groundwater Elevation and Storage Deficit/Stream Gain and Loss Relationship*. Prepared from City of Wichita, Department of Water and Sewer. Kansas City: Published by author.

Burns & McDonnell. (2008c, October). *Streamflow Estimates (14 October 2008 Draft)*. Prepared from City of Wichita, Department of Water and Sewer. Kansas City: Published by author.

Foster, G. (1989). *RESNET: A Reservoir Network Simulation Model*. Unpublished mater’s thesis, University of Kansas, Lawrence.

U.S. Geological Survey. (no date). *National Water Information System* [Database]. Retrieved from <http://water.usgs.gov>.

* * * * *

Attachment B

Supplemental Information on Development of Equus Beds Groundwater Elevation and Storage Deficit/Stream Gain and Loss Relationships

Equus Beds Groundwater Elevation and Storage Deficit/Stream Gain and Loss Relationship

prepared for

**City of Wichita
Wichita, Kansas**



November 2008

Project No. 49305

prepared by

**Burns & McDonnell Engineering Company, Inc.
Kansas City, Missouri**

COPYRIGHT © 2008 BURNS & McDONNELL ENGINEERING COMPANY, INC.



TABLE OF CONTENTS

	<u>Page No.</u>
1.0 INTRODUCTION	1-1
2.0 GROUNDWATER-SURFACE WATER INTERACTION	2-1
2.1 General	2-1
2.2 Groundwater Model	2-2
2.2.1 Initial USGS Model	2-2
2.2.2 USBR Model	2-2
2.2.3 Current Model	2-5
3.0 GROUNDWATER ELEVATION - STREAM GAIN AND LOSS	3-1
3.1 Infiltration from Streams	3-1
3.2 Groundwater Discharge to Streams	3-2
4.0 GROUNDWATER ELEVATION - STORAGE DEFICIT	4-1
4.1 USGS Storage Volume Estimates	4-1
4.2 Detailed Storage Volume Estimates	4-2
4.2.1 Groundwater Model Storage Volume – Groundwater Level Relationship	4-2
5.0 REFERENCES	5-1

APPENDIX A - GROUNDWATER MODEL INFORMATION

* * * * *



LIST OF TABLES

<u>Table No.</u>		<u>Page No.</u>
2.1	2003 Annual Rainfall Totals.....	2-6
4.1	Storage-volume changes in Equus Beds aquifer near Wichita, South-central Kansas, August 1940-January 2006.....	4-4

LIST OF FIGURES

<u>Figure No.</u>		<u>Page No.</u>
2.1	Wichita Well Field Conceptual Model	2-3
2.2	Wichita Well Field Revised Model Grid	2-4
3.1	Modeled Groundwater Elevation at Monitoring Well 886 vs. Aquifer Loss/Gain to Streams.....	3-1
4.1	Hydrograph of Water Levels in Monitoring Well 886	4-2
4.2	Modeled Groundwater Elevation/Storage Deficit Relationship	4-3



1.0 INTRODUCTION

The *Equus* bed aquifer, located northwest of Wichita, supplies municipal and industrial water for the City and for agricultural irrigation. Development for municipal use began in the 1930's. The City owns water rights for up to 40,000 acre-feet per year (AFY) in the *Equus* beds aquifer, one of its major sources of municipal and industrial water.

Equus beds groundwater use for irrigation developed in the 1970's and 1980's with additional water rights granted for an additional amount of about 50,000 AFY. Combined municipal and irrigation pumping is greater than the estimated safe yield of the aquifer, accelerated water level declines resulted, with the greatest decline or deepest groundwater level being recorded in October 1992.

The City has maintained water level measurements from over 100 monitoring wells since before pumping began in 1940. The U.S. Geological Survey (USGS) has been analyzing the data and publishing reports of water-level altitude maps periodically since 1949. More recently, the USGS has been publishing reports of groundwater levels and storage volume in the *Equus* beds aquifer under contract with the City of Wichita.

* * * * *



2.0 GROUNDWATER-SURFACE WATER INTERACTION

2.1 GENERAL

Many studies have addressed the interaction of the *Equus* beds aquifer with the Arkansas and Little Arkansas rivers, including investigations by the U.S. Bureau of Reclamation (USBR) and USGS as reported by Pruitt in 1993 and Myers in 1995.

Prior to groundwater development in the *Equus* beds, there was little exchange of water between the aquifer and the Arkansas River because the groundwater gradient was approximately parallel to the river. The Little Arkansas River, extending from the northern portions of the aquifer to the east and south and paralleling the eastern aquifer boundary, serves as a drain to the aquifer. A relatively large amount of annual precipitation, estimated to be about 20 percent, recharges the aquifer and moves downgradient; that which is not intercepted by pumping ultimately discharges to the Little Arkansas River and lower reaches of the Arkansas River.

With groundwater development, the potentiometric head of the aquifer was lowered; this created a gradient from the Arkansas River toward the aquifer and induced infiltration of saline river water into the aquifer. Additionally, the reduced head in the aquifer reduced the gradient of flow from the aquifer to the Little Arkansas River causing a decline in the river's baseflow.

Concerns that high-chloride water was moving into the aquifer and degrading its excellent water quality led to studies by both the USGS and the USBR. These studies used groundwater modeling to estimate future impacts to the aquifer under various pumping, recharge and management scenarios. The groundwater models used by the agencies were also used to evaluate the feasibility for the Wichita Equus beds aquifer recharge project.

For this analysis, groundwater modeling was used to establish a relationship between water elevation at a representative target well and aquifer-stream interaction. To develop the relationship, the model was run at various pumping stresses to determine aquifer inflow from streams and losses to streams at different elevations at the target well.



2.2 GROUNDWATER MODEL

MODFLOW, a three-dimensional, finite-difference groundwater flow model, was used to simulate the *Equus* Beds aquifer in the vicinity of the City of Wichita well field. MODFLOW is a well-documented groundwater model that is widely used and accepted by many regulatory agencies. The groundwater model currently in use was originally developed by the USGS office in Lawrence, Kansas (Myers et al 1996). The model was refined by the USBR for analysis of chloride migration in the Burton, Kansas area. The model was later further refined by Burns & McDonnell Engineering Company, Inc. (Burns & McDonnell) and used to evaluate the City's Aquifer Storage and Recovery (ASR) Project and later to track recharge credits for the accounting reports required by the Kansas Department of Agriculture Division of Water Resources (DWR).

2.2.1 Initial USGS Model

The USGS groundwater flow model was developed to study the stream-aquifer interaction between the Arkansas River and the *Equus* Beds aquifer and to help evaluate chloride migration into the aquifer. The USGS model area includes the current study area along the Little Arkansas River. The original USGS model grid consists of 34 rows, 42 columns, and 3 layers, and covers an area of approximately 950 square miles. Row spacing varied from 1000 feet to 10,000 feet; column spacing was 5000 feet. A conceptual depiction of the model construction is shown in Figure 2.1. The location and extent of the model area is shown in Figure 2.2.

The model uses constant-head nodes along the margins of the model boundary to represent areas where the aquifer extends beyond the model boundary. No-flow boundaries represent areas where shale provides a natural barrier to groundwater flow. The model includes areal recharge, evapotranspiration, stream flow and well pumpage.

More extensive details of the USGS model including information regarding model set-up, calibration, sensitivity analysis, and model results are contained in Myers et al (1996).

2.2.2 USBR Model

The USBR modified the USGS model for a contaminant transport study for the *Equus* Beds Groundwater Management District No. 2 (GMD2). To improve the accuracy of the transport modeling, the USBR reduced model grid spacing and adjusted the grid cells to a more uniform dimension. This resulted in a

J:\WICHITA\49305_ASR_NEPA\Report\Figures\CONCMODL2.dwg 07-29-2008 12:40 pjt

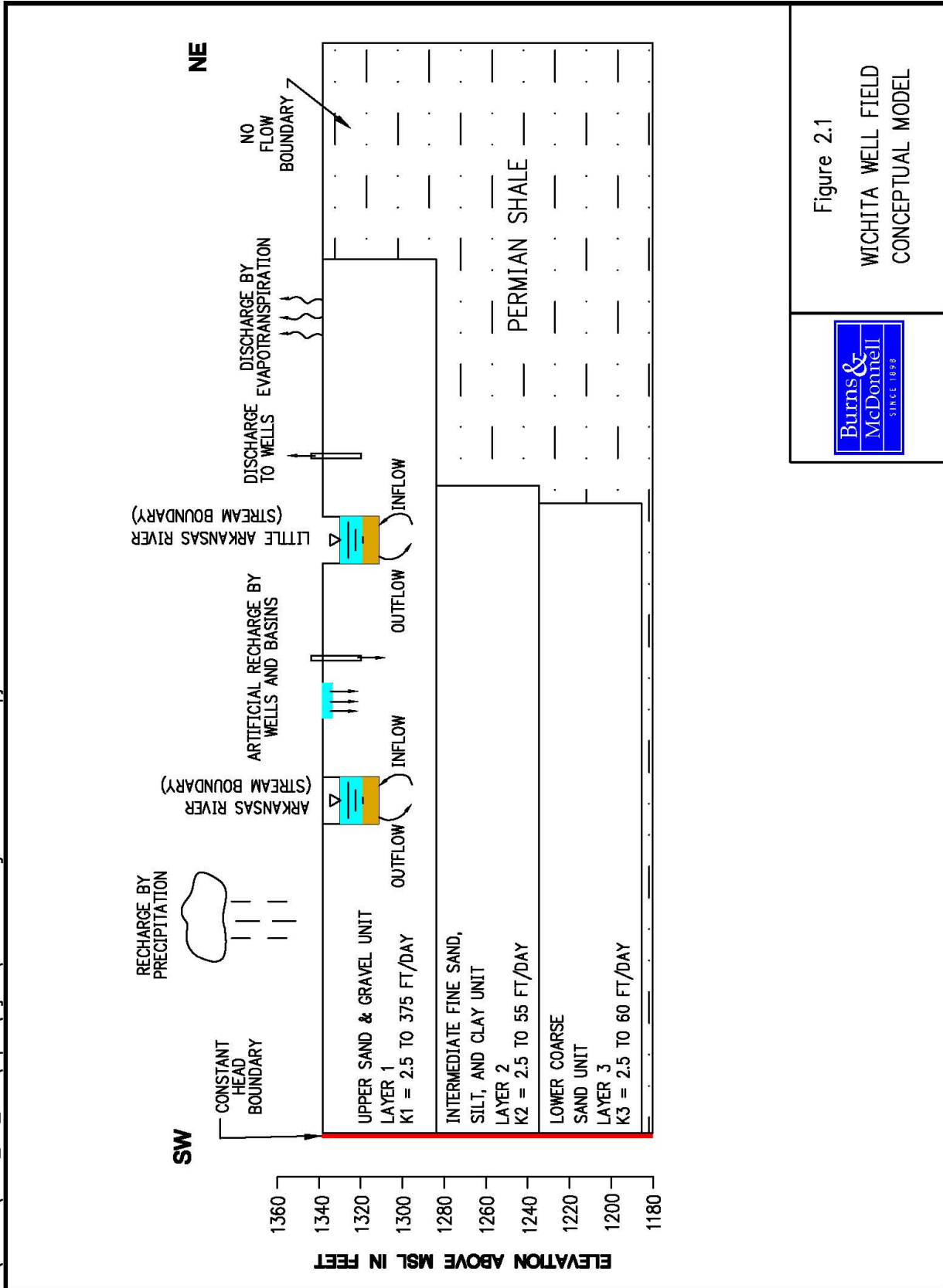
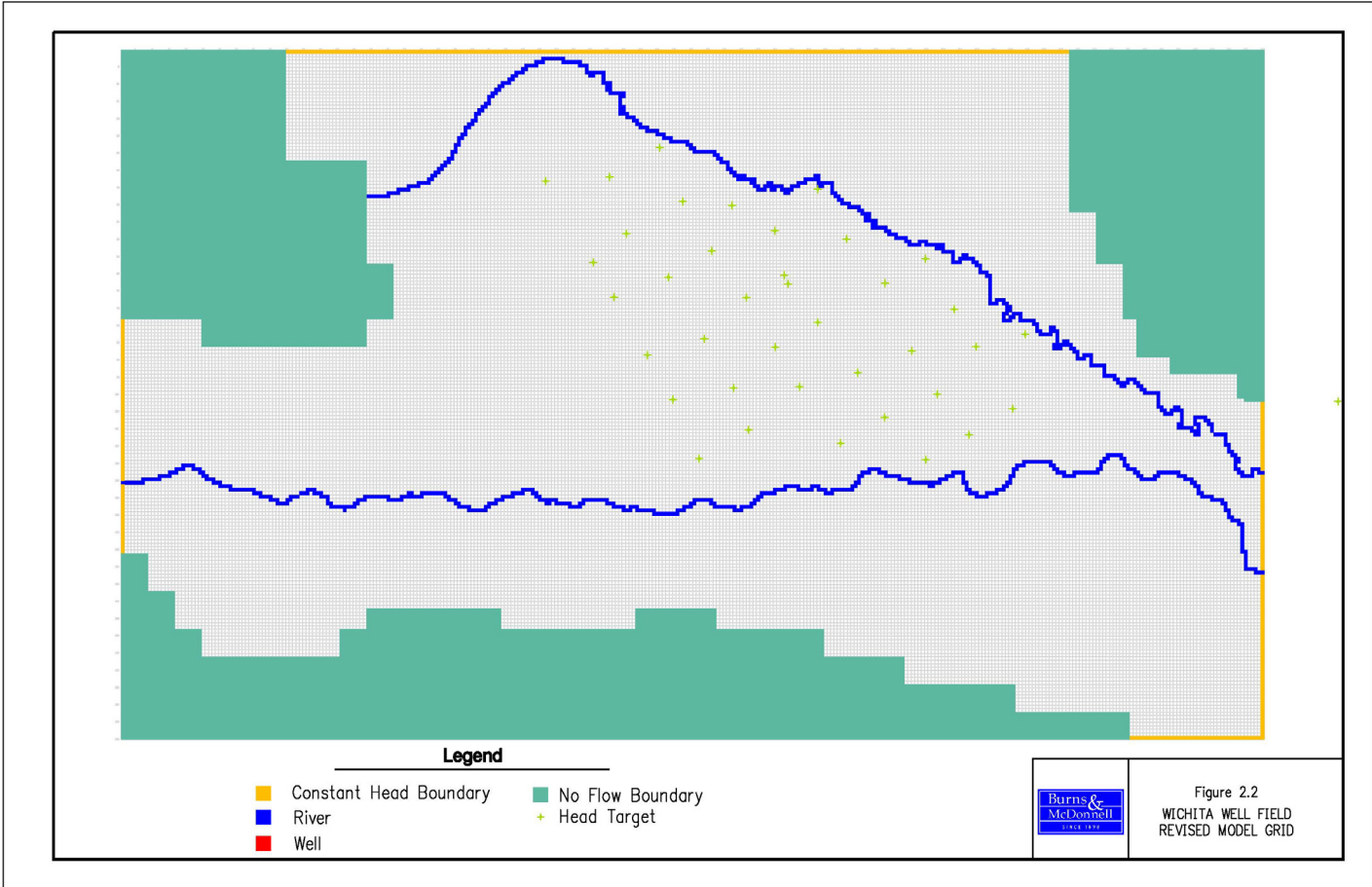


Figure 2.1
 WICHITA WELL FIELD
 CONCEPTUAL MODEL





model grid consisting of 54 rows and 84 columns. Details of the USBR modeling are given in Pruitt (1993).

The primary area of interest during the initial investigation for the ASR Project was the Wichita well field. As a result, the USBR model grid spacing in the well field area was too great for proper analysis, and the model was re-gridded to provide better resolution in this area. The finest grid spacing was 1000 feet by 1000 feet and resulted in a model domain with 84 rows and 120 columns.

2.2.3 Current Model

2.2.3.1 Setup and Implementation

The groundwater model used currently for the Wichita ASR accounting has been upgraded and refined with data acquired during various phases of investigation for the ASR project. Basic model refinements include reducing model cell size to a uniform 632.5 feet by 617.6 feet, resulting in a grid with 200 rows and 340 columns. The reduced cell size required repair of stream parameters. Additionally, some adjustments were made to aquifer parameters in areas where additional data was available.

The original model received from USBR was translated into a pre- and post-processing software program (Groundwater Vistas, V 3.0) and the simulations were performed using MODFLOW 98. The current version of the Wichita *Equus* Beds model was recently upgraded to a newer version of Groundwater Vistas (V 4.0) and is run using MODFLOW 2000.

2.2.3.2 Model Aquifer Parameters

2.2.3.2.1 Hydraulic Conductivity

The current versions of the model used for recharge credit accounting uses a large number of monitoring wells for calibration; however, the calibration at the target well 886 was not particularly good. Well 886 was established by USGS as representative of aquifer heads in the area of greatest historical drawdown in numerous USGS reports describing water level changes and estimate storage volumes (Hansen, 2007). Well 886 was used in the original EIS operation model to identify storage volumes available. Model hydraulic conductivity was reduced by one-half compared to the value used in the USGS model (Myers et al, 1996) to improve calibration at target well 886 for this application. Some pumping test results in the general area suggest that a reduction in hydraulic conductivity is appropriate.



Although these modifications resulted in slight changes to modeled heads, stream gain and loss, and aquifer storage compared to the previous EIS results, the current results are relatively close to the original EIS results. Table A-2 in Appendix A compares stream gain and loss for the two models, and Figure A-4 compares storage deficits calculated from each model and the USGS storage depletion estimates.

2.2.3.2.2 Storativity

Specific yield has been reduced from 0.15 to 0.1, and specific storage for the middle and lower layers was reduced by one-half from 0.0001 ft^{-1} to 0.00005 ft^{-1} compared to the original EIS Model and the USGS transient model (Myers et al, 1996). It should be noted that when computing storage volume changes for the dewatered portions of the aquifer, the USGS has typically used a specific yield value of 0.2 (Hansen, 2007).

2.2.3.2.3 Streambed Conductance and Streambed Roughness

Streambed conductance has been reduced from 50 feet/day to 40 ft/d for the Arkansas River, and from 5.0 ft/d to 4.0 ft/day for the Little Arkansas River compared to the original EIS Model and the USGS transient model (Myers et al). Several model runs varying the streambed conductance showed that the model is not very sensitive to this parameter.

Streambed roughness was not modified in the current version of the model.

2.2.3.3 Area Stresses for Model Input

2.2.3.3.1 Precipitation and Recharge

A percentage of annual precipitation contributes to natural recharge. The USGS used average precipitation from three area weather stations and then distributed the recharge across the model area based on soil type, ground cover, and model calibration. The current model employs data from the same locations used by USGS, plus an additional station added at Newton, Kansas.

2.2.3.3.2 Stream Flow

Stream flow can contribute to aquifer recharge depending on river stage, river bed conductivity, and elevation of the underlying groundwater table. Variations in river stage and flow are considered in the groundwater model using the MODFLOW stream package. In this package, a starting flow is assigned to the upstream river node with MODFLOW assigning river flow and stage in all downstream nodes. The

USGS determined that the appropriate starting river flow was that flow with a 70 percent return interval within the modeled stress period.

The 2007 river flows were used for this model evaluation. At the Alta Mills gage on the Little Arkansas River, a value of 8.5 cubic feet per second (cfs) was determined for the 70 percent return interval. The flow for the Arkansas River was determined to be 263 cfs at Hutchinson.

2.2.3.3.3 Groundwater Pumping

Groundwater pumping data for GMD2 has been from Kansas Department of Agriculture Division of Water Resources (DWR) from the early 1990s. Water use reported in acre-feet by DWR was converted to average daily pumping rates, and well locations reported in geographic coordinates (latitude and longitude) were converted to model coordinates. The converted data was then imported into the model. For this evaluation, pumping data from 2003 was used as the base case. Pumping rates for the stress periods were then set at 0, 10, 30, 50, 70, 90, 115, 130 and 145 percent of the base case to stress the aquifer. The stress period using a pumping rate of 145 percent of the 2003 rates simulated water levels lower than or approximately equal to those recorded in 1992.

2.2.3.3.4 Natural Recharge

The amount of natural recharge entering an aquifer system is based on many factors including the amount of precipitation, the surface conditions of soil texture and slope, and the type and amount of groundcover. The GMD2 has determined that approximately 20 percent of rainfall is recharged to the aquifer. The USGS groundwater model used average rainfall from Wichita, Hutchison, and Mount Hope for model input and distributed recharge based on soil type, slope, and land use. Actual values used in the model are increased or decreased with a ratio of the base case to the precipitation for the current year. Since that time, an additional weather station in Newton has become available. Recharge is distributed across the model based on soil type and other factors. Recharge for 2003 is based on the annual rainfall totals shown in Table 2.1.

2.2.3.3.5 Evaporation and Transpiration

Evapotranspiration is estimated in the model. Earlier USGS studies estimated maximum evapotranspiration to be approximately 3.5 inches per year. The USGS model incorporated a maximum

Table 2.1
2003 Annual Rainfall Totals

<u>Station</u>	<u>2003 Precip. (in.)</u>
Hutchinson E.	35.42
Mount Hope	27.64
Wichita	32.60
<u>Newton</u>	<u>36.05</u>
Average	32.93

value of 3.5 inches per year when the water table is at the surface. The rate is reduced with deeper groundwater levels and is equal to 0 when the water table is 10 feet or more below the surface.

2.2.3.4 Model Calibration

Modeled pumping rates were based on the period (2003) in which the highest observed pumping rates in recent history occurred (where more complete records are available).

Calibration was performed by comparing modeled heads at the end of the 100% stress period (2003) to the observed heads at well 886 at the end of 2003 (actually measured in early 2004).

Reductions in the values for hydraulic conductivity and storage were required to simulate aquifer heads at the target well 886, established by USGS as representative of aquifer heads in the area of greatest historical drawdown (Hansen, 2007). This essentially results in calibrating to a single point as opposed to multiple points in previous versions of the model.

Final calibration resulted in difference of 5.4 feet between the model and observed values (modeled elevation 1384.7 vs. observed 13794 feet).

The current model has a water budget mass balance discrepancy of -0.08 percent, a residual mean of -9.44 feet, and an absolute residual mean (compared to observed January 2004 water level measurements in 38 index monitoring wells) of 9.50 feet. The absolute residual mean is the average absolute difference between measured water levels and computed water levels at the same location. Differences are due to seasonal variations in local weather (recharge), timing of local pumping, and other operations factors.

* * * * *



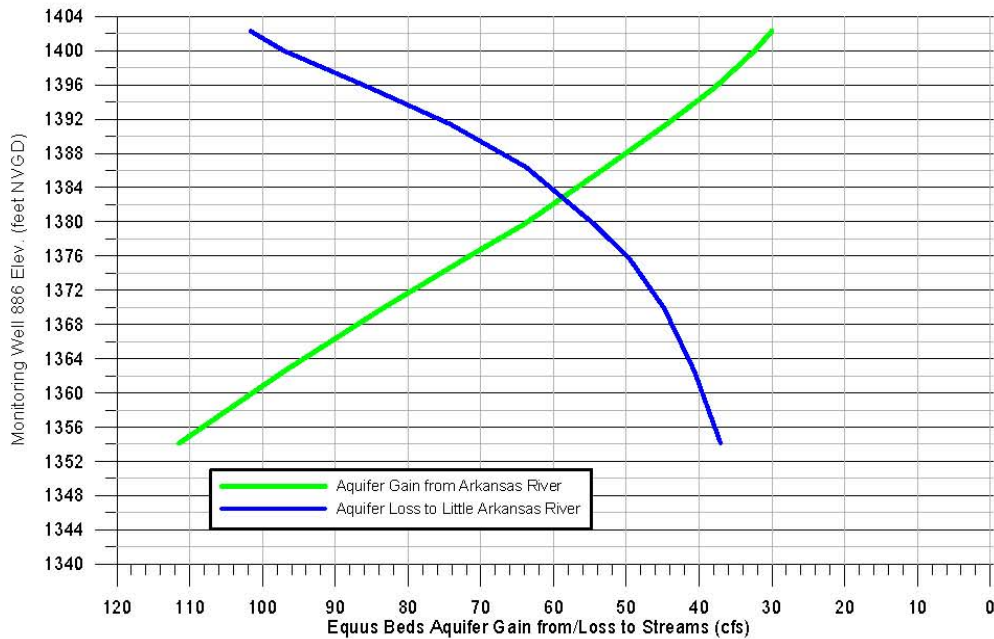
3.0 GROUNDWATER ELEVATION - STREAM GAIN AND LOSS

3.1 INFILTRATION FROM STREAMS

When aquifer levels are lower than water levels in a stream, there is a potential for water inflow or infiltration from the stream to the aquifer. The amount of flow depends on the difference in water levels and the permeability of the streambed. The rate of infiltration from streams is reported in the model water budget for each time and stress period. For this evaluation it is assumed that the infiltration is from the Arkansas River. Minor amounts may actually infiltrate from the Little Arkansas River; however, the amount reported in the model is the net impact on the aquifer. The data from the ten stress periods are graphed with the calculated water level at Monitoring Well 886 to illustrate the change in river inflow dynamics with changes in groundwater elevation (Figure 3.1).

Figure 3.1

**Modeled Groundwater Elevation at Monitoring Well 886
 vs. Aquifer Loss/Gain to Streams**



3.2 GROUNDWATER DISCHARGE TO STREAMS

When aquifer levels are higher than water levels in a stream, there is a potential for water inflow or infiltration from the aquifer to the stream. The amount of flow depends on the difference in water levels and the permeability of the streambed. The rate of aquifer loss to streams is reported in the model water budget for each time and stress period. For this evaluation, it is assumed that aquifer losses are to the Little Arkansas River. Minor amounts may actually be lost to the Arkansas River; however, the amount reported in the model is the net impact on the aquifer. Data from the ten stress periods are graphed with the calculated water level at Monitoring Well 886 to illustrate the change in river inflow dynamics with changes in groundwater elevation (Figure 3.1).

* * * * *



4.0 GROUNDWATER ELEVATION - STORAGE DEFICIT

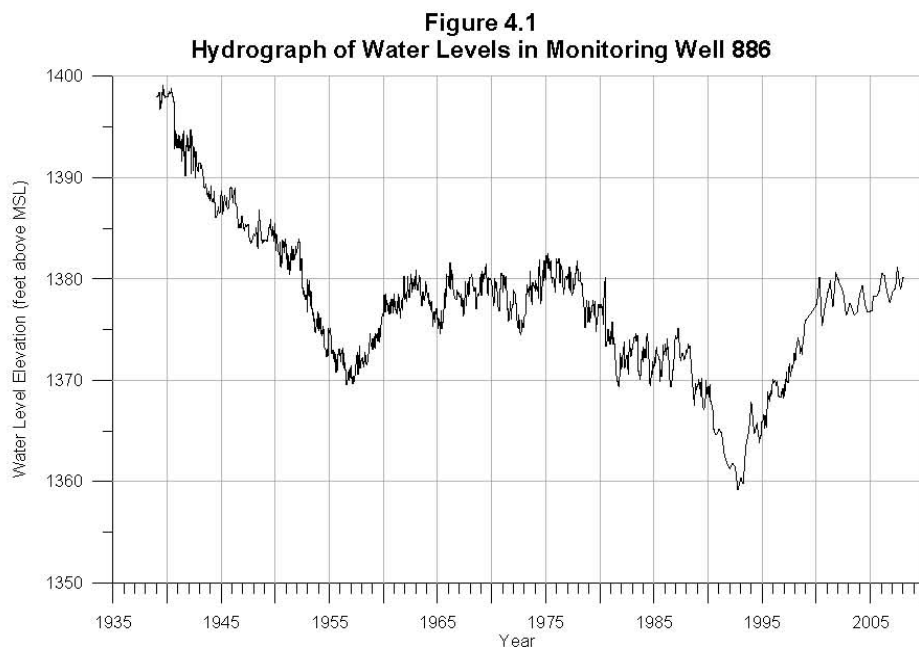
The City of Wichita, GMD2, and the USGS collect water level data in over 100 monitoring wells on a quarterly basis to monitor groundwater level changes. The USGS identified four noteworthy periods of water-level changes. They include the initial period of pumping, the severe drought conditions of the mid-1950's, a period of relatively stable levels from 1958 to 1977, and a period of declines due to increased irrigation pumping from 1978 to 1992. Subsequent to these identified periods, the City has adopted its Integrated Local Water Supply Plan Project (Project) which calls for greater use of water from Cheney Reservoir when available and reduced pumping from the Equus beds aquifer. The reduced withdrawal from the aquifer has resulted in recent rebound of water levels.

4.1 USGS STORAGE VOLUME ESTIMATES

In the current USGS report (Hansen, 2007), three water-level altitude maps of the water level data are presented. These include 1940 (pre-development), 1992 (lowest levels recorded), and current (2006) levels. Additionally, a number of water level change maps showing the difference in water levels for several periods are presented.

The USGS selected monitoring well 886 as a representative descriptor of historical water-level changes in the area of maximum water-level declines which occur in the central part of the study area near the historic center of pumping by the City. Figure 4.1 is a hydrograph of water levels recorded in monitoring well 886.

The USGS has calculated the storage-volume changes for several time periods covering the recorded well field data (Hansen, 2007). USGS defines the changes in storage volume as the change in saturated aquifer volume multiplied by the specific yield of the aquifer; a specific yield of 0.2 has been used by the USGS as representative of the *Equus* beds aquifer. Volume calculations were computed using computer-generated Thiessen polygons based on the measured water-level changes at wells and manually drawn lines of equal water-level change (Hansen, 2007). Table 4.1, developed by the USGS, lists the calculated storage-volume changes in acre-feet and percent for various time periods for the complete study area and the central part of the study area which is the immediate areal extent of the Wichita municipal wells.



4.2 DETAILED STORAGE VOLUME ESTIMATES

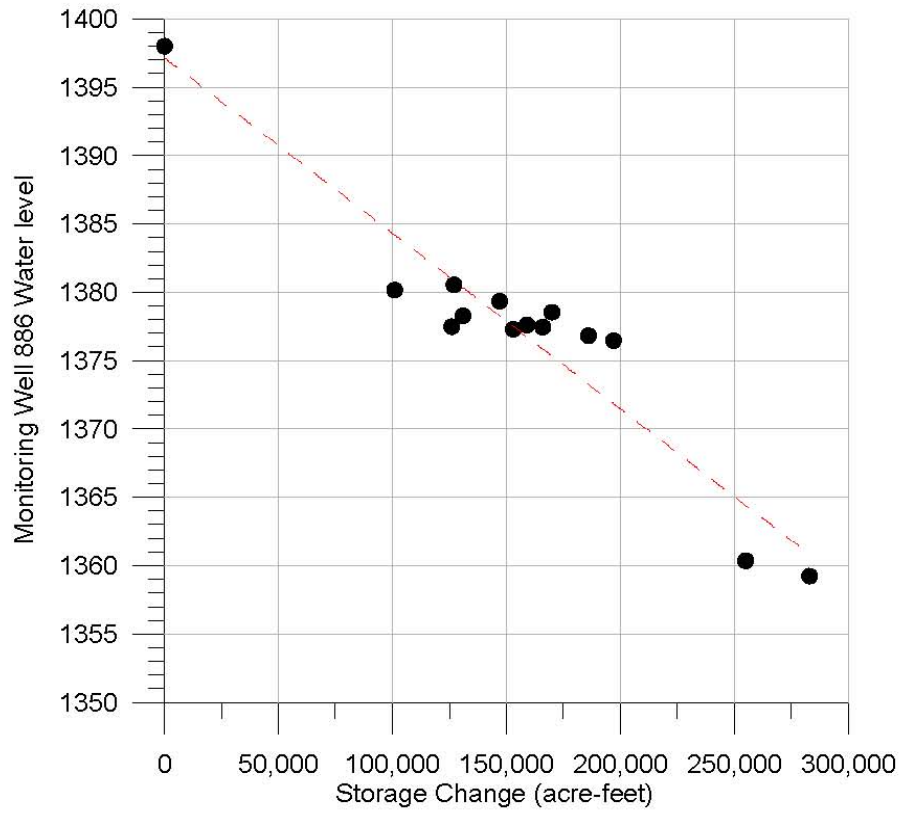
Storage volumes were determined by Burns & McDonnell for each section in the immediate study area, based on drilling and geophysical logs obtained for this project. The total thickness of coarse- and fine-grained material within the allowable vertical ASR zone was determined and storage factors were applied to calculate the total available volume within each section. The calculated total available volume for the immediate study area is about 200,000 acre-feet. This is comparable to the USGS evaluation for a slightly larger study area. Details of the evaluation, drill logs, cross-sections and methods are described in the Concept Design Report (Burns & McDonnell, 2000).

4.2.1 Storage Volume – Groundwater Level Relationship

A relationship between water levels in target well 886 and storage volumes calculated by the USGS is shown in Figure 4.2. The Figure shows the USGS calculated changes in storage from 1940 levels with well 886 elevations for the time of the calculations.

Table A-1 shows the modeled aquifer-stream losses and gains with groundwater elevations at target well 886 and the storage-volume deficit based on the USGS calculations as shown in Figure 4.2. The

Figure 4.2
Well 886 Elevation - Storage Change
USGS SIR 2006-5321



relationship between the storage-volume deficit and the aquifer-stream losses and gains is used directly in the operation model. Table A-2 compares the current model values with the original EIS estimates.

Equus Beds Storage Deficit Relationship

Groundwater Elevation - Storage Deficit

Table 4.1
Storage-volume changes in Equus Beds Aquifer near Wichita,
South-central Kansas, August 1940-January 2006.

End date of time period	Change in storage volume in the study area				Change in storage volume in the central part of the study area			
	Since August 1940 (acre-feet)	Since October 1992 (acre-feet)	Since October 1992 (percent)	Since January 2003 (acre-feet)	Since August 1940 (acre-feet)	Since October 1992 (acre-feet)	Since October 1992 (percent)	Since January 2003 (acre-feet)
October 1992	¹ -283,000	--	--	--	¹ -159,000	--	--	--
January 1993	² -255,000	+28,000	+10	--	² -154,000	+5,000	+3	--
January 2000	¹ -126,000	³ +157,000	+55	--	¹ -70,600	³ +88,400	³ +56	--
April 2000	³ -101,000	³ +182,000	³ +64	--	³ -74,500	³ +84,500	+53	--
January 2003	³ -159,000	³ +124,000	+44	--	³ -83,400	³ +75,600	+48	--
April 2003	-153,000	+130,000	+46	+6,000	-84,400	+74,600	+47	-1,000
July 2003	-197,000	+86,000	+30	-38,000	-89,300	+69,700	+44	-5,900
October 2003	-186,000	+97,000	+34	-27,000	-92,300	+66,700	+42	-8,900
January 2004	-170,000	+113,000	+40	-11,000	-89,900	+69,100	+43	-6,500
April 2004	-147,000	+136,000	+48	+12,000	-83,600	+75,400	+47	-200
July 2004	-166,000	+117,000	+41	-7,000	-86,900	+72,100	+45	-3,500
October 2004	-158,000	+125,000	+44	+1,000	-86,200	+72,800	+46	-2,800
January 2005	-143,000	+140,000	+49	+16,000	-82,700	+76,300	+48	+700
April 2005	-131,000	+152,000	+54	+28,000	-80,500	+78,500	+49	+2,900
July 2005	-137,000	+146,000	+52	+22,000	-74,300	+84,700	+53	+9,100
October 2005	-131,000	+152,000	+54	+28,000	-74,300	+84,700	+53	+9,100
January 2006	-127,000	+156,000	+55	+32,000	-68,900	+90,100	+57	+14,500

¹ Storage-volume change previously reported by Hansen and Aucott (2001).

² Storage-volume change previously reported by Aucott and Myers (1998).

³ Storage-volume change previously reported by Hansen and Aucott (2004).

(Table from USGS Scientific Investigations Report 2006-5321)

* * * * *



5.0 REFERENCES

- Aucott, W.R., and Myers, N.C., 1998, "Changes in ground-water levels and storage in the Wichita well field area, south-central Kansas, 1940–98". U.S. Geological Survey Water-Resources Investigations Report 98-4141, 20 p.
- Aucott, W.R., Myers, N.C., and Dague, B.J., 1998, "Status of ground-water levels and storage in the Wichita well field area, south-central Kansas, 1997". U.S. Geological Survey Water-Resources Investigations Report 98-4095, 15 p.
- Hansen, C.V., and Aucott, W.R., 2001, "Status of ground-water levels and storage volume in the Wichita well field area, south-central Kansas, 1998–2000". U.S. Geological Survey Water-Resources Investigations Report 00-4267, 27 p.
- Hansen, C.V., and Aucott, W.R., 2004, "Status of ground-water levels and storage volume in the *Equus* Beds aquifer near Wichita, Kansas, January 2000–January 2003". U.S. Geological Survey Water-Resources Investigations Report 03-4298, 36 p.
- Hansen, C.V., 2007, "Status of ground-water levels and storage volume in the *Equus* Beds aquifer near Wichita, Kansas, January 2003–January 2006". U.S. Geological Survey Water-Resources Investigations Report 2006-5321, 34 p.
- Myers, N.C., Hargadine, G.D., and Gillespie, J.D., 1996, "Hydrologic and chemical interaction of the Arkansas River and the *Equus* Beds aquifer between Hutchinson and Wichita, south-central Kansas". U.S. Geological Survey Water-Resources Investigations Report 95-4191, 100 p.
- Pruitt, T. 1993. "Arkansas River Water Management Improvement Study, Modeling of Chloride Transport in the Equus Beds Aquifer." U.S. Department of the Interior, Bureau of Reclamation Technical Report.
- Ross, H.C., Myers, N.C., and Aucott, W.R., 1997, "Increased use of Cheney Reservoir for Wichita area water supply benefits *Equus* Beds aquifer". U.S. Geological Survey Fact Sheet 196-97, 2 p.
- U.S. Geological Survey, 2006, "Highlights of *Equus* Beds Ground-Water Recharge Project". Information available on the Web, accessed November 7, 2006, at http://ks.water.usgs.gov/Kansas/studies/equus/equus_hilites.html
- Williams, C.C., and Lohman, S.W., 1949, "Geology and ground-water resources of a part of south-central Kansas, with special reference to the Wichita municipal water supply". Kansas Geological Survey Bulletin 79, 455 p.
- Ziegler, A.C., Christensen, V.G., and Ross, H.C., 1999, "Baseline water quality and preliminary effects of artificial recharge on ground water, south-central Kansas, 1995–98". U.S. Geological Survey Water-Resources Investigations Report 99-4250, 74 p.

* * * * *



APPENDIX A - GROUNDWATER MODEL INFORMATION

Table A-1

Equus Beds Elevation-Storage-Gain-Loss Data

Elevation (feet)*	Storage Deficit (acre-feet)**	Gain from Arkansas River (cfs)	Loss to Little Arkansas River (cfs)
1342	NA	NA	NA
1360	290,000	100	38
1366	245,000	89	43
1370	212,000	82	44
1375	173,000	73	48
1380	135,000	62	53
1385	95,000	54	60
1390	55,000	48	70
1395	20,000	38	82
1396	10,000	36	85
1402	0	29	99

* Aquifer head at monitoring well 886

** Storage deficit read directly from graph and rounded to nearest 1000 ac-ft

Table A-2

Equus Beds Elevation-Storage-Gain-Loss Data

Elevation (feet)*	<u>Original EIS Model</u>		<u>EIS Model Update</u>	
	Gain from Streams (cfs)	Loss to Streams (cfs)	Gain from Streams (cfs)	Loss to Streams (cfs)
1342	138.2	-2.0	NA	NA
1360	90.5	8.2	100	38
1366	74.5	11.6	89	43
1370	63.9	13.9	82	44
1375	57.3	19.8	73	48
1380	50.2	29.2	62	53
1385	40.3	41.9	54	60
1390	29.1	56.3	48	70
1395	17.7	72.0	38	82
1396	15.1	75.2	36	85
1402	NA	NA	29	99

* Aquifer head at monitoring well 886



Figure A-1. Hydraulic Conductivity Zones in Layer 1

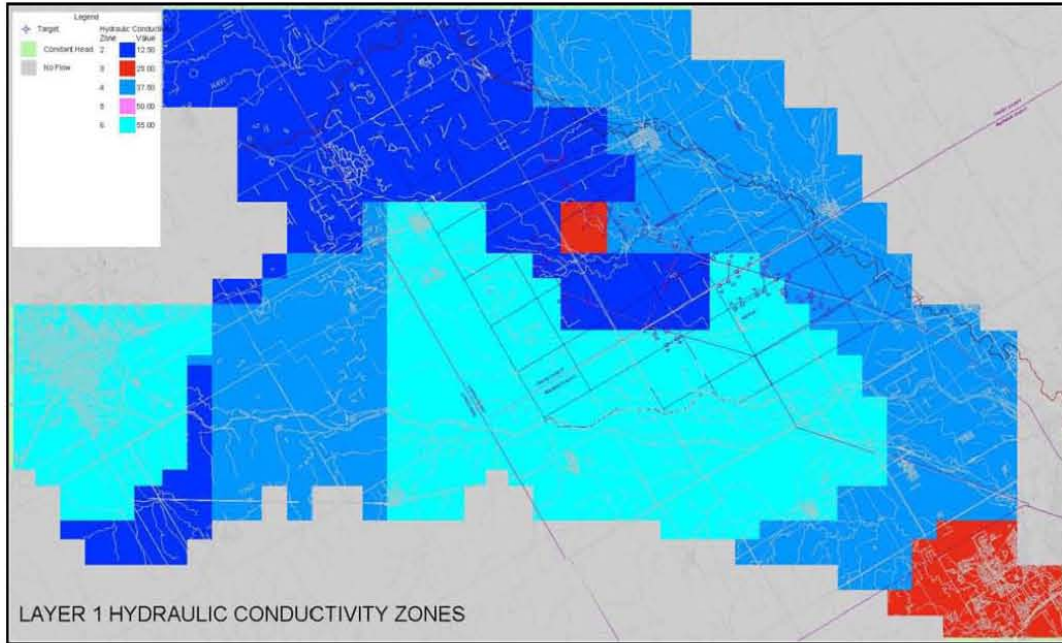


Figure A-2. Hydraulic Conductivity Zones in Layer 2

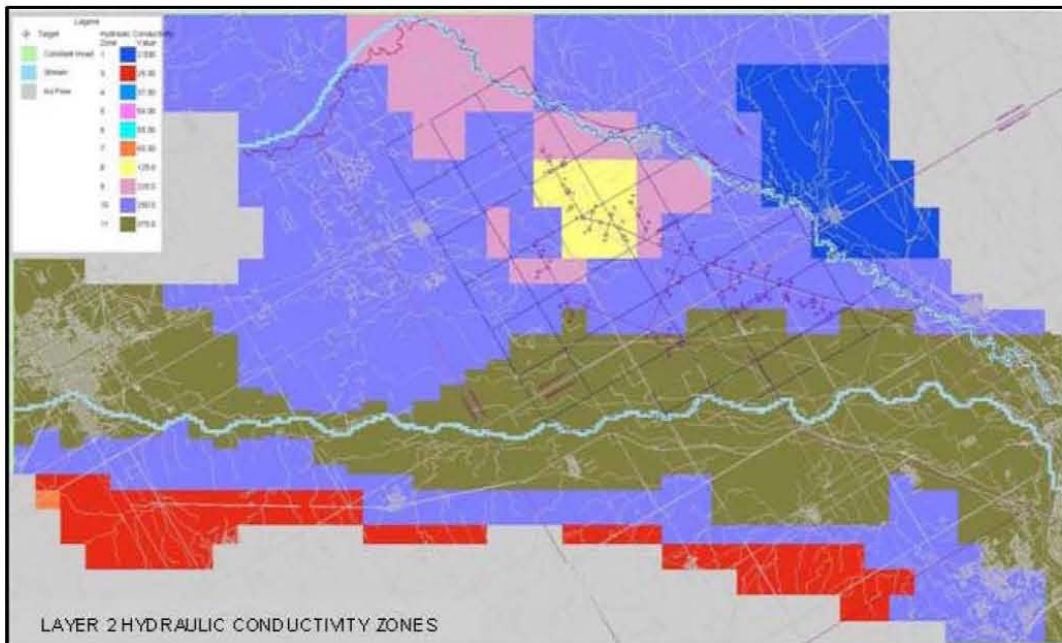


Figure A-3. Hydraulic Conductivity Zones in Layer 3

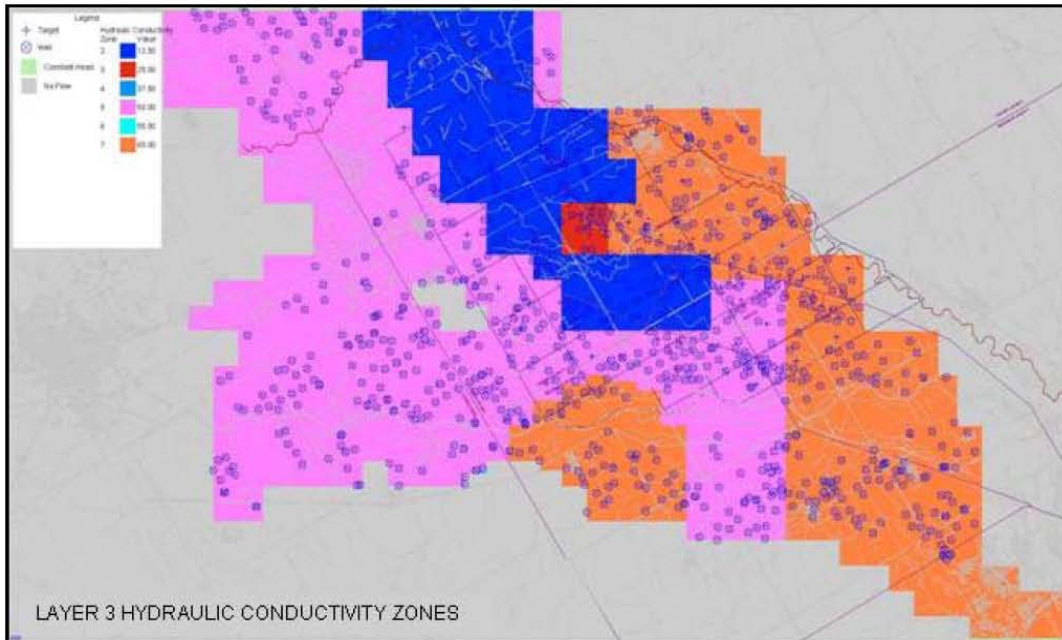
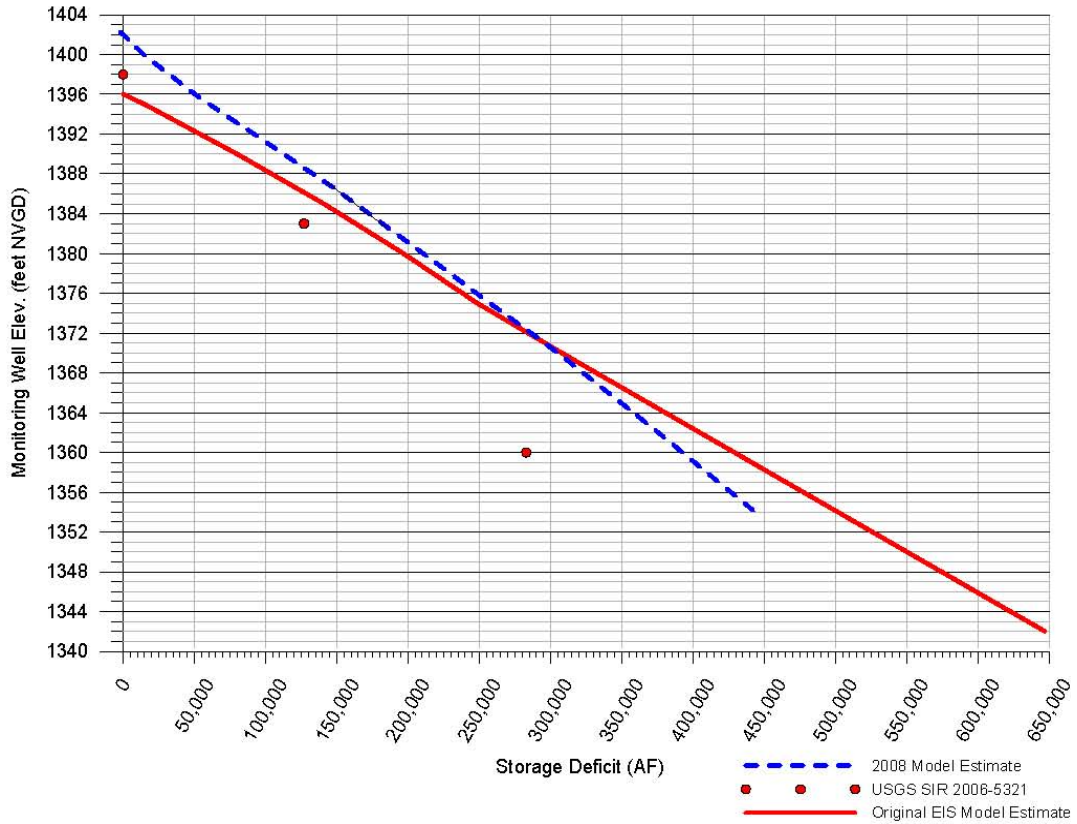


Figure A-4. Comparison of Storage Deficit vs Aquifer Head



Attachment C

Supplemental Information on Cheney Reservoir Evaporation Rates

RESERVOIR EVAPORATION RATES

This appendix documents the reservoir evaporation rate estimates that have been developed for use in planning studies for the City of Wichita’s Integrated Local Water Supply (ILWS) Plan. Discussed below are the base climatic and hydrologic data, the methodology used to develop the evaporation estimates and the resulting estimates.

Background

A computer model was developed to simulate operation of the ILWS system under various scenarios. This operations model was used initially to help with the conceptual design of the ILWS system and later to quantify potential hydrologic impacts for the project’s environmental impact statement (EIS). The operations model calculates a water balance for the ILWS system each day during the 85-year model simulation period (water years [WY] 1923–2007) using the following hydrologic data:

- Historical mean daily stream discharge at selected points within the project area
- Historical monthly reservoir evaporation rates
- Available storage and other physical data for Cheney Reservoir
- Available storage, natural recharge and other parameters for the Equus Beds aquifer
- City’s current and projected water demands
- Irrigation demands for agriculture in the Equus Beds Well Field area
- Minimum desirable streamflow requirements
- Supply capability and other operating parameters for all current and potential water supply sources
- Preferred allocation order for each water supply source

The City’s existing Cheney Reservoir is one of the principal supply sources in the ILWS system. This reservoir is located on the North Fork Ninnescah River (North Fork) about 26 miles west of downtown Wichita. Simulating the operation of this reservoir requires estimates of all significant inflow to and outflow from the reservoir, including the net evaporation from the reservoir surface. The evaporation rate estimates discussed below were used to estimate the net evaporation losses from this reservoir.

Climatic Data

The evaporation rate estimates are based directly or indirectly on recorded climatic data. The climatic data utilized in this analysis are described below:

Pan Evaporation Data

The City of Wichita has collected pan evaporation data at Cheney Reservoir since shortly after the reservoir was placed in service. These data were provided to Burns & McDonnell in the form of monthly pan evaporation rates. The period of record for these data is September 1965 through August 2008; however, there are frequent missing values during the winter months prior to 1975.

Pan evaporation data for two other stations in the vicinity of Cheney Reservoir were also collected for comparison purposes. These data are described below:

- Wichita Weather Service Office: The National Weather Service has developed estimates of average monthly pan evaporation at the Weather Service Office (WSO) in Wichita for the period 1956–1970 (NOAA, 1982b). This office is located near the Wichita airport, which is about 21 miles east-southeast of Cheney Reservoir.
- Fall River Dam: Pan evaporation data were collected at Fall River Dam from 1948–1978. This dam is located approximately 95 miles east of Cheney Reservoir.

The pan evaporation data available from these sources were converted into estimates of lake, or free water surface, evaporation by multiplying by a pan coefficient of 70 percent (NOAA, 1982a). Table 1 and Figure 1 present the average monthly lake evaporation rates calculated from these data. Review of this table and graph show that the recorded monthly evaporation at Cheney Reservoir is typically higher than at the other two locations. This condition is not unexpected because evaporation in Kansas tends to increase in a westerly direction as the climate becomes more arid.

Other Climatic Data

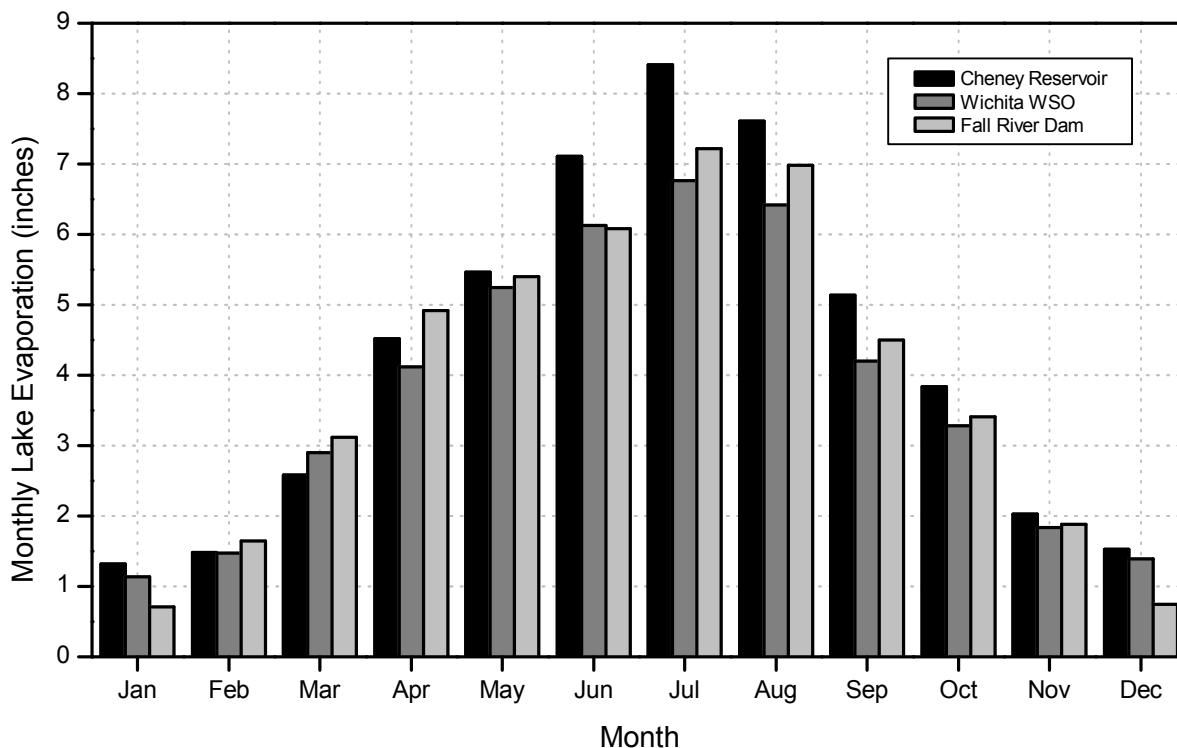
Other types of monthly climatic data were also collected for use in these evaporation rate estimates. These additional data were all collected at the National Weather Service office in Wichita. The available types of climatic data, along with their respective units and periods of record, are listed below:

Table 1: Average Monthly Lake Evaporation Rates (inches)

Month	Cheney Reservoir ^{a,b}	Wichita WSO ^{a,c}	Fall River Dam ^{a,d}
Jan	1.32	1.14	0.71
Feb	1.48	1.47	1.65
Mar	2.58	2.90	3.12
Apr	4.52	4.12	4.92
May	5.46	5.25	5.40
Jun	7.11	6.13	6.08
Jul	8.41	6.76	7.22
Aug	7.61	6.42	6.98
Sep	5.14	4.20	4.50
Oct	3.84	3.28	3.41
Nov	2.03	1.84	1.88
Dec	1.53	1.39	0.75
Annual	51.03	44.90	46.62
May-Oct	37.57	32.04	33.59

- a. Calculated from recorded or estimated pan evaporation data using pan coefficient of 70 percent.
- b. Pan evaporation data collected by City for period Sep 1965-Aug 2007.
- c. National Weather Service estimates of pan evaporation for period 1956–1970.
- d. Pan evaporation data collected for period 1948–1978.

Figure 1: Average Monthly Lake Evaporation Rates



- Average monthly temperature (degrees F.) — Jan 1922–Dec 2007
- Total monthly precipitation (inches) — Jan 1930–Dec 2007
- Average monthly relative humidity (percent) — Jan 1954–Dec 1997
- Average monthly wind speed (miles/hour) — Jan 1954–Dec 1997
- Average monthly barometric pressure (millibars) — Jan 1954–Dec 1997
- Average monthly sunshine (percent of possible sunshine) — long-term averages by month only
- Average solar radiation (megajoules/square meter) — long-term averages by month only

Average monthly values for these data are listed in Table 2. Appendix A contains a complete listing of the data types that have long periods of record: temperature, precipitation, relative humidity, wind speed and barometric pressure. As noted above, many of these data types are only available starting in 1954. For earlier periods when these data types are missing, long-term average monthly values were used as a substitute for actual monthly data.

Table 2: Average Monthly Climatic Data^a

Month	Temperature	Precipitation	Percent Sunshine	Relative Humidity	Solar Radiation	Wind Speed	Baro. Pressure

	(deg. F.)	(inches)		(percent)	(MJ/m ²)	(mph)	(millibars)
Jan	31.3	0.88	61	74.4	9.29	10.0	971.5
Feb	36.5	1.03	61	72.8	11.97	10.9	970.2
Mar	45.0	2.07	61	69.4	15.99	11.6	966.7
Apr	56.2	2.67	64	69.4	19.76	11.8	965.7
May	65.6	4.04	65	74.4	22.78	10.3	965.4
Jun	75.7	4.47	70	72.8	25.20	10.2	965.7
Jul	81.1	3.42	76	67.8	22.12	9.3	967.4
Aug	81.0	3.25	75	68.8	19.32	9.1	967.8
Sep	71.1	3.21	68	72.6	18.71	9.7	968.6
Oct	59.3	2.48	65	71.5	14.40	9.9	969.4
Nov	44.9	1.50	59	73.4	10.26	10.2	969.4
Dec	34.7	1.16	58	75.2	8.29	9.8	970.8

a. All of these data were collected at the Wichita Weather Service Office. The period of record for these data varies. Percent sunshine and solar radiation available only as long-term averages by month.

Evaporation Model

The pan evaporation data collected by the City at Cheney Reservoir are considered to provide the best possible estimates of reservoir evaporation when available (Table B-1 in Appendix B). However, these data start in the mid-1960s when the reservoir was placed in operation and do not cover the entire simulation period used in the operations model (WY1923–2007). For the period prior to 1965, reservoir evaporation rate estimates were calculated for Cheney Reservoir using Burns & McDonnell’s ETCALC computer model. This model uses a form of the Penman Equation to estimate evaporation depths. In general, the ETCALC model uses the following procedure to estimate evaporation rates.

- Advective Losses: The ETCALC model contains a number of relationships to estimate advective, or aerodynamic, losses from the reservoir surface. Advective losses occur as water evaporates from the reservoir into the air immediately over the water surface. This process will occur whenever this air is unsaturated with water vapor (that is, has a relative humidity less than 100 percent). Wind that flows across the reservoir surface will then carry this “wetter” air away and replaces it with air that is

relatively drier, allowing the process to continue. Advective losses are primarily a function of air temperature, relative humidity and wind speed.

- Energy Budget: A substantial amount of heat energy is required to transform water in liquid form into water vapor. The ETCALC model also contains relationships to estimate the amount of evaporation that would occur using an energy budget, or heat balance, methodology. The principal source of heat energy that controls evaporation is the Sun. Incident solar radiation at the reservoir varies seasonally, based on the inclination of the Earth's axis and its distance from the Sun, and with the amount of cloud cover (percent possible sunshine).
- Weighting Function: The Penman Equation uses a weighting function to estimate potential evapotranspiration from the separate advective loss and energy balance estimates. This weighting function is based on the slope of the saturation-vapor-pressure versus temperature curve at the given air temperature. (Linsley, et. al., 1982).

The relationships build into the ETCALC model — the relationships that estimate the advective loss, energy budget and weighting function terms described above — use the types of climatic data listed in the previous section as inputs. For the most accurate evaporation estimates, these inputs should be daily data. However, records of daily climatic data have become widely available only in recent years. Therefore the ETCALC model was designed to use monthly inputs and generate monthly evaporation rate estimates.

Model Calibration

The ETCALC model must be calibrated to yield accurate evaporation estimates. There are two calibration coefficients available in the model that can be used to adjust the resulting evaporation rate estimates. The model was calibrated using the available pan evaporation data collected by the City at Cheney Reservoir, which start in September 1965. When available, the ETCALC model will use recorded evaporation data to calculate a goodness-of-fit statistic based on the differences between monthly recorded and estimated evaporation rates (sum of the squares of the residuals). For calibration, the ETCALC model was executed for a period September 1965–December 1996. The calibration coefficients were adjusted by trial and error until a minimum value for this goodness-of-fit statistic was obtained.

Evaporation RATE Estimates

Once the ETCALC model was successfully calibrated, it was re-executed to estimate monthly evaporation rates for the entire simulation period, WY1923–2007. The evaporation rates estimated in the ETCALC model are gross rates for Cheney Reservoir. These estimated evaporation rates were combined with the data recorded by the City to yield a composite record. That is, whenever recorded evaporation data were available, they were used in preference to values estimated by the ETCALC model. The resulting gross evaporation rate estimates are listed in Table B-2.

Precipitation that falls directly on the surface of Cheney Reservoir will tend to offset some of the gross evaporation from the reservoir. The resulting evaporation — gross evaporation less direct precipitation — is referred to as net reservoir evaporation. Not all of the precipitation that strikes the surface of a reservoir is considered to reduce evaporation. In the absence of the reservoir, some of this precipitation would have run off from the portion of the watershed that is covered by the reservoir itself and contribute to the discharge in the North Fork. This direct runoff was accounted for in the reservoir’s inflow estimates. Therefore, to avoid double counting this water, monthly net evaporation estimates (N) were calculated using the following formula:

$$N = G - P + R$$

In this equation, G is the estimated monthly gross evaporation and P is the estimated total monthly precipitation at Cheney Reservoir. The direct runoff component (R) is also a function of precipitation and was estimated to be 30 percent of direct precipitation. Substituting this relationship for direct runoff ($R = 0.3P$) into the above equation yields the following equation for net evaporation:

$$N = G - 0.7 P$$

Substituting the values of gross evaporation (G) (Table B-2) and precipitation (P) (Table A-2), yields the monthly net evaporation rates estimates. These net evaporation rates are listed in Table B-3. These net evaporation rates can be negative in months when precipitation exceeds evaporation.

Summary

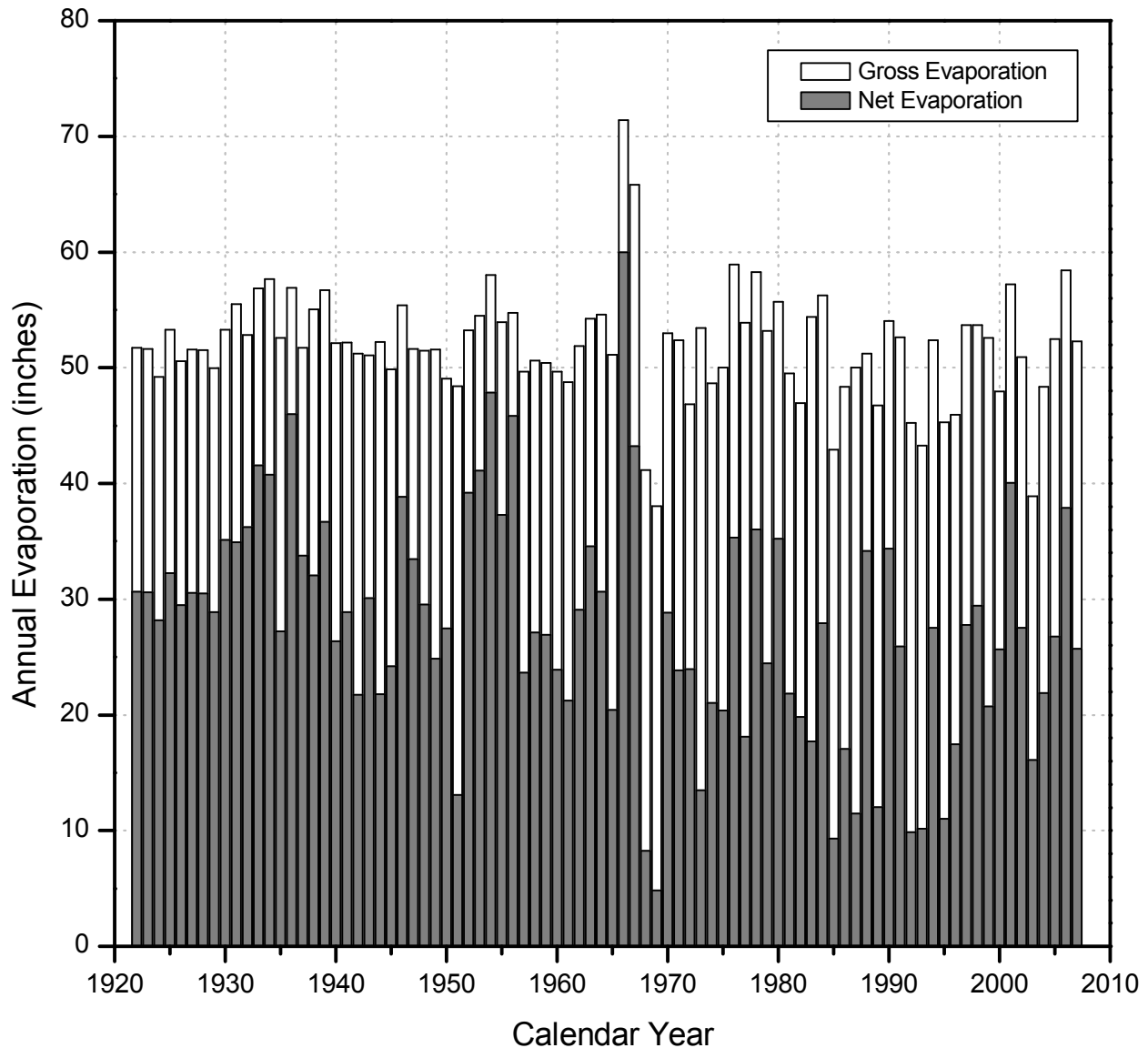
Table 3 is a summary that lists average monthly rates for gross and net evaporation. Figure 2 is a graph of estimated annual gross and net evaporation rates that shows how these rates vary from year to year.

Table 3: Average Monthly Evaporation Rates at Cheney Reservoir

Month	Gross Evaporation (inches)	Net Evaporation (inches)
Jan	1.53	0.85
Feb	1.71	0.92
Mar	2.66	0.94
Apr	4.18	2.04
May	5.25	2.01
Jun	6.88	3.26
Jul	8.31	5.57
Aug	7.86	5.26
Sep	5.47	2.90
Oct	4.08	2.10
Nov	2.27	1.06
Dec	1.68	1.06
Annual	51.88	27.67

Review of Figure 2 shows that annual gross evaporation ranged from a low of 38.02 inches in 1969 to a high of 71.42 inches in 1966; annual gross evaporation averages 51.88 inches. Annual net evaporation is more variable than gross evaporation because it is influenced by precipitation, which can vary significantly from year to year. The range in annual net evaporation was from about 5 to 60 inches, with an average of nearly 28 inches.

Figure 2: Annual Gross and Net Reservoir Evaporation (inches)



The operations model uses a daily time step so it requires estimates of daily evaporation. The daily evaporation rates used in the operations model were estimated from these monthly data by simply dividing the monthly totals by the number of days in each month to yield average daily values by month.

References

Complete citations for the references cited in this document are listed below:

Linsley, R., Kohler, M. & Paulhus, J. (1982). *Hydrology for engineers*. New York: McGraw-Hill Book Company

National Oceanic and Atmospheric Administration (NOAA). (1982a, July). *Evaporation Atlas for the Contiguous United States* [Technical Report NWS 33]. U.S. Department of Commerce, National Oceanic and Atmospheric Administration, National Weather Service: Washington, DC.

NOAA. (1982b, December). *Mean Monthly, Seasonal, and Annual Pan Evaporation for the United States* [Technical Report NWS 34]. U.S. Department of Commerce, National Oceanic and Atmospheric Administration, National Weather Service: Washington, DC.

* * * * *

Attachment D

Supplemental Information on Streamflow Discharge Development for RESNET Model

STREAMFLOW ESTIMATES

This appendix documents the streamflow estimates that have been developed for use in planning studies for the City of Wichita’s Integrated Local Water Supply (ILWS) Plan. Discussed below are the base historical streamflow data, the methodology used to synthesize flow estimates, and the resulting estimates.

Background

A computer model was developed to simulate operation of the ILWS system under various scenarios. This operations model was used initially to help with the conceptual design of the ILWS system; it was later used to quantify potential hydrologic impacts for the project’s environmental impact statement (EIS). The operations model calculates a water balance for the ILWS system each day during the 85-year model simulation period (water years [WY] 1923–2007) using the following hydrologic data:

- Historical mean daily stream discharge at selected points within the project area
- Historical monthly reservoir evaporation rates
- Available storage and other physical data for Cheney Reservoir
- Available storage, natural recharge and other parameters for the Equus Beds aquifer
- City’s current and projected water demands
- Irrigation demands for agriculture in the Equus Beds Well Field area
- Minimum desirable streamflow requirements
- Supply capability and other operating parameters for all current and potential water supply sources
- Preferred allocation order for each water supply source

The ILWS system is represented in the operations model as a network of nodes with connecting links. The majority of the model nodes represent locations on project area streams; the remaining nodes represent off-stream features, such as well fields, treatment plants and pipeline junctions. A schematic of the overall operations model network is shown in Figure 1. The nodes shown in Figure 1 with dark shading are stream nodes that receive unregulated surface runoff. These stream nodes are listed in Table 1 along with their corresponding node numbers.

Figure 1: Operations Model Schematic

(see Page A4 of Attachment A)

Table 1: Model Stream Nodes with Unregulated Inflow

Model Stream Node (Node Number)	Model Stream Node (Node Number)
Arkansas River near Hutchinson (10)	Little Arkansas River at Mouth (70)
Arkansas River near Maize (20)	Arkansas River at Wichita (80)
Little Arkansas River at Alta Mills (30)	NF Ninnescah River at Cheney Reservoir (90)
Little Arkansas River at Halstead (40)	Ninnescah River near Peck (100)
Little Arkansas River near Sedgwick (50)	Arkansas River at Arkansas City (110)
Little Arkansas River at Valley Center (60)	

To maintain a daily water balance for the ILWS system, the operations model requires estimates of mean daily streamflow at each of these stream nodes. As there is no practicable method available that can predict future hydrologic conditions with any certainty, these streamflow estimates are based on historical data. These historical data are used as a surrogate for possible future streamflow. The historical streamflow estimates developed for the operations model are described below.

Recorded Stream Discharge Data

In the United States, stream discharge data are collected primarily by the U.S. Geological Survey (USGS). Although the USGS maintains a network of stream gaging stations located throughout the country, it does not operate gaging stations at each of the stream nodes identified above. Therefore, it was necessary to synthesize some of the stream discharge data used in the operations model from those data that were available. The available stream gages of interest in the project vicinity are listed in Table 2 along with other relevant data. A map showing the locations of these gages is included as Figure 2 (USGS, no date). The recorded mean daily discharge for these gages was downloaded from the USGS' National Water Information System (NWIS), an online database system.

Review of Table 2 shows these streamflow records start as early as 1921 for the Arkansas River; however, only two of these gages, the Little Arkansas River at Valley Center (Station 07144200) and Arkansas River at Arkansas City (Station 07146500), have long continuous records. Under the ILWS plan, the Little Arkansas River is the primary new water source, both for direct use and aquifer recharge; therefore, this gage's period of record was used to define the simulation period for the project operations model: WY 1923-2007 (October 1922–September 2007).

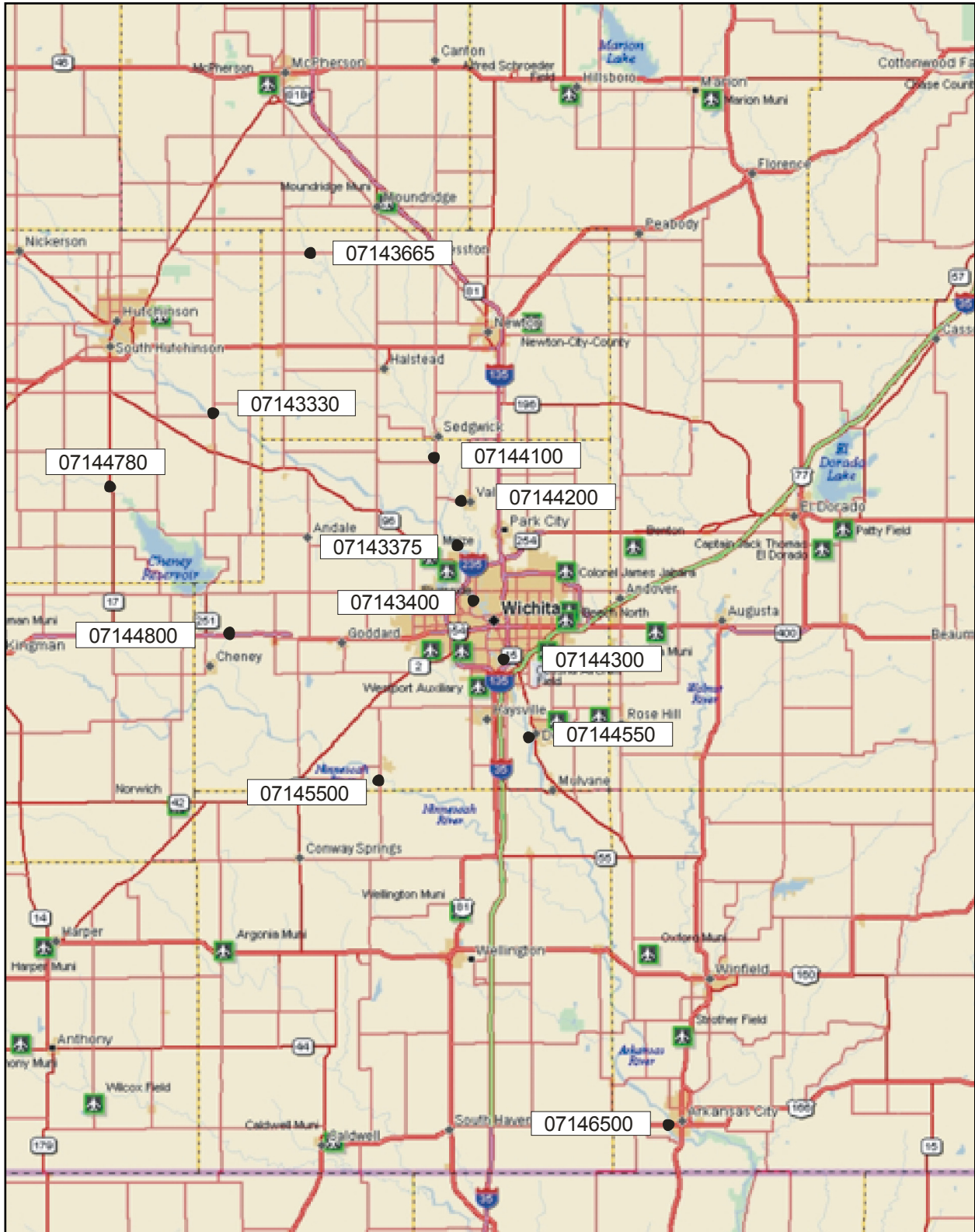
Table 2: USGS Stream Gaging Stations^a

Station Number	Name	Location (Latitude/ Longitude)	Drainage Area ^b (sq. mi.)	Period of Record
07143330	Arkansas River near Huchinson, KS	37°56'47" 97°45'29"	31,724	10/01/59- 09/30/07
07143375	Arkansas River near Maize, KS	37°46'53" 97°23'33"	31,924	03/01/87- 09/30/07
07143400	Arkansas River near Wichita, KS	37°42'30" 97°21'50"	31,978	10/01/21- 03/31/35
07143665	Little Arkansas River at Alta Mills, KS	38°06'44" 97°35'30"	681	06/06/73- 09/30/07
07143672	L. Arkansas River at Hwy 50 near Halstead, KS	38°01'43" 97°32'25"	685	05/01/95 09/30/07
07144100	Little Arkansas River near Sedgwick, KS	37°52'59" 97°25'27"	1,165	10/01/93- 09/30/07
07144200	Little Arkansas River at Valley Center, KS	37°49'56" 97°23'16"	1,253	06/10/22- 09/30/07
07144200	Little Arkansas River Floodway ^c	---	---	---
07144300	Arkansas River at Wichita, KS	37°38'41" 97°20'06"	33,227	10/01/34- 09/30/07
07144300	Big Slough-Cowskin Floodway ^d	---	---	---
07144550	Arkansas River at Derby, KS	37°32'34" 97°16'31"	33,567	10/01/68- 09/30/07
07144780	N. Fork Ninnescah River above Cheney Res., KS	37°50'41" 97°56'09"	550	07/01/65- 09/30/07
07144795	North Fork Ninnescah River at Cheney Dam, KS	37°43'17" 97°47'39"	664	10/01/64- 09/30/07
07144800	North Fork Ninnescah River near Cheney, KS	37°40'00"	685	10/01/50-

		97°46'00"		09/30/64
07145500	Ninnescah River near Peck, KS	37°27'26" 97°25'20"	1,785	04/01/38- 09/30/07
07146500	Arkansas River at Arkansas City, KS	37°03'23" 97°03'32"	36,106	10/01/21- 09/30/07

- a. The available data at these gaging stations were downloaded from USGS NWIS database system.
- b. Contributing drainage area.
- c. During periods of high flow, some of the flow in the Little Arkansas River is diverted through the Little Arkansas Floodway into the Arkansas River. Flow data for Station 07144200 is a composite of flow in main stem of Little Arkansas River and Little Arkansas River Floodway.
- d. During periods of high flow, some of the flow in the Arkansas River is diverted around Wichita through the Big Slough-Cowskin Floodway. These diverted flows re-enter the Arkansas River downstream of Wichita near Derby, KS. Flow data for Station 07144300 is a composite of flow in main stem of Arkansas River and Big Slough-Cowskin Floodway.

Figure 2: Location Map for USGS Stream Gages



Stream discharge can vary significantly from day to day and year to year based on weather patterns and other factors. On an annual basis, this variability is illustrated in a graph of the annual discharge in the Little Arkansas River at Valley Center (Valley Center gage) (Figure 3). These annual discharges have ranged from a low of approximately 18,000 acre-feet in WY 1934 to 1.23 million acre-feet in WY 1993, a factor of more than 100.

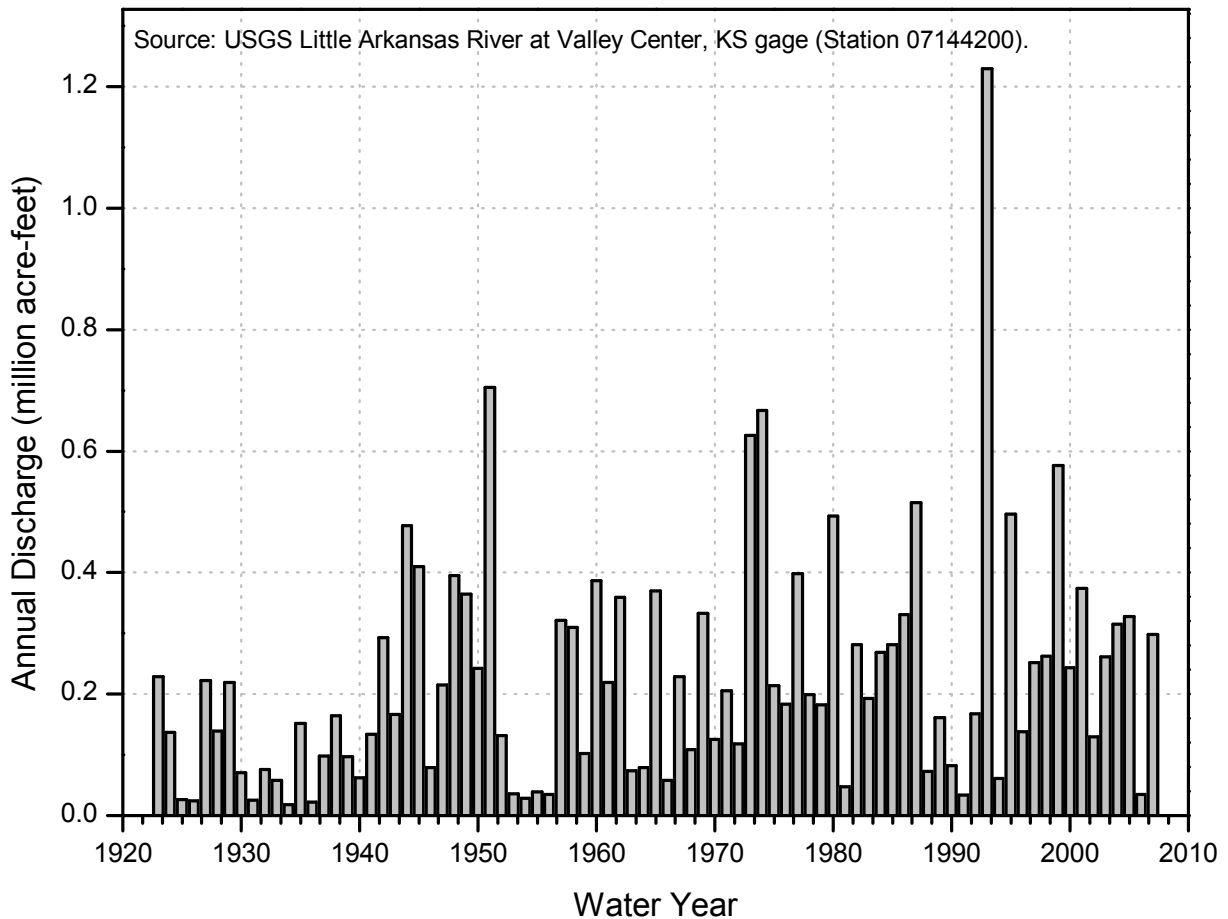


Figure 3: Annual Discharge in Little Arkansas River at Valley Center

For water supply purposes, the most critical periods during the available record are times of drought. In Kansas and much of the central plains region, the drought of record occurred in the mid-1950s. Following widespread flooding in WY 1951 and normal flows in WY 1952, the next four consecutive water years (1953–1956) proved to be exceptionally dry. Individually, there were several water years during the “dust bowl” of the 1920s and 1930s that were drier than these four years (1934, 1936, 1926, 1931, and 1925),

but never more than two in a row. This drought generally ended in February 1957 with heavy rains across the region.

On a daily basis, the mean flow at the Valley Center gage has ranged from 1.1 to 28,600 cubic feet per second (cfs), and averages 315 cfs. Figure 4 is a flow duration curve for this stream gage that shows this daily variability. From this figure, the median (50 percent) discharge in the Little Arkansas River is shown to be 59 cfs, approximately one fifth of the average flow. The 10- and 90-percent flows at this gage are 494 and 21 cfs, respectively.

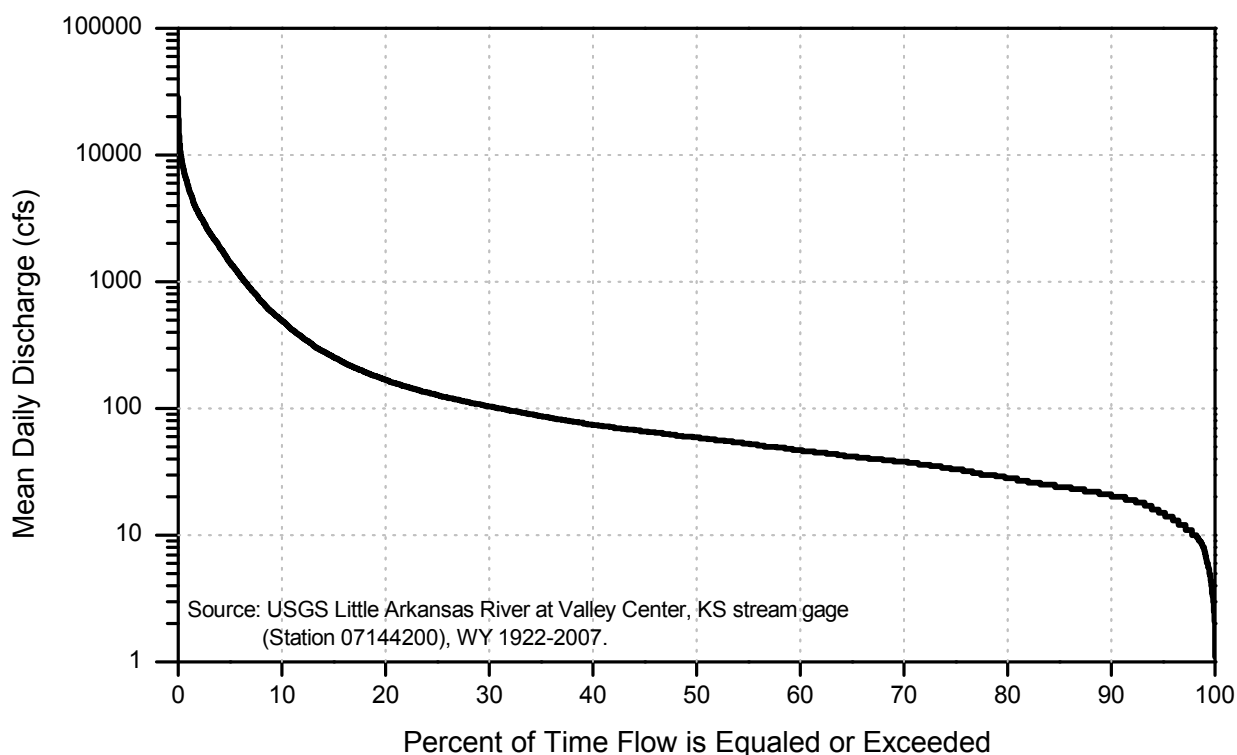


Figure 4: Flow Durations in Little Arkansas River at Valley Center

Natural Stream Discharge

Natural stream discharge is the discharge that would have occurred in a stream without any man-made influences. These influences can include construction of an upstream reservoir, direct withdrawals for water supply or irrigation, or indirect withdrawals caused by groundwater depletions. Over time, these influences tend to become more pronounced as the water resources within a stream’s watershed area are developed.

As a typical first step in the development of a computer model for a water supply system, the available recorded streamflow data are naturalized. That is, they are adjusted to reflect estimated natural conditions by attempting to remove the affects of significant man-made influences. Estimating these influences, however, requires detailed records of applicable stream withdrawals and reservoir operations plus estimates of stream-aquifer interactions (discharges from aquifer to stream and depletions from stream to aquifer). Unfortunately, many of the necessary historical data often do not exist. Even where these data do exist, collection of these data can become a daunting task for a watershed the size of the Arkansas River.

Within the ILWSP project area, there are three primary streams of interest: the North Fork Ninescah, Little Arkansas and Arkansas rivers. Each of these streams is discussed separately below.

North Fork Ninescah River

The North Fork Ninescah River is home to Cheney Reservoir. Other than Cheney Reservoir itself, there is little development within this watershed that would significantly impact streamflow volumes. Land use within the watershed upstream of the reservoir is largely agricultural. Some of this cropland is irrigated but this water is supplied from groundwater and not by diversions from the river. The flow in this river and its tributaries is sporadic enough that surface water diversions have limited utility without accompanying storage. The City has relatively senior surface water rights for Cheney Reservoir and a comprehensive watershed protection program is in place for the reservoir's catchment area.

There are two stream gages on this stream that were used to estimate Cheney Reservoir inflow. The gage near Cheney (Station 07144800) is located below Cheney Dam; this gage was discontinued when the reservoir was placed in service. The other gage of interest (Station 07144780) is located above the reservoir. As a result, neither of these flow records requires adjustment because of the reservoir. Therefore, given there has been little other surface water development in this watershed, the recorded flow at these two gages is considered reasonably equivalent to natural flow.

About 15 miles downstream of Cheney Reservoir, the North and South Forks meet to form the main stem of the Ninescah River. There is another stream gage downstream on the Ninescah River that was included as a stream node in the operations model: Ninescah River near Peck (Station 07145500). About 37 percent of this gage's drainage area is located above Cheney Dam and the recorded flow at this gage has been impacted by operation of the reservoir since it went online in 1964. Therefore, the recorded flows at this gage are generally less than natural in recent years. However, this node was included in the

operations model only to show the impacts (discharge differences) of the various alternatives. For this reason, natural flow at this gage was not estimated.

Little Arkansas River

The Little Arkansas River is the major new water source that will be developed under the ILWS plan. The water in this river will be used directly to meet current City water demands and for aquifer recharge. Land use within this river's watershed is mostly agricultural, except at its extreme northern extent where the City of McPherson is located. Water supplies within this area are derived almost exclusively from groundwater. There are a few small surface water rights on the Little Arkansas River but none result in significant depletions.

There are four USGS stream gages on the Little Arkansas River that were used as stream nodes in the operations model: Alta Mills (Station 07143665), Halstead (Station 07143672), Sedgwick (Station 07144100), and Valley Center (Station 07144200). Given the general lack of significant surface water diversions within the Little Arkansas River watershed and the Alta Mills gage's location relatively high in the watershed, no adjustments were made to this gage's record.

Similarly, the flow record at the Sedgwick, Halstead and Valley Center gages has not been significantly influenced by surface water diversions. However, groundwater discharge from the Equus Beds aquifer does contribute to the base flow in the river at these gages. The operations model includes routines to estimate this groundwater discharge so the incremental runoff between these gages was adjusted later to remove the estimated historical groundwater discharge. This process avoids double counting of this groundwater discharge in the operations model and yields more accurate results.

Arkansas River

The Arkansas River runs through Wichita but because of its poor quality characteristics (high saline content), it is not currently a major water source for the City; use of this water source will increase under the ILWS plan but not significantly. Above Wichita, the Arkansas River drains a contributing watershed that covers more than 33,000 square miles, including about one-half of the State of Kansas. The water resources of the Arkansas River have been extensively developed, with the first ditch diversions for irrigation occurring in the late 1800s.

Although these surface water diversions have impacted the flow in this river, the more significant impacts have occurred because of groundwater development. The High Plains and other aquifers of the central plains states have been developed extensively for irrigation, municipal, and industrial use. This groundwater usage exploded beginning in the late 1960s with the development of reliable center pivot irrigation systems, which encouraged farmers to begin irrigating thousands of square miles of cropland in eastern Colorado and western Kansas. The resulting declines in groundwater levels have turned the Arkansas River into a losing stream; historically, the discharge from alluvial aquifers helped maintain the base flow in this river. Figure 5 provides an illustration of just how significant these flow impacts have been. This graph shows the annual flow in the Arkansas River at Dodge City, which is located about 150 miles west of Wichita. Prior to the 1970s, the discharge at Dodge City was typically 40,000 acre-feet or more even in drier years. By the mid-1970s, typical dry-year flows had dropped to zero or nearly zero.

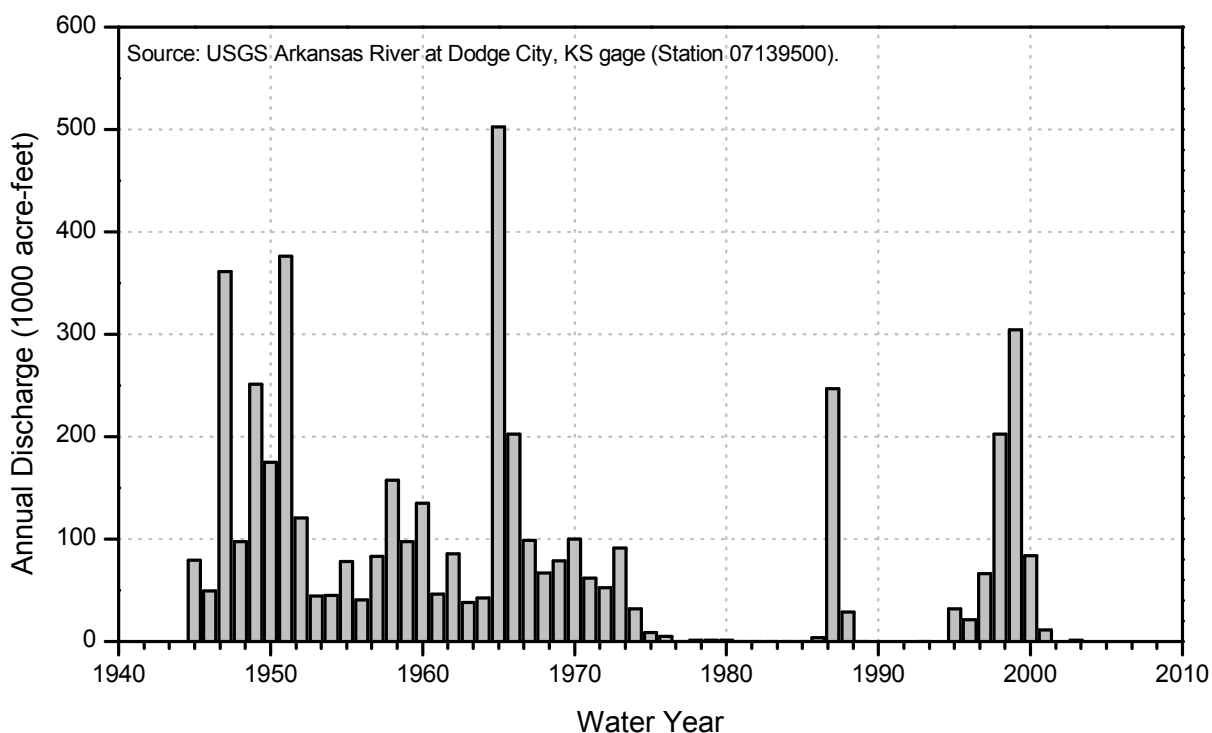


Figure 5: Annual Arkansas River Discharge at Dodge City

Downstream in Wichita, the impacts of stream depletions can be seen when comparing flow durations for periods before and after this groundwater development period. Figure 6 shows two flow duration curves for the Arkansas River at Wichita: one for water years (WY) 1935–1975 and the second for WY 1976–2007. Examination of these graphs show that flows have typically decreased in the midrange, from about 20 to 80 percent. However, the lowest flows — those with durations greater than 85 percent — have

actually increased. This latter observation is counterintuitive but may be a result of increased wastewater or other man-made discharges.

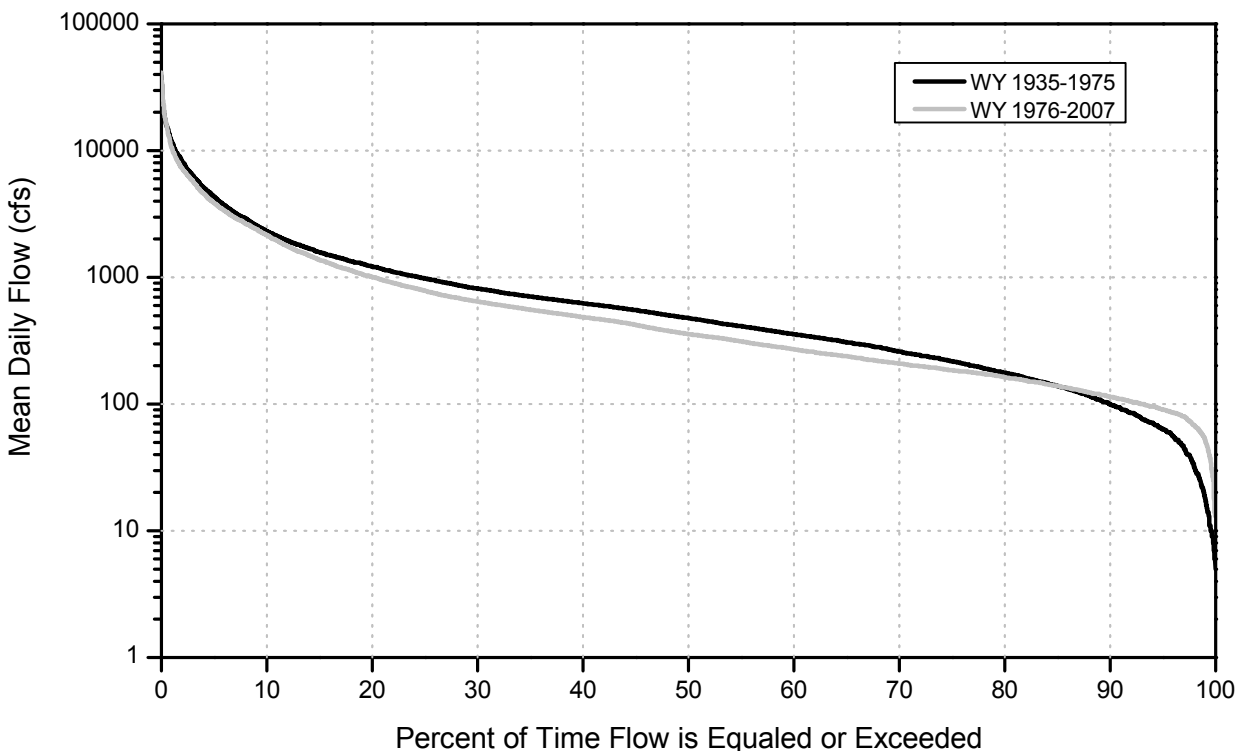


Figure 6: Flow Durations for Arkansas River at Wichita

Naturalizing the flow records for the Arkansas River would require collecting historical data on direct stream diversions from the river and its tributaries, and on groundwater withdrawals plus development of a groundwater model capable of estimating stream-aquifer interactions. Such a major effort was not considered practicable or justifiable given the comparisons presented above and the fact that the Arkansas River is a relatively minor water source for the City of Wichita.

Synthesis of Streamflow Estimates

As mentioned in Section 2, there are only two stream gages in the project vicinity with long continuous records that span the entire model simulation period: the Valley Center and Arkansas River at Arkansas City (Arkansas City) gages. At all other model stream nodes (Table 1), all or portions of the flow data used in the operations model were synthesized. The methods used to synthesize these data are described below:

Methodology

For stream nodes located at stream gages, whether active or discontinued, there are discharge data that cover a portion of the model simulation period. At these locations, it was necessary to fill in the missing data with estimates based on recorded data at other nearby gages. At stream nodes that are not located at an active or discontinued stream gage, a complete 85-year record was generated. In either case, the missing flow data at the target stream node were estimated based on the recorded data at a nearby source gage or gages that have data for the missing period. In selecting source gages, preference was given to gages available on the same stream, located either upstream or downstream of the target stream node, that have comparable drainage areas. For target gages without any nearby upstream or downstream gages, data for a gage on another, nearby stream were used.

For target nodes located at an active or discontinued stream gage, the missing data were estimated by first calculating the average annual unit discharge at the target and source stream gages. Unit discharge was calculated by dividing a gage's flow by its contributing drainage area, yielding values in cfs/square mile. When the target and source gages have an overlapping period of record, regression analyses were used to determine a best-fit line through these data:

$$q_t = a + bq_s$$

Where:

q_t = Recorded average annual unit discharge for target stream node (cfs/square mile)

q_s = Recorded average annual unit discharge for source stream gage (cfs/square mile)

a = Intercept of best-fit line through data

b = Slope of best-fit line through data

When the regression analyses returned a best-fit line with a negative intercept or relatively large positive intercept, an alternate analysis was performed with an intercept forced to go through zero. This adjustment avoided problems later on days when the flow in the source gage was zero or near zero. With a negative intercept, the equation above returns an invalid negative flow estimate. Where the regression analysis returns a large positive intercept, the calculated flows yielded unrealistically high minimum flows. When there is no overlapping period of record for the target and source gages, the intercept and slope were assumed to be zero and one, respectively.

The regression analyses described above were based on average annual flows but later used to develop daily flow estimates. The mean daily discharges at the target stream node were estimated using these regression results in the following equation:

$$Q_t = \left(a + b \times \frac{Q_s}{A_s} \right) * A_t$$

Where:

Q_t = Estimated mean daily discharge at target stream node (cfs)

Q_s = Recorded mean daily discharge at source gage(s) (cfs)

A_s = Contributing drainage area at source gage (square miles)

A_t = Contributing drainage area at target stream node (square miles)

For those source and target gages that have no overlapping period of record, this equation simplifies to a straight drainage area ratio when substituting $a = 0$ and $b = 1$.

Arkansas River near Hutchinson

The uppermost stream node on the Arkansas River is located about 24 miles upstream of Wichita at the USGS' Arkansas River near Hutchinson stream gage (Station 07143330). The period of record at this gage starts in October 1959 and runs through the end of the model simulation period. Prior to October 1959, the flow data for this stream node were estimated from two downstream gages on the Arkansas River: Arkansas River near Wichita and Arkansas River at Wichita. The specifics of these estimates are described below:

- Arkansas River near Wichita gage (Station 07143400): The period of record for this source gage runs from October 1921–March 1934, so it does not overlap the record at the near-Hutchinson gage. Therefore, the flow at this target stream node was estimated from the data at this source gage using a multiplier based on the ratio of the respective drainage areas. The flow estimates derived from this source gage extend from October 1922–September 1934.
- Arkansas River at Wichita gage (07144300): This stream gage began operation in October 1934, replacing the near-Wichita gage discussed in the previous bullet item. This gage has been in continuous operation since that time, so there is an overlapping period of record for the target, near-

Hutchinson stream node and this source gage (October 1959–September 2007). A major tributary, the Little Arkansas River, enters the Arkansas River between the Hutchinson and Wichita gages. The flow in this tributary (as measured at the Valley Center gage) was netted out of the flow at the Wichita gage before making flow comparisons. These comparisons are shown in Figure 7. The best-fit regression line through these points has an intercept of 1.9277E-4 and a slope of 0.80236, with a coefficient of determination (R^2) of about 0.947. For the period October 1934–September 1959, mean daily discharge at the near-Hutchinson stream node was estimated from this source gage using these regression results.

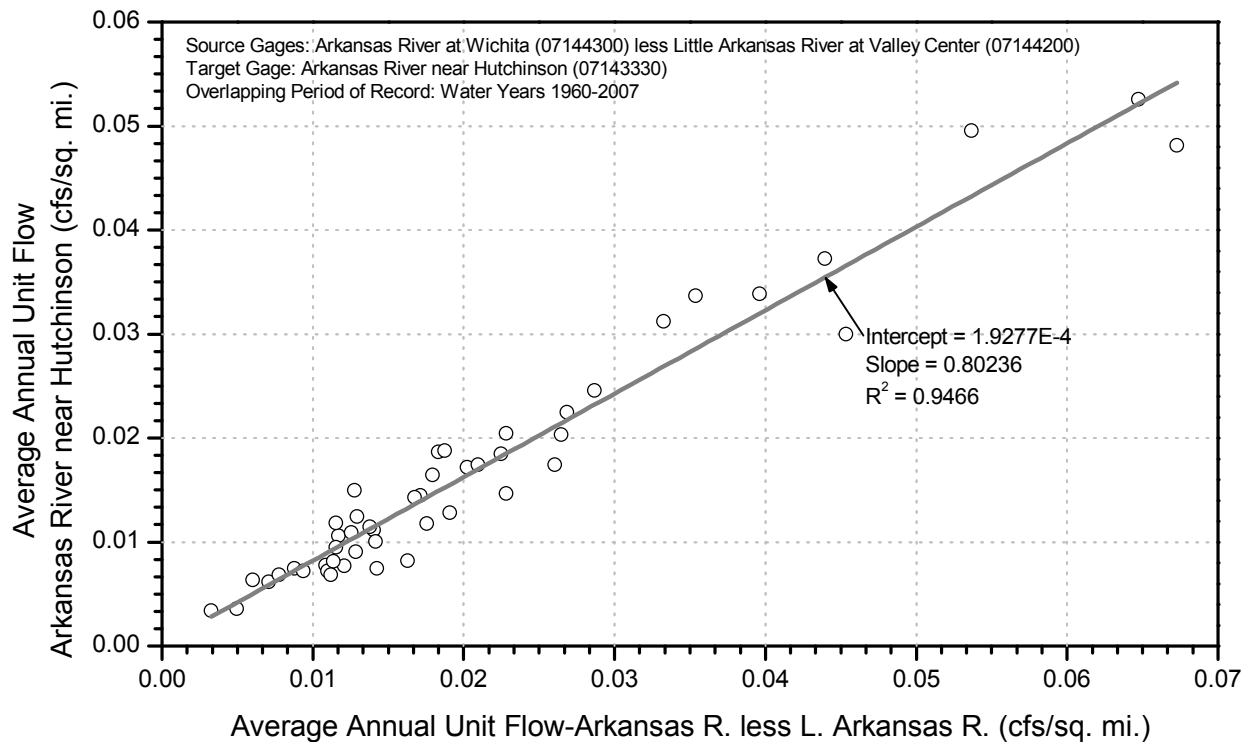


Figure 7: Discharge Comparison–Arkansas River near Hutchinson vs. at Wichita

If the unit runoff at these two Arkansas River gages was equivalent (that is, proportional to their respective drainage areas), the regression line shown in Figure 7 would have an intercept of zero and a slope of one. This seemingly large discrepancy results because the Arkansas River frequently runs dry in central Kansas because of upstream regulation and stream depletions. Therefore, the true effective contributing drainage area for these gages usually starts in central Kansas and not at the continental divide in Colorado.

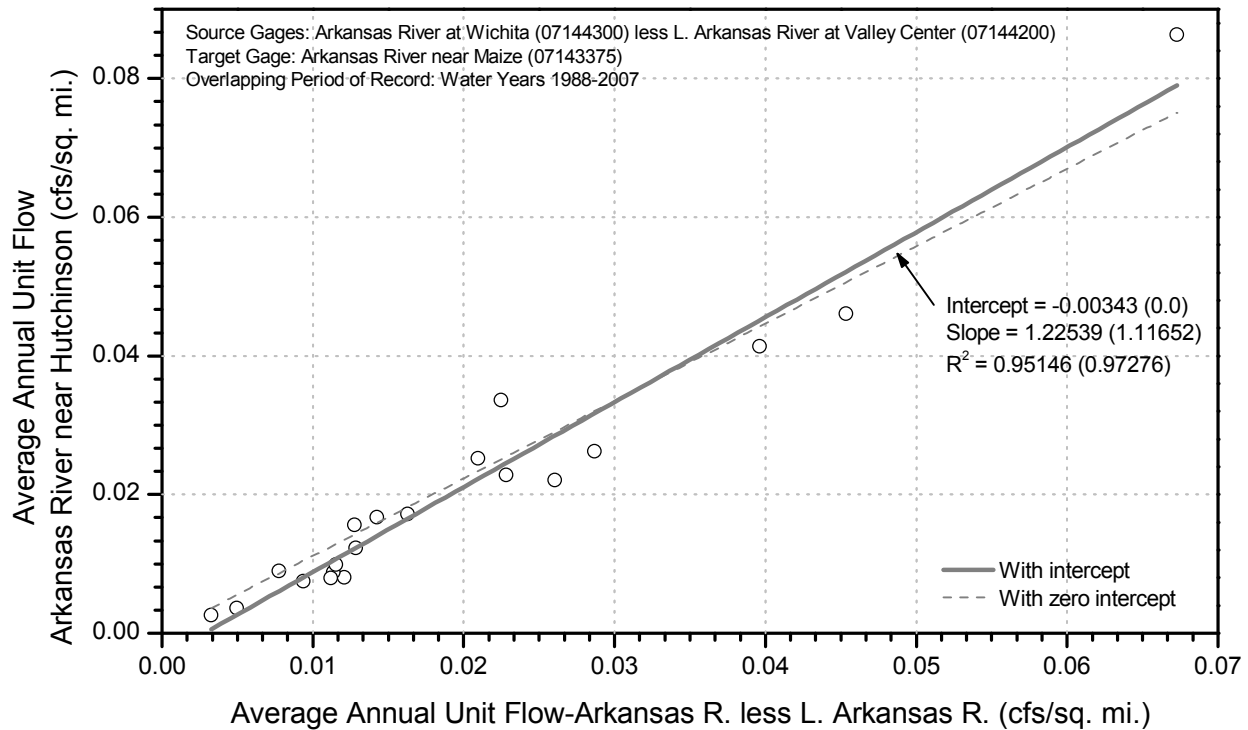
Starting in October 1959, the actual recorded data at the near-Hutchinson stream gage was used for this stream node.

Arkansas River near Maize

The USGS' Arkansas River near Maize, Kansas stream gage (Station 07143375) is located a short distance upstream of the Wichita metropolitan area. The period of record for this gage is March 1987 to present. Prior to March 1987, the flow data for this stream node were estimated using the Arkansas River near Wichita and Arkansas River at Wichita gages. The methods used to estimate the missing flow data at this node are described below:

- Arkansas River near Wichita gage (Station 07143400): The period of record for this source gage runs from October 1921–March 1934; therefore, its record does not overlap that at the near-Maize gage. For this reason, the target node flow estimates derived from this source gage's data were developed using a drainage area ratio. The ratio of the contributing drainage areas at the near-Maize and near-Wichita gages is 0.998 (31,924 square miles/31.978 square miles). The flow estimates developed from this source gage extend from October 1922–September 1934.
- Arkansas River at Wichita gage (Station 07144300): This source gage is the active stream gage on the Arkansas River in Wichita. The period of record for this gage is October 1934 to present. The multiplier used to estimate the flow data at the near-Maize node from this gage's data was derived from regression analyses using average annual unit flow data. Figure 8 is a scatter plot that shows the relationship between the average annual unit flows at the near-Maize gage and the net average annual unit flow at the at-Wichita and Valley Center gages. The best-fit regression line through these points has an intercept of -0.00343 and a slope of 1.22539, with an R^2 of 0.95146. An alternate regression line with a forced intercept of zero yields a slope of 1.11652 and R^2 of 0.97276. These latter regression results were used to generate the flow estimates using this source gage. These estimates start in October 1934 and end in March 1987, when the near-Maize gage became active.

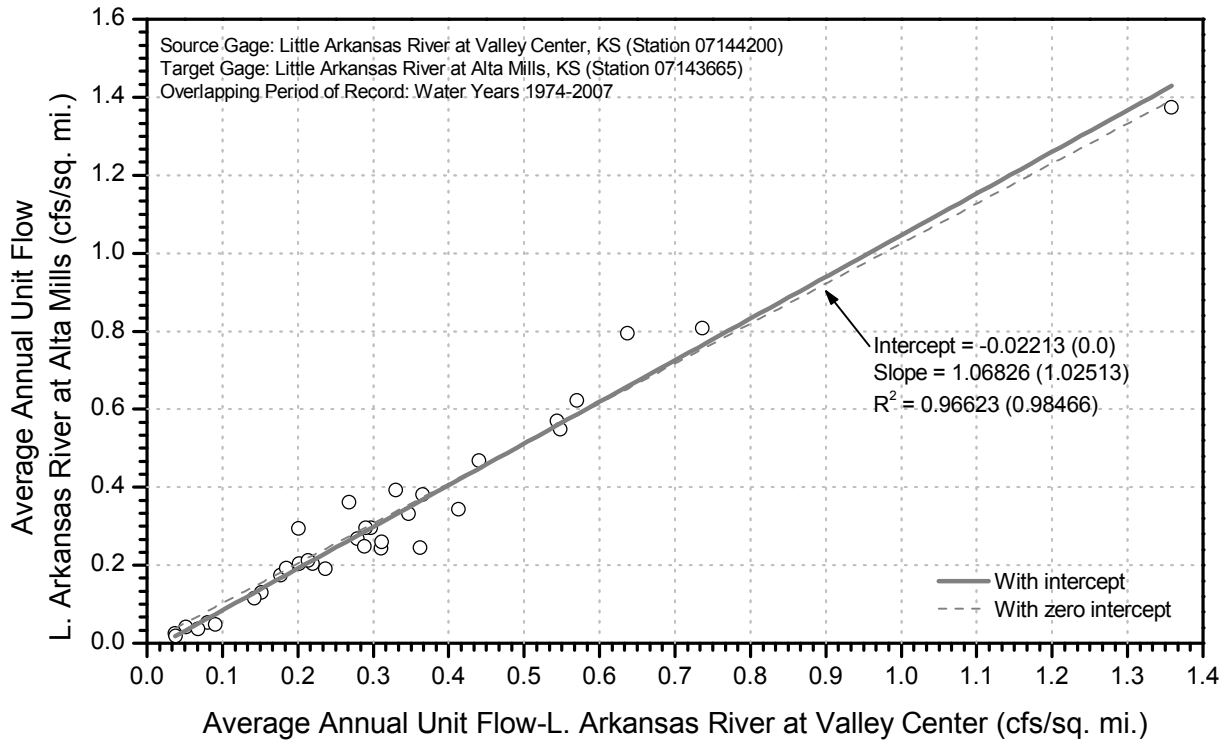
Figure 8: Discharge Comparison-Arkansas River near Maize vs. at Wichita



Little Arkansas River at Alta Mills

The USGS has operated a stream gaging station on the Little Arkansas River at Alta Mills (Station 07143665) since 1973. The location of this gage was selected as the farthest upstream node on the Little Arkansas River. For the balance of the model simulation period, the flow at this gage was estimated from the flow records at the downstream Valley Center gage. A scatter plot that compares the average annual flow at these two gages for the available 34-year overlapping period of record is shown in Figure 9. The best-fit line through these points has an approximate intercept of -0.02213, a slope of 1.06826, and an R² of 0.96623. An alternate regression line with a forced intercept of zero was also added to this graph. This line has a slope of 1.02513 and R² of 0.98466. The results of this alternate regression analysis were used to estimate the discharge at Alta Mills for the missing period, October 1922–June 1973.

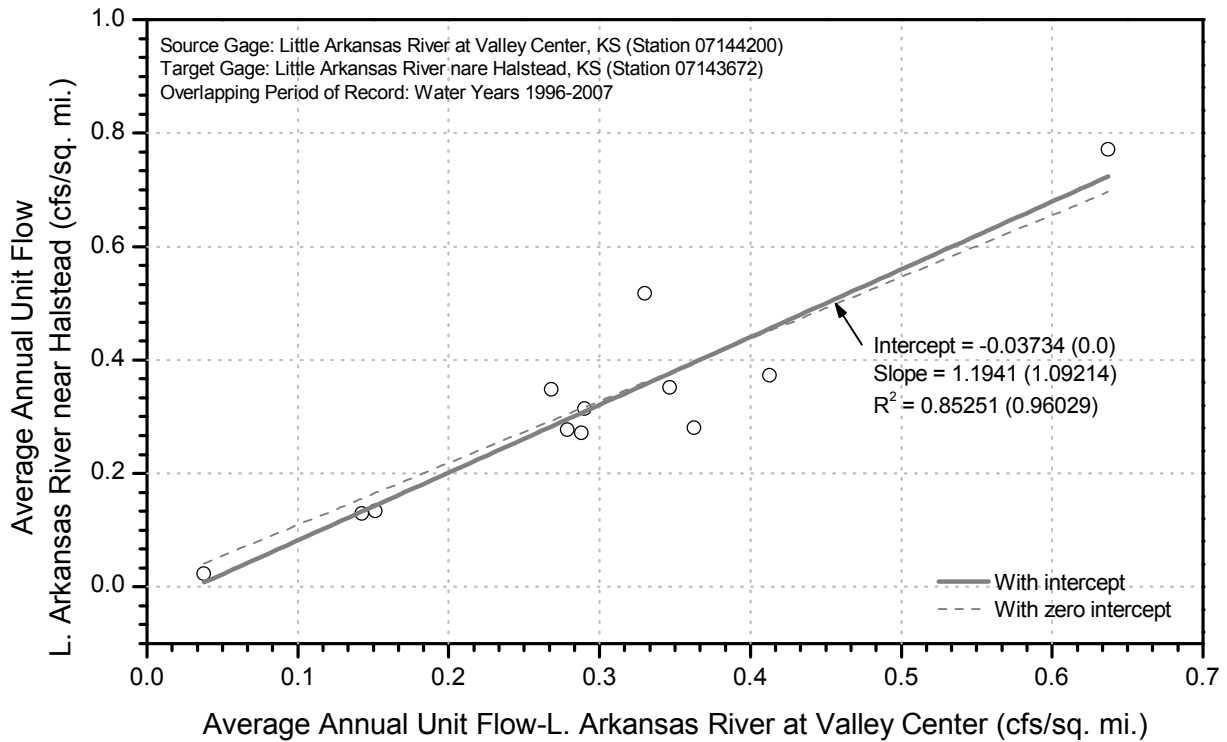
Figure 9: Little Arkansas River Discharge Comparison–Alta Mills vs. Valley Center



Little Arkansas River at Halstead

As originally conceived, the ILWSP included a proposed surface water intake and/or diversion wells on the Little Arkansas River near Halstead. There is a stream gage near this location (Little Arkansas River at Highway 50 near Halstead, Kansas [Station 07143672]); the record at this station begins in May 1995. For the balance of the model simulation period, the flow at this gage was estimated from the flow records at the downstream Valley Center gage. A scatter plot that compares the average annual flow at these two gages for the available 12-year overlapping period of record is shown in Figure 10. The best-fit line through these points has an approximate intercept of -0.03734, a slope of 1.1941, and an R² of 0.85251. An alternate regression line with a forced intercept of zero was also added to this graph. This line has a slope of 1.09214 and R² of 0.96029. The results of this alternate regression analysis were used to estimate the discharge at Halstead for the missing period, September 1922–April 1995.

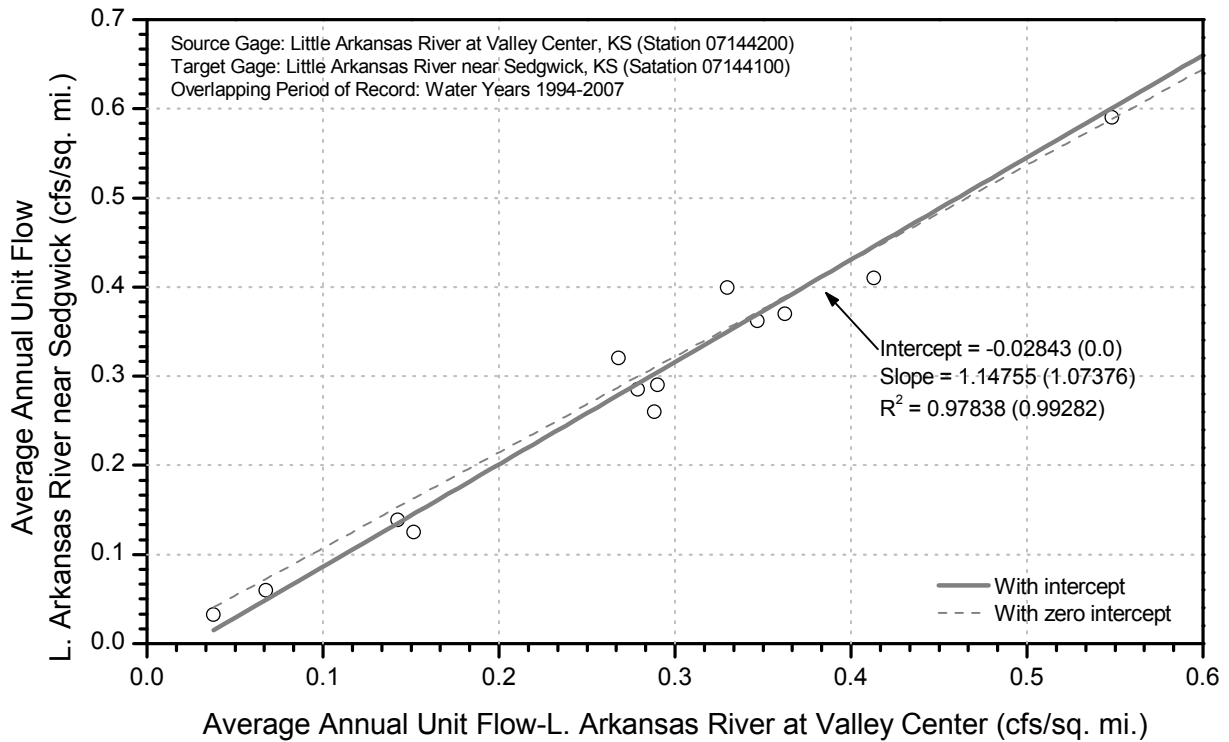
Figure 10: Little Arkansas River Discharge Comparison–Halstead vs. Valley Center



Little Arkansas River near Sedgwick

The USGS’ Little Arkansas River near Sedgwick gage had been in operation since October 1993. Figure 11 shows that the average annual unit flow at the Sedgwick and Valley Center gages has a very nearly linear relationship. The best-fit line through these points has an intercept of -0.02843 and a slope of 1.14755 with an R^2 of 0.97838. An alternate best-fit line with a zero intercept has a slope of 1.07376 and an R^2 of 0.99282. The discharge at this stream node for the period prior to October 1993 was estimated from the data at the Valley Center gage using the results of this latter regression analysis.

Figure 11: Discharge Comparison—Little Arkansas River near Sedgwick vs. at Valley Center



Little Arkansas River at Valley Center

The Valley Center stream node on the Little Arkansas River is located at the USGS’ stream gage of the same name (Station 07144200). The available data at this stream gage cover the entire model simulation period, so no streamflow estimates were necessary.

Little Arkansas River at Mouth

There are no stream gages on the Little Arkansas River below Valley Center; some of the proposed elements of the ILWS plan will impact the flow in the lowest reaches of this river. Therefore, it was necessary to develop flow estimates for the Little Arkansas River near its mouth in downtown Wichita. These flow estimates were developed from the data available at the Valley Center gage using a flow multiplier based on the ratio of the respective drainage areas. The drainage area of the Little Arkansas River at its mouth was estimated as 1,314 square miles, yielding a drainage area ratio of 1.049.

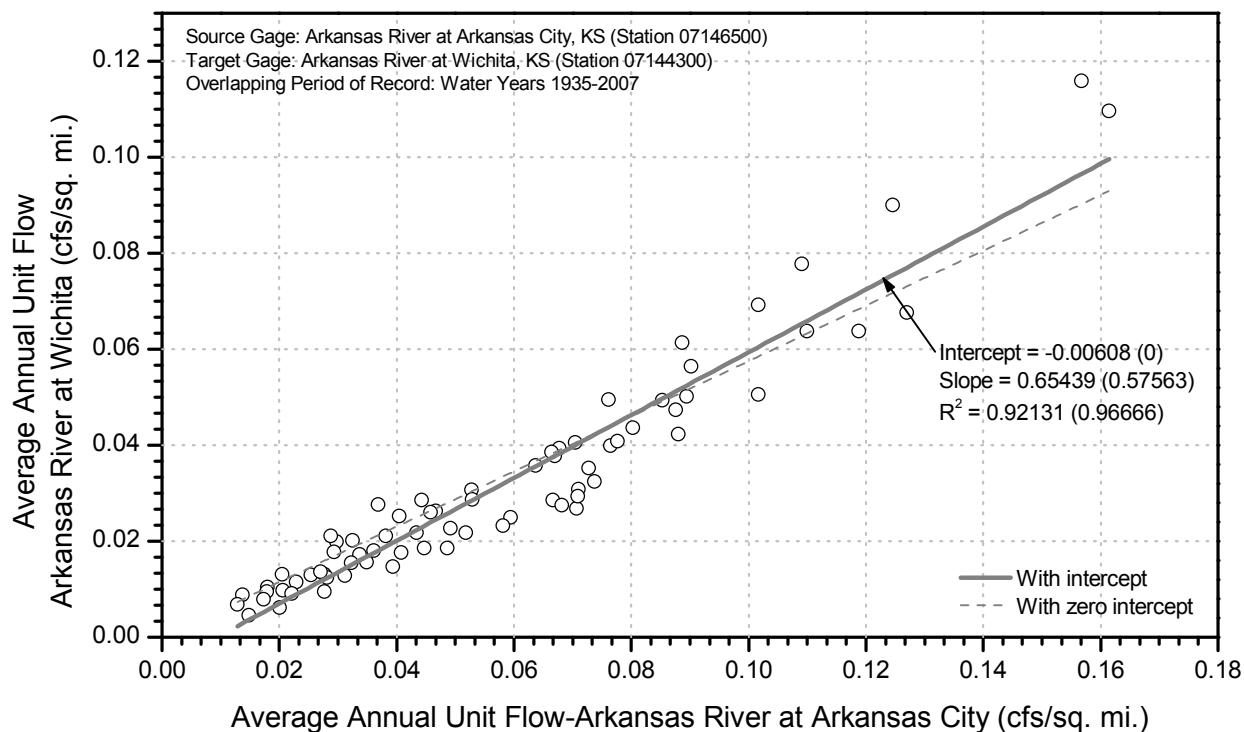
Arkansas River at Wichita

In Wichita, the discharge in the Arkansas River is recorded at a USGS stream gage located at the South Broadway Bridge (Station 07144300). This stream gage (Arkansas River at Wichita) has been in continuous operation since October 1934. Prior to this date, two possible methods were investigated to extend this record back to the start of the model simulation period. These methods are discussed below:

- Arkansas River near Wichita (Station 07143400): There is another stream gage located about six miles upstream of the target stream node that has flow records extending back beyond the start of the model simulation period. This gage (Arkansas River near Wichita) was discontinued shortly after the at-Wichita gage was placed in operation (March 1935). As there are only six months of overlapping data at the near-Wichita and at-Wichita gages, the results of any regression analysis would not be considered to have much validity. Although this gage is located only a short distance upstream, it is also above the confluence of the Little Arkansas River and has a significantly different (smaller) drainage area. Therefore, one method for estimating the flow at this target node would be to total the flow in the Arkansas River at the near-Wichita gage and the estimated flow in the Little Arkansas River at its mouth (Section 4.8).
- Arkansas River at Arkansas City (Station 07146500): The USGS stream gage on the Arkansas River at Arkansas City is one of the few gages with data for the earliest portion of the model simulation period. Figure 12 is a scatter plot that shows the relationship between the average annual unit flows at this gage and the target stream node. Two best-fit regression lines were plotted through these points. The first line has an intercept of -0.00608, an approximate slope of 0.65439, and an R^2 of 0.92131. The second line has a zero intercept, slope of 0.57563 and R^2 of 0.96666.

The flow record at the Wichita stream node was extended using the first method described above — sum of the discharge data for the near-Wichita gage and estimated flow in Little Arkansas River at its mouth.

Figure 12: Discharge Comparison–Arkansas River at Wichita vs. at Arkansas City



North Fork Ninescah River at Cheney Reservoir

Cheney Reservoir is one of the City’s principal water sources. This reservoir is located on the North Fork Ninescah River above Cheney, Kansas. There is a stream gage located at Cheney Dam that was placed in operation at about the same time as the reservoir (October 1964); however, this gage (Station 07144795) records reservoir discharge only. For the operations model, estimates of reservoir inflow are required. These inflow data were estimated from the following sources:

- North Fork Ninescah River near Cheney, Kansas (07144800): This source stream gage was located downstream of Cheney Dam. Its period of record starts in October 1950 and ends in September 1964. The inflow to Cheney Reservoir for this same period was estimated from this gage’s data using a drainage area ratio (664 square miles/685 square miles = 0.969).
- North Fork Ninescah River above Cheney Reservoir (Station 07144780): This source stream gage is located just a few miles upstream of the reservoir. This gage was placed in service after the reservoir became operational (July 1965) and is still active at present. The reservoir inflow estimates developed

from this source gage were developed by multiplying recorded flows by the ratio of contributing drainage areas of the dam and gage (664 square miles/550 square miles = 1.207).

- Little Arkansas River at Valley Center (Station 07144200): Prior to installation of the near-Cheney gage, there are no stream flow records for the North Fork Ninnescah River. For this period, Cheney Reservoir inflow was estimated using data for the Valley Center gage on the Little Arkansas River. Figure 13 is a scatter plot that compares the average annual unit discharge at this gage with those for the near-Cheney and above-Cheney-Reservoir gages. The regression analyses for these data were developed after excluding one outlying data point. This single outlier was shown to have a significant influence on the regression results. The best-fit line through the remaining data points has an intercept of 0.08256 and a slope of 0.62079. Using these regression results to estimate the missing flow data for this target gage results in an unrealistically high minimum reservoir inflow estimate; therefore an alternate regression line with a zero intercept was used to estimate Cheney Reservoir inflow for the period October 1922–September 1950 and October 1964–June 1965. This zero-intercept regression line has a slope of 0.82864 and an R^2 of 0.90329.

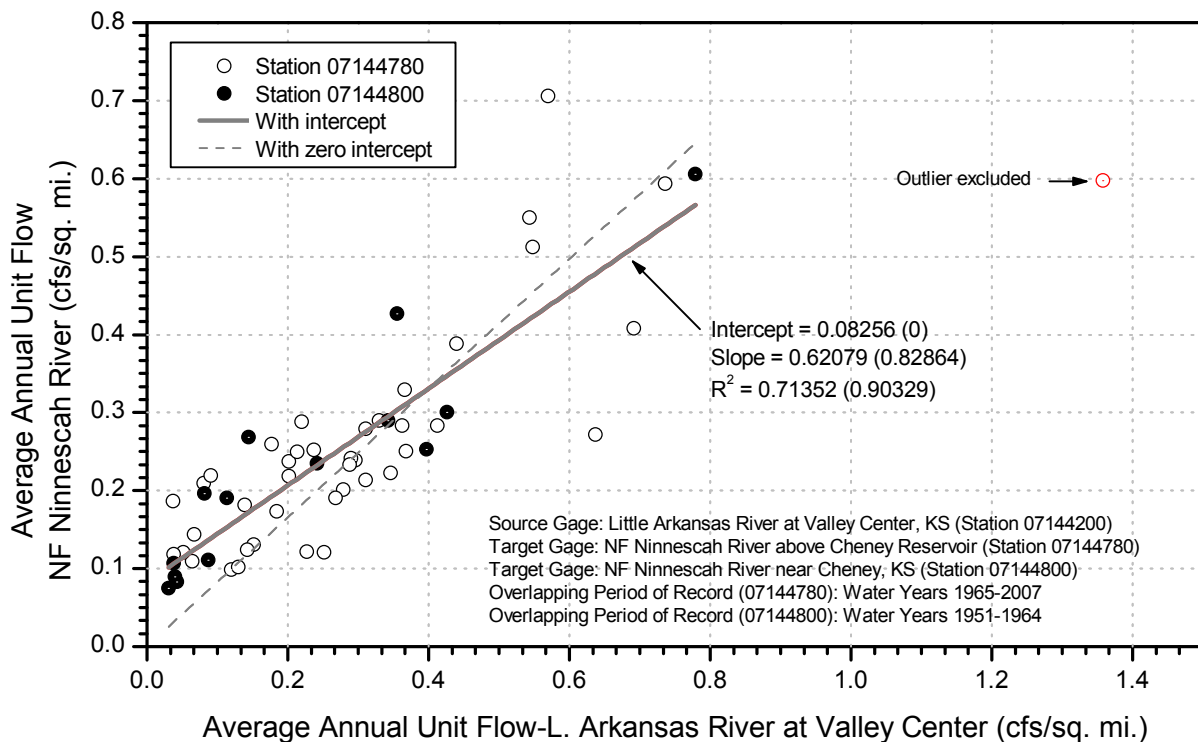


Figure 13: Discharge Comparison–Little Arkansas River vs. NF Ninnescah River

Ninnescah River near Peck

Below Cheney Reservoir on the main stem of the Ninnescah River is a USGS stream gage near Peck (Station 07145500). This gage has a period of record from April 1938 to the present. For the early portion of the model simulation period before this gage became active, these flows were estimated using data for the Arkansas City gage on the Arkansas River (Station 07146500). A scatter plot that compares the average annual unit flow at these source and target gages is included as Figure 14. From regression analyses, the best-fit line through these data points has an intercept of 0.05233, a slope of 4.10385, and an R^2 of 0.84037. The missing data at this stream node were estimated using the results of this regression analysis.

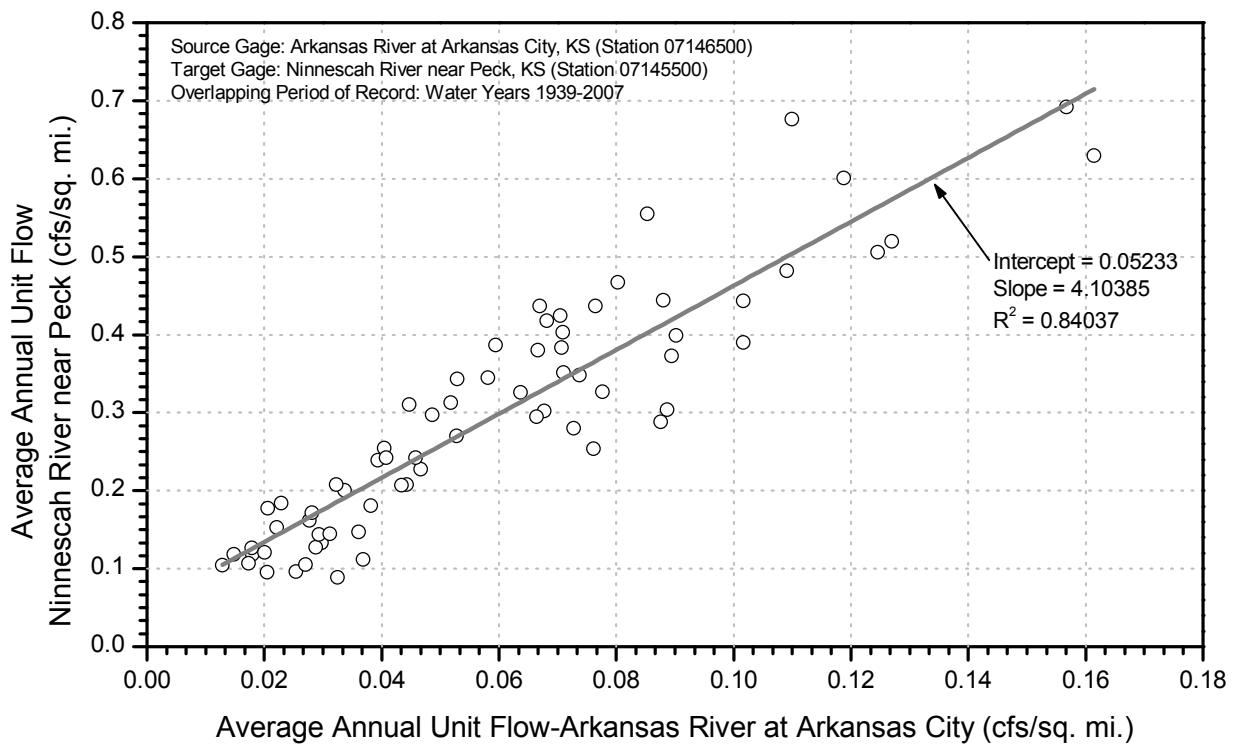


Figure 14: Discharge Comparison–Arkansas River vs. Ninnescah River

Arkansas River at Arkansas City

The last stream node used in the operations model is located on the Arkansas River near the Kansas-Oklahoma state line. This stream node is located at the USGS’ Arkansas River at Arkansas City stream gage (Station 07146500). The available data at this stream gage cover the entire model simulation period so no streamflow estimates were necessary.

Unregulated stream node inflow

The streamflow data presented above includes estimates of the mean daily flow at each stream node for the entire model simulation period. The flow input data required for the operations model, however, are the unregulated inflow at each stream node. The unregulated inflow to a stream node is defined as the net runoff that accrues to the stream between that node and any upstream nodes. For example, the Arkansas River at Wichita stream node is located downstream of two other stream nodes: Arkansas River near Maize and Little Arkansas River at Mouth. Therefore, the unregulated inflow at the Wichita stream node is calculated as the estimated discharge at this node less the estimated discharge at the two upstream nodes. These unregulated inflow data can be negative at times when there are net depletions within a stream reach. These data can also be negative because of differences in the timing of storm hydrographs, which can cause the discharge at an upstream gage to be higher on a given day than the discharge at a downstream gage.

The streamflow estimates at each stream node were converted to unregulated inflow estimates by subtracting the flow from any upstream flow nodes. The upstream nodes at each stream node (if any) can be discovered by examination of Figure 1, but are also listed in Table 4 for convenience.

Table 4: Upstream Nodes at each Stream Node

Node No.	Node Name	Upstream Node(s)	
		Node No.	Node Name
10	Arkansas R. near Hutchinson	---	---
20	Arkansas R. near Maize	10	Arkansas R. near Hutchinson
30	L. Arkansas R. at Alta Mills	---	---
40	L. Arkansas R. at Halstead	30	L. Arkansas R. at Alta Mills
50	L. Arkansas R. near Sedgwick	40	L. Arkansas R. at Halstead
60	L. Arkansas R. at Valley Center	50	L. Arkansas R. near Sedgwick
70	L. Arkansas R. at Mouth	60	L. Arkansas R. at Valley Center
80	Arkansas R. at Wichita	50	L. Arkansas R. near Sedgwick
		70	L. Arkansas R. at Mouth
90	NF Ninescah R. at Cheney Dam	---	---
100	Ninescah R. near Peck	90	NF Ninescah R. at Cheney Dam

110	Arkansas R. at Arkansas City	80	Arkansas R. at Wichita
		100	Ninnescah R. near Peck

Inflow Adjustments for Groundwater Interaction

Groundwater modeling has shown there is a strong hydraulic connection between the Arkansas and Little Arkansas rivers and the Equus Beds aquifer. The rates at which the aquifer gains or loses water to these streams is a function of aquifer water levels and storage. Table 5 lists the estimated rates of aquifer gain from and loss to local rivers as a function of aquifer water levels (Burns & McDonnell, 2008a).

Table 5: Equus Beds Aquifer Gain and Loss Rates

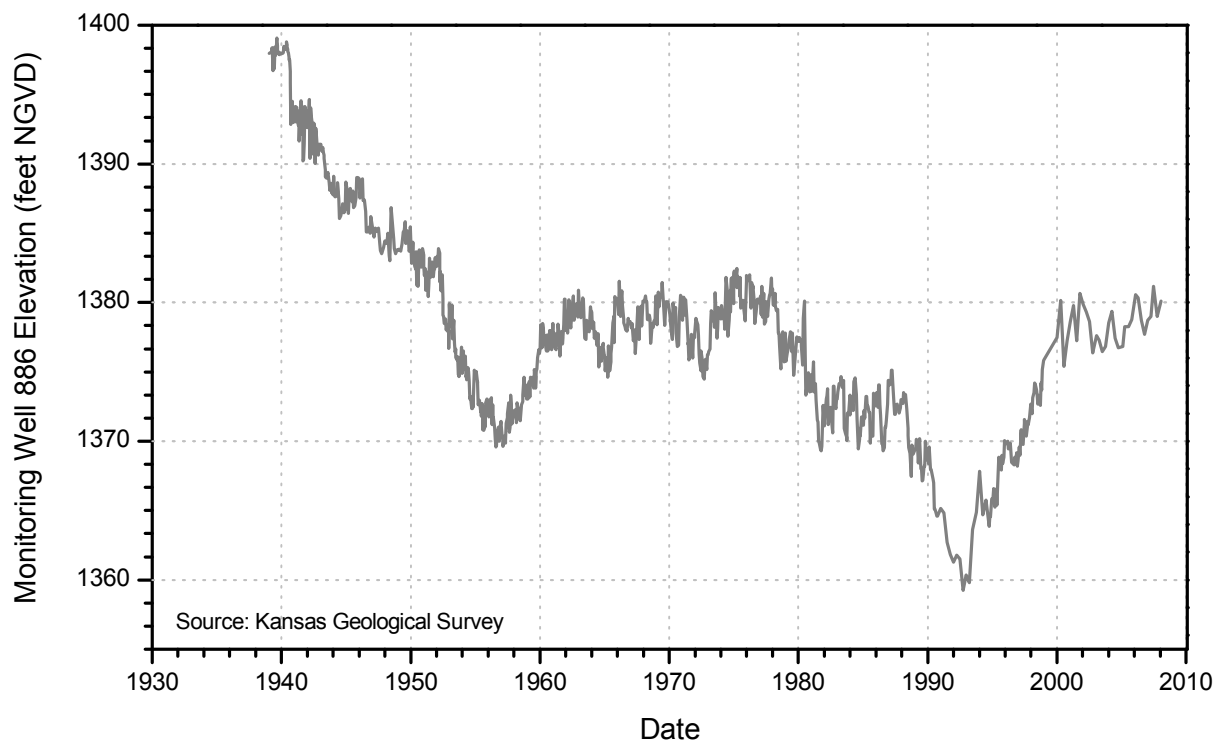
Aquifer Water Level (feet NGVD) ^a	Total Aquifer Gain Rate ^b (cfs)	Total Aquifer Loss Rate ^b (cfs)	Net Aquifer Loss Rate ^c (cfs)
1342	133 ^d	23 ^d	-110
1360	100	38	-62
1366	89	43	-46
1370	82	44	-38
1375	73	48	-25
1380	62	53	-9
1385	54	60	6
1389	48	68	20
1390	46	70	24
1395	38	82	44
1396	36	85	49
1402	29	99	70

- a. Aquifer water level is the water elevation measured in Monitoring Well 886.
- b. Estimates of gains and losses to area streams from MODFLOW groundwater model (Burns & McDonnell, 2008a).
- c. Negative values indicate a net aquifer gain.
- d. Values extrapolated from remaining data.

In past analyses, it has been generally assumed that all Equus Beds aquifer gains come from Arkansas River depletions and all aquifer losses from discharge to the Little Arkansas River. The Little Arkansas River is down gradient of the aquifer so the assumption that all aquifer gains must come from the Arkansas River seems valid. However, review of measured flows in the Little Arkansas River seems at odds with the assumption that all aquifer discharge accrues to this river. The reasons for this conclusion are discussed further below.

The aquifer gain and loss rates listed in Table 5 are relative to aquifer water levels (piezometric water surface elevations) measured in Monitoring Well 886. A hydrograph of historical water levels in this monitoring well is plotted in Figure 14. These measured water levels have ranged from a peak elevation of 1399.09 feet NGVD in August 1939 to a low of 1359.24 feet NGVD in October 1992. From the data in Table 5, the corresponding aquifer discharge would have ranged from a minimum rate of about 37 cfs in 1992 to a maximum of 92 cfs in 1939. With an average water level of nearly 1382 feet, the historical aquifer discharge would have averaged about 56 cfs. If all of this aquifer discharge accrues to the Little Arkansas River then one would expect the baseflow in this stream to be comparable to these groundwater discharge values (that is, to average 56 cfs and never be less than 37 cfs). In fact the measured flow in this river has been less than 56 cfs at Valley Center about 48 percent of the time and less than 37 cfs about 30 percent of the time (Figure 4).

Figure 14: Water Levels in Equus Beds Aquifer



Various methods were tested to find a means to reconcile these estimated Equus Beds aquifer discharge rates with measured flows in the Arkansas and Little Arkansas River, but none of these methods were completely successful. The method that was adopted was to apportion the aquifer discharge between the Little Arkansas and Arkansas rivers in a manner that best balances flows in the Little Arkansas River. Preference was given to balancing flows in the Little Arkansas River because it is the primary new water supply source — both for direct use and aquifer recharge — to be developed under the ILWS plan. This analysis included the following steps:

- The historical water levels measured for Well 886 (Figure 14) were paired with the gain and loss rates listed in Table 5 to yield estimates of historical aquifer gain and loss rates for the entire model simulation period. The first available aquifer level reading (1397.98 feet NGVD) was collected on January 14, 1939. Prior to this date, the aquifer water level was assumed to be a constant 1398 feet NGVD. The recording interval for these data varied from approximately weekly to quarterly. Between sample dates, water levels were assumed to vary linearly with time. After water levels were estimated for each day, the corresponding aquifer gain and loss rates were estimated using these water levels and the data in Table 5.

- The apparent groundwater accretions to the Little Arkansas River were estimated for each day during the 85-year modeling period as the difference in the measured or estimated flows at Alta Mills and Valley Center.
- The apparent net groundwater accretions to the Arkansas River were estimated for each day as the flow at Wichita less the flows at Hutchinson and Valley Center.
- The datasets described above were filtered to eliminate those days when the flow at Valley Center was greater than or equal to its median value of 59 cfs. On the remaining days in these flow records, it was assumed that most of the flow in these streams came from baseflow and not surface runoff.

From the data subsets described above, the following statistics were developed:

- Average total loss from Equus Beds aquifer to rivers: 61.8 cfs
- Average total gain from rivers to Equus Beds aquifer: 60.0 cfs
- Average net loss from Equus Beds aquifer to rivers: 1.8 cfs
- Average flow in Little Arkansas River at Alta Mills: 15.5 cfs
- Average flow in Little Arkansas River at Valley Center: 33.1 cfs
- Average net flow accretion in Little Arkansas River between Alta Mills and Valley Center: 17.6 cfs
- Average flow in Arkansas River near Hutchinson: 197.1 cfs
- Average flow in Arkansas River at Wichita: 254.4 cfs
- Average net flow accretion to Arkansas River between Hutchinson and Wichita: 24.2 cfs

From these statistics, it was concluded that only 28.5 percent of total Equus Beds losses should be assumed to enter the Little Arkansas River ($17.6 \text{ cfs} / 61.8 \text{ cfs} = 0.285$). This percentage of total aquifer losses should approximately preserve the flow balance in the Little Arkansas River. Unfortunately, the same cannot be said for the Arkansas River. These statistics show that, on average, the Arkansas River gains 24.2 cfs through this reach. However, using the remaining gains and losses from the aquifer one would expect a net loss from the Arkansas River ($0.715 * 61.8 \text{ cfs} - 60.0 \text{ cfs} = -15.8 \text{ cfs}$). From these data, there is no apparent way to balance the accretion rates to both the Arkansas and Little Arkansas rivers.

If Equus Beds discharge (loss) is distributed as indicated above, 28.5 percent will accrue to the Little Arkansas River and the remaining 71.5 percent to the Arkansas River. With 100 percent of the aquifer gains assumed to be from the Arkansas River, the resulting net aquifer loss rates are listed in Table 6.

Table 6: Allocation of Equus Beds Aquifer Loss Rates

Aquifer Water Level (feet NGVD) ^a	Net Aquifer Loss to (Gain from) Arkansas River ^b (cfs)	Net Aquifer Loss to Little Arkansas River ^b (cfs)
1342	-116.6	6.6
1360	-72.8	10.8
1366	-58.3	12.3
1370	-50.5	12.5
1375	-38.7	13.7
1380	-24.1	15.1
1385	-11.1	17.1
1389	0.6	19.4
1390	4.1	20.0
1395	20.6	23.4
1396	24.8	24.2
1402	41.8	28.2

- a. Aquifer water level is the water elevation measured in Monitoring Well 886.
- b. All aquifer gains and approximately 71.5 percent of aquifer losses accrue from/to Arkansas River. The remaining 28.5 percent of aquifer losses accrue to the Little Arkansas River.

For the project study period, the estimated historical discharge between the Equus Beds aquifer and the Arkansas and Little Arkansas rivers each day was estimated using the rates in Table 6 and the recorded water levels in Well 886 (Figure 14). These estimates were then used to adjust the unregulated inflow data at three stream nodes. The net losses from the Equus Beds aquifer to the Arkansas River were assumed to occur between the near-Hutchinson and near-Maize stream nodes. Therefore, the unregulated inflow at Maize was adjusted by adding estimated Arkansas River losses (aquifer gains) and subtracting corresponding river gains (aquifer discharge). In the Little Arkansas River, the estimated historical gains from the Equus Beds aquifer were split between two stream nodes. Forty percent of these gains were subtracted from the unregulated inflow at the Halstead stream node and the remaining 60 percent from the

inflow at Sedgwick. If an estimated negative flow adjustment on a particular day was greater than the original recorded or estimated streamflow at the same point, the adjusted inflow on that date was limited to a minimum of zero.

Flow Estimate Spreadsheet

The Microsoft Excel workbook file that accompanies this appendix contains all of the source and estimated flow data described herein. This worksheets included in this workbook are described below:

- Stream Gages — List of USGS stream gages utilized in this streamflow appendix
- Recorded Flows — Copy of USGS flow records for referenced gages
- Flow Estimates — Complete record of flow estimates at model stream nodes. Where applicable, there data are a composite of recorded and estimated flow data.
- Unregulated Inflow — Unregulated inflow estimates used in RESNET operations model
- Equus Beds GainLoss — Estimates of historical Equus Beds aquifer gain and loss rates
- Inflow Adjustments — Groundwater interaction adjustments made to Maize, Halstead and Sedgwick flow data.

References

Complete citations for the references cited in this document are listed below:

Burns & McDonnell. (2003). *Final Environmental Impact Statement for Integrated Local Water Supply Plan, Wichita, Kansas*. Prepared for City of Wichita, Department of Water and Sewer. Kansas City, MO: Published by author.

Burns & McDonnell. (2008a, October). *Equus Beds Groundwater Elevation and Storage Deficit/Stream Gain and Loss Relationship*. Prepared from City of Wichita, Department of Water and Sewer. Kansas City: Published by author.

Burns & McDonnell. (2008b, October). *Operations Model (6 October 2008 Draft)*. Prepared from City of Wichita, Department of Water and Sewer. Kansas City: Published by author.

U.S. Geological Survey. (no date). *National Water Information System* [Database]. Retrieved from <http://water.usgs.gov>.

Memorandum



To: John Christopher, SAIC
From: John Winchester, High Country Hydrology, Inc.
Cc: Mike Jacobs, Deb Ary, Lynn Moore
Subject: Yield Modeling
Date: October 3, 2013

This memo summarizes the yield modeling completed for the City of Wichita's Water Demand Assessment. This involved converting the City's existing RESNET model to MODSIM and running scenarios of new water supply projects.

To derive a critical period of record, we analyzed records of both historical streamflows and paleohydrology to determine the duration and severity of droughts with different recurrence intervals. This resulted in two design droughts, which were used to simulate alternatives with 1- and 2-percent chances of recurring. These are similar to, but not exactly the same as, the historical droughts of the 1930s and 1950s, respectively.

Once the design droughts had been determined, we simulated operations of the existing system, as well as the operations of five additional water supply alternatives to determine the yield through the design droughts. The additional yield for each proposed project was then used by SAIC to determine the unit cost of water for each project, which can be used to compare the costs of the different projects on an equal basis.

Based on the model, this analysis determined that the immediate limitation in the City's ability to meet demands during a drought is the delivery capacity from the Equus Beds Aquifer (62.7 mgd) and Cheney Reservoir (69 mgd). Under current conditions, if the Local well field and the Bentley Reserve well field are unable to deliver water, the maximum peak day supply the system can provide is 131.7 mgd, which with the demand pattern we used, is an annual demand of 71,000 acre-feet/year.

Background

As part of the Water Demand and Supply Assessment performed for the City of Wichita (City), High Country was retained to modify RESNET, the City's existing yield model created by Burns & McDonnell, and make model runs regarding potential raw water supply projects. In talking with city staff, it became clear that the modifications we proposed making to RESNET would not make the model sufficiently user-friendly for City staff's purposes. We recommended that the RESNET model be converted to MODSIM, the parent of RESNET, because MODSIM has a better user interface. The City agreed to this suggestion.

Memorandum

October 3, 2013

Page 2

We converted the RESNET model to MODSIM and verified that the MODSIM model reasonably replicated the RESNET results. MODSIM cannot exactly replicate the RESNET operations due to a variety of reasons. Our verification was based on RESNET run #77, a future condition with anticipated facilities and demands in 2060.

After verifying the operation of the model, we removed the non-existent features and adjusted capacities in the model so it represents the current system as closely as possible, given the data available and the detail in the model. A screen shot of the MODSIM model for the existing system is shown in Figure 1.

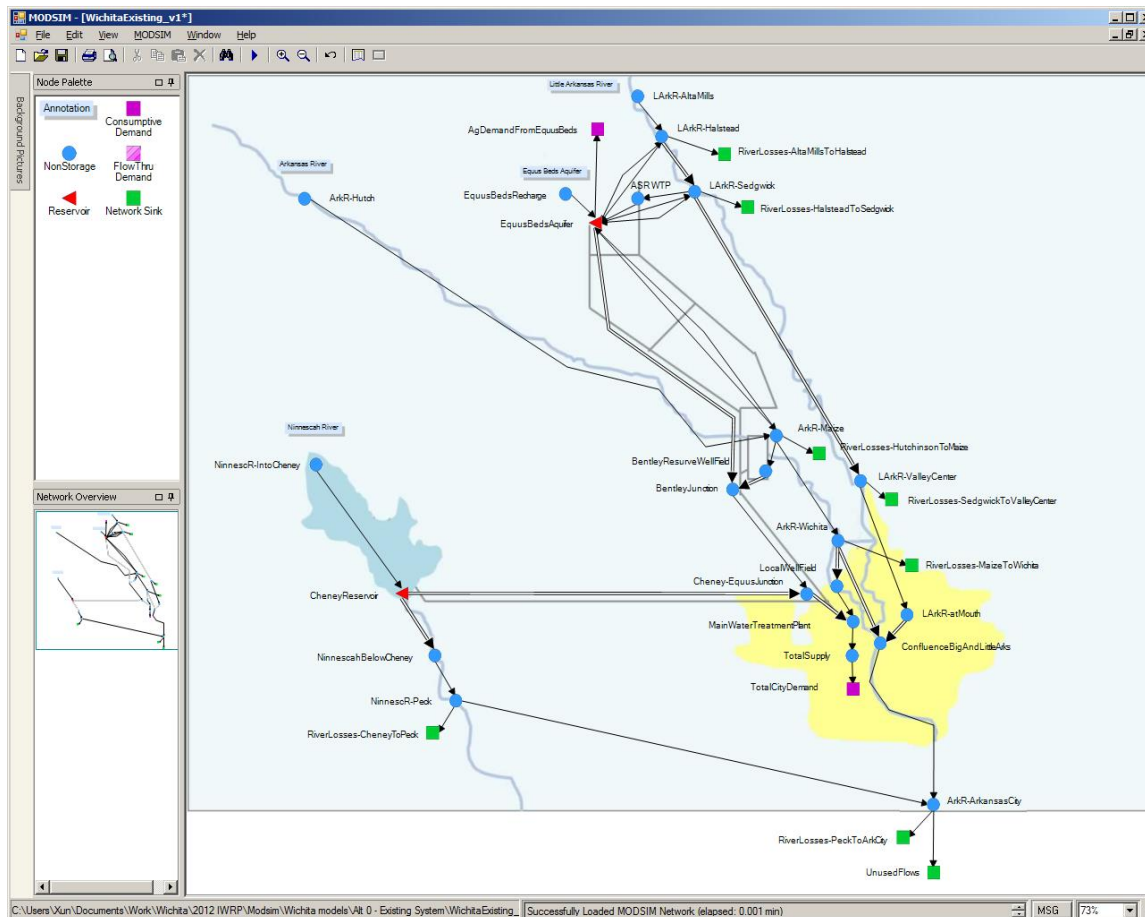


Figure 1. MODSIM Model Wichita Network

We then added each of the proposed projects to the existing system one at a time, and calculated the additional yield each alternative provided.

The results presented in this memo represent our current understanding of the system, but should ultimately be considered preliminary. The results are likely to change when better data for the Equus

Memorandum

October 3, 2013

Page 3

Beds Aquifer becomes available, and if better information regarding El Dorado Reservoir operations is acquired.

Model Conversion

We provided a memo describing the model conversion on Feb 12, 2013.¹

In summary, the RESNET model #77 was the same scenario used in the Integrated Local Water Supply Plan (RESNET ID# 51) except flow and aquifer/river interaction estimates have been updated to 2008 values,^{2,3} and used 2060 demands, projected to be 125,090 acre-feet per year for Wichita's municipal use and 26,500 acre-feet per year for agricultural use from the Equus Beds Aquifer. The municipal and agricultural demands were revised for this analysis, and are described below.

Results between the two models were very similar, though not exactly the same. The primary reason for the difference is that RESNET and MODSIM simulate priorities in slightly different ways, but there are also differences in how the models simulate aquifer gain/loss, and corrections we made to area-capacity curves. While we made the conversion to the best of our ability in the time available, and while there may be other reasons for differences, we did not have the time needed to track down every cause.

Average Verses Peak Day Modeling

The yield model analyzes the system on both a peak day and average (period of record) basis. Modeling was originally anticipated to consist of both an average day analysis, which would determine the amount of water the system could reliably provide, and a peak day analysis, which would determine limitations in the delivery system. This two-step approach is routinely used when a yield model has a monthly or annual time-step, which is insufficient to analyze peak day demands and limitations. Because Wichita's yield model operates on a daily time-step, separate analyses for average and peak day yields were not necessary. Running the model with different levels of demand quantifies both the reliable supply through various levels of drought, as well as identifies where constraints in the raw water supply, storage, and delivery capacity occur on peak days.

City demands for the peak day analysis were based on historical daily pumping data from the Hess Pump Station for 2002. The daily values for 2002 and 2012 were found to have the highest correlation to the mean daily flow for the 2002-2012 period. The 2002 daily pattern is scaled proportionately to generate different levels of annual demand.

¹ Memo from John Winchester to Paul Johnson, "Preliminary Model Results for Current Conditions", Dated February 12, 2013.

² Memo from John Winchester to Andrea Cole, "Equus Beds Ground Water – Surface Water Interaction", dated January 6, 2013. Equus Beds stream interaction.docx.

³ Memo from John Winchester to Paul Johnson, "Resnet Representation of the Equus Beds Aquifer", dated February 7, 2013.

Memorandum

October 3, 2013

Page 4

Model Revisions

Once the MODSIM model was able to reproduce the RESNET results, we made several modifications to the model so it would more accurately simulate Wichita's raw water collection and delivery system. These modifications are described in a memo dated March 21, 2013.⁴

In summary, these changes included:

- Links
 - Removed unnecessary links and nodes to simplify the network;
 - Aggregated link priorities so fewer priorities act in a serial manner, making it easier to follow and adjust network operation;
 - Added a short multi-link at Cheney and Equus Beds, each with ten parallel links limited to 30 acre-feet and 20 acre-feet per day, respectively, with alternating link costs (10, 15, 20, 25, etc). When the reservoirs are in their normal operating range, these direct the model to take 60% of the water from Cheney, 40% from the Equus Beds;
 - Changing link capacities on several pipelines to reflect the current pipeline capacities. Figure 1 shows the capacities used in the model.

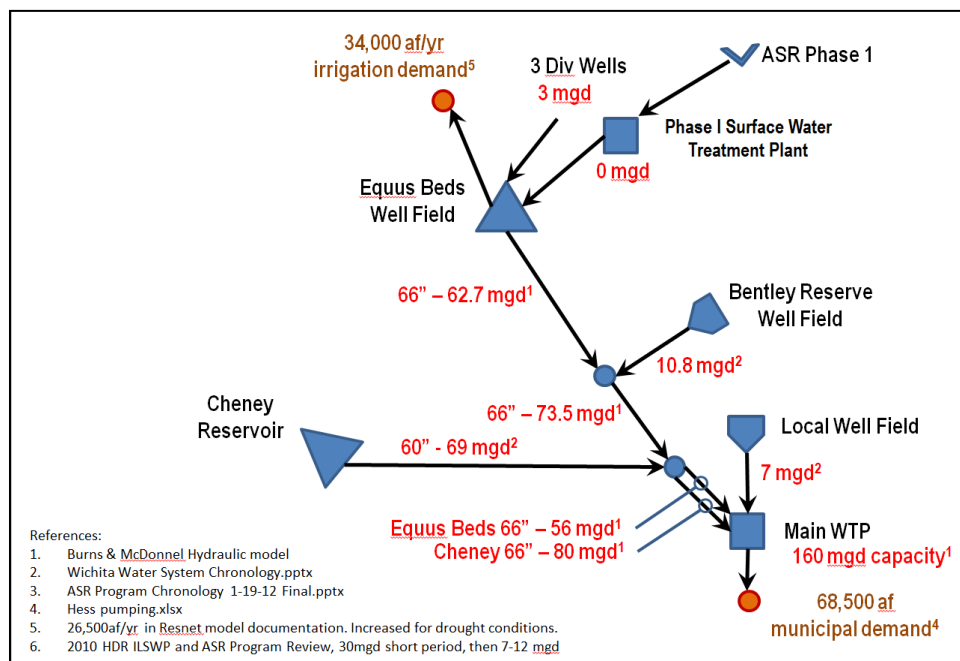


Figure 1. Current System Capacities

⁴ Memo from John Winchester to Paul Johnson, "Modsim Model Modifications", dated March 21, 2013.

Memorandum

October 3, 2013

Page 5

- Modified the available inflows and the period of record;
 - Created two droughts, one with an exceedance probability of 1 percent (one of 1 in 100 years) and 2 percent (1 in 50 years). Generally speaking,
 - The 1-percent drought is the 1930's (eight years: 1933-1940);
 - The 2-percent drought is the 1950's (six years: 1952-1956, 1959);
 - Both drought sequences are preceded by three “average” years and followed by one average year. The average year was constructed based on water year 1981.⁵
- Equus Beds Aquifer
 - The MODSIM model uses more restrictive top and bottom elevations for the Equus Beds Aquifer.
 - Maximum elevation set to 1397' (422,185 af), 13' below top of well M17 (the closest well to 886);
 - Minimum elevation set to 1360' (140,230 af);
 - The stream-aquifer interaction coefficients are the same as in RESNET, but should be re-evaluated when new information becomes available from the USGS;
 - More information about the Equus Beds Aquifer can be found in memos dated Jan 6, 2013⁶ and Feb 7, 2013⁷
- Cheney Reservoir
 - The volume of the conservation pool was slightly revised
 - Maximum elevation set to 1421.6' (247,931 af), top of conservation pool;
 - Minimum elevation set to 1397' (24,817 af), the bottom of the municipal inlet (1393') plus 4' to get above the level of the gate.
- Demands
 - Current demands
 - Wichita municipal demand
 - Based on records from the Hess Pump Station, 2012 demand is 68,520 af/yr⁸
 - Annual demand distributed to daily based on 2002 demand data⁹

⁵ PDSI drought durations - MODSIM inflows for various droughts.xlsx

⁶ Memo from John Winchester to Andrea Cole, “Equus Beds Ground Water – Surface Water Interaction”, dated January 6, 2013. [Tech Memo 1 - Equus Beds stream interaction.docx](#).

⁷ Memo from John Winchester to Paul Johnson, “Resnet Representation of the Equus Beds Aquifer”, dated February 7, 2013. [Tech Memo 2 - Equus Beds characteristics.docx](#).

⁸ Hess Data.xlsx

⁹ [MODSIM daily demand generator.xlsx](#)

Memorandum

October 3, 2013

Page 6

- Ag demand from Equus Beds
 - Set to 20,000 af/yr because demand is expected to be higher during a drought. May 15-Aug 31. Note that agricultural demand in RESNET was 26,500 af/yr.
- Future demands
 - Professional Engineering Consultants (PEC) projects that 2060 demand will be 87,630 af/yr with a peak day to average day demand ratio of 2.07.¹⁰
- Daily demands
 - The daily distribution is based on historical demands from 2002. The value for the peak day (July 28) was adjusted upwards from 109 mgd to 117 mgd so the ratio of peak day to average day is 2.07, the same as the 2060 demand projections by PEC. The value for July 27 was adjusted up to maintain the shape of the original pattern.
- Design Drought
 - Design drought for this analysis would be the drought with a 1-percent chance of exceedance.
 - For additional information about the historical streamflow records, reconstructed drought recurrence intervals from the 1,000-year Palmer Drought Severity Index (PDSI), and the duration and severity of different droughts, see the second technical memo, dated March 14, 2013.¹¹

The model results may differ from actual system operation when system hydraulics are more or less restrictive than what is in the model (such as the delivery capacity out of Cheney Reservoir at very high or very low elevations), when the model over-simplifies the system (e.g., the aquifer gain-loss relationship with the Arkansas rivers), model efficiency (e.g., surface water diversions to the ASR system), or assumptions regarding other uses (e.g., agricultural demand from the Equus Beds Aquifer during droughts).

Modeled Alternatives and Results

Modeling was completed for both the 1-percent and 2-percent droughts for each of the alternatives.

To determine the yield available for each alternative, the model was run repeatedly, increasing demands in 1,000-acre-foot increments until a shortage occurred at the main water treatment plant. The largest demand that could be sustained through the drought without any shortage is considered the sustainable yield the system can provide for the drought being modeled. Because runs with sustainable yields do not have shortages, the primary variable between alternatives is reservoir contents. Graphs of reservoir contents for the sustainable yield are included for each alternative. These graphs show one possible trace of reservoir contents during the drought.

¹⁰ [PEC future demands 2013-01-22.xlsx](#)

¹¹ Memo from John Winchester to Paul Johnson, "Extended drought reconstruction from PDSI", dated March 14, 2013. [Tech Memo 4 - Extended drought reconstruction.docx](#)

Memorandum

October 3, 2013

Page 7

The following sections include discussions about the alternatives, including graphs of reservoir contents for the 1-percent drought. A table with all the results for both the 1-percent and 2-percent droughts is included at the end of this section.

Baseline Scenario - Existing Conditions

Description

During the course of modeling, we made runs using a variety of assumptions. At the City's direction, the final scenarios use the existing pipeline capacities for the delivery system, as shown in Figure 1.

While making these runs, we determined that under both the 1- and 2-percent droughts, the limiting factor on yield at the treatment plant wasn't the supply of water, but is rather restrictions in the delivery system. It appears some of these limitations can be addressed through system modifications rather than laying new pipe.

To determine how much difference this additional capacity would make, we increased the capacities of three of the pipelines in the delivery system and reran the model for the existing condition. These three changes were:

- The Cheney Pipeline currently has a maximum capacity of 69 mgd but has a design capacity of 80 mgd. It is our understanding that the improvements for the Cheney Pipeline have already been approved in the City's Capital Improvement Program. Consequently the run with existing pipeline capacities was made at 69 mgd, while the existing system with improvements was made at 80 mgd.
- The pipeline from the Equus Beds well field to the main WTP has a diameter of 66 inches. The capacity for the Equus Beds pipeline was determined using the City's hydraulic model developed by Burns & McDonnell, which showed that with the Bentley Reserve and Local well fields operating, the capacity of the Equus Beds Pipeline is 62.7 mgd between the Equus Beds and the junction with the Bentley Reserve Well Field, and 73.5 mgd between the Bentley well field and the junction with the Cheney pipeline. For the existing system pipeline run, the capacity of the upper Equus pipeline was assumed to be 62.7 mgd. In the run with the existing system improvements the capacity was assumed to be 73 mgd, which may be possible if the Bentley Reserve well field is not operating or if other modifications can be made.
- There are two 66-inch pipelines from the junction of the Cheney pipeline and the Equus pipeline to the main WTP. According to the hydraulic model, the Cheney pipeline has a capacity of 80 mgd, while the Equus pipeline has a capacity of 56 mgd. Because the pipelines start and end at the same locations and are the same diameter, then it may be possible to configure them to flow the same amount of water. Consequently in the runs with existing system improvements, the pipeline was sized at 80 mgd.

Memorandum

October 3, 2013

Page 8

Key Assumptions for Existing Conditions

In addition to the demands and capacities shown in Figure 1, important assumptions used in this model include:

- Supplies
 - The design drought has an exceedance probability of 1-percent, which equates to a return period of 100 years, is 8 years long and is modeled using the historical data for years 1933-1940.
 - For comparison purposes, the 2-percent drought has a duration of 6 years, and is modeled using the historical data for years 1952-1956 and 1959. This is slightly more severe than the actual drought of the 1950s because 1957-1958 were not drought years and were not included in this analysis.
 - ASR diversions only occur when there is water in the Little Arkansas River. For the existing system, the diversion rate is limited to 3mgd from the diversion wells.
 - Diversions from the Bentley Reserve Well Field and the Local Well Field only occur when there is flow in the Arkansas River.
 - There is only rudimentary accounting in the model for Equus Beds recharge credits. Water stored in the Equus Beds Aquifer is added to a common reservoir that supplies water to the Equus Beds Ag demand and the city of Wichita. The model does limit the rate at which water can be injected, as well as the volume of recharge credits that can be pumped each year due because of the number of wells. The model does not verify that pumping does not exceed the amount recharged, or account for credits lost back to the river.
- Demands
 - The city's daily demand pattern is based on the historical Hess Pumping for 2002. Daily flows are scaled up and down to simulate the various demands. Note that as the daily demands are increased, the peak day increases proportionately. Therefore an alternative that can produce more water in a year can also meet a higher peak day demand than an alternative that produces less water.
 - Ag demands are modeled at 20,000 acre-feet per year. This is higher than the 18,000 acre-feet per year in RESNET, but demands were increased to reflect the increase in demand seen during the 2011-2012 drought.
- Capacities
 - Bentley Reserve Well Field diversions are limited to June 1-Aug 31. This was apparently done in RESNET to approximate the water rights limitations. The MODSIM model also uses this diversion season. MODSIM allows the user to limit flows by annual volume, and we limited diversions from the Bentley Reserve Well Field to 5000 acre-feet per year, but we have since learned that this function does not actually limit flows in daily models due to a problem with the seasonal accounting.

Memorandum

October 3, 2013

Page 9

- Local Well Field diversions can occur year-round at a rate of up to 7 mgd, when there is water in the Arkansas River, without annual volumetric limitations.
- The pipelines between the Cheney-Equis Beds junction are assumed to be interconnected at the Cheney-Equis junction. It is unclear how the interconnect affects hydraulics in the actual system.

Results for Existing Conditions

Annual demands for the existing system model were increased until shortages occurred. Using the assumptions described above, Figure 2 and Figure 3 shows that the existing system with its current capacities can reliably supply 71,000 acre-feet per year through the 2-percent and 1-percent droughts, respectively.

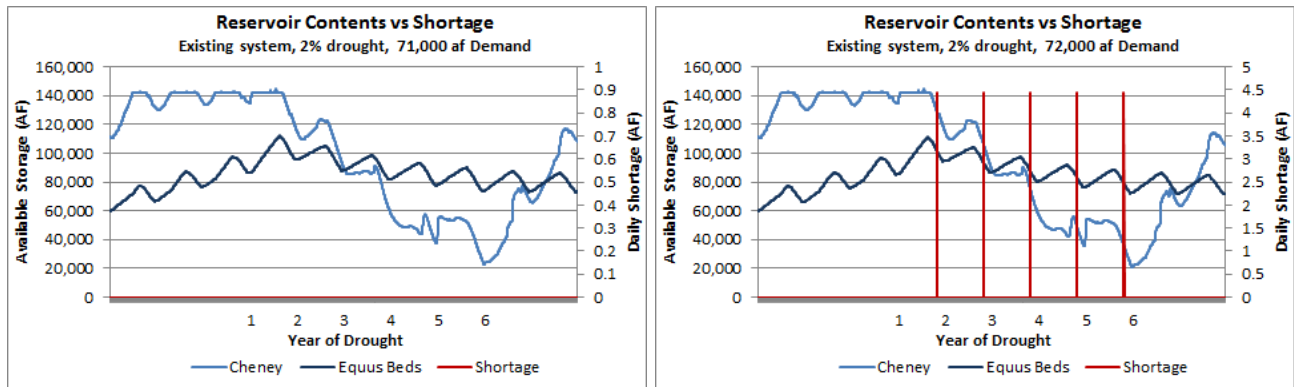


Figure 2. Existing conditions, 2% drought.

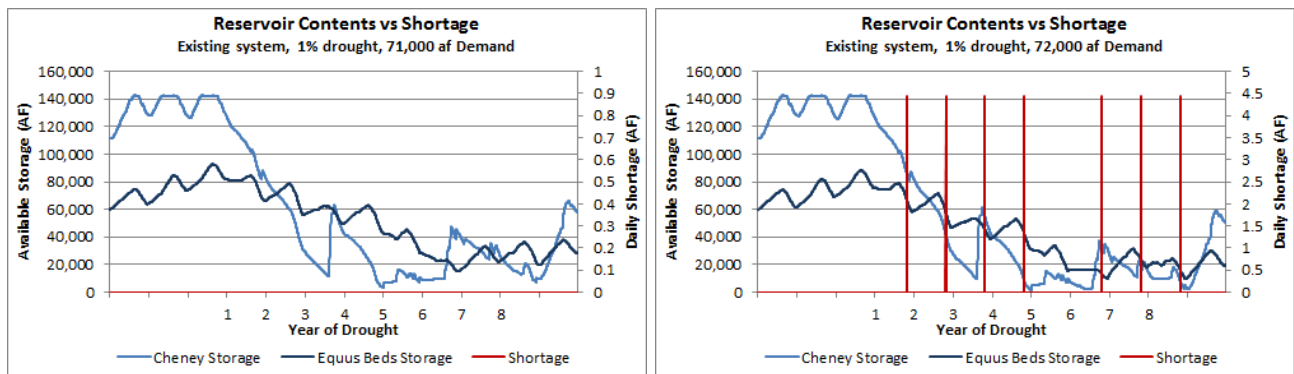


Figure 3. Existing conditions, 1% drought.

Looking at the data used to create Figure 2 and Figure 3, the shortages occurred on the peak days during the drought, when no water was supplied by the Local or Bentley Reserve well fields, and the demand reached 133 mgd, exceeding the Cheney-Equis capacity of 131.7 mgd. As a practical matter, this amount and duration of shortage could likely be avoided through demand management.

Memorandum

October 3, 2013

Page 10

To determine how much additional yield the system is capable of providing if the pipeline capacities were increased to their likely maximums, the capacities for the Cheney, Equus Beds and Cheney-Equus junction-to-main-WTP were increased to the values described above and the model rerun. With the enlarged pipeline capacities the yield of the existing system under the 2% drought increased by 11,000 acre-feet per year to 82,000 acre-feet, as shown in Figure 4. Like the 2% run with the existing pipe sizes, the system ultimately failed to deliver water when the peak day demand exceeded the delivery capacity.

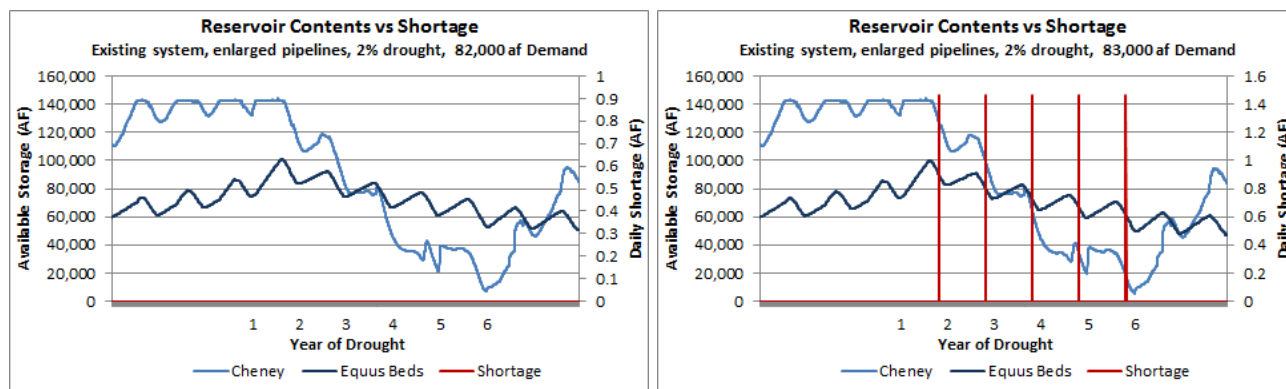


Figure 4. Existing conditions, with enlarged pipeline capacities, 2% drought.

The model was also run for the 1% drought. This model showed that increasing the system’s capacity would allow it to provide an additional 2,000 acre-feet through the drought. The system was eventually unable to deliver water when both Equus Beds and Cheney went dry in the 8th year of the drought.

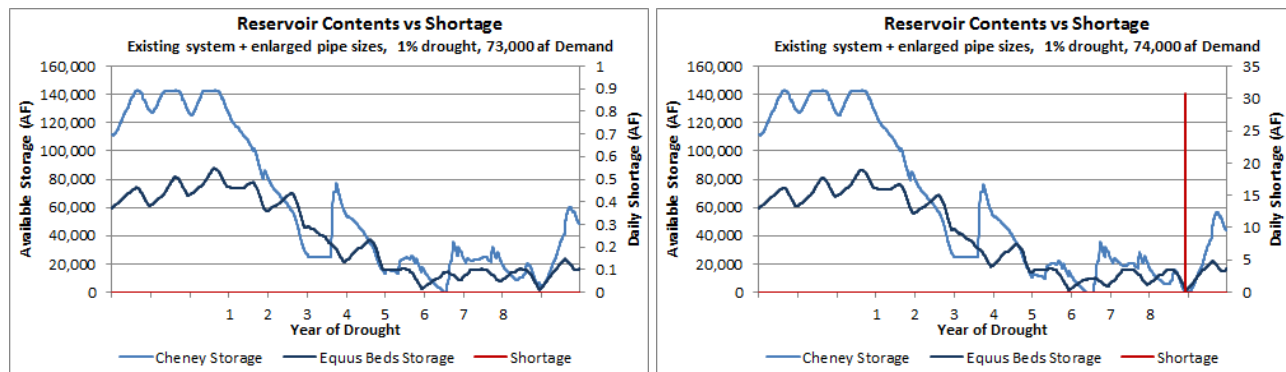


Figure 5. Existing conditions, with enlarged pipeline capacities, 1% drought.

The following sections discuss the additional yield each of the alternatives provides to the City.

Memorandum

October 3, 2013

Page 11

Alternative #1 – Treated Water From El Dorado to Distribution System, and Alternative #2 – Raw Water From El Dorado to Main WTP

Description

These two alternatives include construction of a pipeline from El Dorado Reservoir to Wichita. Alternative #1 would supply treated water to the distribution system, while Alternative #2 would supply raw water to the main water treatment plant. Because the raw water alternative delivers water directly to the water treatment plant and doesn't rely on any part of the existing delivery system, and because the water treatment plant in the yield model has capacity larger than the peak day demand, the additional yield for these two alternatives are the same, regardless of whether water delivered as raw water to the treatment plant or as treated water to the distribution system.

During the course of our work this alternative was modeled using several different assumptions about the amount of water available from El Dorado, including:

1. El Dorado provides water only after its own demand of 13,500 af/yr has been met and when El Dorado Reservoir is full. No storage will be provided for Wichita. As a practical matter, Wichita will receive water that would otherwise spill over the dam. This alternative was eliminated because it supplies Wichita essentially no additional water during drought periods.
2. El Dorado provides Wichita the use of the top 5 feet of the reservoir (36,247 acre-feet), and inflows in excess of its own demands when the reservoir is within the top 5 feet. This alternative was eliminated because it provides so little additional water for Wichita once the drought begins.
3. El Dorado provides Wichita water from storage as long as the reservoir contents are greater than 41,390 acre-feet, enough to provide El Dorado with two years' supply (26,893 af of supply plus 14,497 acre-feet to cover two years of evaporation). This alternative was run to see how sensitive yields were to the volume available to Wichita from storage.
4. El Dorado provides water from storage as long as the reservoir is not empty. If the reservoir is empty, El Dorado will use inflows to satisfy its own needs first, then provide water to Wichita, and lastly refill the reservoir.

Based on direction from the City, the results shown here use the fourth set of assumptions.

Memorandum

October 3, 2013

Page 12

Key Assumptions

- Inflows to El Dorado were developed by pro-rating the Walnut River at Winfield gauge based on drainage basin area.
- El Dorado's municipal demands were developed assuming a demand of 12 mgd x 365 days, which was inferred from the Black & Veatch 2012 report.¹² Because no other information was available, this volume was disaggregated to a daily pattern using the 2002 water year for Wichita. Any reduction in El Dorado's municipal demand would likely increase the amount of water available to Wichita.
- Deliveries from El Dorado Reservoir were not constrained to any level of the conservation pool.
- The pipeline to Wichita was assumed to have a capacity of 10 mgd.

Results

Figure 6 shows the reservoir contents for the alternative when Wichita has 98kaf of storage in El Dorado Reservoir. The sustainable yield of the system under this alternative is 76,000 acre-feet per year. Figure 6 shows the reservoir contents under these operating rules.

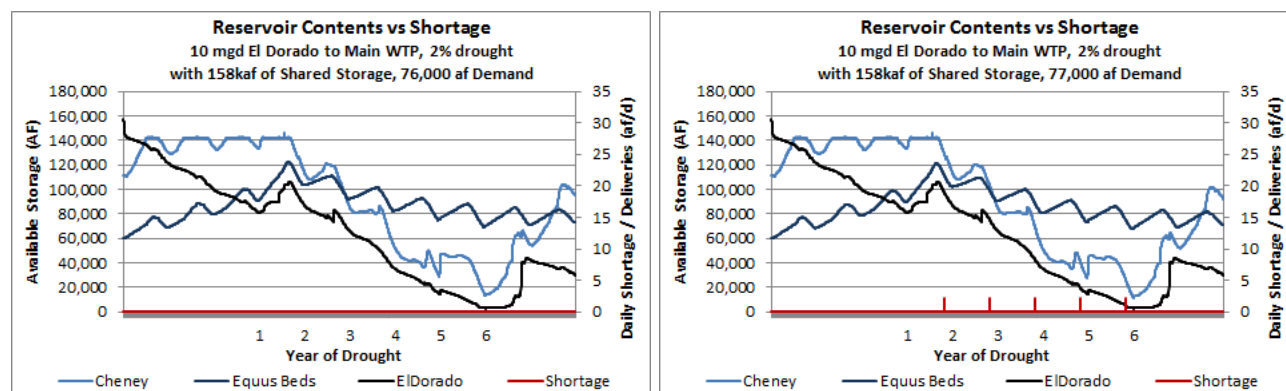


Figure 6. El Dorado to Main WTP, 2% drought.

¹² Black & Veatch, Interim Technical Memo: El Dorado Lake Water Suppl. Jan 9, 2012.

Memorandum

October 3, 2013

Page 13

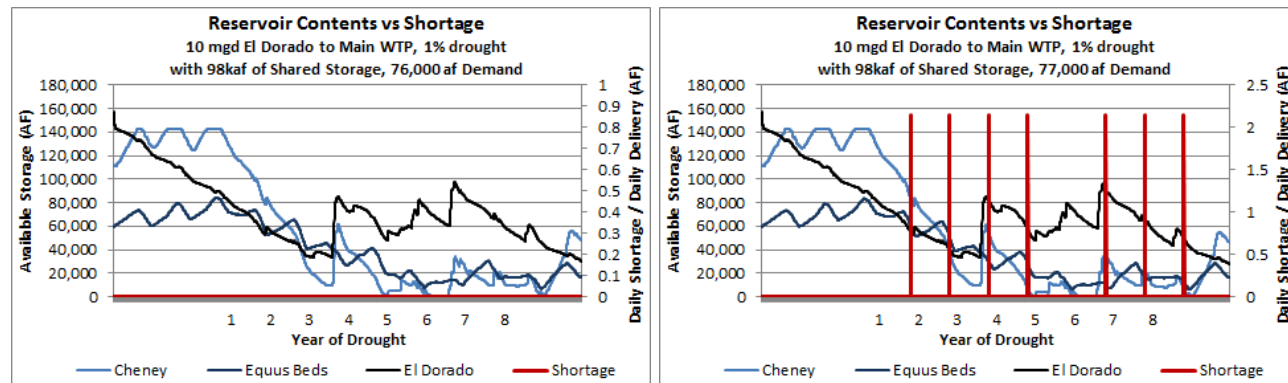


Figure 7. El Dorado to Main WTP, 1% drought.

The El Dorado to downtown alternative is able to increase Wichita's yield for both the 1% and 2% drought to 76,000 acre-feet per year. Both droughts fail to deliver water when the annual demand is set to 77,000 acre-feet per year because the peak day for that demand is 142.3 mgd, which exceeds 141.7 mgd, the sum of the capacity for the Cheney (69 mgd), Equus (62.7 mgd) and the El Dorado (10 mgd) lines. Note there was no shortage at the end of year 5 because there was water available from the Local/Bentley well fields.

This result was obtained by taking as little water from El Dorado as possible to maintain storage that could be used to meet peak demand. The El Dorado alternative could provide a larger volume of water by diverting more water during the three average years preceding the drought, but delivering that water earlier ultimately causes El Dorado to go dry during the drought, leaving no water to meet peak day demands.

Additional analyses of this alternative will require more specific information of how El Dorado would operate the reservoir and how storage and inflows would be allocated to Wichita.

Alternative #3 – El Dorado to ASR WTP

Description

This alternative involves construction of a pipeline from El Dorado to the ASR Phase II water treatment plant. Because the water will be stored in the Equus Beds aquifer, we assumed that no storage would be provided at El Dorado Reservoir, however we did assume that Wichita's water would be delivered after meeting El Dorado's 12 mgd demand but before refilling El Dorado Reservoir.

Key Assumptions

- Inflows to El Dorado were developed by prorating the Walnut River at Winfield gauge based on drainage basin area.

Memorandum

October 3, 2013

Page 14

- El Dorado's municipal demands were developed assuming a demand of 12 mgd x 365 days, which was inferred from the Black & Veatch 2012 report.¹³ Because no other information was available, this volume was disaggregated to a daily pattern using the 2002 water year for Wichita. Any reduction in El Dorado's municipal demand would likely increase the amount of water available to Wichita.
- Water levels in El Dorado Reservoir were constrained to the active conservation pool, from a minimum of 3,359 acre-feet (top of dead pool) to a maximum of 240,559 acre-feet (top of flood pool), with the top of the conservation pool at 158,630 acre-feet.
- Wichita could take any water available in storage, plus any inflows after the City of El Dorado satisfied its demands.
- Demand was varied in 1,000-acre-foot increments. While there was a difference between runs in the number of days Wichita's municipal demand was short under the various alternatives, one or more days of shortage resulted in the demand being reduced and the model run again.
- Pipeline capacity to Wichita is 10 mgd.

Results

Figure 8 shows the storage available in Cheney, Equus Beds and El Dorado. The figure shows that providing additional water to the Equus Beds during the three average years before the drought increases the amount of water available in storage at the beginning of the drought to meet demands during the drought. Because the model has a higher priority for agricultural demands, this increased supply is available to both Ag users as well as the city.

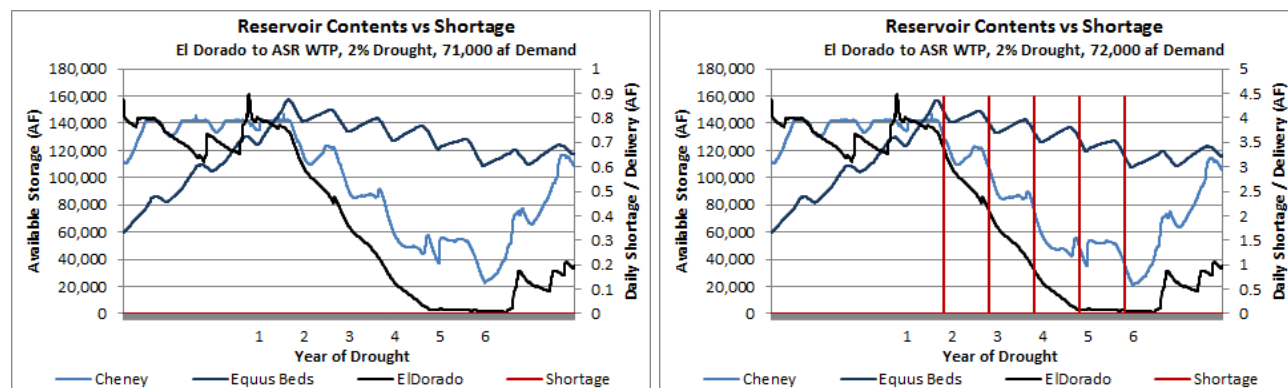


Figure 8. El Dorado to ASR, 2% drought.

Figure 9 shows that if the ASR system is expanded and has three or more average years preceding the drought, the system would be capable of delivering a sustainable yield of 71,000 acre-feet through the 1-percent drought. The right side of Figure 9 shows the shortage on peak days when the demands are increased to 72,000 acre-feet per year.

¹³ Black & Veatch, Interim Technical Memo: El Dorado Lake Water Suppl. Jan 9, 2012.

Memorandum

October 3, 2013

Page 15

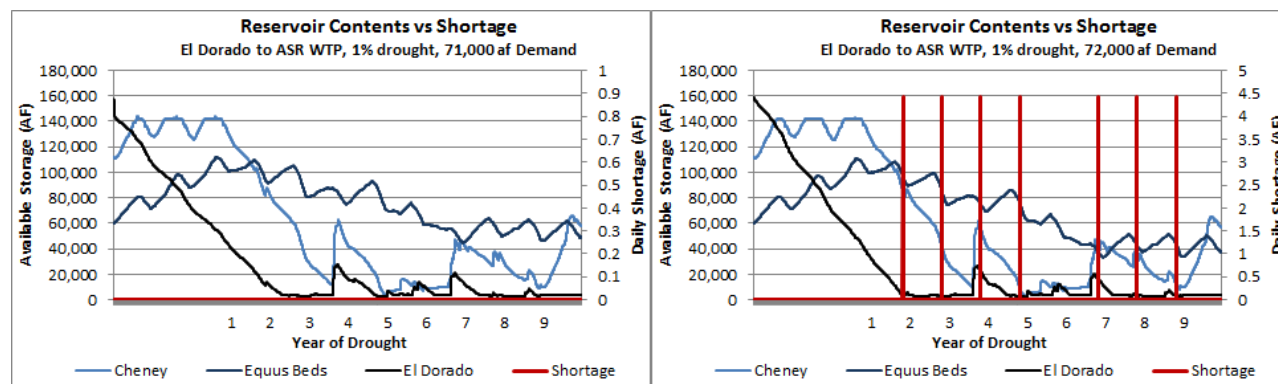


Figure 9. El Dorado to ASR, 1% drought.

This graph shows that the system suffered a shortage on the peak day when there was insufficient capacity to deliver water from Cheney and the Equus Beds.

Alternative #4 – Expanded ASR

Description

This alternative increases the current capacity of the ASR project from 3 mgd to a total diversion and injection capacity of 95 mgd. This was accomplished by increasing the size of the intake at Sedgwick. The model only diverts water when there is more than 40 cfs in the Little Arkansas River below Halstead and 85 cfs below Sedgwick. The ASR project was sized at 95 mgd rather than the design capacity of 100 mgd as a safety factor to compensate for the fact that operations are not 100 percent efficient. For example, there are times when flows are sufficient for operations but operators will decide not start the plant because the start-up time of the system is longer than the anticipated duration of the high flows.

Key Assumptions

- Diversions from the Little Arkansas are available only when there is live streamflow.
- Diversions are junior to an 85 cfs minimum streamflow between Sedgwick and Valley Center.
- River diversions for recharge are limited to 95 mgd.
- Withdrawal of recharge credits is based on the number of wells, which are projected to limit the pumping to 69,500 acre-feet per year. Recharge credits are not accounted for separately in the model, so water put into storage in the Equus Beds Aquifer can be taken by either the City or by agricultural users.

Results

The model simulating the expansion of the ASR system to 95 mgd of recharge capacity had a sustainable yield of 71,000 acre-feet per year.

Memorandum

October 3, 2013

Page 16

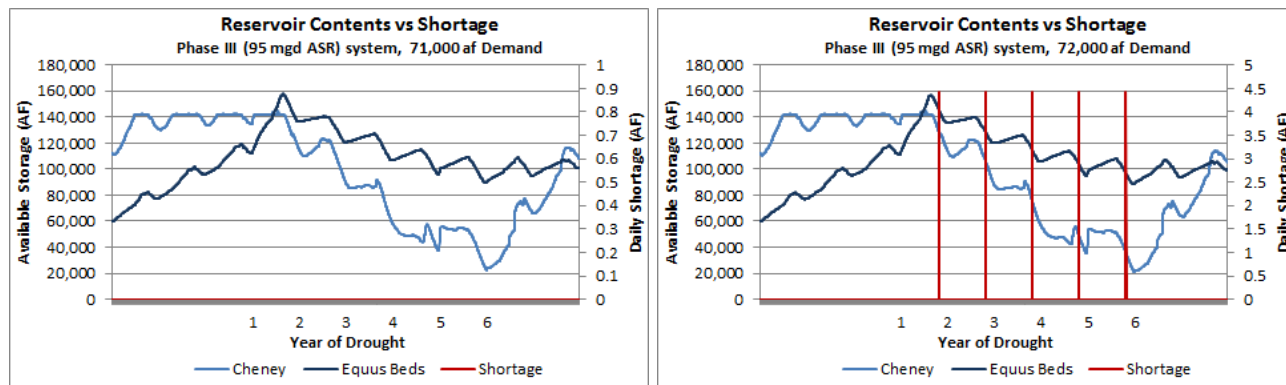


Figure 10. Expansion of ASR to 95 mgd, 2% drought.

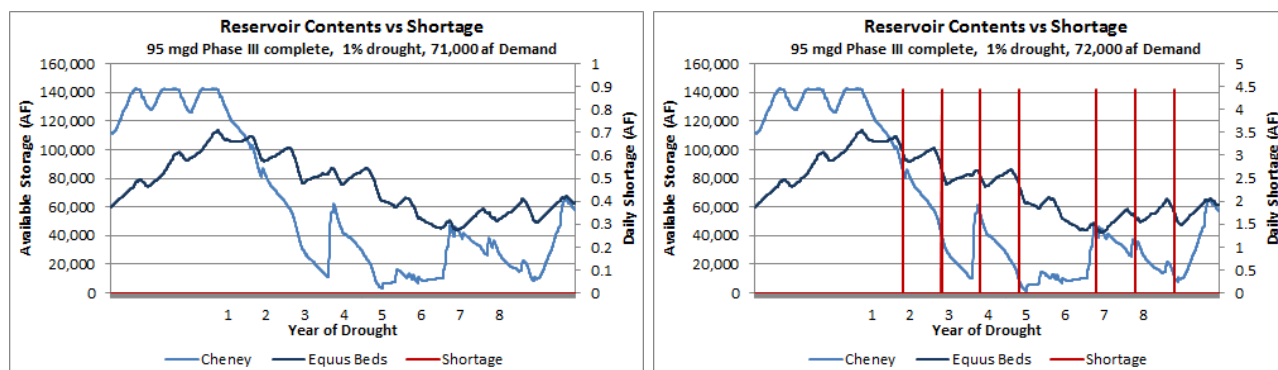


Figure 11. Expansion of ASR to 95 mgd, 1% drought.

The shortages shown in both Figure 10 and Figure 11 indicate that the system is limited in its ability to meet peak day demands.

Alternative #5 – Indirect Potable Reuse

Description

This alternative provides 15 mgd of indirect potable reuse (IPR) water to the main water treatment plant. The water would be diverted from downstream of the wastewater treatment plant through diversion wells, pre-treated to approximately match the existing raw water supplies, then pumped to the main WTP for conventional treatment.

Water pumped from the Equus Beds is legally reusable, which gives the City the right to recapture return flows originally from the Equus Beds and reuse them to extinction (we understand that Wichita is also working with the State of Kansas to make part or all of the water from Cheney also reusable). At the existing demand of 62,000 acre-feet per year, the minimum daily demand is 35

Memorandum

October 3, 2013

Page 17

mgd. Assuming that half of the supply on the minimum day is reusable, 15 mgd is a conservative estimate of reusable water, even on the minimum-use day.

Rather than programming the model to calculate the amount of reusable water available at the wastewater treatment plant, this alternative assumes a steady supply of 15 mgd is available for indirect potable reuse.

Key Assumptions

- A steady flow of 15 mgd is available as a new supply. Because wastewater flows are often higher, this is a conservative assumption.
- Treatment, whether through single or multiple barriers, will be sufficient so that this water can be used in the municipal system.

Results

The model shows that a reuse system can provide a sustainable yield of 79,000 acre-feet through both the 1% and 2% drought, the highest sustainable yield of all the alternatives considered. This is because the yield of 15 mgd is higher than any of the other alternatives, however Figure 12 and Figure 13 show that the addition of a consistently available supply also helps maintain the storage in both Cheney and the Equus Beds, so they could provide even more yield if the existing pipeline capacities were increased.

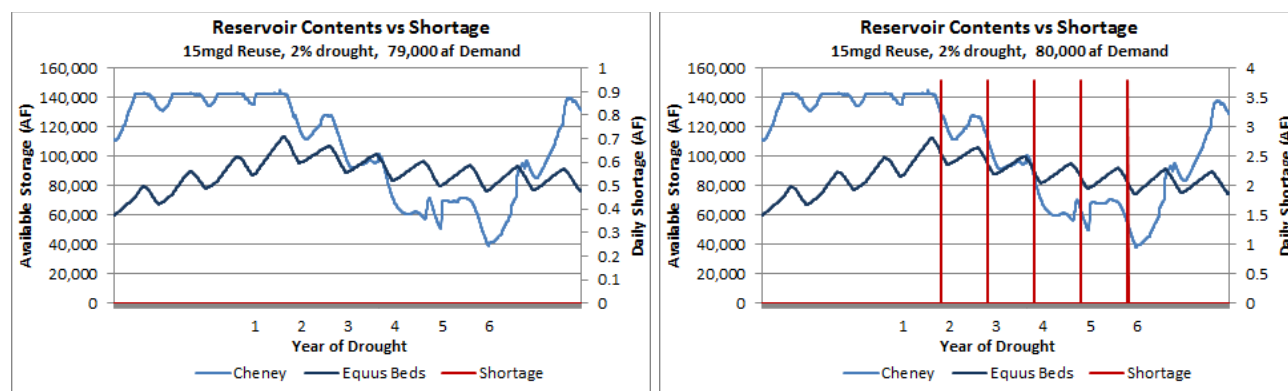


Figure 12. Indirect Reuse, 2% drought.

Memorandum

October 3, 2013

Page 18

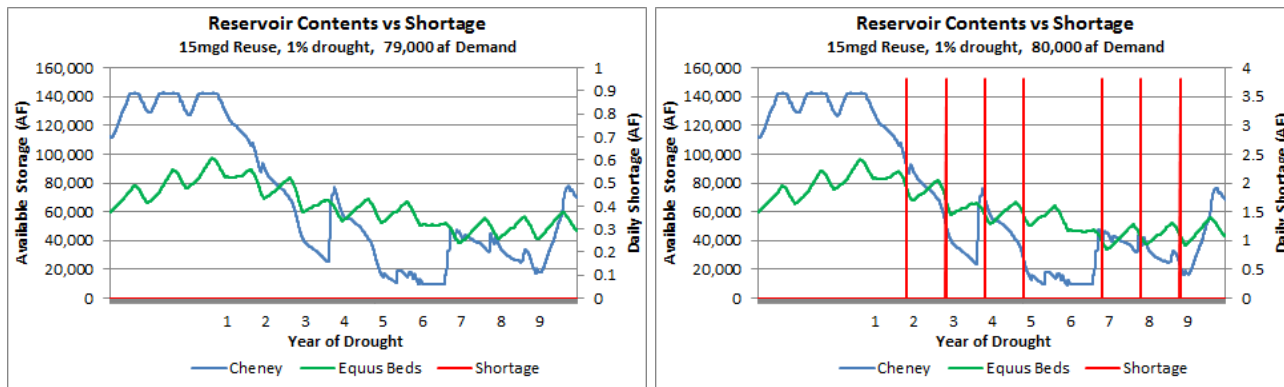


Figure 13. Indirect Reuse, 1% drought.

Both Figure 12 and Figure 13 show the shortage occurs when the combined capacity of the delivery system (146.7 mgd) is exceeded when the demand is set to 80,000 acre-feet per year.

The graphs above show there is still water in storage under both the 1% and 2% droughts. Expanding the pipelines allow the system to provide 89,000 acre-feet/year in the 1% drought and 91,000 acre-feet under the 2% drought.

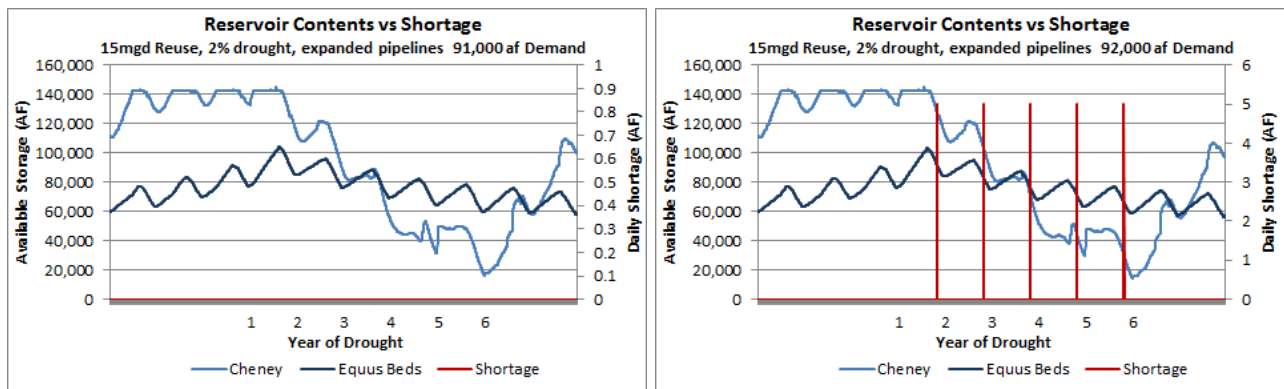


Figure 14. Indirect Reuse, expanded pipeline capacities, 2% drought.

Memorandum

October 3, 2013

Page 19

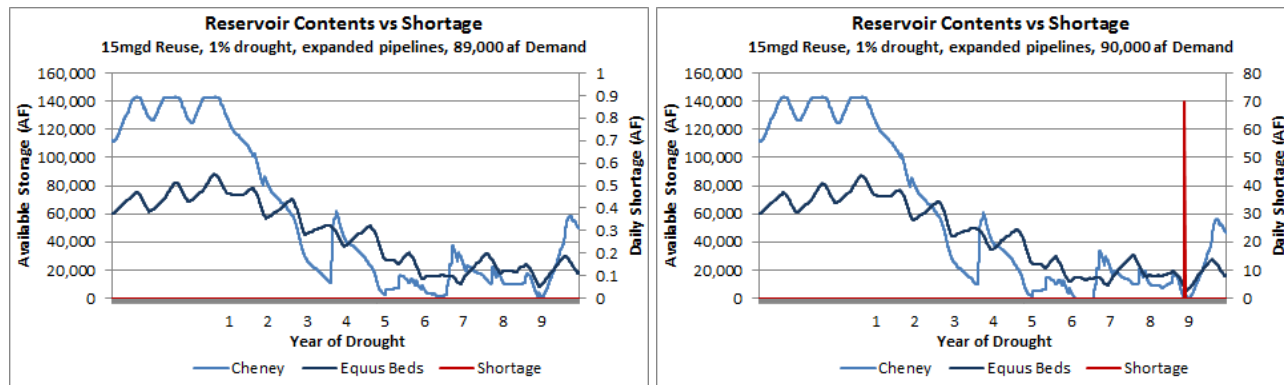


Figure 15. Indirect Reuse, expanded pipeline capacities, 1% drought.

These graphs show that the peak day delivery capacity still controls under the 2% drought, though the physical supply controls under the 1% drought.

Alternative #6 – Cheney Pipeline to ASR

Description

This alternative consists of a pipeline that takes water from Cheney Reservoir to the ASR Phase II surface water treatment plant for treatment and injection into the Equus Beds Aquifer. This is a project similar to the El Dorado to ASR pipeline, except it uses water that Wichita already has the right to divert and use, that would otherwise spill from Cheney Reservoir.

Key Assumptions

- Diversions from the Ninnescah River will be of water that could not be stored in Cheney Reservoir. This could either be water from uncontrolled spills or from water released from the flood control pool.
- The maximum capacity of the pipeline is 10 mgd.

Results

The Cheney alternative had a maximum sustainable yield of 71,000 acre-feet for both the 1% and 2% drought. Available storage is shown in Figure 16 and Figure 17.

Memorandum

October 3, 2013

Page 20

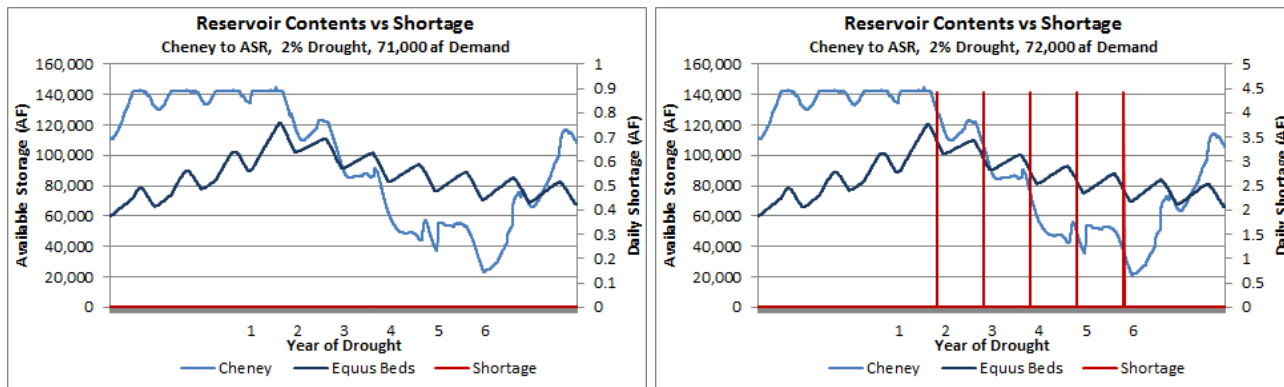


Figure 16. Pipeline from Cheney to ASR WTP, 2% drought.

Increasing demands to 72,000 acre-feet per year causes the system to short the demands because of insufficient delivery capacity on the peak day.

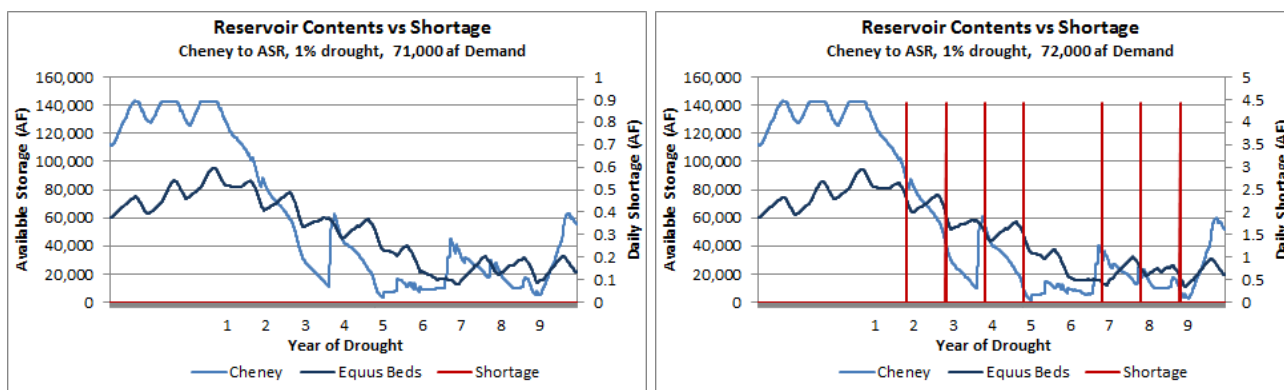


Figure 17. Pipeline from Cheney to ASR WTP, 1% drought.

Memorandum

October 3, 2013

Page 21

Summary of Alternatives

Table 1 summarizes the alternatives described above.

Table 1. Summary of Alternatives.

Yield for Alternatives Under a 1% Drought					
Alternative	Max Yield - no shortage (af/yr)	Peak day demand satisfied (mgd)	Increased yield above existing (af/yr)	2060 demand (af/yr)	2060 shortage (af/yr)
Existing System - current pipeline capacities	71,000	131.2			
<i>Existing System - expanded pipelines</i>	<i>73,000</i>	<i>135.0</i>	<i>2,000</i>	<i>88,000</i>	<i>15,000</i>
ASR Phase 1 Complete	71,000	131.2	0	88,000	17,000
ASR Phase 2 Complete	71,000	131.2	0	88,000	17,000
Alts 1-2, El Dorado to downtown ¹	76,000	140.5	5,000	88,000	12,000
Alt 3 - El Dorado to ASR ¹	71,000	131.2	0	88,000	17,000
Alt 4 - Expanded ASR	71,000	131.2	0	88,000	17,000
Alt 5 - Reuse (15mgd)	79,000	146.0	8,000	88,000	9,000
<i>Alt 5 - Reuse (15mgd) - expanded pipelines</i>	<i>89,000</i>	<i>164.5</i>	<i>18,000</i>	<i>88,000</i>	<i>-1,000</i>
Alt 6 - Cheney to ASR	71,000	131.2	0	88,000	17,000
¹ Assumes 158kaf of storage in El Dorado Reservoir, existing ASR capacity, 20,000 af/yr ag demand.					
Yield for Alternatives Under a 2% Drought					
Alternative	Max Yield - no shortage (af/yr)	Peak day demand satisfied (mgd)	Increased yield above existing (af/yr)	2060 demand (af/yr)	2060 shortage (af/yr)
Existing System - current pipeline capacities	71,000	131.2			
<i>Existing System - expanded pipelines</i>	<i>82,000</i>	<i>151.6</i>	<i>11,000</i>	<i>88,000</i>	<i>6,000</i>
ASR Phase 1 Complete	71,000	131.2	0	88,000	17,000
ASR Phase 2 Complete	71,000	131.2	0	88,000	17,000
Alts 1-2, El Dorado to downtown ¹	76,000	140.5	5,000	88,000	12,000
Alt 3 - El Dorado to ASR ¹	71,000	131.2	0	88,000	17,000
Alt 4 - Expanded ASR	71,000	131.2	0	88,000	17,000
Alt 5 - Reuse (15 mgd)	79,000	146.0	8,000	88,000	9,000
<i>Alt 5 - Reuse (15 mgd) - expanded pipelines</i>	<i>91,000</i>	<i>168.2</i>	<i>20,000</i>	<i>88,000</i>	<i>(3,000)</i>
Alt 6 - Cheney to ASR	71,000	131.2	0	88,000	17,000
¹ Assumes 158kaf of storage in El Dorado Reservoir, existing ASR capacity, 20,000 af/yr ag demand.					

Memorandum

October 3, 2013

Page 22

Given the assumptions in the model about the order in which supplies should be used, the model shows that the majority of shortages will occur on peak days where there is insufficient delivery capacity to meet peak day demands, or, in a few instances, when Cheney and/or the Equus Beds are drawn down to the bottom of their usable pool and there is an insufficient supply. This leads to some general observations:

- Because the delivery capacity is so important for meeting peak day demands, the way to increase the number of days that peak-day yields can be met is to balance the draw-down of Cheney and the Equus Beds so that they go dry at the same time. This allows the maximum use of the City's available resources without instituting any conservation measures. However, drawing down both storage facilities to zero at the same time may result in a sudden shortage of water if reservoir and aquifer inflows do not increase before these storage vessels run dry.

We also recommend that planning be done with some minimum amount of storage held in reserve to guard against a drought with an exceedance probability of less than 1 percent. In systems with terminal storage (storage in the immediate vicinity of the water treatment plant), keeping a year or two of supply in the terminal reservoirs provides protection against failures in the delivery system. Wichita does not have terminal storage, however maintaining a six months or a year's worth of water in storage would provide a pool of water for the city to manage during a severe and sustained drought.

- To provide system redundancy, the delivery capacity from both sources should be increased so that either source can meet peak day demands by itself. If the delivery capacity from the Equus Beds is expanded to meet peak day demands, Cheney could be drawn down first, which has the benefit of minimizing the evaporation loss at Cheney. The disadvantage of relying on one system or the other is that a single source could sufficiently change the water quality at the treatment plant to make treatment difficult, and it would require capital expenditures.
- Of those analyzed, the single project to meet the city's estimated 2060 demands is indirect potable reuse. This is because the yield of this project is constant throughout the drought, it has a higher delivery capacity than other alternatives, and it allows more water to remain in Cheney and the Equus Beds. This supply may have a higher treatment cost than other alternatives, but it does provide the water the city needs.
- Expanding the ASR system by bringing water from Cheney would result in approximately the same amount of water as bringing water from El Dorado. This is because the limited amount of storage in El Dorado limits how much water is available during a 1% drought. The Cheney alternative would likely be easier to complete because the city owns both the facility and the water rights, however the El Dorado alternative would provide greater geographic diversity to the City's water supply system.
- Bringing new water from El Dorado to downtown, either as raw water to the treatment plant, or treated water to the distribution system, would increase the peak day delivery to the City as long as water was held in storage during the drought.

Memorandum

October 3, 2013

Page 23

Suggested Next Steps

The city's potential yield could be further refined by performing the following tasks:

- Determining if the data for the Equus Beds is the best available, and updating the model if it is not. This includes both the elevation-volume relationship, as well as the stream-aquifer interaction. Of particular importance is how far the city can draw down the aquifer.
- Deciding if additional delivery capacity will be built from Cheney and the Equus Beds to the main water treatment plant, and if so, what how much additional capacity will be added. This is particularly important for the 2-percent runs. Adding likely capacity to the model and then re-running the alternatives will quantify how the additional capacity would affect yield.
- Adding more detailed water rights limitations to the model, including limitations on native rights and recharge limits from the Equus Beds Aquifer. Because the allowable volume of recharge credits is tied to the number of wells, determine how many wells will be constructed for each alternative, and modify the annual limit accordingly.
- Obtaining better inflow, use and reservoir management data for El Dorado Reservoir.

These steps could be completed by either a consultant or by City staff.



Memo

Date: January 6, 2013

To: Andrea Cole, SAIC

From: John Winchester, High Country Hydrology, Inc.

Re: Equus Beds Ground Water – Surface Water Interaction

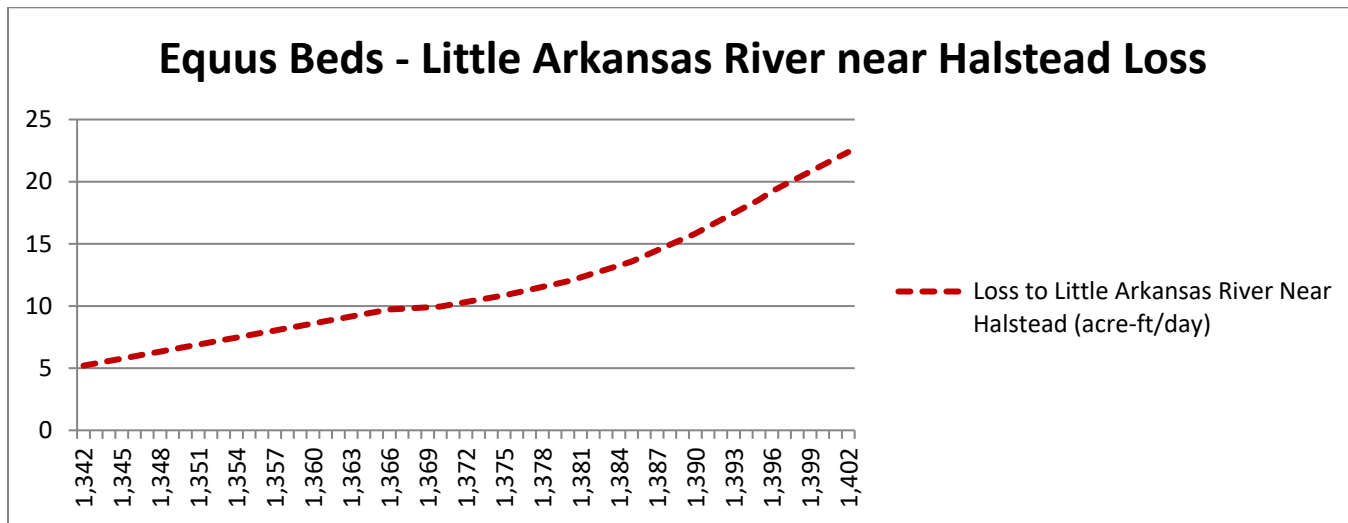
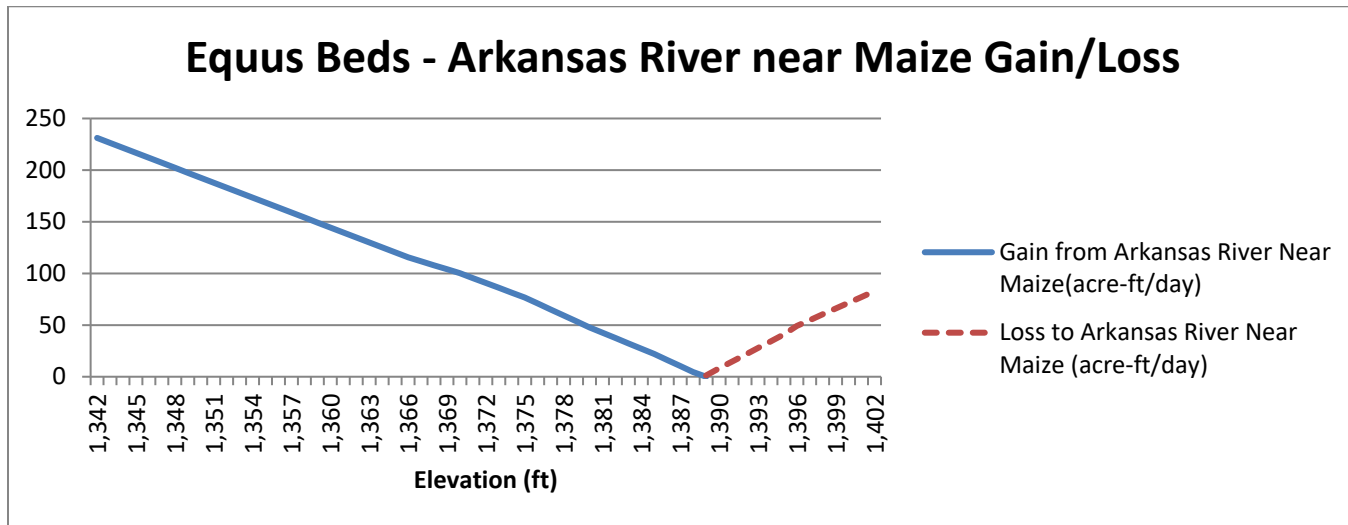
As you requested, we have compiled the data that defines the relationship of the stream gain/loss between the Arkansas, Little Arkansas, and Equus Beds Aquifer.

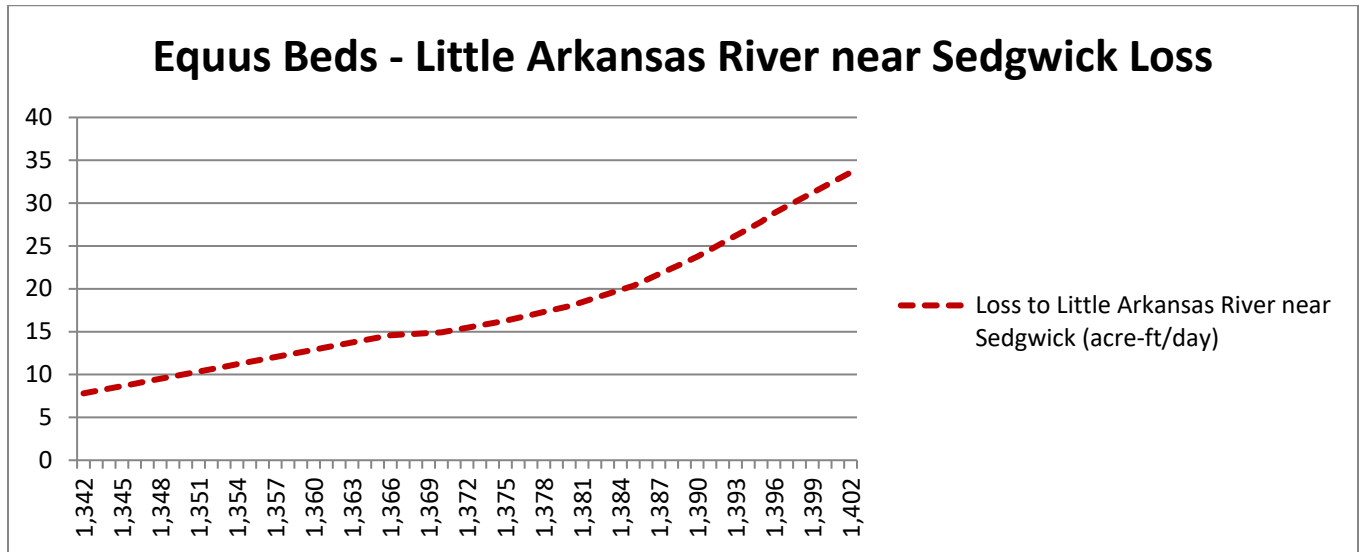
Ground water elevation is based on aquifer head at monitoring well 886. Negative numbers indicate flow from river to the Equus Beds aquifer. The following table is based on data in ResNet models 77, 78, 86. (Documented in Burns & McDonnell Wichita Operations Model Appendix A, Table 9, Page A10)

Elevation (ft)	Storage Deficit (acre-ft)	Gain/Loss to Arkansas River Near Maize (acre-ft/day)	Loss to Little Arkansas River Near Halstead (acre-ft/day)	Loss to Little Arkansas River Near Sedgwick (acre-ft/day)
1,342	429,650.9	-231.1835	5.200661	7.800992
1,343	421,860.3	-226.3653	5.389091	8.083636
1,344	414,069.8	-221.5471	5.577521	8.366282
1,345	406,279.2	-216.7289	5.765951	8.648926
1,346	398,488.6	-211.9108	5.954381	8.93157
1,347	390,698.0	-207.0926	6.14281	9.214215
1,348	382,907.4	-202.2744	6.33124	9.49686
1,349	375,116.8	-197.4562	6.51967	9.779504
1,350	367,326.3	-192.638	6.708099	10.06215
1,351	359,535.7	-187.8198	6.896529	10.34479
1,352	351,745.1	-183.0016	7.084959	10.62744
1,353	343,954.5	-178.1835	7.273388	10.91008
1,354	336,163.9	-173.3653	7.461818	11.19273
1,355	328,373.3	-168.5471	7.650248	11.47537
1,356	320,582.8	-163.7289	7.838677	11.75802
1,357	312,792.2	-158.9107	8.027107	12.04066
1,358	305,001.6	-154.0926	8.215537	12.32331
1,359	297,211.0	-149.2744	8.403967	12.60595
1,360	289,420.4	-144.4562	8.592397	12.8886
1,361	281,629.8	-139.638	8.780827	13.17124
1,362	273,839.3	-134.8198	8.969256	13.45388

1,363	266,048.7	-130.0016	9.157686	13.73653
1,364	258,258.1	-125.1835	9.346115	14.01917
1,365	250,467.5	-120.3653	9.534545	14.30182
1,366	242,677.0	-115.5471	9.722975	14.58446
1,367	234,886.4	-111.7215	9.779504	14.66926
1,368	227,095.8	-107.8959	9.836033	14.75405
1,369	219,305.2	-104.0702	9.892561	14.83884
1,370	211,514.6	-100.2446	9.949091	14.92364
1,371	203,724.1	-95.53983	10.12998	15.19497
1,372	195,933.5	-90.83504	10.31088	15.46631
1,373	188,142.9	-86.13025	10.49177	15.73765
1,374	180,352.3	-81.42547	10.67266	16.00899
1,375	172,561.7	-76.72066	10.85355	16.28033
1,376	164,771.2	-70.93885	11.07967	16.6195
1,377	156,980.6	-65.15703	11.30579	16.95868
1,378	149,190.0	-59.37521	11.5319	17.29785
1,379	141,399.4	-53.59339	11.75802	17.63702
1,380	133,608.8	-47.81157	11.98413	17.9762
1,381	125,818.3	-42.65256	12.30069	18.45104
1,382	118,027.7	-37.49355	12.61726	18.92588
1,383	110,237.1	-32.33455	12.93382	19.40073
1,384	102,446.5	-27.17553	13.25038	19.87557
1,385	94,655.92	-22.01653	13.56694	20.35041
1,386	86,865.34	-16.20496	14.01917	21.02876
1,387	79,074.77	-10.39339	14.47141	21.70711
1,388	71,284.18	-4.581818	14.92364	22.38545
1,389	63,493.60	1.229756	15.37587	23.0638
1,390	55,703.02	8.033055	15.8281	23.74215
1,391	47,912.44	14.61024	16.37078	24.55616
1,392	40,121.86	21.18744	16.91345	25.37018
1,393	32,331.28	27.76462	17.45613	26.1842
1,394	24,540.7	34.34181	17.99881	26.99821
1,395	16,750.12	40.919	18.54149	27.81223
1,396	8,959.534	49.1405	19.21984	28.82975
1,397	7,466.278	54.76364	19.74744	29.62116
1,398	5,973.022	60.38678	20.27504	30.41256
1,399	4,479.767	66.00991	20.80264	31.20397
1,400	2,986.511	71.63306	21.33025	31.99537
1,401	1,493.256	77.2562	21.85785	32.78678
1,402	0.0	82.87934	22.38545	33.57818

The following graphs show that the Equus Beds Aquifer gains or loses water to the Arkansas River depending on the aquifer elevation. The aquifer always loses water to the Little Arkansas River, with higher aquifer levels resulting in higher aquifer losses.







Memo

Date: Feb 7, 2013

To: Nathan Winkley, City of Wichita

Cc: Mike Jacobs, Paul Johnson

From: John Winchester, High Country Hydrology, Inc.

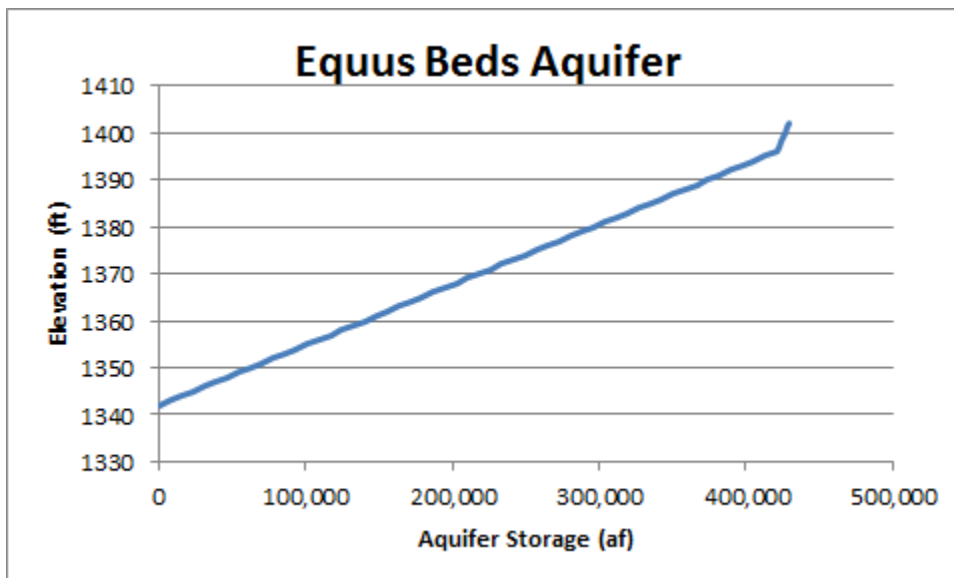
Re: Resnet Representation of the Equus Beds Aquifer

As you requested during our meeting on Wed, Feb 5, the following are some of the characteristics of the Equus Beds Aquifer, as represented in the Resnet model.

Aquifer Elevation-Capacity

The Equus Beds Aquifer is modeled as a reservoir with no surface area. The elevation-capacity curve in Resnet is defined by a table that equates elevation with “storage deficit.” This definition assumes that anytime the aquifer is less than full, there is a deficit in storage. The elevation-capacity data presumes that 429,700 acre-feet of water that could be pumped when the ground water is at an elevation of 1402 feet, and the aquifer would be empty when it is drawn down 60 feet to an elevation of 1342 feet.

As shown in the following graph, the elevation-capacity relationship is linear between the elevation 1343 feet and a capacity of 0 acre-feet, and elevation 1395 feet and a capacity of 412,901 acre-feet (that is, bend in the curve is at 1395 feet). From this, one could suppose that the storage graph was generated from three points (1402:412,901, 1395:412,901, 1343:0).



Recharge and River Gain-Loss

The Equus Beds Aquifer gains water from surface recharge, and gains/loses water to both the Arkansas and Little Arkansas rivers.

RECHARGE

From the Resnet documentation¹

“Natural aquifer recharge was estimated to be 3.2 inches per year by the U.S. Geological Survey. This natural recharge is represented in the operations model as an import to this node (No. 120) of 18,800 acre-feet/year.”

Dividing the recharge volume by the recharge depth results in an aquifer area of 70,500 acres (110 square miles). I have not seen the foundational material from the USGS that supports this

AQUIFER GAIN/LOSS

From the Burns & McDonnell work, the Equus Beds Aquifer both gains and loses water to the Arkansas and Little Arkansas rivers.

From the Resnet model data

“The interaction between the Equus Beds aquifer and local streams was evaluated in the MODFLOW groundwater model. Generally, aquifers receive their recharge from precipitation and streams serve as aquifer drains. The outflow from aquifers supports the baseflow in these streams.”² Aquifer levels are derived from data measured in Monitoring Well 886.³

The river gain/loss is a function of the elevation of the aquifer. In Resnet, this was accomplished with a “leaky reservoir,” where the reservoir seepage rates were adjusted using elevation. In Modsim, the reservoir seepage can only be a positive number, so having a gain (negative loss) was accomplished by setting the capacity on links connecting the aquifer to the river at the beginning of each timestep.

In Resnet, the Equus Beds Aquifer loses water to the Little Arkansas River at all aquifer elevations, loses water to the Arkansas River when aquifer elevations are high, but gains water from the Arkansas River when aquifer elevations are low.

The following table specifies the aquifer elevation-storage relationship and summarizes the aquifer’s gains-lose relationship.

¹ Model documentation final_eis_appendices.pdf. Appendix A, page A10.

² Model documentation final_eis_appendices.pdf. Appendix A, page A10.

³ Model documentation final_eis_appendices.pdf. Appendix A, footnote (a) to Table 5, page D27.



Table 9: Equus Beds Storage Deficit-Gain-Loss Data

Index Well 886 Elevation (feet NGVD)	Storage Deficit (acre-feet)	Total Gain from Rivers (cfs)	Total Loss to Rivers (cfs)	Net Equus Beds Loss Rates (cfs)	
				To Arkansas River	To Little Arkansas River
1,342	429,700	133	23	-116.6	6.6
1,360	289,400	100	38	-72.8	10.8
1,366	242,700	89	43	-58.3	12.3
1,370	211,500	82	44	-50.5	12.5
1,375	172,600	73	48	-38.7	13.7
1,380	133,600	62	53	-24.1	15.1
1,385	94,700	54	60	-11.1	17.1
1,389	63,500	48	68	0.6	19.4
1,390	55,700	46	70	4.1	20.0
1,395	16,800	38	82	20.6	23.4
1,396	9,000	36	85	24.8	24.2
1,402	0	29	99	41.8	28.2

A complete table of stream-aquifer interaction can be found in our memo titled “Equus Beds Ground Water – Surface Water Interaction,” sent to Andrea Cole on January 6, 2013.





Memo

Date: Feb 12, 2013

To: Paul Johnson

Cc: Nathan Winkley, Mike Jacobs, John Christopher, Lynn Moore

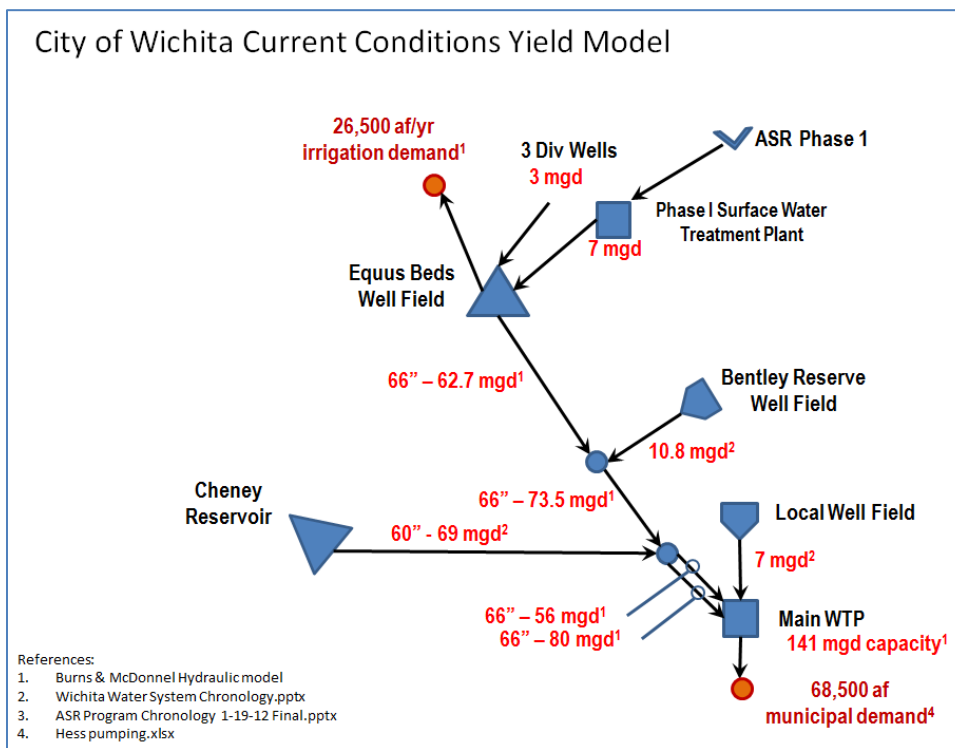
From: John Winchester, High Country Hydrology, Inc.

Re: Preliminary Model Results for Current Conditions

As we discussed during our meeting on Wednesday, February 6, we have successfully ported Wichita's Resnet yield model to Modsim. The calculated reservoir contents are not identical, but for practical purposes are the same. The project does not have the time or budget to exhaustively determine why the models differ. For more information about replicating the Resnet model, see our memo dated February 8, 2013.

The 2008 Resnet model used water supplies and demands projected for 2050, but with new information for the Equus Beds Aquifer. Some of the significant features of this model include an ASR recharge capacity of 100 mgd, an expansion of the local well field, and an annual demand of 125,090 acre-feet, as well as pipeline capacities that are larger than currently exist.

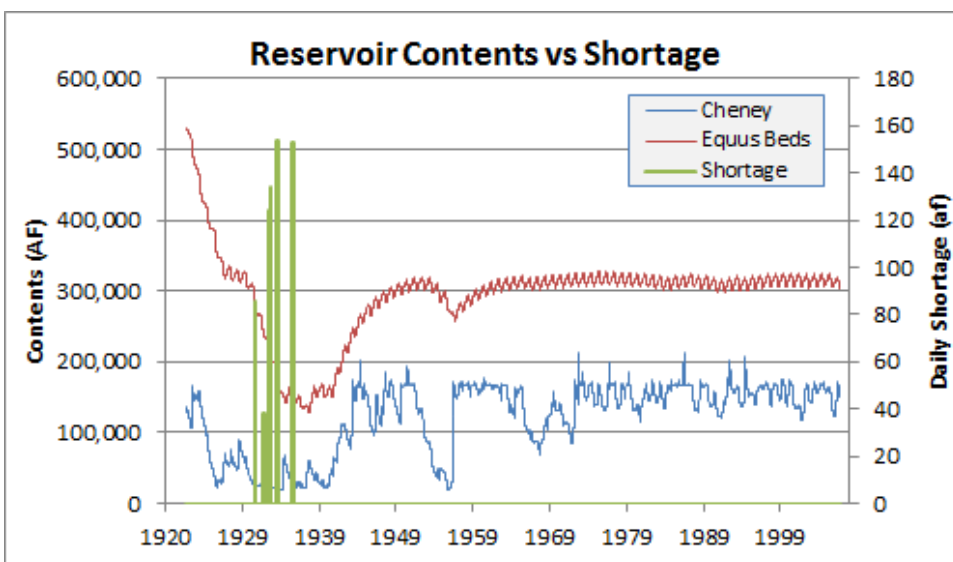
To evaluate the current system's ability to meet demands, we have taken the 2050 model and removed or downsized the facilities and demands so they represent the current system as closely as possible. The following schematic shows our current understanding of capacities of the existing system.



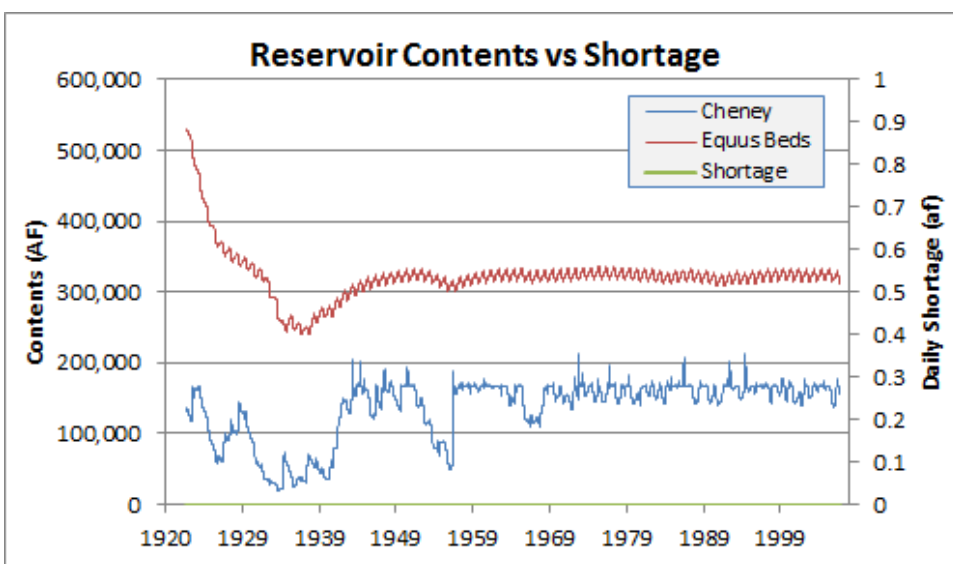
Pipeline capacities in the 2050 model were reduced, where applicable, down to the existing capacity. Some of the pipelines were modeled with parallel links with different costs. Varying costs is one way to balance the flow in the system so one source doesn't deliver all its water before another source begins delivering water (e.g., Cheney Reservoir and the Equus Beds Aquifer). For pipelines modeled using parallel links, the capacity of the link with the lowest priority was reduced first, assuming that this would most accurately preserve the model's allocation of water.

The municipal demand for current conditions comes from the Hess Pump Station for 2012. Daily Hess pumping data was provided by the City for 1989-2012. Because demands have changed over time, the mean daily demand was calculated for the 2002-2012 period. Taking the mean of a series reduces peaks and increases minimums. To maintain actual peak day demands, each of the years was compared to the mean daily demand, and 2012 was found to have the highest correlation. Consequently, the pattern for the daily demand is the 2012 Hess Pump Station data. This pattern is scaled proportionately to generate different levels of annual demand. The annual pattern is repeated for every year of the model's period of record.

After setting the capacities and demands in the model to reflect current conditions, the model was run with a demand of 68,500 acre-feet, the amount actually pumped in 2012. At this demand level, the model had 287 days of shortage, primarily in the 1930s. The following chart shows the reservoir contents and the municipal shortage.



Reducing the demand until there was no shortage, we found that the existing system is capable of delivering water for the historical period of record without any shortage for an annual demand of 45,000 acre-feet per year. The following graph shows the reservoir contents for this demand level.



The following table summarizes how the number of days with municipal shortage are related to the annual demand.

Scenario Summary				
Demand (af)	Minimum Contents (af)		Max Day (mgd)	Days Short
	Cheney	Equus Beds		
68,500	16,672	128,482	118	287
65,000	17,114	143,104	112	203
60,000	17,515	150,737	103	105
50,000	17,922	150,737	86	21
47,500	18,037	150,737	82	14
46,000	18,499	150,737	79	7
45,000	19,065	150,737	77	0

This work is preliminary for two reasons. First, city staff are reviewing the storage characteristics for the Equus Beds Aquifer that are used in the model, and may be providing more accurate data. New data could affect the aquifer's ability to store and/or yield water, which in turn could affect how much demand Wichita's system can provide.

Second, the model's operations showed that under future conditions, the Equus Beds Aquifer was drawn down during the drought of the 1930s, but rebounded to previous levels over the long-term. The model for current conditions shows some rebound, but not as much as the future scenarios. It seems likely that the City would manage the aquifer so the rebound would be more complete than what is currently being show.

Once we receive new aquifer data (or acknowledgement that the existing data is satisfactory), the city may wish to have us adjust the balance of use between Cheney and the Equus Beds so they recover more equally. While rebalancing the distribution of yield may change the result somewhat, the system's ability to meet demand will likely remain approximately the same.





Technical Memorandum

Date: March 14, 2013

To: Paul Johnson, SAIC

Cc: Nathan Winkley, Mike Jacobs, John Christopher, Lynn Moore

From: John Winchester, High Country Hydrology, Inc.

Re: Extended drought reconstruction from PDSI

This memo summarizes the development of long-term reconstructed streamflows.

Background

Stream gauge records in south-central Kansas generally start in the 1920s. These cover the droughts of the 1930s, 1950s and 1990s, but do not necessarily reflect the long-term hydrologic variability.

Our research found that the only long-term surrogate data for south-central Kansas is approximately 1000 years of summer Palmer Drought Severity Index (PDSI) data developed by Dr. Edward Cook at the Lamont-Doherty Earth Observatory of Columbia University.¹ The Palmer soil moisture algorithm is calibrated for relatively homogeneous regions. The Palmer Index varies roughly between -6.0 and +6.0, which Palmer arbitrarily selected based on his original study areas in central Iowa and western Kansas.² The PDSI is a meteorological drought index, and it responds to abnormally wet or dry weather conditions. For example, when precipitation increases from below average to above average, the PDSI shows an end to the drought without considering streamflow, lake and reservoir levels, and other longer-term hydrologic impacts.

The Available PDSI Data

Cook originally produced a gridded network for the continental United States in 1999, based on 388 tree ring chronologies. In 2004 he expanded the spatial and temporal coverage to include 286 points in a 2.5 degree grid covering most of North America, as shown in Figure 1. The 2004 PDSI reconstructions are based on 835 tree-ring chronologies. Figure 2 shows the tree ring sites used for the 1999 network (there was no comparable map for the 2004 chronologies on the NOAA web site). As shown in the figure, in 1999 there are no tree ring sites located in Kansas, so PDSI values for the six locations in Kansas are interpolated from sites in other states.

¹ <http://www.ncdc.noaa.gov/paleo/pdsi.html>

² Palmer, Wayne C., Meteorological Drought – Research Paper No. 45. Office of Climatology, Washington DC. 1965.



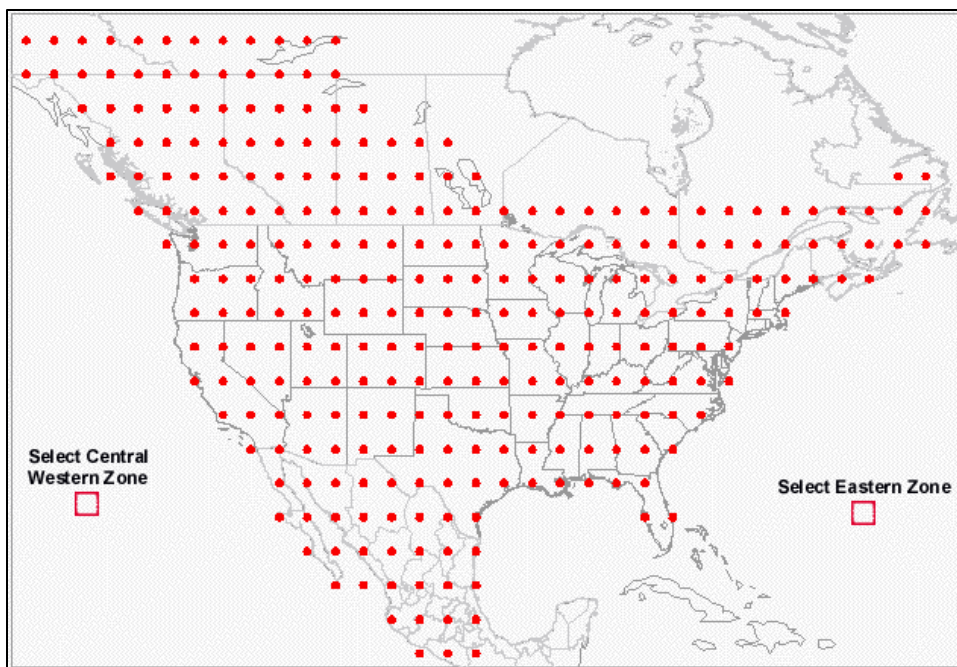


Figure 1. Grid locations where PDSI has been generated (Cook, 2004).

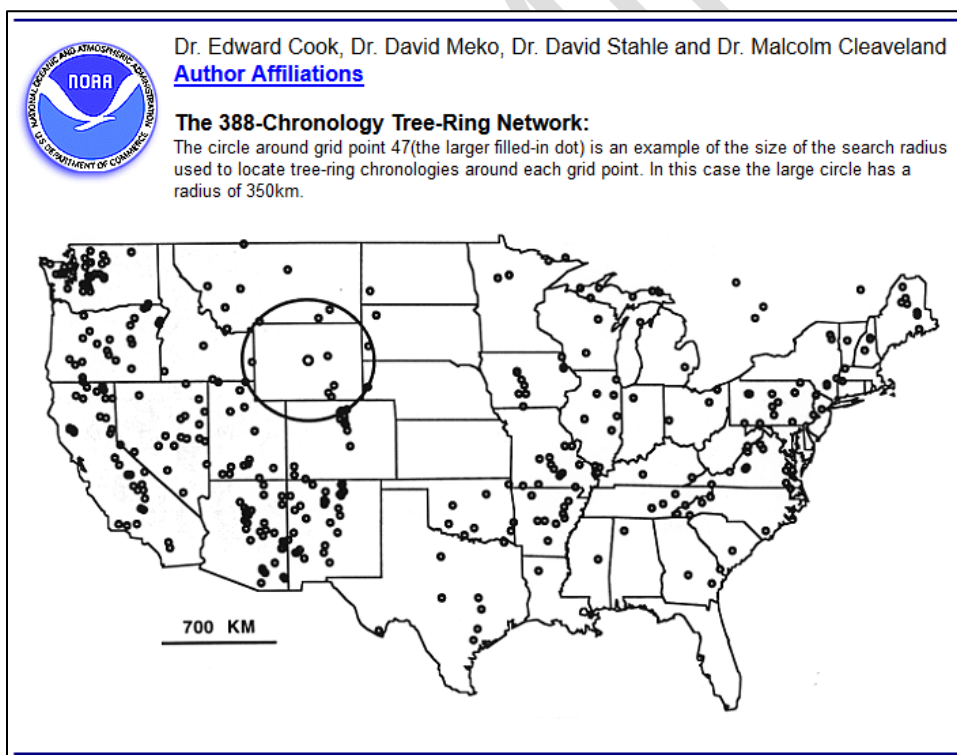


Figure 2. Locations of tree ring chronologies used by Cook in 1999.

The PDSI values generated in 2004 represent the average summer (June-August) PDSI.³ Six of the grid locations published in 2004 fall within Kansas. Comparing the summer PDSI with annual flows for the Little Arkansas River at Valley Center, we found that the best correlation between streamflow and PDSI was obtained when we used the PDSI for southwestern Kansas.

The PDSI data for southwestern Kansas has a period of record from 887 AD – 2003 AD. Figure 3 shows a time series of the PDSI and the number of tree ring sites used to reconstruct the PDSI for the period of record.

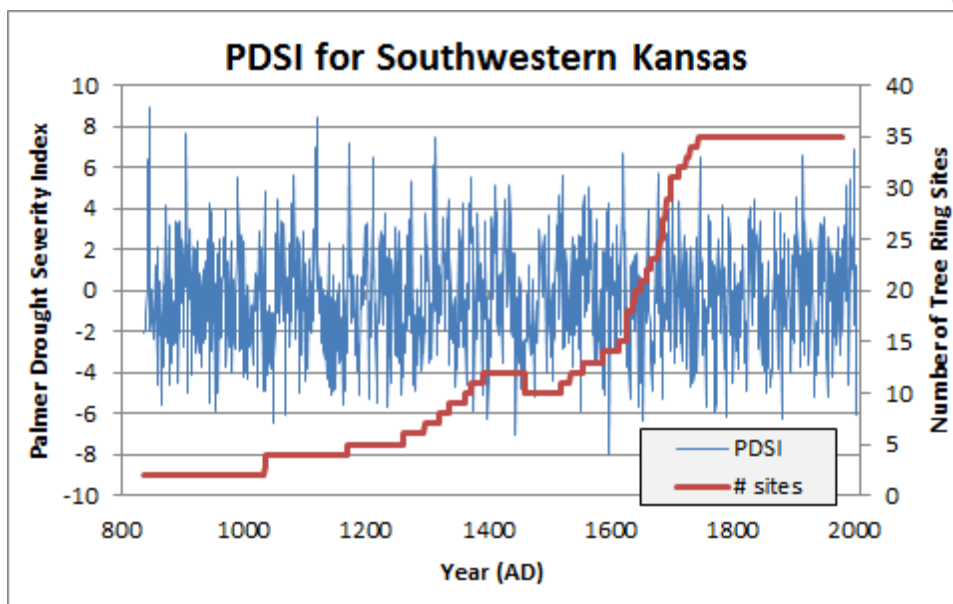


Figure 3. PDSI and number of tree sites.

The Cook data set included both the PDSI calculated from historical records for 1900-2003, and the reconstructed PDSI for 887-2003. The correlation between these two data sets had an r^2 of 0.82. For the following analyses, we used a composite PDSI that was made up of the reconstructed values for the years 887-1899, and actual values for 1900-2003.

Drought Return Period

Using the PDSI data, we calculated the return period for various droughts. While the method for calculating the return period for a single year is well documented, there is no standard method for calculating the return period for multi-year droughts.

We calculated and compared the return period for droughts in three ways: using single years, using the number of consecutive years in a drought, and using the cumulative PDSI.

³ <http://www.ncdc.noaa.gov/paleo/pdsi.html>

Single Year Severity

To calculate the return period of single years, we sorted the annual PDSI values into ascending order, so the most negative values were first. We ranked the data, with 1 being the most negative value.

We applied the equation for recurrence intervals to this data,

$$T = (n+1)/m$$

where

T = recurrence interval in years

n = number of years in the time series

m = rank of the individual year (1, 2, 3...)⁴

While there were drier years before 1900, during the gauged period of record covered by the PDSI (1923-2003), defining droughts based on single years showed that 2002 was the driest single year in the 1900-2003 period of record, followed by 1956 and 1934.

While individual years are interesting, they do not adequately describe the droughts experienced in Kansas.

Number of Drought Years

Counting the number of years with below average precipitation and runoff can be used to determine the duration of a drought.

Rather than simply count the number of sequential years with a PDSI below zero, we modified our calculation of duration to account for variation of average years, and to allow for single years with average conditions that occur in a string of drought years.

Based on Palmer's original paper, the range of -0.49 to 0.49 is considered "near normal." Because there are years with a negative PDSI that are still considered within the normal range, we did not consider a year a drought year until the PDSI was less than -0.5. This assumption eliminated 82 of the 1167 years from the drought classification.⁵

In recognition that droughts can last through a single near-average year, series of drought years were considered unbroken if it contained a single year with a positive PDSI less than 0.5. While there were individual positive years in strings of drought years, this assumption did not change any of the calculated drought durations because all the individual years had a PDSI of greater than 0.5.

⁴ Dunne, Thomas, and Leopold, Luna. Water in Environmental Planning, 1978.

⁵ PDSI drought durations.xlsx

Drought Duration and Severity

City staff at Wichita asked us to analyze surrogate hydrologic data to determine long-term drought durations and severities. This memo discusses long-term droughts and potential data sets that could be used for planning purposes.

Drought Duration and Severity

There are no long-term streamflow reconstructions for south-central Kansas, however Ed Cook and John Krusic have reconstructed annual values of the Palmer Drought Severity Index (PDSI) across North America, including six points in Kansas. We compared the annual values of PDSI with gauged streamflows for 1923-2003, and found that the PDSI for southwest Kansas was the best match for streamflows near Wichita. The PDSI reconstruction for southwest Kansas covers 1166 years, from 837 to 2003.

The PDSI reconstruction for southeast Kansas is based on tree ring chronologies. The number of sites used to develop the PDSI for southwest Kansas ranges from 2 to 35. Statistically comparing different periods of the reconstructed PDSI, we determined that years with more than 15 tree ring sites produced statistics more comparable with the historical record, whereas earlier values based on fewer sites tended to be biased toward drought. Consequently we have limited our use of reconstructed PDSI to the years 1640-2003, which are based on 15 or more tree ring sites.

To determine drought duration, we counted the number of below-average years that occurred in a row, and then calculated the exceedance probability for the different durations using the standard equation,

$$\text{Exceedance} = \text{Rank} / (\text{Sample Size} + 1)$$

Using the same PDSI data, we calculated the total cumulative PDSI for each drought. Because annual PDSI data does not correlate well with historical daily stream gauge data, we suggest that the simplest strategy to generate model input for drought sequences is to use historical streamflow data from years with similar PDSI values. Based on historical PDSI data, we have assembled combinations of gauge data to represent the historical droughts portrayed in the PDSI data. Drought duration, severity and representative years from the historical gauge record are shown in Table 1 for various droughts.

Table 1. Drought Durations and Severity from PDSI Data

Suggested Drought Intervals based on reconstructed PDSI (1640-2003)				Representative Historical Years	
Exceedence Probability	Duration (yrs)	Cumulative PDSI	Mean pdsi	Years	Actual Cum. PDSI
10%	2	-4.4	-2.20	1925-1926	-4.9
4.0%	4	-8.8	-2.21	1925-1926, 1981 x 2	-8.8
2.0%	6	-15.6	-2.60	1952-1956, 1959	-16.1
1.3%	7	-19.6	-2.80	1946, 1952-1956, 1981	-19.6
1.0%	8	-22.4	-2.80	1933-1940	-24.4
0.40%	10	-31.4	-3.14	1952-1956 x 2	-31.1
0.20%	12	-38.2	-3.18	1952-1956 x 2, 1963-1964	-38.4
0.10%	14	-45.0	-3.21	1925, 1933-1940, 1936-1937, 1937, 1940, 1976	-45.0

Design Drought

City staff requested that we fit the drought-duration data to a distribution so they can see how much of the data is included in various multiples of the standard deviation.

The annual PDSI data were classified into wet and dry years, with wet years having a PDSI greater than 1, dry years less than a PDSI of -1, and normal years between 1 and -1. If two dry years were separated by a single wet year with a PDSI of 0.5 or less, the dry streak was considered to be continuous.

Assuming the year counts were divided into 9 bins, the Johnson’s Special Unbounded (SU) distribution best matched the number of consecutive drought years. The analysis of fit was made using sequential years for both wet and dry years (both positive and negative values of PDSI). The red data points show the number of droughts that occurred for each drought duration on the x-axis. Note that the secondary axis only approximately matches the function because it is not possible to mix x-y and bar graph types in Excel.

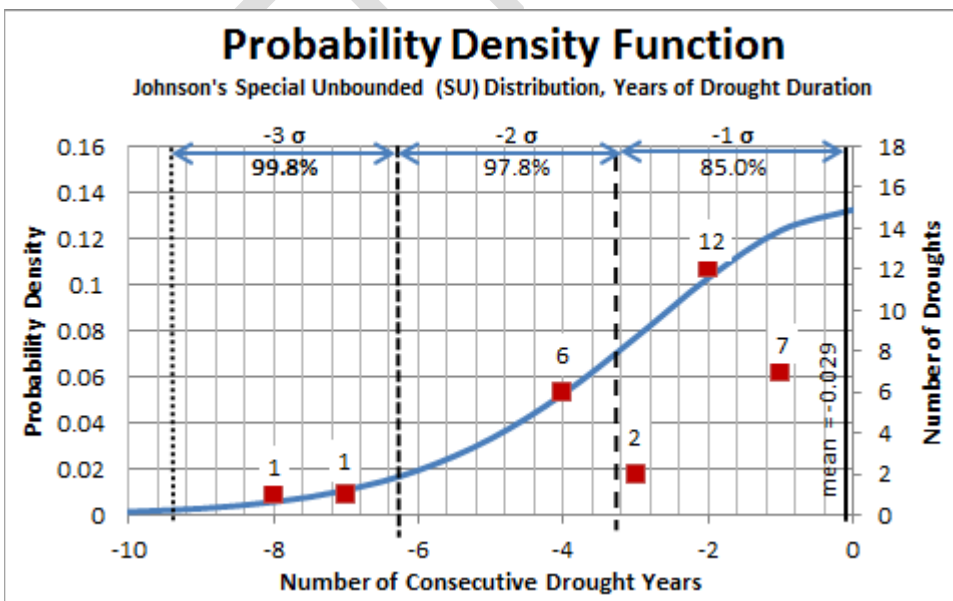


Figure 4. Fitted distribution and actual number of droughts

The graph shows the actual number of droughts for durations of 1, 2, 3... years. The analysis was done using an odd number of bins (9 bins for 16 years), which eliminated the outliers for droughts of 1- and 3-years.

Assuming the distribution represents the data, this graph shows that droughts with durations within 2 standard deviations would represent 97.8 percent of the droughts, including the drought with a 2-percent chance of occurring.



Technical Memorandum

Date: March 21, 2013

To: Paul Johnson, SAIC

Cc: Nathan Winkley, Mike Jacobs, John Christopher, Lynn Moore

From: John Winchester, High Country Hydrology, Inc.

Re: MODSIM Model Modifications

This memo summarizes modifications we have made to the MODSIM yield model since it was converted from RESNET so it would more accurately simulate Wichita's raw water collection and delivery system.

Pipeline Capacities

The pipeline capacities in the RESNET model were set to 2050 conditions. As discussed in other memos, the pipeline capacities were reviewed with the City's consultants and staff to determine the best estimate of current capacity. The original RESNET and revised capacities are shown in the following table.

Pipeline	RESNET Capacity (mgd)	Revised Capacity (mgd)
Cheney to Equus junction	80	69
Equus to Bentley junction	32	62.7
Bentley reserve well field to Equus pipeline	10.8	10.8
Bentley junction to Cheney junction	43	73.5
Local well field to main WTP	36.8	7
Local well field expansion to main WTP	45	0
ASR diversion to ASR WTP	100	3
New pipeline from Equus to main WTP	100	0

These values came from previous work by SAIC or from the Burns&McDonnell hydraulic model.

Wichita Municipal Demand

RESNET used a 2050 demand of 125,100 acre-feet per year. The revised 2060 demand developed by PEC is 87,600 acre-feet per year.

Ag Demand

The agricultural demand from the Equus Beds Aquifer in RESNET was set to 26,500 acre-feet per year, turned on from May 15 to August 15 each year. Because the



simulations for this study focused on drought years, the ag demand was increased to 34,000 acre-feet per year, to reflect increases that have historically been seen during droughts.

Cheney Area-Capacity Curve

Plotting out the area-capacity-elevation curve from RESNET showed that there were two points with typographical errors that created very large deviations from an otherwise smooth curve. The data for these points was interpolated to smooth the curve.

growth. The City believes that the medium growth forecast raw water demands for 2060 may be further reduced to 81,690 AF by implementing planned water use conservation measures, and has utilized this demand forecast to evaluate how water resources will perform under various hydrologic conditions.

2.3 Integrated Water Resources Management During a 1% Drought Using MODSIM-DSS

To evaluate the viability of existing and planned raw water resources versus the projected demands of 81,690 AF by the year 2060, the City developed a dynamic raw water resources model based on MODSIM-DSS (Figure 1). MODSIM-DSS is a water rights planning, water resources management, and river operations decision support system software that can simulate the effects that complex water resource management rules and strategies have on a set of networked raw water resources such as reservoirs, streams, or aquifers. MODSIM-DSS provides for input of variables such as integrated water resources management policy, water rights quantity limitations, water right rate limitations, raw water pipeline capacities, seasonal raw water resource preferences, reservoir conditions, streamflow levels, etc. Using MODSIM-DSS the City can optimize how raw water resources are utilized to meet demand based on any number of management criteria or outcome based goals. To simulate how the raw water demands during a 1% drought should be distributed between Cheney Reservoir, the EBWF, and ASR system, the City utilized the MODSIM-DSS model with the addition of updated drought variables:

1% Drought Simulation MODSIM-DSS Updates

- **Raw water resources include Cheney Reservoir, EBWF, ASR Credits**
 - Cheney Reservoir – existing water rights and a starting storage condition of 110% full based on the reservoir achieving this level during pre-drought conditions
 - EBWF – existing water rights of 40,000 AF
 - ASR Recharge Credits - 60,000 AF of credits available not limited by current minimum index water level restriction
 - E&S Wellfield is not considered a firm source during drought due to water quality and limited capacity during lowered Arkansas River flows
 - Bentley Reserve Wellfield is not considered a firm source during drought due to limiting streamflow triggers and poor water quality during lowered Arkansas River flows
- **Future projected 2060 demand of 81,690 AF**
 - Raw water savings available through DRP added
 - Base demand is reduced depending on Cheney Reservoir condition and associated DRP triggers
- **Simulated 8-Year Drought Hydrologic Components**
 - 1933-1940 stream flows for rivers and streams and Cheney Reservoir
 - 1933-1940 precipitation and evaporation for Cheney Reservoir

Figure 1 - A computer screen capture of the graphical user interface of the City's MODSIM-DSS raw water resources model showing the network of simulated reservoirs, streams, aquifers, interconnections, and sources of demand.



- **Updated Outcome-Based Goals**
 - Prevent economic distress of consumers due to occurrence of DRP Stages 3 and 4
 - Must maintain both Cheney Reservoir and EBWF as viable resources at all times
 - Utilize 40,000 AF per year from EBWF prior to use of ASR Recharge Credits

By running MODSIM-DSS with the updated 1% drought simulation variables, an optimized daily raw water demand is generated for each water resource. The results of the 1% drought MODSIM-DSS simulation indicate that both the EBWF and Cheney Reservoir can be kept viable through the drought by utilizing ASR recharge credits and the City's DRP (Table 2-3). Under these conditions the City must maintain the availability of all raw water resources (EBWF, ASR Recharge Credits, and Cheney Reservoir) to meet daily drought demands and prevent implementation of Stage 3 water restrictions. Further review of the reservoir accounting results indicates that Cheney Reservoir can be balanced such that the calculated minimum reservoir condition during the eight-year drought period is 42% of conservation pool, with an average of 62% (see Figure 2).

Table 2-3: MODSIM-DSS simulation results for the 1% drought utilizing projected 2060 demands

MODSIM-DSS Variable	Drought Year 1	Drought Year 2	Drought Year 3	Drought Year 4	Drought Year 5	Drought Year 6	Drought Year 7	Drought Year 8
Baseline City Demand (AF)	81,690	81,690	81,690	81,690	81,690	81,690	81,690	81,690
Simulated Calendar Year of Drought	1933	1934	1935	1936	1937	1938	1939	1940
Revised City Demand from Drought Response Plan (AF)	81,262	72,492	71,116	71,890	70,812	70,811	71,116	70,664
City Demand Assigned to EBWF & ASR	34,202	45,651	59,907	46,732	56,579	41,980	39,308	39,491
City Demand Assigned to Cheney Reservoir	47,060	26,841	11,209	25,158	14,233	28,831	31,808	31,173
Cheney % of Conservation Pool 12 Month Average	110%	92%	62%	59%	62%	53%	53%	63%

2.4 Groundwater Modeling Setup - 1% Drought Simulation

In 2009, to better understand the regional Equus Beds Aquifer and the effects on water levels due to current and planned ASR activities, the City contracted a study by the USGS. This study developed a three-dimensional finite-difference groundwater-flow model based on MODFLOW-2000. MODFLOW software is broadly recognized as the standard for simulation and prediction of groundwater conditions.

Figure 1 - A computer screen capture of the graphical user interface of the City's MODSIM-DSS raw water resources model showing the network of simulated reservoirs, streams, aquifers, interconnections, and sources of demand.

